Abstracts
The 37th Fullerene-Nanotubes General Symposium

第 37 回フラーレン・ナノチューブ
総合シンポジウム

講演要旨集

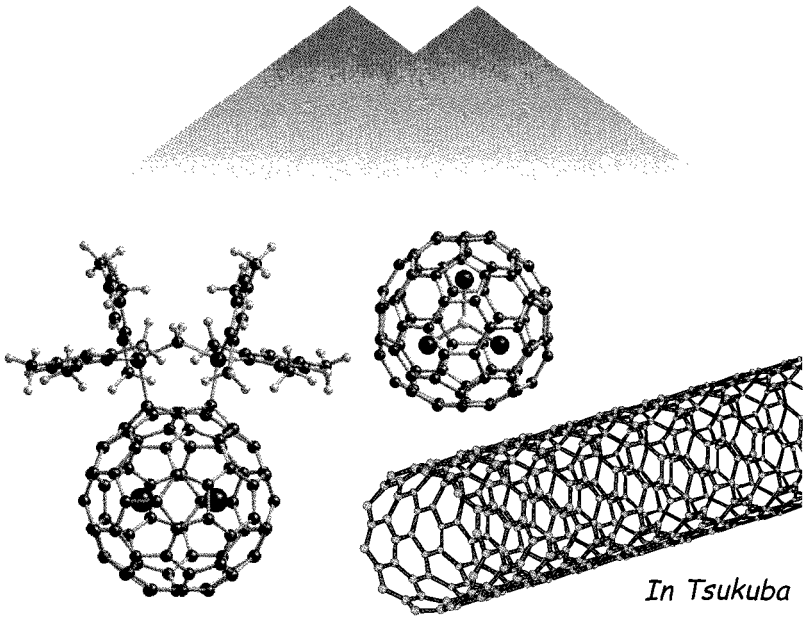

September 1-3, 2009, Tsukuba city, Ibaraki
平成 21 年 9 月 1 日−3 日　つくば国際会議場

The Fullerenes and Nanotubes Research Society
フラーレン・ナノチューブ学会

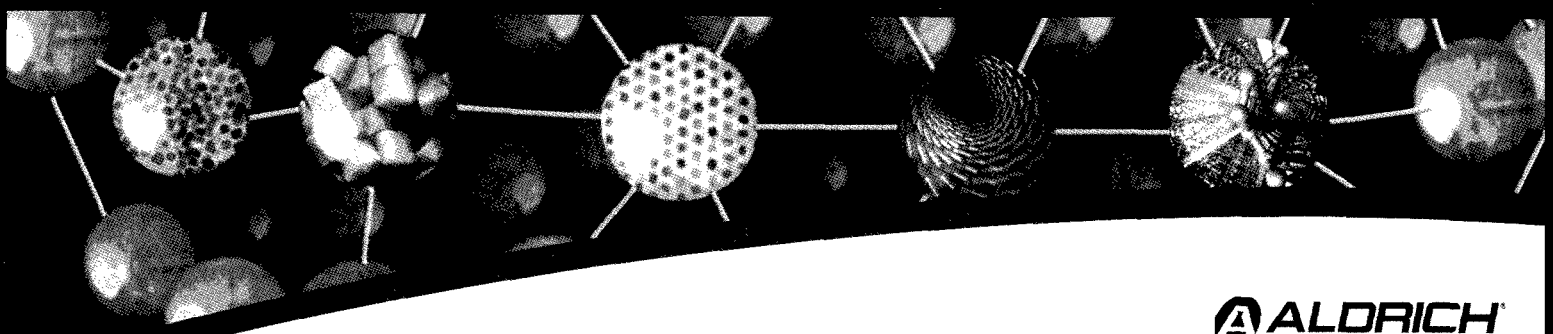

ALDRICH Chemistry

Single-Walled Nanotubes by CoMoCAT® process

- ナノチューブ直径分布が非常に狭い
- 高い単層カーボンナノチューブ含有量
- 高いアスペクト比

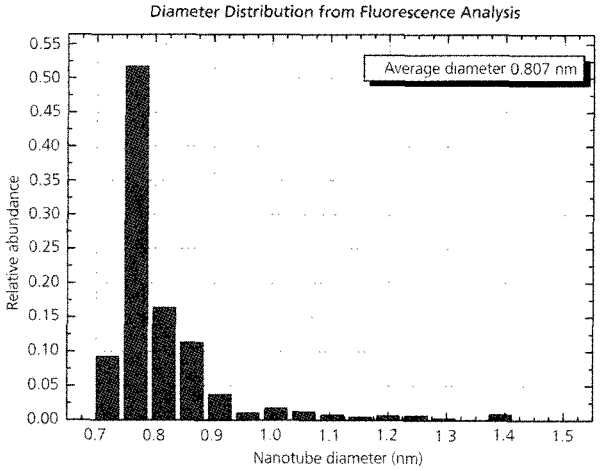

CoMoCATプロセスで作製されたSWNT（SWeNT® SG 65）の直径分布ヒストグラム。

詳しくは ***sigma-aldrich.co.jp/aldrich/nano*** まで

	SWeNT® CG 100	SWeNT® SG 65	SWeNT® SG 76
Aldrich製品番号	704113	704148	704121
容量	250mg, 1g	250mg	250mg
直径[1] (nm)	1.0 ± 0.3	0.8 ± 0.1	0.9 ± 0.2
長さ[2] (nm)	400–2,300 (mode:800)	450–2,000 (mode:900)	300–2,300 (mode:800)
炭素含有量[3] (%)		> 90	
SWCNT含有量[3] (% carbon as SWCNT)	75	80	80
Chirality Distribution[4] (%)	-	> 50 (6,5)	> 50 (7,6)
アスペクト比		> 1,000	

1. ラマンスペクトルとAFMより算出。2. AFMより算出。3. TGAより算出。4. ラマンスペクトルより算出。

SWeNT and CoMoCAT is a registered trademark of SouthWest NanoTechnologies, Inc.

SIGMA-ALDRICH®

シグマ アルドリッチ ジャパン株式会社

〒140-0002 東京都品川区東品川2-2-24
天王洲セントラルタワー4階

■製品に関するお問い合わせは、弊社テクニカルサポートへ
TEL：03-5796-7330 FAX：03-5796-7335
E-mail：sialjpts@sial.com

■在庫照会・ご注文方法に関するお問い合わせは、弊社カスタマーサービスへ
TEL：03-5796-7320 FAX：03-5796-7325
E-mail：sialjpcs@sial.com

http://www.sigma-aldrich.com/japan

Abstracts
The 37th Fullerene-Nanotubes General Symposium

第 37 回フラーレン・ナノチューブ
総合シンポジウム

講演要旨集

The Fullerenes and Nanotubes Research Society

The Chemical Society of Japan
The Physical Society of Japan
Japan Society of Applied Physics
The Society of Polymer Science, Japan
The Electrochemical Society of Japan

主催：フラーレン・ナノチューブ学会

共催：日本化学会
協賛：日本物理学会・応用物理学会・
高分子学会・電気化学会

Date: September 1st(Tue)–3rd(Thu), 2009
Place: Tsukuba International Congress Center
2-20-3 Takezono, Tsukuba, Ibaraki 305-0032
TEL: 029-861-0001
Presentation: Plenary Lecture (40 min presentation, 5 min discussion)
Special Lecture (25 min presentation, 5 min discussion)
General Lecture (10 min presentation, 5 min discussion)
Poster Preview (1 min presentation, no discussion)

日時：平成 21 年 9 月 1 日（火）－3 日（木）
場所：つくば国際会議場（エポカルつくば）
〒305-0032 茨城県つくば市竹園 2-20-3
TEL：029-861-0001
発表時間：基調講演　（発表　40 分・質疑応答　5 分）
特別講演　（発表　25 分・質疑応答　5 分）
一般講演　（発表　10 分・質疑応答　5 分）
ポスタープレビュー（発表　1 分・質疑応答　なし）

展示団体御芳名

（五十音順、敬称略）

ＩＯＰ英国物理学会出版局
(株)あすみ技研
(有)イーアンドティー
(株)イデアルスター
ＨＰＣシステムズ(株)
エスケーバイオ・インターナショナル(株)
コスモ・バイオ(株)
(株)サーモ理工
サイバネットシステム(株)
シグマアルドリッチジャパン(株)
(株)島津製作所
(株)セントラル科学貿易
(株)ダルトン
坪井　利行
東洋炭素(株)
中山商事(株)
ナカライテスク(株)
日本電子(株)
日立工機(株)
日本ベル(株)
(株)堀場製作所
(株)マイクロフェーズ
(株)名城ナノカーボン
ロックゲート(株)
和光純薬工業(株)

広告掲載団体御芳名

（五十音順、敬称略）

(株)アドサイエンス
(株)ＡＴＲ
エクセルソフト(株)
エスケーバイオ・インターナショナル(株)
(株)岡村製作所
コスモ・バイオ(株)
(株)サーモ理工
サイバネットシステム(株)
シグマアルドリッチジャパン(株)
(株)島津製作所
スペクトラ・フィジックス(株)
(株)セントラル科学貿易
坪井　利行
東洋炭素(株)
東ソー(株)
中山商事(株)
ナカライテスク(株)
日本分析工業(株)
日本ベル(株)
ブルカー・エイエックスエス(株)
ブルカー・バイオスピン(株)
フロンティアカーボン(株)
(株)フロンティア出版
(株)マシナックス
(株)リガク
和貴ビジネスグループ

Contents

Time Table ····· i
Chairperson ····· iii
Program Japanese ····· iv
English ····· xvi
Abstracts Plenary Lecture・Special Lecture ····· 1
General Lecture ····· 7
Poster Preview ····· 57
Author Index ····· 201

目次

早見表 ····· i
座長一覧 ····· iii
プログラム 和文 ····· iv
英文 ····· xvi
講演予稿 基調講演・特別講演 ····· 1
一般講演 ····· 7
ポスター発表 ····· 57
発表索引 ····· 201

プログラム早見表

各項目敬称略

9月1日(火)		9月2日(水)		9月3日(木)	
	受付(8:30〜)		受付(8:30〜)		受付(8:30〜)
9:15		9:00		9:00	
	一般講演5件 (グラフェン)		一般講演3件 大澤賞受賞対象者講演		特別講演 (村上睦明)
10:30		10:00		9:30	
10:45	休憩	10:15	休憩		一般講演5件 (ナノチューブの物性)
	一般講演2件 (グラフェン・内包ナノチューブ)		一般講演3件 飯島賞受賞対象者講演	10:45	
11:15		11:15		11:00	休憩
	基調講演 (中村栄一)		特別講演 (澤 博)		ポスタープレビュー
12:00		11:45		12:00	
	昼食		昼食		昼食
		12:45			
		13:00	総会	13:00	
13:00					ポスターセッション
	一般講演7件 (ナノワイヤー・ナノホーン・ナノチューブの生成と精製)		一般講演7件 (ナノ炭素粒子・フラーレンの化学・フラーレンの応用)	14:15	
					特別講演 (畠 賢治)
14:45		14:45		14:45	
15:00	休憩	15:00	休憩		一般講演3件 (ナノチューブの応用)
	一般講演5件 (ナノチューブの生成と精製・フラーレン固体)		一般講演4件 (フラーレンの応用・金属内包フラーレン)	15:30	
				15:45	休憩
16:15		16:00			
	特別講演 (中村洋介)		基調講演 (Harry C. Dorn)		一般講演5件 (ナノチューブの応用)
16:45		16:45		17:00	
	ポスタープレビュー		ポスタープレビュー		
17:45		17:45			
	ポスターセッション		ポスターセッション		
19:00		19:00			
			懇親会		

Time Table

September 1 (Tue)		September 2 (Wed)		September 3 (Thu)	
	Registration (from 8:30)		Registration (from 8:30)		Registration (from 8:30)
9:15		9:00		9:00	
	General Lectures [5] (Graphene)		Lectures by Candidates for the Osawa Award [3]		Special Lecture (Mutsuaki Murakami)
10:30		10:00		9:30	
	Break	10:15	Break		General Lectures [5] (Properties of Nanotubes)
10:45	General Lectures [2] (Graphene・Endohedral Nanotubes)		Lectures by Candidates for the Iijima Award [3]	10:45	
11:15		11:15		11:00	Break
	Plenary Lecture (Eiichi Nakamura)		Special Lecture (Hiroshi Sawa)		Poster Preview
12:00		11:45		12:00	
	Lunch		Lunch		Lunch
13:00		12:45		13:00	
	General Lectures [7] (Nanowires・Nanohorns・Formation and Purification of Nanotubes)	13:00	General Meeting		Poster Session
14:45		14:45	General Lectures [7] (Carbon Nanoparticles・Chemistry of Fullerenes・Applications of Fullerenes)	14:15	
15:00	Break	15:00	Break		Special Lecture (Kenji Hata)
	General Lectures [5] (Formation and Purification of Nanotubes・Fullerene Solids)		General Lectures [4] (Applications of Fullerenes・Endohedral Metallofullerenes)	14:45	General Lectures [3] (Applications of Nanotubes)
16:15		16:00		15:30	
	Special Lecture (Yosuke Nakamura)		Plenary Lecture (Harry C. Dorn)	15:45	Break
16:45		16:45			General Lectures [5] (Applications of Nanotubes)
	Poster Preview		Poster Preview	17:00	
17:45		17:45			
	Poster Session		Poster Session		
19:00		19:00			
			Banquet		

座長一覧

9月1日(火)　　(敬称略)

	時　間	座　長
一般講演	9:15 ～ 10:30	高井和之
一般講演	10:45 ～ 11:15	塩見淳一郎
基調講演(中村栄)	11:15 ～ 12:00	阿知波洋次
一般講演	13:00 ～ 14:00	菅井俊樹
一般講演	14:00 ～ 14:45	片浦弘道
一般講演	15:00 ～ 16:15	鈴木信三
特別講演(中村洋)	16:15 ～ 16:45	田代健太郎
ポスタープレビュー	16:45 ～ 17:45	佐藤義倫
ポスターセッション	17:45 ～ 19:00	斎藤　毅

9月2日(水)

	時　間	座　長
大澤賞対象者講演	9:00 ～ 10:00	若林知成
飯島賞対象者講演	10:15 ～ 11:15	岡田　晋
特別講演(澤)	11:15 ～ 11:45	谷垣勝己
一般講演	13:00 ～ 13:45	兒玉　健
一般講演	13:45 ～ 14:45	若原孝次
一般講演	15:00 ～ 16:00	村田靖次郎
基調講演(Dorn)	16:00 ～ 16:45	赤阪　健
ポスタープレビュー	16:45 ～ 17:45	岸　直希
ポスターセッション	17:45 ～ 19:00	宮田耕充

9月3日(木)

	時　間	座　長
特別講演(村上)	9:00 ～ 9:30	宮本良之
一般講演	9:30 ～ 10:45	大野雄高
ポスタープレビュー	11:00 ～ 12:00	湯村尚史
ポスターセッション	13:00 ～ 14:15	藤本義隆
特別講演(畠)	14:15 ～ 14:45	斎藤　晋
一　般　講　演	14:45 ～ 15:30	湯田坂雅子
一　般　講　演	15:45 ～ 17:00	河合孝純

9月1日(火)

基調講演　発表40分・質疑応答5分
特別講演　発表25分・質疑応答5分
一般講演　発表10分・質疑応答5分
ポスタープレビュー　発表1分・質疑応答なし

一般講演(9:15-10:30)

グラフェン

1-1 Gバンドラマンスペクトルを用いたグラフェンエッジ形状の同定 7
○佐々木健一、森貴紀、高井和之、榎敏明、若林克法

1-2 グラフェンのリチウム二次電池電極応用 8
劉銀珠、金済徳、細野英司、周豪慎、工藤徹一、本間格

1-3 金属-グラフェン界面におけるフェルミ準位ピニング 9
○野内亮、齊藤達也、谷垣勝己

1-4 Hydrazine and Thermal Reduction of Graphene Oxide: Reaction Mechanisms and Design 10
○Xingfa Gao, Shigeru Nagase

1-5 エピタキシャル金属膜上でのグラフェンの触媒成長 11
○吾郷浩樹、田中伊豆美、辻正治、池田賢一

☆☆☆☆☆☆ 休憩 (10:30-10:45) ☆☆☆☆☆☆

一般講演(10:45-11:15)

グラフェン

1-6 長距離弾道的熱伝導をもたらすグラフェン鎖 12
○高橋厚史、伊藤洋平、生田竜也、Xing Zhang、藤井丕夫

内包ナノチューブ

1-7 太いSWCNT内の水の相転移 13
○松田和之、八尋瞳、客野遥、福岡智子、柳和宏、真庭豊、斎藤毅 、大嶋哲 、湯村守雄 、飯島澄男、宮田耕充、片浦弘道

基調講演(11:15-12:00)

1S-1 目で見る有機分子の動き --ナノチューブに発する新しい化学物理学の世界-- 1
中村栄一

☆☆☆☆☆☆ 昼食 (12:00-13:00) ☆☆☆☆☆☆

一般講演(13:00-14:45)

ナノワイヤー

1-8 溶液中におけるポリイン-ヨウ素錯体の光誘起生成 14
○和田資子、長田良一、槐靖範、若林知成、加藤立久

ナノホーン

1-9 ガドリニウム酸化物の内容によるナノホーンの生体分布測定 15
宮脇仁、松村幸子、弓削亮太、村上達也、佐藤重男、冨田章弘、鶴尾隆、市橋鋭也、藤波貴子、入江宏、土田邦博、飯島澄男、芝清隆、○湯田坂雅子

ナノチューブの生成と精製

1-10 単層カーボンナノチューブのカイラリティ制御と成長機構 16
○阿知波洋次、井上亮人、高水直子、児玉健、岡崎俊也

1-11 高効率カーボンナノチューブ成長における一般則 17
二葉ドン、後藤潤大、保田諭、山田健郎、湯村守雄、畠賢治

1-12 大気圧合成法を超える低圧下でのリモートプラズマ法による長尺・垂直配向単層カーボンナノチューブの高速成長 18
○加藤良吾、川原田洋

1-13 単層カーボンナノチューブの酸化反応におけるアルカリ金属塩化物の触媒作用 19
小林雄樹、○佐野正人

1-14 密度勾配超遠心法による(6, 5)カーボンナノチューブ選択単離と分光評価 20
○ツアオ ペイ、村上 陽一、項 榮、エリック エイナルソン、塩見 淳一郎、丸山 茂夫

☆☆☆☆☆☆ 休憩 (14:45-15:00) ☆☆☆☆☆☆

一般講演(15:00-16:15)

ナノチューブの生成と精製

1-15 無単体電気泳動法を用いた単層カーボンナノチューブの半導体・金属分離 21
○井原和紀、當山清彦、遠藤浩幸、二瓶史行

1-16 アガロースゲルを用いた金属型・半導体型カーボンナノチューブの連続分離 22
○田中丈士、卜部泰子、片浦弘道

1-17 フィルタレーションを用いた単層カーボンナノチューブの長さ分離 23
○大森滋和、斎藤毅、シュクラビカウ、湯村守雄、飯島澄男

フラーレン固体

1-18 エピタキシャル成長MgドープC_{60}膜の導電率のMg濃度依存 24
○名取雅人、西誠治、小島信晃、山口真史

1-19 フラーレン/フェロセンハイブリッドナノシートの合成と光学特性 25
○若原孝次、Marappan Sathish、宮澤薫一、Chunping Hu、館山佳尚、根本善弘、佐々木敏雄、伊藤攻

特別講演(16:15-16:45)

1S-2 フラーレンの官能基化と超分子化学 2
中村洋介

ポスタープレビュー(16:45-17:45)

ポスターセッション(17:45-19:00)

フラーレンの化学

1P-1 New 66 π-Electron [70]Fullerene Derivatives as n-Type Materials 57
○Zuo Xiao, Yutaka Matsuo, Eiichi Nakamura

1P-2 フラーレン部位を第二のアクセプター部位としたコバルタジチオレン-TTF-フラーレン錯体の合成と物性 58
○丸山優史、松尾豊、中村栄一

1P-3 シリルメチル二重付加型[60]フラーレン誘導体の合成とLUMO 準位の制御 59
○大山裕美、松尾豊、中村栄一

1P-4 フラーレン-ビスポルフィリン錯体の超分子相互作用を利用した光電変換システム 60
一木孝彦, Xiaoyong Zhang, 松尾 豊, 中村栄一

1P-5 2個の水素分子を内包したフラーレンC_{70}の合成と反応 61
○村田理尚、前田修平、森中裕太、村田靖次郎、小松紘一

1P-6 [60]フラーレンのアミジンによる分子変換 62
○上田展彰、二川秀史、土屋敬広、赤阪健

1P-7 塩化鉄(III)を利用した新規で簡便なフラーレン誘導体の合成 63
○橋口昌彦、渡辺和弘

金属内包フラーレン

1P-8 Why the Isolated-Pentagon-Rule Is Violated by Endohedral Metallofullerenes? A Chemical Answer 64
○Xing Lu, Hidefumi Nikawa, Midori O. Ishitsuka, Takahiro Tsuchiya, Yutaka Maeda, Takeshi Akasaka, Zdenek Slanina, Naomi Mizorogi, Shigeru Nagase

1P-9 La@C_{74}($C_6H_3Cl_2$)の分子変換 65
○赤阪 健、高橋 司、二川秀史、伊藤 剛、久我秀徳、土屋敬広、溝呂木直美、永瀬 茂

1P-10 Sc_2C_2@C_{84}とEr_2C_2@C_{84}の紫外光電子スペクトル 66
○宮崎隆文、青木雄祐、徳本頌治、隅井良平、沖本治哉、梅本 久、伊藤靖浩、篠原久典、日野照純

ナノチューブの物性

1P-11 A scalable route for enrichment of semiconducting from metallic single-walled carbon nanotubes 67
○Hanxun Qiu, Yutaka Maeda, Takeshi Akasaka

1P-12 置換基による単層カーボンナノチューブ側面の修飾率の制御
○加藤敬明、前田優、中村隆之、長谷川正、加固昌寛、赤阪健、永瀬茂 68

1P-13 さまざまな内包単層カーボンナノチューブの高温高圧下での構造変化
○岩田篤志、石井陽祐、廣瀬雅一、川崎晋司 69

1P-14 低温における片持ち梁カーボンナノチューブ振動
○深見瞬、有江隆之、秋田成司 70

1P-15 ○Ahmad R.T. Nugraha, Riichiro Saito, Kentaro Sato, Paulo T. Araujo, Ado Jorio, Mildred S. Dresselhaus 71

1P-16 単一のカーボンナノチューブのサテライト発光ピークの起源
○松永隆佑、松田一成、金光義彦 72

1P-17 カーボンナノチューブ修飾電極のその場ラマン分光電気化学測定
○坂本伸悟、長嶋圭佑、冨永昌人 73

1P-18 カーボンナノチューブのエネルギー論
○加藤幸一郎、斎藤晋 74

1P-19 その場透過電子顕微鏡法による金蒸着したカーボンナノチューブの電界放出評価
○浅井智仁、安坂幸師、中原仁、齋藤弥八 75

1P-20 金属型および半導体型カーボンナノチューブの電子物性
○宮田耕充、P. Ayala、K. de Blauwe、塩沢秀次、柳和弘、馮叶、R. Silva、R. Follath、C. Kramberger、篠原久典、片浦弘道、T. Pichler 76

ナノチューブの応用

1P-21 「複合化燃焼法」と命名した究極のナノ分散評価技術の開発
○坪井利行 77

1P-22 カーボンナノチューブ複合ゲルから成る光駆動熱電変換システムの開発
○都英次郎、廣津孝弘 78

1P-23 Electrical Transport Properties of ssDNA Decorated Single (Double)-Walled Carbon Nanotubes
○Yongfeng Li, Toshiro Kaneko and Rikizo Hatakeyama 79

1P-24 ポリマー/単層カーボンナノチューブ正孔輸送層を用いた有機薄膜太陽電池の作製
○岸直希、加藤慎也、林靖彦、斎藤毅、曽我哲夫、神保孝志 80

1P-25 可溶性ポリベンゾオキサゾール前駆体を用いたカーボンナノチューブの分散
○福丸貴弘、藤ヶ谷剛彦、中島直敏 81

1P-26 印刷型エミッタにおけるシリコーンバインダ添加によるカーボンナノツイストの基板密着性の向上
○横田真志, 須田善行, 桶真一郎, 滝川浩史, 藤村洋平, 伊藤茂生, 植仁志, 盛興昌勝, 清水一樹 82

1P-27 片持ち梁カーボンナノチューブ力センサの設計と作製
○西井亮介、小田康太、有江隆之、秋田成司 83

1P-28 発煙硝酸を用いたMWCNTの官能基化およびポリマーナノコンポジットへの応用
○北村啓、串田信也、関戸大、竹内久人、大野正富 84

1P-29 強磁性電極によるカーボンナノチューブへのスピン注入に関する理論的研究
○加藤良隆、笛野博之、田中一義 85

1P-30 貼付法によるヒューマンモニタリング可能なストレッチャブルセンサーの開発
○山田健郎、山本由貴、牧本なつみ、山田幸子、早水裕平、二葉ドン、畠賢治 86

ナノチューブの生成と精製

1P-31 メスバウアー分光によるSiO_2/Si基板上Fe触媒の挙動解析
○大島久純、島津智寛、シリーミラン、壬生攻 87

1P-32 高配向カーボンナノチューブ液相合成法におけるKOH添加効果
○山口吉弘、山際清史、喜々津智郁、山下俊介、桑野潤 88

1P-33 多糖と界面活性剤混合分散剤を用いた単層カーボンナノチューブのカイラル選択分離
上之薗佳也、内田勝美、土屋好司、石井忠浩、矢島博文 89

1P-34 アーク放電法を用いて作製した単層カーボンナノチューブの電気泳動法を利用した精製
○水澤崇志、鈴木信三、岡崎俊也、阿知波洋次 90

1P-35 成長中自由電子レーザー照射による特定のカイラリティを持った単層カーボンナノチューブの選択成長
○岩田展幸、石塚大祐、境恵二郎、園村拓也、竹下弘毅、金木邦英、矢島博文、山本寛 91

1P-36 アガロースゲルを用いたSWCNT半導体/金属分離のための第一原理計算
○大淵真理 92

1P-37 鉄ペンタカルボニルを用いた高配向カーボンナノチューブの液相一段合成
○喜々津智郁、山際清史、山口吉弘、山下俊介、桑野潤 93

内包ナノチューブ

1P-38 単層カーボンナノチューブ中のγシクロデキストリンでバイキャップされたフラーレンのTEM評価 94
○廣瀬香里、飯泉陽子、岡崎俊也、斎藤毅、末永和知

1P-39 カーボンナノチューブ内部での化学活性種の安定性に関する密度汎関数法計算 95
○湯村尚史

ナノホーン

1P-40 孤立化ナノホーンからの近赤外発光 96
松本響、○佐野正人

1P-41 異なったサイズの単層カーボンナノホーンの細胞特性評価 97
○張民芳、藤波貴子、徐建勛、山口貴司、飯島澄男、湯田坂雅子

グラフェン

1P-42 単層グラフェンへの室温におけるスピン注入手法の確立 98
○三苫伸彦、高野琢、白石誠司、野崎隆行、新庄輝也、鈴木義茂

1P-43 h-BN中の多原子空孔の安定性と構造 99
岡田晋

ナノ炭素粒子

1P-44 ボロンを含む炭素ペレットのレーザー蒸発により作製した強磁性泡状ナノ構造炭素 100
○村木奨、岩田伊織、遠藤宏紀、坂東俊治、飯島澄男

1P-45 炭素ペレットのレーザー蒸発により作製した強磁性泡状ナノ構造炭素 101
○浅野洋仁, 遠藤宏紀, 坂東俊治, 飯島澄男

その他

1P-46 フェムト秒レーザー照射によるナノカーボン構造改変:大型計算機による仮想実験 102
○宮本良之、Hong Zhang

1P-47 希土類金属-黒鉛層間化合物の作製と磁気特性 103
○平郡諭、小林本忠

基調講演　発表40分・質疑応答5分
特別講演　発表25分・質疑応答5分
大澤賞飯島賞対象者講演　発表10分・質疑応答10分
一般講演　発表10分・質疑応答5分
ポスタープレビュー　発表1分・質疑応答なし

大澤賞対象者講演(9:00-10:00)

2-1 単一多層カーボンナノカプセルの合成と力学・電気伝導特性解析 26
○安坂幸師、宮澤薫一、木塚徳志、齋藤弥八

2-2 常磁性金属内包フラーレンの分子変換と物性開拓 27
○高野勇太、山田道夫、二川秀史、ズデネク・スラニナ、溝呂木直美、生沼みどり、土屋敬広、前田優、赤阪健、加藤立久、永瀬茂

2-3 ゲスト封入によりスイッチ可能なホスト-ゲストスピン相互作用 28
○ファティン ハジャジ、田代 健太郎、赤阪 健、加藤 立久、相田 卓三

☆☆☆☆☆☆ 休憩 (10:00-10:15) ☆☆☆☆☆☆

飯島賞対象者講演(10:15-11:15)

2-4 単層カーボンナノチューブの電子準位直接決定 29
○平兮康彦、田中泰彦、加藤幸一郎、斎藤晋、中嶋直敏

2-5 Ink-jet printing of low-voltage SWCNT-thin film transistors using ionic liquid gating 30
○沖本治哉、竹延大志、柳和宏、宮田耕充、片浦弘道、浅野武志、岩佐義宏

2-6 ダイヤモンドナノ粒子を用いたカーボンナノチューブ合成 31
○高木大輔、小林慶祐、本間芳和

特別講演(11:15-11:45)

2S-1 内包C_{60}の精密構造解析 3
澤 博

☆☆☆☆☆☆ 昼食 (11:45-12:45) ☆☆☆☆☆☆

総会(12:45-13:00)

一般講演(13:00-14:45)

ナノ炭素粒子

2-7 ナノダイヤモンドの化学修飾:凝集するナノ粒子に対する表面化学 32
○小澤理樹、Yuejiang Liang、Anke Krueger

フラーレンの化学

2-8 片割れしたフラーレンにおける磁性発現の可能性:理論計算 33
○針谷喜久雄

2-9 近接電子対効果によるフラーレン誘導体のレドックス特性制御 34
○田島右副、沼田陽平

2-10 開口フラーレンの化学変換. 開口部メチレン水素のアルキル化反応. 35
○岩松将一

2-11 ポルフィリンポリマーを利用したフラーレン集合体の形態制御 36
○Xuan Zhang、竹内正之

フラーレンの応用

2-12 キラルな両親媒性ドナー・アクセプターダイアッドの自己組織化による光導電性材料の創成 37
○田代健太郎、樋爪由美、Charvet Richard、山本洋平、関 修平、相田卓三

2-13 水溶性のフラーレン/ポリマーコンプレックスの温度応答挙動とDNAの光切断 38
○遊佐真一、阿波茂樹、川瀬毅、高田忠雄、中島謙一、Dian Liu、山子茂、森島洋太郎

☆☆☆☆☆☆ 休憩 (14:45-15:00) ☆☆☆☆☆☆

一般講演(15:00-16:00)

フラーレンの応用

2-14 ナノメディシンを目指したフラーレン/PEG-b-ポリアミン複合体の設計 39
○長崎幸夫、小高亮輔

2-15 フラーレン誘導体によるTNFα 誘導性NFκB 活性化の抑制 40
○井上巧、伊藤雅之、山名修一、高橋恭子、中村成夫、増野匡彦

金属内包フラーレン

2-16 $LaYC_{80}$の合成と性質 41
○兒玉健、掛田大輔、藤田渉、菊地耕一、鈴木信三、阿知波洋次

2-17 金属内包フラーレンの位置選択的な二段階修飾 42
○佐藤悟、前田優、稲田浩司、二川秀史、山田道夫、溝呂木直美、長谷川正、土屋敬広、赤阪健、加藤立久、Zdenek Slanina、永瀬茂

基調講演(16:00-16:45)

2S-2 Dynamics of Metal Clusters Inside Fullerene Carbon Cages 4
Harry C. DORN

ポスタープレビュー(16:45-17:45)

ポスターセッション(17:45-19:00)

フラーレン固体

2P-1 形態が制御された分散性フラーレン微粒子 104
○高口 豊、藤田泰彦、松川純平、田嶋智之

2P-2 自由電子レーザー照射による溶液中C_{60}ポリマーの合成 105
○岩田展幸、栗原浩平、飯尾靖也、山本寛

2P-3 C_{60}ナノファイバー内部の細孔分布観察 106
○加藤良栄, 宮澤薫一, 王正明

2P-4 アルカリドープフラーレンのフォノンと電子格子相互作用 107
○是常隆、斎藤晋

金属内包フラーレン

2P-5 金属カーバイド内包フラーレン$Sc_2C_2@C_{80}$の構造決定 108
○栗原広樹、山崎裕子、二川秀史、溝呂木直美、土屋敬広、永瀬茂、赤阪健

2P-6 金属内包フラーレンのシラシクロプロパンによる化学修飾 109
○美野輪まり、山田道夫、加固昌寛、土屋敬広、生沼(石塚)みどり、赤阪健

2P-7 Non-IPR構造を有する$La@C_{72}$の二付加体の合成 110
○伊藤剛、二川秀史、赤阪健、土屋敬広、ズネデクスラニナ、溝呂木直美、永瀬茂

2P-8 $La@C_{82}$の安定な[4+2]環化付加体の合成と構造解析 111
○永島佑樹、高野勇太、Zdenek Slanina、土屋敬広、赤阪健、永瀬茂

2P-9 金属内包フラーレン配位子の合成 112
○青山亮、横澤裕也、土屋敬広、赤阪健

2P-10 常磁性金属内包フラーレン / 電子ドナー連結系の合成と性質 113
○田中竜也、土屋敬広、赤阪健、溝呂木直美、永瀬茂

2P-11 ツリウム金属内包フラーレンからの近赤外発光と電荷状態依存 114
○泉乃里子、飯島浩章、岡崎俊也、丹下将克、宮田耕充、篠原久典

2P-12 金属内包フラーレン$M@C_{82}$の放射光X線回折を用いた系統的な結晶構造研究 115
○青野貴行、西堀英治、北浦良、青柳忍、高田昌樹、坂田誠、澤博、篠原久典

2P-13 実験的および理論的考察による$(Lu_2C_2)@C_{88}$の構造解析 116
○塩澤一成、泉乃里子、梅本久、北浦良、篠原久典

2P-14 非経験的分子軌道計算による金属内包フラーレン$Y_2C_2@C_{82}$, $Sc_3N@C_{78}$の電子構造 117
○青木雄祐、宮崎隆文、日野照純

2P-15 $Tm_2@C_{82}$の紫外及びX線光電子分光 118
○徳本頌治、八木創、宮崎隆文、泉乃理子、篠原久典、日野照純

フラーレンの生成

2P-16 窒素原子およびポリイン類のフラーレンおよびナノチューブへの内包 119
○若林知成、手柴雅臣、才川真央、吉川愛里、和田資子

ナノ環境と安全評価

2P-17 マクロファージ様細胞によるフラーレンナノウィスカーの生分解 120
○ぬで島真一、宮澤薫一、奥田順子、谷口彰良

ナノチューブの物性

2P-18 金属型・半導体型単層カーボンナノチューブバッキーペーパーの伝導特性 121
○鵜戸口浩樹、鷺谷智、松田和之、大島勇吾、片浦弘道、竹延大志、柳和宏、真庭豊

2P-19 貴金属粒子から成長した単層ナノチューブのラマンスペクトルにおけるバンドル由来信号の特異な挙動 122
○小林慶裕、高木大輔、庄司 暁、河田 聡

2P-20 還元雰囲気下TGAによるMWNTsの構造評価 123
○本行乾一、松原徹、二井裕之、國重敦弘

2P-21 短尺カーボンナノチューブの光吸収 124
○中西毅, 安藤恒也

2P-22 光光吸収分光法による単層カーボンナノチューブの解析 125
○斎藤毅、シュクラビカウ、大森滋和、湯村守雄、飯島澄男

2P-23 ピリジン型欠陥をもつカーボンナノチューブの原子・電子構造 126
○藤本義隆、斎藤晋

2P-24 マイクロ波プラズマCVD法で合成したカーボンナノチューブの物性評価 127
○渡邊徹、津田俊輔、山口尚秀、高野義彦

2P-25 単層カーボンナノチューブにおける励起子効果とフォトルミネッセンス強度のカイラリティ依存性 128
○佐藤健太郎、齋藤理一郎、丸山茂夫

ナノチューブの応用

2P-26 有機合成のための光駆動カーボンナノヒートシステムの開発 129
○都英次郎、伊藤民武、廣津孝弘

2P-27 Pt/Ruを担持したカーボンナノコイルの透過電子顕微鏡観察 130
○川畑貴博, 横田真志, 瀧本幸太郎, 池田峻, 須田善行, 桶真一郎, 滝川浩史, 藤村洋平, 伊藤茂生, 植仁志, 盛興昌勝, 清水一樹

2P-28 カーボンナノチューブ修飾電極を用いた色素太陽電池の作製 131
○安川幸一、坂本伸悟、冨永昌人

2P-29 カーボンナノチューブ薄膜を用いた太陽電池に関する研究 132
○加藤達也、李永峰、金子俊郎、畠山力三

2P-30 多層カーボンナノチューブ/ポリ乳酸からなる新規人工臓器材料の開発 133
○高橋克宗、矢島博文

ナノチューブの生成と精製

2P-31 吸収測定と発光測定による単層カーボンナノチューブの直径配分の温度依存 134
○井上亮人、鶴岡泰広 、岡崎俊也、阿知波洋次

2P-32 パルスOPOレーザー照射による単層カーボンナノチューブの選択的カイラル分離へのレーザー波長および分散媒の影響 135
○熊沢陽、田島勇、内田勝美、土屋好司、石井忠浩、矢島博文

2P-33 Catalyst deposition by spin-coating for synthesis of vertically-aligned single-walled carbon nanotubes 136
○ティーラポン トゥラキットセーリー、エリック エイナルソン、項榮、趙沛、塩見 淳一郎、丸山 茂夫

2P-34 水平配向カーボンナノチューブの成長中の折り曲げ 137
○吾郷浩樹、今本健太、西徹志、辻正治、生田竜也、高橋厚史、福井宗利

2P-35 アーク放電法によるグラファイト不純物の少ない単層カーボンナノチューブススの合成 138
○佐藤義倫、渡邊 光、名村 優、本宮憲一、田路和幸

2P-36 プラズマCVD法と熱CVD法によるカーボンナノチューブの成長 139
三宅雅人、飯島徹、Kenneth Teo、 Nalin Rupesinghe、小沼賢二郎、堀川和徳、阿部勝義、佐藤正之、林靖彦

2P-37 液相アーク放電によるキシレンからのカーボンナノチューブの合成 140
○木津たきお、相川慎也、西川英一

2P-38 ポリカルバゾール誘導体を用いたSWNTの選択的可溶化 141
小澤寛晃、井出奈都子、藤ヶ谷剛彦、Suhee Song、Hongsuk Suh、 中嶋直敏

内包ナノチューブ

2P-39 共鳴ラマン分光による単層カーボンナノチューブと内包フラーレン間のホスト-ゲスト相互作用の直径依存性 142
○鄭淳吉、岡崎俊也、岡田晋、飯島澄男

2P-40 単層カーボンナノチューブに内包させたペリレン分子における室温でのY発光
○丹下将克、岡崎俊也、劉崢、末永和知、飯島　澄男 143

2P-41 コロネン内包ナノチューブのエネルギー論と電子構造
岡田晋 144

ナノホーン

2P-42 Ceramide-conjugated PEG: an Outstanding Dispersant for SWNHs
○Jianxun Xu, Sumio Iijima, Masako Yudasaka 145

グラフェン

2P-43 ナノ多孔質アルミナ膜を用いたグラフェン上への蜂の巣状ナノ細孔アレイの形成とエッジ電子構造
○中村仁、春山純志、清水台生、及川進規、榎本翔太 146

2P-44 走査電子顕微鏡によるグラフェンの評価
○日浦英文、塚越一仁、宮崎久生 147

2P-45 グラフェンナノリボンの作製とそれらの構造及び電気的性質の観測
○清水台生、春山純志、中村仁、田邊裕喜、山川雄祐 148

ナノ炭素粒子

2P-46 レーザー蒸発による多面体グラファイト成長のケイ素またはホウ素添加による促進
千種甫、野崎伊織、小塩明、○小海文夫 149

2P-47 溶液内での光誘起によるポリイン－臭素錯体形成
○槐靖範、加藤立久、和田資子、若林知成 150

2P-48 熱処理したランタンフラーレン煤のラマンとTEMによる研究
○山本和典、社本真一、赤阪健、若原孝次、宮澤薫一 151

9月3日(木)

特別講演　発表25分・質疑応答5分
一般講演　発表10分・質疑応答5分
ポスタープレビュー　発表1分・質疑応答なし

特別講演(9:00-9:30)

3S-1 高分子を原料とする高品質・高配向性グラファイトの作製と応用 5
村上睦明

一般講演(9:30-10:45)

ナノチューブの物性

3-1 孤立分散させた単層カーボンナノチューブにおける超高速コヒーレント非線形光学応答 43
○田尾祥一、宮田耕充、柳和宏、片浦弘道、岡本博

3-2 半導体ナノチューブから金属ナノチューブへの励起キャリアの拡散:時間依存密度汎関数法による数値計算 44
○河合孝純、宮本良之

3-3 電極間に架橋したカーボンナノチューブの高速・高分解能ラマンイメージング 45
○内山知也、小林実、太田泰輔、吉村雅満

3-4 単層カーボンナノチューブ/オリゴDNA複合体の安定性と光学特性評価 46
○山本悠喜、藤ヶ谷剛彦、中嶋直敏

3-5 金属性カーボンナノチューブのRBMバンドにおけるフェルミエネルギー依存性 47
○朴珍成、佐々木健一、齋藤理一郎、Gene Dressselhaus, Mildred S. Dresselhaus

☆☆☆☆☆☆ 休憩 (10:45-11:00) ☆☆☆☆☆☆

ポスタープレビュー(11:00-12:00)

☆☆☆☆☆☆ 昼食 (12:00-13:00) ☆☆☆☆☆☆

ポスターセッション(13:00-14:15)

フラーレンの化学

3P-1 ドナー部位を有する軸分子を用いたフラーレン系インターロック化合物の合成 152
○坂本千佳、室谷直輝、中村洋介、西村　淳

3P-2 種々の連結部位を有するオリゴカルバゾール部位-[60]フラーレン付加体の合成と光物理的性質 153
○小林浩之佑、木下恵介、中村洋介、西村　淳

3P-3 シアノビフェニル基を末端に持つフラロデンドロンの合成と液晶性 154
○高口　豊、酒向祐輝、田嶋智之

3P-4 シリカゲル内部を反応場とするC_{60}と共役ジエンとのDiels-Alder反応 155
南方聖司○長町俊希、中山和之

3P-5 有機電子デバイスに用いる新規フラーレン誘導体の合成およびモルフォロジ制御 156
○松尾敬子, 松尾豊, 中村栄一

3P-6 新規開口C_{60}誘導体の合成と性質 157
○黒飛敬、村田理尚、村田靖次郎

3P-7 Construction of Ordered Fullerene Arrays by Supramolecular Fullerene-Perfluorobenzene interaction 158
李昌治、松尾豊、中村栄一

3P-8 スルフィルイミンを用いたC_{60}の位置選択的アジリジン化 159
○石塚みどり、岡田光了、仲程　司、二川秀史、土屋敬広、赤阪　健、藤江哲夫、吉村敏章、Zdenek Slanina、永瀬　茂

3P-9 Behavior of the photocurrent on Mg-doped C_{60} films 160
Crisoforo Morales, Nobuaki Kojima, Masato Natori, Seiji Nishi, Masafumi Yamaguchi

フラーレンの応用

3P-10 溶液から電極間に直接成長したC_{60}結晶 161
○岩田展幸、栗原浩平、飯尾靖也、山本寛

金属内包フラーレン

3P-11 フラーレンの抽出選択性:溶媒依存性 162
○井上崇、田尾理恵、瀧本裕治

3P-12 バルクヘテロ型有機薄膜太陽電池の高効率化へ向けての金属内包フラーレンの応用 163
○才田守彦、大泉春菜、相模寛之、溝渕裕三、表研次、笠間泰彦、横尾邦義、小野昭一、山本恵彦、桑原貴之、高橋光信

3P-13 高対称C_{60}に内包された水素分子の回転エネルギー副準位 164
○谷垣勝己、小濱芳允、良知 健、ジュ ジン、リ ザオフェイ、タング ジュン、熊代良太郎、泉澤 悟、川路宏、阿竹 徹、澤 宏、村田靖次郎、小松紘一

3P-14 Structure and Relative Stabilities of $Sc_2@C_{74}$ and $La_2@C_{74}$ 165
○T. Ren, X. Zhao, H. Zheng, J. S. Dang

ナノチューブの物性

3P-15 紫外ラマン分光法による多層カーボンナノチューブの評価 166
○二井裕之、本行乾一、中川浜三

3P-16 単層カーボンナノチューブの超強磁場下近赤外吸収特性 167
○横井裕之、小嶋映二、嶽山正二郎、南信次

3P-17 多糖類のカーボンナノチューブへの吸着の分子動力学シュミレーション 168
○篠宮弘行、内田勝美、土屋好司、矢島博文

3P-18 多層カーボンナノチューブからの電界放出に及ぼすチタン蒸着の効果 169
○山本雄太、劉華栄、野村航大、中原仁、齋藤弥八

3P-19 有機溶媒中における単層カーボンナノチューブの還元 170
○前田優、田代敦士、長谷川正、土屋敬広、赤阪健、ジンルウ、永瀬茂

3P-20 有機溶媒中における単層カーボンナノチューブの溶媒効果 171
○沖田朋久、前田優、岨手勝也、長谷川正、土屋敬広、赤阪健、永瀬茂

3P-21 SWNTと周囲材料の界面熱コンダクタンスのメカニズム 172
○車振赫、 塩見淳一郎、 丸山茂夫

3P-22 鉄触媒を用いて水素ガスアーク放電で作られたMWNTs・SWNTsで観察された鎖状炭素物質のラマン散乱 173
○神野誠、安藤義則

ナノチューブの応用

3P-23 単層カーボンナノチューブを用いた帯電防止性を有する眼鏡用プラスチックレンズの作製 174
○高橋宏寿、深川剛、橋本剛

3P-24 スーパーグロース:As grownカーボンナノチューブからの、低閾値電圧・均一・安定な電界放出特性 175
○木村寛恵、二葉ドン、山田健郎、樋田竜男、趙斌、倉知宏行、上村佐四郎、畠賢治

3P-25 SWNT配向プリプレグシートとその補強効果 176
○小橋和文、西野秀和、山田健郎、二葉ドン、畠賢治

3P-26 色素増感太陽電池(酸化スズ/p3HT電極)に対するMWCNT添加効果 177
○新井徹、古田篤志、倉本竜典

3P-27 meso-meso結合ポルフィリンオリゴマーによる単層カーボンナノチューブの可溶化 178
○内海剛志、藤ヶ谷剛彦、中嶋直敏

3P-28 ポリアニリンスルホン酸及び単層カーボンナノチューブから成る導電性フィルムの作製 179
○栗山智行、小野淑、上之薗佳也、内田勝美、土屋好司、石井忠浩、矢島博文

3P-29 As-grownの単層カーボンナノチューブを用いた容易な電界効果トランジスタの作製とその特性評価 180
○相川慎也, 項榮, エリック エイナルソン, 塩見淳一郎, 西川英一, 丸山茂夫

ナノチューブの生成と精製

3P-30 Sn薄膜状へのFe触媒形成によるカーボンナノコイルの収率の向上 181
○瀧本幸太郎、篠原雄一郎、横田真志、川畑貴博、須田善行、桶真一郎、滝川浩史、藤村洋平、山浦辰雄、伊藤茂生、植仁志、盛興昌勝

3P-31 ブラシ状カーボンナノチューブの嵩密度の向上 182
○久保元、有江隆之、秋田成司

3P-32 高真空中でのアルコールガスソース法によるカーボンナノチューブ成長への水添加の効果 183
○佐藤一徳、丸山隆弘、成塚重弥

3P-33 金触媒利用単層カーボンナノチューブ成長におけるプラズマの発光分光測定 184
○ Z. Ghorannevis, T. Kato, T. Kaneko and R. Hatakeyama

3P-34 スーパーグロース:高純度カーボンナノチューブのさらなる高速成長法の開発 185
○佐藤潤一、保田諭、二葉ドン、山田健郎、湯村守雄、畠賢治

3P-35 CCVCD法によるCNT合成における担体効果 186
○中山拓哉、北浦良、篠原久典

3P-36 直交した単層カーボンナノチューブ・アレーの直接合成 187
○西徹志、吾郷浩樹、カルロ オロフェオ、石神直樹、辻正治、生田竜也、高橋厚史

3P-37 High Precision Site-selective Growth of SWNTs and its Applications 188
○項栄、相川慎也、エイナルソン エリック、塩見淳一郎、丸山茂夫

内包ナノチューブ

3P-38 高分解能透過型電子顕微鏡による単層カーボンナノチューブに内包した分子の光反応過程の観察 189
○小林慶太、末永和知、斎藤毅、飯島澄男

3P-39 発光および光吸収法によるアザフラーレンピーポッドの電子構造解析 190
○飯泉陽子、岡崎俊也、Liu Zhen、末永和知、中西毅、飯島澄男、Tagmatarchis Nikos

3P-40 カルシウム内包単層カーボンナノチューブの形成と特性評価 191
○小山内陽祐、清水哲弘、加藤俊顕、大原渡、畠山力三

3P-41 高充填率なユーロピウムナノワイヤー内包単層カーボンナノチューブの分光分析 192
○中西亮、北浦良、吉本隆久、斎藤毅、宮田耕充、篠原久典

3P-42 2層カーボンナノチューブ内における直線状ポリイン分子の成長と進化 193
○趙晨、北浦良、原裕訓、ステファン・イレ、篠原久典

ナノホーン

3P-43 ナノホーンの構造解析 194
入江路子、徐建勛、弓削亮太、飯島澄男、○湯田坂雅子

3P-44 ナノホーンの細胞毒性 195
藤波貴子、徐建勛、○茗原侑里、飯島澄男、湯田坂雅子

グラフェン

3P-45 グラフェンのラマン分光における端形状依存性 196
○森貴紀、高井和之、佐々木健一、若林克法、榎敏明

3P-46 アモルファスカーボン薄膜のポストアニールによるナノ結晶化と巨大な表面形状変化 197
○野口卓也、島田敏宏、千葉貴史、寺田真男、長谷川哲也

3P-47 折り畳まれたグラフェンの電子状態 198
○高木祥光、岡田晋

その他

3P-48 コンビナトリアル手法による$Fe-SnO_2$触媒を用いたカーボンナノコイル合成 199
○藤田博、有江隆之、秋田成司

特別講演(14:15-14:45)

3S-2 スーパーグロースの進捗 -成長・応用・デバイス- 6
畠 賢治

一般講演(14:45-15:30)

ナノチューブの応用

3-6 フラロデンドロン/単層カーボンナノチューブ超分子複合体を利用した光水素発生 48
○高口 豊、坂田和歌子、田嶋智之

3-7 高次フラーレンと単層カーボンナノチューブの複合クラスター 49
○梅山有和、手塚記庸、俣野善博、今堀博

3-8 多層カーボンナノチューブフィルムセンサを用いた脳波の検出 50
○川本昂、北井隆平、久保田紀彦

☆☆☆☆☆☆ **休憩 (15:30-15:45)** ☆☆☆☆☆☆

一般講演(15:45-17:00)

ナノチューブの応用

3-9 垂直配向カーボンナノチューブへの高速原子ビームを用いた表面処理の影響 51
○藤野真久、須賀唯知、塩見淳一郎、丸山茂夫、曽我育生、近藤大雄、石月義克、岩井大介、水越正孝

3-10 電解質プラズマ中で形成されたDNA内包単層カーボンナノチューブの電気特性 52
○金子俊郎, 李永峰, 畠山力三

9月3日(木)

3-11 DNA-単層カーボンナノチューブ複合物質の薄膜トランジスタへの応用 53
○浅田有紀、宮田耕充、大野雄高、北浦良、菅井俊樹、水谷孝、篠原久典

3-12 ITO上へのC_{60}-SWNTハイブリッド薄膜生成 54
○王　奇観、森山広思

3-13 金属表面上の単層カーボンナノチューブの第一原理計算 55
○高木祥光、岡田晋

Plenary Lecture: 40 min (Presentation) + 5 min (Discussion)
Special Lecture: 25 min (Presentation) + 5 min (Discussion)
General Lecture: 10 min (Presentation) + 5 min (Discussion)
Poster Preview: 1 min (Presentation), No Discussion

General Lecture (9:15-10:30)

Graphene

1-1 Identifying the shape of graphene edge using G band Raman spectra
○Kenichi Sasaki, Takanori Mori, Kazuyuki Takai, Toshiaki Enoki, Katsunori Wakabayashi 7

1-2 Graphene as advanced rechargeable Li battery electrode materials
EunJoo Yoo, Jedeok Kim, Eiji Hosono, H.S. Zhou, Tetsuichi Kudo and Itaru Honma 8

1-3 Fermi-Level Pinning at Metal-Graphene Interfaces
○Ryo Nouchi, Tatsuya Saito, Katsumi Tanigaki 9

1-4 Hydrazine and Thermal Reduction of Graphene Oxide: Reaction Mechanisms and Design
○Xingfa Gao, Shigeru Nagase 10

1-5 Catalytic Growth of Graphene over Epitaxial Metal Film
○Hiroki Ago, Izumi Tanaka, Masaharu Tsuji, Ken-ichi Ikeda 11

☆☆☆☆☆☆ **Coffee Break (10:30-10:45)** ☆☆☆☆☆☆

General Lecture (10:45-11:15)

Graphene

1-6 Graphene Chain as a Long Distance Ballistic Heat Conductor
○Koji Takahashi, Yohei Ito, Tatsuya Ikuta, Xing Zhang, Motoo Fujii 12

Endohedral Nanotubes

1-7 Phase transition of water inside large-diameter SWCNTs
○Kazuyuki Matsuda, Hitomi Yahiro, Haruka Kyakuno, Tomoko Fukuoka, Kazuhiro Yanagi, Yutaka Maniwa, Takeshi Saito, Satoshi Ohshima, Motoo Yumura, Sumio Iijima, Yasumitu Miyata, Hiromichi Kataura 13

Plenary Lecture (11:15-12:00)

1S-1 Imaging Organic Molecules in Motion - A New World of Chemical Physics as Viewed through a Nanotube -
Eiichi Nakamura 1

☆☆☆☆☆☆ **Lunch Time (12:00-13:00)** ☆☆☆☆☆☆

General Lecture (13:00-14:45)

Nanowires

1-8 Photo-Induced Formation of Polyyne-Iodine Complex in Solution
○Yoriko Wada, Ryoichi Osada, Yasunori Kai, Tomonari Wakabayashi, Tatsuhisa Kato 14

Nanohorns

1-9 Biodistibution and Ultrastructural Localization of Single-walled Carbon Nanohorns Determined In Vivo with Embedded Gd_2O_3 Labels
Jin Miyawaki, Sachiko Matsumura, Ryota Yuge, Tatsuya Murakami, Shigeo Sato, Akihiro Tomida, Takashi Tsuruo, Toshinai Ichihashi, Takako Fujinami, Hiroshi Irie, Kunihiro Tsuchida, Sumio Iijima, Kiyotaka Shiba, ○Masako Yudasaka 15

Formation and Purification of Nanotubes

1-10 The role of cap structure formation on the chirality selective formation of single-walled carbon nanotubes
○Yohji Achiba, Akihito Inoue, Naoko Takamizu, Takeshi Kodama, Toshiya Okazaki 16

1-11 General Rules Governing the Highly Efficient Growth of Carbon Nanotubes
○Don N. Futaba, Jundai Gotou, Satoshi Yasuda, Takeo Yamada, Motoo Yumura and Kenji Hata 17

1-12 High Rate Growth of Long Vertically Aligned Single-Walled Carbon Nanotubes by Remote Plasma in Low Pressure Beyond the Atmospheric Pressure Synthesis 18
○Ryogo Kato, Hiroshi Kawarada

1-13 Catalytic Effects of Alkali Metal Chlorides on Thermal Oxidation of Single-Walled Carbon Nanotubes 19
Yuki Kobayashi, ○Masahito Sano

1-14 Optical Spectroscopy of (6,5) Carbon Nanotubes Sorted by Density Gradient Ultracentrifugation 20
○Pei Zhao, Yoichi Murakami, Rong Xiang, Erik Einarsson, Junichiro Shiomi, Shigeo Maruyama

☆☆☆☆☆ **Coffee Break (14:45-15:00)** ☆☆☆☆☆

General Lecture (15:00-16:15)

Formation and Purification of Nanotubes

1-15 Metallic-semiconducting separation of single-walled carbon nanotubes by using free-flow electrophoresis 21
○Kazuki Ihara, Kiyohiko Toyama, Hiroyuki Endoh, and Fumiyuki Nihey

1-16 Continuous Separation of Metallic and Semiconducting Carbon Nanotubes Using Agarose Gel 22
○Takeshi Tanaka, Yasuko Urabe and Hiromichi Kataura

1-17 Length Fractionation of SWCNTs by Using Filtration Method 23
○Shigekazu Ohmori, Takeshi Saito, Bikau Shukla, Motoo Yumura, Sumio Iijima

Fullerene Solids

1-18 Mg concentration dependence of conductivity in epitaxial-grown Mg-doped C_{60} thin films 24
○Masato Natori, Seiji Nishi, Nobuaki Kojima and Masafumi Yamaguchi

1-19 Preparation and Optical Properties of Fullerene/Ferrocene Hybrid Hexagonal Nanosheets 25
○Takatsugu Wakahara, Marappan Sathish, Kun'ichi Miyazawa, Chunping Hu, Yoshitaka Tateyama, Yoshihiro Nemoto, Toshio Sasaki, Osamu Ito

Special Lecture (16:15-16:45)

1S-2 Exohedral Functionalization of Fullerenes and Supramolecular Chemistry 2
Yosuke Nakamura

Poster Preview (16:45-17:45)

Poster Session (17:45-19:00)

Chemistry of Fullerenes

1P-1 New 66π-Electron [70]Fullerene Derivatives as n-Type Materials 57
○Zuo Xiao, Yutaka Matsuo, Eiichi Nakamura

1P-2 Synthesis and Electronic Properties of a Cobaltadithiolene-TTF-Fullerene Complex: Fullerene Moieties as Secondary Acceptor Units 58
○Masashi Maruyama, Yutaka Matsuo, Eiichi Nakamura

1P-3 Synthesis and LUMO-level Control of 1-Aryl-4-silylmethyl[60]fullerene Derivatives 59
○Hiromi Oyama, Yutaka Matsuo, Eiichi Nakamura

1P-4 Photocurrent Generating Systems of Fullerene-bisporphyrins with Supramolecular Interaction 60
Takahiko Ichiki, Xiaoyong Zhang, Yutaka Matsuo, Eiichi Nakamura

1P-5 Synthesis and Reaction of Fullerene C_{70} Encapsulating Two Molecules of H_2 61
○Michihisa Murata, Shuhei Maeda, Yuta Morinaka, Yasujiro Murata, Koichi Komatsu

1P-6 Chemical Functionalization of [60]fullerene with Amidine 62
○Nobuaki Ueda, Hidefumi Nikawa, Takahiro Tsuchiya, Takeshi Akasaka

1P-7 A Novel and Simple Synthesis of Fullerene Derivatives using $FeCl_3$ 63
○Masahiko Hashiguchi and Kazuhiro Watanabe

Endohedral Metallofullerenes

1P-8 Why the Isolated-Pentagon-Rule Is Violated by Endohedral Metallofullerenes? A Chemical Answer 64
○Xing Lu, Hidefumi Nikawa, Midori O. Ishitsuka, Takahiro Tsuchiya, Yutaka Maeda, Takeshi Akasaka, Zdenek Slanina, Naomi Mizorogi, Shigeru Nagase

1P-9 Chemical Understanding of $La@C_{74}(C_6H_3Cl_2)$ 65
○Takeshi Akasaka, Tsukasa Takahashi, Hidefumi Nikawa, Tsuyoshi Ito, Hidenori Kuga, Takahiro Tsuchiya, Naomi Mizorogi, Shigeru Nagase

1P-10 Ultraviolet Photoelectron Spectroscopy of $Sc_2C_2@C_{84}$ and $Er_2C_2@C_{84}$
○Takafumi Miyazaki, Yusuke Aoki, Youji Tokumoto, Ryohei Sumii, Haruya Okimoto, Hisashi Umemoto, Yasuhiro Ito, Hisanori Shinohara, Shojun Hino 66

Properties of Nanotubes

1P-11 A scalable route for enrichment of semiconducting from metallic single-walled carbon nanotubes
○Hanxun Qiu, Yutaka Maeda, Takeshi Akasaka 67

1P-12 Control of the Degree of Functionalization on Single-walled Carbon Nanotubes Sidewall by the Substituents
○Takaaki Kato, Yutaka Maeda, Takayuki Nakamura, Tadashi Hasegawa, Masahiro Kako, Takeshi Akasaka, Shigeru Nagase 68

1P-13 Structural changes of several kinds of endohedral SWCNTs under high-pressure and at high-temperature
○Atsushi Iwata, Yosuke Ishii, Shinji Kawasaki 69

1P-14 Cantilevered Carbon Nanotube Oscillation at Low Temperature
○Shun Fukami, Takayuki Arie, Seiji Akita 70

1P-15 Exciton Environmental Effect for Optical Transition Energy of Single Wall Carbon Nanotubes
○Ahmad R.T. Nugraha, Riichiro Saito, Kentaro Sato, Paulo T. Araujo, Ado Jorio, Mildred S. Dresselhaus 71

1P-16 Origin of the Satellite Photoluminescence Peaks in Single SWNTs
○Ryusuke Matsunaga, Kazunari Matsuda, and Yoshihiko Kanemitsu 72

1P-17 In-situ Raman Spectroelectrochemical Measurements at Carbon Nanotubes Modified Electrode
○Shingo Sakamoto, Keisuke Nagashima, Masato Tominaga 73

1P-18 Energetics of Single-Walled Carbon Nanotubes
○Koichiro Kato, Susumu Saito 74

1P-19 In-situ transmission electron microscopy of field emission from a gold coated carbon nanotube
○Tomohito Asai, Koji Asaka, Hitoshi Nakahara, Yahachi Saito 75

1P-20 Electronic properties of metallic and semiconducting carbon nanotubes
○Y. Miyata、P. Ayala、K. de Blauwe、H. Shiozawa、K. Yanagi、Y. Feng、R. Silva、R. Follath、C. Kramberger、H. Shinohara、H. Kataura、T. Pichler 76

Applications of Nanotubes

1P-21 Development of a novel technique for evaluating nanodispersion: "composite combustion method"
○Toshiyuki Tsuboi 77

1P-22 Light-Triggered Thermoelectric Conversion Based on Carbon Nanotube Hybrid Gels
○Eijiro Miyako, Takahiro Hirotsu 78

1P-23 Electrical Transport Properties of ssDNA Decorated Single (Double)-Walled Carbon Nanotubes
○Yongfeng Li, Toshiro Kaneko and Rikizo Hatakeyama 79

1P-24 Fabrication of Organic Solar Cells with Polymer/SWCNT Composite Hole Transport Layer
○Naoki Kishi, Shinya Kato, Yasuhiko Hayashi, Takeshi Saito, Tetsuo Soga, Takashi Jimbo 80

1P-25 Dispersion of Single-Walled Carbon Nanotubes using polybenzoxazoles precursor
○Takahiro Fukumaru, Tsuyohiko Fujigaya, Naotoshi Nakashima 81

1P-26 Enhancement of adhesion between carbon nanotwist and substate in printed field emitter by adding silicone binder
○Masasgi Yokota, Yoshiyuki Suda, Shinichiro Oke, Hirofumi Takikawa, Youhei Fujimura, Shigeo Itoh, Hitoshi Ue, Masakatsu Morioki, Kazuki Shimizu 82

1P-27 Design and Fabrication of Cantilevered Carbon Nanotube Force Sensor
○Ryosuke Nishii, Kota Oda, Takayuki Arie, Seiji Akita 83

1P-28 Sidewall Functionalization of MWCNT with Fuming Nitric Acid and Its Application to Polymer-Nanocomposite
○Hiroshi Kitamura, Shinya Kushita, Masaru Sekido, Hisato Takeuchi, Masatomi Ohno 84

1P-29 Theoretical Study of Spin Injection from Ferromagnetic Electrodes into Carbon Nanotube
○Yoshitaka Kato, Hiroyuki Fueno, Kazuyoshi Tanaka 85

1P-30 Fully-Stretchable Sensors for Human Motion Sensing by "Sticking" SWNT Films to Arbitrary Substrates
○Takeo Yamada, Yuki Yamamoto, Natsumi Makimoto, Sachiko Yamad, Don N. Futabaa, Yuhei Hayamizu, Kenji Hata 86

Formation and Purification of Nanotubes

1P-31 Analysis of Fe Catalyst Behavior on SiO_2/Si Substrates for CNT Growth Using Mössbauer Spectroscopy
○Hisayoshi Oshima, Tomohiro Shimazu, Milan Siry and Ko Mibu 87

1P-32 Effects of KOH Addition on Liquid-phase Synthesis of Highly Aligned Carbon Nanotubes
○Yoshihiro Yamaguchi, Kiyofumi Yamagiwa, Tomoka Kikitsu, Shunsuke Yamashita, Jun Kuwano 88

1P-33 Chiral Selective Separation for Single-walled Carbon Nanotubes Using both dispersants of Polysaccharide and Surfactant 89
Yoshiya Kaminosono, Katsumi Uchida, Koji Tsuchiya, Tadahiro Ishii and Hirofumi Yajima

1P-34 Purification of single-walled carbon nanotubes generated with arc-burning apparatus by utilizing electrophoresis technique 90
○Takashi Mizusawa, Shinzo Suzuki, Toshiya Okazaki, Yohji Achiba

1P-35 Selective SWNTs Growth with Specific Chirality by Irradiating Free Electron Laser during Growth
○Nobuyuki Iwata, Daisuke Ishiduka, Keijiro Sakai, Takuya Sonomura, Hiroaki Takeshita, Kunihide Kaneki, Hirofumi Yajima, Hiroshi Yamamoto 91

1P-36 Ab Initio Study toward Separation of Metallic and Semiconducting Single-Wall Carbon Nanotubes with Agarose Gel 92
○Mari Ohfuchi

1P-37 One-step Liquid-phase Synthesis of Highly Aligned Carbon Nanotube Arrays with Iron Pentacarbonyl 93
○Tomoka Kikitsu, Kiyofumi Yamagiwa, Yoshihiro Yamaguchi, Shunsuke Yamashita and Jun Kuwano

Endohedral Nanotubes

1P-38 TEM characterization of gamma-cyclodextrin bicapped C_{60}-fullerene in single-walled carbon nanotubes 94
○Kaori Takai Hirose, Yoko Iizumi, Toshiya Okazaki, Takeshi Saito, Kazu Suenaga

1P-39 Chemically Reactive Species Remain Alive inside Carbon Nanotubes: A Density Functional Theory Calculation Study 95
○Takashi Yumura

Nanohorns

1P-40 Photoluminescence from Isolated Individual Carbon Nanohorns 96
HIbiki Matsumoto, ○Masahito Sano

1P-41 Cytotoxicity of Single-Wall Carbon Nanohorns with Different Sizes 97
○Minfang Zhang, Takako Fujinami, Jianxun Xu, Takashi Yamaguchi, Sumio Iijima, Masako Yudasaka

Graphene

1P-42 Establishment of injecting spins into a single layer graphene
○Nobuhiko Mitoma, Takumi Takano, Masashi Shiraishi, Takayuki Nozaki, Teruya Shinjo, Yoshishige Suzuki 98

1P-43 Stability and Atomic Structures of Mult-Vacancies in Hexagonal Boron Nitride 99
Susumu Okada

Carbon Nanoparticles

1P-44 Ferromagnetic carbon nano-foam formed from boron containing composite carbon target by the pulsed laser vaporization in Ar/H_2 mixture 100
○Susumu Muraki, Iori Iwata, Hiroki Endo, Shunii Bandow, Sumio Iiiima

1P-45 Ferromagnetic carbon nano-foam prepared by the pulsed laser vaporization of pure carbon in Ar/H_2 mixture 101
○Hirohito Asano, Hiroki Endo, Shunji Bandow, Sumio Iijima

Miscellaneous

1P-46 Structural Change in Nano-carbon by Femtosecond Laser Shots:Virtual Experiments Using Supercomputers 102
○Yoshiyuki Miyamoto, Hong Zhang

1P-47 Synthesis and Magnetic Properties of Rare Earth Metal Graphite Intercalation Compounds 103
○Satoshi Heguri, Mototada Kobayashi

Plenary Lecture: 40 min (Presentation) + 5 min (Discussion)
Special Lecture: 25 min (Presentation) + 5 min (Discussion)
General Lecture by Candidates
for the Osawa and Iijima Award: 10 min (Presentation) + 10 min (Discussion)
General Lecture: 10 min (Presentation) + 5 min (Discussion)
Poster Preview: 1 min (Presentation), No Discussion

General Lecture by Candidates for the Osawa Award (9:00-10:00)

2-1 Synthesis, Mechanical and Electric Characterization of a Multiwall Carbon Nanocapsule Studied by in-situ Transmission Electron Microscopy 26
○Koji Asaka, Kun'ichi Miyazawa, Tokushi Kizuka, Yahachi Saito

2-2 Pioneering Research on the Properties and the Methods for Chemical Modification of Paramagnetic Endohedral Metallofullerenes 27
○Yuta Takano, Michio Yamada, Hidefumi Nikawa, Zdenek Slanina, Naomi Mizorogi, Midori O. Ishitsuka, Takahiro Tsuchiya, Yutaka Maeda, Takeshi Akasaka, Tatsuhisa Kato, Shigeru Nagase

2-3 Host-Guest Spin Communication Switchable by Guest Confinement 28
○Fatin Hajjaj, Kentaro Tashiro, Takeshi Akasaka, Tatsuhisa Kato, Takuzo Aida

☆☆☆☆☆☆ **Coffee Break (10:00-10:15)** ☆☆☆☆☆☆

General Lecture by Candidates for the Iijima Award (10:15-11:15)

2-4 Direct Determined Precise Electronic States of Isolated (n, m) Single-Walled Carbon Nanotubes 29
○Yasuhiko Hirana, Yasuhiko Tanaka, Koichiro Kato, Susumu Saito, Naotoshi Nakashima

2-5 Ink-jet printing of low-voltage SWCNT-thin film transistors using ionic liquid gating 30
○Haruya Okimoto, Taishi Takenobu, Kazuhiro Yanagi, Yasumitsu Miyata, Hiromichi Kataura, Takeshi Asano, Yoshihiro Iwasa

2-6 Carbon Nanotube Growth from Diamond Nanoparticles 31
○Daisuke Takagi, Yoshihiro Kobayashi, Yoshikazu Homma

Special Lecture (11:15-11:45)

2S-1 Precise Structural Analysis of Endohedral C_{60} Compounds 3
Hiroshi Sawa

☆☆☆☆☆☆ **Lunch Time (11:45-12:45)** ☆☆☆☆☆☆

General Meeting (12:45-13:00)

General Lecture (13:00-14:45)

Carbon Nanoparticles

2-7 Functionalisation of Nanodiamonds: Surface Tailoring of Agglomerating Nanoparticles 32
○Masaki Ozawa, Yuejiang Liang, Anke Krueger

Chemistry of Fullerenes

2-8 Possible Magnetic States in Buckybowl Molecules 33
○Kikuo Harigaya

2-9 Control of Redox Properties of Fullerene Derivatives by Lone Pair Proximity Effect 34
○Yusuke Tajima, Youhei Numata

2-10 Chemical Transformation of the Open-Cage Fullerenes. Alkylation Reactions of the Methylene Protons on the Opening Moieties 35
○Sho-ichi Iwamatsu

2-11 Porphyrin Polymer Assisted Self-Assembly of C_{60} to Silk Ball-Shaped Microspheres 36
○Xuan Zhang, Masayuki Takeuchi

Applications of Fullerenes

2-12 Self-Assembly of A Chiral Donor-Acceptor Amphiphilic Dyad For Molecular Design of Photoconducting Materials 37
○Kentaro Tashiro, Yumi Hizume, Charvet Richard, Yohei Yamamoto, Shu Seki, Takuzo Aida

2-13 Thermo-Responsive Behavior and DNA Photocleavage of Water-Soluble Fullerene/Polymer Complex 38
○Shin-ichi Yusa, Shigeki Awa, Takeshi Kawase, Tadao Takada, Kenichi Nakashima, Dian Liu, Shigeru Yamago and Yotaro Morishima

☆☆☆☆☆☆ **Coffee Break (14:45-15:00)** ☆☆☆☆☆☆

General Lecture (15:00-16:00)

Applications of Fullerenes

2-14 Design of Fullerene/PEG-b-polyamine Complex for Nanomedicine 39
○Yukio Nagasaki, Ryosuke Kodaka

2-15 TNFα-induced NFκB activation is attenuated by Fullerene Derivatives 40
○Takumi Inoue, Masayuki Ito, Shuichi Yamana, Kyoko Takahashi, Shigeo Nakamura, Tadahiko Mashino

Endohedral Metallofullerenes

2-16 Production and Characterization of $LaYC_{80}$ 41
○Takeshi Kodama, Daisuke Kakeda, Wataru Fujita, Koichi Kikuchi, Shinzo Suzuki, Yohji Achiba

2-17 Two Step Regioselective Exohedral Functionalization of Endohedral Metallofullerene 42
○Satoru Sato, Yutaka Maeda, Koji Inada, Hidefumi Nikawa, Michio Yamada, Naomi Mizorogi, Tadashi Hasegawa, Takahiro Tsuchiya, Takeshi Akasaka, Tatsuhisa Kato, Zdenek Slanina, Shigeru Nagase

Plenary Lecture (16:00-16:45)

2S-2 Dynamics of Metal Clusters Inside Fullerene Carbon Cages 4
Harry C. DORN

Poster Preview (16:45-17:45)

Poster Session (17:45-19:00)

Fullerene Solids

2P-1 Dispersion of Morphology-Controlled Fullerene Particles 104
○Yutaka Takaguchi, Yasuhiko Fujita, Junpei Matsukawa, Tomoyuki Tajima

2P-2 C_{60} Polymerization in Solution with Free Electron Laser Irradiation 105
○Nobuyuki Iwata, Kohei Kurihara, Yasunari Iio, Hiroshi Yamamoto

2P-3 Observation of Pore Size Distribution Inside C_{60} Nanofibers 106
○Ryoei Kato and Kun'ichi Miyazawa and Zheng-Ming Wang

2P-4 Phonon and electron-phonon coupling in alkali-doped fullerides 107
○Takashi Koretsune, Susumu Saito

Endohedral Metallofullerenes

2P-5 Structural Determination of Metal Carbide Endofullerene $Sc_2C_2@C_{80}$ 108
○Hiroki Kurihara, Yuko Yamazaki, Hidefumi Nikawa, Naomi Mizorogi, Takahiro Tsuchiya, Shigeru Nagase and Takeshi Akasaka

2P-6 Chemical modification of $La_2@C_{80}$ with Silacyclopropane 109
○Mari Minowa, Michio Yamada, Masahiro Kako, Takahiro Tsuchiya, Midori O. Ishitsuka, Takeshi Akasaka

2P-7 Bis-adduct of Non-IPR $La@C_{72}$ 110
○Tsuyoshi Ito, Hidefumi Nikawa, Takeshi Akasaka, Takahiro Tsutiya, Zdenek Slanina, Naomi Mizorogi, Shigeru Nagase

2P-8 Synthesis and characterization of stable [4+2] derivatives of $La@C_{82}$ 111
○Yuki Nagashima, Yuta Takano, Zdenek Slanina, Takahiro Tsuchiya, Takeshi Akasaka, Shigeru Nagase

2P-9 Synthesis and properties of endohedral metallofullerene ligand 112
○Ryo Aoyama, Yuya Yokosama, Takahiro Tsuchiya, Takeshi Akasaka

2P-10 Synthesis and properties of paramagnetic metallofullerene/electron donor dyad 113
○Tatsuya Tanaka, Takahiro Tsuchiya, Takeshi Akasaka, Naomi Mizorogi, Shigeru Nagase

2P-11 Valence States-Dependent Photoluminescence from Thulium Atoms Encapsulated in Fullerenes 114
○Noriko Izumi, Hiroaki Iijima, Toshiya Okazaki, Masayoshi Tange, Yasumitsu Miyata, Hisanori Shinohara

2P-12 Systematic X-Ray Diffraction Studies on Crystal Structure of Mono-Metallofullerene $M@C_{82}$ 115
○Takayuki Aono, Eiji Nishibori, Ryo Kitaura, Shinobu Aoyagi, Masaki Takata, Makoto Sakata, Hiroshi Sawa, Hisanori Shinohara

2P-13 Isolation and structure determination of $(Lu_2C_2)@C_{88}$: Experimental and theoretical analyses 116
○Kazunari Shiozawa, Noriko Izumi, Hisashi Umemoto, Ryo Kitaura, Hisanori Shinohara

2P-14 Electronic structure of endohedral fullerenes$Y_2C_2@C_{82}$, $Sc_3N@C_{78}$ obtained by ab initio molecular orbital calculation 117
○Yusuke Aoki, Takafumi Miyazaki, Shojun Hino

2P-15 Ultraviolet and X-ray photoelectron spectra of C_{3v}-$Tm_2@C_{82}$ 118
○Youji Tokumoto, Hajime Yagi, Takafumi Miyazaki, Noriko Izumi, Hisanori Shinohara, Shojun Hino

Fullerene Formation

2P-16 Encapsulation of Atomic Nitrogen into C_{60} and Polyynes into SWNTs 119
○Tomonari Wakabayashi, Masashi Teshiba, Mao Saikawa, Airi Yoshikawa, Yoriko Wada

Environmental/Safety Characterization of Nanomaterials

2P-17 Biodegradation of Fullerene Nanowhiskers by Macrophage-like Cells 120
○Shin-ichi Nudejima, Kun'ichi Miyazawa, Junko Okuda-Shimazaki and Akiyoshi Taniguchi

Properties of Nanotubes

2P-18 Conductivity of metallic and semiconducting single wall carbon nanotube buckypaper 121
○Hiroki Udoguchi, Satoshi Sagitani, Kazuyuki Matsuda, Yugo Oshima, Hiromichi Kataura, Daishi Takenobu, Kazuhiro Yanagi, Yutaka Maniwa

2P-19 Anomalous behavior of bundle-related Raman signals from carbon nanotubes grown by noble-metal particles 122
○Yoshihiro Kobayshi, Daisuke Takagi, Satoru Shoji, Satoshi Kawata

2P-20 Structure Analysis of Multi-Walled Carbon Nanotubes by TGA in the Reductive Atmosphere 123
○Ken-ichi Hongyou, Tohoru matsubara, Hiroyuki Nii, Atsuhiro Kunishige

2P-21 Optical absorption in short metallic carbon nanotubes 124
○Takeshi Nakanishi, Tsuneya Ando

2P-22 Chirality Distribution and Hidden Features of SWCNTs Explored by Optical Absorption Spectroscopy 125
○Takeshi Saito, Bikau Shukla, Shigekazu Ohmori, Motoo Yumura, Sumio Iijima

2P-23 Atomic geometry and electronic structure of pyridine-type defects in carbon nanotube 126
○Yoshitaka Fujimoto, Susumu Saito

2P-24 Physical properties of Carbon nanotube grown by Microwave Plasma CVD method 127
○Tohru Watanabe, Shunsuke Tsuda, Takahide Yamaguchi, Yoshihiko Takano

2P-25 Excitonic effects and chirality dependence of photoluminescence intensity of single wall carbon nanotubes 128
○Kentaro Sato, Riichiro Saito, Shigeo Maruyama

Applications of Nanotubes

2P-26 Development of Light-Driven Carbon Nanoheat System for an Organic Reaction 129
○Eijiro Miyako, Tamitake Itoh, Takahiro Hirotsu

2P-27 Transmission electron microscopic observation of Pt/Ru-supported carbon nanocoil 130
○Takahiro Kawabata, Masashi Yokota, Kotaro Takimoto, Takashi Ikeda, Yoshiyuki Suda, Shinichiro Oke, Hirofumi Takikawa, Yohhei Fujimura, Shigeo Itoh, Hitoshi Ue, Masakatsu Morioki, Kazuki Shimizu

2P-28 Carbon nanotubes modified electrode for a dye-sensitized solar cell 131
○Koichi Yasukawa, Shingo Sakamoto, Masato Tominaga

2P-29 Investigation on Solar Cell Fabricated by Carbon Nanotube Thin Film 132
○Tatsuya Kato, Yongfeng Li, Toshiro Kaneko, Rikizo Hatakeyama

2P-30 Development of Novel Artificial Organ Biomaterial Composed of Multi-walled Carbon Nanotubes and Poly(L-lactic acid) 133
○Katsumune Takahashi, Hirofumi Yajima

Formation and Purification of Nanotubes

2P-31 Temperature dependence of diameter distributions of SWNTs revealed by optical absorption and photoluminescence mesurements 134
○Akira Inoue, Yasuhiro Tsuruoka, Toshiya Okazaki, Yohji Achiba

2P-32 Effect of Laser Wavelength and Dispersed Agents to Selective Chiral Separation of Single-walled Carbon Nanotubes by Pulsed OPO Laser Irradiation 135
○Akira Kumazawa, Isa, Katsumi Uchidamu Tajima, Koji Tsuchiya, Tadahiro Ishii, Hirofumi Yajima

2P-33 Catalyst deposition by spin-coating for synthesis of vertically-aligned single-walled carbon nanotubes 136
○Theerapol Thurakitseree, Erik Einarsson, Rong Xiang, Pei Zhao, Junichiro Shiomi, Shigeo Maruyama

2P-34 Bending Horizontally-Aligned Carbon Nanotubes during Growth 137
○Hiroki Ago, Kenta Imamoto, Tetsushi Nishi, Masaharu Tsuji, Tatsuya Ikuta, Koji Takahashi, Munetoshi Fukui

2P-35 Synthesis of Single-Walled Carbon Nanotube Soot with Few Impurity Graphites by Arc Discharge 138
○Yoshinori Sato, Hikaru Watanabe, Masaru Namura, Kenichi Motomiya, Kazuyuki Tohji

2P-36 Growth of carbon nanotubes by plasma enhanced and thermal chemical vapor depositions 139
○Masato Miyake, Toru Iijima, Kenneth Teo, Nalin Rupesinghe, Kenjirou Onuma, Kazunori Horikawa, Katsuyoshi Abe, Masayuki Satoh and Yasuhiko Hayashi

2P-37 Carbon Nanotubes Synthesis in Liquid Xylene by Arc Discharge Using Metal Electrodes 140
○Takio Kizu, Shinya Aikawa, Eiichi Nishikawa

2P-38 Selective dispersion of single-walled carbon nanotubes using polycarbazole derivative 141
Hiroaki Ozawa, Natsuko Ide, Tsuyohiko Fujigaya, Suhee Song, Hongsuk Suh and Naotoshi Nakashima

Endohedral Nanotubes

2P-39 Diameter-Dependence of Host-Guest Interaction between Single-Wall Carbon Nanotubes and Encapsulated Fullerenes Probed by Resonance Raman Spectroscopy 142
○Soon-Kil Joung, Toshiya Okazaki, Susumu Okada and Sumio Iijima

2P-40 Room-Temperature Y-Emission from Perylene Molecules Confined in Single-Wall Carbon Nanotubes 143
○Masayoshi Tange, Toshiya Okazaki, Zheng Liu, Kazu Suenaga, Sumio Iijima

2P-41 Energetics and Electronic Structure of Carbon Nanotube Encapsulating Coronene 144
Susumu Okada

Nanohorns

2P-42 Ceramide-conjugated PEG: an Outstanding Dispersant for SWNHs 145
○Jianxun Xu, Sumio Iijima, Masako Yudasaka

Graphene

2P-43 Formation of honeycomb nano-pore array on graphene using by nanoporous alumina template and edge electronic structures 146
○J.Nakamura, J. Haruyama, T. Shimizu, S.Oikawa, S.Enomoto

2P-44 Characterization of Graphene by Scanning Electron Microscopy 147
○Hidefumi Hiura, Hisao Miyazaki and Kazuhito Tsukagoshi

2P-45 Fabrication of graphene nano-ribbons and observation of those structures and electrical features 148
○Taisei Shimizu, Junji Haruyama, Jin Nakamura, Yuki Tanabe, Yusuke Yamakawa

Carbon Nanoparticles

2P-46 Promotion of polyhedral graphite growth in laser vaporization by adding silicon or boron 149
Hajime Chigusa, Iori Nozaki, Akira Koshio, ○Fumio Kokai

2P-47 Photo-induced formation of Polyyne-Bromine Complex in Solution 150
○Yasunori Kai, Tatsuhisa Kato, Yoriko Wada, Tomonari Wakabayashi

2P-48 Raman and TEM Studies of Heat-Treated La Fullerene Soot 151
○Kazunori Yamamoto, Shin-ichi Shamoto, Takeshi Akasaka, Takatsugu wakahara and Kun'ichi Muyazawa

Special Lecture: 25 min (Presentation) + 5 min (Discussion)
General Lecture: 10 min (Presentation) + 5 min (Discussion)
Poster Preview: 1 min (Presentation), No Discussion

Special Lecture (9:00-9:30)

3S-1 Synthesis and Applications of High-quality and Highly Oriented Graphite from Polyimide Films
Mutsuaki Murakami 5

General Lecture (9:30-10:45)

Properties of Nanotubes

3-1 Ultrafast exciton level modulation due to coherent optical nonlinearity in isolated semiconducting SWNTs
○Shoichi Tao, Yasumitsu Miyata, Kazuhiro Yanagi, Hiromichi Kataura, Hiroshi Okamoto 43

3-2 Excited Carrier Diffusion for Bundle of Semiconductive and Metallic Carbon Nanotubes: Time-Dependent Density Functional Calculations
○Takazumi Kawai, Yoshiyuki Miyamoto 44

3-3 The fastest high definition Raman imaging of carbon nanotubes bridged between electrodes
○Tomoya Uchiyama, Minoru Kobayashi, Taisuke Ota and Masamichi Yoshimura 45

3-4 Stability and optical propeties of Single-walled carbon nanotubes/oligo-DNA hybrid
○Yuki Yamamoto, Tsuyohiko Fujigaya, Naotoshi Nakashima 46

3-5 Fermi energy dependence of radial breathing mode in metallic single-wall carbon nanotubes
○Jin Sung Park, Kenich Sasaki, Riichiro Saito, Gene Dresselhaus, Mildred S. Dresselhaus 47

☆☆☆☆☆☆ **Coffee Break (10:45-11:00)** ☆☆☆☆☆☆

Poster Preview (11:00-12:00)

☆☆☆☆☆☆ **Lunch Time (12:00-13:00)** ☆☆☆☆☆☆

Poster Session (13:00-14:15)

Chemistry of Fullerenes

3P-1 Preparation of [60]Fullerene-Based Interlocked Compounds Using Axle Molecules Including Donor Units
○Chika Sakamoto, Naoki Muroya, Yosuke Nakamura and Jun Nishimura 152

3P-2 Synthesis and Photophysical Properties of Oligocarbazole-[60]Fullerene Adducts Bearing Various Spacer Units
○Kounosuke Kobayashi, Keisuke Kinoshita, Yosuke Nakamura and Jun Nishimura 153

3P-3 Synthesis and Liquid Crystallinity of Fullerodendron Having Cyanobiphenyl Groups at the Terminals
○Yutaka Takaguchi, Yuuki Sako, Tomoyuki Tajima 154

3P-4 The Diels-Alder Reaction of C_{60} and Dienes in Mesoporous Silica as a Reaction Medium
Satoshi Minakata ○Toshiki Nagamachi and Kazuhisa Nakavama 155

3P-5 Synthesis and Thermally Morphological Control of 1,4-Bis(silylmethyl)[60]fullerene Derivatives
○Keiko Matsuo, Yutaka Matsuo, Eiichi Nakamura 156

3P-6 Synthesis and Properties of Novel Open-Cage C_{60} Derivatives
○Kei Kurotobi, Michihisa Murata, Yasujiro Murata 157

3P-7 Construction of Ordered Fullerene Arrays by Supramolecular Fullerene-Perfluorobenzene interaction
○Chang-Zhi Li, Yutaka Matsuo, Eiichi Nakamura 158

3P-8 Highly Regioselective Adiridination of C_{60} with Sulfilimines
○Midori O. Ishitsuka, Mitsunori Okada, Tsukasa Nakahodo, Hidefumi Nikawa, Takahiro Tsuchiya, Takeshi Akasaka, Tetsuo Fujie, Toshiaki Yoshimura, Zdenek Slanina, Shigeru Nagase 159

3P-9 Behavior of the photocurrent on Mg-doped C_{60} films
Crisoforo Morales, Nobuaki Kojima, Masato Natori, Seiji Nishi, Masafumi Yamaguchi 160

Applications of Fullerenes

3P-10 C_{60} Crystal Growth Directly between Electrodes from Solution
○Nobuyuki Iwata, Kohei Kurihara, Yasunari Iio, Hiroshi Yamamoto 161

Endohedral Metallofullerenes

3P-11 Extraction Selectivity of Fullerenes: Dependence on Solvents
○Takashi Inoue, Rie Tao, Yuji Takimoto 162

3P-12 Application of Metal Endohedral Fullerenes for High Power Conversion Efficiency in Bulk-heterojunction Solar Cells
○Morihiko Saida, Haruna Oizumi, Hiroyuki Sagami, Yuzo Mizobuchi, Kenji Omote, Yasuhiko Kasama, Kuniyoshi Yokoo, Shoichi Ono, Shigehiko Yamamoto, Takayuki Kuwabara, Kohshin Takahashi 163

3P-13 Rotational Sub-levels of Ortho-Hydrogen Molecule Encapsulated in Isotropic C_{60} Fullerene Cages
○Katsumi Tanigaki, Yoshimitsu Kohama, Takeshi Rachi, Jing Ju, Zhaofei Li, Jun Tang, Ryotaro Kumashiro, Satoru Izumisawa, Hitoshi Kawaji, Tooru Atake, Hiroshi Sawa, Yasuiiro Murata and Koichi Komatsu 164

3P-14 Structure and Relative Stabilities of $Sc_2@C_{74}$ and $La_2@C_{74}$
○T. Ren, X. Zhao, H. Zheng, J. S. Dang 165

Properties of Nanotubes

3P-15 Evaluation of Multi-Walled Carbon Nanotubes by Ultraviolet Raman Spectroscopy
○Hiroyuki Nii, Ken-ichi Hongyou, Hamazo Nakagawa 166

3P-16 Near-infrared Absorption Properties of Single-walled Carbon Nanotubes under Ultra-high Magnetic Fields
Hiroyuki Yokoi, Eiji Kojima, Shojiro Takeyama, Nobutsugu Minami 167

3P-17 Molecular Dynamics Simulation of Adsorption of Polysaccharide on Carbon Nanotubes
○Hiroyuki Shinomiya, Katsumi Uchida, Koji Tsuchiya, Tadahiro Ishii and Hirofumi Yajima 168

3P-18 Field emission study on a single Ti-coated multi-wall carbon nanotube
○Yuuta Yamamoto, Huarong Liu, Koudai Nomura, Hitoshi Nakahara, Yahachi Saito 169

3P-19 Reduction of Single-walled Carbon Nanotubes in Organic Solvent
○Yutaka Maeda, Atsushi Tashiro, Tadashi Hasegawa, Takahiro Tsuchiya, Takeshi Akasaka, Jing Lu, Shigeru Nagase 170

3P-20 Solvent Effect On Single-walled Carbon Nanotubes in Organic Solvent
○Tomohisa Okita, Yutaka Maeda, Katsuya Sode, Tadashi Hasegawa, Takahiro Tsuchiya, Takeshi Akasaka, Shigeru Nagase 171

3P-21 Mechanism of thermal boundary conductance between SWNTs and surrounding materials
○Jin Hyeok Cha, Junichiro Shiomi, Shigeo Maruyama 172

3P-22 The Raman scattering of chain like carbon materials observed in MWNTs and SWNTs produced by hydrogen gas arc discharge using Fe catalyst
○Makoto Jinno, Yoshinori Ando 173

Applications of Nanotubes

3P-23 Fabrication of plastic lens for glasses with anti-static property using single wall carbon nanotubes.
○Hirotoshi Takahashi, Tsuyoshi Fukagawa, Takeshi Hashimoto 174

3P-24 Super-growth: Low Threshold Voltage, High Uniformity and High Stability Field Emission from As-Grown Carbon Nanotubes
○Hiroe Kimura, Don N. Futaba, Takeo Yamada, Tatsuo Toida, Bin Zhao, Hiroyuki Kurachi, Sashiro Uemura and Kenji Hata 175

3P-25 Aligned SWNT Prepreg Sheets and Their Reinforcing Effects
○Kazufumi Kobashi, Hidekazu Nishino, Takeo Yamada, Don N. Futaba, Kenji Hata 176

3P-26 Enhanced Photocurrent in a Dye-Sensitized Solar Cell Consisting of an FTO glass/SnO_2/p3HT Electrode by Coating with MWCNTs
○Toru Arai, Atsushi Furuta, Tatsunori Kuramoto 177

3P-27 Solubilization of Single-walled Carbon Nanotubes by Using meso-meso Linked Porphyrin oligomer
Takeshi Uchinoumi, Tsuyohiko Fujigaya, Naotoshi Nakashima 178

3P-28 Preparation of Conductive Film Composed of Polyaniline Sulfonic Acid and Single-walled Carbon Nanotubes
○Tomoyuki Kuriyama, Syuku Ono, Yosiya Kaminosono, Katsumi Uchida, Koji Tsuchiya, Tadahiro Ishii and Hirofumi Yajima 179

3P-29 Facile Fabrication and Characterization of a Field Effect Transistor using As-grown Single-Walled Carbon Nanotubes
○Shinya Aikawa, Rong Xiang, Erik Einarsson, Junichiro Shiomi, Eiichi Nishikawa, Shigeo Maruyama 180

Formation and Purification of Nanotubes

3P-30 Improvement of carbon nanocoil yeild by using vacuum-evaporated Sn thin film
○Koraro Takimoto, Yuichiro Shinohara, Masashi Yokota, Takahiro Kawabata, Yoshiyuki Suda, Shinichiro Oke, Hirofumi Takikawa, Youhei Fujimura, Tatsuo Yamaura, Shigeo Ito, Hitoshi Ue, Masakatu Morioki 181

3P-31 Improvement of bulk-density of brush-like carbon nanotubes
○Gen Kubo, Takayuki Arie, Seiji Akita 182

3P-32 Influence of Water Addition on Carbon Nanotube Growth by Alcohol Gas Source Method in High Vacuum 183
○Kuninori Sato, Takahiro Maruyama, Shigeya Naritsuka

3P-33 Optical Emission Spectroscopy Study of Plasmas during the growth of Single-Walled Carbon Nanotubes with Au Catalyst 184
○ Z. Ghorannevis, T. Kato, T. Kaneko and R. Hatakeyama

3P-34 Super-growth:How to Make Fast Growth Even Faster (and keep its quality) 185
○Junichi Sato, Satoshi Yasuda, Don N. Futaba, Takeo Yamada, Motoo Yumura and Kenji Hata

3P-35 Effect of the support materials on catalyst chemical vapor deposition (CCVD) growth of carbon nanotubes 186
○Takuya Nakayama, Ryo Kitaura, Hisanori Shinohara

3P-36 Direct Growth of Orthogonal Single-Walled Carbon Nanotube Arrays 187
○Tetsushi Nishi, Hiroki Ago, Carlo M. Orofeo, Naoki Ishigami, Masaharu Tsuji, Tatsuya Ikuta, Koji Takahashi

3P-37 High Precision Site-selective Growth of SWNTs and its Applications 188
○Rong Xiang, Shinya Aikawa, Erik Einarsson, Junichiro Shiomi, Shigeo Maruyama

Endohedral Nanotubes

3P-38 Observation of Photoreaction Process of Molecules within Single-Wall Carbon Nanotube by High Resolution Transmission Electron Microscopy 189
○Keita Kobayashi, Kazutomo Suenaga, Takeshi Saito and Sumio Iijima

3P-39 Host-Guest Interaction between Azafullerene And Single-Wall Carbon Nanotubes in Peapod Structure 190
○Yoko Iizumi, Toshiya Okazaki, Zhen Liu, Kazu Suenaga, Takeshi Nakanishi, Sumio Iijima, Nikos Tagmatarchis

3P-40 Creation and Property Evaluation of Calcium Encapsulated Single-Walled Carbon Nanotubes 191
○Yosuke Osanai, Tetsuhiro Shimizu, Toshiaki Kato, Wataru Oohara, Rikizou Hatakeyama

3P-41 Spectroscopic Characterization on the High-Yield Filling of Eu-Nanowires inside Single-Wall Carbon Nanotubes. 192
○Ryo Nakanishi, Ryo Kitaura, Takahisa Yoshimoto, Takeshi Saito, Miyata Yasumitsu, Hisanori Shinohara

3P-42 Evolution and Growth of Linear-Polyynes Inside Thin Double-Wall Carbon Nanotubes 193
○Chen Zhao, Ryo Kitaura, Hironori Hara, Stephan Irle and Hisanori Shinohara

Nanohorns

3P-43 Structure Analysis of Single-Wall Carbon Nanohorns 194
M. Irie, J. Xu, R. Yuge, S. Iijima, ○M. Yudasaka

3P-44 Cytotoxicity of Single-Wall Carbon Nanohorns 195
Takako Fujinami, Jianxun Xu, ○Yuri Myouhara, Sumio Iijima, Masako Yudasaka

Graphene

3P-45 The edge-shpae dependence of Raman spectra for graphene 196
○T. Mori, K. Takai, K. Sasaki, K. Wakabayashi and T. Enoki

3P-46 Nano-graphitization and mesoscopic large corrugation of amorphous carbon thin films by high temperature post-annealing 197
○Takuya Noguchi, Toshihiro Shimada, Takashi Chiba, Masao Terada, Tetsuya Hasegawa

3P-47 Electronic Structures of Folded Graphene 198
○Yoshiteru Takagi, Susumu Okada

Miscellaneous

3P-48 Combinatorial study on Fe-SnO_2 catalyst for synthesis of carbon nanocoils 199
○Hiroshi Fuiita. Takavuki Arie. Seiii Akita

Special Lecture (14:15-14:45)

3S-2 Advances in Supergrowth - Growth, Application and Devices 6
Kenji Hata

General Lecture (14:45-15:30)

Applications of Nanotubes

3-6 Photosensitized Hydrogen Evolution from Water Using Fullerodendron/SWNT Supramolecular Nanocomposite 48
○Yutaka Takaguchi, Wakako Sakata, Tomoyuki Tajima

3-7 Composite Clusters of Higher Fullerenes and Single-Walled Carbon Nanotubes 49
○Tomokazu Umeyama, Noriyasu Teduka, Yoshihiro Matano, Hiroshi Imahori

3-8 Brain wave detection using a multi-wall carbon nanotube film sensor
○Akira Kawamoto, Ryuhei Kitai, Toshihiko Kubota 50

☆☆☆☆☆☆ **Coffee Break (15:30-15:45)** ☆☆☆☆☆☆

General Lecture (15:45-17:00)

Applications of Nanotubes

3-9 Evaluation of Ar Fast Atom Bombardment Process on Vertically Aligned Carbon Nanotubes
○Masahisa Fujino, Tadatomo Suga, Junichiro Shiomi, Shigeo Maruyama, Ikuo Soga, Daiyu Kondo, Yoshikatsu Ishizuki, Taisuke Iwai and Masataka Mizukoshi 51

3-10 Electrical Characteristics of DNA Encapsulated Single-Walled Carbon Nanotubes Created in Electrolyte Plasmas
○Toshiro Kaneko, Yongfeng Li, Rikizo Hatakeyama 52

3-11 Sorting and integration of DNA-wrapped single-wall carbon nanotubes for thin film transistors
○Yuki Asada, Yasumitsu Miyata, Yutaka Ohno, Ryo Kitaura, Toshiki Sugai, Takashi Mizutani, Hisanori Shinohara 53

3-12 [60]-Fullerene and Single-Walled Carbon Nanotube-Based Hybrid Ultrathin Films on ITO
○Qiguan Wang, Hiroshi Moriyama 54

3-13 First-Principles study for Single-Walled Carbon Nanotube on Metal
○Yoshiteru Takagi, Susumu Okada 55

基調講演
Plenary Lecture

特別講演
Special Lecture

1S – 1 ～ 1S – 2
2S – 1 ～ 2S – 2
3S – 1 ～ 3S – 2

1S-1

Imaging Organic Molecules in Motion
- A New World of Chemical Physics as Viewed through a Nanotube -

Eiichi Nakamura

Department of Chemistry and Nakamura Functional Carbon Cluster ERATO Project
The University of Tokyo, Bunkyo-ku, Tokyo 113-0033, Japan

Chemists are "molecular architects". They enjoy building molecular architectures, and feel happy about learning whether or not they behave as expected. However, the molecules are too small and too fast moving to see directly their dynamic behavior. Therefore, the concept of molecules has remained very hard to understand even for chemistry students, not to mention, lay people. How many of us would really understand the molecular mechanism of the action of a pill for curing your headache?

For sometime, we ponder the possibility of taking a look at molecules by a high-resolution transmission electron microscope, and succeeded very recently in obtaining time-resolved, near atomic resolution images of organic molecules in action (see below). The talk will be describe such molecular images that have just become available as well as some discussions of implications of the new finding.

Corresponding Author: Eiichi Nakamura
TEL and FAX: +81-3-5800-6889, E-mail: nakamura@chem.s.u-tokyo.ac.jp

1S-2

Exohedral Functionalization of Fullerenes and Supramolecular Chemistry

Yosuke Nakamura

Department of Chemistry and Chemical Biology, Graduate School of Engineering, Gunma University, Kiryu, Gunma 376-8515, Japan

The suitable functionalization of fullerenes using the supramolecular approaches as well as the conventional covalent bondings is necessary for the application of fullerenes into functional materials. We have so far developed new functionalization methods using covalent bonds and clarified the properties of obtained adducts. Especially, we have examined the multiple functionalization including the regioselective synthesis of bisadducts, the elucidation of their properties, and the optical resolution of chiral bisadducts [1]. In the course of our studies, we have also engaged in the supramolecular functionalization of fullerenes. This lecture presents the recent examples of the fullerene functionalization or supramolecular approaches leading to some functional materials.

Fullerene bisadduct **1** bearing a dibenzo-18-crown-6 moiety was obtained with a high regioselectivity by the Diels-Alder reaction of the corresponding *o*-quinodimethane precursor with [60]fullerene. Intriguingly, **1** complexed with K^+ ion with extremely high selectivity among alkali metal ions.

Recently, we have developed new synthetic strategies of neutral fullerene-based [2]catenanes and [2]rotaxanes, consisting of a fullerene derivative carrying an aromatic diimide moiety as another electron-acceptor and an electron-donating macrocycle such as a dibenzocrown ether [2]. In the presence of 1,5-dinaphtho-38-crown-10 ether at low temperatures, the *inter*molecular Bingel reactions of [60]fullerene monoadducts bearing a naphthalenetetracarboxylic diimide moiety with [60]fullerene successfully afforded novel [2]rotaxanes **2**, while their *intra*molecular Bingel reactions gave [2]catenanes **3** with D–A–D–A stacking structure. These rotaxanes and catenanes are applicable to molecular machines and molecular switches.

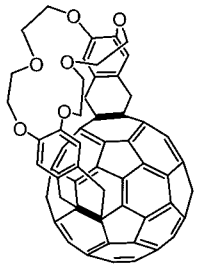

1

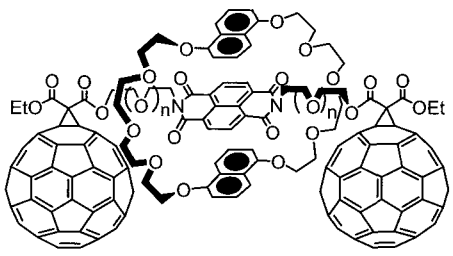

2: n = 2, 3

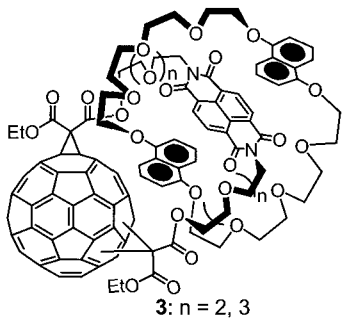

3: n = 2, 3

[1] Y. Nakamura, K. O-kawa, and J. Nishimura, *Bull. Chem. Soc. Jpn.*, **76**, 865–882 (2003).

[2] Y. Nakamura, S. Minami, K. Iizuka, and J. Nishimura, *Angew. Chem., Int. Ed.*, **42**, 3158–3162 (2003).

Corresponding Author: Yosuke Nakamura

Tel: +81-277-30-1310, Fax: +81-277-30-1314, E-mail: nakamura@chem-bio.gunma-u.ac.jp

2S-1

Precise Structural Analysis of Endohedral C_{60} Compounds

Hiroshi Sawa

Department of Applied Physics, Nagoya University, Nagoya 464-8603, Japan

Many types of endohedral metallofullerenes have been synthesized and structurally characterized in the past 10 years. In particular, interesting behavior of metal atoms trapped inside carbon cages were revealed by physical measurements, e.g. giant thermal motion, formation of metal clusters, and so on. These characteristic features were able to specify by the full-filled endohedral metallofullerenes and high quality crystalline specimen. However, metallofullerenes have higher cages (the so-called higher fullerenes) such as C_{82} and C_{84} have been isolated and structurally characterized[1].

On the other hand, C_{60} is the most promising material for the wide range of practical applications owing to their high productivity and the highest structural symmetry. Recent developments on fabrication of non-metal endohedral fullerenes have provided macroscopic amounts of C_{60} based endofullerenes. For example, He@C_{60}, Ar@C_{60} and H_2@C_{60}, have been successfully produced by a high-pressure gas reaction [2], the ion implantation [3] and molecular surgery techniques [4].

It has not been possible to specifically locate the electron-density of such a small scattering cross section of a H_2 molecule by the conventional X-ray source. In order to observe the endohedral atom/molecule directly, the X-ray diffraction measurements using synchrotron radiation were carried out. We observed a single H_2 molecule and an Ar atom encapsulated in fullerene cage using structure analysis and maximum entropy method (Figure.1). The each endohedral element is floating at the center of the C_{60} cage and considered to be completely isolated from the outside[3,5].

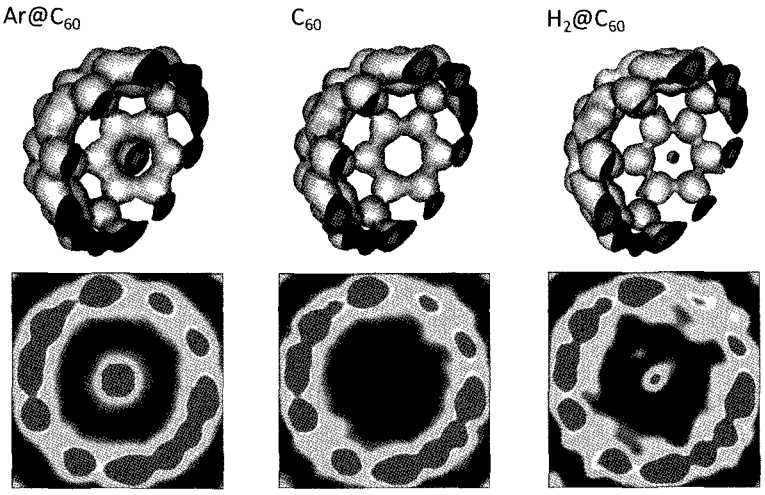

Figure 1. MEM electron density of Ar@C_{60} (left), pristine C_{60} (center), and H_2@C_{60} (right) as an equal-density contour surface (upper), which equicontour level is 0.8 [e/Å^3], and cross sections 0.1-1.0 [e/Å^3] (lower).

[1] H. Shinohara, *Rep. Prog. Phys.* **63**, 843 (2000).

[2] M. Saunders, R. J. Cross, H. A. Jiménez-Vázquez, R. Shimshi, A. Khong, *Science* **271**, 1693 (1996).

[3] K. Yakigaya et al., *New J. Chem.* **31**, 973 (2007).

[4] K. Komatsu, M. Murata, Y. Murata, *Science* **307**, 238 (2005).

[5] H. Sawa, Y. Wakabayashi, Y. Murata, M. Murata, K. Komatsu, *Angew. Chem. Int. Ed.* **44**, 1981 (2005).

Corresponding Author: Hiroshi Sawa
TEL: +81-52-789-4453, FAX: +81-52-789-3724, E-mail: hiroshi.sawa@cc.nagoya-u.a.jp

2S-2

Dynamics of Metal Clusters Inside Fullerene Carbon Cages

Harry C. Dorn

Carbonaceous Nanomaterials Center and Department of Chemistry, Virginia Tech
Blacksburg, VA, USA 24060-0212

Although there has been considerable progress in characterizing fullerene carbon cages and their corresponding motional processes in solution and the solid-state, progress toward understanding the dynamics of metal cluster motion inside these fullerenes (endohedral metallofullerenes) has not been as clearly described in the literature. The trimetallic nitride templated endohedral metallofullerenes (TNT EMFs) clearly contain metal clusters with a range of different metals as well as larger cages $M_3N@C_{2m}$ (m=40-50) available for study. [1-5] In addition, $M_n@C_{2m}$ (n=1-2, m=40-50) and metal carbide $M_2C_2@C_{2m}$ (m=40-50) systems provide an array of novel systems for study.[6-9] This presentation will discuss recent results from our laboratory describing the preparation, properties, and reactions of large cage endohedral metallofullerenes. We will focus our presentation on the motional processes of the corresponding encapsulated metal clusters in these metallofullerenes.

[1] Stevenson, S.; Rice, G.; Glass, T.; Harich, K.;Cromer, F.; Jordan, M. R.; Craft, J.; Hadju, E.; Bible, R.; Olmstead, M. M.; Maltra, K.; Fisher, A. J.; Balch, A. L.;Dorn, H. C. *Nature* **1999** *401*, 55-57.

[2] Yang, S.; Dunsch, L. *Angewandte Chemie,International Edition* **2006** 45(8), 1299-1302.

[3] Beavers, C. M.; Zuo, T.; Duchamp, J. C.; Harich, K.; Dorn, H. C.; Olmstead, M. M.; Balch, A. L. *JACS* **2006** 128(35), 11352-11353.

[4] Zuo, T.; Beavers, C. M.; Duchamp, J. C.; Campbell, A.; Dorn, H. C.; Olmstead, M. M.; Balch, A. L. *JACS* **2007** 129(7), 2035-2043.

[5] Chaur, M. N.; Melin, F.; Ashby, J.; Elliott, B.; Kumbhar, A.; Rao, A. M.; Echegoyen, L. *Chemistry-A European Journal* **2008** 14(27), 8213-8219.

[6] Yang, H.; Lu, C.; Liu., Z.; Jin, H.; Che, Y.; Olmstead, M. M.; Balch, A. L. *JACS* **2008** 130(51), 17296-17300.

[7] Iiduka, Y.; Wakahara, T.; Nakahodo, T.; Tsuchiya, T.; Sakuraba, A. Maeda, Y.; Akasaka, T.; Yoza, K.; Horn, E.; Kato , T.; Liu, M. T. H.; Mizorogi, N.; Kobayashi, T.; Nagase, S. *J. Am. Chem. Soc.* **2005**, 127, 12500-12501.

[8] Shi, Z. Q. ; Wu, X.; Wang, C. R.; Lu, X.; Shinohara, H. *Angew. Chem. Int. Ed.* **2006,** 45, 2107-2111.

[9] Yamazaki, Y.; Nakajima, K.; Wakahara, T.; Tsuchiya, T.; Ishitsuka, M. O.; Maeda, Y.; Akasaka, T.; Waelchli, M.; Mizorogi, N.; Nagase, S. *Angew. Chem. Int. Ed.* **2008,** 47, 7905-7908.

Corresponding Author: Harry C. Dorn
TEL: 1-540-231-5953, FAX: 1-540-231-5385, E-mail: hdorn@vt.edu

3S-1

Synthesis and Applications of High-quality and Highly Oriented Graphite from Polyimide Films.

Mutsuaki Murakami

New Business Development Group and Frontier Materials Development Laboratories, KANEKA Corporation
5-1-1 Torikai-nishi, Settsu Osaka 566-0072, Japan

The method of making high-quality graphite by using the polymer as a raw material was developed for the first time by authors in 1986. [1] A high-temperature (3000℃) heat treatment of polyimide(PI) film with high molecular orientation (for example PMDA-ODA type PI) yielded a high quality graphite film, The hexagonal lattice formation of graphite depends on the heat treated temperature (HTT), and the orientation of the graphite layer preferentially proceeds from the surface of the film. [2] Various forms, such as a sheet, a large block, and bent block can be produced from thin polyimide films.

The graphite films composed of thin graphite layers with 6～7nm in thickness containing minute vesicles within the film were obtained, which yielded flexible graphite sheet with excellent physical and mechanical properties.[3] The sheet is promising in wide technical applications where light weight, flexibility, high purity and high electrical or thermal conductivity are required. Now, the film was widely used as a heat spreader for electronic devices such as a mobile phone.

High-quality and highly oriented graphite block having physical properties close to those of single-crystal graphite was produced from a thousand of PI films of 25μm thick. Graphite blocks as large as 150×50×13 mm^3 were prepared, and the mosaic spread (the degree of preferred orientation) attained was 0.4°. [4] The block is particularly suitable for making optical components for X-ray, neutron and SOR optics, such as monochromators and filters. In addition, we developed single-bent and double-bent graphite X-ray condenser devices, which enabled X-ray condensation by up to a factor of 10 times for a single-bent and about 220 times for a toroidal type condenser device. [5]

(References)

[1]M. Murakami, K. Watanabe, and S. Yoshimura, Appl. Phys. Lett., **48(23)**, 1594 (1986)

[2]N. Nishiki, H. Taka, K. Watanabe, M. Murakami, S. Yoshimura and K. Yoshino, IEE. J Trans. FM, **124**(9), 812(2004)

[3]N. Nishiki, H. Taka, M. Murakami, S. Yoshimura and K. Yoshino, IEE. J Trans. FM, **123**(11), 1116(2003)

[4]M. Murakami, N. Nishiki, K. Nakamura, J. Ehara, H. Okada, T. Kouzaki, K. Watanabe, T. Hoshi, and S. Yosimura. *Carbon* **30(2)**, 255 (1991).

[5] N.Nishiki, T.Kawashima, M. Murakami, S. Yoshimura, and K. Yoshino, IEEJ Trans. FM. 124(11), 1059(2004)

Corresponding Author: Mutsuaki Murakami
TEL: +81-80-240-18238, E-mail: Mutsuaki_murakami@kn.kaneka.co.jp

3S-2

Advances in Supergrowth - Growth, Application and Devices

Kenji Hata○

[1]*Nanotube Research Center, National Institute of Advanced Industrial Science and Technology (AIST), 1-1-1 Higashi, Tsukuba, Ibaraki 305-8565, Japan*

Abstract: Throughout the history of materials, synthesis had always played the limiting factor, and often a breakthrough in synthesis paved the way for breakthroughs in the entire field. The CVD concept has expanded by the addition of a almost background level of (100-200 ppm) water into the growth ambient of normal hydrocarbon CVD, which dramatically increased the growth efficiency to unprecedented levels Since the development of the water-assisted chemical vapor deposition in 2004 [1], we have extensively pursued the possibility of the synthesis, to understand the mechanism and kinetics [2-5], to expand the CVD world [6], to improve the yield, control the structure of nanotubes [7], developed post-growth process to develop various forms such as carbon nanotube solid [8], and nanotube wafers [9]. .
The SWNTs by the super-growth possess exceptional properties of high purity, high surface area, long length, and alignment. These properties has opened up new opportunities for CNTs, exemplified by CNT black body absorbers [10], light mechanical beams [11], stretchable conductors [12], high power and density super-capacitors, fast-moving, low-voltage actuators [14], and the possibility for mass production.

References: *[1] Science 2004, 306, 1362, [2] Phys. Rev. Lett.2005, 95, 5 056104-1,[3] Nano Lett. 2008, 8, 4288., [4] Nano Letters, 9 (2), 769-773 (2009), [5] ACS Nano, 3 (1), 108-114 (2009), [6] in print in Advanced Materials, [7] Nature Nanotechnology. 1, 131-136,(2006), [8] Nature Material. 5, 987-994,(2006), [9] Nature Nanotechnology. 3, 289-294 (2008), [10] Proceedings of the National Academy of Sciences, 106 (15), 6044-6047 (2009), [11] Physical Review Letters, 102, 175505 (2009), [12] Science, 321, 1468(2008), [13] Nature Materials, 8 (6), 494-499 (2009)*

Corresponding Author Kenji Hata
TEL: +81-29-861-4654, FAX: +81-29-861-4851, E-mail: kenji-hata@aist.go.jp

一般講演
General Lecture

1 – 1 ～ 1 – 19
2 – 1 ～ 2 – 17
3 – 1 ～ 3 – 13

1-1

Identifying the shape of graphene edge using G band Raman spectra

○K. Sasaki[1], T. Mori[2], K. Takai[2], T. Enoki[2], and K. Wakabayashi[1,3]

[1]*National Institute for Materials Science, Namiki, Tsukuba 305-0044, Japan*

[2]*Department of Chemistry, Tokyo Institute of Technology, Ookayama, Meguroku, Tokyo 152-8551, Japan*

[3]*PRESTO, Japan Science and Technology Agency, Kawaguchi 332-0012, Japan*

The physics near the edge of graphene has attracted much attention [1]. It is partly because of that the electronic properties depend strongly on the "chirality" of the hexagonal carbon lattice of the edge as well as that single wall nanotubes (SWNTs) exhibit either metallic or semiconducting behavior depending on the chirality of the tube. In fact, it has been predicted that the localized edge states appear near the zigzag edge, while they are absent near the armchair edge. Thus the characterization of the shape of edge of graphene is an important issue as well as the characterization of SWNTs.

Raman spectroscopy has been widely used for the characterization of SWNTs. In this presentation, we report on our theoretical and experimental studies of the G-band Raman spectroscopy near the edge of graphene. It is known that the G-band consists of the longitudinal optical (LO) and transverse optical (TO) phonon modes. We find that the TO (LO) mode is Raman active near the zigzag (armchair) edge, while it is not Raman active near the armchair (zigzag) edge. This is exactly the same as the chirality dependent G-band Raman intensity in SWNTs, [3] that is, for armchair (zigzag) SWNT, only the TO (LO) mode is Raman active. We also find that, regardless the shape of edge, the LO mode can undergo Kohn anomaly (KA) effect, [2] while the TO mode does not. KA makes the frequency of the LO mode down shift as compared with that of the TO mode. Thus, the G-band spectra near the zigzag edge consist only of the TO mode and appear above the G-band that is taken near the armchair edge, which is consistent with our experimental results. We consider that the G-band Raman spectra can be used to identify the shape of edge of graphene sample.

[1] Kosynkin *et al.*, Nature **458**, 872 (2009) ; Jiao *et al.*, Nature **458**, 877 (2009) ; Jia *et al.*, Science **323**, 1701 (2009) ; Girit *et al.*, Science **323**, 1705 (2009).

[2] Sasaki *et al.*, Phys. Rev. B **77**, 245441 (2008), ibid. **78**, 235405 (2008).

[3] Saito *et al.*, Phys. Rev. B **64**, 085312 (2001).

Corresponding Author: Ken-ichi Sasaki

TEL: +81-29-851-3354(Ex.8315), FAX: +81-29-860-4706, E-mail: SASAKI.Kenichi@nims.go.jp

1-2

Large reversible Li storage of Graphene Nanosheets

EunJoo Yoo[a], Jedeok Kim[b], Eiji Hosono[a], H.S. Zhou[a], Tetsuichi Kudo[a] and Itaru Honma[a]*

[a]Energy Technology Research Institute, National Institute of Advanced Industrial Science and Technology (AIST), Umezono 1-1-1, Central 2, Tsukuba, Ibaraki 305-8568 Japan
[b]Nano Ionics Mareials Group, National Institute of Materials Science (NIMS), Namiki 1-1, Tsukuba, Ibaraki 305-0044 Japan, e-mail: i.homma@aist.go.jp

Keywords: Graphene, Li storage, Lithium battery, anode materials

The lithium storage properties of graphene nanosheet (GNS) materials as high capacity anode materials for rechargeable lithium secondary batteries (LIB) were investigated. Graphite is a practical anode material used for LIB, because of its capability for reversible lithium ion intercalation in the layered crystals, and the structural similarities of GNS to graphite may provide another type of intercalation anode compound. While the accommodation of lithium in these layered compounds is influenced by the layer spacing between the graphene nanosheets, control of the inter-graphene sheet distance through interacting molecules such as carbon nanotubes (CNT) or fullerenes (C_{60}) might be crucial for enhancement of the storage capacity. The specific capacity of GNS was found to be 540 mAh/g, which is much larger than that of graphite, and this was increased up to 730 mAh/g and 784 mAh/g, respectively, by the incorporation of macromolecules of CNT and C_{60} to the GNS.

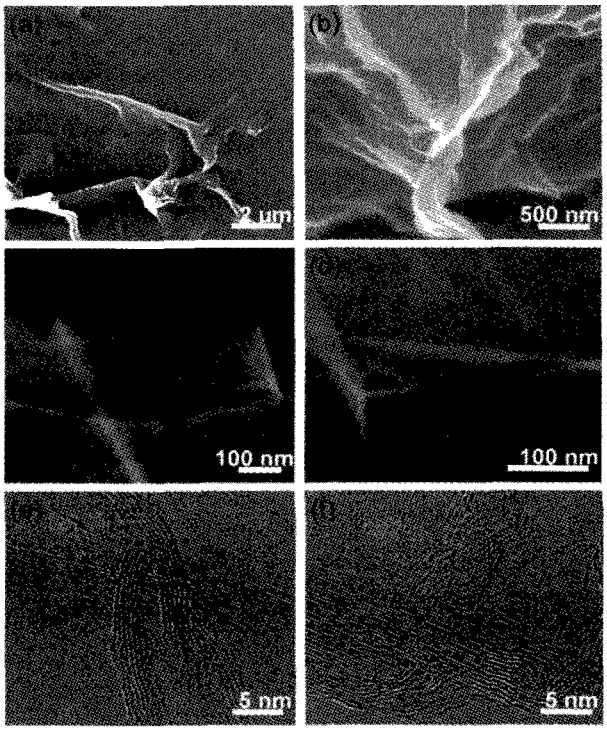

Fig.1 SEM and TEM observation of OGS and GNS. (a) and (b) SEM images of GNS. TEM images of (c) OGS, and (d) GNS. (e) and (f) Cross-sectional TEM images of GNS.

References

1. EunJoo Yoo, Jedeok Kim, Eiji Hosono, Hao-shen Zhou, Tetsuichi Kudo and Itaru Honma, Nano Letters, **8,** 2277 (2008).
2. Seung-Min Paek, EunJoo Yoo and Itaru Honma, Nano Letters, **9,** 72 (2009)

1-3

Fermi-Level Pinning at Metal-Graphene Interfaces

○Ryo Nouchi[1], Tatsuya Saito[2] and Katsumi Tanigaki[1,2]

[1]*WPI-Advanced Institute for Materials Research, Tohoku University, Sendai 980-8577, Japan*
[2]*Department of Physics, Tohoku University, Sendai 980-8578, Japan*

Graphene, one-atom-thick carbon sheet with a honeycomb structure, have been attracting incredible attention for its unique physical properties such as a massless Dirac fermion system [1]. This material shows an extraordinary high charge carrier mobility of higher than 200,000 $cm^2 V^{-1} s^{-1}$ [2], and is considered to be a major candidate for a future high-speed transistor material. In addition, graphene has shown its ability to transport charge carriers with spin conservation even at room temperature, and is regarded as a pivotal material in the emerging field of molecular spintronics [3]. In order to construct such electronic devices, metallic materials should make a contact with the graphene layers. We have studied the effect of such metal contacts to transfer (drain current, I_D, versus gate voltage, V_G) characteristics of graphene field-effect transistors (FETs).

Graphene layers were formed onto a highly-doped Si substrate with a 300-nm-thick thermal oxide layer on top of it by a conventional mechanical exfoliation from a bulk graphite crystal [4]. These layers were determined to be single layer graphene from the optical contrast. Metal electrodes were fabricated onto the graphene layers by electron beam lithography and lift-off techniques. While graphene devices with inert metals (e.g. Au) displayed conventional transfer characteristics, those with more reactive metals (e.g. ferromagnetic metals) showed anomalous distorted characteristics as is displayed in Fig. 1 [5]. Simulated transfer characteristics that assume a simple diffusive transport exhibit such distortion if Fermi-level pinning at the metal-graphene interfaces is excluded [6]. Ordinary Ti/Au contacts have been found to pin the Fermi level of graphene [7]. Our results indicate a possible *depinning* of Fermi level at the ferromagnet-graphene interfaces.

[1] A. H. Castro Neto, F. Guinea, N. M. R. Peres, K. S. Novoselov and A. K. Geim, *Rev. Mod. Phys.* **81**, 109 (2009).

[2] K. I. Bolotin, K. J. Sikes, Z. Jiang, M. Klima, G. Fudenberg, J. Hone, P. Kim and H. L. Stormer, *Solid State Comm.* **146**, 351 (2008).

[3] M. Ohishi, M. Shiraishi, R. Nouchi, T. Nozaki, T. Shinjo and Y. Suzuki, *Jpn. J. Appl. Phys.* **46**, L605 (2007).

[4] K. S. Novoselov, D. Jiang, F. Schedin, T. J. Booth, V. V. Khotkevich, S. V. Morozov and A. K. Geim, *Proc. Natl. Acad. Sci. USA* **102**, 10451 (2005).

[5] R. Nouchi, M. Shiraishi and Y. Suzuki, *Appl. Phys. Lett.* **93**, 152104 (2008).

[6] R. Nouchi, T. Saito and K. Tanigaki, *in preparation*.

[7] E. J. H. Lee, K. Balasubramanian, R. T. Weitz, M. Burghard and K. Kern, *Nat. nanotechnol.* **3**, 486 (2008).

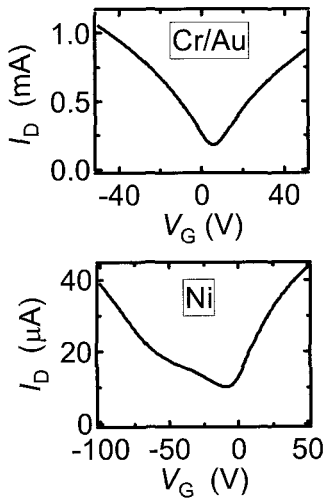

Fig.1 Transfer characteristics of graphene FETs with (top) Cr/Au and (bottom) Ni source/drain electrodes. The distances between the electrodes were around 4 μm.

Corresponding Author: Ryo Nouchi
TEL: +81-22-795-6468, FAX: +81-22-795-6470, E-mail: nouchi@sspns.phys.tohoku.ac.jp

1-4

Hydrazine and Thermal Reduction of Graphene Oxide: Reaction Mechanisms and Design

Xingfa Gao and Shigeru Nagase

Department of Theoretical and Computational Molecular Science, Institute for Molecular Science, Myodaiji, Okazaki 444-8585, Japan

For decades, researchers have been attempting to develop materials that are cheap and capable of broad applications. Recent studies have established that graphene is a promising candidate of such material, provided that its large-scale synthesis is reliazed.[1] So far, it is still a challenge to produce high-quality graphene in large scale. Several methods have been used in laboratory to generate graphene and graphene derivatives, each with advantages and shortcomings.[2] Among them, the chemical reduction of graphene oxide (GO) is noticeable for intriguing merits: being cheap and easily scalable to high-volume production, and in particular, such solution-based approach being well suited to chemical modification and other subsequent processing.[2] As a result, reducing GO has been widely applied in experiments to obtain chemically converted graphene (CCG) for device applications. Optimizations of the reaction conditions have shown that the reduction via hydrazine and thermal treatment gives rise to the best efficiency of deoxygenation.

However, CCG obtained from the chemical reduction of GO is recognized to differ considerably from defect-free graphene. CCG contains, apart from structural disorder and defects inherited from the pristine GO, a marked amount of residual oxygen functionalities. In the case of hydrazine reduction, CCG also contains a marked amount of nitrogen-containing groups. As a result of CCG's amorphous nature, experimental characterizations of CCG's detailed structures have been severely suspended. Consequently, to date, little has been know about reduction process of GO at the atomic level. "*Understanding of the structure(s) of CMG sheets and their reaction mechanisms*" has become a "*critical issue*" for making better graphene-based functional materials via the chemical reduction route.[2]

Using density functional theory method, we study reactions of GO's oxygen functionalities—epoxide, hydroxyl, carbonyl, and carboxyl—in the conditions of hydrazine and heat treatments. We answer the questions portrayed in the right figure. GO fragments with various sizes are adopted in the study to model the structures of amorphous GO. Our results provide an atomic-leveled understanding for GO's reduction, and give suggestions on how to further optimize the reaction conditions.

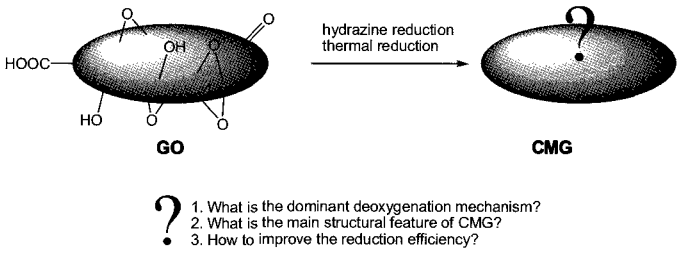

References:

1. Service R. F. *Science* **2009**, *324*, 875.
2. Park, S.; Ruoff, R. S. *Nat. Nanotechnol.* **2009**, *4*, 217 and references therein.
3. Gao X.; Zhou Z.; Zhao Y.; Nagase S.; Zhang S. B.; Chen Z. *J. Phys. Chem. C* **2008**, *112*, 12677.
4. Gao, X; Wang, L.; Ohtsuka, Y.; Jiang, D.-E.; Zhao, Y.; Nagase, S.; Chen, Z. *J. Am. Chem. Soc.* **2009**, doi: 10.1021/ja902878w.

1-5

Catalytic Growth of Graphene over Epitaxial Metal Film

○Hiroki Ago,[*,1,2,3] Izumi Tanaka,[1] Masaharu Tsuji,[1,2] and Ken-ichi Ikeda[2]

[1] *Institute for Materials Chemistry and Engineering, Kyushu University*
[2] *Graduate School of Engineering Sciences, Kyushu University, Fukuoka 816-8580, Japan*
[3] *PRESTO, Japan Science and Technology Agency*

Graphene is emerging as a new building block of future nanoelectronics and microelectro-mechanical systems. Catalytic growth has attracted recent interest as a powerful means to produce highly crystalline large-area graphene sheets [1-3]. In addition, studies on the catalytic growth of graphene are expected to give new insights in the growth of single-walled carbon nanotubes (SWNTs), which may stimulate further control of the SWNT structure.

The catalytically-grown graphene films are usually not uniform, because the employed catalyst films are polycrystalline [1,2]. On the other hand, the growth on single crystal substrates, such as Ni (111) [4], Ir (111) [5], and Ru (0001) [6], are very expensive, and thus not practical for electronic applications.

In this study, we investigated the growth of graphene films over the epitaxial Co or Ni metal films deposited on single crystalline substrates. The Co (or Ni) metal films were epitaxially deposited on single crystalline substrates as revealed by X-ray diffraction (XRD) and electron backscatter diffraction (EBSD) measurements. We found that the epitaxial metal films gave unique micro-pits having square or triangular shape, depending on the crystallographic orientation of the substrate. Interestingly, thin films of graphene were preferentially formed inside these pits. The graphene film was transferred onto a SiO_2/Si substrate, and the Raman spectra and AFM data confirmed the formation of a few layers (1-5 layers) of graphene.

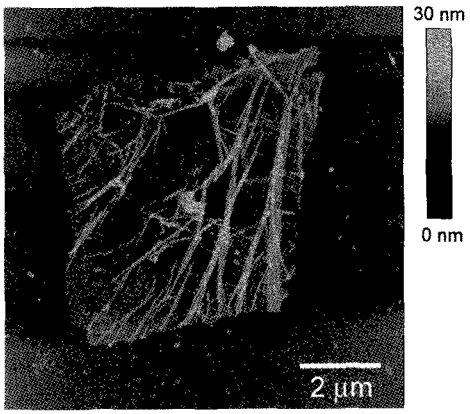

Figure 1. AFM image of the square shaped graphene film transferred onto a SiO_2/Si substrate. The thickness of this film is around 1.3 nm.

References

[1] A. Reina *et al.*, *NanoLett.*, **9**, 30 (2009). [2] K. S. Kim *et al.*, *Nature*, **457**, 706 (2009). [3] X. Li *et al.*, *Science*, **324**, 1312 (2009). [4] Y. Gamo *et al.*, *Surf. Sci.*, **374**, 61 (1997). [5] A. T. N'Diaye *et al.*, *Phys. Rev. Lett.*, **97**, 215501 (2006). [6] P. T. Sutter *et al.*, *Nature*, **7**, 406 (2008).

Corresponding Author: Hiroki Ago (Tel&Fax: +81-92-583-7817, E-mail: ago@cm.kyushu-u.ac.jp)

1-6

Graphene Chain as a Long Distance Ballistic Heat Conductor

○Koji Takahashi[1], Yohei Ito[1], Tatsuya Ikuta[1], Xing Zhang[2], Motoo Fujii[3]

[1]*Department of Aeronautics and Astronautics, Kyushu University, Fukuoka 819-0395, Japan*
[2]*Institute of Engineering Thermophysics, Tsinghua University, Beijing 100084, China*
[3]*AIST, Fukuoka 819-0395, Japan*

A potential to conduct heat ballistically over a long distance has been discovered for a fibrous nanomaterial, named as cup-stacked carbon nanofiber. This fiber consists of a stacked graphene cups and its longitudinal heat transport ability had been forecast to be extremely poor due to the weak van der Waals force operating between the cups. However our measurements of individual nanofiber samples [1] showed that its thermal conductivity is much higher than that along the c-axis of bulk graphite, and is even higher than that of a single-crystal silicon wire of the same characteristic size. This unexpected result can be understood by its similarity to the one-dimensional harmonic-chain where no phonon is scattered even for an infinite length [2]. The current graphene-based nanofiber resembles this type of super-thermal-conductive chain due to the huge difference between the stiff covalent bonding in each cup and the weak inter-cup interaction. In other words, the effect of the three-dimensionality of this size is negligible for heat conduction and highly-ballistic phonon transport can occur in this fiber. In order to validate this hypothesis, a non-equilibrium molecular dynamics simulation was also conducted. Numerical results revealed a uniform temperature distribution in the intermediate cups between hot and cold reservoirs, which means that the phonon scattering there is very few. Further analysis on atomic and cup motions in this graphene chain suggest that its heat conduction is mainly caused by the longitudinal vibration and other phonon modes have weak effects. Though the computational task of MD simulation limits the cup number in our calculation, obtained data of up to 8 cups made it clear that this graphene chain has the highest similarity to the ballistic 1D harmonic chain in the existing real materials. The findings we report here should pave the way for the construction of a new phonon wave guide with the highest ever thermal conductivity via future improvements of the synthesis technology.

[1] M. Fujii, X. Zhang, H. Xie, H. Ago, K. Takahashi, T. Ikuta, H. Abe and T. Shimizu, Phys. Rev. Lett. **95** 065502 (2005).
[2] R. Livi and S. Lepri, Nature **421**, 327 (2003).

Corresponding Author: Koji Takahashi
TEL: +81-92-802-3015, FAX: +81-92-802-3017, E-mail: takahashi@aero.kyushu-u.ac.jp

1-7

Phase transition of water inside large-diameter SWCNTs

○Kazuyuki Matsuda[1], Hitomi Yahiro[1], Haruka Kyakuno[1],Tomoko Fukuoka[1], Kazuhiro Yanagi[1,4], Yutaka Maniwa[1,4]Takeshi Saito[2], Satoshi Ohshima[2], Motoo Yumura[2], Sumio Iijima[2], Yasumitu Miyata[3], and Hiromichi Kataura[3,4]

[1] *Faculty of Science, Tokyo Metropolitan University, 1-1 Minami-osawa, Hachioji, Tokyo 192-0397, Japan*

[2] *Research Center for Advanced Carbon Materials, National Institute of Advanced Industrial Science and Technology (AIST), Tsukuba 305-8565, Japan*

[3] *Nanotechnology Research Institute, National Institute of Advanced Industrial Science and Technology (AIST), Central 4, Higashi 1-1-1, Tsukuba, Ibaraki 305-8562, Japan*

[4] *JST, CREST, Kawaguchi, 332-0012, Japan*

Single-walled carbon nanotubes (SWCNTs) encapsulate many kinds of materials in their inner hollow cavities. Materials confined in such small cavities are expected to show novel features that are not observed in bulk materials. In previous works [1-3], it has been revealed that water confined inside SWCNTs with diameters (D) below ~1.5nm arranges in tubule structures so-called ice nanotubes (ice-NTs) at low temperatures. The melting temperature (T_m) of the ice-NTs decreases with increasing the SWCNT diameter. Here, we have investigated phase transition behavior of water confined inside large-diameter SWCNTs with D=1.6~2.4 nm by means of x-ray diffraction and ^{1}H,^{2}H-NMR. The obtained phase diagram of water confined inside SWCNT as a function of D is shown in Fig. 1. As for the large diameter-SWCNTs, it was found that the T_m substantially deviates from T_m vs D curve of ice-NT formed inside the small-diameter SWCNTs with D<~1.5 nm. Instead, it seems to follow a variation of the Kelvin equation ($273-T_m \propto 1/D$) for the depression of T_m in capillary. This suggests that a crossover from microscopic to macroscopic phenomena occurs at D_C ~1.5 nm. The details will be presented in the conference.

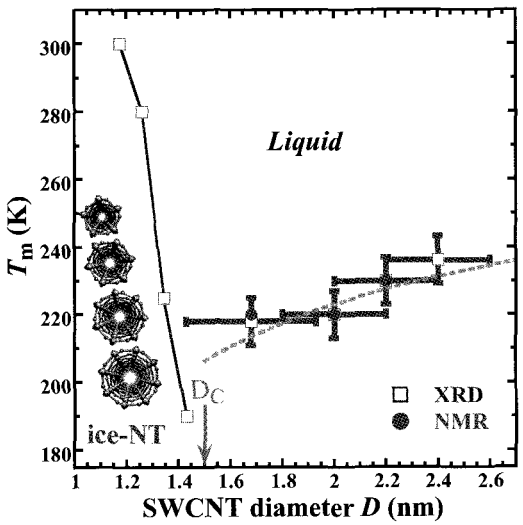

Fig. 1. Phase diagram of water in single-walled carbon nanotubes.

[1] K. Koga et al., Nature 412, 802-805 (2001).

[2] Y. Maniwa et al., Chem. Phys. Lett. 401, 534-538 (2005).

[3] K. Matsuda et al., Phys. Rev. B 74, 073415 (2006).

Corresponding Author: Kazuyuki Matsuda

E-mail: matsuda@phys.metro-u.ac.jp, TEL: +81-426-77-2498, FAX +81-426-77-2483

1-8

Photo-Induced Formation of Polyyne-Iodine Complex in Solution

○Yoriko Wada[1], Osada Ryouichi[2], Yasunori Kai[2], Tomonari Wakabayashi[1]*, Tatsuhisa Kato[2]*

[1]*Department of Chemistry, Kinki University, Higashi-Osaka 577-8502, Japan*
[2]*Department of Chemistry, Josai University, Sakado, Saitama 350-0295, Japan*

Polyynes, $H(C{\equiv}C)_nH$ ($n{\geq}2$), are sp-hybridized carbon chain molecules with two hydrogen atoms at both ends. Those molecules exhibit electric-dipole allowed transitions in the UV and forbidden transitions in the near UV. In the present work, we found that, by adding I_2 molecules into a solution of polyyne, the intensity of absorption bands in the UV decreased and those in the near UV increased. This observation suggests that polyyne and iodine form a stable complex in solution.

We found that the reaction was promoted by irradiation with visible light. Figure 1 shows time profile for the intensity of the UV absorption band of $C_{10}H_2$ at 252 nm following mixing of iodine with polyyne in a solution. Open circles correspond to the condition with photo-irradiation, while closed circles without irradiation. The absorption intensity was decreasing only in the period under irradiation. On the other hand, the absorption intensity at 252 nm was constant under the condition without photo-irradiation. This result clearly suggests that the formation of polyyne-iodine complex is induced by photo-irradiation.

Polyyne/iodine solution was photo-irradiated at selected wavelengths to clarify the relationship between the photo-induced reaction and the wavelength. Figure 2 shows the intensity for the UV absorption band at 252 nm during irradiation of selected wavelengths using long-pass filters. This result suggests that formation of polyyne-iodine complexes was followed by absorption of visible light (440-640 nm) by iodine molecules.

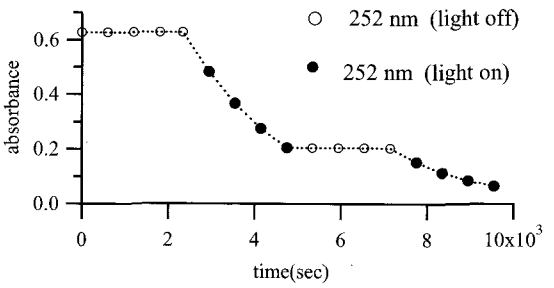

Figure 1. Absorbance of $C_{10}H_2/I_2$ solution at 252 nm with (●) and without (○) light irradiation.

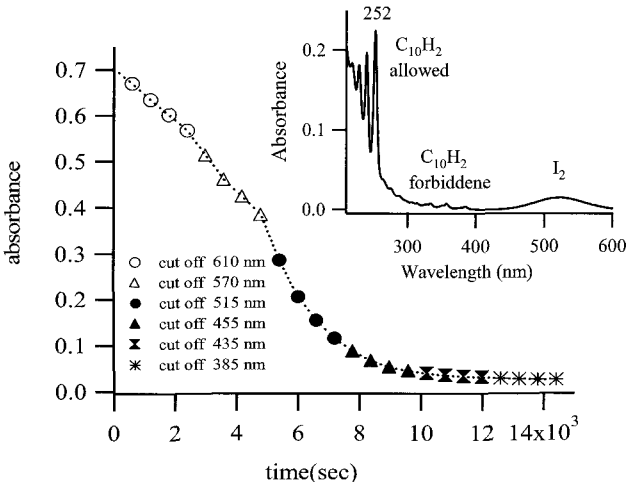

Figure 2. Absorbance of $C_{10}H_2/I_2$ solution at 252 nm after during light irradiation. Inset shows spectrum of $C_{10}H_2/I_2$ solution.

Corresponding Author: Tomonari Wakabayashi
E-mail: Wakaba@chem.kindai.ac.jp
Tel: 06-6730-5880 (ex.4101) / Fax 06-6723-2721

1-9

Biodistibution and Ultrastructural Localization of Single-walled Carbon Nanohorns Determined *In Vivo* with Embedded Gd_2O_3 Labels

Jin Miyawaki,[†,¶], Sachiko Matsumura,[†,‡,¶] Ryota Yuge,[§] Tatsuya Murakami,[⊥,$] Shigeo Sato,[‡] Akihiro Tomida,[‡] Takashi Tsuruo,[‡] Toshinai Ichihashi[§], Takako Fujinami[‖], Hiroshi Irie,[#] Kunihiro Tsuchida,[⊥] Sumio Iijima,[†,§,‖] Kiyotaka Shiba,[‡,*] ○Masako Yudasaka,[†,§,‖,*]

[†] *Japan-Science and Technology Agency.* [‡] *Japanese Foundation for Cancer Research, 3-10-6 Ariake, Koto-ku, Tokyo 135-8550.* [§] *NEC, 34 Miyukigaoka, Tsukuba 305-8501.* [⊥] *Fujita Health University, Toyoake, Aichi, 470-1192.* [#] *Teikyo University School of Medicine, 2-11-1 Kaga, Itabashi-ku, Tokyo 173-8605.* [‖] *National Institute of Advanced Industrial Science and Technology, Central 5, 1-1-1 Higashi, Tsukuba, 305-8565.*

[¶] *J. Miyawaki and S. Matsumura equally contributed to this research.*
[$] *Current address: J. Miyawaki, Institute for Materials Chemistry and Engineering, Kyushu University.; T. Murakami, Institute for Integrated Cell-Material Sciences (iCeMS), Kyoto University.*

We have been reported that single-walled carbon nanohorns (SWNHs) have high potential in application to drug delivery system (DDS). For the further study toward the practical applications, we need to clarify biodistribution and ultrastructural localization of SWNHs *in vivo*, which enables researches of appropriate sizes and chemical modifications of SWNHs for DDS. For these measurements and observation, we used Gd_2O_3 nanoparticles as labels that were embedded in the SWNH aggregate (Gd_2O_3@SWNHag).

Gd_2O_3@SWNH was prepared by heating the Gd acetate incorporated SWNH at 1200°C in Ar [1]. The dispersion of Gd_2O_3@SWNH in glucose solution was intravenously injected from the mice tails, and the quantities of Gd in the internal organs were measured by inductively-coupled plasma atomic emission spectroscopy. The results showed that 70 to 80% of the total injected was accumulated in livers. Since Gd has high electron scattering ability and can be confirmed with energy dispersive X-ray spectroscopy, ultrastructural localization of individual Gd_2O_3@SWNH with transmission electron microscopy was easy. In the liver, they were localized in the Kupffer cells. In the Kupffer celss, most of the Gd_2O_3@SWNHs existed inside the phagosomes, and some were in another cytoplasm, which is likely to be phagolysosomes. According to these results, Gd_2O_3 is the excellent label, and will be useful to study the influence of the size and chemical modification of SWNHs on the biodistribution.

References:

[1] Yuge et al. J. Phys. Chem. C **2009**, *113*, 2741-2744.

[2] Miyawaki, Matsumura et al. ACS Nano 2009.*3*,1399-1406

Corresponding Authors: K. Shiba (kshiba@jfcr.co.jp) and M. Yudasaka (m-yudasaka@aist.go.jp)

1-10

The role of cap structure formation on the chirality selective formation of single- walled carbon nanotubes

○Yohji Achiba[1)], Akihito Inoue, Naoko Takamizu[1)], Takeshi Kodama[1)] and Toshiya Okazaki[2)]

1) Department of Chemistry, Tokyo Metropolitan University, Minami-Osawa 1-1, Hachioji, 192-0397 Tokyo Japan

2) Advanced Industrial Science and Technology (AIST), Tsukuba 305-8565, Ibaragi, Japan

The control of chirality distribution of single-walled carbon nanotubes is undoubtedly one of the most important issues from the view points both basic science and applied technology of the carbon nanotubes. Particularly, in aid of future applications to very fine industrial products such as electronic, optoelectronics and bio-electronic devices, it is strongly required to prepare the sample with chirality-pure and no structural defects. In order to overcome the difficulty in developing a production method by which the sample is prepared as the one consisting of very limited numbers of chiral species or of single chirality species, it is desirable to obtain further understanding of the growth process of single-walled carbon nanotubes in detail.

In the present paper, on the basis of experimental results revealed by both CVD and laser vaporization methods, we will demonstrate how atmospheric temperature difference or catalyst change gives significant effect on the size and chirality distribution of single-walled carbon nanotubes and we will discuss such a significant effect on the production of SWNTs in terms of cap structure formation in the very early stage of the growth process.

The carbon nanotubes were prepared by the following two methods; alcohol CVD with Pt catalyst embedded on the porous glass and laser vaporization with the catalyst of Ni/Co or Rh/Pd. In order to understand the size and chirality distribution of the sample, all the samples were characterized by the following optical measurement procedures: 1) Resonance Raman scattering measurements were carried out for the sample as prepared form with use of two laser lines, 488nm and 633nm. 2) The crude sample was dispersed in solution by the conventional procedures described elsewhere; homozinization, sonication and centrifugation and SDBS or PFO polymer as surfactants. 3) Optical measurements in solution were carried out by conventional absorption and photoluminescence spectroscopy.

One of the significant aspects deduced by the present experiments is that selective production of near arm-chair chirality is very much pronounced under the extreme condition such as low temperature and low pressure condition in the CVD experiments and rapid cooling condition of ablated species in the laser vaporization. All these experimental evidence strongly suggests that the pentagon-hexagon cap structures formed in the very early growth stage play a role on determining size and chiral distribution of the nanotubes.

Corresponding Author Yohji Achiba
E-mail Achiba-yohji@tmu.ac.jp
Tel&Fax 042-677-2534 and 042-677-2525

1-11

General Rules Governing the Highly Efficient Growth of Carbon Nanotubes

○ Don N. Futaba[1], Jundai Gotou[1], Satoshi Yasuda[1], Takeo Yamada[1], Motoo Yumura[1], and Kenji Hata[1,2]

[1]*National Institute of Advanced Industrial Science and Technology (AIST), Tsukuba, 305-8565, Japan*
[2]*Japan Science and Technology Agency (JST), Kawaguchi, 332-0012, Japan*

In water-assisted chemical vapor deposition (CVD), the addition of a growth enhancer, e.g. water, to the ambient of normal hydrocarbon CVD dramatically improved growth efficiency resulting in vertically aligned forests [1]. Here, we present a generalized picture of water-assisted chemical vapor deposition (Super-growth) by demonstrating that highly efficient growth of carbon nanotubes (CNTs) is possible using, essentially, a countless number of growth enhancers, e.g. alcohols, ethers, esters, ketones, aldehydes, and even carbon dioxide [2]. Importantly, we uncovered the general rules governing the highly efficient growth of carbon nanotubes and the fundamental reasons from which they arose. Specifically, we found that the key for highly efficient growth is to include two essential ingredients in the growth ambient: a carbon source not containing oxygen and a minute quantity of a secondary gas, i.e. growth enhancer, containing oxygen. Exclusively for all combinations of carbon sources and growth enhancers following these rules, we could achieve highly efficient growth.

References:

[1] K. Hata *et al*, Science, **306**, 1241 (2004).

[2] D. N. Futaba *et al*, Adv. Mater *(in press)*.

Corresponding Author: Don N. Futaba

TEL: (029) 861-44402, FAX: (029) 861-4851, E-mail: d-futaba@aist.go.jp

1-12

High Rate Growth of Long Vertically Aligned Single-Walled Carbon Nanotubes by Remote Plasma in Low Pressure Beyond the Atmospheric Pressure Synthesis

○Ryogo Kato, Hiroshi Kawarada

School of Science and Engineering, Waseda university, Tokyo 169-8555, Japan

We have succeeded in enhancing the growth rate of SWNTs without sacrificing catalyst conversion ability in a remote plasma deposition. Normally SWNT length was been limited to 2-3 mm because of catalyst life time. In this work the SWNTs growth rate at 60 Torr in a remote plasma increases to 3mm/h, which is 10 times higher in the SWNTs growth rate (270μm/h)[1] at lower pressure (20Torr) in the same remote plasma and is comparable with the growth rate of SWNTs by the water-assisted synthesis method at the atmospheric pressure [2] We have achieved the enhanced growth rate of SWNTs by raising microwave power and total gas pressure up to 60 Torr. The maximum length of SWNTs is 5mm after 2.5 h deposition and can be extended to centimeters because the catalyst particles preserving high conversion ability[3,4] because water vpaour has not been introduced.

Si substrates are coated with a sandwich-like structure Al2O3 /Fe /Al2O3 (/Si). Al2O3 between Si and Fe is a buffer layer to suppress the interdiffusion On the other hand, Al2O3 above the Fe film works as a barrier of the surface diffusion of catalytic atoms so that the aggregation of Fe atoms can be controlled during the pre-heating time. As a result, high dense catalytic particles can be formed and extremely dense and vertically aligned SWNTs can be synthesized. The substrate was heated up to 690°C within a few minutues by an induction heater to form catalytic nanoparticles, and then plasma was turned on in a gas mixture of H2 and CH4 for the growth of SWNTs. The microwave power and total gas pressure were 120W and 60Torr, respectively. We can control the diameter and layer number of CNTs by adjusting thickness of Fe films and Al2O3 films. Specifically, SWNTs are grown at below 0.5 nm in Fe film thickness. From the result of Raman spectroscopy of as-grown vertically aligned SWNTs(Fe film thickness 0.2-0.5nm), our SWNTs have diameters of 0.8-1.2nm and High G- to D-peak ratio which indicates the high quality of our SWNTs despite high growth rate synthesis.

[1] G. Zhong, H.Kawarada et al., Jpn. J. Appl. Phys., 44, 1558 (2005).[2] D.Futaba, K. Hata et al., PRL 95,056104 (2005).[3] G. Zhong, H.Kawarada et al., J. Phys. Chem. B, 111, 1907 (2007).[4] T. Iwasaki, H.Kawarada et al., Nano Lett. 8, 886 (2008).

Corresponding Author: H.Kawarada E-mail :kawarada@waseda.ac.jp Tel&Fax: +81-3-5286-3391

1-13

Catalytic Effects of Alkali Metal Chlorides on Thermal Oxidation of Single-Walled Carbon Nanotubes

Yuki Kobayashi and Masahito Sano

Department of Polymer Science and Engineering, Yamagata University, Yonezawa, Yamagata 992-8510, Japan

Many chemical reactions involving single-walled carbon nanotubes (SWCNTs) are dependent on diameter, defect, and bundling. There are numerous reports on the diameter dependence on oxidation using thin SWCNTs with the consistent result that the smaller diameter tubes are oxidized faster. This is explained by the increasing strain on carbon bonds as the tube diameter decreases for thin SWCNTs. Defects are often terminated by various oxide groups and have an effect of localizing electrons. They can initiate or promote organic reactions, with a consequence that SWCNTs with more defects tend to be more reactive. Due to close packed structures of tubes in bundles, reactant molecules cannot access tubes inside bundles unless they are very small. As a result, bundling tend to lower the reactivity as a whole. In this study, we report an exception to these ordinary characteristics. Alkali metal chlorides act as catalysts in thermal oxidation of SWCNTs.

A typical TGA graph is shown in Figure 1. The combustion temperature of the acid-treated SWCNTs is lowered more than 100 °C by the presence of NaCl. Raman spectroscopy shows that, while D-band and BWF shoulder increases relative to G-band as oxidation proceeds for the acid-treated SWCNTs, relative intensities of all three remains the same for SWCNTs with NaCl. This indicates that either defects are oxidized as fast as they are produced or the oxidation has not created any new defects. RBM peaks of the acid-treated SWCNTs tend to show the faster disappearance of smaller diameter tubes as already reported by many others. Relative peak intensities of SWCNTs with NaCl, however, have no such regularity and fluctuate randomly. Consistent with these results, SEM reveals no significant deposition of ashes with NaCl, in contrast with significant deposition in oxidation of pure SWCNTs. NaCl promotes "clean burning" of SWCNTs. On the other hands, O_{1s} and C_{1s} peaks of XPS indicate no strong interaction between SWCNTs and NaCl. Thus, NaCl act as a catalyst in thermal oxidation of SWCNTs.

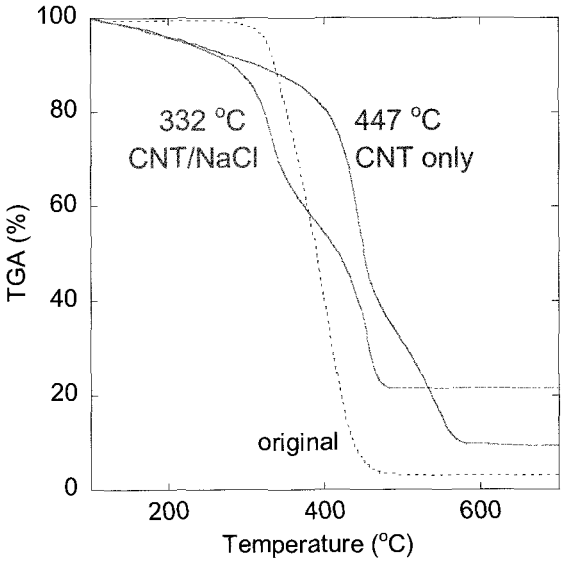

Figure 1. TGA curves of the original, the acid-treated, and the salted SWCNTs. Due to bundling, not all tubes in the salted sample are covered by NaCl.

Corresponding Author: Masahito Sano
TEL: +81-238-26-3072, FAX: +81-238-26-3072, E-mail: mass@yz.yamagata-u.ac.jp

1-14

Optical Spectroscopy of (6,5) Carbon Nanotubes Sorted by Density Gradient Ultracentrifugation

○Pei Zhao[1], Yoichi Murakami[2], Rong Xiang[1], Erik Einarsson[1], Junichiro Shiomi[1], Shigeo Maruyama[1]

[1]*Department of Mechanical Engineering, The University of Tokyo*
[2]*Global Edge Institute, Tokyo Institute of Technology*

We present a protocol to selectively isolate single-walled carbon nanotubes (SWNTs) with a chirality of (6,5) using density gradient ultracentrifugation (DGU)[1]. Starting with SWNTs synthesized by the alcohol catalytic chemical vapor deposition (ACCVD) method, we used sodium deoxycholate (DOC), sodium dodecyl sulfate (SDS) and sodium cholate (SC) as co-surfactant encapsulating agents[2] to isolate (6,5) SWNTs. In addition to observation by transmission electron microscopy (TEM), the high purity of (6,5) SWNTs was shown by various spectroscopic methods, such as optical absorbance, photoluminescence excitation (PLE), and resonance Raman spectra (RRS, 488 nm laser excitation) . Evaluation before and after DGU process revealed that the resulting sample contained a high concentration of (6,5) SWNTs, but other chiralities were also present at low concentrations. Unlike previous studies[1] using CoMoCAT SWNTs—of which (6,5) SWNTs are known to be one of the dominant chiral species—this effective extraction of a minority fraction of the pristine sample clearly shows the efficient chirality-selection by this dispersion process, without the existence of metallic nanotubes. This illustrates the potential for complete isolation, which we hope to achieve by further refinement of this process.

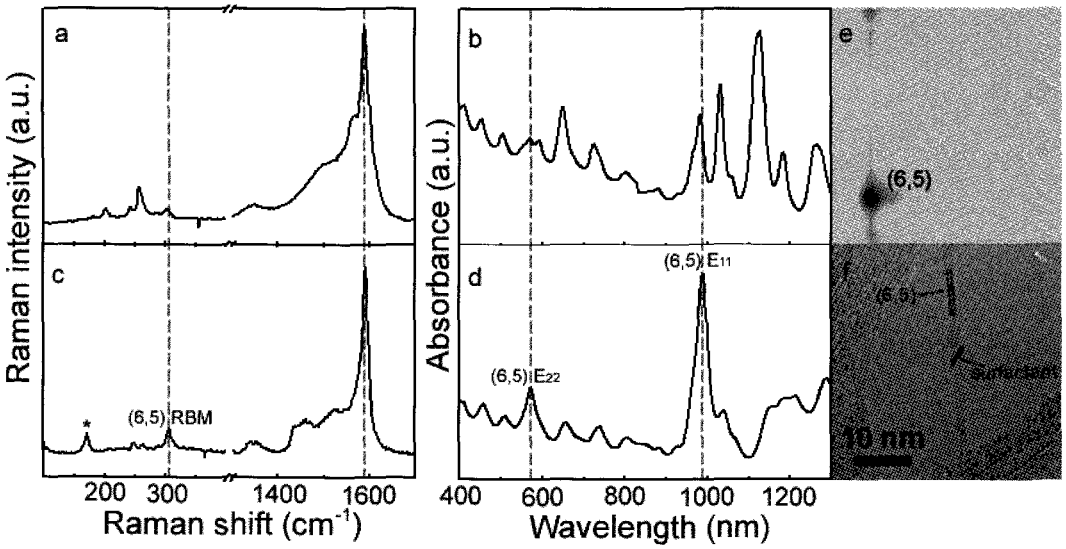

Figure 1: Optical spectroscopy showing the selective isolation of (6,5) SWNTs from ACCVD SWNTs by density gradient ultracentrifugation. (a) Resonance Raman spectra (b) Optical absorbance of pristine ACCVD SWNTs; (c) Resonance Raman spectra (d) Optical absorbance (e) Photoluminescence excitation map (f) TEM image of isolated (6,5) SWNTs after DGU process.

[1] M. Arnold, A. Green, J. Hulvat, S. Stupp and M. Hersam. *Nat. Nanotechnol.* **1**, 60 (2006)
[2] K.Yanagi, Y. Miyata and H.Kataura, *Appl. Phys. Express* **1**, 034003 (2008)

Corresponding Author: Shigeo Maruyama
TEL: +81-3-5841-6421, FAX: +81-3-5841-6983, E-mail: maruyama@photon.t.u-tokyo.ac.jp

1-15

Metallic-semiconducting separation of single-walled carbon nanotubes by using free-flow electrophoresis

○Kazuki Ihara*, Kiyohiko Toyama, Hiroyuki Endoh, and Fumiyuki Nihey*

Nano Electronics Res. Labs., NEC Corp., Tsukuba 305-8501, Japan

Since the single-walled carbon nanotube (SWCNT) was discovered, it has attracted much attention as a novel electrical material because of its excellent properties such as mechanical stability, chemical stability, and high conductivity [1]. Carbon-nanotube field effect transistors (CNT-FETs) have been widely studied because of their very high mobility and remarkably large current capacity. However, there is a brick wall for applying the electronic devices because as-produced material contains both metallic and semiconducting SWCNTs at a statistical ratio of 1:2.

We have investigated a novel method for separating metallic and semiconducting SWCNTs by using free-flow electrophoresis. Both the buoyancy of SWNT-micelles and electrophoretic force were utilized for the separation. We confirmed that metallic-semiconducting separation of HiPCO SWCNTs was successful by performing UV-vis-NIR absorption spectroscopy and Raman spectroscopy measurements.

Figure 1 plots UV-vis-NIR absorbance spectra of pristine (P), fractionated samples from anode (A) and cathode (C) regions. The intensity of the peaks in the range of 2-3 eV was suppressed for Sample A. On the other hand, the peaks were emphasized for Sample C. Because these peaks originated from the absorption of metallic SWCNT for HiPCO, this result suggests that semiconducting and metallic SWCNTs were respectively condensed in the anode and cathode regions.

Figure 2 plots Raman spectra in the radial breathing mode region excited by a 488-nm laser. Peaks at 245, 260, and 305 cm^{-1}, assigned as metallic, were totally suppressed on the anode side. This result supports the results of UV-vis-NIR absorbance spectra.

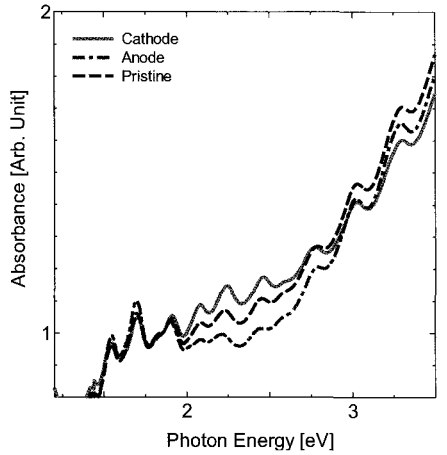

Fig. 1 UV-vis-NIR absorption spectra of pristine, fractionated samples from anode and cathode regions

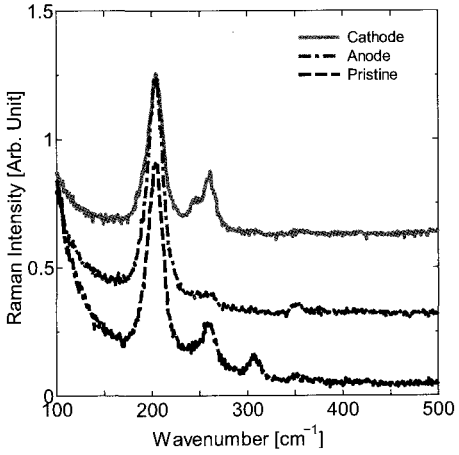

Fig. 2 Raman spectra of pristine, fractionated samples from anode and cathode regions

References: [1] Saito, R. *et al.*, *Appl. Phys. Lett.* **60**, 2204-2206 (1992).

Corresponding Author: Kazuki Ihara

E-mail: k-ihara@aist.go.jp, Tel: +81-29-861-6357, Fax: +81-29-861-4413

***Present Address:** Nanotube Research Center, AIST, Tsukuba 305-8565, Japan

1-16

Continuous Separation of Metallic and Semiconducting Carbon Nanotubes Using Agarose Gel

○Takeshi Tanaka[1], Yasuko Urabe[1] and Hiromichi Kataura[1,2]

[1]*Nanotechnology Research Institute, National Institute of Advanced Industrial Science and Technology (AIST), Tsukuba, Ibaraki 305-8562, Japan*
[2]*JST, CREST, Kawaguchi, Saitama, 332-0012, Japan*

Single wall carbon nanotubes (SWCNTs) have attracted a great deal of attention towards versatile applications, especially in the field of electronics, such as flexible transistor and transparent conducting film. However, electrical heterogeneity of as-produced SWCNTs (metal/semiconductor) is one of the most crucial problems preventing useful application of SWCNTs. Previously, we reported novel separation methods of metallic and semiconducting SWCNTs (MS separation) using agarose gel[1,2]. In this presentation, we report an improved method for the MS separation using agarose gel.

SWCNTs/SDS (sodium dodecyl sulfate) dispersion was applied to a column filled with agarose gel beads (Fig. 1). Only semiconducting SWCNTs (S) were trapped the beads, while metallic SWCNTs (M) passed through the column. After washing the column with SDS solution, semiconducting SWCNTs in the beads were eluted with sodium deoxy cholate (DOC) solution. After washing with DOC and re-equilibrating with SDS, the column could be used for repeated separation. Because this continuous and repeatable separation method can be applied to a low-cost and large-scale process, it is expected that industrial production of metallic and semiconducting SWCNTs can be realized.

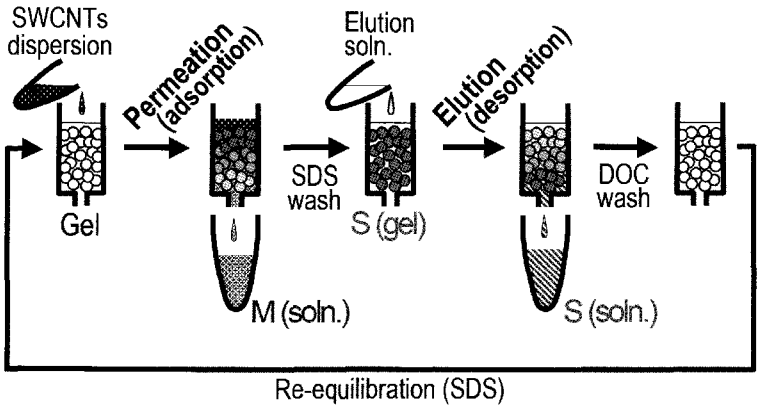

Fig. 1. Continuous and repeatable MS separation using column.

This study was supported by the industrial technology research grant program of the New Energy and Industrial Technology Development Organization (NEDO) of Japan.

[1] T. Tanaka et al., *Appl. Phys. Express* 2008, **1**, 114001.
[2] T. Tanaka et al., *Nano Lett.* 2009, **9**, 1497

Corresponding Author: T. Tanaka
Tel: +81-29-861-2903, Fax: +81-29-861-2786, E-mail: tanaka-t@aist.go.jp

1-17

Length Fractionation of SWCNTs by Using Filtration Method

○Shigekazu Ohmori[1], Takeshi Saito[1,2], Bikau Shukla[1], Motoo Yumura[1], Sumio Iijima[1]

1: Natioanl Institute of Advanced Industrial Science and Technology (AIST), Tsukuba, 305-8565, Japan
2: PRESTO, Japan Science and Technology Agency (JST), Tokyo 102-0075, Japan

Length is an important structural parameter in SWCNTs, especially for the preparation of their dispersed inks used in the printable electronics application. Although controlling diameter of SWCNTs that is another important one of their structural parameters has been reported frequently and has become possible to a considerable extent in the SWCNT production [1], previous studies on sorting SWCNTs by their length is quite few and limited in low-throughput methods. Thus, a high-throughput method of sorting SWCNTs by length is still needed for some applications.

Motivated by this need, we have developed a novel length fractionation system by the multi-steps cross-flow filtration of SWCNT dispersed suspensions. The cross-flow filtration was carried out by using a handmade filteration apparatus converted from the tangential flow filtration system, VIVAFLOW 50 (Sartorius Stedim Biotech) in which effective filtration area is 50cm^2. SWCNTs were dispersed in aqueous solutions of sodium carboxymethylcellrose salt (CMC) and sodium dodecylbenzene sulfate (SDBS) with the help of bath sonication and these suspensions were loaded in this system as source suspensions. The source suspension was flowed by a peristalic pump at the flow rate of 1ml/sec. In this work, we have constructed 3-steps cross-flow filtration system by using three membrane filters of different pore sizes, 0.2μm, 0.45μm, 1.0μm.

By the abovementioned closs-flow filtration system, the source suspension of SWCNTs dispersed by CMC was separated into four samples A~D, that is, three different retentates and one permeate of the last step. Those separated samples were characterized by optical absorption spectroscopy and atomic force microscope (AFM) measurements. Filtration efficiencies and relative amounts of SWCNTs were calculated from observed absorption spectra. The length distribution profiles of SWCNTs were obtained from direct measurements of individual SWCNT lengths in topographical images of AFM. It was found that length distribution peaks in profiles of four separated samples approximately agree with the expected ranges from used pore sizes of filters. On the other hand, this length fractionation phenomenon was not observed in the SDBS suspension, suggesting that polymer type detergent is suitable for sorting of SWCNTs by length.

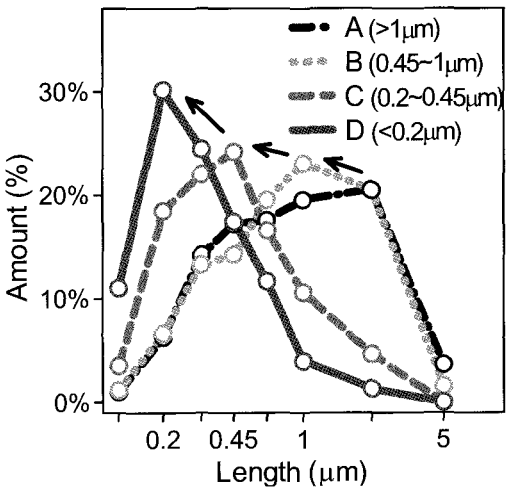

Figure 1. The length distribution profiles of A~D.

References:
[1] T. Saito, et. al., J. Nanosci. Nanotech., 8, 6153 (2008)

Corresponding Author: Takeshi Saito
E-mail: ohmori-sh@aist.go.jp
Tel: 029-861-6276 Fax: 029-861-4413

1-18

Mg concentration dependence of conductivity in epitaxial-grown Mg-doped C_{60} thin films

○Masato Natori, Seiji Nishi, Nobuaki Kojima and Masafumi Yamaguchi
Toyota Technological Institute, 2-12-1 Hisakata Tenpaku, Nagoya 468-8511, Japan

C_{60} solids have been known as high resistive semiconductor materials. For organic solar cell applications, such high resistivity is one of the reasons of low charge transport efficiency in a C_{60} accepter layer. Impurity doping in organic semiconductor can increase conductivity, and control band profile at the interface between organic/metal or organic/organic materials. For the semiconductor device application, the search for new guest materials is necessary. Mg is one of the promising materials for guest metal showing semiconductor property. However, the detailed investigation of semiconductor properties of Mg-doped C_{60} films has not been reported yet.

The electric conduction of organic materials is also affected by the crystal quality. The increase of conductivity and electron mobility of C_{60} thin films with the grain size was reported. In this paper, we investigate the epitaxial growth of Mg-doped C_{60} films to obtain the well-crystalline films, and electric properties of the epitaxial Mg-doped C_{60} films.

C_{60} and Mg-doped C_{60} films were grown on mica (001) or quarts glass substrates by molecular beam epitaxy. The film composition of Mg/C_{60} was changed by the beam flux ratio of Mg/C_{60} sources. The resulted film composition of Mg/C_{60} was confirmed by X-ray photoelectron spectroscopy. (111)-oriented crystalline Mg-doped C_{60} can be grown on mica (001) at the growth temperature of 165°C. For the conductivity measurements, bottom electrode structure was used. The conductivity was estimated from I-V characteristics between the adjacent bottom electrodes under the vacuum condition.

Figure 1 shows Mg concentration dependence of the conductivity σ in comparison between glass and mica substrates. For mica substrate, epitaxial growth was confirmed by XRD measurement. The conductivity increases with increasing Mg concentration in both substrates. Furthermore, significant increase in conductivity can be seen in Mg-doped C_{60} film on mica substrate. It is considered that such significant increase is caused by the drastic improvement of crystal quality realized by epitaxial growth. Figure 2 shows relationship between the conductivity and Mg concentration in Mg-doped C_{60} films on mica substrates. The values of $\sigma^{1/2}$ increase linearly with Mg concentration. This result may suggest that two electrons per Mg atom contribute the electrical conduction.

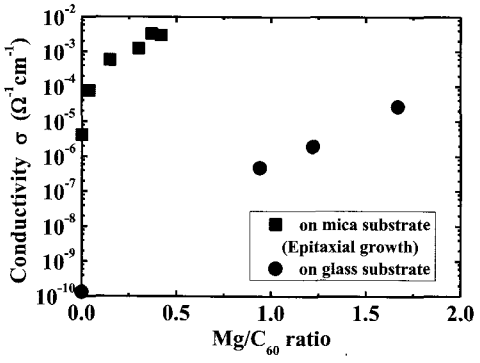

Figure 1. Mg concentration dependence of the conductivity in comparison between mica and glass substrates.

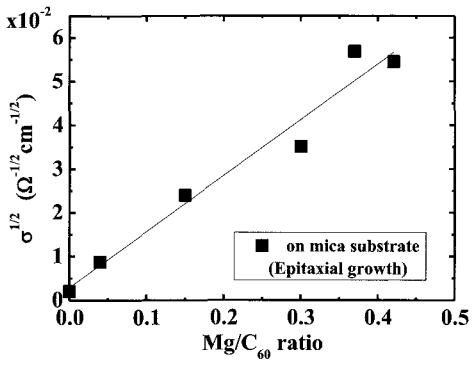

Figure 2. Relationship between $\sigma^{1/2}$ and Mg concentration in Mg-doped C_{60} films on mica substrates.

Corresponding Author: Masato Natori
E-mail: sd08427@toyota-ti.ac.jp **Tel&Fax:** +81-52-809-1877, +81-52-809-1879

1-19

Preparation and Optical Properties of Fullerene/Ferrocene Hybrid Hexagonal Nanosheets

○Takatsugu Wakahara,[1] Marappan Sathish,[1] Kun'ichi Miyazawa,[1] Chunping Hu,[2] Yoshitaka Tateyama,[2,3] Yoshihiro Nemoto,[2] Toshio Sasaki[4] and Osamu Ito[5]

[1]*Fullerene Engineering Group, Exploratory Nanotechnology Research Laboratories, National Institute for Materials Science, 1-1 Namiki, Tsukuba, Ibaraki 305-0044, Japan*
[2]*International Center for Materials Nanoarchitectonics (MANA), National Institute for Materials Science, 1-1 Namiki, Tsukuba, Ibaraki 305-0044, Japan*
[3]*PRESTO, Japan Science and Technology Agency, 4-1-8 Honcho, Kawaguchi, Saitama 333-0012, Japan*
[4]*ICYS, National Institute for Materials Science, 1-1 Namiki, Tsukuba, Ibaraki 305-0044, Japan*
[5]*CarbonPhotoScience Institute, Kita-Nakayama2-1-6, Izumi-ku, Sendai, 981-3215*

Fullerenes form a wide variety of donor-acceptor complexes with different classes of organic and organometallic donors. [1] These complexes show a wide range of physical properties. Ferrocene (Fc) is one of such very important donors because of its strong electron-donating ability and high stability under redox conditions. Therefore, supramolecular hybrids formed by the combination of fullerene and Fc are expected to have fascinating properties. Indeed, C_{60}/Fc hybrid molecules have been reported to show interesting properties. [2]

We herein report a simple method for the preparation of C_{60}/Fc hybrid nanowhiskers [3] and hexagonal nanosheets [4] by a liquid-liquid interfacial precipitation (LLIP) method. The highly crystallized C_{60}/ferrocene hexagonal nanosheets had the formulation C_{60}(ferrocene)$_2$. A strong charge-transfer (CT) band between ferrocene and C_{60} was observed at 782 nm, indicating the presence of donor-acceptor interaction in the nanosheets. Upon heating the nanosheets to 150 °C, the CT band disappeared due to the sublimation of ferrocene from the C_{60}/ferrocene hybrid, and C_{60} nanosheets with an fcc crystal structure and the same shape and size as the C_{60}/ferrocene nanosheets were obtained.

References

[1] D. V. Konarev, R. N. Lyubovskaya, N. V. Drichko, E. I. Yudanva, Y. M. Shul'ga, A. L. Litvinov, V. N.Semkin, and B. P. Tarasov, *J. Mater. Chem.* **2000**, *10*, 803-918.

[2] Y. Matsuo, K. Kanaizuka, K. Matsuo, Y-W. Zhong, T. Nakae, and E. Nakamura, *J. Am. Chem. Soc.*, **2008**, *130*, 5016-5017.

[3] T. Wakahara, M. Sathish, K. Miayzawa, and T. Sasaki, *Nano* **2008**, *3*, 351-354.

[4] T. Wakahara, M. Sathish, K. Miayzawa, C. Hu, Y. Tateyama, Y. Nemoto, T. Sasaki and O. Ito, *J. Am. Chem. Soc. in press.*

Corresponding Author; Takatsugu Wakahara
E-mail; WAKAHARA.Takatsugu@nims.go.jp
Tel; +81-29-860-4846, Fax: +81-29-860-4667

2-1

Synthesis, Mechanical and Electric Characterization of a Multiwall Carbon Nanocapsule Studied by *in-situ* Transmission Electron Microscopy

○Koji Asaka[1], Kun'ichi Miyazawa[2], Tokushi Kizuka[3] and Yahachi Saito[1]

[1]*Department of Quantum Engineering, Nagoya University, Nagoya 464-8603, Japan*
[2] *National Institute for Materials Science, 1-1, Namiki, Tsukuba, 305-0044, Japan*
[3] *Institute of Materials Science, Graduate School of Pure and Applied Sciences, University of Tsukuba, Tsukuba 305-8573, Japan*

We have developed *in-situ* high-resolution transmission electron microscopy for a mechanical and an electron transport testing of individual nanometer-sized materials using a nanometer-sized tip. We synthesized carbon nanocapusles, which are giant multiwall fullerene molecules with diameters of several nanometers. Here, we used this microscopy to demonstrate atomistic structural dynamics of the single nanocapsules during the repetitive compressive deformation and the conductance measurement. Simultaneously, we measured the subnanonewton force and the electric current acting on the nanocapsules. The results showed the surprising toughness and the metallic-type electron transport of the nanocapsules owing to size reduction on a nanometer scale.

We synthesized crystalline whiskers composed of C_{60} molecules with submicrometer diameters by a liquid-liquid interfacial precipitation method. The crystalline whiskers were heated in high vacuum at 1173 K for 30 min to transform them into amorphous carbon whiskers. The amorphous whiskers were dispersed on a tip of a gold plate of 50 μm thickness. The gold plate was mounted on a specimen holder of a transmission electron microscope. A cantilever tip used for atomic force microscopy was coated with a gold film of 5 - 10 nm thickness, and was mounted in front of a tube type piezoelectric element on another specimen holder. The cantilever tip was brought into contact with one of the amorphous whiskers in the microscope. We impressed a current into the whisker at room temperature in a vacuum of 1 x 10^{-5} Pa, and synthesized multiwall carbon nanocapsules aggregating on the whisker. We picked one of the nanocapsules on the whisker using the cantilever tip, and transferred it to the surface of the gold plate beside the whisker. The atomistic structural dynamics was observed by the lattice imaging of transmission electron microscopy using a television system, with simultaneous force, current, and voltage measurements.

Figure 1 shows a time-sequence series of high-resolution images of a nanocapsule during manipulation. The nanocapsule is supported between two gold surfaces A and B. In Fig. 1(c), we applied a bias voltage to the nanocapsule. The current increased linearly from 0 to 0.20 V, and no gap was observed in current around 0 V. The conductance in this region is estimated to be 0.5 G_0, where $G_0 = 2e^2 / h$ is the conductance quantum (e is the electron charge, h is Planck's constant). The results show the metallic-type electron transport for the single nanocapsules. The mechanical properties of the single nanocapsules are also reported in this presentation.

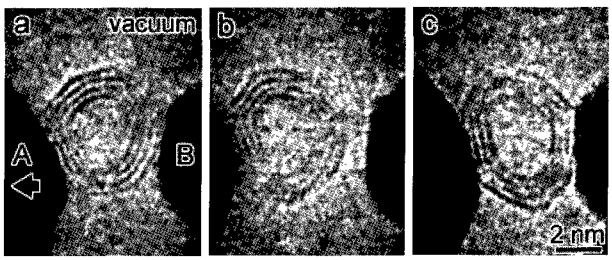

Fig.1 Time-sequential high-resolution images of a nanocapsule during manipulation. The outer diameter is ~ 5.3 nm, and the capsule is constructed of four graphene shells.

Corresponding Author: Koji Asaka
TEL: +81-52-789-3714, FAX: +81-52-789-3703,
E-mail: asaka@nuqe.nagoya-u.ac.jp

2-2

Pioneering Research on the Properties and the Methods for Chemical Modification of Paramagnetic Endohedral Metallofullerenes

○Yuta Takano,[1] Michio Yamada,[1] Hidefumi Nikawa,[1] Zdenek Slanina,[1] Naomi Mizorogi,[1] Midori O. Ishitsuka,[1] Takahiro Tsuchiya,[1] Yutaka Maeda,[2] Takeshi Akasaka,[1] Tatsuhisa Kato,[3] Shigeru Nagase.[4]

[1]*Center for Tsukuba Advanced Research Alliance, University of Tsukuba, Tsukuba, Ibaraki 305-8577,* [2]*Department of Chemistry, Tokyo Gakugei University, Koganei, Tokyo 184-8501,* [3]*Department of Chemistry, Josai University, Sakaido, Saitama 350-0295, Japan,* [4]*Department of Theoretical and Computational Molecular Science, Institute for Molecular Science, Okazaki, Aichi 444-858.*

Among many kinds of endohedral metallofullerenes (EMFs), paramagnetic EMFs have attracted special interest as new spherical molecules because of their unique properties that are not expected from empty fullerenes.[1] M@C_{82} (M = La, Ce, Gd, etc.) is one of the most abundantly produced EMFs, having the electronic state described by $[M]^{3+}[C_{82}]^{3-}$ because of electron transfer from the M atom onto the C_{82} cage.[2] As the result, M@C_{82} has an open-shell electronic structure of C_{82} with an unpaired electron being widely delocalized on the surface of the C_{82} cage. Those paramagnetic features of this kind of EMFs are expected to develope wide range of potential applications in chemistry, physics, medicinal chemistry, and nanomaterial science.

In this series of research, we revealed the characteristics of paramagnetic EMFs by using La@C_{82} and Ce@C_{82}. i) The addition reaction of radical groups to La@C_{82} occurred regioselectively, affording stable and novel monoadducts (Figure 1a), which have a closed-shell electronic structure.[3] The DFT calculation suggests that the radical coupling reactions take place at the cage carbons that have high spin densities. ii) Two isomers of Ce@C_{82}Ad (Ad = adamantylidene) were synthesized in high yields by a carbene addition reaction (Figure 1b).[4] The chemical reactivity of Ce@C_{82} was found to be similar to that of La@C_{82}, although the encapsulated metals are different. Paramagnetic shifts in ^{1}H and ^{13}C NMR spectra reflecting the anisotropic behavior of the f-electron spin on the Ce atom were observed for the two isomers of [Ce@C_{82}Ad]$^{-}$, which were prepared by controlled potential bulk electrolysis.

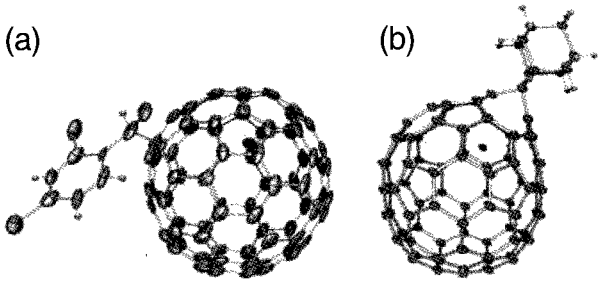

Figure 1. ORTEP drawings of the derivatives of (a) La@C_{82} and (b) Ce@C_{82}.

It is expected that the selective radical reactions of paramagnetic EMFs will open a new methodology in preparing functionalized metallofullerenes. In addition, the observations of the anisotropic magnetic behavior on the derivatives of Ce@C_{82} reveal the promising magnetic properties of metal-encapsulating carbon clusters of EMFs.

References: [1] *Endofullerenes: A New Family of Carbon Clusters*; T. Akasaka, S. Nagase, Eds.; Kluwer Academic Publisher: Dordrecht, 2002. [2] (a) D. S. Bethune, et al. *Nature* **1993**, *366*, 123-128. (b) K. Kobayashi et al. *Chem. Phys. Lett.* **1998**, *282*, 325-329. [3] Y. Takano et al. *J. Am. Chem. Soc.* **2009**, *131*, DOI: 10.1021/ja902106a. [4] Y. Takano et al. *J. Am. Chem. Soc.* **2008**, *130*, 16224-16230.

Corresponding Author: Takeshi Akasaka

E-mail: akasaka@tara.tsukuba.ac.jp, **Tel&Fax:** +81-29-853-6409.

2-3

Host-Guest Spin Communication Switchable by Guest Confinement

○Fatin Hajjaj[1], Kentaro Tashiro[2], Takeshi Akasaka[3], Tatsuhisa Kato[4], Takuzo Aida[1]

[1]*School of Engineering and Center for NanoBio Integration, The University of Tokyo 7-3-1 Hongo, Bunkyo-ku, Tokyo 113-8656, Japan*
[2]*National Institute for Materials Science, Tsukuba 305-0044, Japan*
[3]*Center for Tsukuba Advanced Research Alliance, University of Tsukuba, Tsukuba Ibaraki 305-8577, Japan*
[4]*Department of Chemistry, Josai University, Sakado, Saitama 350-0295, Japan*

Supramolecular architectures consisting of a cyclodimeric Cu(II) porphyrin and endohedral metallofullerene La@C_{82} (**Chart 1**) have been constructed to investigate through space host-guest spin communication. Electron spin transient nutation (ESTN) spectroscopy of ***open*-Cu** revealed that the spin ground state is doublet, indicating that the two spins behave independently. Drastic ESR spectral change of ***open*-Cu**, upon inclusion of La@C_{82}, strongly suggests that the spins on ***open*-Cu** and La@C_{82} are coupled to form a new spin state. ESTN spectroscopy of the inclusion complex revealed that the spin ground state of ***open*-Cu⊃**La@C_{82} is quartet, demonstrating that spins on the host and guest are coupled ferromagnetically. To the best of our knowledge, this is the first example of host-guest ferromagnetic spin communication. Ring closing metathesis reaction of ***open*-Cu⊃**La@C_{82} afforded guest-confined complex ***close*-Cu⊃**La@C_{82}, which does not show any signs of dissociation of the components under chromatographic and mass spectrometric conditions. Very interestingly, ESR spectrum of ***close*-Cu⊃**La@C_{82} obviously differed from that of ***open*-Cu⊃**La@C_{82}, indicating that the host-guest spin communication is switched by the guest confinement. These spectral comparisons, together with the spin-doublet ground state of the complex, as determined by ESTN spectroscopy, allowed us to conclude that the spins on the host and guest of ***close*-Cu⊃**La@C_{82} are not ferromagnetically but ferrimagnetically coupled.[1]

Chart 1

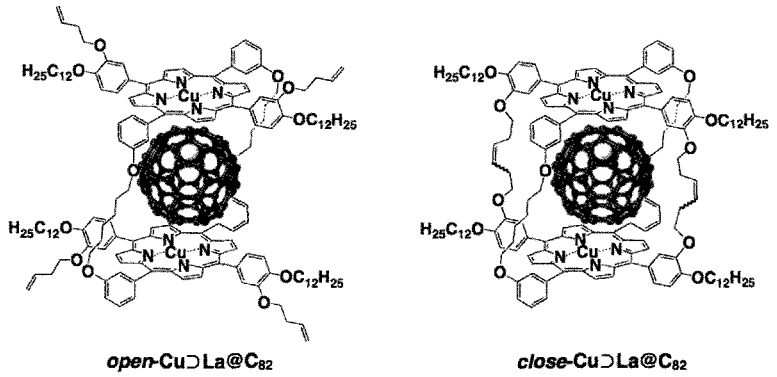

(1) Fatin Hajjaj, Kentaro Tashiro, Hidefumi Nikawa, Takeshi Akasaka, Ko Furukawa, Tatsuhisa Kato, Takuzo Aida. *Submitted.*

Corresponding Authors: Takuzo Aida and Kentaro Tashiro
E-mail: fatin@nanospace.miraikan.jst.go.jp
Tel & Fax: 03-3570-9182; 03-3570-9183

2-4

Direct Determined Precise Electronic States of Isolated (n, m) Single-Walled Carbon Nanotubes

○Yasuhiko Hirana[1], Yasuhiko Tanaka[1], Koichiro Kato[2],
Susumu Saito[2] and Naotoshi Nakashima[1,3]

[1]*Department of Applied Chemistry, Graduate School of Engineering, Kyushu University, Fukuoka 819-0395, Japan.*
[2]*Department of Physics, Tokyo Institute of Technology, 2-12-1 Oh-okayama, Meguro-ku, Tokyo 152-8551, Japan*
[3]*CREST, Japan Science and Technology Agency, 5 Sanbancho, Chiyoda-ku, Tokyo 102-0075, Japan*

Electronic structures of CNTs, one of the most fundamental features of nanotubes, strongly depend on their diameter and chirality. For many practical applications of nanotubes, redox behavior of nanotubes plays a central role. Here we report the in situ near-IR photoluminescence (PL) spectroelectrochemical method to determine the redox potentials of isolated single-walled carbon nanotubes (SWNTs) having their own chirality indices. It was found that PL signals from the isolated SWNTs showed strong applied-potential dependence and that the potential dependence of PL intensity was exactly Nernst response. Using the Nernst equation analysis of the PL data, the precise redox potentials of fifteen SWNTs have been determined (Figure 1, Table 1).

We will present details about this method and compare our data with other experimental data previously reported by other groups.

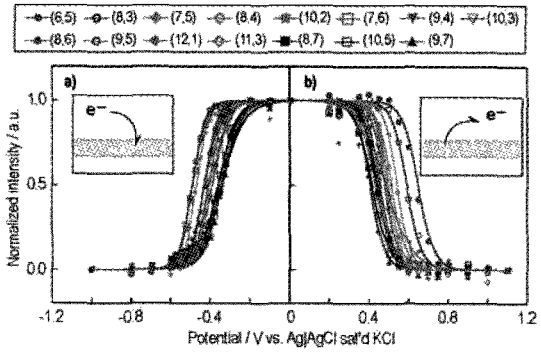

Figure 1. Normalized PL intensity of a film containing fifteen isolated SWNTs on an ITO electrode as a function of external applied potential and the Nernst analysis curves

Table 1. Experimentally determined electronic states of fifteen isolated SWNTs.

chirality index (n,m)	nanotube diameter (nm)	$E^{0'}_{ox}$ (V vs. vacuum)	$E^{0'}_{red}$ (V vs. vacuum)	Fermi level (E_f) (V vs. vacuum)	bandgap (eV)
(6,5)	0.757	5.08	4.01	4.55	1.07
(8,3)	0.782	5.03	3.95	4.49	1.08
(7,5)	0.829	4.98	3.97	4.48	1.01
(8,4)	0.840	4.96	4.05	4.50	0.91
(10,2)	0.884	4.93	3.95	4.44	0.98
(7,6)	0.895	4.94	4.03	4.49	0.91
(9,4)	0.916	4.92	4.01	4.47	0.91
(10,3)	0.936	4.89	4.09	4.49	0.81
(8,6)	0.966	4.90	4.05	4.47	0.85
(9,5)	0.976	4.89	4.09	4.49	0.79
(12,1)	0.995	4.93	4.03	4.48	0.90
(11,3)	1.014	4.87	4.05	4.46	0.82
(8,7)	1.032	4.88	4.09	4.49	0.79
(10,5)	1.050	4.86	4.08	4.47	0.78
(9,7)	1.103	4.85	4.10	4.47	0.75

Corresponding Author: Yasuhiko Hirana
Tel&FAX: +81-92-802-2842, E-mail: yhirana1116@ mail.cstm.kyushu-u.ac.jp

2-5

Ink-jet printing of low-voltage SWCNT-thin film transistors using ionic liquid gating

○Haruya Okimoto[1], Taishi Takenobu[1], Kazuhiro Yanagi[2,3], Yasumitsu Miyata[2], Hiromichi Kataura[2,3], Takeshi Asano[4], Yoshihiro Iwasa[1]

[1]*Institute for Materials Research (IMR), Tohoku University, Sendai 980-8577, Japan*
[2]*Nanotechnology Research Institute, AIST, Tsukuba, Ibaraki 305-8562, Japan,*
[3]*CREST/JST,* [4]*Brother Industries, Ltd., Nagoya 467-0855, Japan*

An important strategy for realizing flexible electronics is to use solution-processable materials that can be directly printed and integrated into high-performance electronic components. For these points, single-walled carbon nanotube (SWCNT) is very attractive materials which have a significant advantage in transport properties and chemical stability. Recently, we have reported an ink-jet printing of flexible and high performance SWCNT thin-film-transistors (TFTs) [1,2]. However, to exploit the exceptional electronic properties of printed SWCNTs in network–based devices, several challenges need to be overcome. Here we report a fabrication of all ink-jet printing, low-voltage and less hysteresis SWCNT-TFTs using ionic liquid gating, which have high capacitance.

Figure 1 shows a schematic illustration of fabrication procedure. First, conducting SWCNT thick film was printed as source, drain and gate electrodes. In addition, thin SWCNT film was printed as semiconducting layer. In second step, *N,N*-Diethyl-N-methyl-N-(2-methoxy-ethyl) ammonium bis (tri-fluoro-methane-sulfonyl)imide(DEME-TFSI) was printed as gate dielectric between gate electrode and semiconducting layer. Figure 2 shows the transfer characteristics of printed SWCNT-TFTs using back gating and ionic liquid gating. The operation gate voltage (-20 to 1 V) and the large hysteresis was observed for the back-gating SWCNT-TFTs. On the other hand, ionic liquid gating SWCNT-TFTs was operated -1 to 1 V as gate voltage and reduced the hysteresis from 15 V to 0.1 V. Importantly, this ionic liquid gating SWCNT-TFTs was fabricated by only ink-jet printing.

In summary, we fabricated the all ink-jet printing SWCNT-TFTs using ionic liquid gating. Use of ionic liquid as gate dielectric can be drastically reduced an operation voltage and hysteresis than that of back gating SWCNT-TFTs. In the future, it is easy to expand this technique to several substrates, especially flexible substrate for realization of all ink-jet printed flexible SWCNT-TFTs.

This study has been supported by Industrial Technology Research Grant Program in 2006 from NEDO of Japan.

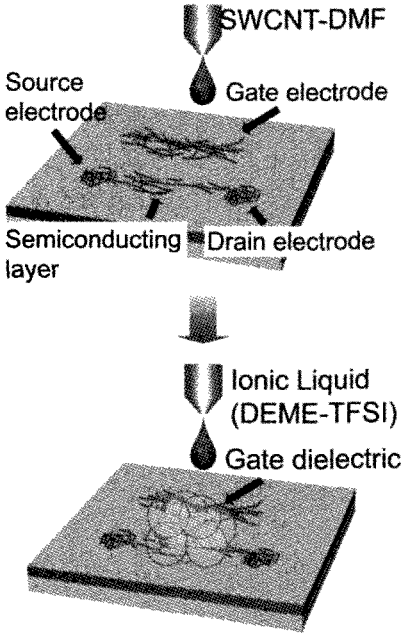

Fig.1
Schematic illustration of all ink-jet printed SWCNT-TFTs .

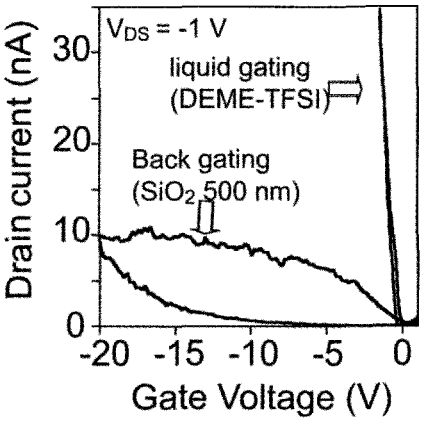

Fig.2 Transfer characteristics of printed SWCNT-TFTs with (a)back gating and (b) ionic liquid gating.

[1] T. Takenobu *et al., Appl. Phys. Express.*, **2**, 025005(2009).
[2] H. Okimoto *et al., Jpn. J. Appl. Phys.*, in press. [3] T. Ozel *et al., Nano Lett.*, **5**, 905(2005).

Corresponding Author: Haruya Okimoto
E-mail: haruya@imr.tohoku.ac.jp Tel: +81-22-215-2033 FAX: +81-22-215-2031

2-6

Carbon Nanotube Growth from Diamond Nanoparticles

○Daisuke Takagi[1], Yoshihiro Kobayashi[1†], Yoshikazu Homma[2]

[1]*NTT Basic Research Laboratories, NTT Corporation, Atsugi, Kanagawa 243-0198, Japan*
[2]*Department of Physics, Tokyo University of Science, Shinjuku, Tokyo 162-8601, Japan*

Here, we demonstrate that nanosize diamond particles can act as carbon nanotube (CNT) growth nuclei in chemical vapor deposition (CVD)[1].

Metal, semiconductor, and metal-oxide nanoparticles have been found to act as CNT growth nuclei[2,3]. Since semiconductor and metal-oxide nanoparticles maintain a solid phase even during CVD, they are expected to be useful for chirality-controlled CNT growth based on the epitaxial relationship between CNT-cap and a particle surface. However, their surface structure and composition can be altered by reactions with carbon atoms during CVD. Furthermore, since they can not be formed in a high density on substrate, they are not suitable for massive CNT growth. We show that diamond, carbon allotrope, can solve these issues.

The size of the diamond is the key to CNT synthesis (1-5 nm). To satisfy this condition, we used diamond particles produced by the detonation method (NanoCarbon Research Institute Co., Ltd., Japan)[4,5]. Most of the diamond particles produced by this technique have a size of 4-5 nm. CNTs were synthesized by CVD with ethanol vapor at 850 °C. The grown CNTs and nanodiamond particles were characterized by SEM, TEM, Raman spectroscopy, and EDX.

The TEM images of grown CNTs and diamond particles are shown in Figs. 1a and b, and a FFT image of Fig. 1b is shown in Fig. 1c. These images clearly indicate that grown CNTs are single-walled carbon nanotubes (SWCNTs) and that the nanosized diamond particles can act as SWCNT growth nuclei. Since diamond particles retain the solid phase during the CVD process, they do not fuse to each other and can maintain their original sizes. This nonfusion characteristic of nanodiamond particles allows massive SWCNT growth from high-density and three-dimensionally aggregated particles as shown in Fig. 1d (SEM image).

Carbon atoms can not diffuse inside the diamond at the CVD temperature. This means that SWCNT nucleation on diamond is dominated not by the usual bulk diffusion but by a novel mechanism via surface diffusion of carbon. Since the composition of diamond is not altered by carbon absorption and the surface structure of diamond has been extensively studied, nanodiamond is a potentially promising material for chirality-controlled SWCNT growth.

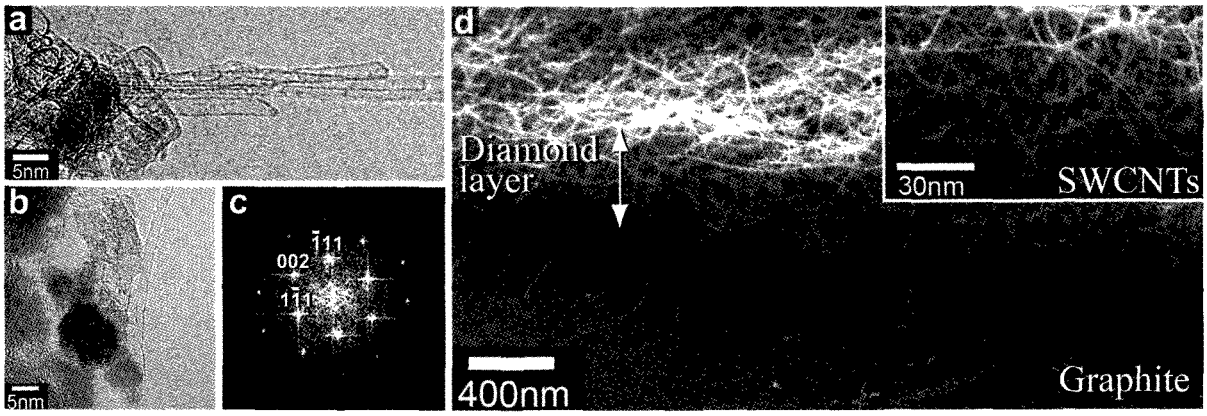

Figure 1. SWCNT growth from diamond nanoparticles

[1] Takagi, D. et al. *J. Am. Chem. Soc.* **2009**. *131*, 6922. [2] Takagi, D. et al. *Nano Lett.* **2006**, *6*, 2642, **2007**, *7*, 2272, **2008**, *8*, 832. [3] Liu, H. et al. *Appl. Phys. Express*. **2008**, *1*, 014001. [4] Danilenko, V. V. *Phys. Sol. Stat.* **2004**, *46*, 595. [5] Ōsawa, E. *Diam. Rel. Mat.* **2007**, *16*, 2018.

†*Present address: Dept. of appl. Phys. Osaka Univ. Suita, Osaka 565-0871, Japan*

Corresponding Author: Daisuke Takagi
TEL: +81-3-5228-8244, FAX +81-3-5261-1023, E-mail: daisuke@will.brl.ntt.co.jp

2-7

Functionalisation of Nanodiamonds: Surface Tailoring of Agglomerating Nanoparticles

○Masaki Ozawa[1], Yuejiang Liang[2], and Anke Krueger[2]

[1]*Department of Materials Science and Engineering, Meijo University, Nagoya 468-8520, Japan*

[2]*Institut für Organische Chemie der Julius-Maximilians-Universität Würzburg Am Hubland, 97074 Würzburg, Germany*

The successful history of wet chemistry has been proving its validity in synthesising soluble compounds. It seems a key also for nanoparticles to enable various sophisticated applications by tailoring the vast surface areas. Nevertheless, their insolubility and spontaneous agglomeration make it fairly challenging. Especially for persistently agglomerating nanoparticles like detonation nanodiamonds, surface modification of primary particles must be performed within narrow experimental windows allowing colloidal stability. Otherwise, it ends up only surfaces of the agglomerates. The simplest solution to widen the windows is likely integration of a high energy deagglomeration process in chemical reactions.

Recently we have disclosed bead-assisted sonic disintegration (BASD) using a powerful sonicator equipped with a horn-type sonotrode in the presence of ceramic beads as a novel deagglomeration technique. Contrarily to stirred-media milling, BASD is applicable to the conventional chemistry systems in a simple way, as shown in the figure. Such a setup allows atmospheric and temperature control, use of toxic chemicals, irradiation, electrochemical treatments etc.

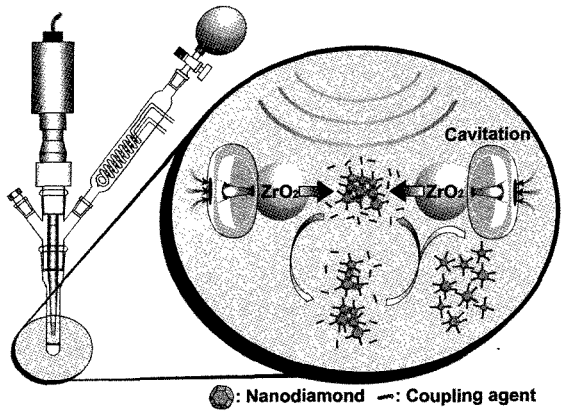

Here we demonstrate two different reactions on detonation nanodiamonds: a simple condensation reaction yielding silanisation and arylation with diazonium salts. The former performed in dry THF, where as purchased powder immediately precipitate, exhibited gradual deagglomeration and dispersion in the solvent, finally yielding a dark brownish clear colloid. The latter reaction also started under flocculating conditions in water due to the coupling agents. Although no improvement in dispersion was obtained throughout the reaction, purified products dispersed well in water with drastic change in zeta potential from the pristine positive value to negative. Dynamic light scattering measurements, infra-red spectroscopy, transmission electron microscopy, etc. proved deagglomeration and simultaneous surface functionalisation of primary nanoparticles.

[1] M. Ozawa, M. Inaguma, M. Takahashi, F. Kataoka, A. Krueger and E. Ōsawa, *Adv. Mater.*, **19**, 1201 (2007).

[2] Y. Liang, M. Ozawa and A. Krueger, *submitted to ACS Nano.*

Corresponding Author: Masaki Ozawa

TEL: +81-52-838-2410, FAX: +81-52-832-1170, E-mail: mozawa@ccmf.s.meijo-u.ac.jp

2-8

Possible Magnetic States in Buckybowl Molecules

Kikuo Harigaya○

Nanotechnology Research Institute, AIST, Tsukuba 305-8568

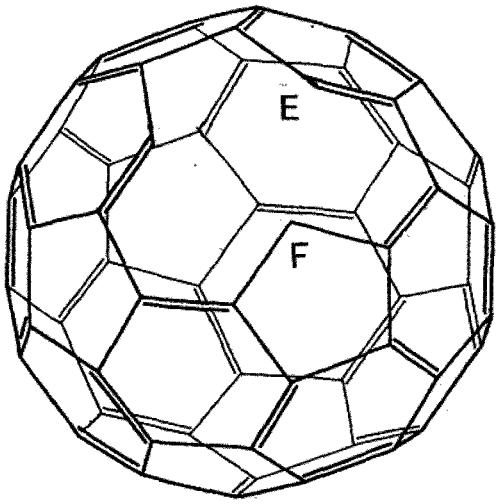

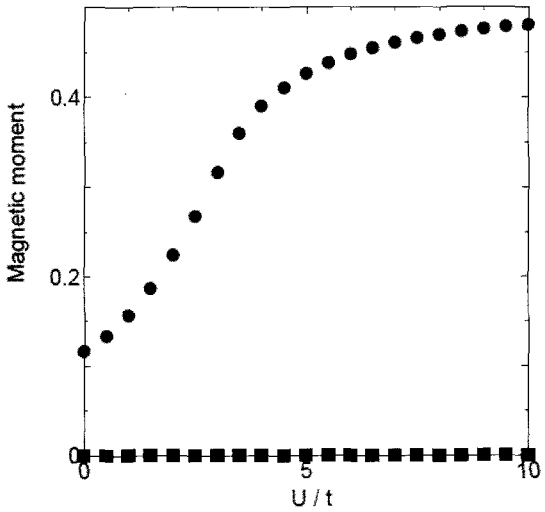

Abstract: We investigate possible magnetic states in buckybowl structures, where the sumanene and a part of C_{60} (p-C_{60}) are considered. We also consider cluster effects of the empty atoms, later, in this presentation (left figure). We shall use the Hubbard model with the mean field theory. We show that the magnetic property of the sumanene molecule reflects the structure of the molecule. On the other hand, we have found, that the larger buckybowls show the crossover properties with respect size effects, from molecules to materials with zigzag edge states known in nanographene. The defects of the C_{60} give rise to magnetic properties owing to the symmetries of the molecules (right figure).

Corresponding Author: K. Harigaya
E-mail: k.harigaya@aist.go.jp

2-9

Control of Redox Properties of Fullerene Derivatives by Lone Pair Proximity Effect

○Yusuke Tajima[1] and Youhei Numata[2]

[1]*Supramolecular Science, RIKEN, 2-1 Hirosawa, Wako, Saitama 351-0198, Japan*
[2]*Advanced Photovoltaics Center, National Institute for Materials Science, 1-2-1 Sengen, Tsukuba, Ibaraki, 305-0047 Japan*

Bulk hetero-junction (BHJ) organic photovoltaic devices offer several advantages over the current inorganic devices, including fabrication with flexible substrates, lightweight, and production by inexpensive processes. But the power conversion efficiencies of the BHJ devices must make great stride to realize widespread commercialization of them, and such improvements will require new semiconductor materials constituting the active layer. One problem on BHJ devices is the low open-circuit voltage which believed to originate from the difference in energy between the HOMO of the donor and the LUMO of the acceptor. This work aimed to research on the development of a new class of fullerene derivatives controlled the redox properties, which can be used as n-type organic semiconductors.

Recently, we developed synthetic strategy of indolino-type fullerene derivatives from fullerene oxide, $C_{60}O$, and could obtain several fullerene derivatives with low reduction potential such as PCBM, which is widely used as n-type semiconductors for BHJ devices [1]. Furthermore, we found a much more effective approach to raise the LUMO by altering the atomic charge on fullerene cage under the influence of substituent due to lone pair proximity effect. The first reduction potentials (E^1_{red}) of 4'-substituted indolino[60]fullerene (**1b**) is significantly lower than indolino[60]fullerene (**1a**) or yet PCBM; **1b** is expected to be an electron-acceptor material with superior LUMO level in BHJ OPV use. With the present approach we have finally succeeded in altering the redox properties of the fullerene derivatives sufficiently for a significant improvement in BHJ device performance. This new technique for control of redox properties in fullerene materials may even offer notable advantages in the organic semiconductor field.

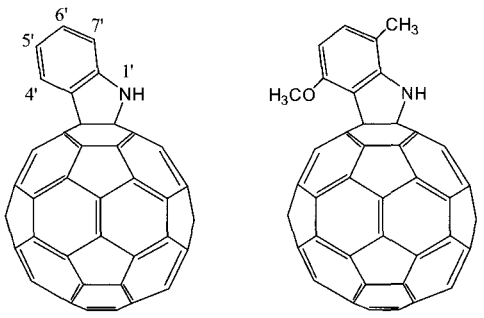

1a **1b**

Fig. 1 Indolino[60]fullerenes

Table 1. First reduction potentials (E^1_{red} vs. Fc/Fc^+) of **1** and PCBM.

Substituent	E^1_{red} / V
5'-NO2	-1.090
5'-MeO	-1.112
5'-F	-1.127
4',6'-Me	-1.134
5'-*n*-Bu	-1.135
5'-Me	-1.138
1a	-1.141
5'-*n*-C12H25	-1.143
6'-MeO-7'-Me	-1.149
PCBM	-1.166
4',6'-MeO	-1.175
4'-MeO-7'-Me (**1b**)	-1.189

Reference : [1] Y. Numata, *et al.*, *Chem. Lett.*, **37** (2008) 1018.

Corresponding Author: Yusuke Tajima
E-mail: tajima@riken.jp
Tel: +81-48-467-9309, Fax: +81-48-462-4702

2-10

Chemical Transformation of the Open-Cage Fullerenes. Alkylation Reactions of the Methylene Protons on the Opening Moieties

○Sho-ichi Iwamatsu[1]

[1]*Graduate School of Environmental Studies (c/o School of Informatics and Sciences), Nagoya University, Nagoya 464-8601, Japan*

Among chemically modified fullerenes, hole-opened, open-cage fullerenes have attracted much attention because these derivatives can be easily filled inside with an atom or a small molecule. We have synthesized open-cage C_{60} derivatives **1** and **2** by multiple carbon–carbon bond scissions, and achieved encapsulations of H_2, H_2O, CO, N_2, NH_3, CH_4 and noble gas atoms [1,2]. To expand the fullerene cage area by organic synthesis, for a larger guest, recently we are investigating chemical reactivity of the substituents on the orifices. Herein, we report the alkylation reactions on the methylene protons in **1** and **2**.

The reaction of **1a** with allyl bromide proceeded at 100 °C in the presence of potassium *tert*-butoxide, and the allylated product **3a** was obtained in 50% yield. In the same manner, the reaction of **2** with allyl bromide gave the di-allylated product **4** in 37% yield. In each cases, ^{1}H NMR spectra suggested that outer protons were converted into allyl substituents. Same as in the case of **2**, compound **4** encapsulates one water molecule to form H_2O@**4**, which shows characteristic sharp singlet at δ -11.4 ppm in the ^{1}H NMR spectrum. Scope of the reactions and inclusion property of the products will be discussed in this session.

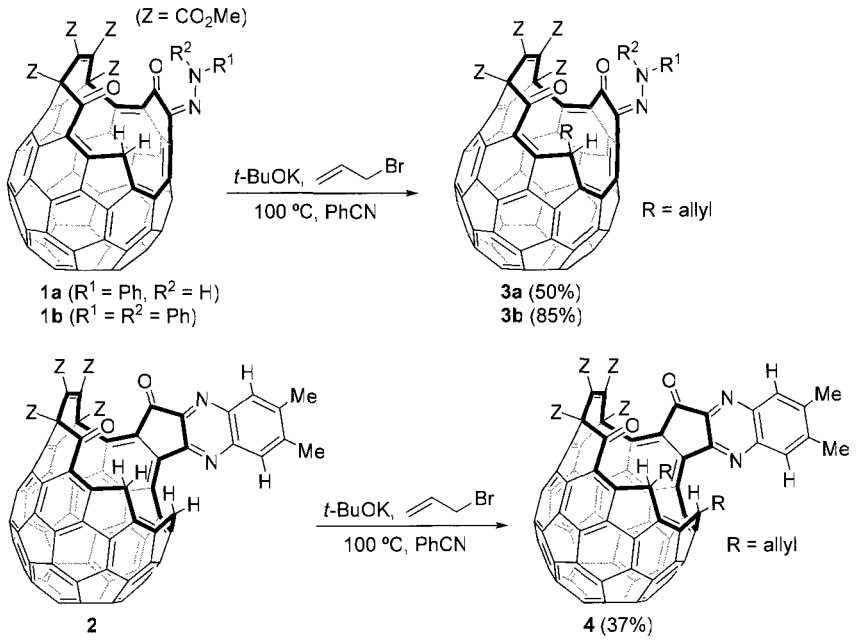

[1] S.-i. Iwamatsu and S. Murata, *Synlett*, 2127–2129 (2005).

[2] K. E. Whitener, R. J. Cross, M. Saunders, S.-i. Iwamatsu, S. Murata, N. Mizorogi, and S. Nagase, *J. Am. Chem. Soc*, **131**, 6338–6339 (2009) and references cited therein.

Corresponding Author: Sho-ichi Iwamatsu
TEL: +81-52-789-4849, FAX: +81-52-789-4765, E-mail: iwmt@urban.env.nagoya-u.ac.jp

2-11

Porphyrin Polymer Assisted Self-Assembly of C_{60} to Silk Ball-Shaped Microspheres

○ Xuan Zhang, Masayuki Takeuchi

Macromolcules Group, Organic Nanomaterials Center (ONC), National Institute for Materials Science (NIMS), 1-2-1 Sengen, Tsukuba 305-0047, Japan

Due to the excellent electronic and mechanical properties of fullerene (C_{60}), C_{60} has drawn much attention in the material science since its discovery in 1985 [1]. As a key component, C_{60} has been found many potential applications in fabrication of various devices, such as solar cells, organic transistors, superconductors, and sensors. Recently, it has been recognized that the device performance, for example, the power conversion efficiency in solar cell, strongly depends on the morphology of C_{60} active film [2]. As a consequence, much effort has been devoted to controlled synthesis of well-defined C_{60} nano/microstructures. One-dimensional (1D) C_{60} rods, wires, whiskers, tubes, and 2D sheets structures have been achieved by slow evaporation of pristine C_{60} solution in various solvents. However, there was usually a limitation on shape and dimensionality modulation and the original face-centered cubic (fcc) structure of pristine C_{60} crystal was also lost. Very recently, diverse-shaped C_{60} crystal has been prepared by this approach but there is no detailed structure information. The self-assembly of amphiphilic C_{60} derivatives can create controlled diverse supramolecular architectures. As an excellent example, 1D fibers, 2D sheets, and 3D spheres and flowerlike objects have been successfully obtained in a C_{60} derivative bearing multiple alkyl chains tail. The alternative way is noncovalent functionalization of C_{60} by making supramolecular composite to control the morphology. The whiskers and spheres have been obtained by making conjugated polymer-C_{60} blend whereas the fcc structure of C_{60} packing was completely disappeared [3].

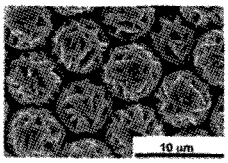

Figure 1 SEM images of novel silk ball-like microspheres of porphyrin polymer-C_{60} composite.

In this presentation, we will report porphyrin polymer assisted self-assembly of C_{60} to diverse shapes of 1D rods, 2D sheets and discs, 3D flower-, sphere-, and shuttle-like objects, and especially the controlled synthesis of novel silk ball-like microspheres (Figure 1) in detail. The obtained superstructures were characterized by SEM, TEM, Raman spectroscopy and XRD. The nice single crystal and fcc structure characters were confirmed and the formation mechanism was also discussed.

[1] H. W. Kroto, J. R. Heath, S. C. O'Brien, R. F. Curl, R. E. Smalley, *Nature*, **318**, 162 (1985).

[2] M. Campoy-Quiles, T. Ferenczi, T. Agostinelli, P. G. Etchegoin, Y. Kim, T. D. Anthopoulos, P. N. Stavrinou, D. D. C. Bradley, J. Nelson, *Nature Mat.*, **7**, 158 (2008).

[3] M. H. Nurmawati, P. K. Ajikumar, R. Renu, C. H. Sow, S. Valiyaveettil, *ACS Nano*, **2**, 1429 (2008).

Corresponding Author: Masayuki Takeuchi

TEL: +81-29-859-2110, FAX: +81-29-859-2101, E-Mail: TAKEUCHI.Masayuki@nims.go.jp

2-12

Self-Assembly of A Chiral Donor-Acceptor Amphiphilic Dyad For Molecular Design of Photoconducting Materials

○Kentaro Tashiro[1], Yumi Hizume[2], Charvet Richard[1], Yohei Yamamoto[3], Shu Seki[4] and Takuzo Aida[2,3]

[1]*National Institute for Materials Science, Tsukuba 305-0044, Japan*
[2]*Department of Chemistry & Biotechnology, the University of Tokyo, Tokyo 113-8656, Japan*
[3]*JST ERATO-SORST NANOSPACE PROJECT, Tokyo 135-0064, Japan*
[4]*Department of Applied Chemistry, Osaka University, Osaka 565-0871, Japan*

Controlled supramolecular assemblies of donor-acceptor dyads are important for the design of photoconductive and photovoltaic materials. Although stereochemistry of molecules has a lot of effects on the structures of their assemblies, there is no report that studies the stereochemical effects of the components on the physical properties of their assemblies. Here we report novel chiral donor-acceptor amphiphilic dyad **1** (Figure 1) composed of porphyrin and fullerene units. We found that the enantiomers of this compound self-assemble into cylindrical nanofibers with a length up to 10 μm under appropriate conditions. Furthermore, a drop-cast film of these cylindrical nanofibers is photoconductive with ambipolar nature. In contrast, the racemic mixture of this compound self-assembles into spherical objects, whose drop-cast film does not show any photoconduction.

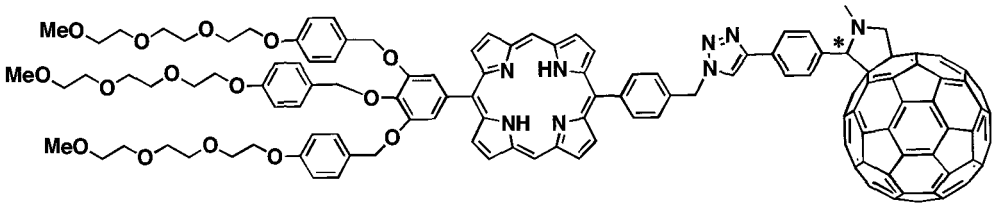

Fig.1 Molecular Structure of Porphyrin-Fullerene Dyad **1**

Corresponding Authors: Takuzo Aida and Kentaro Tashiro
E-mail: TASHIRO.Kentaro@nims.go.jp
Tel +29-851-3354-8429; Fax + 29-860-4706

2-13

Thermo-Responsive Behavior and DNA Photocleavage of Water-Soluble Fullerene/Polymer Complex

Shin-ichi Yusa[1], Shigeki Awa[1], Takeshi Kawase[1], Tadao Takada[1], Kenichi Nakashima[2], Dian Liu[2], Shigeru Yamago[3] and Yotaro Morishima[4]

[1]*Department of Materials Science and Chemistry, Graduate School of Engineering, University of Hyogo, 2167 Shosha, Himeji, Hyogo 671-2280, Japan*
[2]*Departments of Chemistry, Faculty of Science and Engineering, Saga University, Honjo-machi, Saga 840-8502, Japan*
[3]*Institute for Chemical Research, Kyoto University, Uji, Kyoto 611-0011, Japan*
[4]*Faculty of Engineering, Fukui University of Technology, 6-3-1 Gakuen, Fukui 910-8505, Japan*

Water-soluble diblock copolymers, poly(*N*-isopropylacrylamide)-*block*-poly(*N*-vinyl-2-pyrroridone) (PNIPAM$_m$-*b*-PNVP$_n$) with well-defined block lengths were prepared via the organotellurium-mediated radical polymerization (TERP) method (Figure 1). The PNVP block is interacted with fullerene (C_{60}), and hence C_{60} can be solubilized in water with the diblock copolymer to form the C_{60}/PNIPAM$_m$-*b*-PNVP$_n$ complex. The complex formed core-shell micelle-like aggregate comprising the hydrophobic core of C_{60}/PNVP and thermoresponsive PNIPAM shell. Thermoresponsive behavior of the complex was studied by temperature dependence on percent transmittance, light scattering, ^{1}H NMR measurements. The hydrodynamic radius (R_h) of the complex slightly increases with increasing temperature due to the hydrophobic interaction between dehydration of the PNIPAM chains above the lower critical solution temperature (LCST). ^{1}H NMR data suggest that the motion of PNIPAM block is restricted above LCST due to dehydration of the PNIPAM block in water. It is known that photoexcited C_{60} is a highly efficient photosensitizer to produce singlet oxygen. The singlet oxygen was generated on irradiation of the C_{60}/PNIPAM$_m$-*b*-PNVP$_n$ complex in water, which was confirmed by the 9,10-anthracenedipropionic acid (ADPA) bleaching experiments. Furthermore, to clarify the effective singlet oxygen actually responsible for the biological action of photoexcited C_{60}, the DNA cleaving experiments were performed under the several conditions. The complex can cleave DNA under visible light irradiation. Pharmaceutical application of the C_{60} complex to cancer photodynamic therapy (PDT) appears promising.

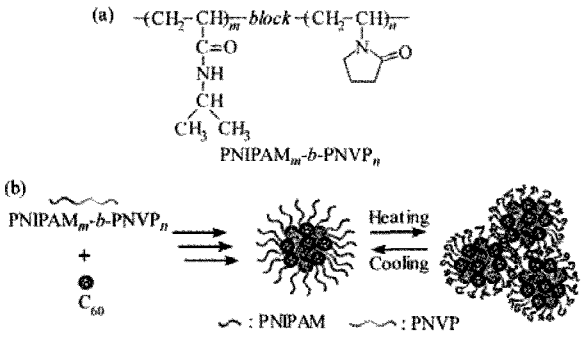

Figure 1. (a) Chemical structure of thermoresponsive diblock copolymer (PNIPAM$_m$-*b*-PNVP$_n$) used in this study. (b) Conceptual illustration of complexation of PNIPAM$_m$-*b*-PNVP$_n$ with C_{60} and thermoresponsive behavior of the complex.

Corresponding Author: Shin-ichi Yusa
E-mail: yusa@eng.u-hyogo.ac.jp
Tel&Fax: +81-79-267-4954, +81-79-266-8868

2-14

Design of Fullerene/PEG-b-polyamine Complex for Nanomedicine

○Yukio Nagaskai, Ryosuke Kodaka

Graduate School of Pure and Applied Sciences, Tsukuba Research Center for Interdisciplinary Materials Science (TIMS), Center for Tsukuba Advanced Research Alliance (TARA), Satellite Laboratory of International Center for Materials Nanoarchitechtonics, National Institute for Materials Science and Master's School of Medical Sciences, Graduate School of Comprehensive Human, University of Tsukuba, Tennoudai 1-1-1, Tsukuba, Ibaraki 305-8573, Japan.

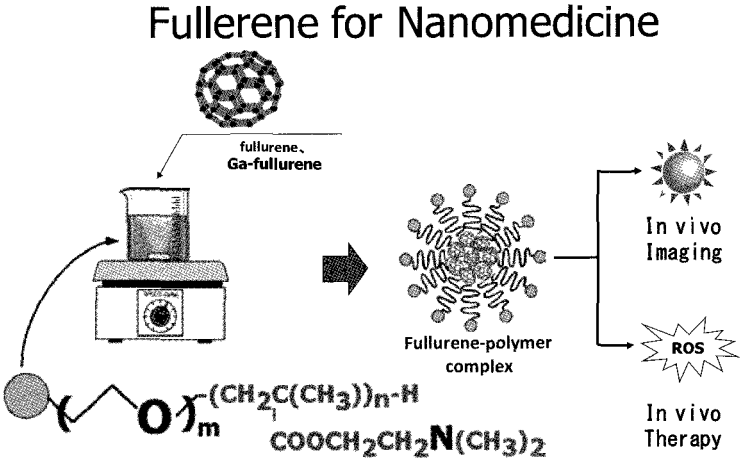

Fullerene, C60 has attracted much attention due to its unique cage structure, chemical and physical properties. In addition, fullerenes and their derivatives exhibit high biological activity in vitro and in vivo. Their poor solubility behavior in aqueous media, however, prevents their biological applications. The objective of this study was to improve the solubility of fullerene using our original water soluble block copolymer, acetal- poly(ethylene glycol)-b-poly(N,N-dimethylaminoethyl methacrylate) (acetal-PEG-b-PAMA) block copolymer. The acetal-PEG-b-PAMA thus prepared can be utilized for a solubilization of fullerenes in aqueous media with the size of several nanometer (Figure 1). The obtained complex was fairly high dispersion stability at high ionic strength. The complex was confirmed to show an oxidization ability of superoxide(Figure 2). When Ga incorporated-fullerene was used, the pH dependent relaxation time of water molecule was observed(data now shown).

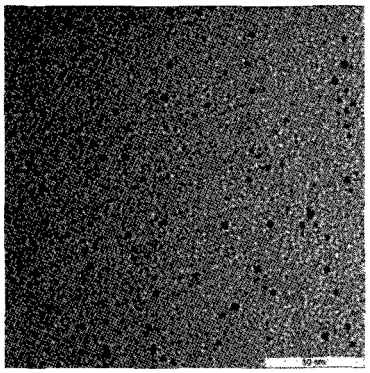

Figure 1. Transmission electron microscope image of C60/acetal-PEG-b-PAMA complex

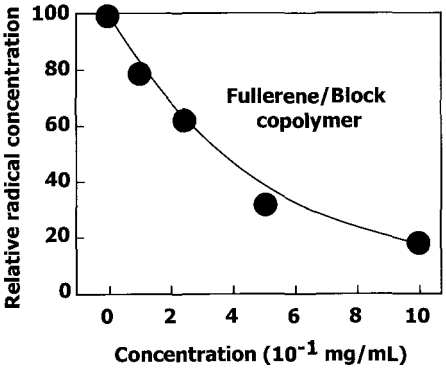

Figure 2. Quenching of superoside by C60/acetal-PEG-b-PAMA complex

Corresponding Author: Yukio Nagasaki
e-mail yukio@nagalabo.jp, Tel&Fax +81-29-853-5749

2-15

TNFα-induced NFκB activation is attenuated by Fullerene Derivatives

○ Takumi Inoue[1] , Masayuki Ito[2] , Shuichi Yamana[2] , Kyoko Takahashi[1] , Shigeo Nakamura[1] , Tadahiko Mashino[1]

[1]*Department of Pharmaceutical Sciences, Faculty of Pharmacy, Keio University, Tokyo 105-8512, Japan*
[2]*Vitamin C60 BioResearch Corporation, Tokyo 103-0028, Japan*

Inflammatory response is one of the biological defence systems against foreign substances including bacterial infection and is usually activated when they invade into the body. But excessive inflammation damages self tissue and exerts a harmful influence on the body. Recently, nuclear factor κB(NFκB), one of the major transcriptional factor in the inflammatory signal pathway, has been revealed that its transcriptional activation is regulated by reactive oxygen species(ROS) [1].

Until now, we have focused on redox property of fullerene and have synthesized various soluble fullerene derivatives. We have already reported that fullerene bismalonic acid derivative (**1**) and bispiperadinium derivative (**2**) (Fig. 1) showed high antioxidative properties [2]. So we investigated inhibition of NFκB transcriptional activation by these fullerene derivatives. As a result, these derivatives significantly attenuated tumor necrosis factor α (TNFα)-induced expression of inflammatory chemokine (CCL2/MCP-1). Moreover, these derivatives showed low cell cytotoxicity. We also evaluated inhibition of NFκB transcriptional activation by Radical Sponge®, fullerene solubilized by polyvinylpyrrolidone (PVP) and used ingredient of cosmetics. As a result, Radical Sponge® significantly attenuated CCL2/MCP-1 expression and the effect was not caused by PVP (Fig. 2). These results suggest that fullerene is potent lead compound against inflammatory diseases.

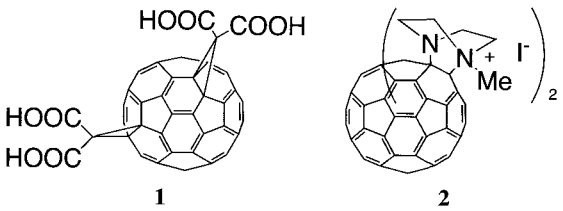

Fig. 1 Fullerene derivatives

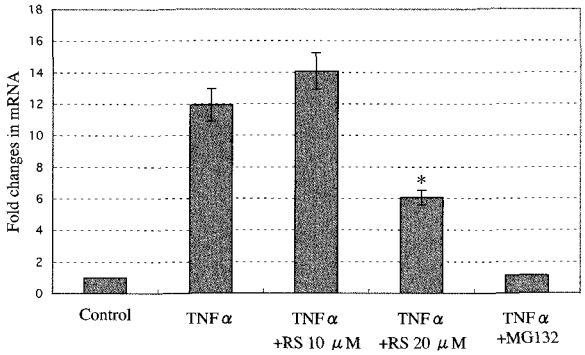

Fig. 2 Inhibition CCL2/MCP-1 expression by Radical Sponge®; * $p < 0.02$ (v.s. TNFα)

[1] A. Bowie, L. A. J. O'Neill, *Biochem Pharmacol.*, **2000**, *59*, 13-23.
[2] K. Okuda, T. Mashino, M. Hirobe, *Bioorg. Med. Chem. Lett.*, **1996**, *6*, 539-542.

Corresponding Author: Tadahiko Mashino
E-mail: mashino-td@pha.keio.ac.jp
Tel: +81-3-5400-2694, **Fax:** +81-3-5400-2691

2-16

Production and Characterization of $LaYC_{80}$

○Takeshi Kodama[1], Daisuke Kakeda[1], Wataru Fujita[1], Koichi Kikuchi[1],
Shinzo Suzuki[2], Yohji Achiba[1]

[1]*Department of Chemistry, Tokyo Metropolitan University, Hachioji, 192-0397, Japan*
[2]*Department of Physics, Kyoto Sangyo University, Kamigamo-Motoyama, Kita-ku, Kyoto, 603-8555, Japan*

So far, two types of di-metllofullerenes have been reported: one is that two metal atoms are encapsulated mainly in C_{78} and C_{80} cage, and the other is that two metal atoms are encapsulated in different carbon cages, such as C_{82} and C_{84}. For the former case, La_2C_{78}, La_2C_{80}, Ce_2C_{78}, and Ce_2C_{80} are representative, and for the latter case, Y_2C_{82}, Y_2C_{84}, Er_2C_{82}, and Er_2C_{84} are representative. As for the case of the hetero two metal atoms encapsulation, two different metal atoms that favor the same type of carbon cage are encapsulated in the favorite cages, such as $LaCe\underline{C_{80}}$ and $ErY\underline{C_{82}}$. Until now, the production of the hetero-di-metallofulleres whose two metal atoms favor the different type of carbon cage has not been reported.

In this study, we tried to produce the hetero-di-metallofullerene with the combination of two different type of metals, La and Y, and investigated the following two points; 1) whether $LaYC_n$ is produced or not, and 2) if produced, which type of cage structure is favorably formed, or both type of cage structure are formed.

Soot containing metallofullerenes was produced by direct-current (65A) arc discharge of La/Y/C composite rods (La:Y:C=1:1:98) under a 500 torr He atmosphere. Both empty fullerenes and metallofullerenes were extracted from the raw soot by refluxing with 1,2,4-trichlorobenzene for 8h. The extract was separated by multi-stage high performance liquid chromatography (HPLC). The presence of $LaYC_n$ was investigated by LD-TOF-MS.

The presence of La-Y combination encapsulated in fullerene cage was confirmed as $LaYC_{80}$ species by MS. In the HPLC separation, the $LaYC_{80}$ appears at the same retention time as Y_2C_{80}, not as La_2C_{80}. This result suggests the cage structure of $LaYC_{80}$ is identical to Y_2C_{80}, not to La_2C_{80}.

Corresponding Author: Takeshi Kodama
E-mail: kodama-takeshi@c.metro-u.ac.jp
Tel:+81-42-677-2530, Fax:+81-42-677-2525

2-17

Two Step Regioselective Exohedral Functionalization of Endohedral Metallofullerene

○Satoru Sato,[a] Yutaka Maeda,[b] Koji Inada,[b] Hidefumi Nikawa,[a] Michio Yamada,[a] Naomi Mizorogi,[a] Tadashi Hasegawa,[b] Takahiro Tsuchiya,[a] Takeshi Akasaka,*[a] Tatsuhisa Kato,[c] Zdenek Slanina,[a] Shigeru Nagase[d]

[1]Center for Tsukuba Advanced Research Alliance, University of Tsukuba, Tsukuba, Ibaraki 305-8577, Japan, [2]Department of Chemistry, Tokyo Gakugei University, Koganei, Tokyo 184-8501, Japan, [3]Department of Chemistry, Josai University, Sakado, Saitama 350-0295, Japan, [4]Department of Theoretical and Computational Molecular Science, Institute for Molecular Science, Okazaki, Aichi 444-8585, Japan

Endohedral metallofullerenes have attracted much attention because of their novel properties due to the intramolecular electron transfer between the metal atom and the fullerene cage.[1] Structural analyses of mono-adducts of endohedral metallofullerenes reveal how the chemical reactivity and selectivity of empty fullerenes change upon endohedral metal-doping and how the electronic properties of endohedral metallofullerenes change upon chemical functionalization. We have reported highly regioselective reactions of La@C_{82} and demonstrated that the local strain and charge density on the carbons control the reactivity toward nucleophilic[2] and electrophilic[3] reagents. Multiple functionalization of fullerenes has become an important topic because regioselectivity provides fundamental information about their chemical properties. Moreover, it would be attractive for practical application of fullerenes.

Herein, we present the formation of bis-adducts of La@C_{82} with different addenda. We chose 1,2,3,4,5-pentamethylcyclopentadiene (Cp*) and 2-adamantane-2,3-[3H]-diazirine (AdN_2) as reactants because cyclopentadiene (Cp) and AdN_2 afford the corresponding regioselective mono-adducts of La@C_{82}.[2,4] The addition position of Cp has not been clarified yet because the retro reaction of La@C_{82} with Cp proceeds readily at room temperature.[4] In this work, structural analysis of the mono-adduct of La@C_{82} with Cp* was also conducted.

The bis-adducts of La@C_{82} with Cp* and adamantylidene were synthesized by two different route (Scheme) and characterized. Furthermore, the addition position and the regioselectivity in functionalization of La@C_{82} derivatives were also discussed on the basis of spectroscopic analysis and theoretical calculation.

Scheme

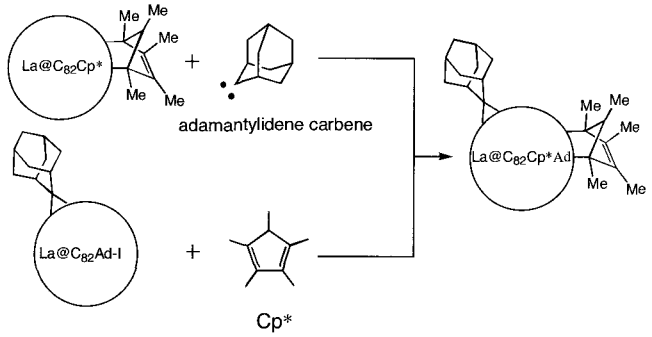

References:

[1] *Endofullerenes: A New Family of Carbon Clusters*; Akasaka, T., Nagase, S., Eds.; Kluwer Academic Publishers: Dordrecht, The Netherlands, 2002. [2] Y. Maeda, et al., *J. Am. Chem. Soc.* 2004, **126**, 6858. [3] L. Feng, et al., *J. Am. Chem. Soc.* 2005, **127**, 17136. [4] Y. Maeda, et al., *J. Am. Chem. Soc.* 2005, **127**, 12190.

Corresponding Author: Takeshi Akasaka
E-mail: akasaka@tara.tsukuba.ac.jp **TEL & FAX**: +81-29-853-6409

3-1

Ultrafast exciton level modulation due to coherent optical nonlinearity in isolated semiconducting SWNTs

○Shoichi Tao[1], Yasumitsu Miyata[2], Kazuhiro Yanagi[3], Hiromichi Kataura[4] and Hiroshi Okamoto[1,5]

[1]*Department of Advanced Materials Science, Univ. of Tokyo, Kashiwa 277-8561, Japan*
[2]*Department of Chemistry, Nagoya University, Nagoya 464-8602, Japan*
[3]*Department of Physics, Tokyo Metropolitan University, Hachioji 192-0397, Japan*
[4]*Nanotechnology Research Institute, National institute of Advanced Industrial Science and Technology, Tsukuba 305-8562, Japan*
[5]*CREST, Japan Science and Technology Corporation, Kawaguchi 332-0012, Japan*

Optical nonlinearity is one of the most attracting properties of SWNTs because exciton absorption in bundled SWNTs shows large absorption saturation and short relaxation time ~1 picosecond (ps) of excition transitions. However, it is well known that relaxation time of excitons in isolated SWNTs is on the order of 10 ps and is much longer than that of bundled tubes. This difference arises from the lack of exciton/charge transfer from semiconducting tubes to metallic tubes.

Recently, it has been reported that large coherent optical nonlinearity occurs in semiconducting SWNTs and dominates their nonlinear responses even under the resonant excitation conditions [1]. This phenomenon was attributed to the optical Stark effect and characterized by a photoinduced shift of exciton transition due to strong exciton-photon coupling [2, 3]. This coherent optical nonlinearity appears only during an irradiation of a laser pulse, so that it would be a possible mechanism for sub-ps optical switching.

In this study, we have investigated ultrafast coherent nonlinear optical responses in well-isolated semiconducting SWNTs (micellar suspension of CoMoCAT SWNTs in gelatin) using femtosecond pump-probe spectroscopy. The sample in this study shows sharper absorption peaks and lower absorption background than samples in previous studies, so that we can observe fine structures of photoinduced absorption changes, which are often obscured by inhomogeneous broadening of the absorption spectra.

Transient absorption change spectra were measured under various excitation energies. For all excitation energies, large absorption change appears just after the photoexcitation and disappears within 0.2 ps. Such ultrafast absorption changes are attributable to the coherent optical nonlinearity. The detailed spectral analyses have revealed that the observed spectral changes consist of not only the blue shift of exction transition due to the optical Stark effect but also the spectral broadening. The broadening signal is attributable to the effect of exciton-exciton scattering. It should be emphasized that such a broadening-type coherent nonlinear optical response is observed for the first time not only in SWNTs but also in semiconductor quantum structures. The physical mechanisms of these two responses will be discussed on the basis of the excitation energy dependence of transient absorption changes.

[1] A. Maeda *et al.*, Phys. Rev. Lett. **94**, 047404 (2005).
[2] A. Maeda *et al.*, J. Phys. Soc. Jpn. **75**, 043709 (2006).
[3] S. Matsumoto *et al.*, Jpn. J. Appl. Phys. **45**, L513 (2006).

Corresponding Author: Shoichi Tao
E-mail: tao@okalab.k.u-tokyo.ac.jp Tel&Fax: +81-4-7136-3773

3-2

Excited Carrier Diffusion for Bundle of Semiconductive and Metallic Carbon Nanotubes: Time-Dependent Density Functional Calculations

○Takazumi Kawai, Yoshiyuki Miyamoto

Nano Electronics Research Laboratories, NEC Corporation, 34 Miyukigaoka, Tsukuba 305-8501, Japan

There is no fluorescence from the bundle of carbon nanotubes. The reason is understood by the transport of excited carrier from semiconductive to metallic carbon nanotubes in the same bundle [1]. However, the actual mechanism of carrier diffusion is not clarified, where the excited carrier (hole and charge) should diffuse over the inter-wall distance of 3.4 A.

Using time-dependent density functional method [2,3], we demonstrate the time-evolution of carrier diffusion for the bundle of (8,0) and (9,0) nanotubes. Throughout the molecular dynamics simulations at room temperature, we found that the excited states in the (8,0) nanotube hybridize to those of the (9,0) nanotube. Those hybridizations suggest easy transport of excited carriers through the metallic nanotube. We will further present the dynamics of the carrier diffusion in detail.

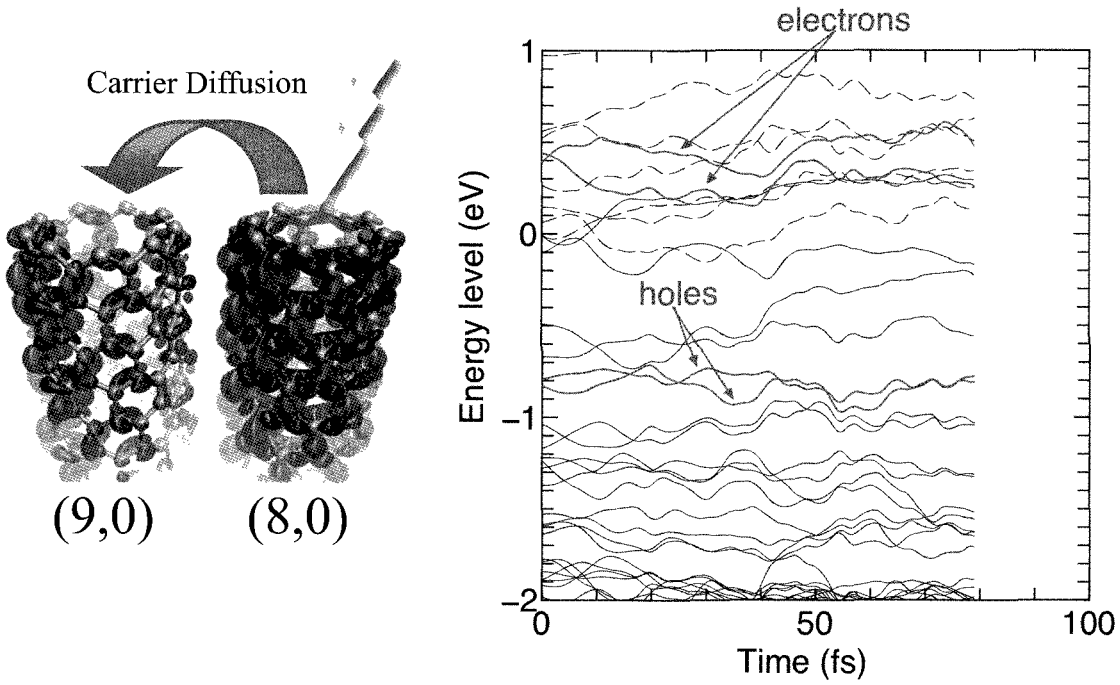

References

[1] M.J. O'Connell, et al., Science 297 (2002) 593.

[2] O. Sugino and Y. Miyamoto, Phys. Rev. B 59, 2579 (1999).

[3] Y. Miyamoto, A. Rubio, and D. Tomanek, Phys. Rev. Lett. 97, 126104 (2006).

Corresponding Author: Takazumi Kawai

E-mail: takazumi-kawai@mua.biglobe.ne.jp

Tel&Fax: 029-850-1554 (029-856-6136)

3-3

The fastest high definition Raman imaging of carbon nanotubes bridged between electrodes

○Tomoya Uchiyama[1], Minoru Kobayashi[1], Taisuke Ota[1] and Masamichi Yoshimura[2]

[1]*Nanophoton Corporation, Suita 565-0871, Japan*
[2]*Research Center for Local Structural Control, Toyota Technological Institute, Nagoya 468-8511, Japan*

The Raman spectrum of carbon nanotube (CNT) contains a wealth of information such as the radial breathing modes (RBMs), G- and G+-band and D-band. The conventional Raman instruments detect an extremely weak Raman signal from one point on the sample, and as a result, it takes huge time to construct high-definition Raman spectral images. The innovative technology which enables the high speed Raman imaging has been needed to meet the needs of CNTs distribution imaging.

We developed a new laser Raman microscope by combining the line illumination and multi-spectrum simultaneous measurement. By using this method, the incident laser can excite the Raman scattering from the sample surface along the line illuminated area and measure it as 400 Raman scattered lights while each light is dispersed spectrally by 1340-400 pixels electrically cooled CCD detector. Additionally, our Raman microscope scans the line-shaped laser by laser beam scanning method and realizes high-speed and vibration-free imaging compared to the stage scanning method. We developed original optics (patented) to avoid a non-uniform intensity illumination along the line caused by the cylindrical lens (conventional line illumination method). Also, we adopted slit confocal optics to keep the three-dimensional spatial resolution when we use line illumination. By these means, we succeeded in speeding up the Raman imaging speed about several hundred times faster than that of conventional method while keeping the high definition imaging performance.

CNTs distribution between electrodes is previously imaged by using scanning electron microscope; however it cannot tell us the property of CNTs. We observed the distribution of CNTs bridged between electrodes by our Raman microscope and obtained the high definition Raman image at a diffraction-limited resolution of 532nm excitation laser in only 8 minutes. The Raman image reveals not only the distribution of CNTs bridged between electrodes but also the distribution of CNTs which have a different RBM peak with high S/N.

Corresponding Author: Tomoya Uchiyama
TEL: +81-6-6878-9911, FAX: +81-6-6878-9912, E-mail: uchiyama@nanophoton.jp

3-4

Stability and optical properties of oligo-DNA /Single-walled carbon nanotube hybrids

○Yuki Yamamoto[1], Tsuyohiko Fujigaya[1], Naotoshi Nakashima[1,2]

[1]*Department of Applied Chemistry, Graduate School of Engineering, Kyushu University, Fukuoka 819-0395, Japan*
[2]*Science and Technology Agency, CREST, 5 Sanbancho, Chiyoda-ku, Tokyo 102-0075, Japan*

Since the discovery that double-strand DNA (dsDNA)[1]-[3] and single-strand DNA (ssDNA)[4] solubilize single-walled carbon nanotubes (SWNTs) in water, many groups have endeavored to understand the fundamental properties of the SWNTs/DNA nanobio hybrids and their applications in nano- and nanobio-related materials science. However, one must pay attention to the fact that large amounts of unbound (free) DNA molecules exist in SWNTs/DNA aqueous solutions. Are the hybrids containing no free DNAs in the bulk stable enough for use in many experiments? Do we need to consider the desorption of the bound DNA molecules from the hybrids to the bulk solutions to reach thermodynamic equilibrium? We undertake this fundamental issue in the present study. For this purpose, we first completely separated free dsDNA from an aqueous solution of the DNA/SWNT hybrids using size exclusion chromatography (SEC), and then examined the stability of the bulk DNA-free SWNTs/dsDNA hybrids using SEC. In our previous work, we found that the bulk DNA-free SWNTs/dsDNA solutions are stable for more than one month[4]. DNA we used then was native DNA (about 300 bp). In this work, we carried out the same measurement using oligo-DNA (20 mer) instead of native DNA. Consequently, SWNTs/oligo-DNA hybrids have been found to be stable in water for at least a month. Oligo-DNA is length- and sequence-controllable and SWNTs/oligo-DNA hybrids is expected to be used for various applications. This observation indicates that we virtually need not consider the desorption of bound oligo-DNA from the nanohybrids in water for at least a month, which is of great advantage to the utilization of the hybrids in wide areas of science.

[1] N. Nakashima, S. Okuzono, H. Murakami, T. Nakai and K. Yoshikawa. *Chem. Lett.*,**32**, 456 (2003).
[2] Y. Noguchi, T. Fujigaya, Y. Nidome and N. Nakashima, *Chem. Eur. J.*, **14**, 5966 (2008)
[3] Y. Noguchi, T. Fujigaya, Y. Nidome and N. Nakashima, *Chem. Phys. Lett.*, **455**, 249 (2008)
[4] M. Zheng, A. Jagota, E. D. Semke, B. A. Diner, R. S. Mclean, A. R. Lusitg, R. E. Richardson and N. G. Tassi, *Nature Mater.*, **2**, 338 (2003)
Corresponding Author: Naotoshi Nakashima
Tel/FAX: +81-92-802-2840, E-mail: nakashima-tcm@mail.cstm.kyushu-u.ac.jp

3-5

Fermi energy dependence of radial breathing mode in metallic single-wall carbon nanotubes

* Jin Sung Park[1], Kenich Sasaki[2], Riichiro Saito[1], Gene Dressselhaus[3], Mildred S. Dresselhaus[3]

[1] Tohoku University, Japan, [2] NIMS, Japan, [3] Massachusetts Institute of Technology, Cambridge, MA 02139-4307, USA

The radial breathing mode (RBM) of single-wall carbon nanotubes (SWNTs) arises from the first-order, one-phonon and intra-valley Raman scattering process, which is used to assign the diameter and chirality of a SWNT. For metallic SWNTs, the curvature effect induces a small energy gap except for armchair SWNTs. Since the curvature-induced energy gap is similar to the RBM phonon energy for nanotubes with diameter range, $0.7<d_t<2$ nm (15~40 meV), the curvature-induced energy gap may affect the phonon softening of the RBM, so called the Kohn anomaly effect. The Kohn anomaly effect can be explained by the self-energy correction to the RBM phonon mode in which the virtual excitation of an electron-hole pair causes a softening of the RBM phonon frequencies. Recently an experimental group has observed the Fermi energy (E_F) dependence of the phonon-softening effect of M-SWNTs by electrochemical doping, and their result clearly shows the RBM phonon softening as a function of E_F [1]. The frequency shift of the RBM is produced by electron-phonon interaction [2]. The RBM Raman spectrum for the M-SWNTs depends on chirality and diameter. While a zigzag SWNT shows the maximum RBM frequency shift, an armchair SWNT does not show any frequency shift. It has been known that the k-dependent electron-phonon (el-ph) interaction of the RBM gives rise to the chirality dependence [3]. Although the RBM Raman intensity has been calculated by the el-ph and electron-photon (el-op) interactions, the RBM Raman spectra has not been calculated yet. In this paper, the RBM Raman spectra will be shown by including the Kohn anomaly effect and the resonance window values [4]. Further we will consider exciton-phonon and exciton-photon interactions, too, and compare the calculated results with those by el-ph and el-op interactions. The Fermi energy dependence of the RBM Raman spectra for metallic nanotubes is also directly compared to the experiment in which the Kohn anomaly effect appears by change of the gate voltage.

Reference:

[1] H. Farhat et al., Phys. Rev. Lett., 102, 126804 (2009).

[2] K. Sasaki et al., Phys. Rev. B, 78, 235405 (2008).

[3] J. Jiang et al., Phys. Rev. B, 72, 235408 (2005).

[4] J. S. Park et al., Phys. Rev. B, 74, 165414 (2006).

Corresponding Author:

Email: park@flex.phys.tohoku.ac.jp

3-6

Photosensitized Hydrogen Evolution from Water Using Fullerodendron/SWNT Supramolecular Nanocomposite

○Yutaka Takaguchi, Wakako Sakata, Tomoyuki Tajima

Graduate School of Environmental Science, Okayama University, Okayama 700-8530, Japan

Since their discovery in 1991[1], single-walled carbon nanotubes (SWNTs) have attracted intensive interest because of their peculiar one-dimensional structure with the rolled-up graphene sheet in nanoscale diameter. Despite their intensive application to devices such as solar cells, fuel-cell electrodes, microactuators, and sensors, SWNTs have not yet been explored as an active component in sensitizing the H_2 evolution from water owing to insolubility in water. Recently, we have reported SWNTs easily dispersed in water via supramolecular nanocomposite formation with fullerodendron[2]. Here we report the fabrication of silica-composite of SWNTs/fullerodendron supramolecular nanocomposite and highlight their high activities for the photosensitized H_2 evolution from water. To our best knowledge, this is the first example of photocatalytic H_2 evolution using SWNTs nanocomposites.

High-efficiency light-driven hydrogen evolution from water was demonstrated by using supramolecular nanocomposites, SWNT/fullerodendron (**1**) and SWNT/fullerodendron/SiO_2 (**2**), of which structures were shown in Figure 1. Under visible light irradiation ($\lambda > 420$ nm), photocatalytic water reduction for hydrogen generation was achieved using photocatalyst (**1**) or (**2**) in the presence of a mixture of methyl viologen (MV^{2+}), 1-benzyl-1,4-dihydronicotinamide (BNAH; sacrificial electron donor), and a colloidal PVA-Pt.

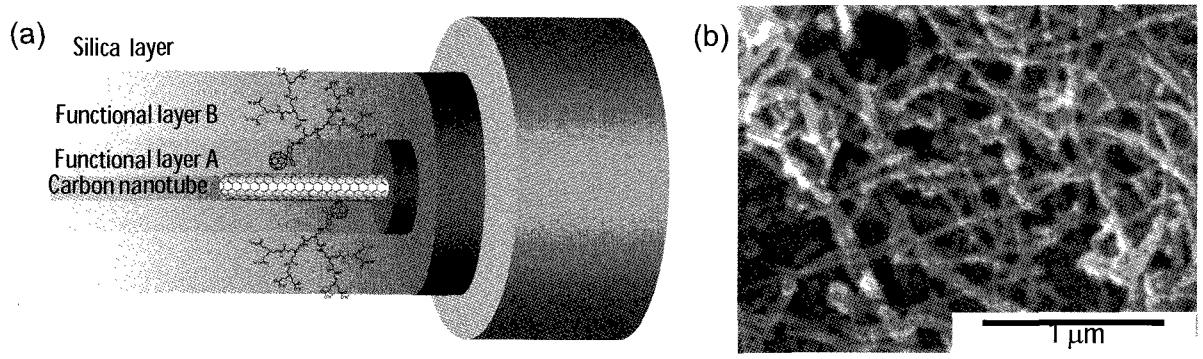

Figure 1. (a) Schematic illustration of SWNT/fullerodendron/SiO_2 nanocomposite (**2**). (b) SEM image of the nanocomposite (**2**).

[1] S. Iijima, *Nature*, **1991**, 354, 56.

[2] Y. Takaguchi, M. Tamura, Y. Sako, Y. Yanagimoto, S. Tsuboi, T. Uchida, K. Shimamura, S. Kimura, T. Wakahara, Y. Maeda and T. Akasaka, *Chem. Lett.*, **2005**, 34, 1608.

Corresponding Author: Yutaka Takaguchi
TEL: +81-86-251-8903, FAX: +81-86-251-8903, E-mail: yutaka@cc.okayama-u.ac.jp

3-7

Composite Clusters of Higher Fullerenes and Single-Walled Carbon Nanotubes

○Tomokazu Umeyama[1], Noriyasu Tezuka[1], Yoshihiro Matano[1] and Hiroshi Imahori[1,2]

[1]*Graduate School of Engineering, Kyoto University, Kyoto 615-8510, Japan*
[2]*Institute for Integrated Cell-Material Sciences, Kyoto University, Kyoto 615-8510, Japan*

The cluster formation, electrophoretically deposited film structures, and photoelectrochemical properties of the composites consisting of single-walled carbon nanotube (SWNT) with C_{60}, C_{70}, or C_{84} have been systematically compared for the first time. In *ortho*-dichlorobenzene (ODCB)–acetonitrile mixture, the higher fullerenes (i.e., C_{70} and C_{84}) were found to form single composite clusters exclusively with highly soluble SWNT with bulky swallow-tailed substituents (f-SWNT), which is in marked contrast with the unselective formation of three different clusters in the C_{60}–f-SWNT composites [1]. The density functional theory calculations supported the preference of complexation between C_{70} and SWNT. Electrophoretic deposition of the composite clusters yielded the corresponding films on nanostructured SnO_2 electrodes (denoted as FTO/SnO_2/$(C_{70}$+f-SWNT$)_m$ and FTO/SnO_2/$(C_{84}$+f-SWNT$)_m$, Figure 1). The C_{70}–f-SWNT photoelectrochemical device exhibited the highest incident photon-to-current efficiency (IPCE) value (26% at 400 nm) ever reported for analogous SWNT-based photoelectrochemical cells. The highest IPCE value results from selective formation of the single composite film, in which the SWNT network is covered with C_{70} molecules, and the high electron mobility (2.4 cm^2 V^{-1} s^{-1}) through the C_{70}–SWNT network. On the other hand, similar selective complexation of C_{84} with f-SWNT led to the poor IPCE value (4.8% at 400 nm) because of the inability of C_{84} radical anion to donate electrons to the conduction band (CB) of f-SWNT as well as the poor electron injection from C_{84} radical anion to the CB of the SnO_2 electrode.

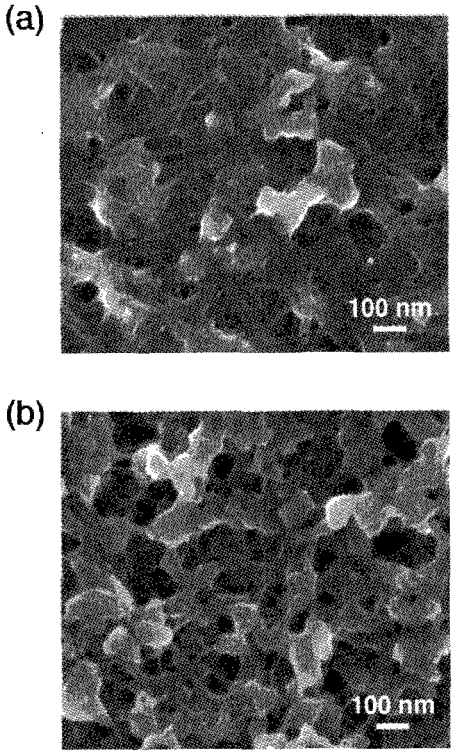

Figure 1. FE-SEM images of (a) FTO/SnO_2/$(C_{70}$+f-SWNT$)_m$ and (b) FTO/SnO_2/$(C_{84}$+f-SWNT$)_m$ electrodes.

References: [1] (a) Umeyama, T.; Tezuka, N.; Fujita, M.; Hayashi, S.; Kadota, N.; Matano, Y.; Imahori, H. *Chem. Eur. J.* **2008**, *14*, 4875-4885. (b) Umeyama, T.; Imahori, H. *Energy Environ. Sci.* **2008**, *1*, 120-133.

Corresponding Author: Tomokazu Umeyama
E-mail: umeyama@scl.kyoto-u.ac.jp
Tel: +81-75-383-2568, Fax: +81-75-383-2571

3-8

Brain wave detection using a multi-wall carbon nanotube film sensor

○Akira Kawamoto[1], Ryuhei Kitai[2], Toshihiko Kubota[2]

[1]*Department of Electrical and Electronic Engineering, Fukui National College of Technology, Geshi, Sabae, Fukui 916-8507, Japan*

[2]*Department of Neurosurgery, Fukui University, 23-3 Matsuoka, Eiheiji, Fukui 910-1193, Japan*

In order to operate safely on the brain in accordance with the surgical plan, both morphological and functional information should be intraoperatively monitored. Brain morphology can be imaged in real time by X-ray computed tomography (CT) or magnetic resonance imaging (MRI). Conversely, functional information comprising electrophysiological data is obtained from the relevant brain regions and the cranial nerves using a disk electrode to record electroencephalic activity. To date, disk electrodes have been made from silver; however, silver distorts X-ray CT and MRI-generated images, preventing visualization of areas in the vicinity of the electrodes. Fig. 1 shows the resulting artifact in an X-ray CT image. X-ray permeability around the silver disk electrode is reduced, causing the area in the electrode shadow to be represented as white lines (artifact) radiating out from the electrode. This hinders the operative procedure. Furthermore, the multiple silver disk electrodes currently utilized during surgery are reused repeatedly due to their high cost. This poses the danger of inter-patient infection, including viral hepatitis C. Therefore, there is a need for the development of novel electroencephalographic electrodes to overcome these issues.

In the present study, we constructed film sensors (electroencephalographic electrodes) from multi-wall carbon nanotube-dispersed polymethylmethacrylate (PMMA) thin films. These films were prepared using a solution casting method on Teflon FEP substrates whereby a mixture of PMMA, multi-wall carbon nanotubes and methyl ethyl ketone were dispersed onto thin film using ultrasonic waves. We found that film sensors using multi-wall carbon nanotubes can detect encephalographic activity without distorting X-ray CT or MRI images and actually exhibit greater detection sensitivity than conventional silver disk electrodes. They can also be disposed of after a single use [1].

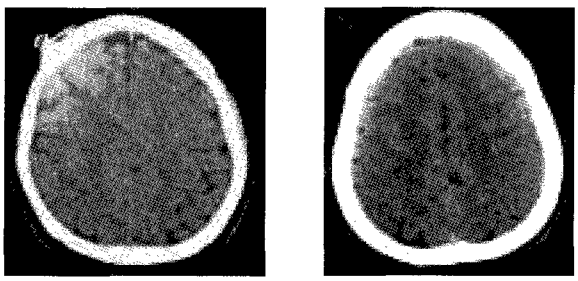

(1) Artifact (silver electrode) (2) No Artifact (multi-wall carbon nanotube electrode)

Fig.1. X-ray CT images

References:

[1]A. Kawamoto, R. Kitai, Appl. No.:2009-98098

Corresponding Author: Akira Kawamoto
E-mail:kawamoto@fukui-nct.ac.jp
Tel/ Fax:+81-778-62-2849

3-9

Evaluation of Ar Fast Atom Bombardment Process on Vertically Aligned Carbon Nanotubes

○Masahisa Fujino[1], Tadatomo Suga[1], Junichiro Shiomi[2], Shigeo Maruyama[2]
Ikuo Soga[3], Daiyu Kondo[3], Yoshikatsu Ishizuki[3], Taisuke Iwai[3] and Masataka Mizukoshi[3]

[1]*Department of Precision Engineering, The University of Tokyo, Tokyo 113-8656, Japan*
[2]*Department of Mechanical Engineering, The University of Tokyo, Tokyo 113-8656, Japan*
[3]*FUJITSU Laboratories Ltd. and FUJITSU Ltd., Kanagawa 243-0197, Japan*

Carbon Nanotubes (CNTs), especially Multi-walled Carbon Nanotubes (MWNT) are the high conductivity materials and they are expected to be applied conductive material such as VIA in high-density integrate circuits, but the interconnection between CNTs and metal substrate are still electrically high resistance, hundreds of kOhm, that are provided the catalyst adhesion to the growth substrate, or metal sputtering deposition on CNTs [1]. Therefore, in order to reduce the contact resistance, we suggested direct bonding between CNTs and metal substrate by surface activated bonding (SAB) method, that surface of bonding materials is sputter etched by Ar fast atom beam (FAB) at room temperature [2]. Though this sputter etching removes the surface layer such as contaminations and also activates sputter etched surface, it damages also body layer.

In this research, we evaluated and optimized this FAB process to vertically aligned CNTs with X-ray photoelectron spectroscopy and Raman shift spectroscopy. Vertically aligned CNTs were fabricated by acethylene-CVD with Fe catalyst, which formed MWNTs with 1-2 nm diameter, 120-150 μm height. 1.5 keV - 15 mA energized FAB was processed in ca. 10^{-4} Pa vacuum. Fig.1 (a) shows that Oxygen was removed around 5-7 min. FAB irradiation, and Fig.2 (b) shows that *G/D* ratio decreased from 2.6 to 0.9 by 1min. FAB irradiation, but *G/D* ratio was saturated after 1min. Therefore FAB process for cleaning surface of CNTs was necessary around 5 min.

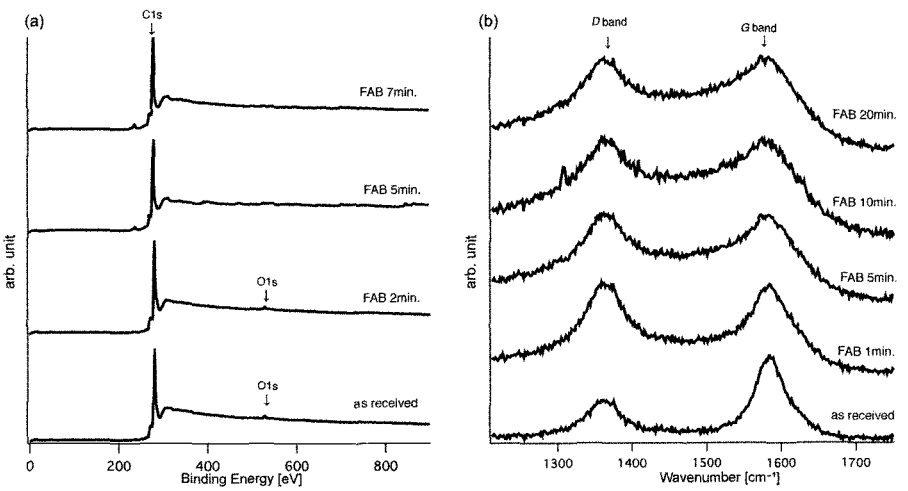

Figure 1 (a)XPS of CNTs (b)Raman Shift Spectra around *G*-band and *D*-band of CNTs

[1] M. Nihei, D. Kondo, A. Kawabata, S. Sato, H. Shioya, M. Sakaue, T. Iwai, M. Ohfuti, and Y. Awano, *Proc. Interconnect Technology Conference 2005*. 234 (2005)
[2] H. Takagi, R. Maeda, N. Hosoda and T. Suga, *Appl. Phys. Lett.*, **74**, 2387 (1999)

Corresponding Author: Masahisa Fujino
TEL: +81-3-5842-6495, FAX: +81-3-5842-6485, E-mail: fujino.masahisa@su.t.u-tokyo.ac.jp

3-10

Electrical Characteristics of DNA Encapsulated Single-Walled Carbon Nanotubes Created in Electrolyte Plasmas

○T. Kaneko, Y. F. Li, and R. Hatakeyama

Department of Electronic Engineering, Tohoku University, Sendai 980-8579, Japan

We direct our attention to the biomolecule such as DNA, as a functional material encapsulated inside single-walled carbon nanotubes (SWNTs) because DNA consists of four kinds of bases, each of which has a different electronic property [1], and the control of the electronic properties in nano scale can be performed by selecting the base sequence of DNA. Since DNA is stable and easily forms negative ions in solution, we apply the ion irradiation method to the electrolyte solutions with DNA which mainly consist of negative (DNA^-) and positive (hydrogen H^+) ions, and neutral particles (H_2O), and consequently can be regarded as "electrolyte plasmas" [2].

After the irradiation of DNA to the SWNTs, the electrical characteristics of the SWNTs are investigated under a field effect transistor (FET) configuration by measuring a source-drain current (I_{DS}) as a function of gate voltage (V_G) or source-drain voltage (V_{DS}). The characteristic of pristine semiconducting SWNTs is well known to exhibit the p-type behavior which is shown as a dotted line in Fig. 1(a), where the characteristic curve of I_{DS} - V_G is described for V_{DS} = 1 V. The characteristic of the C_{30} irradiated SWNTs is presented as a solid line in Fig. 1(a). The typical p-type characteristic is observed, but the threshold voltage for hole conductance is found to shift from −20 V to −10 V compared with that of the pristine SWNTs, indicating that the p-type behavior of the SWNTs is enhanced by the encapsulation of C_{30} as an electron acceptor. In contrast, the characteristic of the G_{30} irradiated SWNTs drastically changes to an n-type semiconductor [Fig. 1(b)]. This n-type characteristic is attributed to the charge transfer between the SWNTs and G_{30} as an electron donor. These phenomena are explained by the difference in work functions between SWNTs and the bases of DNA measured by ultraviolet photoelectron spectroscopy.

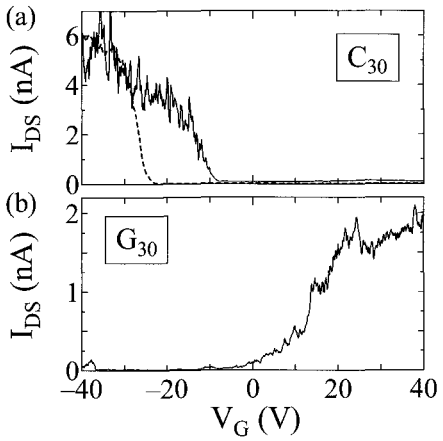

Fig. 1: I_{DS}-V_G characteristics of (a) pristine (dotted line) and C_{30} irradiated (solid line) SWNTs, (b) G_{30} irradiated SWNTs.

[1] D. Kato *et al.*, *J. Am. Chem. Soc.*, **130**, 3716 (2008).

[2] T. Kaneko, T. Okada and R. Hatakeyama, *Contrib. Plasma Phys.*, **47**, 57 (2007).

Corresponding Author: Toshiro Kaneko

TEL: +81-22-795-7046, FAX: +81-22-263-9375, E-mail: kaneko@ecei.tohoku.ac.jp

3-11

Sorting and integration of DNA-wrapped single-wall carbon nanotubes for thin film transistors

○Yuki Asada[1], Yasumitsu Miyata[1], Yutaka Ohno[2], Ryo Kitaura[1], Toshiki Sugai[1*], Takashi Mizutani[2] and Hisanori Shinohara[1]

[1]*Department of Chemistry & Institute for Advanced Research, Nagoya University, Nagoya 464-8602, Japan*
[2] *Department of Quantum Engineering, Nagoya University, Nagoya 464-8603 Japan*

The networks of single-wall carbon nanotubes (SWCNTs) have attracted much attention because of their potential applications in thin film transistors (TFTs) and chemical/biological sensors. To realize high-performance devices, it is essential to control the chirality, length, and the extent of aggregation of SWCNTs and to develop a preparation method of their networks. Here we show that the DNA-wrapped SWCNTs (DNA-SWCNTs) provide an effective way to fabricate the uniform networks of highly isolated, structure-sorted nanotubes for TFTs. In this work, the SWCNTs were dispersed with commercial salmon DNA in water and separated by length incorporating size-exclusion high-performance liquid chromatography (HPLC, COSMOSIL CNT columns, nacalai tesque Inc.). To fabricate TFTs, DNA-SWCNT network was formed on an amino-coated SiO_2 substrate, followed by depositing Au/Ti electrodes on it. Figure 1 shows an AFM image of the network, indicating that the nanotubes deposited are individual SWCNTs. Figure 2 presents the typical output characteristic of DNA-SWCNT TFTs. The devices show p-type behavior with an on/off ratio of 10^5. In this presentation, the detailed characteristics of DNA-SWCNT TFTs will be discussed.

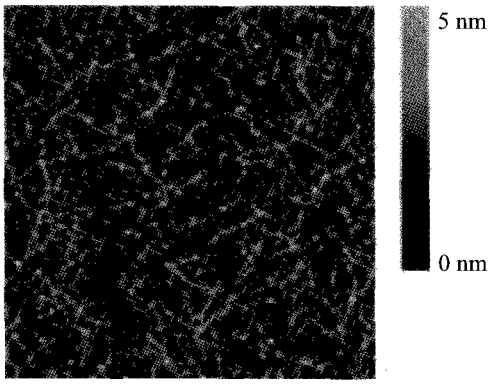

Figure 1. AFM image of DNA-SWCNT networks. The scale bar is 500 nm.

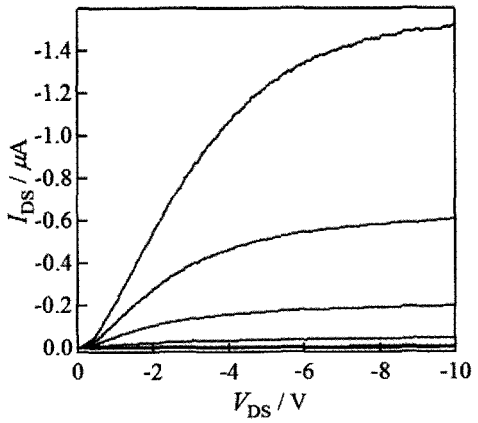

Figure 2. Output characteristic of DNA-SWCNT TFT measured at gate voltages of -10 (top) to 0 V (bottom) in 2 V steps.

* Present address: Department of Chemistry, Toho University
Corresponding Author: Hisanori Shinohara
E-mail: noris@nagoya-u.jp, **TEL**: +81-52-789-2482, **FAX**: +81-52-747-6442

3-12

[60]-Fullerene and Single-Walled Carbon Nanotube-Based Hybrid Ultrathin Films on ITO

○Qiguan Wang[1], Hiroshi Moriyama[1,2]

[1]*Research Center for Materials with Integrated Properties, Toho University, Miyama 2-2-1, Funabashi, 274-8510 Japan*
[2]*Deparment of Chemistry, Toho University, Miyama 2-2-1, Funabashi, 274-8510 Japan*

Because carbon nanotubes and fullerenes both showed photocurrent generation effects [1.2], the combination of these two carbon allotropes, has been extensively investigated by different methods. The C_{60} or SWNT films on an optically transparent electrode were generally prepared using electrophoretic deposition; however, for the C_{60}–SWNT two-component film, this technique results in a layer-by-layer structure because of the faster deposition of SWNT than of C_{60} [3]. To increase the lifetime of excitons during the photoexcitation, the bundling of SWNT and the clustering of C_{60} should be decreased. Therefore, designing a more uniformly distributed C_{60}–SWNT film on a solid substrate is required for future research.

Recently, a stable electroactive SWNT monolayer endcapped by a conductive oligomer was prepared in our group that showed potential application in electrochemical nanoarchitectures [4]. In view of the intriguing electrochemical properties of C_{60}, introducing C_{60} in the SWNT film may be a good way to modify SWNTs. From the viewpoint of morphology control, here, we report a more homogeneous SWNT–C_{60} film covalently grafted onto an optically transparent SAM–ITO surface using a step-by-step method, in which the SWNTs were anchored to the unreacted amines of the SAM–ITO as well as to C_{60} aggregates functionalized by amine groups (Scheme 1), which is expected to fabricate chemically stable composite films for future research in photoactive systems. The obtained film was s investigated by using AFM, SEM, XPS, FTIR, etc.

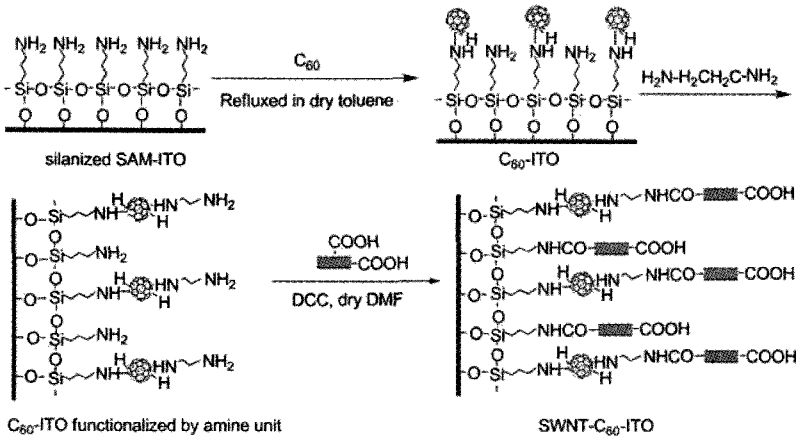

Scheme 1. Schematic illustration of the preparation route to C_{60}–SWNT ultrathin film grafted on ITO step-by-step.

[1] S. Barazzouk, S. Hotchandani, K. Vinodgopal, P. V. Kamat, *J. Phys. Chem. B*, **108**, 17015–17018 (2004).
[2] P. V. Kamat, S. Barazzouk, K. G. Thomas, S. Hotchandani, *J. Phys. Chem. B*, **104**, 4014–4017 (2000).
[3] T. Umeyama, N. Tezuka, M. Fujita, S. Hayashi, N. Kadota, Y. Matano, H. Imahori, *Chem. Eur. J.*, **14**, 4875–4885 (2008). [4] Q. Wang, H. Moriyama, *Bull. Chem. Soc. Jpn.*, **82**, 743–749 (2009).

Corresponding Author: Hiroshi Moriyama
TEL: +81-47-472-1211, FAX: +81-47-476-9449, E-mail: moriyama@chem.sci.toho-u.ac.jp

3-13

First-Principles study for Single-Walled Carbon Nanotube on Metal Surface

Yoshiteru Takagi[1,2] and Susumu Okada[1,2]

[1]*Center for Computational Sciences and Graduate School of Pure and Applied Science, University of Tsukuba, Tsukuba 305-8577, Japan*

[2]*CREST, Japan Science and Technology Agency, 4-1-8 Honcho, Kawaguchi, Saitama 332-0012, Japan*

Carbon nanotubes (CNTs) are promising materials for nano-scale electronic device such as field emission transistors (FET) because of their one-dimensional structures and ballistic conductivity. There are many studies for realizing the FETs using CNT. These studies reported that the FETs exhibit different properties depending on the metal species of the electrode. For instance, CNT-FET with Pd electrodes shows *p*-type conduction behavior. In contrast to CNT-FET with Pd electrodes, CNT-FET with Mg electrodes shows bipolar conduction behavior [1]. However, origin of the dependency on contact metal species has not been elucidated yet. Thus, we investigated the electronic properties of single-walled carbon nanotube adsorbed on metal surfaces (Au, Ag, Pd, Pt, Mg) based on the first-principle total-energy calculations. Our calculations clearly show that the optimized structure and electronic properties of the hybrid structure of CNT and metal surfaces depend on metal species. Figure 1(a) and 1(b) show the optimized structure of CNT on Au and CNT on Pt, respectively. Optimized structures and distance between CNT and metal surface depend on metal species. The Au surface almost keeps their original structure. While, Pt surface is highly reconstructed due to the substantial interaction between Pt surface and CNT. In addition, the electronic structure of the hybrid systems also strongly depends on the metal species. Our calculations clearly show that the Fermi level pinning in the hybrid structure of CNT and metals does not take place.

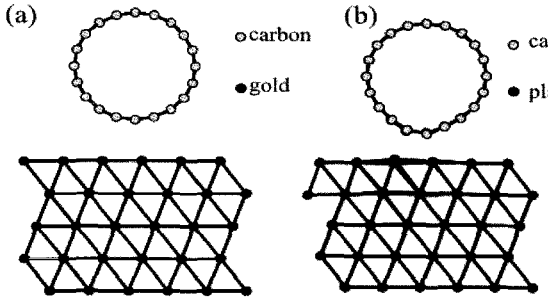

Fig.1 Side view of optimized structure of (a) CNT/Au and (b) CNT/Pt.

[1] Y.Nosho, Y.Ohno, S.Kishimoto, and T.Mizutani, Nanotecnology **17** (2006) 3412.

Corresponding Author: Yoshiteru Takagi

E-mail: ytakagi@comas.frsc.tsukuba.ac.jp, TEL: +81-29-853-5600(8233), FAX:+81-29-853-5924

ポスター発表
Poster Preview

1P – 1 ～ 1P – 47
2P – 1 ～ 2P – 48
3P – 1 ～ 3P – 48

1P-1

New 66π-Electron [70]Fullerene Derivatives as n-Type Materials

○ Zuo Xiao[1], Yutaka Matsuo[1,2], Eiichi Nakamura[1,2]

[1]*Nakamura Functional Carbon Cluster Project, ERATO, Japan Science and Technology Agency (JST), Hongo, Bunkyo-ku, Tokyo 113-0033, Japan*
[2]*Department of Chemistry, The University of Tokyo, Hongo, Bunkyo-ku, Tokyo 113-0033, Japan*

Abstract: Organic photovoltaic (OPV) devices have attracted considerable interest as a potential cost-efficient alternative to silicon solar cells. The [60]fullerene and its derivative PCBM are commonly used n-type materials in OPV devices due to their high electron affinity. However, their low absorbance in the solar spectrum limits their potential. In contrast, [70]fullerene and its derivatives have stronger absorbance especially in the 500-700 nm range. It was reported that the higher absorption of C_{70} can lead to high external quantum efficiencies of the devices.[1] A recently reported bulk heterojunction solar cell using $PC_{70}BM$ as the n-type material has achieved ca. 6% power conversion efficiency.[2]

We have developed an efficient method to synthesize 66π-electron C_{70} derivatives $C_{70}Ar_3H$ in quantitative yield. However, the low solubility, low thermo- and electrochemical stability limit their application in OPV devices. Starting from $C_{70}Ar_3H$, we disclosed a method to synthesize a new type of 66π-electron C_{70} derivatives $C_{70}Ar_3Ar'$ (Scheme 1). These derivatives are thermo- and electrochemical stable, and some of them exhibit good solubility for device processing. These improvements make them a promising candidate for OPV n-type materials.

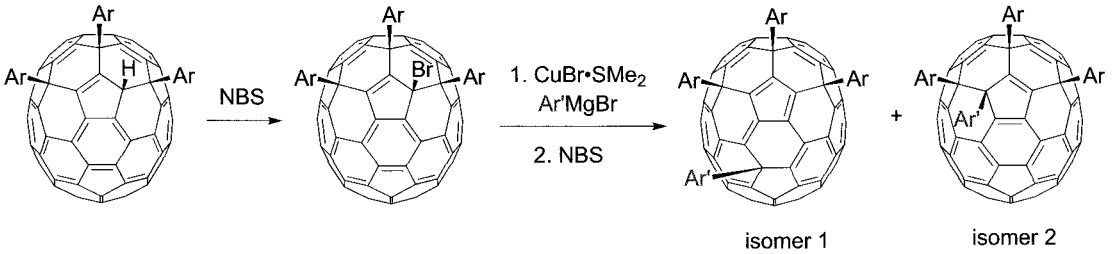

Scheme 1

References:
1. S. Pfuetzner, J. Meiss, A. Petrich, M. Riede, and K. Leo, *Appl. Phys. Lett.* **2009**, *94*, 223307.
2. S. H. Park, A. Royl, S. Beaupre, S. Cho., N. Coates, J. S. Moon, D. Moses, M. Leclerc, K. Lee, and A. J. Heeger, *Nature Photonics* **2009**, *3*, 297.

Corresponding Authors: Yutaka Matsuo and Eiichi Nakamura
E-mail: matsuo@chem.s.u-tokyo.ac.jp; nakamura@chem.s.u-tokyo.ac.jp
Tel & Fax: +81-3-5841-1477

1P-2

Synthesis and Electronic Properties of a Cobaltadithiolene-TTF-Fullerene Complex: Fullerene Moieties as Secondary Acceptor Units

○Masashi Maruyama[†], Yutaka Matsuo[†,‡], and Eiichi Nakamura[†,‡]

[†] *Department of Chemistry, The University of Tokyo, Hongo, Bunkyo-ku, Tokyo 113-0033, Japan*

[‡] *Nakamura Functional Carbon Cluster Project, ERATO, Japan Science and Technology Agency, Hongo, Bunkyo-ku, Tokyo 113-0033, Japan*

Donor-acceptor systems are known to serve as semiorganic conductors, near-infrared dyes, nonlinear optical materials, and so on. Rational design of functional molecules and construction of ordered structures in solid states by the use of fullerene derivatives are extensively investigated. We herein report synthesis and properties of a multi-functional cobaltadithiolene-TTF-fullerene complex, which has one donor part (TTF moiety) and two acceptor parts (cobaltadithiolene and fullerene moieties). A reaction of dicarbonyl complex **1** with bis(carbonyldithio)tetrathiafulvalene produced a donor-acceptor array **2** (Scheme 1). The structure of **2** was determined by X-ray crystallographic analysis to reveal packing structures in solid states.

As shown in Figure 1, complex **2** showed a characteristic absorption band in near-infrared region, which is attributed to a charge-transfer transition between TTF and cobaltadithiolene moieties. Electrochemical properties of **2** were characterized with cyclic voltammogram exhibiting two reversible one-electron oxidation processes due to the TTF moiety, two reversible one-electron reduction processes due to the cobaltadithiolene moieties, and one reversible two-electron reduction process due to the fullerene moieties.

We will discuss the significant effects of the terminal fullerene moieties as secondary acceptor units on the electronic properties. We will also report transient absorption spectra and third-order nonlinear susceptibility measurements data to discuss the time-resolved photophysical dynamics of excited states and the electronic interactions within the chromophore of **2**.

Scheme 1

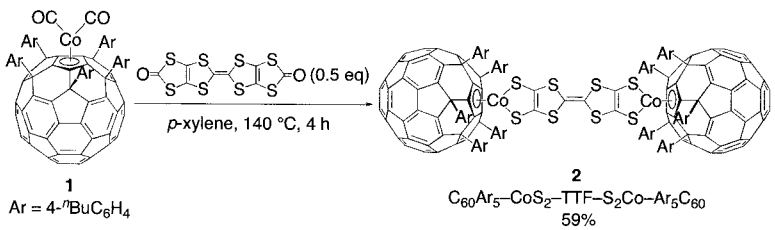

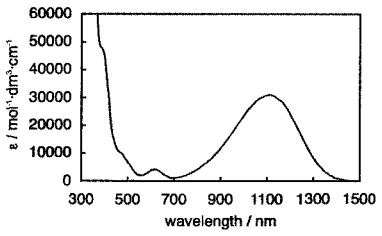

Figure 1. UV-*vis*-NIR absorption spectrum of **2** in CH_2Cl_2.

Corresponding Authors: Yutaka Matsuo and Eiichi Nakamura
TEL/FAX: +81-3-5841-1476; E-mail: matsuo@chem.s.u-tokyo.ac.jp; nakamura@chem.s.u-tokyo.ac.jp

1P-3

Synthesis and LUMO-level Control of 1-Aryl-4-silylmethyl[60]fullerene Derivatives

○Hiromi Oyama[†], Yutaka Matsuo[†,‡], and Eiichi Nakamura[†,‡]

[†] *Department of Chemistry, The University of Tokyo, Hongo, Bunkyo-ku, Tokyo 113-0033, Japan*

[‡] *Nakamura Functional Carbon Cluster Project, ERATO, Japan Science and Technology Agency, Hongo, Bunkyo-ku, Tokyo 113-0033, Japan*

Abstract:

The excellent electron-accepting capability of fullerene has received much attention as n-type materials for organic photovoltaic cells. However, there are only a few examples such as PCBM and fulleropyrrolidines to be used for OPV applications. Recently, we have synthesized 1,4-diadduct [60]fullerene derivatives, bis(silylmethyl)[60]fullerenes,[1] which contribute to high power conversion efficiency in the OPV devices. To achieve higher performance, control of LUMO levels of the [60]fullerene core and high solubility in various organic solvents are required.

Inspired by the efficient synthesis of mono-adducts **1** that can be obtained very good yield,[1] we designed 1,4-di(organo)[60]fullerene **2** with an aryl group and a silylmethyl group (Scheme 1). A directly attached aryl group on [60]fullerene is expected to change greatly the electrochemical property. In addition, the silylmethyl group on the [60]fullerene cage is expected to give high solubility in various organic solvents. We report here the electrochemical and thermal properties of **2**.

Scheme 1

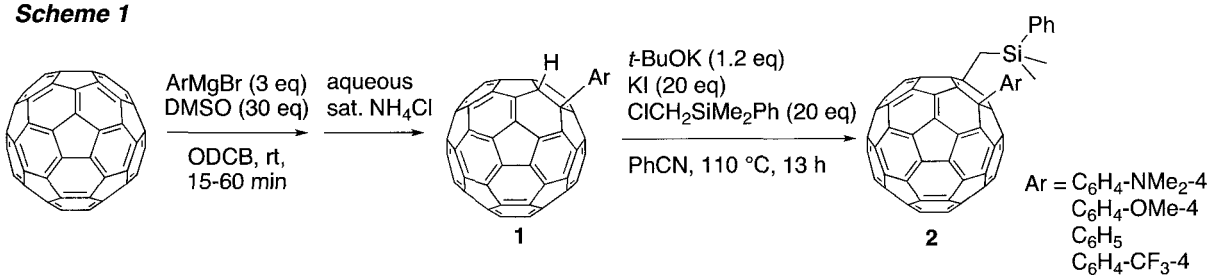

References:

Y. Matsuo, A. Iwashita, Y. Abe, C.-Z. Li, K. Matsuo, M. Hashiguchi, E. Nakamura, *J. Am. Chem. Soc.* **2008**, *130*, 15429.

Corresponding Authors: Yutaka Matsuo and Eiichi Nakamura

TEL/FAX: +81-3-5841-1476;

E-mail: matsuo@chem.s.u-tokyo.ac.jp; nakamura@chem.s.u-tokyo.ac.jp

1P-4

Photocurrent Generating Systems of Fullerene-bisporphyrins with Supramolecular Interaction

○Takahiko Ichiki,[†] Xiaoyong Zhang,[‡] Yutaka Matsuo[†,‡] and Eiichi Nakamura[†,‡]

[†]*Department of Chemistry and The University of Tokyo, 7-3-1 Hongo, Bunkyo-ku, Tokyo 113-0033, Japan, and* [‡]*Nakamura Functional Carbon Cluster Project, ERATO, JST, 7-3-1 Hongo, Bunkyo-ku, Tokyo 113-0033, Japan*

Fullerene-porphyrin hybrid systems have attracted much attention due to their unique properties including photoinduced energy and electron transfer as well as their structures [1,2]. Additionally, they can show non-covalent supramolecular interaction through their porphyrin moieties. This property provides great possibility for fabrication of new optoelectronic devices.

We synthesized fullerene-bisporphyrin conjugate (**F2ZnP**). Electrochemical, light-absorbing, and photoluminescent properties for these compounds were investigated. Their two hand-like porphyrins not only enhance the absorption but also capsulate guest molecules with large binding constants. We will report host-guest chemistry of **F2ZnP** with guest molecules such as pyradine and DABCO, and their application to surface chemistry to construct photocurrent generating supramolecular self-assembled monolayer systems. Remarkably, we achieved the control of configurations of the systems by changing the length of pyradine linkers, giving high performance in photocurrent generations.

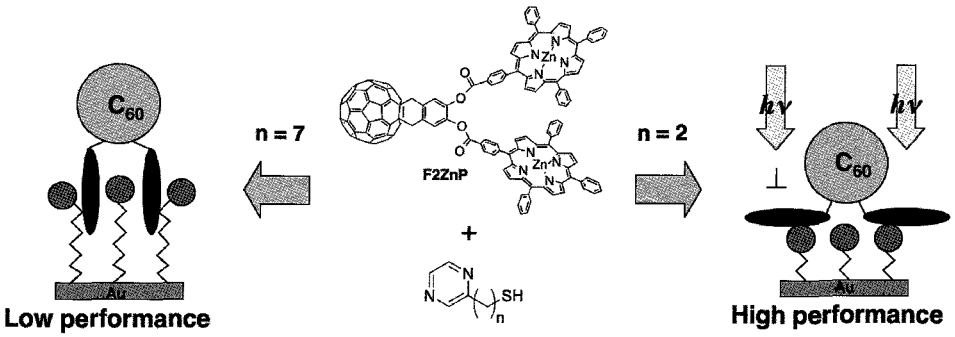

References

1. Liddell, P. A.; Sunida, J. P.; McPherson, A. N.; Noss, L.; Seely, G. R.; Clark, K. N.; Moore, A. L.; Moore, T. A.; Gust, D. *Photochem. Photobiol.* **1994**, *60*, 537.

2. Imahori, H.; Sakata, Y. *Adv. Mater.* **1997**, *9*, 537.

Corresponding Authors: Yutaka Matsuo and Eiichi Nakamura

E-mail: matsuo@chem.s.u-tokyo.ac.jp; nakamura@chem.s.u-tokyo.ac.jp

Tel&Fax: +81-(0)3- 5841-1476

1P-5

Synthesis and Reaction of Fullerene C_{70} Encapsulating Two Molecules of H_2

○Michihisa Murata,[1] Shuhei Maeda,[1] Yuta Morinaka,[1] Yasujiro Murata,[1]
Koichi Komatsu[2]

[1]*Institute for Chemical Research, Kyoto University, Uji, Kyoto 611-0011, Japan*
[2]*Department of Environmental and Biotechnological Frontier Engineering, Fukui University of Technology, Gakuen, Fukui 910-8505, Japan*

Endohedral fullerene C_{60} encapsulating one molecule of H_2 ($H_2@C_{60}$) has become an attractive object for fundamental studies since its organic synthesis by the technique of "molecular surgery" [1]. The encapsulated H_2 has served as a powerful NMR probe to study aromaticity of ionic C_{60} derivatives and to follow chemical reactions taking place at the exterior of the cage. The synthesis of $H_2@C_{60}$ has also opened up the way to elucidate the intrinsic nature of a single H_2 molecule surrounded by the carbonaceous cage.

In the present research, the scope of the molecular surgery method is extended to the representative higher fullerene, C_{70}, to provide a novel endohedral fullerene C_{70} encapsulating one and two molecules of H_2 from their cage-opened C_{70} derivatives [2]. Actually, $H_2@C_{70}$ and $(H_2)_2@C_{70}$ were synthesized, separated, and characterized [3]. Although the interaction between the encapsulated H_2 and C_{70} cage is quite minute for $H_2@C_{70}$, there is still a possibility that a difference in chemical reactivity of the C_{70} cage becomes appreciable when two molecules of H_2 are incorporated inside the cage. To clarify this, the equilibrium constants for the Diels-Alder reaction of $H_2@C_{70}$ and $(H_2)_2@C_{70}$ with 9,10-dimethylanthracene (DMA) shown in Scheme 1 have been determined at 30, 40, and 50 °C. It was found that the equilibrium constants for $(H_2)_2@C_{70}$ is smaller than that for $H_2@C_{70}$ by more than 15% at each temperature, demonstrating the "*apparently*" decreased reactivity of $(H_2)_2@C_{70}$ toward DMA [3].

Scheme 1

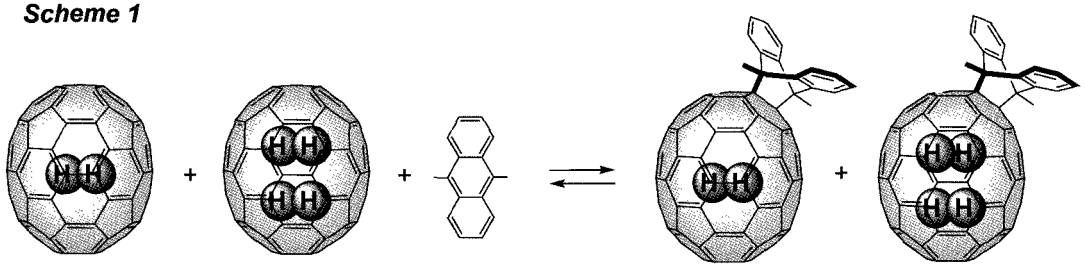

References:

[1] M. Murata, Y. Murata, and K. Komatsu, *Chem. Commun.*, 6083 (2008).

[2] Y. Murata, S. Maeda, M. Murata, and K. Komatsu, *J. Am. Chem. Soc.*, **130**, 6702 (2008).

[3] M. Murata, S. Maeda, Y. Morinaka, Y. Murata, and K. Komatsu, *J. Am. Chem. Soc.*, **130**, 15800 (2008).

Corresponding Author: Yasujiro Murata
E-mail: yasujiro@scl.kyoto-u.ac.jp
Tel: +81-774-38-3172, Fax: +81-774-38-3178

1P-6

Chemical Functionalization of [60]fullerene with Amidine

○Nobuaki Ueda, Hidefumi Nikawa, Takahiro Tsuchiya, and Takeshi Akasaka

Center for Tsukuba Advanced Research Alliance, University of Tsukuba, Tsukuba, Ibaraki 305-8577, Japan

Functionalizaiton of fullerene is one of the most interesting things regarding to the developmetnt of new materials with unique properties. A variety of methods for the addtion of functional groups to the spherical double bond have been developed in these yerars. Especially, the amination of fullerene is expected to develop in medical applications. [1]

Amidines are one of very versatile species, because they are utilized not only as a base but also recently as a precursor of carbene. We carried out the photochemical reaction of C_{60} with several kinds of linear amidines. In the reaction of C_{60} with amidine **2** (R = 2, 6-diisopropylphenyl), C_{60}-amidine adduct **3** was obtained, and the structure of which was determined by the spectroscopic analysis and the single crystal X-ray analysis to be a unique β-lactam-like structure.

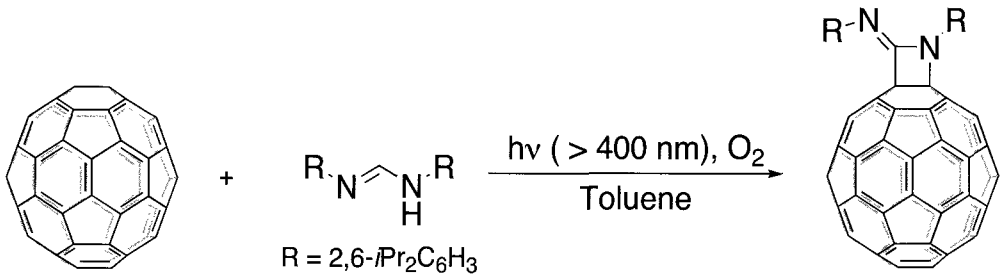

References

[1] T. Nakahodo, M. Okada, H. Morita, T. Yoshimura, M. O. Ishitsuka, T. Tsuchiya, Y. Maeda, H. Fujihara, T. Akasaka, X. Gao, S. Nagase, *Angew. Chem. Int. Ed.* **2008**, 47, 1298-1300.

Corresponding Author: Takeshi Akasaka
E-mail: akasaka@tara.tsukuba.ac.jp
Tel: +81-29-853-6409

1P-7

A Novel and Simple Synthesis of Fullerene Derivatives using $FeCl_3$

○Masahiko Hashiguchi, and Kazuhiro Watanabe

Fullerene Development Group, Mitsubishi Chemical Corporation
1-1, Shiroishi, Kurosaki, Yahatanishi-ku, Kitakyushu 806-0004, Japan

A concise and low-cost synthesis of fullerene derivatives is required for its wide application in the industry. Several low-cost production[1,2] and purification[3] of fullerenes have been reported before now, and less expensive synthesis methods of fullerene derivatives as typified by polyhydroxylation have been developed. For the application of fullerene derivatives, arylated[60]fullerenes are remarkable materials not only in organic chemistry but also in nanoscale materials science[4]. The arylation of C_{60} is usually achieved using organometallic reagents, therefore the synthesis method is not suitable for industrial-scale applications. On the other hand, although $AlCl_3$-mediated Friedel-Crafts type reaction[5] is the easiest method for the synthesis of arylated[60]fullerenes, it is impossible to introduce only aryl groups into C_{60} selectively because hydrogenation also proceeds in parallel with arylation.

Here we report a new class of method, $FeCl_3$-mediated multiarylation of C_{60}, which can be achieved by a simple procedure without expensive reagents. By this simple reaction of a [60]fullerene with chlorobenzene in the presence of $FeCl_3$, C_{60} can be converted into the pentaaryl and multiaryl[60]fullerene without hydrogenation (Scheme 1). And our method is a single-step synthesis of pentaarylmonocholoro[60]fullerenes (**1**) from C_{60} without requiring any complicated procedure, although these type of derivatives are usually obtained by multistep synthesis.

Scheme 1. Synthesis of Compound **1**.

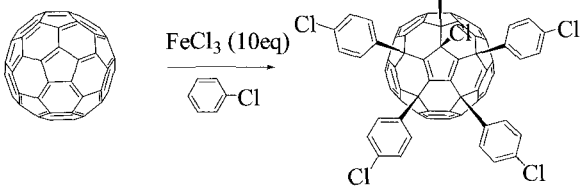

1

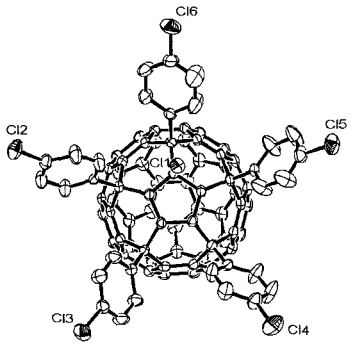

Figure 1. ORTEP drawing of Compound **1**.

[1] J. B. Howard, J. T. McKinnon, Y. Makarovsky, Y. Lafleur, M. E. Johnson, *Nature* **352**, 139(1991).

[2] H. Takehara, M. Fujiwara, M. Arikawa, M. D. Diener, J. M. Alford, *Carbon* **43**, 311(2005).

[3] K. Nagata, E. Dejima, Y. Kikuchi, M. Hashiguchi, *Chem. Lett.* **34**, 178(2005).

[4] For examples, see: (a) M. Sawamura, K. Kawai, Y. Matsuo, K. Kanie, T. Kato, and E. Nakamura, *Nature* **419**, 702(2002); (b) H. Isobe, T. Homma and E. Nakamura, *Proc. Natl. Acad. Sci. USA* **104**, 14895(2007).

[5] G. A. Olah, I. Bucsi, C. Lambert, R. Aniszfeld, N. J. Trivedi, D. K. Sensharma, G. K. S. Prakash, *J. Am. Chem. Soc.*, **113**, 9387 (1991).

Corresponding Author: Masahiko Hashiguchi
TEL: +81-93-643-4402, FAX: +81-93-643-4401, E-mail: 6206530@cc.m-kagaku.co.jp

1P-8

Why the Isolated-Pentagon-Rule Is Violated by Endohedral Metallofullerenes? A Chemical Answer

○Xing Lu[1], Hidefumi Nikawa[1], Midori O. Ishitsuka[1], Takahiro Tsuchiya[1], Yutaka Maeda[2], Takeshi Akasaka[1], Zdenek, Slanina[1], Naomi Mizorogi[1] and Shigeru Nagase[3]

[1]*Center for Tsukuba Advanced Research Alliance, University of Tsukuba, Tsukuba, Ibaraki 305-8577, Japan,*
[2]*Department of Chemistry, Tokyo Gakugei University, Tokyo 184-8501, Japan,*
[3]*Department of Theoretical and Computational Molecular Science, Institute for Molecular Science, Okazaki 444-8585, Japan*

Fullerenes violating the isolated-pentagon-rule (IPR) are only obtained in the form of their derivatives.[1] Non-IPR endohedral metallofullerenes (EMFs), however, still have unsaturated sp^2-carbons on the [5,5]-bond junctions, which enables to probe their chemical properties, and the interactions between inner metals and [5,5]-bond junctions as well.[1] Herein, we presented the first experimental evidences of the stabilization of encapsulated metals on the fused-pentagon bonds in EMFs by functionalization of the non-IPR $La_2@C_{72}$ with a carbene reagent. X-ray structural results unambiguously elucidate that the fused-pentagon sites are still very reactive, but the carbons making the [5,5]-junctions are less reactive than the adjacent ones, confirming that they interact strongly with the encaged metals, and thus are stabilized by the metals.[2,3]

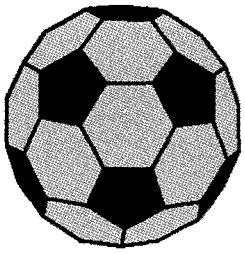

IPR-obeying C_{60}

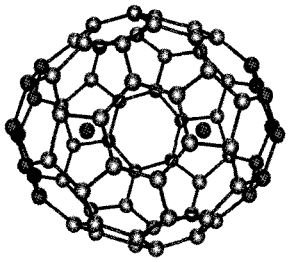

IPR-violating $La_2@C_{72}$

References:

[1] T. Akasaka and S. Nagase, *Endofullerenes: A New Family of Carbon Clusters;* Kluwer: Dordrecht, The Netherlands, **2002**.

[2] X. Lu *et al, J. Am. Chem. Soc., 130*(28), 9129-9136, **2008.**

[3] X. Lu *et al, Angew. Chem. In. Ed., 47*(45), 8642-8645, **2008.**

Corresponding Author: Xing Lu
TEL& FAX: +81-29-853-7289, E-mail: lux@tara.tsukuba.ac.jp

1P-9

Chemical Understanding of $La@C_{74}(C_6H_3Cl_2)$

○Takeshi Akasaka[1], Tsukasa Takahashi[1], Hidefumi Nikawa[1], Tsuyoshi Ito[1], Hidenori Kuga[1], Takahiro Tsuchiya[1], Naomi Mizorogi[1] and Shigeru Nagase[2]

[1]*Center for Tsukuba Advanced Research Alliance, University of Tsukuba, Tsukuba, Ibaraki 305-8577, Japan*
[2]*Institute for Molecular Science, Okazaki, Aichi 444-8585, Japan*

The chemical modifications of endohedral metallofullerenes have attracted much attention because the chemical properties of endohedral metallofullerenes are different from those of empty fullerenes due to the electron transfer from the encaged metals to fullerene cage and the derivatives are also useful than the parent endohedral metallofullerenes in several fields.[1,2] Most reported studies are focused on the mono-adduct of endohedral metallofullerenes, while only a few papers are available for the bis-adduct of endohedral metallofullerenes.[3,4] The controlled synthesis of the bis-adducts of the endohedral metallofullerene open the door to form the basis for the tailor-made design of a large variety of functional endohedral metallofullerene derivatives. Apparently, the investigation on the bis-adducts of endohedral metallofullerenes is a new hot topic in the fullerene chemistry

The reaction of $La@C_{74}(C_6H_3Cl_2)$ with diethyl bromomalonate in the presence of sodium hydride in *o*-dichlorobenzene(*o*-DCB) has been performed. Sodium hydride (18 equiv) was added dropwise to a mixture of $La@C_{74}(C_6H_3Cl_2)$ (1 equiv) and diethyl bromomalonate (20 equiv). The total yield of Bingel adducts was about 65% based on the $La@C_{74}(C_6H_3Cl_2)$. The four mono-adducts were revealed to be the major products of this reaction. They were successfully isolated from the mixture by multistage high-performance liquid chromatography (HPLC).

Herein, we report the Bingel reaction of $La@C_{74}(C_6H_3Cl_2)$. It proceeds effectively to afford the corresponding adducts, which have been successfully isolated by HPLC and characterized by a variety of spectroscopic analyses. As a result, the chemical reactivity of $La@C_{74}(C_6H_3Cl_2)$ has been clarified.

[1] *Endofullerenes: A New Family of Carbon Clusters;* Akasaka T. and Nagase S., Eds.; Kluwer: Dordrecht, The Netherlands, 2002.

[2] Tsuchiya, T.; Sato, K.; Kurihara, H.; Wakahara, T.; Nakahodo, T.; Maeda, Y.; Akasaka, T.; Ohkubo, K.; Fukuzumi, S.; Kato, T.; Mizorogi, N.; Kobayashi, K.; Nagase, S. *J. Am. Chem. Soc.* **2006**, *126*, 6699-6703.

[3] Stevenson, S.; Stephen, R. R.; Amos, T. M.; Cadorette, V. R.; Reid, J.E.; Phillips, J. P. *J. Am. Chem. Soc.* **2005**, *127*, 12776-12777

[4] Cai, T.; Xu, L.; Shu, C.; Reid, J. E.; Anklin, C.; Gibson, H. W.; Dorn, H. C. *J. Am. Chem. Soc.* **2008**, *130*, 2136-2137.

Corresponding Author: Takeshi Akasaka
TEL & FAX: +81-29-853-6409, E-mail: akasaka@tara.tsukuba.ac.jp

1P-10

Ultraviolet Photoelectron Spectroscopy of $Sc_2C_2@C_{84}$ and $Er_2C_2@C_{84}$

○Takafumi Miyazaki[1], Yusuke Aoki[1], Youji Tokumoto[1], Ryohei Sumii[2], Haruya Okimoto[3], Hisashi Umemoto[3], Yasuhiro Ito[3], Hisanori Shinohara[3], Shojun Hino[1]

[1] *Graduate School of Science and Engineering, Ehime University*
[2] *Institute for Molecular Science*
[3] *Graduate School of Science, Nagoya University*

Ultraviolet photoelectron spectra (UPS) of endohedral metallofullerenes have been measured to determine their electronic structure. In this study the UPS of $Sc_2C_2@C_{84}$ and $Er_2C_2@C_{84}$ were measured and compared with other metallofullerenes.

Figure 1 shows the UPS of $Sc_2C_2@C_{84}$ and $Er_2C_2@C_{84}$ at $h\nu$ = 40 eV irradiation. The UPS of three $Y_2C_2@C_{82}$ isomers [1], empty C_{82} and C_{84} are also shown in Figure 1 for comparison. The spectral onset (E_{onset}) of $Sc_2C_2@C_{84}$ and $Er_2C_2@C_{84}$ is much smaller than that of other metallo-fullerenes (E_{onset}= 0.4 ~ 0.9 eV) and the empty C_{82} and C_{84} (E_{onset}= 1.2 eV). Principally the spectra of fullerenes deeper than 5 eV resemble, but the UPS of $Sc_2C_2@C_{84}$ and $Er_2C_2@C_{84}$ are quite different. In the UPS of empty fullerenes and endohedral fullerenes, there is a characteristic structure at around 5.3 eV accompanied by deeps dips (located at 4.2 and 6.1 eV) beside the structure. In the UPS of $Sc_2C_2@C_{84}$ and $Er_2C_2@C_{84}$, the structure could be discernible but it did not accompany the higher binding energy side dip. The electronic structure of C_{84} metallo- fullerenes might be different categories from other endohedral metallofullerenes.

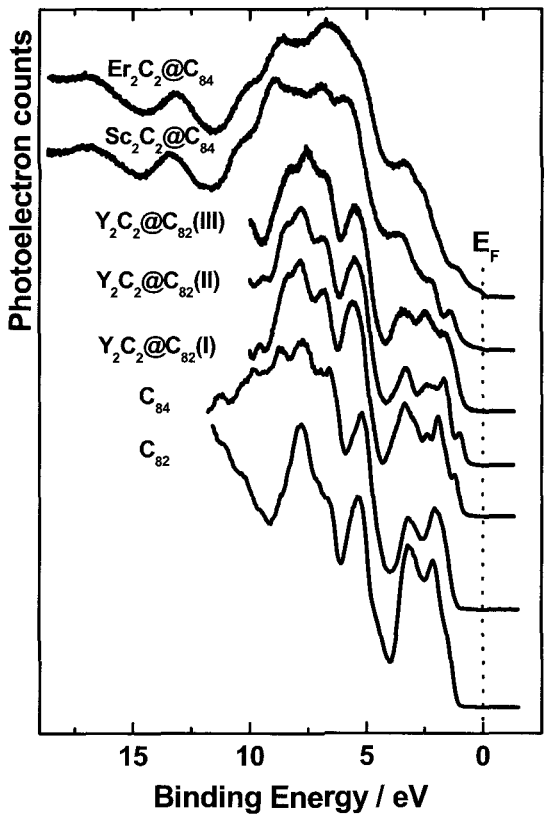

Figure 1. UPS of $Sc_2C_2@C_{84}$ and $Er_2C_2@C_{84}$, and empty C_{82} and C_{84}.

[1] S. Hino et al., Bull. Chem. Soc. Jpn., in press.

Corresponding Author: S. Hino, E-mail: hino@eng.ehime-u.ac.jp, phone: 089-927-9924

1P-11

A scalable route for enrichment of semiconducting from metallic single-walled carbon nanotubes

○Hanxun Qiu,[1] Yutaka Maeda,[2] Takeshi Akasaka,[1]

[1]*Center for Tsukuba Advanced Research Alliance, University of Tsukuba, Tsukuba, Ibaraki 305-8577, Japan*

[2]*Department of Chemistry, Tokyo Gakugei University, Tokyo 184-8511, Japan*

PRESTO, Japan Science and Technology Agency, Chiyoda, Tokyo 102-0075, Japan

Single-walled carbon nanotubes (SWNTs) keep on fascinating the scientific community mainly because of their unique electronic properties of semiconducting SWNTs (s-SWNTs). However no pure s-SWNTs over metallic counterparts, so far, could be obtained directly from synthetic procedures, as has extremely hindered their studies and applications as promising electronics. Therefore separation of nanotubes aimed at obtaining a single type of SWNTs is of great importance.[1] Recently we developed a more facile and easily scalable approach which involved mixed acid-assisted dispersion and microwave irradiation procedures, as has proved efficient for enrichment of s-SWNTs.[2] With this technique, both electronic type-dependent (metallic versus semiconducting) and diameter-dependent separations of SWNTs were realized simultaneously by an one-step treatment.

By applying microwave irradiation to the acids solution containing homogeneously dispersed HipCo SWNTs in an isothermal setup, different types of carbon nanotubes were well discriminated. As a result, the metallic nanotubes (m-SWNTs) and smaller s-SWNTs were preferentially destroyed after an appropriate time treatment and removed by filtration and thermal treatment, retaining fully semiconductor-yield and optimum-diameter nanotubes (see in Fig.1). Most importantly, the chemical and electronic structures of the resulting material were completely restored just following a high temperature annealing step, as evidenced by Raman and UV absorption investigations, as well as SEM observations. These strongly suggest the method employed is effective for enrichment of s-SWNTs without introducing great damages to the carbon nanotubes.

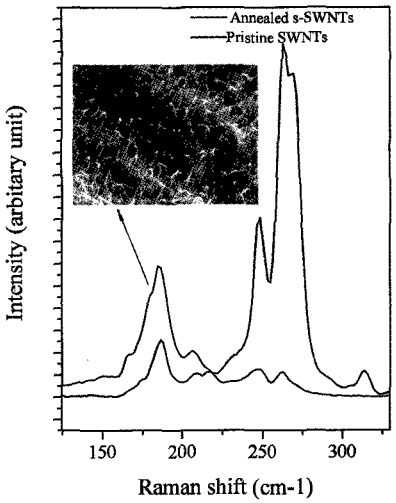

Figure 1. RBMs of the pristine and s-SWNTs recorded at 514.5 nm. Inset shows the cross sectional profile of s-SWNTs.

The dual effects of semiconducting enrichment and diameter distribution narrowing, as well as the facile procedures involved make this method promising for large-scaled separation of SWNTs and thus industrial fabrication of nanotube-based electronics.

References

[1] Maeda, Y.; Kimura, S.; Akasaka, T. *etal. J. Am. Chem. Soc.* **2005**, *127*, 10287-10290. Maeda, Y.; Kanda, M.; Akasaka, T. *etal. J. Am. Chem. Soc.* **2006**, *128*, 12239-12242.

[2] Qiu, H.; Maeda, Y.; Akasaka, T. Submitted.

Corresponding Author: Takeshi Akasaka

E-mail: akasaka@tara.tsukuba.ac.jp, **Tel & Fax:** +81-29-853-6409

1P-12

Control the Degree of Functionalization on Single-walled Carbon Nanotubes Sidewall by the Substituents

○Takaaki kato[1], Yutaka Maeda[1,2], Takayuki Nakamura[1], Tadashi Hasegawa[1], Masahiro Kako[3], Takeshi Akasaka[4], Shigeru Nagase[5]

[1]*Department of Chemistry, Tokyo Gakugei University, Koganei 184-8501, Japan*
2PRESTO, Japan Science and Technology Agency, Chiyoda, Tokyo 102-0075, Japan
[3]*The University of Electro-Communications, Tokyo 182-8585, Japan*
[4]*Center for Tsukuba Advanced Research Alliance, University of Tsukuba, Tsukuba, Ibaraki 305-8577, Japan*
[5]*Department of Theoretical and Computational Molecular Science, Institute for Molecular Science, Okazaki, Aichi 444-8585,Japan*

Single-walled carbon nanotubes (SWNTs) have excellent mechanical and electrical properties that have given rise to many potential applications. The functinalization of SWNTs, which controls their solubility and electrochemical properties, is a current subject of intense research.Hirsch et al. reported the sidewall functionalization of SWNTs by an addition reaction. After treatment of SWNTs with *t*-butyllithium, the resultant *t*-butylated-SWNTs$^-$ anion intermediate was then oxidized by oxygen.[1] They repeated the addition-oxidation or addition-protonation cycle three times because the efficiency of the functionalization in one cycle is not high. Billups et al. reported that reductive alkylation of SWNTs using lithium and organic halides in liquid ammonia yields SWNTs functionalized by corresponding alkyl or aryl groups via electron-transfer pathway.[2] Prato et al. reported a new strategy for a synthesis of multi-functionalized SWNTs.[3] They prepared SWNTs having two different functional groups through two chemical reaction processes. The functionalization introducing more than one group would be useful for practical applications.

We investigate a novel one-pot synthesis of SWNTs having two different functional groups using alkyllithium and alkyl halide. One-pot dialkylation of SWNTs shows strong substituent effect on the degree of functionalization of SWNTs. Because influence of degree of functionalization on SWNTs sidewall upon SWNTs characteristic properties is high, it is noteworthy to control the degree of functionalization on SWNTs sidewall by the substituents.

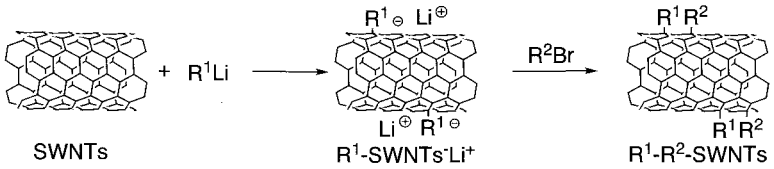

1. A. Hirsch, *J. Am. Chem. Soc.*, 2006, **128**, 6683-6689

2. W. E. Billups, *Nano Lett.*, 2004, **4**, 1257-1260

3. E. Vázquez, *J. Am. Chem. Soc.*, 2008, **130**, 8094-8100.

Corresponding Author Yutaka Maeda
E-mail ymaeda@u-gakugei.ac.jp
Tel&Fax +81-42-329-7512

1P-13

Structural changes of several kinds of endohedral SWCNTs under high-pressure and at high-temperature

○A.Iwata[1], Y. Ishii[2], M. Hirose[2], S. Kawasaki[2]

[1]*Department of Frontier Materials, Nagoya Institute of Technology, Japan*
[2]*Department of Materials Science and Technology, Nagoya Institute of Technology, Japan*

We have investigated the structural changes of SWCNTs and C_{60}-peapods by high pressure and high temperature (HPHT) treatments [1]. It was found that the stractural behavior of the C_{60}-peapods under high pressure was quite different from that of the SWCNTs. It indicates that the encapsulated molecules strongly affect the structure of SWCNTs under high pressure. Therefore, it is very interesting to perform structural investigations of SWCNTs containing various materials inside the tubes. SWCNTs filled with thinner SWCNTs, namely DWCNTs, which were produced by the CVD method [2], was supplied from Prof. Endo (Shinshu Univ.). We prepared SWCNTs filled with KI, NaI [3], and water [4] according to the previously reported methods. In situ XRD measurements of the samples under high pressure and at high temperatures were performed at AR-NE5C and at BL-18C of KEK in Tsukuba. As shown in Fig.1, it was found that the change in Raman spectra of DWCNTs under high pressure as a function of temperature was different from that of SWCNTs. The figure indicates that the DWCNTs are less reactive for the HPHT treatments than the SWCNTs [5]. We will discuss the phenomena and will report on the high pressure structural changes of the SWCNTs containing KI, NaI and H_2O inside the tubes in the symposium.

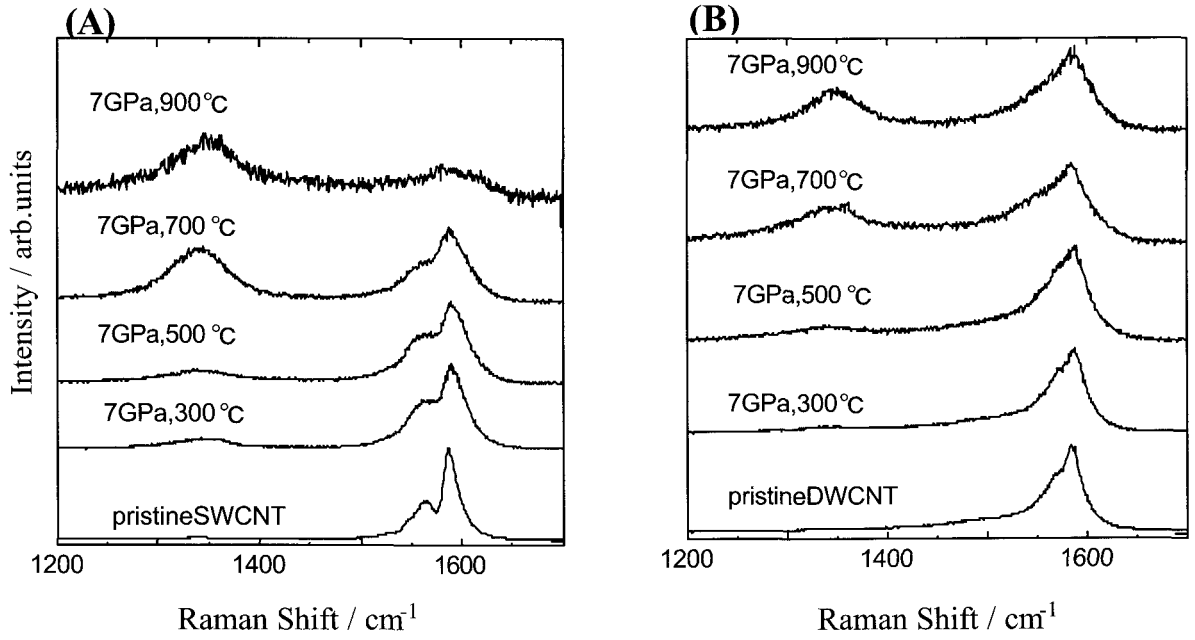

Fig. 1 Raman spectra of the HPHT treated (A) SWCNTs and (B) DWCNTs.

[1] S. Kawasaki et al., Carbon, **43**, (2005) 37 [2] M. Endo et al., Nature, **433**, (2005) 476 [3] Y. Maniwa et al., J. Phys. Soc. Jpn, **71**, (2002) 12 [4] L. Shao, et al., Carbon, **44**, (2006) 2855 [5] S. Kawasaki, et al., J. NanoSci. NanoTech., accepted.

Corresponding Author: Shinji Kawasaki Fax: +81-(52)-735-5221, E-mail: kawasaki.shinji@nitech.ac.jp

1P-14

Cantilevered Carbon Nanotube Oscillation at Low Temperature

○Shun Fukami, Takayuki Arie, and Seiji Akita

[1]*Department of Physics and Electronics, Osaka Prefecture University, 1-1 Gakuen-cho, Naka-ku, Sakai, Osaka 599-8531, Japan.*

In order to achieve highly sensitive force sensing using cantilevered CNT, the origin of dissipation of oscillating cantilevered CNT should be clarified. In this study, we investigate the temperature dependence of the energy loss of cantilevered CNT resonators.

Multiwall CNTs examined in this study were synthesized by arc discharged method. The temperature dependence of the frequency response was measured using a cryostage with a scanning electron microscope or a cryostat with an optical microscope, where the temperature was varied from 4.2 to 300 K. CNTs were oscillated mechanically by a piezo device in a vacuum. Thus, we can ignore the loss factor induced by the collision to gas molecules.[1]

As shown in Fig. 1, the resonant frequencies around 10 K are higher than that at room temperature and become maximum at certain temperature, T_{max}, around 150 K. It is noted that the temperature dependence less than 10% was observed in this experiment. This indicates that the Young's modulus, which corresponds to the sound velocity, is varied within 20 % for the temperatures from 4.2 to 300 K. Figure 2 shows a log-log plot of the temperature dependence of Q factors. The dependence can be divided in two parts around T_{max} mentioned before; high and low temperature regimes. The Q factor depends weakly on the temperature lower than T_{max}, whereas the strong dependence is appeared at the higher temperature than T_{max}. Thus the softening of the CNT shown in Fig. 1 induces the Q factor degradation at higher temperatures.

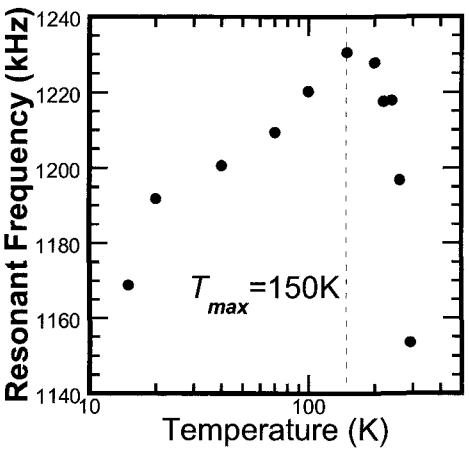

Fig.1 Temperature dependence of Resonant Frequency.

The thermoelastic loss, which is one of the important loss factors, depends not only on the temperature, but also on the thermal relaxation time which also depends on the temperature. However, the thermoelastic loss may be negligible if the parameter for the graphite is applicable to the CNTs. It was revealed by molecular dynamics simulations that the loss due to the interlayer interaction strongly contributes to the dissipation. Thus, the possible mechanisms for the temperature dependence of the dissipation are the clamping loss and/or the interlayer interaction for the multiwall of the CNT.

Acknowledgement This study is supported by Grant-in-Aid for Scientific Research on Priority Area of the Ministry of Education, Culture, Sports, Science and Technology of Japan.

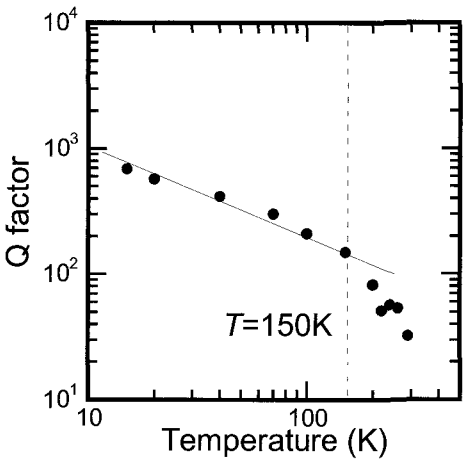

Fig.2 Temperature dependence of Q factor

[1] Fukami et al, Jpn. J. Appl. Phys. **48** (2009) 06FG04.

Corresponding Author: Seiji Akita,
E-mail: akita@pe.osakafu-u.ac.jp, Tel&Fax: 072-254-9261

1P-15

Exciton Environmental Effect for Optical Transition Energy of Single Wall Carbon Nanotubes

○ Ahmad R.T. Nugraha[1], Riichiro Saito[1], Kentaro Sato[2], Paulo T. Araujo[3], Ado Jorio[3], Mildred S. Dresselhaus[4]

[1]*Department of Physics, Tohoku University, Sendai 980-8578, Japan*
[2]*Department of Mechanical Engineering, University of Tokyo, Tokyo113-8656, Japan*
[3]*Department of Physics, UFMG, Belo Horizonte 30123-970, Brazil*
[4]*Department of Physics, MIT, Cambridge, MA 02139-4307, USA*

Optical transition energies of single wall carbon nanotubes (SWNTs) depend on the surrounding materials, which we call environmental effect [1]. In SWNTs, photo-excited electrons and holes form excitons which are stable even at the room temperature because of large binding energy. The optical transition energy is calculated using Bethe-Salpeter (B-S) equation within extended tight-binding approximation [2]. The exciton binding energy and the self energy appeared in B-S equation are Coulomb energies which are sensitive to the dielectric response of nanotube itself and surrounding materials. In the B-S equation, we consider polarization function $\Pi(q)$ for dielectric response of π-electrons and the remaining dielectric response is expressed by a parameter κ. The κ value should depend on the nanotube diameter d_t and the exciton size. However, a functional form of κ is not well-understood for reproducing many transition energies of resonance Raman spectroscopy (RRS) and photoluminescence experiments with different environments.

In the previous paper [3], diameter dependent κ could reproduce experimental RRS data. However, the functional form of $\kappa(d_t)$ is different for (E_{11}^{S}, E_{22}^{S}, E_{11}^{M}) relative to (E_{33}^{S}, E_{44}^{S}). The reason for the presence of the two $\kappa(d_t)$ functions is due to the exciton size effect corresponding to the reduced mass μ of an e-h pair. In order to incorporate the effect of the exciton size, κ values which reproduce the experimental results are now expressed in terms of both d_t and μ for a wide range of energies and diameters. This treatment can give one fitting line for different transition energies and the energy calculated using this $\kappa(d_t, \mu)$ function has a better accuracy within 60 meV than the previous results.

[1] Y. Miyauchi, R. Saito, K. Sato, Y. Ohno, S. Iwasaki, T. Mizutani, J. Jiang, and S. Maruyama, *Chem. Phys. Lett.* **442**, 394-399 (2007).

[2] J. Jiang, R. Saito, Ge. G. Samsonidze, A. Jorio, S. G. Chou, G. Dresselhaus, and M. S. Dresselhaus, Phys. Rev. B **75**, 035407 (2007)

[3] P. T. Araujo, A. Jorio, M.S. Dresselhaus, K. Sato, R. Saito, *unpublished.*

Corresponding Author: Riichiro Saito
TEL: +81-22-795-7754, FAX: +81-22-795-6447, E-mail: rsaito@flex.phys.tohoku.ac.jp

1P-16

Origin of the Satellite Photoluminescence Peaks in Single SWNTs

○Ryusuke Matsunaga, Kazunari Matsuda, and Yoshihiko Kanemitsu

Institute for Chemical Research, Kyoto University, Uji, Kyoto 611-0011, Japan

Optical properties of single-walled carbon nanotubes (SWNTs) originating from one-dimensional excitons have attracted much attention, because the degenerated band structure creates multiple exciton states; optically-allowed (bright) and optically-forbidden (dark) excitons. We have directly observed photoluminescence (PL) peak arising from the even-parity singlet dark exciton state a few meV below the bright exciton state through the Aharonov-Bohm effect [1]. Very recently, other satellite PL peaks have been observed much lower (> 100 meV) than the bright exciton peak [2-4]. Because the lowest exciton state has great influence on the optical properties of SWNTs, the origin of the satellite PL peaks has been a matter of intense debate [2-4]. However, detailed information of the satellite PL peaks has not been reported.

In this work, we investigated the temperature and tube-diameter dependence of the PL spectra by single SWNT spectroscopy [1,5]. Sharp PL spectra of single SWNTs provide clear feature of the satellite peaks for various chiralities. We found that there are at least two different types of the satellite PL peaks far below the bright exciton peak. A weak PL peak about 140 meV below the bright exciton state is observed in almost all SWNTs and disappears with decreasing temperature. These experimental results clearly show that the satellite PL peak comes from the phonon sideband of the dark exciton state with non-zero angular momentum above the bright exciton state [3]. On the other hand, by strong pulsed-laser irradiation [4], another PL peak appears and become strong with decreasing temperature. Moreover, we found that the energy separation between the laser-induced PL and the bright exciton peak is strongly dependent on the tube diameter. This behavior cannot be explained by the phonon sideband. Our results suggest that the laser-induced PL peak may arise from the triplet exciton state.

[1] R. Matsunaga, K. Matsuda, and Y. Kanemitsu, *Phys. Rev. Lett.* **101**, 147404 (2008).

[2] O. Kiowski, K. Arnold, S. Lebedkin, F. Hennrich, and M. M. Kappes, *Phys. Rev. Lett.* **99**, 237402 (2007).

[3] O. N. Torrens, M. Zheng, and J. M. Kikkawa, *Phys. Rev. Lett.* **101**, 157401 (2008).

[4] H. Harutyunyan, T. Gokus, A. A. Green, M. C. Hersam, M. Allegrini, and A. Hartschuh, *Nano Lett.* **9**, 2010 (2009).

[5] R. Matsunaga, Y. Miyauchi, K. Matsuda, and Y. Kanemitsu, *submitted* (2009).

Corresponding Author: Ryusuke Matsunaga

TEL: +81-774-38-4513, FAX: +81-774-38-4511, E-mail: matsunagaryusuke@2059.mbox.media.kyoto-u.ac.jp

1P-17

In-situ Raman Spectroelectrochemical Measurements at Carbon Nanotubes Modified Electrode

○Shingo Sakamoto, Keisuke Nagashima, Masato Tominaga

Graduate School of Science and Technology, Kumamoto University, Kumamoto 860-8555, Japan

Carbon nanotubes (CNTs) are expected for a platform electrode as charge storage and various electronic devices. It is important to understand the CNT/liquid interfacial behaviors during applying potential, because understanding the interfacial reactions such as electron transfer reactions and specifically adsorbed ions is key knowledge to achieve a high performance demonstration. In the present study, the interfacial behaviors at CNTs-modified electrode were investigated by an in-situ Raman spectroelectrochemical measurement.

CNTs were synthesized onto a gold electrode surface by CVD method. The average size in diameter was evaluated to be *ca.* 1. Cyclic voltammetric measurements were performed to investigate the electrochemical interfacial behaviors of CNTs. An Ag/AgCl (saturated KCl) electrode and a platinum electrode were used as the reference and counter electrodes, respectively.

Fig. 1 shows the cyclic voltammogram at CNTs-modified electrode in a neutral aqueous solution. Large oxidation peak was observed around 1.1 V, which would be due to the oxidation of CNTs. Fig. 2 shows in-situ Raman spectra at CNTs-modified electrode during applying potential at 0 and 1.4 V. The decreasing G-band and increasing D-band were observed at 1.4 V in comparison with those at 0 V.

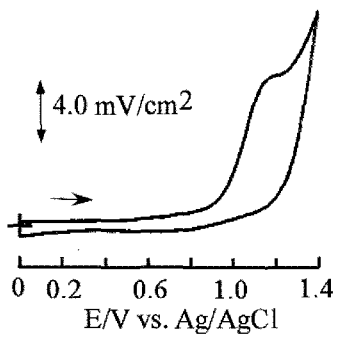

Fig. 1. Cyclic voltammogram at CNTs-modified electrode in a phosphate buffer (pH 7).

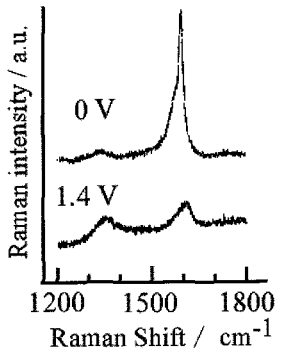

Fig. 2. In-situ Raman spectra at CNTs-modified electrode at 0 and 1.4 V in a phosphate buffer (pH 7).

Corresponding Author: Masato Tominaga
E-mail: masato@gpo.kumamoto-u.a.jp
TEL&FAX: 096-342-3656

1P-18

Energetics of Single-Walled Carbon Nanotubes

○Koichiro Kato and Susumu Saito

Department of Physics, Tokyo Institute of Technology
2-12-1 Oh-okayama, Meguro-ku, Tokyo 152-8551, Japan

Carbon nanotube (CNT) has been considered to be one of the most important materials in nanoscience and nanotechnology. The reason of this attention mainly comes from their unique electronic properties. The electronic structure of CNTs sensitively depends on the diameter and chirality. Therefore, it is very important to know the accurate electronic properties of CNTs for any possible electronic application. However, the synthesizing technique with the diameter and chirality control of CNT has not been established so far. Hence, the accurate measurements of the electronic properties of CNTs have been reported scarcely. Recently, however, some interesting studies were reported and it has been reviled that near-armchair CNTs are relatively abundant in yield CNT samples [1, 2].

In the present work, we study the energetics of single-walled CNTs in the framework of the density functional theory. We perform the complete structural relaxations and compare the total energies about 44 kinds of CNTs including some near-armchair nanotubes. We define the near-armchair nanotubes as (n, n-1) tubes. The diameters of calculated nanotubes are in the range from 0.3 nm to 2.0 nm. It is confirmed that the total energies of CNTs obtained is mostly proportional to the inverse square of their diameters. This tendency has already been reported by using Tersoff's potential [3] and by using density functional theory for zigzag nanotubes [4]. In this study, we compare the proportionality coefficients of armchair, zigzag and near-armchair nanotubes in detail. It is found that the coefficients of near-armchair CNTs are lower than those of armchair and zigzag CNTs in the whole diameter region. This result suggests that near-armchair nanotubes are relatively stable among various type CNTs. We also discuss the posiibilities of helical relaxation of chiral nanotubes and its importance in the energetics.

[1] S. M. Bachilo, L. Balxano, J. E. Herrera, F. Pompeo, D. E. Resasco and R. B. Weisman : *J. Am. Chem. Soc.* **125** 11186 (2003)

[2] Y. Miyauchi, S. Chiashi, Y. Murakami, Y. Hayashida and S. Maruyama : *Chem. Phys. Lett.* **387** 198 (2004)

[3] S. Sawada and N. Hamada : *Solid. State. Commun.* **83** 917 (1992)

[4] K. Kanamitsu and S. Saito : *J. Phys. Soc. Jap* **71** 483 (2002)

E-mail: kato@stat.phys.titech.ac.jp (K. Kato)

1P-19

In-situ transmission electron microscopy of field emission from a gold-coated carbon nanotube

○Tomohito Asai, Koji Asaka, Hitoshi Nakahara and Yahachi Saito

Department of Quantum Engineering, Nagoya University, Furo-cho, Nagoya 464-8603

Field emission (FE) characteristics from carbon nanotubes (CNTs) are influenced by their tip structures and materials deposited on the CNT surface. In order to clarify the role of gold (Au) deposited on CNTs, we carried out an *in-situ* transmission electron microscopy (TEM) study on the FE properties of Au-coated CNTs.

A multi-walled CNT, synthesized by an arc discharge method, was mounted on a tungsten (W) needle, and used as an emitter. The emission current-voltage (*I-V*) of this emitter was measured in the microscope. During the measurement, the variation in the CNT structure was observed using a television camera.

Fig. 1 shows a TEM image of an emitter. The length and the diameter of the CNT are 0.8 μm and 20 nm, respectively. The Au deposited on the CNT surface forms particles with an average diameter of 4 nm. Fig. 2 shows the *I-V* characteristic for this emitter with a CNT tip to anode distance of 0.6 μ m. The emission current gradually rose with increasing the applied voltage, and suddenly jumped from 5 to 40 μA at 107 V. The reduction in the size of Au particles was observed at an emission current of 40 μ A. We ascribe this reduction to the evaporation of Au particles by the Joule resistive heating effect.

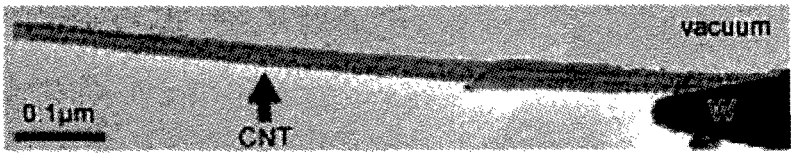

Fig. 1 TEM image of a CNT.

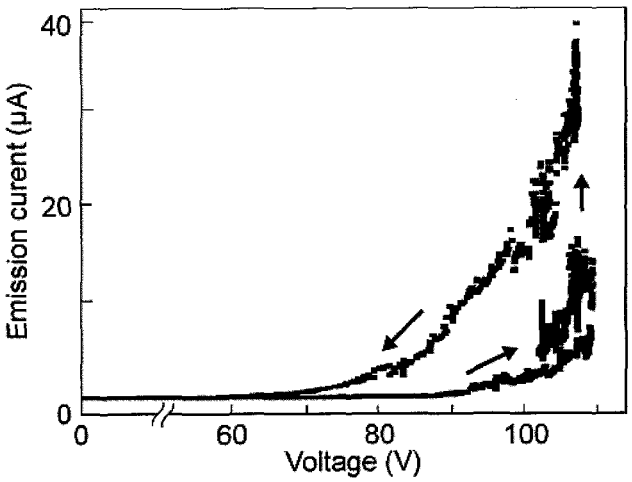

Fig. 2 Emission current-voltage curve.

Corresponding author: Tomohito Asai
E-mail: asai@surf.nuqe.nagoya-u.ac.jp
TEL: +81-52-789-3714
FAX: +81-52-789-3703

1P-20

Electronic properties of metallic and semiconducting carbon nanotubes

○Y. Miyata[1,2], P. Ayala[3], K. de Blauwe[3], H. Shiozawa[4], K. Yanagi[2], Y. Feng[2], R. Silva[4], R. Follath[5], C. Kramberger[3], H. Shinohara[1], H. Kataura[2,6], and T. Pichler[3]

[1]*Department of Chemistry, Nagoya University, Nagoya, Japan*
[2]*Nanotechnology Research Institute, AIST, Tsukuba, Japan*
[3]*Faculty of Physics, University of Vienna, Wien, Austria*
[4]*University of Surrey, Advanced Technology Institute, Guildford, United Kingdom*
[5]*BESSY II, Berlin, Germany,*
[6]*JST, CREST, Kawaguchi, Japan*

Single-wall carbon nanotubes (SWCNTs) are representative one-dimensional solids with van Hove singularities (vHs) in their density of states (DOS) and a Tomonaga-Luttinger liquid (TLL) behavior. Valence band and core level photoemission spectroscopy (PES) and X-ray absorption (XAS) are versatile tools to probe the occupied and unoccupied DOS, respectively. However, previous experiments were complicated by unavoidable mixed signals from the co-existing semiconducting and metallic SWCNTs in as-produced samples. Recently, density gradient centrifugation has been shown to be one of the most effective ways to separate SWCNTs by electronic structure [1] and was applied to produce dense mats of metallicity selected SWCNTs [2,3]. In this study, we have investigated the bulk electronic properties of high-purity metallic and semiconducting SWCNTs using high-resolution PES and XAS. The obtained spectra reveal the distinct differences in the vHs in π-band DOS (Fig. 1), a C1s response, work function, and the TLL behavior between the two samples. Our results are a clear experimental assessment of their electronic ground state and provide a solid basis for a detailed insight into the influence of chemical interactions and the transport properties of SWCNTs.

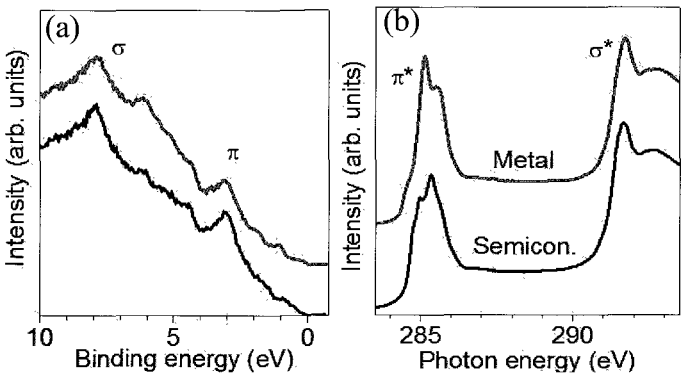

Fig. 1. (a) Valence band photoemission spectra and (b) XAS response of metallic (upper curve) and semiconducting (lower curve) SWCNTs.

References: [1] M.S. Arnold et al., Nat. Nanotechnol. 1 (2006) 60. [2] K. Yanagi, et al. Appl. Phys. Express 1 (2008) 034003. [3] Y. Miyata et al., J. Phys. Chem. C 112 (2008) 3591., **Corresponding Author: Hiromichi Kataura, E-mail: h-kataura@aist.go.jp, Tel: +81-29-861-2551, Fax: +81-29-861-2786**

1P-21

Development of a novel technique for evaluating nanodispersion: "composite combustion method"

Toshiyuki Tsuboi

No affiliation available, 1-6-9-4 Toubudai, Mobara-shi, Chiba 297-0015

Dispersion is one of the most important technologies in nanotechnology. However, techniques for evaluating dispersion in order to obtain information that helps determine an optimum dispersion condition have not yet been developed. Here, I present a novel technique for evaluating nanodispersion. I serendipitously developed this technique by myself around 2005.

In my technique, when multi-walled carbon nanotubes (MWCNTs) with good crystallinity (produced by arc discharge) are dispersed by ultrasonication, an equal amount of carbon black (BP2000; CABOT) is added to them. BP2000 is a conductive carbon black with an extremely high structure and small particle size (diameter: 12 nm).

BP2000 has good dispersibility due to its high porosity (oil absorption) and tends to aggregate due to its small particle size. BP2000 particles are rapidly dispersed upon ultrasonication and rapidly aggregate when ultrasonication is stopped. Due to their high structure, BP2000 particles aggregate to form highly porous three-dimensional structures that resemble intertwined lint (I call it the "magical 3-D net effect.").

The aggregation rate of BP2000 is higher than that of MWCNTs because the particle size of BP2000 is smaller than that of MWCNTs. Therefore, BP2000 aggregates and forms magical 3-D nets before MWCNTs aggregate. In other words, BP2000 and MWCNTs form a composite that consists entirely of carbon atoms, and in this composite, the state of dispersed MWCNTs does not change after ultrasonication is stopped.

The state of dispersed MWCNTs can be observed by scanning electron microscope (SEM) observation. However, this is a subjective analysis technique and is not conclusive. Thermogravimetry/differential thermal analysis (TG-DTA) of the composite shows that BP2000 ignites spontaneously at approximately 600 °C. Although MWCNTs should ignite spontaneously at 800 °C, they are thermally damaged by heat from BP2000 combustion, resulting in a decrease in their combustion temperature; the degree of this decrease indicates the dispersibility of MWCNTs. The combustion temperature of thermally damaged MWCNTs is between 650 °C and 750 °C; the lower the combustion temperature, the better the dispersibility of the MWCNTs.

The method presented here is called the "composite combustion method." This method yielded a lot of useful information on dispersion, e.g., information on an ideal dispersion medium, an ideal treatment vessel, the performance of an ultrasonic generator, and the importance of limiting the amount of materials treated.

The observation of change with the passage of time by using the composite combustion method showed that the ultrasonic dispersion of MWCNTs involved two types of dispersion—splitting dispersion and peeling dispersion—and that the treatment conditions determined the dominant dispersion type. Further, objective evidence for the dominance of peeling dispersion under the ideal dispersion condition was obtained.

Corresponding Author: Toshiyuki Tsuboi TEL: +81-47-526-2002, E-mail: marobonta@yahoo.co.jp

1P-22

Light-Triggered Thermoelectric Conversion Based on Carbon Nanotube Hybrid Gels

○Eijiro Miyako, Takahiro Hirotsu

Health Technology Research Center, National Institute of Advanced Industrial Science and Technology (AIST), 2217-14, Hayashi-cho, Takamatsu 761-0395, Japan

Energy problems can be solved by developing a new energy generator. Thermoelectric (TE) conversion elements can directly convert thermal energy to electricity by the Seebeck effect, without involving mechanical or chemical conversion processes. Although TE conversion elements are well-known as clean-energy generators, their heat energy sources are limited to waste, geothermal, and solar heat. On the other hand, nanocarbons, such as carbon nanotubes (CNTs), carbon nanohorns, fullerenes, and their composites have gained importance because of their physicochemical properties. In particular, the photothermal property of nanocarbons is one of the most desirable characteristics for various thermal applications.[1] In the present study, we have developed a near-infrared (NIR) laser-triggered TE conversion system based on CNT gel composites (Figure). Our concept may be applied to conventional TE module as well as other applications such as the remote control of biorobots and spaceflight power-generation systems.

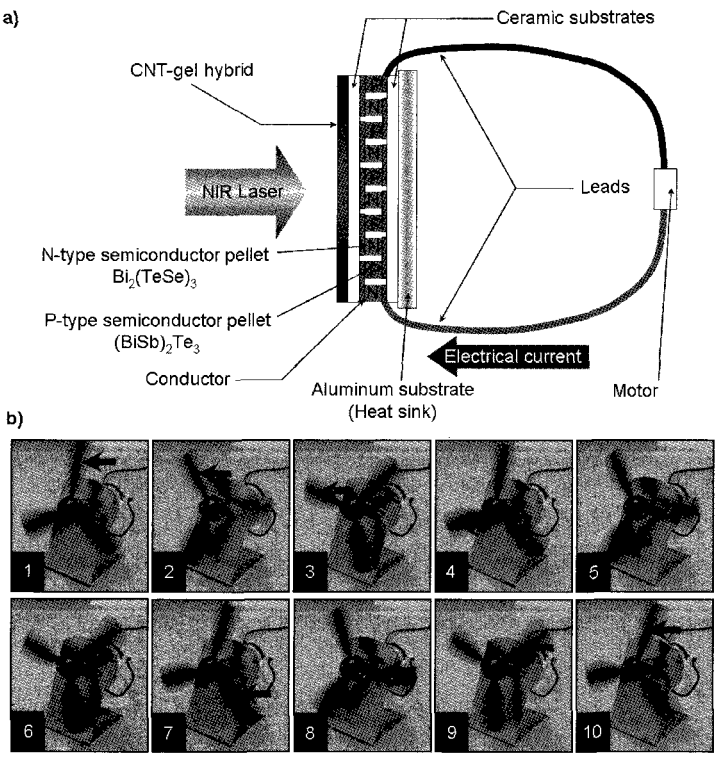

Figure. Light-driven thermoelectric conversion. a) Schematic illustration of the nanotube–gel hybrid for photoinduced TE conversion. e) Direct observation of the rotation of a propeller driven by a photoinduced nanotube–gel hybrid TE conversion module. The arrows indicate the observed propeller rotation.

[1] E. Miyako et al. *Angew. Chem. Int. Ed.*, **47**, 3610–3613 (2008); E. Miyako et al. *Adv. Mater.*, in press (2009); E. Miyako et al. *Chem. Eur. J.*, in press (2009); E. Miyako et al. *Lab Chip*, **9**, 788–794 (2009); E. Miyako et al. *Small*, **4**, 1711–1715 (2008); E. Miyako et al. *ChemSusChem*, **2**, 419–422 (2009); E. Miyako et al. *ChemSusChem*, in press (2009); E. Miyako et al. *Nanotechnology*, **18**, 475103–475109 (2007); E. Miyako et al. *Nanotechnology*, **19**, 075106–075111 (2008); E. Miyako et al. *Chem. Phys. Lett.*, **456**, 220–222 (2008).

Corresponding Author: Eijiro Miyako
TEL: +81-87-869-3574, FAX: +81-87-869-3550, E-mail: e-miyako@aist.go.jp

1P-23

Electrical Transport Properties of ssDNA Decorated Single (Double)-Walled Carbon Nanotubes

○Y. F. Li, T. Kaneko, and R. Hatakeyama

Department of Electronic Engineering, Tohoku University, Sendai 980-8579, Japan

In this work, we have studied the electrical transport properties of single-strand DNA (ssDNA) decorated single (double)- walled carbon nanotubes (SWNTs and DWNTs), which are prepared by applying a DC electric field in ssDNA solution [1]. Our results demonstrate that the diameters of nanotubes show a significant effect on the morphologies of ssDNA modified carbon nanotubes. Owing to their small diameter, ssDNA molecules are usually found to be adsorbed onto the outside of SWNTs, which is characterized by atomic force microscopy (AFM). For example, Fig. 1(a) shows 30-base-long cytosine (C_{30}) ssDNA wrapping a SWNT, revealing a regular pattern of ssDNA on the surface of the SWNT. On the other hand, ssDNA molecules are found to be easily encapsulated inside large diameter DWNTs, which is confirmed evidently by transmission electron microscopy (TEM) observations, as seen in Fig. 1(b), where C_{30} molecules distribute well inside a DWNT.

In either case, the electrical transport properties of SWNTs or DWNTs are found to be changed drastically due to the ssDNA modification. Importantly, it is found the charge transfer between the ssDNA bases and nanotubes is highly dependent on the type of the DNA bases, which is possibly explained in terms of their different redox potentials. Moreover, at low temperatures, ssDNA wrapping SWNTs shows a clear single-electron tunneling feature, as reflected in the observation of Coulomb oscillation peaks at temperatures up to 130 K. Our results indicate that it is also possible to create quantum dots by ssDNA modification.

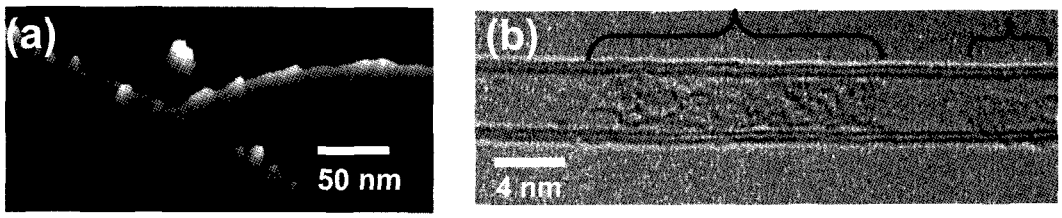

Fig.1: (a) An AFM image of C_{30} ssDNA wrapping a SWNT. (b) A TEM image of C_{30} ssDNA encapsulated a DWNT.

[1] T. Okada, T. Kaneko, R. Hatakeyama, and K.Tohij, *Chem. Phys. Lett.*, **417**, 288 (2006).

Corresponding Author: Yongfeng Li

Tel : +81-22-795-7046, FAX: +81-22-263-9225, E-mail: yfli@plasma.ecei.tohoku.ac.jp

1P-24

Fabrication of Organic Solar Cells with Polymer/SWCNT Composite Hole Transport Layer

○Naoki Kishi[1], Shinya Kato[1], Yasuhiko Hayashi[1], Takeshi Saito[2,3], Tetsuo Soga[1] and Takashi Jimbo[1]

[1]*Department of Frontier Materials, Nagoya Institute of Technology, Nagoya 466-8555, Japan*
[2]*Nanotube Research Center, National Institute of Advanced Industrial Science and Technology (AIST), Tsukuba 305-8565, Japan*
[3]*PRESTO, Japan Science and Technology Agency, Kawaguchi 332-0012, Japan*

Organic solar cells have attracted much attention in recent years for their potential application as a low cost approach to solar energy conversion. Hole transport layer, which is formed between hole correcting anode and organic active layer, plays an important roll on the controlling the hole injection conditions to the anode. Several kinds of conducting polymers such as PEDOT:PSS(poly-(3,4-ethilenedioxy-thiophene):poly(styrenesulfonate))[1] have been investigated as materials for hole transport layer of polymer solar cells. To enhance conversion efficiency of organic solar cells, it is important to improve carrier transport properties of each layer because of the low conductivity of organic semiconductors.

In the present study, we report that performances of polymer solar cells can be improved by introducing the highly conductive polymer/SWCNTs (single-wall carbon nanotubes) composite film as hole transport layer. The composite hole transport layer was fabricated by spin-casting of dispersion of PEDOT:PSS and SWCNTs synthesized by e-DIPS method[2]. The conductivity of composite films increases with increasing the amount of loaded SWCNTs. SWCNT concentration dependence of the performances of the solar cells (e.g. conversion efficiency) will be discussed in detailed.

References:

[1] L. S. Roman *et. al.*, Appl. Phys. Lett., 75, 3557 (1999).
[2] T. Saito *et. al.*, J. Nanosci. Nanotech., 8, 6153 (2008).

Corresponding Author : Naoki Kishi
E-mail : kishi.naoki@nitech.ac.jp
Tel&Fax : 052-735-5147

1P-25

Dispersion of Single-Walled Carbon Nanotubes Using Soluble Polybenzoxazoles Precursor

○Takahiro Fukumaru[1], Tsuyohiko Fujigaya[1] and Naotoshi Nakashima[1,2]

[1]*Department of Applied Chemistry, Graduate School of Engineering, Kyushu University, 744 Motooka, Fukuoka 819-0395, Japan*

[2]*Japan Science and Technology Agency, CREST, 5 Sanbancho, Chiyoda-ku, Tokyo, 102-0075, Japan*

Carbon nanotubes (CNTs) possess remarkable electrical, mechanical, and thermal properties. The superior properties make CNTs excellent candidates to substitute for the conventional fillers in the fabrication of polymer nanocomposites [1]. CNTs usually form bundled structure but the homogeneous dispersion of CNTs in polymer matrix is essential to maximize the CNTs' properties of the polymer composites. On the other hand, polybenzoxazoles (PBO) are known to have excellent mechanical strength and thermal stability to organic solvents. CNT/PBO nanocomposites expect to have excellent properties that enable field of application such as super high mechanical strength nanofibers and high thermal conductive films. However, the poor solubility of PBO hinders the fabrication of CNT/PBO nanocomposites.

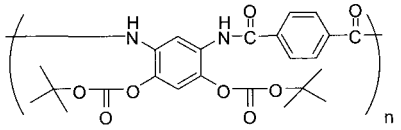

Fig. 1. Chemical structure of ^{t}Boc-prePBO.

To enhance the solubility of PBO precursor, we introduced *tert*-butyl carbonyl group to the PBO precursor by two-step reaction in organic solvent such a NMP. The obtained PBO precursor (^{t}Boc-prePBO) (**Fig. 1.**) shows excellent solubility to common organic solvent and the PBO were successfully obtained by the heating of the PBO precursor under vacuum.

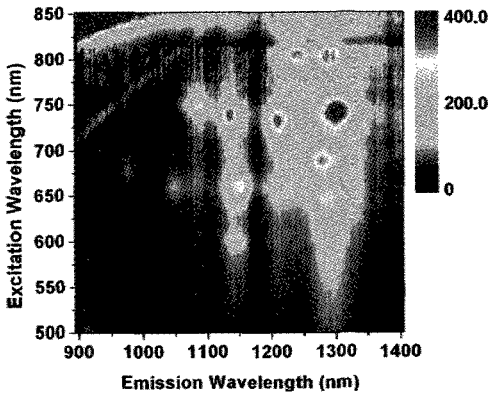

Fig. 2. Counter plot of the PL spectrum of SWNT/^{t}Boc-prePBO supernatant.

Here we report that SWNTs are well dispersed by the use of ^{t}Boc-prePBO (**Fig. 2.**) in organic solvent.

[1] (a) T. Fujigaya, S. Haraguchi, T. Fukumaru, N. Nakashima, *Adv. Mater.* **2008**, *20*, 2151.

(b) T. Fujigaya, T. Fukumaru, N. Nakashima, *Synthetic Metals.* **2009**, *159*, 827.

Corresponding Author: Naotoshi Nakashima

E-mail: nakashima-tcm@mail.cstm.kyushu-u.ac.jp Tel&Fax: +81-92-802-284

1P-26

Enhancement of adhesion between carbon nanotwist and substate in printed field emitter by adding silicone binder

○M. Yokota[1], Y. Suda[1], S. Oke[1], H. Takikawa[1],
Y. Fujimura[2], S. Itoh[2], H. Ue[3], M. Morioki[4], K. Shimizu[5]

[1] *Department of Electrical and Electronic Engineering, Toyohashi University of Technology*
[2] *Research and Development Center, Futaba Corporation*
[3] *Fuji Research Laboratory, Tokai Carbon Co., Ltd.*
[4] *Fundamental Research Department, Toho Gas Co., Ltd.*
[5] *Development Department, Shonan Plastic Mfg. Co., Ltd.*

Carbon nanotwist (CNTw) is one of fibrilliform carbon nanomaterials with helical shape, and one of the applications is an electron field emitter. To produce the CNTw printed field emitters, the paste including organic binder and CNTw is squeegee-printed on ITO glass and the binder is to be calcined at 400°C. CNTws printed on the substrate are made to be stand-up by a filament-discharge (FD) treatment [1] and dispersed and relocated by gas flowing [2]. When CNTws printed are detached from the substrate by electromagnetic force, those CNTws may cause spark or short out during field emission demonstration. In this study, the CNTw field emitters were produced by adding silicone binder to organic one for enhancement of the adhesion between CNTws and substrate. Fig. 1 shows the surfaces of CNTw emitter after FD treatment. The relocated CNTws in the silicone-binder-added (SBA) emitter were less than those in the organic-binder-only (OBO) one. Fig. 2 shows field emission characteristics of the CNTw emitters. Though turn on voltage of the OBO emitter was about 3.8 V/μm and less than that of the SBA one, the OBO emitter shorted out at 4.8 V/μm. Filed emission of the SBA emitter continued until 10 V/μm without spark and short out.

This work has been partly supported by the Outstanding Research Project of the Research Center for Future Technology, Toyohashi University of Technology (TUT); the Research Project of the Venture Business Laboratory (TUT); Global COE Program "Frontiers of Intelligent Sensing" from the Ministry of Education, Culture, Sports, Science and Technology (MEXT); The Japan Society for the Promotion of Science (JSPS) and Core University Programs (JSPS-CAS program in the field of "Plasma and Nuclear Fusion").

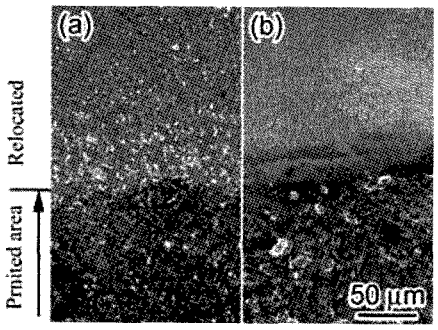

Fig. 1. SEM images of emitter surfaces (a) OBO, (b) SBA after FD treatment.

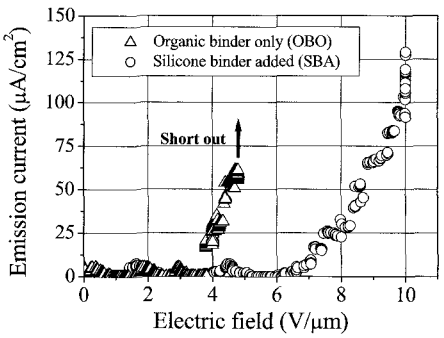

Fig. 2. Field emission characteristics of CNTw emitters.

[1] Y. Hosokawa, et al: J. Phys. D: Appl. Phys., 41, (2008) 205418
[2] Y. Shinohara, et al: Application of Plasma Process, accepted
Corresponding Author: Yoshiyuki Suda
E-mail: suda@eee.tut.ac.jp, Tel: +81-532-44-6726

1P-27

Design and Fabrication of Cantilevered Carbon Nanotube Force Sensor

○Ryosuke Nishii[1], Kota Oda[1], Takayuki Arie[1,2], and Seiji Akita[1,2]

1 Department of Physics and Electronics, Graduate School of Engineering, Osaka Prefecture University, 1-1 Gakuen-cho, Naka-ku, Osaka 599-8531, Japan
2 CREST, Japan Science and Technology Agency

Mechanical vibration of cantilevered carbon nanotubes (CNTs) enables highly sensitive mass measurement with high sensitivity of 10^{-21} g order in vacuum. In order to apply this method to biological samples, it is necessary to realize the electrical detection of the mechanical vibration in air and/or in liquid. In this study, we propose a fabrication procedure of a nano-electro-mechanical -system (NEMS) device, called "Cantilevered Carbon Nanotube Force Sensor". This device consists of a carbon nanotube field effect transistor (CNT-FET) and a cantilevered carbon nanotube functioning as a gate electrode. We also calculate the device performance using a finite element method (FEM).

Figure 1 shows a structure of the proposed "Cantilevered Carbon Nanotube Force Sensor". On the SiO_2 substrate, we fabricated a side gate CNT-FET through conventional photolithography process. A catalyst for single-walled carbon nanotubes (SWCNTs) was a Co thin layer with a thickness of 8 nm, which was formed by the electron beam (EB) evaporation. SWCNTs were synthesized by alcohol chemical vapor deposition method. Source and drain electrodes consisting of Pt/Ti were fabricated. On the channel of CNT-FET, a Si_3N_4 layer was deposited in order to protect SWCNTs from an electron beam during nano-manipulation under the direct view of scanning electron microscopy (SEM). Following these processes, a side gate electrode was fabricated near the SWCNT channel. Finally, a cantilevered multiwall CNT was attached on the gate by the nano-manipulation technique. Figure 2 shows an SEM image of a device thus fabricated.

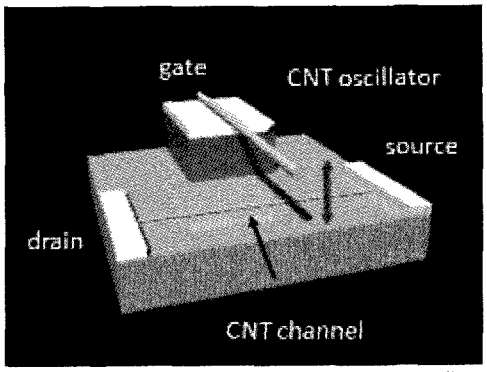

Fig.1 Cantilevered Carbon Nanotube Force Sensor

To evaluate the device performance, we performed the FEM calculation to estimate the moving gate capacitance consisting of a single multiwall CNT. It is noted that this device can detect the movement of the cantilevered CNT as the change of the drain current. The sensitivity for detecting the cantilever displacement in air was estimated to be 0.17 nA/nm from the results of the FEM calculations and the static characteristics of the side gate FETs. This sensitivity is sufficient to detect the movement of the cantilevered CNT.

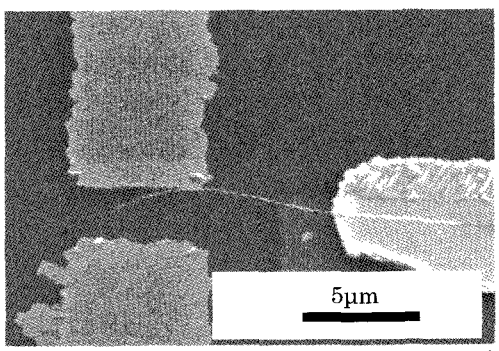

Fig.2 SEM Image of a fabricated force sensing device.

Corresponding Author: Seiji Akita
E-mail: akita@pe.osakafu-u.ac.jp,
Tel & Fax: 072-254-9261

1P-28

Sidewall Functionalization of MWCNT with Fuming Nitric Acid and Its Application to Polymer-Nanocomposite

○Hiroshi Kitamura[1], Shinya Kushita[1], Masaru Sekido[2], Hisato Takeuchi[3], Masatomi Ohno[1]

[1]*Department of Advanced Science and Technology, Toyota Technological Institute, Tempaku, Nagoya 468-8511*
[2]*Department of Materials Science and Engineering, Miyagi National College of Technology, Natori, Miyagi 981-1239*
[3]*Materials Fundamental Research Department, Toyota Central R &D Labs. Inc, Nagakute, Aichi 480-1192*

The structural uniqueness of CNT induces some useful properties; for example, mechanical strengthening has attracted considerable attention in nanotechnological application of CNT as a filler in polymer matrix. Nevertheless, its application is often limited by the low solubility due to easy aggregation to bundles. One of the overcoming methods for this problem is sidewall functionalization of CNT, which may destruct the bundle structure, allowing desirable dispersion into polymer.

For this aim, the reaction of SWCNT with fuming HNO_3 was studied in our group, and the results showed that introduction of functional groups could be performed on the surface of SWCNT and such modification enabled dispersion of SWCNT in polar solvents [1]. In our continuing work, we wish to report extension of this methodology to the sidewall functionalization of MWCNT besides its application to MWCNT-polyvinyl alcohol (PVA) nanocomposite.

For example, MWCNT (NANOCYL® ϕ=9.5 nm, l=1.5 μm) was reacted with fuming HNO_3 under ultrasonic irradiation, and the product was treated with aq. NH_3 to give water soluble MWCNT. The structure of thus modified MWCNT was elucidated by IR, XPS and TGA analyses and solubility in water was estimated to be around 25 mg ml^{-1}. The modified MWCNT dispersed in water was simply mixed with PVA also in water, and drying of the resulting mixture on the glass plate at room temperature gave the MWCNT-PVA composite film. Tensile strength of 0.1-1 wt.% MWCNT-PVA composite film was found to be ca. 30 % higher than that of the standard PVA film.

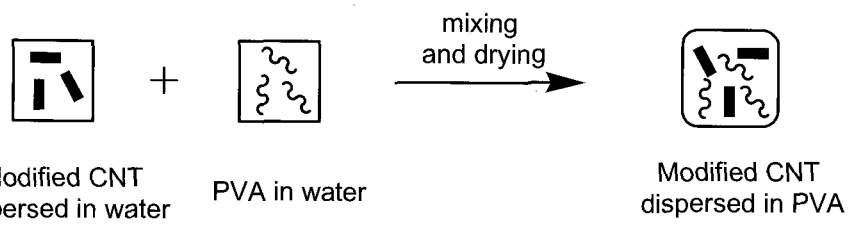

[1] H. Kitamura, M. Sekido, H. Takeuchi, M. Ohno The 36th symposium abstract p. 85.

Corresponding Author: Masatomi Ohno

TEL: +81-52-809-1889, FAX: +81-52-809-1721, E-mail: ohno@toyota-ti.ac.jp

1P-29

Theoretical Study of Spin Injection from Ferromagnetic Electrodes into Carbon Nanotube

○Yoshitaka Kato, Hiroyuki Fueno and Kazuyoshi Tanaka

Department of Molecular Engineering, Graduate School of Engineering, Kyoto University, Kyoto 615-8510, Japan

In addition to charge, electron has another attribute 'spin' which dominates magnetism. Only characteristics of charge have been mainly utilized for electronic devices. But recently, many researchers have been studying 'spintronics' which utilizes both charge and spin characteristics. Magnetoresistance effect (MR effect) is one such example. It is a phenomenon that resistance becomes larger when magnetization of electrodes is relatively anti-parallel than parallel. By use of spintronics, we could expect development of newer electronic devices.

In this study, we theoretically considered spin injection from ferromagnetic electrodes into carbon nanotube (CNT) and estimated the MR effect. The nonequilibrium Green's function method based on the density functional theory (DFT) is used to compute the spin transport properties by the ATK (Atomistix ToolKit) program package. DFT calculation was performed based on the generalized gradient approximation (GGA) and we chose single zeta polarized function for the basis set.

We chose Fe for ferromagnetic electrodes and semiconducting (7,0) CNT for object of spin injection (Fig. 1). We obtained I-V (current-voltage) characteristics when magnetization of electrodes is relatively parallel and anti-parallel (Fig. 2). From Fig. 2, we confirmed to obtain MR effect that resistance becomes larger when parallel than anti-parallel. And we got up to 80 % MR ratio

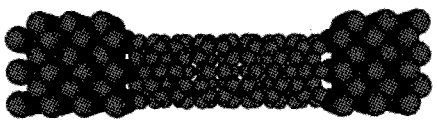

Fig. 1 CNT bridged between Fe ferromagnetic electrodes.

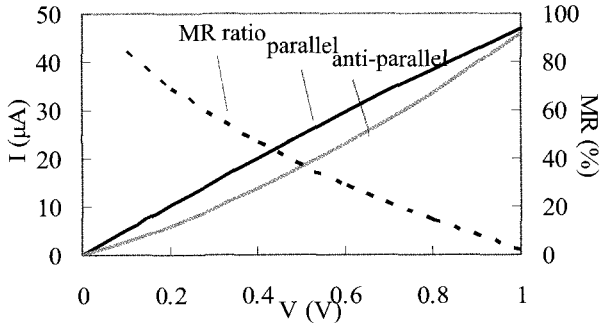

Fig. 2 I-V characteristics for each magnetization scheme and MR ratio.

Corresponding author: Yoshitaka Kato

TEL: 075-383-2551, Fax: 075-383-2556, E-mail: kato-yoshitaka@mail.goo.ne.jp

1P-30

Fully-Stretchable Sensors for Human Motion Sensing by "Sticking" SWNT Films to Arbitrary Substrates

○Takeo Yamada[1], Yuki Yamamoto[1], Natsumi Makimoto[1], Sachiko Yamada[1], Yuhei Hayamizu[1], Don N. Futaba[1], and Kenji Hata[1, 2]

[1]*Research Center, National Institute of Advanced Industrial Science and Technology (AIST), 1-1-1 Higashi, Tsukuba, Ibaraki 305-8565, Japan*
[2]*Japan Science and Technology Agency (JST), Kawaguchi, 332-0012, Japan*

Previously, we presented "Super-growth," (water-assisted chemical vapor deposition) which enabled the highly efficient growth of vertically-aligned, single-walled carbon nanotubes (SWNT forest) [1]. Later, we demonstrated the controlled, high-densely packing of the SWNT forest structure using liquids to create shape-engineerable SWNT bulk solids ("CNT-solid") [2]. More recently, we introduced a methodology to assemble and process SWNT thin films ("CNT-wafer") to realize complex, multi-dimensional microelectromechanical devices [3]. Here, we present the next step forward [4].

We demonstrate a CNT-based, fully-stretchable device (i.e. all device components are stretchable). We achieve this by overcoming the constraint of using rigid silicon substrates by developing a method to "stick" various CNT structures to arbitrary substrates. From the varied structure and composition of CNTs-aggregates, we observed both ductile and brittle mechanical properties, which opened an opportunity to make fully-stretchable devices. As an example, we fabricated CNT-based strain sensor which showed great performance range with a long cyclic life, particularly when compared to conventional metal-based strain sensors. Because of the wide performance range, we applied this toward the sensing of human motion, an application only possible by complex or computer-intensive methods.

References:

[1] K. Hata, D.N. Futaba, K. Mizuno, T. Namai, M. Yumura, and S. Iijima, Science **306**, 1362 (2004).

[2] D.N. Futaba, K. Hata, T. Yamada, T. Hiraoka, Y. Hayamizu, Y. Kakudate, O. Tanaike, H. Hatori. M. Yumura, and S. Iijima, Nature Mater. **5**, 987 (2006).

[3] Y. Hayamizu, T. Yamada, K. Mizuno, R.B. Davis, D.N. Futaba, M. Yumura, and K. Hata, Nature Nanotech. **3**, 289 (2008)

[4] T. Yamada, Y. Yamamoto, Y Hayamizu, D.N. Futaaba, Y. Yomogida, A. Sekiguti, M. Yumura, and K. Hata, Science submitted.

Corresponding Author: Takeo Yamada
E-mail: takeo-yamada@aist.go.jp
Tel: +81-29-8614654, Fax: +81-29-8614851

1P-31

Analysis of Fe Catalyst Behavior on SiO_2/Si Substrates for CNT Growth Using Mössbauer Spectroscopy

Hisayoshi Oshima[1], Tomohiro Shimazu[1], Milan Siry[1] and Ko Mibu[2]

[1]*Research Laboratories, DENSO CORPORATION*
500-1 Minamiyama, Komenoki, Nisshin-shi, Aichi 470-0111, Japan
[2] *Graduate School of Engineering, Nagoya Institute of Technology*
Showa-ku, Nagoya 466-8555, Japan

Great efforts have been expended for understanding of catalysts behavior during the growth of carbon nanotubes (CNTs) in order to control CNT features such as diameter, chirality, length and so on. However, there are few reports describing chemical states of the catalysts during the CNT growth. One of the reasons is difficulty to detect catalyst signals using standard analytical instruments such as XPS, because catalysts are covered with CNT and/or carbon. We have demonstrated that conversion electron Mössbauer spectroscopy (CEMS) is a powerful tool for the analysis of the CNT catalyst, when Fe is employed as a catalyst. [1]

In this study, we applied CEMS to the analysis of Fe chemical states on SiO_2/Si substrates from the deposition of Fe to the end of CNT growth.

Samples for the investigation were prepared as follows. ^{57}Fe was deposited on thermally oxidized Si substrates by an evaporator. Film thicknesses of ^{57}Fe were changed from 1 nm to 20 nm. CNTs were grown at 1113 K under C_2H_4 gas flow with an addition of H_2 and water vapor. Annealing of a substrate was also performed for reference using the growth tube at 1113 K under atmospheric pressure of flowing Ar gas for 5 min.

Figure 1a shows the CEMS spectrum of ^{57}Fe after annealing. The result of curve fitting revealed that the spectrum consisted of α-Fe (+) and three additional components, indicated as (#), (*) and ($). (#) is attributed to γ-Fe. (*) and ($) are similar to the reported peaks from Fe_2SiO_4 and an alleged super-paramagnetic phase.[2] After CVD, the intensities of α-Fe and Fe_2SiO_4 rapidly decreased and Fe_3C (o) phase appeared. (Figure 1b) During the CNT growth, it was found from in-situ TEM observation [3] that the catalyst shows a metal-carbide phase. Therefore, some portion of Fe_3C formed from α-Fe and Fe_2SiO_4 could act as CNT growth catalyst. The assignment of the peak ($) needs further investigations with consideration of the super-paramagnetic effect of ultra fine magnetic particles.

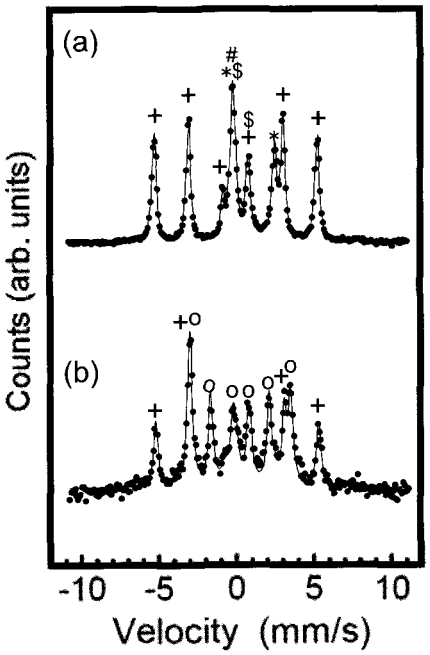

Fig.1 CEMS spectra of ^{57}Fe on SiO_2/Si substrates, (a); annealed at 1113 K in Ar, (b); CNT grown for 3 min. (+); α-Fe, (o); Fe_3C, (*); Fe_2SiO_4, (#); γ-Fe, and ($); unknown nonmagnetic phase. Solid lines indicate the result of curve fitting. The initial film thickness of ^{57}Fe was 5 nm.

References: [1] H. Oshima et al., *The 36th Fullerene-Nanotubes General Symposium,* (2009) 3P-15.
[2] M. Pe´rez-Cabero et. al., *Phys. Chem. Chem. Phys.*, **8**, 1230 (2006).
[3] Yoshida et al., *Nano Lett.*, **8**, 2082 (**2008**)

Corresponding Author: Hisayoshi Oshima
E-mail: hoosima@rlab.denso.co.jp Tel.: +81-561-75-1860 Fax.: +81-561-75-1193

1P-32

Effects of KOH Addition on Liquid-phase Synthesis of Highly Aligned Carbon Nanotubes

○Yoshihiro Yamaguchi, Kiyofumi Yamagiwa, Tomoka Kikitsu, Shunsuke Yamashita and Jun Kuwano

Department of Industrial Chemistry, Faculty of Engineering, Tokyo University of Science, 12-1 Ichigayafunagawara-machi, Shinjuku-ku, Tokyo 162-0826, Japan

Ando *et al.* have reported the liquid-phase synthesis of highly aligned carbon nanotubes arrays (HA-CNTAs) on Si substrates [1]. Our group has also developed one-step liquid-phase synthesis of HA-CNTAs with a stainless steel substrate and a homogeneous alcoholic solution of metallocene catalysts [2,3]. No catalyst preparation process is necessary for this method, which is the simplest and lowest cost among known synthetic methods of CNTs. Furthermore, the liquid-phase reaction field has other advantages including high density of the liquid carbon souse and a wide choice of additives which can be dissolved into the solvents.

We here select KOH as an additive, which is a well-known chemical activator for preparation of activated carbons, and examine effects on the growth.

A plate of commercially available stainless steel (SUS304, 5×25×0.1 mm) was resistance-heated at 800°C for 15 min in 10 mM ferrocene methanol solution (200 mL) with an Ar flow. One of additives of MOH(M=Li,Na,K) and CH_3COOK was added to the solution to elucidate the roles of K and OH ions in the HA-CNTAs growth.

Fig. 1 shows SEM images of the products in the cases of (a) no addition of KOH and (b) addition of KOH. HA-CNTAs were grown in both cases: the height increased ten times by adding KOH, (a) 10 μm and (b) 100 μm.

On the other hand, no such effects were observed with addition of LiOH, NaOH or CH_3COOK. This indicates that neither K nor OH alone accelerates the growth of CNTs. The added KOH presumably acts as a chemical activator, that is, the KOH would remove amorphous carbons deposited on the surface of the catalyst particles and probably prevent the inactivation, resulting in the acceleration of the HA-CNTAs growth.

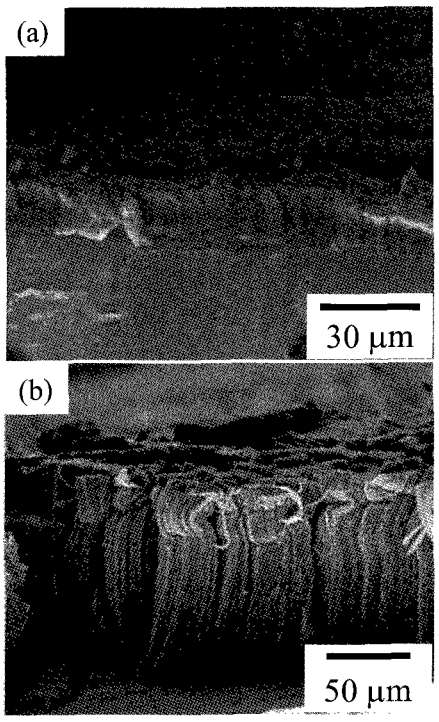

Fig. 1. SEM images of HACNTs prepared a) without addition of KOH, b) with addition of KOH.

[1] Y. F. Zhang, M et al., *Physica B*, **323**, 293 (2002): *Jpn. J. Appl. Phys.*, **41**, L408 (2002).
[2] K. Yamagiwa *et al.*, *Key Eng. Mater.*, **350**, 19 (2007). [3] M. Mikami *et al.*, *ibid.*, **350**, 23 (2007).

Corresponding Author: Jun Kuwano
TEL/FAX: +81-3-5228-8314, E-mail: kuwano@ci.kagu.tus.ac.jp

1P-33

Chiral Selective Separation for Single-walled Carbon Nanotubes Using both dispersants of Polysaccharide and Surfactant

Yoshiya Kaminosono, Katsumi Uchida, Koji Tsuchiya, Tadahiro Ishii, and Hirofumi Yajima*
Department of Applied Chemistry, Faculty of Science, Tokyo University of Science
12-1 Funagawara-machi, Shinjyuku-ku, Tokyo 162-0826, Japan

The electronic properties of single-walled carbon nanotubes (SWNTs) vary from metal to semiconductor depending on their chirality. As-synthesized SWNTs contain various chiralities, namely, both metallic and semiconducting SWNTs. Thus, for application of the SWNTs to electronic devices such as field emission transistor, it's absolutely imperative to separate metallic from semiconducting SWNTs, or to pick out specific chirality. To overcome this problem, many researchers have been focusing on the effective chiral separation of SWNTs using various dispersants such as DNA, polymer, and surfactant, with various separation techniques such as density gradient ultracentrifugation (DGU), laser ablation, ion-exchange chromatography and electrophoresis. We have investigated the dispersion of SWNTs in water using polysaccharide such as carboxymethylcellulose (CMC) and chitosan. In result, CMC possessed the high ability to disperse SWNTs. Additionally, by means of DGU for the SWNTs dispersed by using CMC, the metal-to-semiconducting ratio for the treated SWNTs was changed, indicating that CMC was an effective agent for chiral separation of SWNTs. In this study, we have investigated the chiral separation of the HiPco SWNTs using the mixed dispersants of both CMC and sodium dodecyl sulfate (SDS) with DGU. The HiPco SWNTs were dispersed in the mixed dispersants aqueous solution with changing the mixture ratio of CMC and SDS by ultrasonication. The dispersed solution was then ultracentrifuged to remove the bundles of SWNTs. The supernatant solution was added in the iodixanol solution in the centrifuge tube. The chiral separation of the dispersed SWNTs was conducted with the DGU treatment using the density gradient (d = 1~1.4 g /cm^3) solution of iodixanol. In result, one of fractions of the SWNTs aqueous solutions treated by DGU was colored not black but blue. From visible-NIR absorption spectra, the metal-to-semiconducting (Metal/Semi) ratio for the SWNTs fractionated by DUG was changed, comparing with SWNTs by not treated DUG. Using mixture of 1 wt% SDS and 1 wt% CMC, the Metal/Semi ratio was significantly changed, resulting in only increasing the ratio of (7, 5) SWNT. This result indicates that the use of the mixed dispersing agents and DGU is a promising method for chiral selective separation.

Corresponding Author: Hirofumi Yajima
TEL: +81-3-3260-4272(ext.5760), FAX: +81-3-5261-4631, E-mail: yajima@rs.kagu.tus.ac.jp

1P-34

Purification of Single-walled Carbon Nanotubes Generated with Arc-burning Apparatus by Utilizing Electrophoresis Technique

○Takashi Mizusawa[1], Shinzo Suzuki[1], Toshiya Okazaki[2], and Yohji Achiba[3]

[1]*Department of Physics, Kyoto Sangyo University, Kyoto 603-8555, Japan*
[2]*Nanotube Research Center, AIST, Tsukuba 305-8565, Japan*
[3]*Department of Chemistry, Tokyo Metropolitan University, Tokyo 192-0397, Japan*

Abstract: In these few years, purification process of single-walled carbon nanotubes (SWNTs) has been extensively developed by several groups, where new technique such as density-gradient ultra-centrifugation [1] or electrophoresis technique [2] has been incorporated, in order to separate semi-conductive and metallic SWNTs from the mixture in mono-dispersed surfactant solution.

Recently, SWNTs generated with arc-burning apparatus in nitrogen atmosphere [3] or in helium atmosphere [4] were found to be well mono-dispersed in surfactant solution, suggesting that even raw carbon materials containing few amounts of SWNTs could give SWNTs of higher quality after purification/separation process was applied. Since the diameter distribution of SWNTs is different between SWNTs prepared in nitrogen and in helium atmosphere, respectively, it is expected that the diameter distribution of semi-conductive and metallic SWNTs can also be controlled by utilizing arc-burning technique.

In this presentation, a tentative result of separation of SWNTs prepared with arc-burning technique into semi-conductive and metallic SWNTs by utilizing electrophoresis technique is presented. The difference seen in the experimental condition between our result and ref. [2] will be discussed. Additionally, the effectiveness of density-gradient technique applied to the solution with mono-dispersed SWNTs prepared by arc-burning technique will also be presented.

References:

[1] M. S. Arnold, A. A. Green, J. F. Hulvat, S. I. Stupp, and M. C. Hersam, *Nature Nanotech.*, **1**, 60-65(2006).

[2] T, Tanaka, H, Jin, Y, Miyata, and H, Kataura, *Appl. Phys. Express*, **1**, 114001-1(2008).

[3] S. Suzuki , T. Mizusawa, T. Okazaki, and Y. Achiba, *Eur. Phys. J. D*, **52**, 83-86(2009).

[4] S. Suzuki, K. Hara, T. Fujita, T. Mizusawa, T. Okazaki, and Y. Achiba, *J. Nanosci. Nanotechnol.*, in press.

Corresponding Author: Shinzo Suzuki
E-mail: suzuki-shinzo@cc.kyoto-su.ac.jp
Tel: 075-705-1631, **FAX:** 075-705-1640

1P-35

Selective SWNTs Growth with Specific Chirality by Irradiating Free Electron Laser during Growth

○Nobuyuki Iwata[1], Daisuke Ishiduka[1], Keijiro Sakai[1], Takuya Sonomura[1], Hiroaki Takeshita[1], Kunihide Kaneki[2], Hirofumi Yajima[2], and Hiroshi Yamamoto[1]

[1]*Department of Electronics & Computer Science, College of Science & Technology, Nihon University, 7-24-1 Narashinodai, Funabashi-shi, Chiba, 274-8501 Japan*
[2]*Department of Applied Chemistry, Faculty of Science, Tokyo University of Science, 1-3 Kagurazaka, Shinjuku-ku, Tokyo, 162-8601 Japn*

For field effect transistor using single-walled carbon nanotubes (SWNTs) with extremely dense packed electronic devices, the diameter, the alignment, and the chirality of the SWNTs should be controlled. The diameter might be determined by the size of the catalyst and the in-plane alignment was also reported in growth on sapphire and SiO_2, and using the flow of the feeding gas[1]. The separation of metallic and semiconducting SWNTs has been also investigated by electrophoresis, polymer wrapping, and so on[2] However the separation and/or selective growth of SWNTs with specific chirality have not been achieved. We propose a novel technique to grow the selective SWNTs with specific chirality using free electron laser (FEL) irradiation during growth[3]. The features of the variable wavelength(0.3-6μm) and the very sharp pulse width approximately 500 ps of FEL are able to enhance the SWNTs growth with specific chirality, because absorption wavelength depends on the individual chirality.

The Co/Mo catalyst was dispersed on quartz substrates by dipping technique with the speed of 600 μm/s. The annealed substrate at 400°C in air for 5 min was loaded to alcohol catalytic chemical vapor deposition (ACCVD) chamber. The ACCVD with ethanol growth was carried out for 30 min at 1000°C after deoxidization with H_2. The irradiated wavelength of FEL was 800 nm during growth. In figure 1, Raman spectra of SWNTs are shown. The excitation lasers are 532 nm in Fig.1(a-1) and (b-1), and 785 nm in Fig.(a-2) and (b-2). The spectra of Fig. 1(a-1,-2) are of specimen without FEL, and of Fig.1(b-1,-2) are with 800 nm-FEL irradiation. The diameter of SWNTs were approximately 1.5 nm, 1.3 nm and 1.0 nm, the chirality of which are (10,7), (14,1), (12,4), (12,3), (11,5), (14,0), (10,6), (9,7), (11,4), (10,5), (13,1), (9,6) in the specimen without FEL. From the result of Fig.1(b-1), the metallic SWNTs disappeared, and the spectrum of Fig.1(b-2) showed the growth of only semiconducting SWNTs with (14,0), (10,6), (9,7) with 1.1 nm in diameter.

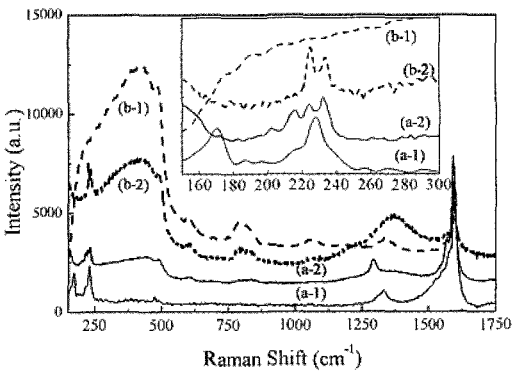

Fig.1 Raman spectra of specimens (a-1,-2) without FEL and (b-1,-2) with 800-FEL.

[1] H. Ago et al., Appl. Phys. Lett. 90 (2007) 123112.
[2] T. Tanaka et al., APEX 1 (2008) 114001.
[3] N. Iwata et al., Jpn. J. Appl. Phys. **47** (2007) 1412

iwata@ecs.cst.nihon-u.ac.jp

1P-36

Ab Initio Study toward Separation of Metallic and Semiconducting Single-Wall Carbon Nanotubes with Agarose Gel

Mari Ohfuchi

Nanoelectronics Research Center, Fujitsu Laboratories Ltd.,
10-1 Morinosato-Wakamiya, Atsugi 243-019, Japan

Recently experiments on separation of metallic and semiconducting single-wall carbon nanotubes (SWCNTs) with agarose gel have been reported [1, 2]. In the separation, an anionic surfactant, sodium dodecyl sulfate (SDS) also seems to play an important role by interacting more strongly with metallic tubes than with semiconducting ones. In this study, we examine both of the adsorption energies between SWCNTs and agarose and between SWCNTs and SDS, toward understanding and controlling the separation process.

We adopt *ab initio* method using localized basis functions optimized for biological molecules [3, 4]. The real and reciprocal space grids are set to ensure accuracy within 0.01eV of the adsorption energy per unit cell. The basis set superposition error, which is peculiar to the localized basis set, is corrected for all calculations using the counterpoise method [5].

Zigzag (n, 0) SWCNTs are selected so as to have both of metallic and semiconducting properties depending on n, which is from 8 to 13. Several directions and distances of SWCNTs with respect to agarose are examined and all SWCNTs have been found to have the same adsorption energy within the accuracy of calculation. The SDS molecule fully screened with a sodium ion also gives the same adsorption energy for all SWCNTs.

On the other hand, the SDS anion completely unscreened with a uniform background charge of opposite sign makes a large difference between metallic and semiconducting SWCNTs. The adsorption energies for the metallic tubes are 0.1 eV stronger than for the semiconducting ones. This can be attributed to the larger charge transfer from the SDS anion to the metallic SWCNTs as also shown using metallic armchair and semiconducting zigzag tubes previously [6]. This is only the result that shows a difference between metallic and semiconducting tubes for the moment. To confirm this, however, we need to examine SWCNTs wrapped by SDS anions in solution.

[1] T. Tanaka, H. Jin, Y. Miyata, and H. Kataura, Appl. Phys. Express 1, 114001 (2008).
[2] T. Tanaka *et al.*, Nano Lett. 9, 1497 (2009).
[3] T. Ozaki, Phys. Rev. B 67, 155108 (2003).
[4] T. Ozaki and H. Kino, J. Chem. Phys. 121, 10879 (2004).
[5] S. F. Boys and F. Bernardi, Mol. Phys. 19, 553 (1970).
[6] M. Ohfuchi, The 36th Fullerene-Nanotubes General Symposium 3-9 (2009).
Corresponding Author: Mari Ohfuchi
Tel: +81-46-250-8843, Fax: +81-46-250-8844, E-mail: mari.ohfuti@jp.fujitsu.com

1P-37

One-step Liquid-phase Synthesis of Highly Aligned Carbon Nanotube Arrays with Iron Pentacarbonyl

○Tomoka Kikitsu, Kiyofumi Yamagiwa, Yoshihiro Yamaguchi, Shunsuke Yamashita and Jun Kuwano

Department of Industrial Chemistry, Faculty of Engineering, Tokyo University of Science, 12-1 Ichigayafunagawara-machi, Shinjuku-ku, Tokyo 162-0826, Japan

Recently, highly aligned carbon nanotube arrays (HACNTAs) have been synthesized by resistance-heating of Si substrates in liquid-phase [1,2]. Our group has also developed one-step liquid-phase synthesis of HACNTAs on stainless steel substrates with an alcoholic solution of metallocene catalyst precursors such as ferrocene $Fe(C_5H_5)_2$ [3,4].

Iron pentacarbonyl $Fe(CO)_5$ has been often used as a precursor of ultrafine particles and catalysts. In this study, we used the carbonyl complex as a catalyst precursor for the one-step liquid-phase synthesis of HACNTAs.

Pieces cut from commercially available stainless steel (SUS304) plates were used as substrates. A substrate was resistance-heated at 800°C for 15 min by applying an alternate current in methanol containing $Fe(CO)_5$ or $Fe(C_5H_5)_2$.

Figs. 1 (a) and (b) show the HACNTAs prepared from 0.01 mM $Fe(CO)_5$ methanol solution and the dispersed CNTs specimen of the HACNTAs. In contrast, as shown in Fig. 2 (a), no HACNTAs was prepared from 0.01 mM $Fe(C_5H_5)_2$ methanol solution. In the case of the $Fe(C_5H_5)_2$ precursor, the concentration necessary for HACNTAs growth was 0.01 M (Fig. 2 (b)), which was 1000 times of that of $Fe(CO)_5$.

We presumed that the low optimal $Fe(CO)_5$ concentration for growth of HACNTAs was attributed to its decomposition temperature as low as below 100°C. It is much lower than that of $Fe(C_5H_5)_2$ of *ca.* 500°C. Probably, $Fe(CO)_5$ is able to produce many Fe catalyst nanoparticles enough for the HACNTAs growth readily even at the low concentration. The pentacarbonyl of $Fe(CO)_5$ was found to be an excellent catalyst precursor for the one-step liquid-phase synthesis of HACNTAs.

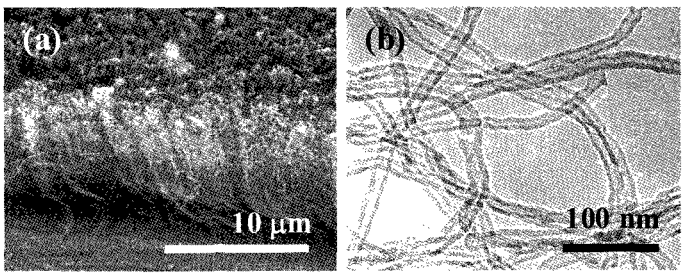

Fig. 1. (a) SEM and (b) TEM images of CNTs prepared from methanol containing 0.01 mM $Fe(CO)_5$.

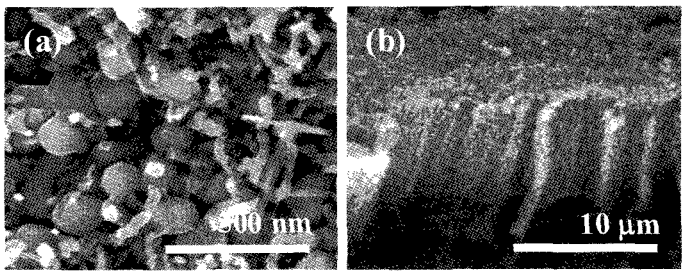

Fig. 2. SEM images of products prepared from methanol containing (a) 0.01 mM and (b) 0.01 M $Fe(C_5H_5)_2$.

[1,2] Y. F. Zhang et al., *Physica B*, **323**, 293 (2002); *Jpn. J. Appl. Phys.*, **41**, L408 (2002).
[3] K. Yamagiwa *et al.*, *Key Eng. Mater.*, **350**, 19 (2007). [4] M. Mikami *et al.*, *ibid.*, **350**, 23 (2007).

Corresponding Author: Jun Kuwano TEL/FAX: +81-3-5228-8314, E-mail: Kuwano@ci.kagu.tus.ac.jp

1P-38

TEM characterization of gamma-cyclodextrin bicapped C_{60}-fullerene in single-walled carbon nanotubes

○Kaori Takai Hirose[1], Yoko Iizumi[2], Toshiya Okazaki[1,2], Takeshi Saito[1] and Kazu Suenaga[1]

[1] *Nanotube Research Center, National Institute of Advanced Industrial Science and Technology (AIST), Tsukuba, 305-8565, JAPAN*
[2] *Department of Chemistry, University of Tsukuba, Tsukuba, JAPAN*

Cyclodextrin (CD) s are known as one of the host molecules in host-guest inclusion complex groups and have cyclic oligosaccharides with a hydrophobic interior and a hydrophilic exterior. Due to the hydrophilic exterior, therefore, the CDs show wide practical applications with various materials such as foods and chemicals to facilitate them to be solved in water. The size of guest molecules depends on a size of CD's internal diameter. Three typical CDs, namely alpha, beta and gamma, consist of six, seven and eight glucopyranoses, respectively.

In order to directly recognize such a host-guest interaction of the CDs at individual molecular basis, we focus on the C_{60}-fullerene and gamma-cyclodextrin (γCD) as a model of the host-guest inclusion complex. In a previous study, a crystal of C_{60}-γCD complex was shown to have a 1:2 compositon of C_{60} and γCD after using high-speed vibration milling (HSVM) suggesting a bicapped structure [1].

In this study we prepared the C_{60}-γCD complex by using HSVM and capsulated the complex into the SWNTs with mean diameters of 1.7 and 2.0 nm with the vapor deposition(Fig. 1). We will show the HR-TEM images of the C_{60}-γCD in SWNTs (Fig. 2).

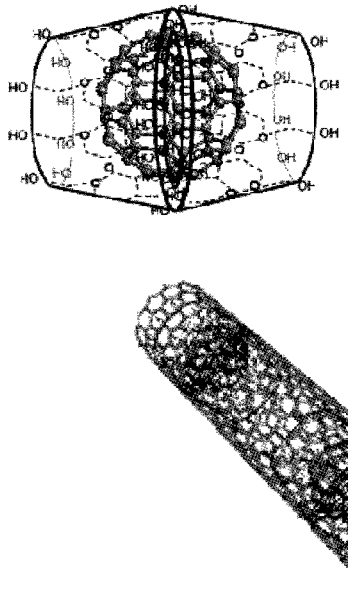

Fig. 1 Schematic representation of C_{60}-2γCD and C_{60}-2γCD in SWNT

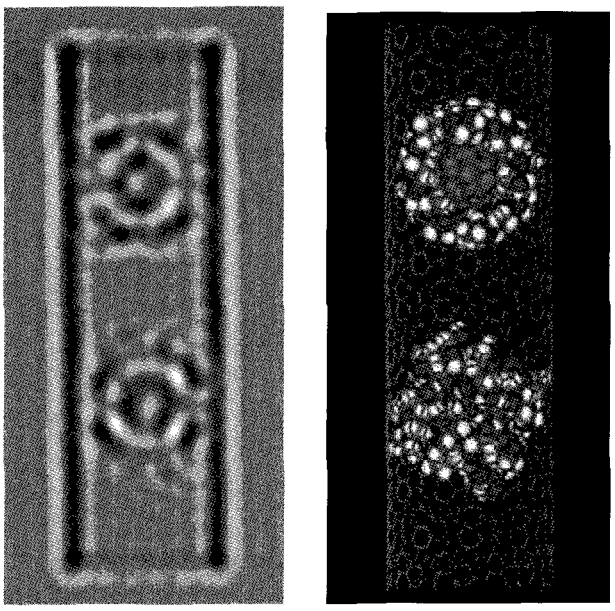

Fig. 2 Simulated TEM image and model of C_{60}-2γCD in SWNT

[1] K. Komatsu, K. Fujiwara, Y. Murata and T. Braun, *J. Chem. Soc., Perkin Trans.*, **1**, 2963-2966 (1999)

Corresponding Author: Kazu Suenaga
TEL: +81-29-861-6850, FAX: +81-29-861-4806, E-mail: suenaga-kazu@aist.go.jp

1P-39

Chemically Reactive Species Remain Alive inside Carbon Nanotubes: A Density Functional Theory Calculation Study

○Takashi Yumura

Department of Chemistry and Materials Technology, Kyoto Institute of Technology, Matsugasaki, Sakyo-ku, Kyoto, 606-8585, Japan

Abstract: Inside a carbon nanotube host, chemical reactions occur smoothly [1]. During the reactions, reactive guest species should be formed as a reaction intermediate. Judging from a lot of experiments, the reactive species seem to react with adjacent guests, despite the possibility that the reactive species are inactivated by forming the inner covalent bond with a tube host. Here a question arises as to whether the inner reactions are distracted by the formation of a covalent bond between a reactive guest and a tube host. To answer the intriguing question, we employed density functional theory (DFT) calculation based on PW91 functional. In this study, an alkyl radical guest is supposed to be formed by the removal of one H atom from its corresponding alkane due to heating or irradiation with light according to a text book. Here methyl, ethyl, isopropyl, and tert-butyl radicals were considered as guest radicals, and (8,8), (10,10), and (12,12) tubes as tube hosts.

According to DFT calculations, we obtained two types of optimized geometries of an alkyl radical inside a nanotube in Fig. 1: one is that an alkyl radical is bound to an inner tube wall, and the other is that an alkyl radical remains alive freely without the inner bond formation. Surprisingly the structures without the inner bond are more stable than those with the inner bond in energy. The energy differences are more pronounced, when an alkyl radical is encapsulated inside a tube with its smaller diameter. Stabilizing an isolate radical species inside a tube is reasonable, because the energy gain by the formation of the inner bond being strikingly weak [2] cannot compensate for the energy loss by tube deformations induced by the bond formation.

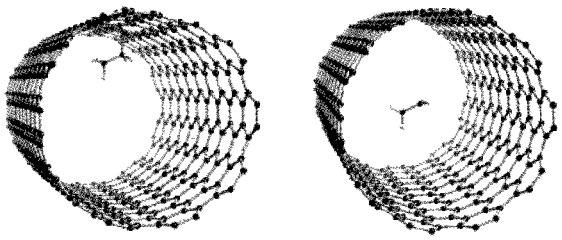

Figure 1 Optimized structures of an ethyl radical inside a (10,10) tube.

References: [1] Khlobystov, A. N.; Britz, D. A.; Briggs, A. D. *Acc. Chem. Res.*, **2005**, *38*, 901.
[2] (a) Yumura, T.; Kertesz, M.; Iijima, S. *J. Phys. Chem. B*, **2007**, *111*, 1099. (b) Yumura, T.; Kertesz, M.; Iijima, S. *Chem. Phys. Lett.* **2007**, *444*, 155.

Corresponding Author Takashi Yumura
E-mail yumura@chem.kit.ac.jp
Tel&Fax +81-75-724-7571

1P-40

Photoluminescence from Isolated Individual Carbon Nanohorns

Hibiki Matsumoto and Masahito Sano

Department of Polymer Science and Engineering, Yamagata University, Yonezawa, Yamagata 992-8510, Japan

A carbon nanohorn (CNHorn) is often described as a single-walled carbon nanotube (SWCNT) with conical tips. The diameters range from 2 to 5 nm and the lengths are of the order of 50 nm. When they are synthesized, they always form a 100 nm wide spherical aggregate of the secondary structure as if each CNHorn radiates from the common center. It is not known how each CNHorn is connected. Raman spectroscopy shows D-band that is as intense as G-band, indicating that a significant amount of non-crystalline carbons are present. Whereas SWCNTs are stable at high temperatures in vacuum, CNHorn "melts" to condensed spheres. These observations suggest that CNHorn is a full of defects. It is, then, a natural question to ask whether CNHorn is a kind of SWCNTs, or how close they are each other.

Photoluminescence (PL) spectroscopy is a powerful technique to characterize SWCNTs. In particular, chirality can be assigned to individual SWCNT, based on the excitonic interactions produced by light absorption of each chiral SWCNT. In this study, we have examined PL from purified, isolated CNHorn.

CNHorns can be freed from the secondary aggregates easily by an application of ultrasonic in acids. Freed CNHorns are collected by centrifugation. One of the main differences between CNHorn and SWCNT is the fact that a stable solution of CNHorn is obtainable without using any kinds of surfactants or additives. We think that the small size and the large defect density are responsible for this. Thus, the supernatant behaves as if it is a usual molecular solution, which allows us to perform various techniques that are common in organic chemistry. The supernatant was injected to gel-permeation chromatography (GPC) and the first two portions are collected (Figure 1). Because we used UV absorption as a detecting signal, all portions have strong UV absorption at 300 nm. The concentration of each portion, however, was so low that any UV spectroscopic feature was discernible. The first portion did not yield any PL. The second portion, marked as 5.2 min, produced PL around 800 nm. Unlike SWCNTs, it is excited by a wide range of wavelengths. This behavior is similar to ordinary organic molecules or super-oxide defects in inorganic compounds.

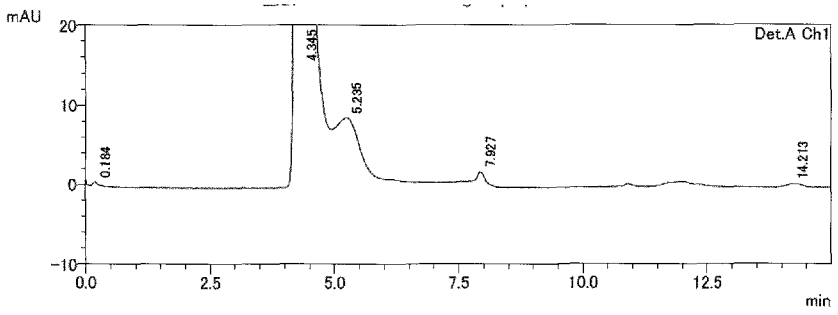

Figure 1. GPC chromatograph of the supernatant containing individual CNHorn..

Corresponding Author: Masahito Sano
TEL: +81-238-26-3072, FAX: +81-238-26-3072, E-mail: mass@yz.yamagata-u.ac.jp

1P-41

Cytotoxicity of Single-Wall Carbon Nanohorns with Different Sizes

○M. Zhang[1], T. Fujinami[1], J. Xu[1], T. Yamaguchi[2], S. Iijima[1,2], M. Yudasaka[1]

AIST, Tsukuba, Nagoya University

Application of single wall carbon nanohorns (SWNHs) to drug delivery system (DDS) has been studied recently and SWNHs are found to be useful due to their unique structures. The fundamental study such as the cytotoxicity of SWNH aggregates with sizes of about 100 nm has also been investigated. However, the cytotoxicities of SWNH aggregates with other different sizes were not clear, especially those of the small sized aggregates or individual SWNHs that are believed to be more useful in DDS than aggregates with 100 nm sizes. In this study, we investigate the cytotoxicity of SWNH aggregates with different sizes and individual SWNTs that were separated from as-produced aggregates by sucrose gradient centrifugation (SGC).

We separated SWNHs from as-produced aggregates by using SGC method as reported previously [1]. We prepared three types of SWNHs dispersions. The first one had individual tubes and small-aggregate of SWNHs. The shapes of individual SWNHs were straight or branched. Lengths of straight SWNHs or of each arm of the branched types were 10-70 nm and their diameters were 2-10 nm. The small aggregates have diameter about 30-40 nm. The second and third ones were SWNHs with size-distribution about 70 nm and 100 nm, respectively. We incubated two cell lines of HeLa and NIH 3T3 cells with culture medium solution containing three types of dispersions of SWNHs (1 to 20 μg/ml) for 24 hours. The cytotoxicities of the three types of SWNH specimens were examined by using WST-1. The results showed that the three types of SWNHs with different sizes are not cyototoxic in the condition of this study. The cell uptake of the individual SWNHs observed with confocal microscopy will be presented in symposium.

References:

[1] M. Zhang, T. Yamaguchi, S. Iijima, M. Yudasaka, J. Phys. Chem. C 113 (2009) 11184

Corresponding Author: M. Zhang, M. Yudasaka

E-mail: m-zhang@aist.go.jp; m-yudasaka@aist.go.jp

Tel&Fax: 029-861-6290

1P-42

Establishment of spin injection into a single layer graphene at room temperature

○Nobuhiko Mitoma[1], Takumi Takano[1], Masashi Shiraishi[1,2], Takayuki Nozaki[1], Teruya Shinjo[1], Yoshishige Suzuki[1]

[1]*Graduate school of engineering science, Osaka University, Toyonaka 560-8531, Japan*
[2]*JST-PRESTO, Kawaguchi 332-0012, Japan*

Graphene has been attracted much interests as an exciting potential candidate for spintronic device due to its high mobility and weak spin-orbit interaction. So far, several research groups have succeeded in demonstrating spin injection into a single layer graphene (SLG) [1,2]. However, mechanisms of spin injection through the interface between ferromagnetic electrode and SLG is still remained as a controversial problem; while Tombros *et al.* claimed that Al oxide tunneling barrier plays a crucial role for spin injection, Cho *et al.* observed spin signal in a SLG at low temperature without using tunnrling barrier, and furthermore Han *et al.* reported spin injection into a SLG at room temperature using transparent Co/SLG interface with MgO masking layer [3].

Here, in this presentation, we firstly demonstrate room temperature spin injection into a SLG without any tunneling barrier nor masking layer. Non-local magnetoresistance measurement revealed an obvious spin signal at room temperature, and gate voltage dependence of the signal showed systematic increase with decreasing the carrier concentration. These results indicate that neither tunneling barrier nor masking layer is crucial and spin injection into a SLG can be realized by more simplified fabrication process, which would be an encouraging progress for a research field of graphene spintronics.

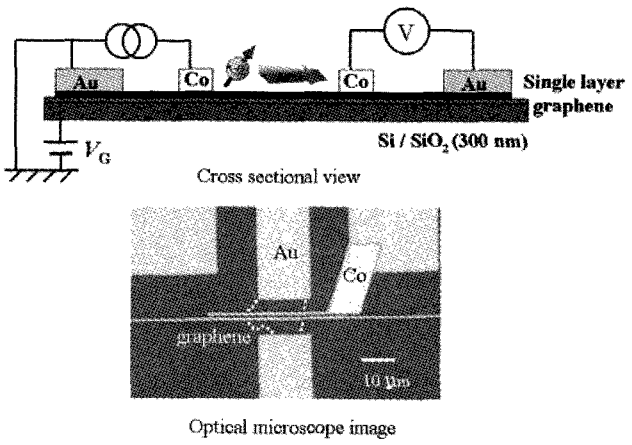

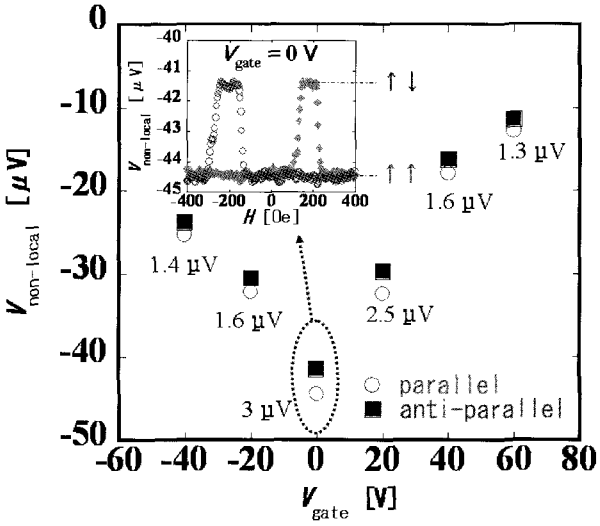

Fig.: sample image (left) and a gate voltage dependence of the spin signal (right).

[1] N.Tombros *et al.*, *Nature* **448** 571 (2007).
[2] S.Cho *et al.*, *Appl.Phys.Lett.* **91** 123105 (2007).
[3] W.Han *et al.*, *Appl.Phys.Lett.* **94** 222109 (2009).

Corresponding Author: Nobuhiko Mitoma
TEL: +81-6-6850-6427, FAX: +81-6-6850-6427, E-mail: mitoma@spin.mp.es.osaka-u.ac.jp

1P-43

Stability and Atomic Structures of Multi-Vacancies in Hexagonal Boron Nitride

Susumu Okada

Graduate School of Pure and Applied Sciences, Center for Computational Sciences, University of Tsukuba, Tennodai, Tsukuba 305-8577, Japan
CREST, JST, 4-1-8 Honcho, Kawaguchi, Saitama 332-0012, Japan

Atomic-scale intrinsic defects in graphene and carbon nanotubes are known to influence electronic and mechanical properties of such systems. Many theoretical and experimental works have reported the modulation of these properties in these materials possessing hexagonally bonded network. Boron nitride is the other example for planer and tubular structure of honeycomb network. In the case, due to the ambivalent nature characterized by ionicity and covalency, a recent transmission electron microscopic study has shown the interesting variations of the atomic structure for the multi-vacancies introduced into h-BN sheet [1]. However, theoretical investigations on electronic and atomic structure of the intrinsic defects are not addressed yet.

Here we perform the total energy calculation on multi-vacancies in h-BN based on the local density approximation. The atomic structures of the vacancies in h-BN are considerably different from that in graphene due to the ambivalent nature of the material. Furthermore, our calculation clearly show that nitrogen terminated edges are energetically favorable for the multi-vacancies in h-BN under the electron rich condition. The results agree well with the experimentally observed structure.

[1] K. Suenaga, private communications.

Corresponding Author: Susumu Okada, sokada@comas.frsc.tsukuba.ac.jp

1P-44

Ferromagnetic carbon nano-foam formed from boron containing composite carbon target by the pulsed laser vaporization in Ar/H_2 mixture

○Susumu Muraki, Iori Iwata, Hiroki Endo, Shunji Bandow, Sumio Iijima

Department of Materials Science and Engineering, Meijo University, 1-501 Shiogamaguchi, Tenpaku, Nagoya 468-8502, Japan

Vaporization of composite carbon pellet including ~1 wt % of B_2O_3 in depressurized Ar/H_2 mixture was carried out by using Nd:YAG pulsed laser at various temperatures between 400 and 1000 °C. Generated materials were looks like amorphous carbon material but the graphitization was progressed. Transition metals such as Fe, Ni, Co and other ferromagnetic elements have not been detected by EELS. In addition, even the boron was used for the sample preparation B-element was not detected. So that we consider if the B was doped in the carbon network, the rate is far below the detection limit of EELS (< 1000 ppm).

As mentioned above, TEM observation reveals that the structure of present products resembles amorphous carbon with somewhat graphitized, and it is similar to the foam. Hence we call the present materials as boron doped carbon nanofoam (B-CNF).

Magnetization curves taken at 4.2 K were indicated in Fig. 1. From this figure, all of the B-CNF have ferromagnetic feature with clear hysteresis, and the magnitude of the saturation magnetization (M_s) slightly depend on the formation temperature under the same preparation pressure. On the other hand, the magnitude of the coercivity increased as the preparation temperature increased. The largest M_s was obtained when the sample was prepared in 760 torr at 1000 °C.

Fig. 2 shows the temperature dependence of the magnetic susceptibility. The value of χ decreases as the temperature increased, obeying the Cure law. Since the *M-H* carves at 280 K did not give hysteresis, this spin system behaves superparamagnetism near RT.

Quantitative discussion will be presented at the symposium.

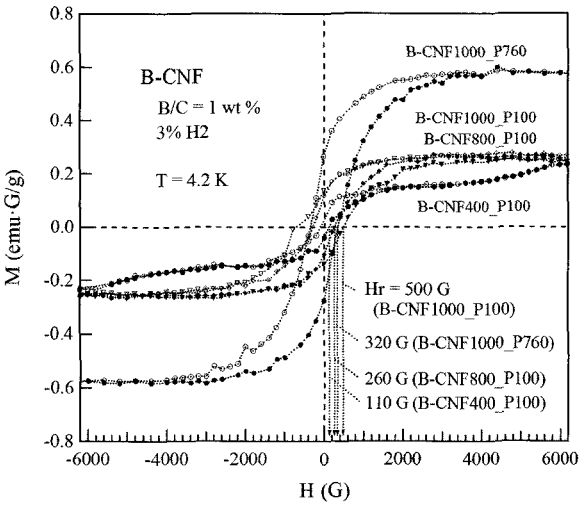

Fig. 1. *M-H* curves taken for the samples of B doped carbon nanofoam (B-CNF) produced at the temperatures of 400, 800, 1000 °C. P100 and P760 in the sample codes mean, respectively, the environment pressures in torr. H_r is coercivity.

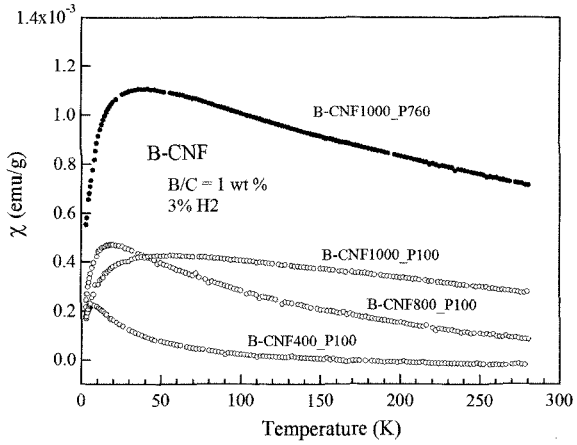

Fig. 2. Temperature dependences of the magnetic susceptibility. Magnitude of χ decreases at low temperatures and which is explainable by the blocking effect.

Corresponding Author: Shunji Bandow, **E-mail:** bandow@ccmfs.meijo-u.ac.jp, **Tel&Fax:** +81-52-834-4001

1P-45

Ferromagnetic carbon nano-foam prepared by the pulsed laser vaporization of pure carbon in Ar/H_2 mixture

○Hirohito Asano, Hiroki Endo, Shunji Bandow, Sumio Iijima

Department of Materials Science and Engineering, Meijo University, 1-501 Shiogamaguchi, Tenpaku, Nagoya 468-8502, Japan

Pulsed laser vaporization of pure carbon target in the mixture of Ar/ H_2 at 1000 °C was carried out and the magnetic feature of the products was examined. TEM image of the product in 3 % of H_2 was seen in Fig. 1. One can recognize that the structure of the sample looks like the foam, so that we call here the sample as carbon nanofoam (CNF). In addition, the elemental analysis using EELS did not give any extrinsic element such as Fe, Ni and Co etc; only carbon has been detected.

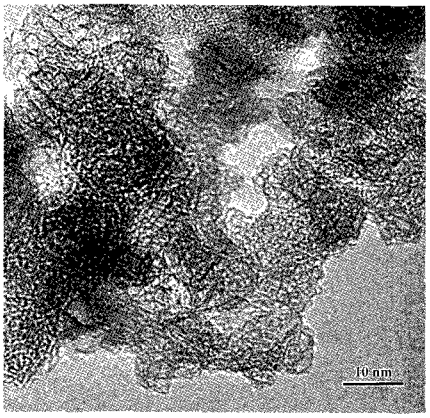

Fig. 1. TEM of all carbon nanofoam.

Magnetization curves are in Fig. 2, which indicate clear hysteresis loops. Although the same value for the coercivity of 350 G was observed, the magnitude of the saturation

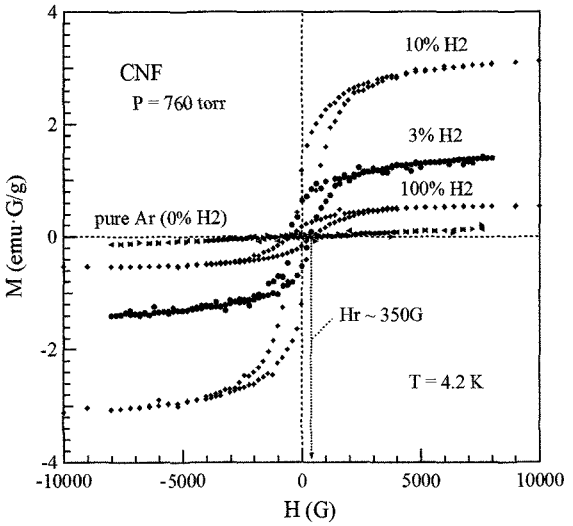

Fig. 2. *M-H* curves taken for CNF prepared in pure Ar (0% H_2), 3 % H_2, 10 % H_2 and 100 % H_2 at 1000 °C. The values of the saturation magnetization were increased upon increasing H_2 concentration up to 10 % but it decreased when the CNF was prepared in 100 % of H_2. H_r is coercivity and is independent on the preparation condition.

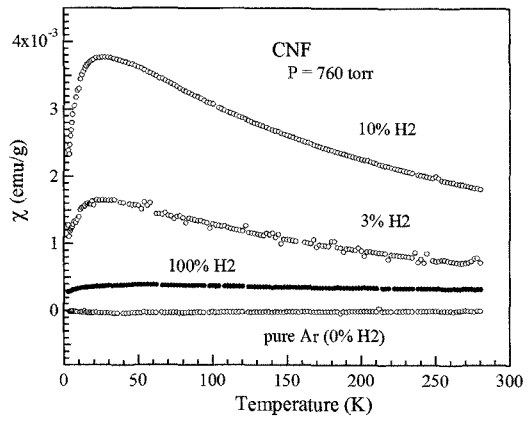

Fig. 3. Temperature dependences of the magnetic susceptibility. Note that all traces resemble well with almost the same blocking temperature of ~20 K.

magnetization largely depends on the H_2 concentration. Fig. 3 is the temperature dependence of the magnetic susceptibility. All traces have similar feature. According to the results appeared in Figs. 2 and 3, it is natural to consider that only the difference in the magnetic feature among the samples is the magnitude of M and χ. Hence we conclude that the yield of ferromagnetic CNF is a function of H_2 concentration. Analyses in detail will be discussed in the symposium.

Corresponding Author: Shunji Bandow,
E-mail: bandow@ccmfs.meijo-u.ac.jp, **Tel&Fax:** +81-52-834-4001

1P-46

Structural Change in Nano-carbon by Femtosecond Laser Shots: Virtual Experiments Using Supercomputers

○Yoshiyuki Miyamoto[1], and Hong Zhang[2]

[1]*Nano Electronics Research Laboratories, NEC, 34 Miyukigaoka, Tsukuba, 305-8501, Japan*
[2]*School of Physical Science and Technology, Sichuan University, Chengdu 610065, China*

Carbon materials with high melting temperatures are hard to fabricate just by thermal processes. Recent experiments using the Femtosecond laser opened a door for controlled fabrication of material with such high melting temperatures. We are seeking on efficient method of controlling the structure of graphene and nanotube by means of the femtosecond laser shot. Instead of real experiment, we are performing virtual experiment using supercomputers.

A computational method mimicking strong laser shot has been developed combining the real-time propagation method within the time-dependent density functional theory [1], which satisfies energy conservation rule throughout the molecular dynamics simulation upon pulse laser shot and is convenient for performing long-time simulation with numerical stability. Exfoliation of graphene layer and destruction of carbon nanotube will be demonstrated in our presentation. By changing the power and pulse-shape of the femtosecond laser, the resulting structural change can be designed and will be applicable to predict and analyze recent experiments [2-4].

All calculation presented here were performed by using the Earth Simulator.

[1] Y. Miyamoto and H. Zhang, *Phys. Rev. B***77**, 165123 (2008).

[2] F. Carbone, P. Baum, P. Rudolf, and A. H. Zewail, Phys. Rev. Lett. **100**, 035501 (2008).

[3] R. K. Raman, Y. Murooka, C.-Y. Ruan, T. Yang, S. Berber, and D. Tománek, Phys. Rev. Lett. **101**, 077401 (2008).

[4] J. Kanasaki, E. Inami, K. Tanimura, H. Ohnishi and K. Nasu, Phys. Rev. Lett. **102**, 087402 (2009).

Corresponding Author: Yoshiyuki Miyamoto
TEL: +81-29-850-1586, FAX: +81-29-856-6136, E-mail: y-miyamoto@ce.jp.nec.com

1P-47

Synthesis and Magnetic Properties of Rare Earth Matel Graphite Intercalation Compounds

○Satoshi Heguri, Mototada Kobayashi

Department of Material Science, Graduate School of Material Science
University of Hyogo, Ako, Hyogo 678-1297, Japan

Recently, graphite intercalation compounds (GICs) have attracted great attention due to the discovery of superconductivity in CaC_6 and YbC_6 with fairly high transition temperatures T_c of 11.5 and 6.5K, respectively [1,2]. The magnetic behavior of GIC is a good model for low dimensional magnetism and is interesting subjects from experimental and theoretical viewpoints.

There have been many studies on transition metal chloride GICs [3]. In those chloride compounds, however, the effect of the magnetic transition metal ions on the magnetic properties is not so simple because the magnetic ions are surrounded by chlorine ions. The first stage Eu-GIC EuC_6 was expected to be simple system due to including only bare magnetic ions. However, EuC_6 showed the peculiar magnetic behavior [4]. The magnetic properties in the higher stage of Eu-GIC have not been reported.

In this work, we report synthesis and magnetic properties of Sm- or Tm-GICs. We expect that those GICs show various magnetic characteristics of great interest depending on their number of f-electrons and graphene layer.

Sm and Tm-GICs were synthesized from highly oriented pyrolytic graphite (grade ZYA), and excess Sm metal (99.9%) or Tm metal (99.9%). They were sealed into quartz tube after evacuating. Thermal treatment was performed in a furnace at 893~1023K for several weeks. After the reaction, the surface color of compounds changed from that of graphite and the sample thickness was found to be increased. Sm and Tm-GICs show ferromagnetic characteristics at low temperature.

Further details will be discussed together with the results of the x-ray diffraction profiles and the magnetic susceptibility at the meeting.

References: [1] T. E. Weller et al., Nature Physics 1 (2005) 39.
[2] N. Emery et al., Phys. Rev. Lett. 95 (2005) 087003.
[3] K. Ohhashi et al., J. Phys. Soc. Japan 37 (1974) 63.
[4] H. Suematsu et al., Synthetic Metals 8 (1983) 23.

Corresponding Author: Satoshi Heguri
E-mail: rk07d004@stkt.u-hyogo.ac.jp
Tel&Fax: +81-791-58-0156/+81-791-58-0131

2P-1

Dispersion of Morphology-Controlled Fullerene Particles

○Yutaka Takaguchi, Yasuhiko Fujita, Junpei Matsukawa, Tomoyuki Tajima

Graduate School of Environmental Science, Okayama University, Okayama 700-8530, Japan

Morphology control of fullerene particles is an important advance in materials chemistry. Several reports described nano-sized C_{60} particles having controlled morphology, such as spherical colloids and nanocrystals. However, the examples of micron-sized C_{60} particles, of which morphologies are well controlled, are quite rare. Furthermore, water or organic solvent dispersion of C_{60} microparticles has not yet been well explored. Here we report morphology controlled C_{60} microparticles easily dispersed in water or organic solvent by an appropriate surface modification by the use of photoirradiation or fullerodendron.

Although the nanoparticles of fullerene remain dispersed in water even without the aid of a dispersant, water dispersion of fullerene whiskers, fibrous crystals made of C_{60} having submicron diameters and length of more than 5 μm, has never been reported. We found that photoirradiation by a fluorescent lamp made the whisker dispersible in water. Figure 1a shows the SEM image of water-dispersed fullerene whisker. Interestingly, negative zeta potential of the whisker increased with increasing photoirradiation time and reached −42.1 mV after 24 h. The concentration of C_{60} in water was 1.4 mg/mL which is 5 times higher than Deguchi's hand grinding method[1].

Meanwhile, we have reported that fullerodendrons act as a dispersant of single-walled carbon nanotubes (SWNTs) via supramolecular nanocomposite formation owing to strong interaction of their C_{60} moiety with the surface of SWNTs[2]. That result prompted us to investigate the interaction and influence of fullerodendrons upon C_{60} particle formation. Surprisingly, the control over micron-sized C_{60} morphology was achieved in the presence of fullerodendrons during particle formation to yield C_{60} microspheres, which have uniform size (0.5 – 3.0 μm; depend on the conditions) and spherical morphology observed by SEM and TEM (Figure 2b and c).

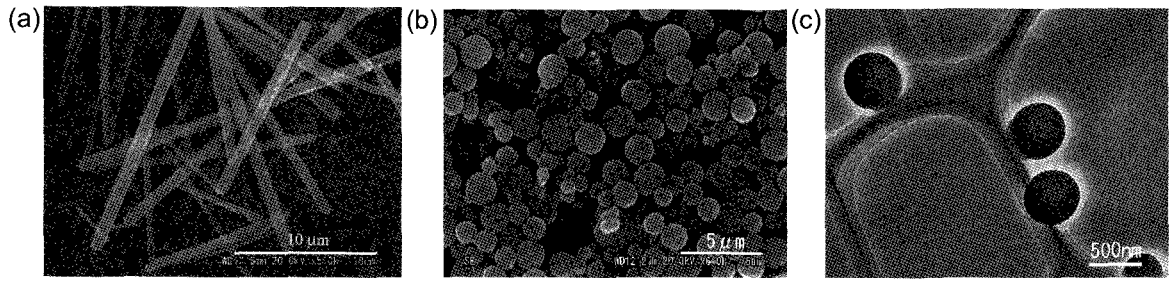

Figure 1. (a) SEM image of water-dispersible fullerene whisker, (b) SEM and (c) TEM images of fullerene microspheres dispersed in toluene/2-propanol.

[1] S. Deguchi, S. Mukai, M. Tsudome, K. Horikoshi, *Adv. Mater.*, **18**, 729 (2006).

[2] Y. Takaguchi, M. Tamura, Y. Sako, Y. Yanagimoto, S. Tsuboi, T. Uchida, K. Shimamura, S. Kimura, T. Wakahara, Y. Maeda, T. Akasaka, *Chem. Lett.*, **34**, 1608 (2005).

Corresponding Author: Yutaka Takaguchi
TEL: +81-86-251-8903, FAX: +81-86-251-8903, E-mail: yutaka@cc.okayama-u.ac.jp

2P-2

C_{60} Polymerization in Solution with Free Electron Laser Irradiation

○Nobuyuki Iwata, Yasunari Iio, and Hiroshi Yamamoto

Department of Electronics & Computer Science, College of Science & Technology, Nihon University, 7-24-1 Narashinodai, Funabashi-shi, Chiba, 274-8501 Japan

Polymerization processes for C_{60} molecules have been developed for photo-, electron-beam-, pressure-, and plasma-induced methods. Among them, a crystalline three-dimensional (3D) C_{60} polymer can be obtained at 15 GPa and approximately 650°C, but the 2D polymer remains in part and includes a graphite like amorphous phase[1]. The aim of our study is to synthesize an amorphous 3D C_{60} polymer on the bulk scale for various applications by free electron laser (FEL) irradiation. The FEL has unique features: a tunable wavelength in the infrared range, and a 20 μs macropulse containing several hundred micropulses with a pulse width less than one ps[2]. We expect the features of the polymer to be the hardness higher than diamond, the flexibility like organic material owing to the amorphous phase of C_{60} polymer with 2+2 cycloaddition, and the density lower than that of alloys. In the previous reports, the 450 and 500 nm wavelength is most efficient for polymerization[3-6]. However, the grain size of C_{60} polymer was limited to μm order in a pressed C_{60} powder. The most likely explanation of the limitation of the polymer size is the directivity of polymerization. Therefore inserting some molecules with double bonds between C_{60} molecules is expected to reduce the directivity of polymerization and then amorphous C_{60} polymer with macro scale is anticipated.

The C_{60} powder was pressed at 600 MPa in vacuum. The pressed powder was soaked in C_{60} saturation m-xylene solution for one week, and then the 500 nm-FEL was irradiated at the surface of the specimen for one hour. The sample surface and the height of the solution surface were almost same. Figure 1 shows the Raman spectrum after FEL irradiation. Two peaks around 1460 cm^{-1} and 1465 cm^{-1} were obtained. The pristine Ag(2) mode of C_{60} molecule appears at 1469 cm^{-1}. Almost all of surface of the C_{60} specimen was polymerized. During the irradiation of FEL, C_{60} precipitates on the surface due to evaporation of the solvent. We expect that C_{60} polymer become thicker continuing the irradiation.

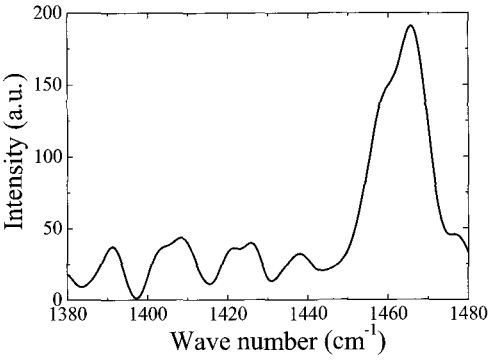

Figure 1 : Raman spectrum of the specimen after 500nm-FEL irradiation.

[1] S. Yamanaka and A. Syouji: Kotai Butsuri **41**, 407 (2006) [in Japanese].

[2] Y. Hayakawa, et al., Nucl. Instrum. Methods Phys. Res., Sect. A **507**,404 (2003).

[3] H. Yamamoto, et al., Appl. Surf. Sci. **253**,7977 (2007).

[4] S. Ando et al., Trans. Mater. Res. Soc. Jpn. 32, 1251 (2007).

[5] N. Iwata et al., S. Ando, R. Nokariya, and H. Yamamoto, Jpn. J. Appl. Phys. **47** (2007) 1412-1415.

[6] N. Iwata et al., Mater. Res. Soc. 2007 Fall Proc. 1057-II05-48.

iwata@ecs.cst.nihon-u.ac.jp

2P-3

Observation of Pore Size Distribution Inside C_{60} Nanofibers

○Ryoei Kato[1] and Kun'ichi Miyazawa[1] and Zheng-Ming Wang[2]

[1]*Fullerene engineering group, National institute for Materials Science, Tsukuba, Ibaraki, 305-0044, Japan*

[2]*Energy Technology Research Institute, National Institute of Advanced Industrial Science and Technology, Tsukuba, Ibaraki 305-8569, Japan*

The fullerene nanofibers are the fine crystalline fibers composed of fullerene molecules with the diameter less than a few hundred nm and the length more than several μm [1, 2].

In this study, thin slices of cross-section of C_{60} nanofibers were obtained by means of focused ion beam (FIB) lithography to observe directly the cross-sectional inner structure of C_{60} nanofibers in order to understand their three-dimensional morphology, inner structure [3], and the pore size distribution inside C_{60} nanofibers.

The C_{60} nanofibers were fabricated by the liquid-liquid interfacial precipitation method. The grown C_{60} nanofibers were embedded in a polyvinyl alcohol (PVA) mold on a Si plate to obtain a sample for the cross-sectional observation. The cutting of designated parts of the sample and fixing of them on the holder for thinning was conducted by means of the FIB (Hitachi, FB-2100). The thickness of the slice was 50 nm which was thin enough for TEM observation.

The cross-sectional morphology and structure were observed by transmission electron microscopy (JEOL, JEM-2010), and the pore size distribution was investigated by gas/vapor adsorption techniques (BELSORP, 18A).

Many pores were generated inside C_{60} nanofibers. The pore size decreases towards the whisker surface, indicating a structural difference between the surface part and the inside part of the fibers. These results support that the fullerene nanofibers have the core-shell structure [2, 4].

[1] K. Miyazawa, A. Obayashi, and M. Kuwabara, *J. Am. Ceram. Soc.*, **84**, 3037 (2001).

[2] K. Miyazawa, J. Minato, T. Yoshii, M. Fujino and T. Suga, *J. Mater. Res.*, **20**, 3, 688 (2005).

[3] S. Q. Feng, D. P. Yu, G. Hu, X. F. Zhang and Z. Zhang, *J. Phys. Chem. Solids*. **58**, 1887 (1997).

[4] K. Saito, K. Miyazawa and T. Kizuka, *Jpn. J. Appl. Phys.*, **48**, 010217 (2009).

Corresponding Author: Ryoei Kato

Tel: +81-029-851-3354 ext. 8462, Fax: +81-029-860-4667, E-mail: KATO.Ryoei@nims.go.jp

2P-4

Phonon and electron-phonon coupling in alkali-doped fullerides

○Takashi Koretsune and Susumu Saito

Department of Physics, Tokyo Institute of Technology
2-12-1 Oh-okayama, Meguro-ku, Tokyo 152-8551, Japan

Recent discovery of superconductivity at Tc=38K in bulk Cs_3C_{60}[1] renewed interest in superconductivity in alkali-doped fullerides. It is usually assumed that the intramolecular phonon caused superconductivity in these systems. Thus, to predict the critical temperature theoretically, it is important to clarify the electron-phonon couplings as well as the density of states at the Fermi level. The accurate calculation of the electron-phonon couplings is, however, a hard task and the previous calculations[2] adopted the several simplifications; for examples, phonons dispersion (momentum dependences) are neglected. In this work, we perform more sophisticated calculation of the electron-phonon coupling using the density functional theory.

We first calculate the phonon dispersion and the electron-phonon coupling constant of fcc A_3C_{60} (A=K, Rb, Cs) with full momentum dependence. Originally, the critical temperature should be calculated with Eliashberg theory. In practical calculation, however, the McMillan's formula, the numerical approximation for the Eliashberg theory, is usually used to estimate the critical temprature. Therefore, we first evaluate the critical temperature using McMillan's formula and discuss the effect of momentum dependences. Note that in the alkali-doped fullerides, the phonon energy scale cannot be neglected compared with electron energy scale, indicating that McMillan's formula may not be a good approximation for the Eliashberg theory. Thus, we also estimate the critical temperature using Eliashberg theory. Furthermore we will discuss the possibility of higher critical temperature in the viewpoint of the electron-phonon coupling.

References:

[1] A. Y. Ganin *et. al.* Nature mat. **7** (2008) 367

[2] O. Gunnarsson, Rev. Mod. Phys. **69** (1997) 575 and references there in.

Corresponding Author: Takashi Koretsune
E-mail: koretune@stat.phys.titech.ac.jp

2P-5

Structural Determination of Metal Carbide Endofullerene $Sc_2C_2@C_{80}$

○ Hiroki Kurihara[1], Yuko Yamazaki[1], Hidefumi Nikawa[1], Naomi Mizorogi[1], Takahiro Tsuchiya[1], Shigeru Nagase[2] and Takeshi Akasaka[1]

[1]*Center for Tsukuba Advanced Research Alliance, University of Tsukuba, Tsukuba, Ibaraki 305-8577, Japan*
[2]*Department of Theoretical and Computational Molecular Science, Institute for Molecular Science, Okazaki, Aichi 444-8585, Japan*

Endohedral metallofullerenes have attracted special attention as new spherical molecules with unique properties that are unexpected for empty fullerenes [1]. Scandium metallofullerenes are of special interest because of the high variety of fullerene sizes and of encapsulated structures inside a hollow fullerene cage. Recently, it was corrected that the structure of several Scandium metallofullerenes encage not only metal, but also metal carbide inside hollow fullerenes ($Sc_2C_2@C_{84}$ [2], $Sc_2C_2@C_{82}$ [3], $Sc_3C_2@C_{80}$ [4] etc) confirmed by both NMR spectroscopic and single crystal X-ray structural analyses.

Metallofullerene Sc_2C_{82}, however, was only characterized by UV/Vis/NIR absorption spectrometric measurements and theoretical calculation[5]. No experimental evidence for its structure has been reported yet.

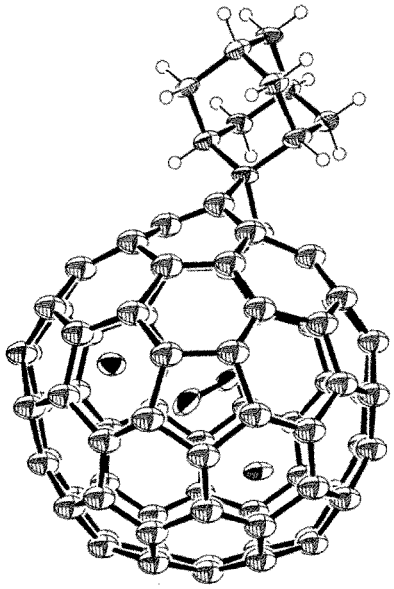

Figure. ORTEP drawing of **1**.

We report here the structural determination of the Sc_2C_{82} derivative (**1**) by the ^{13}C NMR spectroscopy and single crystal X-ray structural analysis. It is remarkable that the endohedral structure of Sc_2C_{82} is not $Sc_2@C_{82}$, but $Sc_2C_2@C_{80}$.

References

[1] Endofullerenes: A New Family of Carbon Clusters; *Akasaka, T., Nagase, S.; Eds.; Kluwer: Dordrecht, 2002.*

[2] Wang, C. R. et al. *Angew. Chem. Int. Ed.* **2001**, *40*, 397.

[3] Iiduka, Y. et al. *Chem. Commun.* **2006**, 2057.

[4] Iiduka, Y. et al. *J. Am. Chem. Soc.* **2005**, *127*, 12500.

[5] Wang, C. R. et al. *Chem. Phys. Lett.* **1999**, *300*, 379.

Corresponding Author: Takeshi akasaka

Tel & Fax : +81-298-53-6409, E-mail : akasaka@tara.tsukuba.ac.jp

2P-6

Chemical Modification of $La_2@C_{80}$ with Silacyclopropane

○Mari Minowa[1], Michio Yamada[1], Masahiro Kako[2],
Takahiro Tsuchiya[1], Midori O. Ishitsuka[1], Takeshi Akasaka[1]

[1]*Center for Tsukuba Acvanced Research Alliance, University of Tsukuba, Tennodai 1-1-1, Tsukuba, Ibaraki 305-8577, Japan*
[2]*Department of Applied Physics and Chemistry, University of Electro-Communications, Chofu, Tokyo 182-8585, Japan*

It is well-known that endohedral metallofullerenes have fascinating electronicproperties owing to the electron transfer from the encapsulated metal atoms to the carbon cage [1]. Meanwhile, reactions of endohedral metallofullerenes with organosilicon compounds have been studied with special interests since silylation can modify the electronic properties of the carbon cage. In this context, it can be expected that the combination of organosilicon compounds with endohedral metallofullerenes provides a new class of fullerene-organosilicon hybrid. However, reactions with organosilicon compounds have been limited to bissilylation so far [2]. Here we report for the first time the carbosilylation of $La_2@C_{80}$.

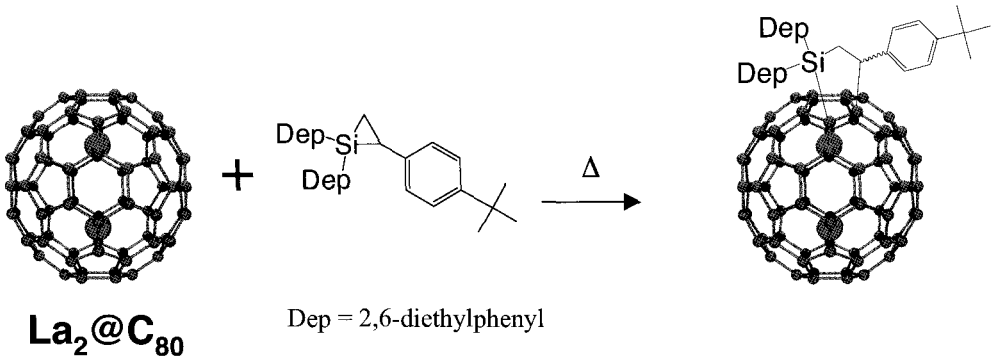

$La_2@C_{80}$

Dep = 2,6-diethylphenyl

[1] *Endofullerenes: A New Family of Carbon Clusters*; Akasaka, T., Nagase, S., Eds.; Kluwer, Dordrecht, theNetherlands, 2002.

[2] a) Akasaka, T. et al. *Nature* **1995**, *374*, 600-601, b) Yamada, M. et al. *J. Phys. Chem. B.* **2005**, *109*, 6049-6051. c) Iiduka, Y. et al. *J. Am. Chem. Soc.* **2005**, *127*, 9956-9957. d) Yamada, M. et al. *J. Am. Chem. Soc.* **2005**, *127*, 14570-14571. e) Wakahara, T. et al. *J. Am. Chem. Soc.* **2006**, *128*, 9919-9925.

Corresponding Author: Takeshi Akasaka

Tel&Fax: 029-853-6409, E-mail: akasaka@tara.tsukuba.ac.jp

2P-7

Bis-adduct of Non-IPR La@C_{72}

○ Tsuyoshi Ito[1], Hidefumi Nikawa[1], Takeshi Akasaka[1], Midori O. Ishitsuka[1], Takahiro Tsutiya[1], Zdenek Slanina[1] ,Naomi Mizorogi[2], Shigeru Nagase[2]

[1]Center for Advanced Research Alliance, University of Tsukuba, Tsukuba, Ibaraki 305-8577, Japan, [2]Department of Theoretical and Computational Molecular Science, Institute for Molecular Science, Okazaki, Aichi 444-8585, Japan

The chemical modifications of endohedral metallofullerenes have attracted great attention because the chemical properties of endohedral metallofullerenes are different from those of empty fullerenes due to the electron transfer from the encaged metals to fullerene cage and the derivatives are more useful than the parent endohedral metallofullerenes in several fields[1]. Since the first exohedral adduct of La@C_{82} was reported in 1995,[2] the various kinds of endohedral metallofullerene derivatives have been successfully synthesized from the several reactions, and some of these have been isolated and structurally characterized. [2,3] Most reported studies are focused on the mono-adduct of endohedral metallofullerenes, while only a few papers are available for the bis-adduct of endohedral metallofullerenes.[4,5] The controlled synthesis of the bis-adducts of the endohedral metallofullerene open the door to form the basis for the tailor-made design of a large variety of functional endohedral metallofullerene derivatives. Apparently, the investigation on the bis-adducts of endohedral metallofullerenes is a new hot topic in the fullerene chemistry. However, the bis-adduct of endohedral metallofullerenes with different substituents have not yet been reported. Meanwhile, we have succeeded in the extraction, isolation and characterization of La@C_{72} as a derivative, La@C_{72}($C_6H_3Cl_2$),[6] that has non-IPR cage. Non-IPR metallofullerene is one of the most interesting topics in the fullerene science. In our knowledge, there is no report for the reactivity of non-IPR fullerene.

We herein report the synthesis and characterization of the bis-adduct of endohedral metallofullerene, La@C_{72}($C_6H_3Cl_2$)Ad that La@C_{72}($C_6H_3Cl_2$)Ad was synthesized from the selective photochemical reaction of non-IPR metallofullerene derivative, La@C_{72} ($C_6H_3Cl_2$), with 2-adamantane-2,3-[3H]-diazirine. The reactivity of non-IPR metallofullerene derivative, La@C_{72}($C_6H_3Cl_2$), was discussed on the basis of the theoretical study.

1. Tsuchiya, T. et al. *J. Am. Chem. Soc.* **2006**, *126*, 6699-6703.
2. Akasaka, T. et al. *Nature* **1995**, *374*, 600-601.
3. Mikawa, M. et al. *Bioconjugate Chem.* **2001**, *12*, 510-514.
4. Stevenson, S. et al. *J. Am. Chem. Soc.* **2005**, *127*, 12776-12777
5. Cai, T. et al. *J. Am. Chem. Soc.* **2008**, *130*, 2136-2137.
6. Wakahara, T. et al. *J. Am. Chem. Soc.* **2006**, *128*, 14228

Corresponding Author: Takeshi Akasaka
E-mail: akasaka@tara.tsukuba.ac.jp, Tel&Fax: +81-29-853-6409

2P-8

Synthesis and characterization of stable [4+2] derivatives of La@C_{82}

○Yuki Nagashima[1], Yuta Takano[1], Satoru Sato[1], Zdenek Slanina[1], Takahiro Tsuchiya[1], Takeshi Akasaka*[1], Shigeru Nagase[2]

[1]*Center for Tsukuba Advanced Research Alliance, University of Tsukuba, Tsukuba 305-8577*
[2]*Depertment of Theoretical Molecular Science, Institute of Molecular Science, Okazaki 444-8585*

Endohedral metallofullerenes have attracted special attention because of the unique properties unexpected from empty fullerenes[1]. In particular, the lanthanum metallofullerene, La@C_{82} is very interesting to be a stable radical molecule. Although La@C_{82} reacts with various reagents to form La@C_{82} derivatives, it affords several isomers in general with different addition positions. Recently, we have reported that the [4+2]-type cycloaddition of La@C_{82} is highly selective giving only one regioisomer[2]. In the previous report, however, there was problem that the reaction is reversible and the product is unstable.

We here report the synthesis of stable [4+2]-type monoadducts of La@C_{82} (**2a**, **2b**) by using sultines(**1a**, **1b**). The adducts were characterized by vis-near-IR absorption and electron spin resonance (ESR) spectroscopies, and cyclic and differential pulse voltammetries.

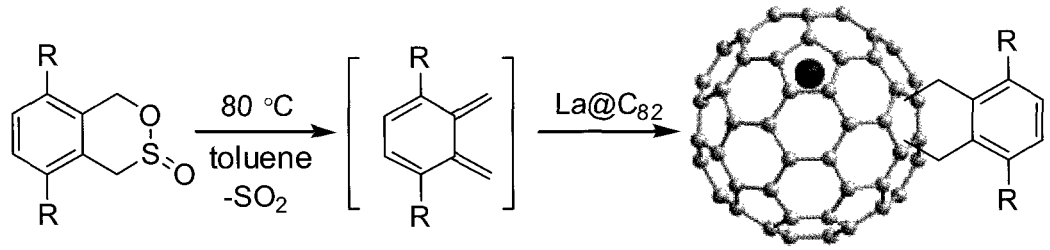

1a: R = H
1b: R = OCH_3

2a: R = H
2b: R = OCH_3

References:

[1] *Endofullerenes: A New Family of Carbon Clusters;* Akasaka. T, Nagase. S, Eds; Kluwer: Dordrecht, 2002.

[2] Maeda. Y. et al., *J. Am. Chem. Soc.* **2005**, *127*, 12190-12191.

Corresponding Author: Takeshi Akasaka

E-mail: akasaka@tara.tsukuba.ac.jp

Tel & Fax: +81-29-853-6409

2P-9

Synthesis and Properties of An Endohedral Metallofullerene Ligands

○Ryo Aoyama, Yuya Yokosawa, Takahiro Tsuchiya, and Takeshi Akasaka*

Center for Tsukuba Advanced Research Alliance, University of Tsukuba, Tsukuba, Ibaraki 305-8577, Japan

Studies on donor-acceptor dyads capable of undergoing photoinduced electron or energy transfer are of current interest to mimic the primary events of the photosynthetic reaction center and also to develop molecular electronic devices.[1,2] Toward constructing such dyads, fullerenes are particularly appealing as electron acceptors because of their three-dimensional structure, low reduction potential, and absorption spectra extending over most of the visible region. The preparation of various non-covalently linked donor-acceptor systems by coordination of fullerene derivatives bearing a pyridine unit to metal porphyrins have been reported.[2] On the other hand, endohedral metallofullerenes have lower reduction potentials and form more stable anions compared to the empty fullerenes, which is because of an intramolecular electron transfer from encapsulated metal(s) to the carbon cage.[3] Recently, we have found the complexation behavior of endohedral metallofullerene $La_2@C_{80}$ with the organic molecules by electron transfer between them.[4,5] The facile electron transfer is one of the characteristic features of endohedral metallofullerenes.

In this context, we synthesized the endohedral metallofullerene ligand, which has a pyridine moiety as a ligand part to metal complexes.

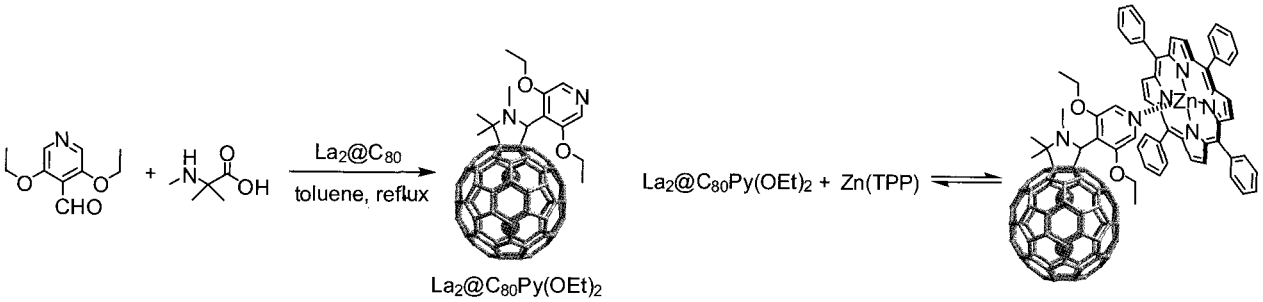

[1] H. Imahori et al. *Eur. J. Org. Chem.* **1999**, 2445-2457.
[2] F. D'Souza et al. *J. Phy. Chem. B.* **2006**, *110*, 25240-25250
[3] T. Akasaka et al. *J. Am. Chem. Soc.* **2000**, *122*, 9316-9317
[4] T. Tsuchiya et al. *J. Am. Chem. Soc.* **2006**, *128*, 14418-14419
[5] T. Tsuchiya et al. *Bull. Chem. Soc. Jpn.* **2009**, *82*, 171.

Corresponding Author: Takeshi Akasaka
E-mail: akasaka@tara.tsukuba.ac.jp
Tel&Fax: +81–298–53–6409

2P-10

Synthesis and properties of paramagnetic metallofullerene/electron donor dyad

○Tatsuya Tanaka[1], Takahiro Tsuchiya[1], Takeshi Akasaka[1],
Naomi Mizorogi[1], Shigeru Nagase[2]

[1]Center for Tsukuba Advanced Research Alliance, University of Tsukuba, Ibaraki 305-8577, Japan, [2]Institute for Molecular Science, Aichi 444-8585, Japan

Fullerenes have attracted special attention as the component of supramolecular system. In particular, fullerene have been well studied in photoinduced donor-acceptor dyads because of their special three-dimensional structure, absorption spectra extending over visible region and low reduction potential[5]. Endohedral metallofullerene, La@C_{82}, shows lower reduction potential than empty fullerenes due to the three electron transfer from encapsulated metal to carbon cage. In addition, it has an open-shell electronic structure, formally described as $La^{3+}C_{82}^{3-}$, exhibiting paramagnetic nature. Therefore, La@C_{82} is easily reduced to form the stable anion, $[La@C_{82}]^-$, having a closed-shell electronic structure[1]. Recently, we have found the intermolecular electron transfer from donor molecules to $La@C_{82}$[2-4].

Herein, we report the synthesis of donor- La@C_{82} dyad and its properties.

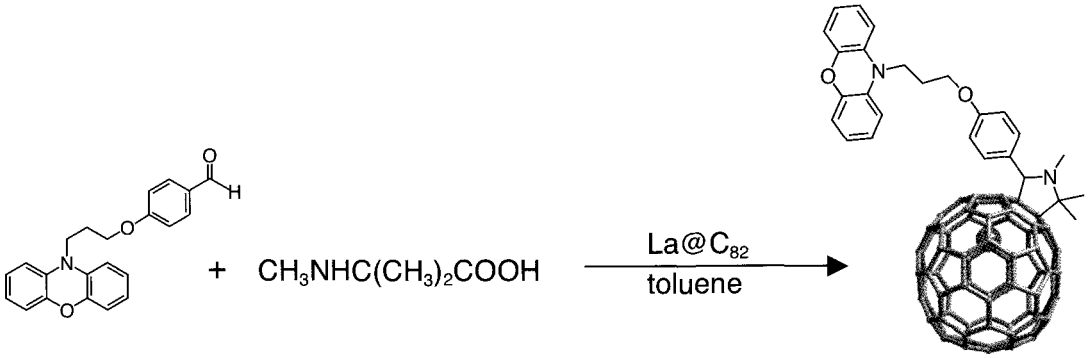

[1] T. Akasaka et al. *J. Am. Chem. Soc.* **2006**, *128*, 6699
[2] T. Tsuchiya et al. *J. Am. Chem. Soc.* **2006**, *128*, 6699.
[3] T. Tsuchiya et al. *Chem. Commun.* **2006**, 3585.
[4] T. Tsuchiya et al. *J. Am. Chem. Soc.* **2006**, *128*, 14418.
[5] K. G. Thomas, et al. *ChemPhysChem* **2003**, *4*, 1299.

Corresponding Author: Takeshi Akasaka
TEL: +81-293-53-6409, FAX: +81-293-53-6409
E-mail: akasaka@tara.tsukuba.ac.jp

2P-11

Valence States-Dependent Photoluminescence from Thulium Atoms Encapsulated in Fullerenes

○Noriko Izumi[1], Hiroaki Iijima[1], Toshiya Okazaki[2], Masayoshi Tange[2], Yasumitsu Miyata[1] and Hisanori Shinohara[1]

[1]*Department of Chemistry & Institute for Advanced Research, Nagoya University, Nagoya 464-8602, Japan*
[2]*Research Center for Advanced Carbon Materials, National Institute of Advanced Industrial Science and Technology (AIST), Tsukuba 305-8565, Japan*

Photoluminescence (PL) properties on thulium (Tm) atoms in fullerenes are interesting because of the unique valence states of encapsulated metal atoms compared to those in the conventional bulk state[1]. To date, it has been reported that the PL from thulium ion depends on its valence state, i.e. Tm^{2+} vs. Tm^{3+}. However, the intrinsic effect of the Tm valence state on PL is still unclear because of the known high sensibility to the surrounding environment of Tm^{2+}[2]. To investigate this issue, metallofullerenes, which can isolate Tm ions, are expected to be an ideal system. It has been reported that encapsulated thulium ions show trivalent states in $Tm_2@C_{82}$ [3]. Recently, we have found the presence of divalent states of Tm ions in $Tm@C_{88}$. By using these Tm metallofullerenes, the PL properties of Tm^{3+} can be well compared with that of Tm^{2+} under a similar environment.

Here we report the production, isolation and observation of unique PL properties of series of Tm metallofullerenes: $Tm@C_{88}$(I, II, III, IV), $Tm_2@C_{82}$(C_s(6), C_{2v}(9), C_{3v}(8)) and $(Tm_2C_2)@C_{82}$(C_s(6), C_{2v}(9), C_{3v}(8)). Figure1 shows emission spectra of $Tm@C_{88}$(III) and $(Tm_2C_2)@C_{82}$(C_{3v}(8)) in CS_2 solution at room temperature. The observed PL at 1,200 nm arises from the $^2F_{5/2}\rightarrow{}^2F_{7/2}$ transition of Tm^{2+} in $Tm@C_{88}$(III), whereas the 1,800 nm PL peak corresponds to the $^3F_4\rightarrow{}^3H_6$ transition of Tm^{3+} in $(Tm_2C_2)@C_{82}$(C_{3v}(8)). These results provide a conclusive evidence for the influence of valence states on PL of Tm atoms in almost the same environments. In the presentation, we will discuss the observed unique relationship between the electronic state and PL properties for a series of Tm metallofullerenes.

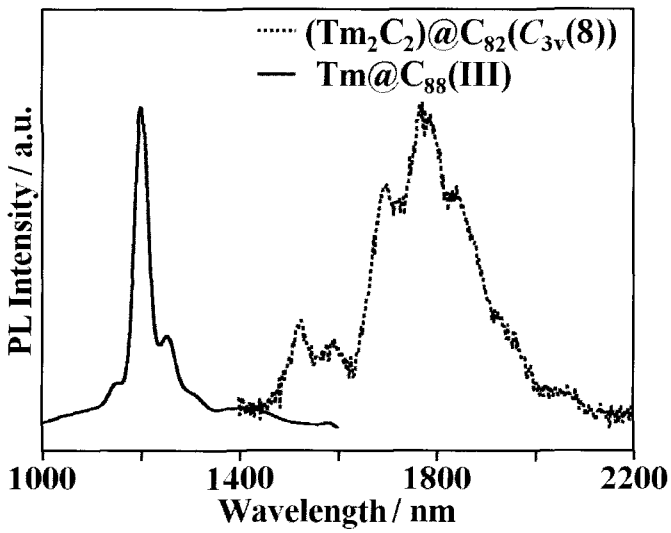

Figure 1
Emission spectra of $Tm@C_{88}$(III) and $(Tm_2C_2)@C_{82}$(C_{3v}(8)) .

[1] H. Shinohara, *Rep. Prog. Phys.*, **63**, 843 (2000).
[2] Z. J. Kiss, *Phys. Rev.*, **127**, 3 (1962).
[3] K. Kikuchi, *et al.*, *Chem. Phys. Lett.*, **319**, 472 (2000).
[4] X. Ding, *et al.*, *Chem. Phys. Lett.*, **269**, 72 (1997).

Corresponding Author: Hisanori Shinohara
E-mail: noris@nagoya-u.jp
Tel: +81-52-789-2482 **Fax**: +81-52-747-6442

2P-12

Systematic X-Ray Diffraction Studies on Crystal Structure of Mono-Metallofullerene M@C_{82}

○Takayuki Aono[1], Eiji Nishibori[2], Ryo Kitaura[1], Shinobu Aoyagi[2], Masaki Takata[3], Makoto Sakata[2], Hiroshi Sawa[2] and Hisanori Shinohara[1,4]

[1]*Department of Chemistry, Nagoya University, Nagoya 464-8602, Japan*

[2] *Department of Applied Physics, Nagoya University, Nagoya 464-8603, Japan*

[3]*RIKEN SPring-8 Center, 1-1-1 Kouto, Sayo-cho, Sayo-gun, Hyogo 679-5148, Japan*

[4]*Institute for Advanced Research, Nagoya University, Nagoya 464-8602, Japan*

The endohedral metallofullerenes, M@C_{82}, have attracted interests due to their unique structural and electronic properties [1]. It is known that M@C_{82} is one of the most abundant metallofullerenes so far synthesized and structurally characterized. The M@C_{82} has been widely used for applications such as MRI contrast agents and FET devices. Although the molecular structures of M@C_{82} metallofullerenes might be similar with each other, many of those for M@C_{82} have not yet been determined experimentally except for several examples. We have been carried out systematic structural studies of M@C_{82} by using synchrotron X-ray powder diffraction (SXRD) at SPring-8 incorporating the MEM/Rietveld analysis [2, 3]. Powder diffraction at SPring-8 enables us to measure high quality powder data from a small amount of powder samples. In this study, we report the powder structural studies of series of a M@C_{82} metallofullerenes at low temperature.

We used the samples M@C_{82} (M=La, Ce, Sm, Tm, Yb, Lu) with C_{2v} or C_S symmetry. Powder samples of M@C_{82}/$C_6H_5CH_3$ were crystallized from toluene solvent. The XRD patterns were collected at SPring-8 BL02B2 beamline. A remarkable peak split indicating a phase transition from orthorhombic to monoclinic is observed in the powder data of M@C_{82} (C_{2v}) and M@C_{82} (C_S) (M=Sm, Tm, Yb) (cf. **Fig.1 and 2**). In the cases of powder data for M@C_{82} (C_{2v}) and M@C_{82} (C_S) (M=La, Ce, Lu), such a split has never been observed at temperatures from 90K to 300K. The detail of result will be discussed at the meeting.

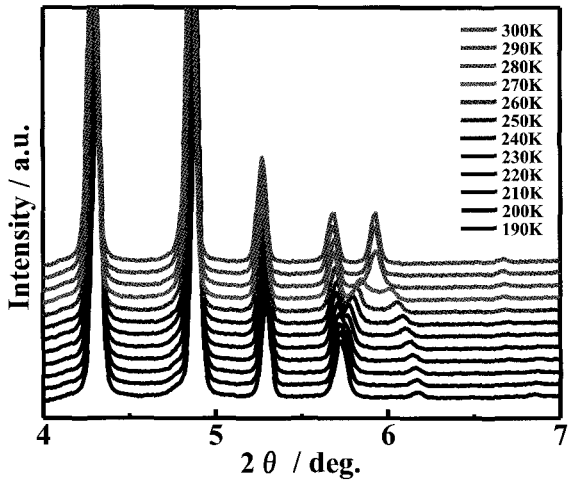

Fig.1 The X-ray powder diffraction patterns of Sm@C_{82} (C_S) on cooling process. The peaks around 2θ=6° were splitted by cooling.

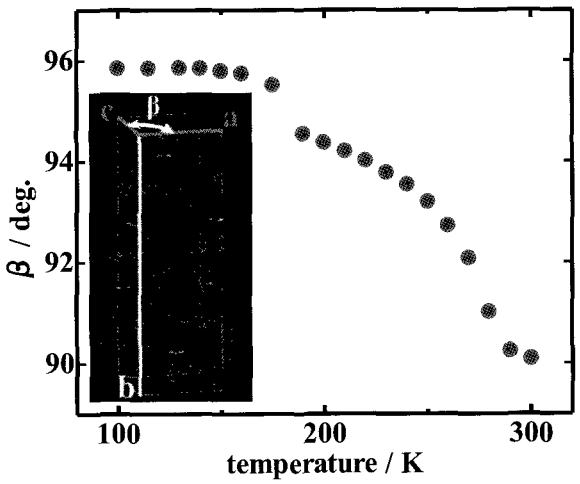

Fig.2 The β angle of the monoclinic unit cell of Sm@C_{82} (C_S) on cooling process. The angles drastically changed at around 190K and 280K.

[1] H. Shinohara, ***Rep. Prog. Phys.***, 63, 843 (2000) [2] M. Takata *et al.*, ***Nature***, 377, 46 (1995)

[3] E. Nishibori *et al.*, ***Chem. Phys. Lett.*** 330, 497 (2000)

Corresponding Author: Hisanori Shinohara **E-mail:** noris@nagoya-u.jp

Tel: +81-52-789-2482 **Fax:** +81-52-747-6442

2P-13

Isolation and structure determination of $(Lu_2C_2)@C_{88}$: Experimental and theoretical analyses.

○Kazunari Shiozawa, Noriko Izumi, Hisashi Umemoto, Ryo Kitaura and Hisanori Shinohara

Department of Chemistry and Institute for Advanced Research, Nagoya University, Nagoya 464-8602, Japan

During the formation of endohedral metallofullerenes, shrinkage of giant endohedral metallofullerenes induces pop-outs of C_2 units, which plays an important role in the stabilization of metallofullerenes[1]. Therefore, structural characterization of metallofullerenes with large cage size (higher metallofullerenes) may provide a clue as to the formation mechanism of metallofullerenes. However, the structure determination of higher metallofullerenes using x-ray diffraction (XRD) is difficult because of very low production yield. Hence, we have focused on ^{13}C nuclear magnetic resonance (NMR) combined with theoretical calculations (GAIO method) to further elucidate the structure of higher metallofullerenes.

In this study, we selected $(Lu_2C_2)@C_{88}$ isomers (I) and (II) as higher metallofullerenes to avoid undesirable peak broadening of NMR. Separation of $(Lu_2C_2)@C_{88}$ isomer (I) and (II) was achieved by recycling HPLC using Cosmosil columns (5PYE, Buckyprep, Buckyprep-M and 5PBB) and toluene as eluent. Figure1(a) shows the experimental ^{13}C NMR spectrum of isomer (I). The spectrum shows 42 lines with equal intensity and 4 lines with half in intensity (square in Fig.1). This indicates that the isomer (I) corresponds to one of the five isomers with C_s symmetry among 35 possible IPR isomers of C_{88}. To determine the cage structure, the chemical shifts of 5 isomers were calculated using the GIAO method (Fig.1(b)). The comparison between theoretical and experimental NMR spectra strongly supports that $(Lu_2C_2)@C_{88}$(I) is isomer **24**(C_s) (Fig.2(a)). Using the same procedure, the fullerene cage of $(Lu_2C_2)@C_{88}$(II) was determined to be isomer **35**(D_2) (Fig.2(b)).

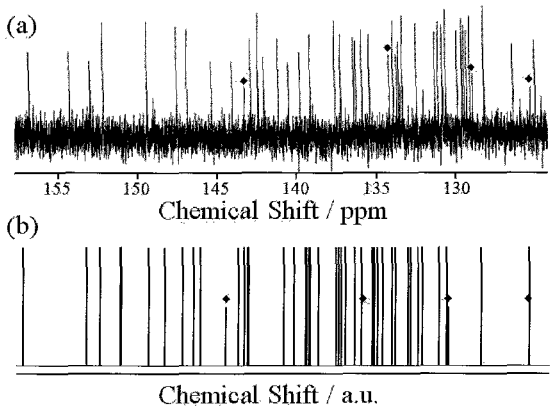

Figure 1. Comparison between two ^{13}C NMR spectra. (a)^{13}C NMR spectrum of $(Lu_2C_2)@C_{88}$(I) (b) theoretical ^{13}C NMR spectrum of C_{88}^{6-}

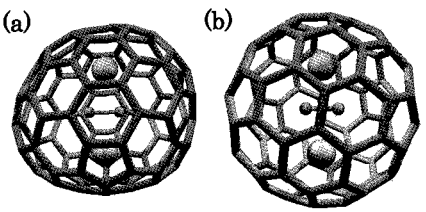

Figure 2. Structure of two isomers (a) $(Lu_2C_2)@C_{88}$(I) (b) $(Lu_2C_2)@C_{88}$(II)

[1] T.Inoue *et al.*, ***Chem. Phys. Lett.***, 382, 226-231 (2003)

Corresponding Author: Hisanori Shinohara
TEL: +81-52-789-2482, FAX: +81-52-747-6442, E-mail: noris@nagoya-u.jp

2P-14

Electronic structure of endohedral fullerenes$Y_2C_2@C_{82}$, $Sc_3N@C_{78}$ obtained by *ab initio* molecular orbital calculation

○Yusuke Aoki, Takafumi Miyazaki, Shojun Hino

Graduate School of Science & Engineering, Ehime University

Ultraviolet photoelectron spectra (UPS) of endohedral fullerenes have been measured and comparison of the UPS with theoretical calculation gave the clue to elucidate the cage structure as well as the structure of entrapped atoms. Further, it has been found that entrapped species do not induce serious effect to the electronic structure of endohedral fullerenes but cage symmetry (structure) strongly affects the electronic structure. We present a theoretical study on endohedral fullerenes, C_{2v}-$Y_2C_2@C_{82}$ and D_{3h}-$Sc_3N@C_{78}$, and examine the structure of entrapped cluster in the fullerene cage with comparison of their UPS.

The calculation was performed with a Gaussian 03 program module. The structure of endohedral fullerenes was optimized at HF (Hatree-Fock) level, and the electronic structure was obtained by using density functional theory level calculation (B3LYP). The 6-31g (d) basis sets were used for carbon and nitrogen, and TZP basis sets were used for scandium and yttrium.

Figure 1 shows the UPS and calculated simulation spectra. The simulated spectra denoted by isomer 1 – isomer 3 were obtained with the different initial Y_2C_2 positions. The isomer 3 spectrum reproduces UPS spectrum very well. The structure of isomer 3 is that Y atoms are on the six-membered ring and they bond to three carbon atoms of the six-membered ring. The spectrum isomer 2 also reproduces the UPS fairly well. Isomer 3 has the smallest formation energy and the formation energy difference between isomer 2 and isomer 3 is only 8.38kcal/mol. The actual structure of C_{2v}-$Y_2C_2@C_{82}$ might be the one shown in Fig. 2 (isomer 3). The electronic structure of $Sc_3N@C_{78}$ will also be presented in the symposium.

Fig. 1 UPS and the calculated simulation spectra of $Y_2C_2@C_{82}$.

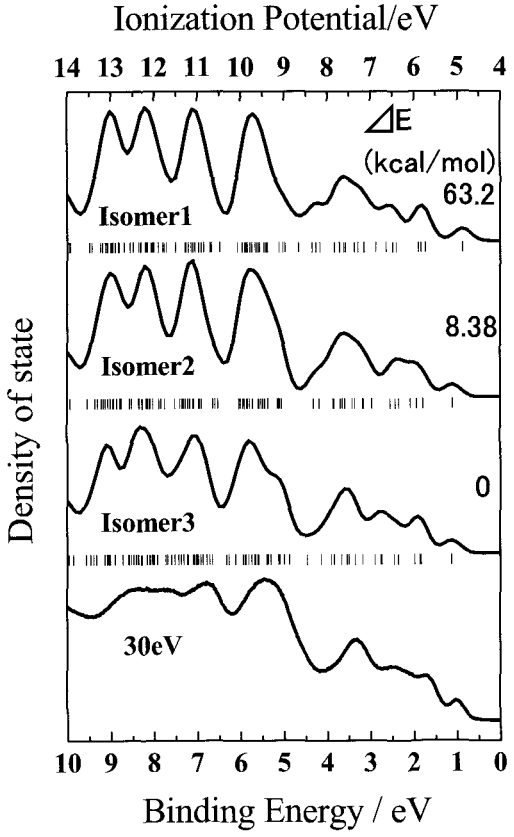

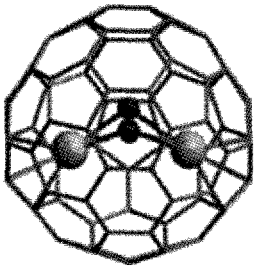

Isomer 3

Fig. 2 Endohedral fullerenes of $Y_2C_2@C_{82}$.

Corresponding Author: S.Hino; E-mail: hino@eng.ehime-u.ac.jp; Phone: 089-927-9924

2P-15

Ultraviolet and X-ray photoelectron spectra of C_{3v}-$Tm_2@C_{82}$

○Youji Tokumoto[1], Hajime Yagi[1], Takafumi Miyazaki[1], Noriko Izumi[2], Hisanori Shinohara[2], Shojun Hino[1]

[1]*Graduate School of Science and Engineering, Ehime University*
[2]*Graduate School of Science, Nagoya University*

In this study ultraviolet and X-ray photoelectron spectra (UPS and XPS) of $Tm_2@C_{82}$ will be presented and the oxidation state of Tm atoms in the C_{82} fullerene cage will be discussed. Symmetry of measured $Tm_2@C_{82}$ is C_{3v}-C_{82} (82:8).

Figure 1 shows the UPS of C_s- and C_{3v}-$Er_2@C_{82}$, C_{2v}- and C_{3v}-$Lu_2@C_{82}$, C_{3v}-$Tm_2@C_{82}$. The spectral onset (E_{onset}) of $Tm_2@C_{82}$ is 0.88 eV at 40 eV irradiation. The UPS deeper than 5 eV of these endohedral fullerenes resemble. On the other hand, these UPS shallower than 5 eV differ except for the UPS of those fullerenes having the same C_{3v}-cage symmetry. That is, endohedral fullerenes $M_2@C_{82}$ of the same symmetry have analogous electronic structure. Figure 2 shows Tm4d XPS of $Tm_2@C_{82}$ and those of Tm4d of Tm_2O_3 (Tm^{3+}) [1], TmSe (Tm^{2+} and Tm^{3+}) [2] and TmTe (Tm^{2+}) [2] for comparison. The peak position of Tm4d of $Tm_2@C_{82}$ located at 177.8 eV, which suggests Tm^{3+} oxidation state. The oxidation state of Tm in $Tm@C_{82}$ was +2. Present finding is note worthy since the oxidation state of entrapped atoms changes in accordance with environment change of the fullerene inner space.

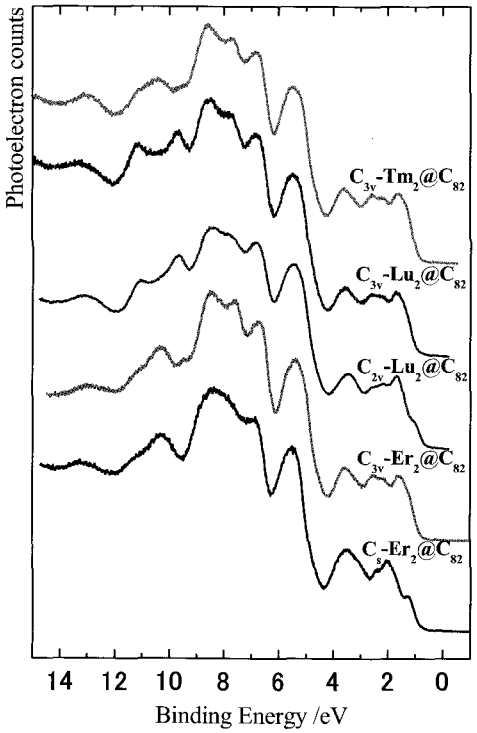

Figure 1 UPS of $Er_2@C_{82}$, $Lu_2@C_{82}$ and $Tm_2@C_{82}$

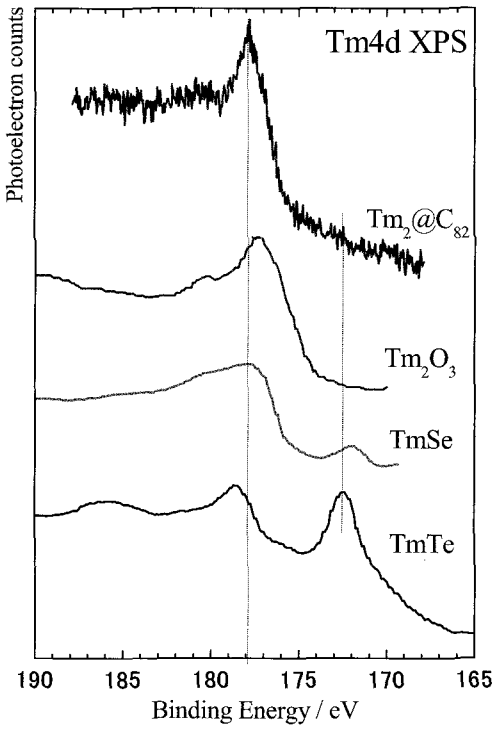

Figure 2 Tm4d XPS of $Tm_2@C_{82}$, Tm_2O_3, TmSe and TmTe.

[1] H. Ogasawara et al., Physical Review B 50, 12332 (1994).
[2] K.G. Nath et al., Journal of Electron Spectroscopy and Related Phenomena, 88-91 369-375 (1998).
Corresponding Author : S.Hino, E-mail:hino@eng.ehime-u.ac.jp, phone:089-927-9924

2P-16

Encapsulation of Atomic Nitrogen into C_{60} and Polyynes into SWNTs

○Tomonari Wakabayashi, Masashi Teshiba, Mao Saikawa, Airi Yoshikawa, Yoriko Wada

Department of Chemistry, School of Science and Engineering, Kinki University

Abstract: Atoms and molecules composed of main group elements can be encapsulated into a hollow space inside fullerenes and nanotubes. The hybrid system is demanded for precise control of electronic and optical properties of fullerenes and nanotubes. In addition, accommodating reactive species inside, fullerenes and nanotubes can be a best spectroscopic capsule for the study of magnetic as well as optical properties of rarely obtainable samples.

We have produced fullerene C_{60} with a nitrogen atom inside, N@C_{60}, for the study of the electronic structure as atomic nitrogen as well as its magnetic properties inside the fullerene cage, and single-wall carbon nanotubes with size-selected polyyne molecules inside, $HC_{2n}H$@SWNTs (n=4-8), for the study of vibrational as well as electronic properties for the polyyne molecules inside SWNTs. The key for the study of these hybrid system is to prepare well-defined samples in purity and concentration. We will discuss on the preparation scheme in more detail.

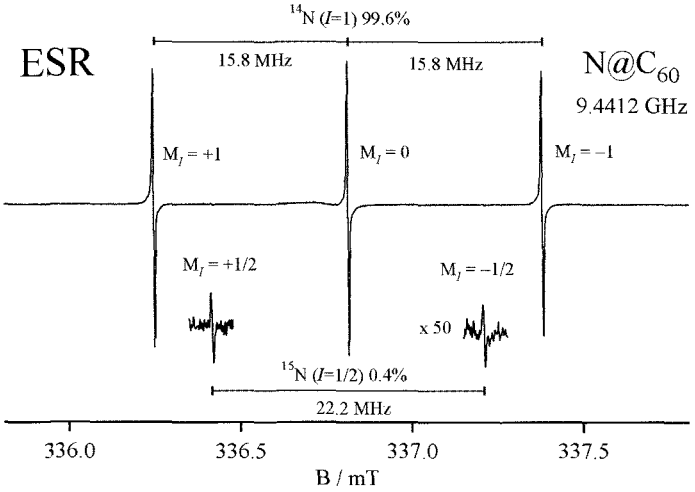

Figure 1. Electron spin resonance spectra of N@C_{60}. The triplet is due to the hyperfine structure for ^{14}N isotope inside a C_{60} cage, while the weaker doublet for ^{15}N with a natural abundance of 0.4 %.

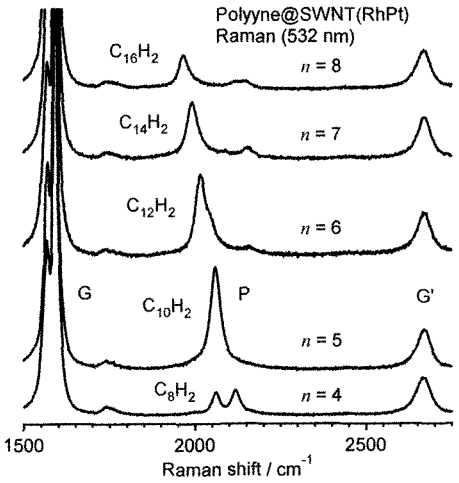

Figure 2. Raman spectra of size-selected polyyne molecules encapsulated in SWNTs, $HC_{2n}H$@SWNTs (n=4-8). Signals for totally symmetric stretching modes of the polyynic carbon chain are discernible.

Corresponding Author: Tomonari Wakabayashi
E-mail: wakaba@chem.kindai.ac.jp
Tel: 06-6730-5880 (ex. 4101)

2P-17

Biodegradation of Fullerene Nanowhiskers by Macrophage-like Cells

○Shin-ichi Nudejima[1], Kun'ichi Miyazawa[1],
Junko Okuda-Shimazaki[2] and Akiyoshi Taniguchi[2]

[1]*Fullerene Engineering Group, Exploratory Nanotechnology Research Laboratories, National Institute for Materials Science (NIMS), Tsukuba 305-0044, Japan*
[2]*Advanced Medical Material Group, Biomaterials Center, NIMS, Tsukuba 305-0044, Japan*

Fullerene nanowhiskers (FNWs) are one of the most hopeful nanomaterials for various applications such as low dimensional semiconductors, field emission tips, nanoprobes for microdevices, fiber-reinforced nanocomposites, composite elements for lubrication, and so on [1]. FNWs are composed of fullerene molecules that are usually bonded via van der Waals forces and synthesized by the liquid-liquid interfacial precipitation method.

But the biological impact of FNWs is pointed out as a problem to be studied before the practical use of them because the nanosized needle-like structure resembling asbestos may be hazardous to human lungs via inhalation. The needle-like structure has been suspected to induce the asbestosis. It is confirmed in some studies that the asbestos-like pathogenic behavior of carbon nanotubes (CNTs) depended on their length in the case of CNTs [2]. For these reasons, it is imperative to evaluate the biological impact of FNWs.

Macrophages are one of the immune system cells and defend the host against the foreign materials by uptake and digest them in a nonspecific manner during the early phase of infection. In our previous pilot study, we observed the macrophage-like cells exposed to 0.1, 1 and 10 μg/mL of the C_{60} fullerene nanowhiskers (C_{60}NWs) with the average length of 6.0 μm and the average diameter of 660 nm by use of an inverted optical microscope for 48 h [3]. The macrophage-like cells were observed to internalize the C_{60}NWs gradually, but the exposed C_{60}NWs didn't affect the morphology of the cells.

According to some previous studies, C_{60} may be non-toxic against mammalian cells [4, 5, 6] and C_{60} was dissolved inside the lipid droplets in a rat liver [7]. Macrophages may be able to decompose C_{60}NWs into individual C_{60} molecules as the primary immune response owing to their weak van der Waals bonding forces, and the C_{60}NWs may exert the effect which is not similar to that of the needle-like structure but is similar to that of C_{60} molecules on organisms. To examine the basis of this assumption (biodegradability), we performed the co-culture of macrophage-like cells and 10 μg/mL of C_{60}NWs for 4 weeks and got the result suggesting the decomposition of C_{60}NWs by the cells.

[1] K. Miyazawa, Y. Kuwasaki, A. Obayashi and M. Kuwabara, J. Mater. Res., **17 [1]**, 83 (2002).
[2] C. A. Poland, R. Duffin, I. Kinloch, A. Maynard, W. A. H. Wallace, A. Seaton, V. Stone, S. Brown, W. Macnee and K. Donaldson, Nature Nanotechnol., **3**, 423 (2008).
[3] S. Nudejima, K. Miyazama, J. Okuda-Shimazaki and A. Taniguchi, J. Physics: Conf. Series, **159**, 012008 (2009).
[4] S. Fiorito, A. Serafino, F. Andreola, P. Bernier, Carbon, **44**, 1100 (2006).
[5] F. Moussa, P. Chretien, P. Dubois, L. Chuniaud, M. Dessante, F. Trivin, P. Y. Sizaret, V. Agafonov, R. Ceolin, H. Szwarc, V. Greugny, C. Fabre, A. Rassat, Fullerene Sci. Technol., **3**, 333 (1995).
[6] T. Baierl, E. Drosselmeyer, A. Seidel, S. Hippeli, Exp. Toxic. Pathol., **48**, 508 (1996).
[7] N. Gharbi, M. Pressac, M. Hadchouel, H. Szwarc, S. R. Wilson and F. Moussa, Nano Lett., **5**, 2578 (2005).
Corresponding Author: Shin-ichi Nudejima
TEL: +81-29-851-3354 (EXT: 8463), FAX: +81+29-860-4667, E-mail: NUDEJIMA.Shinichi@nims.go.jp

2P-18

Conductivity of metallic and semiconducting single wall carbon nanotube buckypaper

○H. Udoguchi,[1] S. Sagitani,[1] K. Matsuda,[1] Y. Oshima,[2] H. Kataura,[3,4] T. Takenobu,[5] K. Yanagi,[1,4] Y. Maniwa[1,4]

1. Department of Physics, Tokyo Metropolitan University
2. RIKEN
3. Nanotechnology Research Institute, National Institute of Advanced Industrial Science and Technology (AIST)
4. JST-CREST
5. Institute for Materials Research, Tohoku University

Abstract: Single wall carbon nanotubes (SWCNTs) have superior electrical characteristics, however, a mixture state of the metallic and semiconducting types of nanotubes has impeded their applications in a large scale. Moreover, the mixed state has made it difficult to understand the detailed mechanisms of carrier transport processes in nanotube networks. One of approaches to overcome these problems is to prepare a large amount of high-purity SWCNT samples, such as a form of buckypaper with a single electronic type. In this study, we prepared metallic or semiconducting SWCNT buckypaper (paper size; 700 mm^2) in high-purity,[1] and investigated their conductive characteristics. The purity of the samples was estimated to be more than 90 % from their optical absorption spectra. Figure 1 shows the temperature dependence of the resistance of the metallic and semiconducting buckypaper. At 4 K, the resistance of the semiconducting type was six orders of magnitude larger than that of the metallic type, clearly reflecting the difference of their electronic types. Remarkably, the resistance increased at low temperature in both samples. The increase in the metallic type would be caused by the following possible factors, (1) influence of semiconducting SWCNTs existing as impurity in the buckypaper, (2) hopping barriers between the metallic bundles, (3) presence of small gap caused by Mott transition,[2] and (4) presence of residual metal catalysts. Analysis results of the temperature dependence suggested that the resistance at low temperature was mainly influenced by 2 D variable range hopping in both samples, indicating strong effects of the second factor.

This study was supported by Industrial Technology Research Grant Program in 2007 from New Energy and Industrial Technology Development Organization (NEDO) of Japan

References: [1] Yanagi et al., Appl. Phys. Express 1 (2008) 034003, [2] Deshpande et al., Science 323 (2009) 106.

Corresponding Author: Kazuhiro Yanagi
E-mail: yanagi@phys. metro-u.ac.jp
Tel&Fax: 042-677-2494 (& 2483)

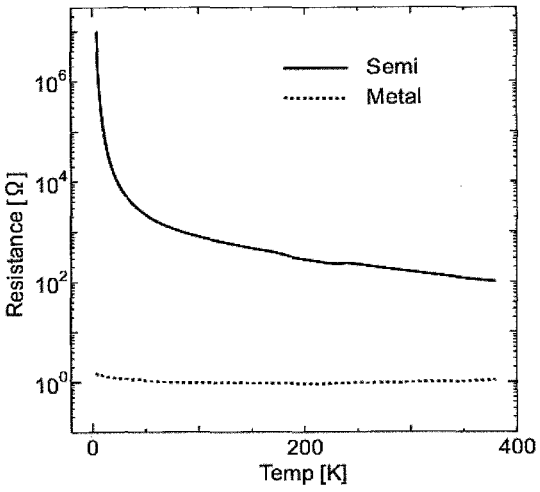

Fig. 1: Resistance of metallic (Metal, dotted line) and semiconducting (Semi, solid line) SWCNT buckypaper as a function of temperature

2P-19

Anomalous behavior of bundle-related Raman signals from carbon nanotubes grown by noble-metal particles

○Yoshihiro Kobayshi[1], Daisuke Takagi[2], Satoru Shoji[1] and Satoshi Kawata[1]

[1]*Department of Applied Physics, Osaka University, Suita 565-0871, Japan*
[2]*NTT Basic Research Laboratories, NTT Corporation, Atsugi 243-0198, Japan*

Raman spectroscopy is a powerful tool for characterizing single-wall carbon nanotubes (SWNTs) since Raman spectra are very sensitive to their structures, such as chirality, and to their environments, including inter-nanotube interaction due to bundle formation. It has been reported that Raman signals of the radial breathing modes (RBMs), which should be off-resonance for individual SWNTs under a specific measurement condition, are occasionally observed from bundled samples, owing to red-shifting and broadening of the electronic transition by bundle formation [1]. In this work, we analyzed in detail the spatial distribution of RBM signals and G-bands from bundled SWNTs grown using noble-metal nanoparticles.

Dense SWNTs were grown from Au and Ag nanoparticles formed on porous Al-hydroxide surface (Fig. 1) [2], and Raman images of both RBM and G-band regions were mapped using Raman-11 microscope (Nanophoton Co.) with 785-nm excitation. Figure 2 shows typical Raman images of RBM signals obtained from a 10 μm x 100 μm area with 40 x 400 measurement points. It can be recognized that intensity distribution is highly inhomogeneous and bundle-related signals from (10,2) and/or (9,4) nanotubes appear around 265 cm^{-1}, in addition to the usual RBM signals resonant with 785-nm excitation. As shown in Fig. 3, spatially resolved Raman spectra obtained from a very limited area (4x4 pixels) indicate that the bundle-related signals are anomalously intense compared with previous reports [1] and associated with a remarkable G-band shift to lower frequency of about 10 cm^{-1}. Considering the Ag/Au nanoparticle size (~5 nm) and excitation power dependence, possibilities of surface-enhanced Raman scattering (SERS) with the electromagnetic mechanism due to surface plasmon excitation, trivial sample heating effects, or the stimulated Raman effect should be ruled out for explaining the phenomena observed here. The G-band shift suggests that the anomalous intensity enhancement is caused by combination of the usual resonance effects by bundle formation and SERS originating from the charge transfer between metal particles and SWNTs. Further study using non-metal seeds is necessary to address this issue.

[1] M. J. O'Connell et al., PRB **69**(2004)235415, D. A. Heller et al., JPC B **108**(2004)6905. [2] D. Takagi et al., Nano Lett. **6**(2006)2642.

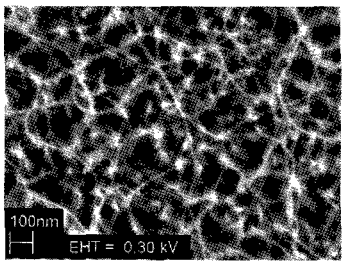

Fig.1. SEM image of SWNTs grown from Ag nanoparticles.

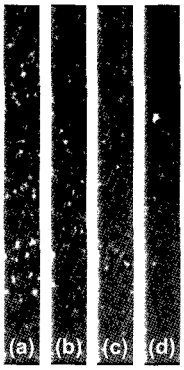

Fig.2. Intensity maps for RBM signals of around (a) 150, (b) 205, (c) 235, and (d) 265 cm^{-1}.

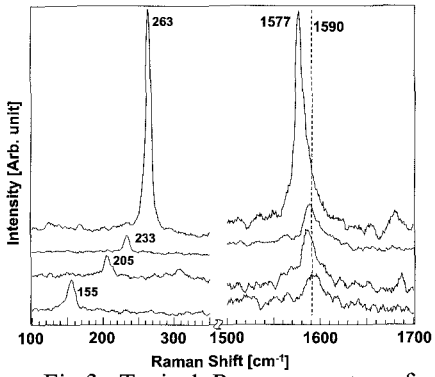

Fig.3. Typical Raman spectra of RBM and G-band regions

Corresponding Author: Y. Kobayashi, TEL/FAX:+81-6-6879-7833, E-mail:kobayashi@ap.eng.osaka-u.ac.jp

2P-20

Structure Analysis of Multi-Walled Carbon Nanotubes by TGA in the Reductive Atmosphere

○Ken-ichi Hongyou, Tohoru matsubara, Hiroyuki Nii, Atsuhiro Kunishige

UBE Scientific Analysis Laboratory, Inc., 1978-5 Kogushi, Ube, Yamaguchi 755-8633, Japan

Thermogravimetric Analysis(TGA) is an analytical technique used for characterization of CNTs. In general, measurements are carried out in the oxidative atmosphere such as air, for evaluation of decomposition temperature and quantification of inorganic compounds including catalyst residues. Under this condition, however, it is difficult to investigate the detailed composition of carbon materials such as amorphous carbon, SWNTs, DWNTs and MWNTs by this method, because of the combustion heat caused by oxidative reaction during the experiment. In this report, we tried TGA on MWNT samples in the reductive atmosphere for the purpose of avoiding the high combustion heat.

The CNTs used in this study were the mixtures of SWNTs, DWNTs and MWNTs. In order to investigate the detailed carbon materials composition, measurements on CNT samples were carried out in the reductive atmosphere with dynamic temperature mode in which the temperature increase rate was controlled according to the weight decrease rate. While the TGA curve in the oxidative atmosphere(Fig.1) showed one-step weight decrease at about 500℃, the other one in the reductive atmosphere(Fig.2) showed two-step weight decreases at about 700℃ and 850℃. It suggests that there are two different type decompositions in the reductive atmosphere. From TEM observation, we found that there were linear type CNTs, which seemed to be defect free, and aggregations of carbon materials in the pristine sample, and the former still existed but the latter decreased drastically after the first step. In addition to that, metal particles of grown up catalysts were also observed. Other results and detailed analysis will be presented in the symposium.

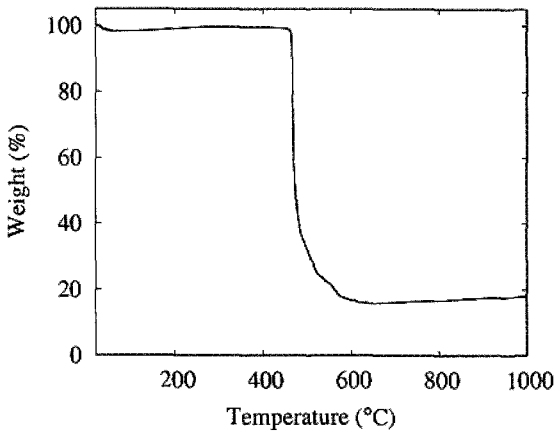

Fig.1 TGA curve of MWNTs sample in the oxidative atmosphere

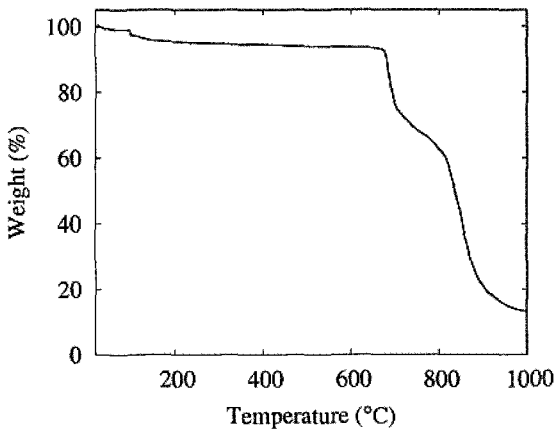

Fig.2 TGA curve of MWNTs sample in the reductive atmosphere

Corresponding Author:Ken-ichi Hongyou
E-mail:kenichi.hongiyou@ube-ind.co.jp
Tel:0836-31-6568/Fax:0836-31-6601

2P-21

Optical absorption in short metallic carbon nanotubes

Takeshi NAKANISHI[1] and Tsuneya ANDO[2]

[1]*Nanotube Research Center, AIST*
1-1-1 Higashi, Tsukuba 305-8565, Japan

[2]*Department of Physics, Tokyo Institute of Technology*
2-12-1 Ookayama, Meguro-ku, Tokyo 152-8551, Japan

Carbon nanotubes are a one-dimensional conductor consisting of rolled graphene sheets. Recently, cutting and length selection of single-wall carbon nanotubes have been studied [1-3]. Optical absorption in low-frequency region was recently reported in such nanotubes [4-6]. In short carbon nanotubes with good conductivity, depolarization field in the axis direction becomes important due to the accumulated charge at both ends of nanotubes in optical absorption [7]. The purpose of this paper is to calculate a low-frequency optical response in metallic carbon nanotubes with finite length.

We consider a metallic carbon nanotube with finite length l under an external electric field in the axis direction. We solve the electrostatic equations instead of full Maxwell's equation, which is justified by the fact that the plasmon velocity in carbon nanotubes is much smaller than the light velocity. The response of the system can generally be described by a nonlocal conductivity. We consider the case that the length of the nanotube is much larger than the mean free path. Thus, we can neglect effects of edges on the conductivity and use the Boltzmann conductivity in infinitely long nanotubes, employing a relaxation-time approximation. In actual numerical calculations, we consider a periodic array of the nanotubes and calculate an effective electric field including effects of polarization charges.

Calculated power absorption oscillates with decreasing $\sim\omega^{-2}$ in the low frequency region. The frequency of the peaks is inversely proportional to the length of nanotubes. Calculated power absorption is compared with that in a single-mode approximation in which a resonance occurs at frequency $\omega=v_Q Q_n$ with $Q_n\approx(2n+1)\pi/l$ $(n=0,1,\cdots)$, where v_Q is a plasmon velocity and a few times larger than the Fermi velocity in carbon nanotubes. We find that the calculated peaks are shifted significantly from those in the single-mode estimation, except for the main peak $(n=0)$. Actually, the electric field shows significant mixture of other modes, which are involved to form the induced electric field at the both ends of the nanotubes.

References

[1] K. J. Ziegler, D. J. Schmidt, U. Rauwald, K. N. Shah, E. L. Flor, R. H. Hauge, and R. E. Smalley: Nano Lett. **5**, 2355 (2005).

[2] F. Hennrich, R. Krupke, K. Arnold, J. A. Rojas Stultz, S. Lebedkin, T. Koch, T. Schimmel, and M. M. Kappes: J. Phys. Chem. B **111**, 1932 (2007).

[3] J. A. Fagan, M. L. Becker, J. Chun and E. K. Hobbie: Adv. Mater. **20**, 1609 (2008).

[4] M. E. Itkis, S. Niyogi, M. E. Meng, M. A. Hamon, H. Hu, and R. C. Haddon: Nano Lett. **2**, 155 (2002).

[5] N. Akima, Y. Iwasa, S. Brown, A. M. Barbour, J. Cao, J. L. Musfeldt, H. Matsui, N. Toyota, M. Shiraishi, H. Shimoda, and O. Zhou: Adv. Mater. **18**, 1166 (2006).

[6] T. Kampfrath, K. von Volkmann, C. M. Aguirre, P. Desjardins, R. Martel, M. Krenz, C. Frischkorn, M. Wolf, and L. Perfetti: Phys. Rev. Lett. **101**, 267403 (2008).

[7] G. Ya. Slepyan, M. V. Shuba, S. A. Maksimenko, and A. Lakhtakia: Phys. Rev. B **73**, 195416 (2006).

2P-22

Chirality Distribution and Hidden Features of SWCNTs Explored by Optical Absorption Spectroscopy

○Takeshi Saito[1,2], Bikau Shukla[1], Shigekazu Ohmori[1], Motoo Yumura[1] and Sumio Iijima[1]

[1]*Nanotube Research Center, AIST, Tsukuba 305-8565, Japan*
[2]*PRESTO, Japan Science and Technology Agency, Kawaguchi 332-0012, Japan*

Optical absorption spectroscopy has been frequently used as one of the most versatile characterization tools for the evaluation of purity [1], metal/semiconductor ratio [2], diameter [3] and chirality distribution of single-wall carbon nanotubes (SWCNTs) [4]. Up to date, the optical absorption properties of SWCNTs in near-infrared (NIR) region have been extensively investigated theoretically and experimentally, from the interband transitions near Fermi level to the dominant effect of excitons. On the other hand, their optical absorption in the ultraviolet (UV) region has not been fully investigated due to the analytical difficulty arising from the overlapped background that is typically attributed to collective excitations (π-plasmons). Because the featureless and broad UV absorption of the π-plasmon can be superposed even upon the NIR absorption peaks as a background, it is inevitable to eliminate the background from observed spectra in order to obtain the absorption attributed by isolated SWCNTs for reliable characterizations and detailed analyses, especially in the UV region. With respect to the background absorption, one should be worth considering the component originated from bundled SWCNTs besides that from π-plasmons of graphitic impurities.

In this work, we have investigated the variation in optical absorption spectra of SWCNTs based on the degree of debundling modulated by centrifugation timing. As a result, we have decomposed the observed spectrum into the background and the absorption component of isolated SWCNTs. More interesting is the estimation of chirality distribution by deconvoluting the spectrum into Lorentzian profiles.

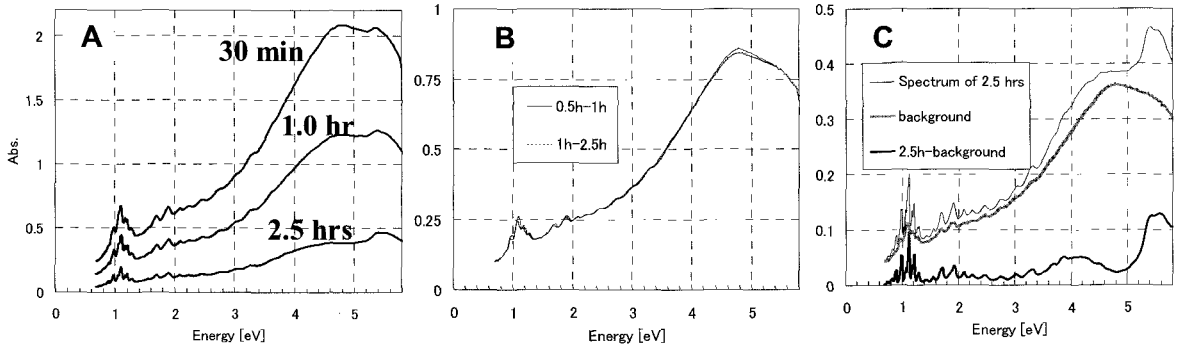

Figure 1. Optical absorption spectra of SWCNT dispersions prepared by different centrifugation times (A), difference spectra calculated by their subtraction attributed to the precipitates (B), and the decomposed spectrum of isolated SWCNTs obtained by the subtraction of B from A (C).

References

[1] M. E. Itkis et al., J. Am. Chem. Soc., 127(2005) 3439. [2] Y. Miyata et al., J. Phys. Chem. C, 112 (2008) 13187. [3] T. Saito et al., J. Nanosci. Nanotech., 8 (2008) 6153. [4] N. Nair et al., Anal. Chem. 78(2006) 7689.

Corresponding Author: Takeshi Saito

E-mail: takeshi-saito@aist.go.jp, Tel: +81-29-861-4863, Fax: +81-29-861-4413

2P-23

Atomic Geometry and Electronic Structure of Pyridine-Type Defects in Carbon Nanotube

○Yoshitaka Fujimoto and Susumu Saito

Department of Physics, Tokyo Institue of Technology, Tokyo 152-8551, Japan

Carbon nanotubes (CNTs) have been studied extensively since they are expected to be the potential applications in nano-electronic devices, such as a field effect transistor, a field emission display and so on. One of the efficient way to modify the electronic properties of CNT is to introduce dopants and defects. The nitrogen atom is considered to be a good candidate as a dopant. The nitrogen-doped CNT has been synthesized experimentally so far, and it is reported that the nitrogen-doped CNT constitutes the pyridine-type configuration [1,2].

We study atomic geometries, energetics, and electronic structures of the nitrogen-doped CNTs using the first-principles total-energy calculations within the framework of the density-functional theory. We here focus on the pyridine-type configuration in the carbon nanotube. In this talk, we will report on effects of the pyridine-type configuration formed in the carbon nanotube.

This work was partly supported by grants-in-aid from MEXT Japan through Global Center of Excellence Program of Nanoscience and Quantum Physics of Tokyo Institute of Technology.

[1] R. Czerw, M. Terrones, J. C. Charlier, X. Blasé, B. Foley, R. Kamalakaran, N. Grobert, H. Terrones, D. Tekleab, P. M. Ajayan, W. Blau, M. Ruhle, M. Ruhler, and D. L. Carroll, *Nano. Lett.* **1**, 457 (2001).

[2] M. Terrones, P. M. Ajayan, F. Banhart, X. Blasé, D. L. Carroll, J. C. Charlier, R. Czerw, B. Foley, N. Grobert, R. Kamalakaran, P. Kohler-Redlich, M. Ruhler, T. Seeger, and H. Terrones, *Appl. Phys. A* **74**, 355 (2002).

Corresponding Author: Yoshitaka Fujimoto
TEL: +81-3-5734-2368, FAX: +81-3-5734-2368, E-mail: fujimoto@stat.phys.titech.ac.jp

2P-24

Physical properties of Carbon nanotube grown by Microwave Plasma CVD method

○Tohru Watanabe[1,2], Shunsuke Tsuda[1,3], Takahide Yamaguchi[1], Yoshihiko Takano[1,2]

[1]*National Institute for Materials Science, 1-2-1, Sengen, Tsukuba, Ibaraki, 305-0047*
[2]*Tsukuba University, 1-1-1, Tennodai, Tsukuba, Ibaraki, 305-8577*
[3]*WPI-MANA, 1-1, Namiki, Tsukuba, Ibaraki, 305-0044*

Carbon nanotube (CNT), which has low resistivity, is expected to be applied to various devices, for example, transparent electrodes, nanowiring for future LSIs, probes for scanning probe microscopes and so on. However, CNT shows semiconducting and metallic behavior depending on the chiral vector. Then, to synthesized CNT, which have low resistivity, we tried to dope boron and injected careers into CNT, referring to boron-doped diamond. CNT and diamond are composed of only carbon atom. Pure diamond is an insulator, however by lightly doping of boron, it becomes semiconductor. And hevily boron-doped diamond becomes superconductor at low temperature [(1)].

We synthesized boron-doped CNT with microwave plasma chemical vapor deposition (MWCVD) method. Methane and tri-methyl-borate gases were used to CNT synthesis as source materials. CNTs were grown on the SiO_2 substrate. We synthesized various boron concentration CNT, and we succeeded to obtain very long and vertically aligned CNT. It is advantageous to mass production and direct wiring. Obtained CNT were characterized by Raman spectroscopy. And electrical property of individual CNT was measured by four terminals method. Four terminals were established using electron beam lithography technique. Our boron-doped CNT has lower resistivity than commercial pure CNT.

References: (1) Y.Takano et al. Appl. Phys. Lett., Vol. 85, No. 14, 4

Corresponding Author: WATANABE TOHRU
E-mail: WATANABE.Tohru@nims.go.jp
Fax: 029-859-2601

2P-25

Excitonic effects and chirality dependence of photoluminescence intensity of single wall carbon nanotubes

○Kentaro Sato[1], Riichiro Saito[2], Shigeo Maruyama[1]

[1]*Department of Mechanical Engineering, The University of Tokyo, 7-3-1 Hongo, Bunkyo-ku, Tokyo 113-8656, Japan*
[2]*Department of Physics, Tohoku University, Aramaki, Aoba-ku, Sendai 980-8578, Japan*

Photoluminescence (PL) has been widely used for the optical characterization of semiconducting single wall carbon nanotubes (SWNTs) because the PL intensity and PL energy depend on the diameter and chirality of SWNTs [1,2]. The optical absorption and emission energies of the PL of SWNTs, which are corresponding to the PL peak positions, are also known the exciton energies. Experiments and theoretical studies have been demonstrated that the excitonic effect in the presence of electron-hole and electron-electron interaction and the screening from the environment occurs to the change of the PL intensity and the energy shift of the PL peak position [3,4]. In the previous theoretical work [2], the chirality dependence of the PL intensity was calculated by multiplying the photon absorption, relaxation and photon emission matrix elements in the frame work of the tight-biding scheme in the one-electron picture. To consider the excitonic effect in the PL, we need to consider and calculate the PL intensity in the exciton picture.

In this paper we will discuss that the excitonic effect of the PL intensity and the dependence of the PL intensity on the diameter and chirality. The PL intensity is considered from the photon absorption, relaxation and photon emission in the exciton picture. Here we use the exciton-phonon and exciton-photon matrix elements in the framework of the tight-binding scheme [5]. The exciton energy dispersion of SWNTs in order to calculate the PL intensity is calculated by solving the Bethe-Salpeter equation in which the one particle energies are given by the tight-binding method [3,6]. Here the screening from environment and nanotubes itself is expressed by the dielectric constant. The relation between the exciton energy and dielectric constant is also discussed. We compare our calculation results with the experimental results.

References:

[1] O'Connell et al., Science **297**, 593 (2002).

[2] Y. Oyama et al., Chem. Phys. Lett. **44**, 873 (2006).

[3] T. Ando, J. Phys. Soc. Jpn. **66**. 1066 (1997).

[4] Y. Ohno et al., Phys. Rev. B **73**, 235427 (2006).

[5] J. Jiang et al., Phys. Rev. B **75**, 035405 (2007).

[6] J. Jiang et al., Phys. Rev. B **75**, 035407 (2007).

Corresponding Author: Kentaro Sato
E-mail: kentaro@photon.t.u-tokyo.ac.jp
Tel: +81-3-5841-6408

2P-26

Development of Light-Driven Carbon Nanoheat System for an Organic Reaction

○Eijiro Miyako, Tamitake Itoh, Takahiro Hirotsu

Health Technology Research Center, National Institute of Advanced Industrial Science and Technology (AIST), 2217-14, Hayashi-cho, Takamatsu 761-0395, Japan

Carbon nanotubes (CNTs) and their composites are very attractive for various research fields because of their unique physicochemical properties. In particular, the photodynamic properties of CNTs have potential for allowing various applications.[1] On the other hand, room temperature ionic liquids (RTILs) have attracted considerable attention because of their interesting physicochemical characteristics: no significant vapour pressure, non-flammability, good thermal stability, a wide useable temperature range etc.. Hence, RTILs are attracting great interest as environmentally friendly replacements for traditional organic solvents used in chemical processes. We believe that precise thermal control of RTILs is one of the most important tasks for expanding not only potential thermal applications of RTILs but also future chemistry utilizing RTILs. Here we show that a new photoinduced CNT composite can successfully achieve not only ultrarapid thermal control of RTILs but also polymerization of *N*-isopropylacrylamide (NIPAM) as a model monomer (Figure). By in situ microscopy, we demonstrate that when triggered by very low powered near-infrared (NIR) laser irradiation, photo-immobilized single-walled CNT (SWNT) composite arrays can achieve ultrafast thermal control of various RTILs as well as water and produce many PNIPAM microspheres quickly in water-in-RTIL (W/R) emulsions without conventional polymerization initiators and accelerators.

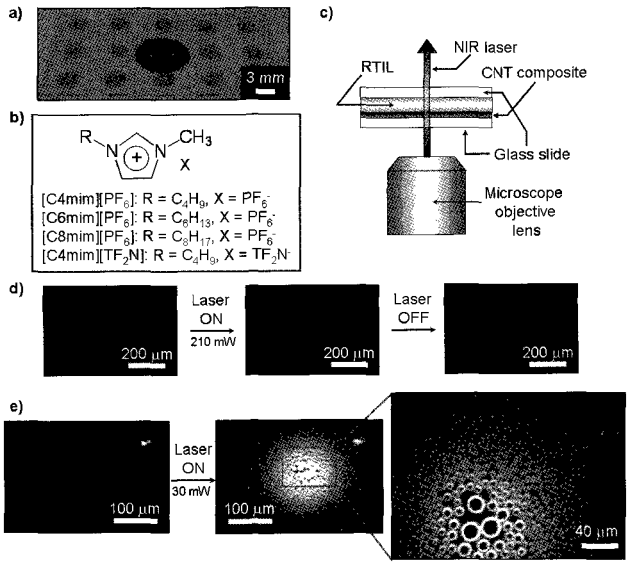

Figure. Ultrafast thermal control of RTILs and remote polymerization of NIPAM through a photoinduced CNT composite. (a) Image of transparent CNT composite arrays on a glass slide. (b) Chemical structure of RTILs. (c) Laser irradiation setup. (d) A direct observation of ultrafast temperature change of RTIL. Temperature change is evident by the ability to rapidly switch the fluorescence of temperature sensitive chemical. (e) Remote synthesis of PNIPAM microspheres.

[1] E. Miyako et al. *Angew. Chem. Int. Ed.*, **47**, 3610–3613 (2008); E. Miyako et al. *Adv. Mater.*, in press (2009); E. Miyako et al. *Chem. Eur. J.*, in press (2009); E. Miyako et al. *Lab Chip*, **9**, 788–794 (2009); E. Miyako et al. *Small*, **4**, 1711–1715 (2008); E. Miyako et al. *ChemSusChem*, **2**, 419–422 (2009); E. Miyako et al. *ChemSusChem*, in press (2009); E. Miyako et al. *Nanotechnology*, **18**, 475103–475109 (2007); E. Miyako et al. *Nanotechnology*, **19**, 075106–075111 (2008); E. Miyako et al. *Chem. Phys. Lett.*, **456**, 220–222 (2008).

Corresponding Author: Eijiro Miyako
TEL: +81-87-869-3574, FAX: +81-87-869-3550, E-mail: e-miyako@aist.go.jp

2P-27

Transmission electron microscopic observation of Pt/Ru-supported carbon nanocoil

○T. Kawabata[1], K. Takimoto[1], M. Yokota[1], T. Ikeda[1], Y. Suda[1], S. Oke[1], H. Takikawa[1], Y. Fujimura[2], S. Itoh[2], H. Ue[3], M. Morioki[4], K. Shimizu[5]

[1] *Department of Electrical and Electronic Engineering, Toyohashi University of Technology*
[2] *Research and Development Center, Futaba Corporation*
[3] *Fuji Research Laboratory, Tokai Carbon Co., Ltd.*
[4] *Fundamental Research Department, Toho Gas Co., Ltd.*
[5] *Development Department, Shonan Plastic Mfg. Co., Ltd.*

In direct methanol fuel cell (DMFC), there is a problem that flow of fuel and air is disturbed when catalyst-support material has too high density. The catalyst efficiency may be decreased. When carbon nanocoil (CNC) is used as a catalyst-support material, the flow is expected to be easy because CNC has a helical structure and hole inside it. In this study, we supported Pt/Ru catalyst on CNC and observed the Pt/Ru-supported CNC by transmission electron microscopy (TEM). CNCs are synthesized by chemical vapor deposition on a graphite substrate using a composite catalyst, Fe-Sn. The catalyst-loaded substrate was placed in the center of a quartz-made reaction tube. The reaction temperature, the gas flow rates of nitrogen as a dilution gas and acetylene as a source gas, and the reaction time were 780°C, 1400 ml/min, 350 ml/min, and 10 min, respectively. Then the CNC surface was treated by 15 wt% H2O2 solution and Pt/Ru was supported on CNC [1]. Fig. 1 shows TEM image of the Pt/Ru-supported CNC. Catalyst particles were clearly observed and the particle size was 3-8 nm diameter. Pt and Ru were confirmed by the energy-dispersive X-ray spectrometer (EDS) as shown in Fig. 2.

This work has been partly supported by the Outstanding Research Project of the Research Center for Future Technology, Toyohashi University of Technology (TUT); the Research Project of the Venture Business Laboratory (TUT); Global COE Program "Frontiers of Intelligent Sensing" from the Ministry of Education, Culture, Sports, Science and Technology (MEXT); The Japan Society for the Promotion of Science (JSPS) and Core University Programs (JSPS-CAS program in the field of "Plasma and Nuclear Fusion").

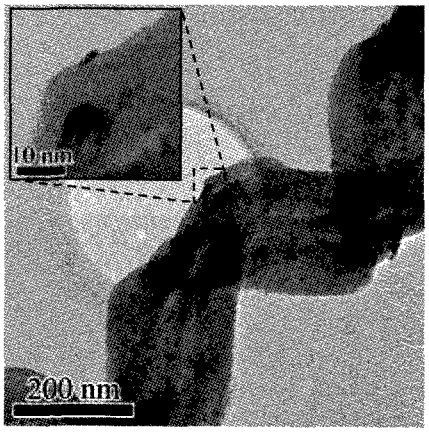

Fig. 1 TEM image of Pt/Ru-supported CNC.

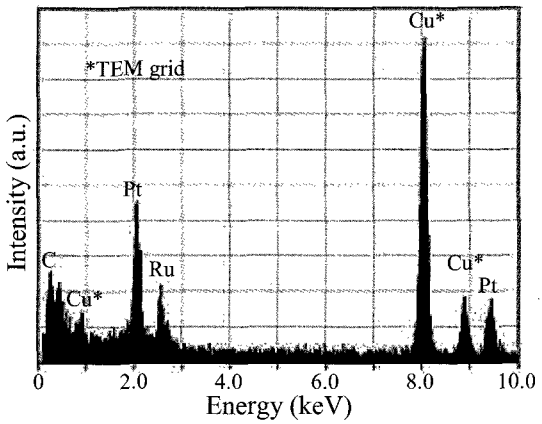

Fig. 2 EDS spectrum of Pt/Ru-supported CNC.

[1] S. Oke, et al., *Chem. Eng. J.*, Vol. **143**, pp. 225–229 (2008)

Corresponding Author: Yoshiyuki Suda
E-mail: suda@eee.tut.ac.jp, Tel: +81-532-44-6726

2P-28

Carbon Nanotubes Modified Electrode for a Dye-Sensitized Solar Cell

○Koichi Yasukawa, Shingo Sakamoto, Masato Tominaga

Graduate School of Science and Technology, Kumamoto University, Kumamoto 860-8555, Japan

Carbon nanotubes (CNTs) are expected to be applied to electric devices for its specific properties. We try to fabricate a dye-sensitized solar cell using CNTs as both counter electrode and photoelectrode. Fast charge transfer reaction at electrode interface and high conductivity are required for a counter electrode. Effective exciton generation induced by photoelectric conversion at dye molecular-modified elecrode interface is required for photoelectrode. In the present study, we prepared CNTs-modified quartz electrode as a counter and photoelectode for dye-sensitized solar cell.

CNTs were synthesized onto a flat quartz glass surface by chemical vapor deposition method using Co-Mo alloy nanoparticles as a catalyst. The thickness of catalyst layer was controlled by the dipping time of the quartz plate to the catalyst solution. Fig. 1 shows a plot of sheet resistance vs. CNT thickness. The sheet resistance reached to almost constant value of ca. 130 $\Omega\square^{-1}$ at ca 30 μm of CNT thickness. The details will be discussed.

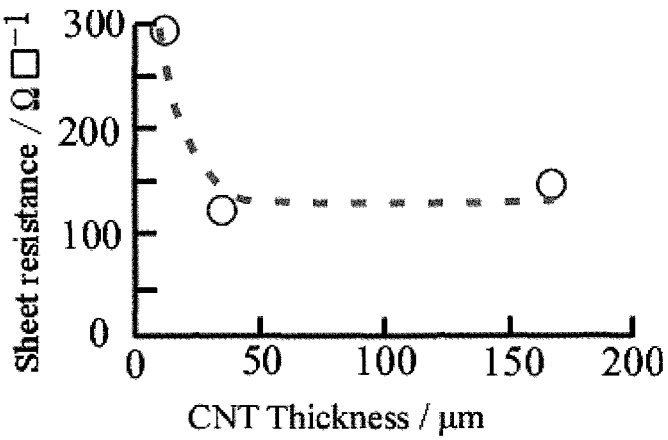

Fig.1 A plot of sheet resistance vs. CNT thickness.

Corresponding Author: Masato Tominaga
E-mail: masato@gpo.kumamoto-u.ac.jp
Tel&Fax: 096-342-3656

2P-29

Investigation on Solar Cell Fabricated by Carbon Nanotube Thin Film

○T.Y. Kato, Y.F. Li, T. Kaneko and R. Hatakeyama

Department of Electronic Engineering, Tohoku University, Sendai 980-8579, Japan

Carbon nanotubes (CNTs) have a great potential application for solar cells due to their absorption bands in the infrared light range as well as other advantages such as large surface areas, enormous current carrying capability, high mechanical strength, chemical stability, and etc. In this study, as a crucial step toward the realization of high-efficiency solar cells composed of CNTs, the electrical properties of p-n junction fabricated using the combination of a thin film of CNTs, including pristine (empty) single-walled carbon nanotubes (SWNTs) or fullerene (C_{60}) encapsulated SWNTs (C_{60}@SWNTs) prepared by either a thermal diffusion method or a plasma irradiation method [1], and an n-doped silicon (n-Si) are investigated.

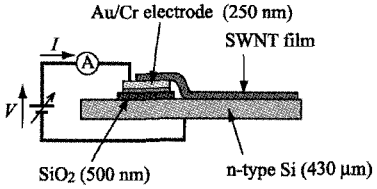

Fig. 1. The structure of p-n junction device made by SWNT film/n-Si.

Figure 1 shows a schematic illustration of p-n junction device structure fabricated using the pristine SWNT or C_{60}@SWNT film and the n-Si, which is fabricated by a spin-coating method. An Au/Cr electrode deposited on a SiO_2 insulator is formed on an n-Si substrate. Then, SWNTs suspended by sonication in N, N-dimethylformamide (DMF) are dropped and spin-coated on the substrate for several times to make the SWNT film.

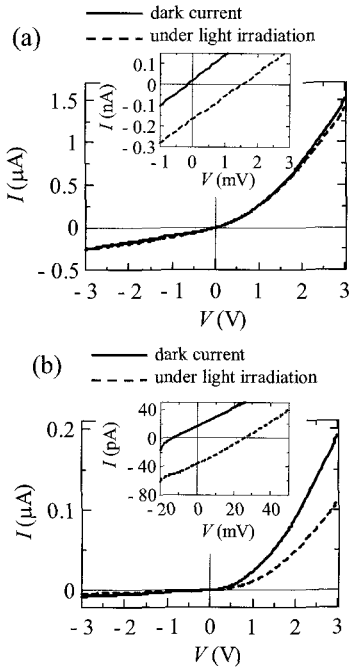

Fig. 2. The *V-I* characteristics of (a) pristine SWNT film/n-Si and (b) C_{60}@SWNT film/n-Si with or without light irradiation.

Figure 2 shows *V-I* characteristics of (a) pristine SWNT film/n-Si and (b) C_{60}@SWNT film/n-Si with or without light irradiation. The electrical properties of these CNT film/n-Si devices show an obvious rectifying characteristic, and a short-circuit current I_{SC} and an open-circuit voltage V_{OC} through a downward shift of *I-V* curves are observed under light irradiation. Moreover, it is found that the device fabricated with the C_{60}@SWNT film has a larger V_{OC} caused possibly by a large diffusion voltage in the interface of p-n junction compared with the device fabricated with the pristine SWNT film, due to the enhanced p-type behavior of SWNTs after C_{60} encapsulation.

[1] Y.F. Li, T. Kaneko, and R. Hatakeyama, *Nanotechnol.* **19**, 415201 (2008).

Corresponding Author: Tatsuya Kato
TEL: +81-22-795-7046, FAX: +81-22-263-9225, E-mail: tkato@plasma.ecei.tohoku.ac.jp

2P-30

Development of Novel Artificial Organ Biomaterial Composed of Multi-walled Carbon Nanotubes and Poly(L-lactic acid)

○Katsumune Takahashi[1,2],and Hirofumi Yajima[1]

1 Department of Applied Chemistry, Faculty of Science, Tokyo University of Science, 1-3 Kagurazaka, Shinjyuku, Tokyo 162-0825, Japan

2 Center for Colloid and Interface Science, Tokyo University of Science, 2641 Yamazaki, Noda, Chiba 278-8510, Japan

Multi-walled carbon nanotubes (MWNT) have attracted much attention for biomaterials. Recently, it has been reported that MWNT enhanced cell attachment, proliferation [1], and adsorption of extra-cellular matrix protein [2], whereas inhibited blood platelets adhesion, aggregation, and activation [3], respectively. The objective of this study is to fabricate the artificial organ material with both cyto and blood compatibility by using MWNT. Therein, poly(L-lactic acid) (PLLA), which is biodegradable polymer, was used as a substrate for the materials.

PLLA/MWCNT membranes were prepared by using spin-coating. Surface characterization was performed by the various analytical techniques such as Raman spectroscopy, X-ray photoelectron spectroscopy, contact angle, and surface zeta potential measurements. Bovine aortic endothelial cells (BAECs) and human blood platelets were used to evaluate biocompatibility.

BAEC attachment on the composite membrane after 24 h cultivation was lower compared to that of PLLA as control. However, BAEC proliferation was observed on the composite membrane after 7 days culturing. Blood platelets experiments revealed that composite membrane inhibited platelets adhesion and activation.

In conclusion, we have fabricated PLLA/MWNT composite membranes with cyto and blood compatibility by simple and safety method. The composite membranes are high potential and promising biomaterials for artificial blood vessel.

References

[1] L. Bacakova et al., Diamond Relat. Mater. 16 (2007) 2133-2140.

[2] D. Khang et al., Biomaterilas 28 (2007) 4756-4768.

[3] J. Meng et al., J. Biomed. Mater. Res. 74A (2005) 208-214.

Corresponding Author: Hirofumi Yajima

Tel: +81-3-5228-8705

E-mail: yajima@rs.kagu.tus.ac.jp

2P-31

Temperature dependence of diameter distributions of SWNTs revealed by optical absorption and photoluminescence mesurements

○Akira Inoue[1)], Yasuhiro Tsuruoka[1)], Toshiya Okazaki[2)] and Yohji Achiba[1)]

1) Department of Chemistry, Tokyo Metropolitan University, Hachioji, Tokyo 192-0397, Japan

2) Advanced Industrial Science and Technology (AIST), Tsukuba 305-8565, Japan

Controlling chiral distribution of single-walled carbon nanotubes must be one of the most important issues in the science and technology of SWNTs, particularly in aid of application to the field of nano-eletcronics, nano-optoelectronics as well as bio-electronics. In order to obtain the SWNTs with a specific chirality, recently a lot of tasks have been appeared in the research work of the separation and purification of the specific chiral species from the crude sample originally containing many kinds of (n,m) species. Under such circumstance, it is strongly demanded to develop a new method by which we can obtain the crude sample containing only limited numbers of (n,m) species or single chiral species. In the present paper, we will demonstrate how furnace temperature makes effect on the size and chirality distributions of single-walled carbon nanotubes in the laser vaporization experiments.

The crude soot was prepared at different furnace temperature (950℃-1250℃) by using Ni/Co catalyst and Nd/YAG pulsed laser. After conventional homozinization and sonication procedures, the isolated SWNTs were dispersed in the solution of SDBS/H2O or PFO(poly-9, 9-di-n-octyl-fluorenyl-2, 7-diyl)[1]/toluene system.

Figure1 shows absorption spectra of the semiconducting SWNTs prepared at different furnace temperature. The sample prepared at the lower temperature shows that the absorption spectrum mostly consists of near-armchair type nanotubes, but those pepared at the higher furnace temperature, the absorption consists of broadly distributed chiral species. Photoluminescence measurements also support such tendency (see Fig.2).

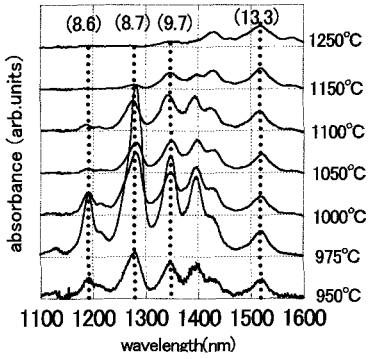

Fig.1 Absorption spectra in the E_{11} energy of semiconducting SWNTs by changing temperature from950℃ to1250℃

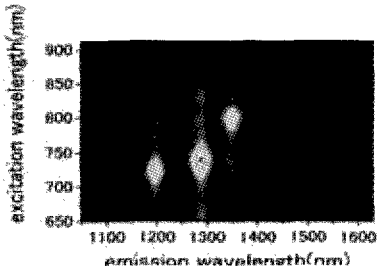

Fig.2 photoluminescence spectra of the sample prepared at 975℃.

References: A. Nish, et al., nature nanotechnology. 2, 290 (2007)

Corresponding Author Yohji Achiba
E-mail achiba-yohji@tmu.ac.jp TEL042-677-2534

2P-32

Effect of Laser Wavelength and Dispersed Agents to Selective Chiral Separation of Single-walled Carbon Nanotubes by Pulsed OPO Laser Irradiation

○ Akira Kumazawa, Isamu Tajima, Katsumi Uchida, Koji Tsuchiya, Tadahiro Ishii, Hirofumi Yajima

Department of Applied Chemistry, Faculty of Science, Tokyo University of Science
12-1 Funagawara-machi, Shinjyuku-ku, Tokyo 162-0826, Japan

As-synthesized single-walled carbon nanotubes (SWNTs) contain various chiralities, namely, both metallic and semiconducting SWNTs. Thus, for application of SWNTs to electronic devices such as field emission transistor, it's absolutely imperative to separate metallic from semiconducting SWNTs, or to pick out specific chirality. Thus, we have investigated about a new selective separation method for metallic (m-) and semiconducting (s-) SWNTs with nanosecond pulsed optical parametric oscillator (OPO) laser, which could control wavelength and pulse-number of laser irradiation. In this study, we have reported about the influence of dispersing agent to sorting of SWNTs by laser ablation using carboxymethylcellulose (CMC) or dodecylbenzensulfonic acid sodium salt (NaDDBS). The aqueous solutions of SWNTs dispersed by CMC or NaDDBS were irradiated by the OPO laser with laser wavelength corresponding to typical absorption peaks in m-SWNTs first transition region (M11), and s-SWNTs first and second transition band region (S22, S11), respectively. The SWNTs in the solutions before and after laser irradiation was estimated with UV-vis-NIR absorption and resonance Raman scattering spectra, and AFM. By irradiation of laser with wavelength in M11 region, the optical absorption intensity of the SWNT dispersed by CMC or NaDDBS was reduced in all regions of M11, S11, and S22. Irradiation of laser in S11 or S22 region induced to reduction of the absorption intensity in S11 and S22 region, however, the adsorption intensity in M11 region was almost constant. Additionally, the adsorption intensity of the SWNTs was dependent on the pulse number of laser irradiation. From AFM, the amount of the SWNTs destroyed by laser irradiaition was dependent on wavelength and dispersing agent. Irradiation of laser with wavelength in S22 region caused to the extensive damage to the SWNTs dispersed by CMC. On the other hand, the SWNTs dispersed by NaDDBS were damaged significantly by irradiation of laser with wavelength in M11 region. Now, we have been investigating about the effect of wavelength and pulse number of laser, and dispersing agent to selection of SWNTs by laser ablation in detail.

Corresponding Author: Hirofumi Yajima

TEL: +81-3-3260-4272(ext.5760), FAX: +81-3-5261-4631, E-mail: yajima@rs.kagu.tus.ac.jp

2P-33

Catalyst deposition by spin-coating for synthesis of vertically-aligned single-walled carbon nanotubes

○ Theerapol Thurakitseree, Erik Einarsson, Rong Xiang, Pei Zhao,
Junichiro Shiomi, Shigeo Maruyama

Department of Mechanical Engineering, The University of Tokyo, Tokyo 113-8656, Japan

In our conventional alcohol catalytic CVD method [1,2], vertically aligned single-walled carbon nanotubes (VA-SWNTs) are synthesized from catalyst nanoparticles deposited onto Si or quartz substrates by a dip-coating process [3]. Here we present a spin-coating method as an alternative to dip-coating, where cobalt and molybdenum metals were deposited onto Si substrates by spin-coating a solution containing 0.01 %wt of each metal species dissolved in ethanol. The SWNT arrays were characterized by SEM observation (Fig. 1a) and resonance Raman spectroscopy (Fig. 1b). The results from this method were compared with the standard dip-coating method, and we found the spin-coating method resulted in higher yield of VA-SWNTs. Based on SEM observation, it was clear that the VA-SWNT array thickness is dependent on the thickness of the spin-coated film, and its uniformity could be optimized by tuning the spinning conditions. Furthermore, we found the RBM region of the resonance Raman spectra is very similar to that of VA-SWNTs synthesized from dip-coated catalyst.

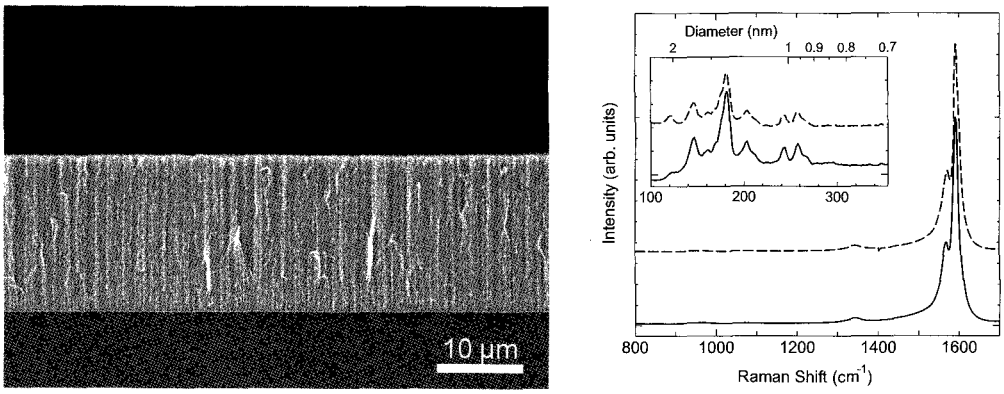

Fig. 1. (a) SEM image of VA-SWNTs synthesized from spin-coated catalyst; (b) resonance Raman spectra (488 nm?) of SWNTs from catalyst prepared by dip-coating (dashed line) and spin-coating (solid line)

[1] S. Maruyama, R. Kojima, Y. Miyauchi, S. Chiashi, M. Kohno, *Chem. Phys. Lett.* **360** (2002) 229.

[2] Y. Murakami, S. Chiashi, Y. Miyauchi, M. Hu, M. Ogura, T. Okubo, S. Maruyama, *Chem. Phys. Lett.* **385** (2004) 298.

[3] Y. Murakami, Y. Miyauchi, S. Chiashi, S. Maruyama, *Chem. Phys. Lett.* **377** (2003) 49.

Corresponding Author: Shigeo Maruyama
TEL: +81-3-5841-6421, FAX: +81-3-5800-6983, E-mail: maruyama@photon.t.u-tokyo.ac.jp

2P-34

Bending Horizontally-Aligned Carbon Nanotubes during Growth

○Hiroki Ago,[*,1,2,3] Kenta Imamoto,[2] Tetsushi Nishi,[2] Masaharu Tsuji,[1,2]
Tatsuya Ikuta,[4] Koji Takahashi,[4] and Munetoshi Fukui[5]

[1]*Institute for Materials Chemistry and Engineering, Kyushu University,* [2]*Graduate School of Engineering Sciences, Kyushu University,* [3]*PRESTO, Japan Science and Technology Agency,* [4]*Graduate School of Engineering, Kyushu University,* [5]*Hitachi High-Technologies Corporation*

There are two different mechanisms of horizontally-aligned growth of single-walled carbon nanotubes (SWNTs) on single crystalline substrates; lattice-oriented [1-3] and step-templated growth [4]. We reported that the height of the atomic steps of sapphire (α-Al_2O_3) determines the alignment direction, and the higher steps with > 0.5 nm gave the step-templated growth [5]. More recently, we succeeded in growing the aligned SWNTs on SiO_2/Si wafers by making artificial nanoscale trenches [6]. The combination of two growth mechanisms, lattice-oriented and step-templated growth, is expected to offer further control of SWNT structure.

By making artificial steps on sapphire surfaces, bending of horizontally-aligned SWNTs was achieved. The SWNTs grown on the r-plane sapphire are originally aligned along the specific crystallographic [$1\bar{1}0\bar{1}$] direction due to the lattice-oriented growth, and we created artificial step structures perpendicular to this SWNT growth direction. These steps changed the nanotube growth direction from [$1\bar{1}0\bar{1}$] to the step direction with bending angle of nearly 90° (Figure 1a) [7]. Effects of the bending structure on electron transport property were studied by using a nanoprobing scanning system, and we found that the bending part showed higher resistivity than the straight part (Figure 1b,c). Our approach to combine the lattice-oriented growth with the step-templated growth will offer a new route towards the growth of two-dimensionally controlled SWNT architectures for future nanoelectronics.

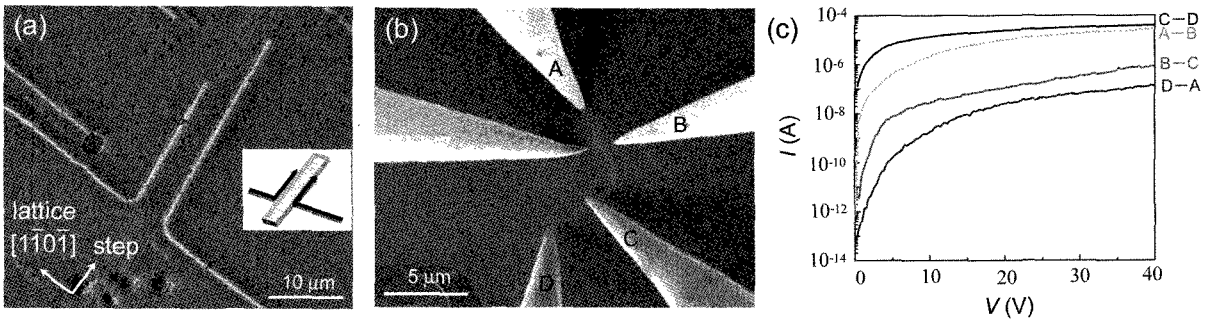

Figure 1. (a) SEM image of bent SWNTs observed at the patterned steps with ~8 nm height. Inset shows the schematic image of the bent SWNTs. (b,c) Resistivity measurement of a bent SWNT with four probes.

Reference

[1] H. Ago *et al.*, *Chem. Phys. Lett.* (2005). [2] S. Han *et al.*, *J. Am. Chem. Soc.* (2005). [3] C. Kocabas *et al.*, *J. Phys. Chem. C* (2007). [4] A. Ismach *et al.*, *Ang. Chem. Int. Ed.* (2004). [5] H. Ago *et al.*, *Appl. Phys. Lett.* (2007). [6] C. M. Orofeo *et al.*, *Appl. Phys. Lett.* (2009). [7] H. Ago *et al.*, *J. Phys. Chem. C*, in press.

Corresponding Author: Hiroki Ago (Tel&Fax: +81-92-583-7817, E-mail: ago@cm.kyushu-u.ac.jp)

2P-35

Synthesis of Single-Walled Carbon Nanotube Soot with Few Impurity Graphites by Arc Discharge

○ Yoshinori Sato[1,2], Hikaru Watanabe[1], Masaru Namura[1], Kenichi Motomiya[1], and Kazuyuki Tohji[1]

[1]*Graduate School of Environmental Studies, Tohoku University, Sendai, 980-8579, Japan*
[2]*PRESTO, Japan Science and Technology Agency, 4-1-8 Honcho Kawaguchi, Saitama, Japan.*

Single-walled carbon nanotube (SWCNT) is an intriguing material for its mechanical, electrical, or chemical properties due to one-dimension structure. SWCNTs have been successfully synthesized in large quantities using a direct current arc discharge method, anode graphite electrode mixed with several metallic species, predominantly transition metals such as Fe, Co, Ni, and Y. The SWCNTs synthesized by this method coexist with impurities such as metals, amorphous carbon, and graphite. We have developed the easy purification method for SWCNTs incorporating the air oxidation and acid treatment. However, graphite remains in the purified SWCNTs, which comes from the anode electrode made from graphite. Here, we tried to produce SWCNT soot with few impurity graphites using an arc discharge by changing a carbon material of anode. The obtained SWCNT soot were discussed by characterizing the intermediate products using X-ray diffraction (XRD), Raman scattering spectroscopy, scanning electron microscopy (SEM), extend X-ray absorption fine structure (EXAFS), thermogravimetric analysis (TGA), inductively coupled plasma - Mass Spectrometry (ICP-MS), and high resolution transmission electron microscopy (HRTEM) with energy dispersive X-ray spectroscopy (EDX). The result will be reported in detail and discussed.

Corresponding Author: Yoshinori Sato
E-mail: hige@bucky1.kankyo.tohoku.ac.jp
Tel&Fax: +81-22-795-3868

2P-36

Growth of carbon nanotubes by plasma enhanced and thermal chemical vapor depositions

○Masato Miyake[a)], Toru Iijima[b)], Kenneth Teo[c)], Nalin Rupesinghe[c)], Kenjirou Onuma[a)], Kazunori Horikawa[a)], Katsuyoshi Abe[a)], Masayuki Satoh[a)] and Yasuhiko Hayashi[b)]

a) AIXTRON K.K, 9F Davinci Shinagawa II, 1-8-11, Kita-shinagawa Shinagawa-ku Tokyo 140-0001, Japan

b) Department of Frontier Materials, Nagoya Institute of Technology, Gokiso Showa Nagoya 466-8555, Japan

c) AIXTRON Ltd, Anderson Road, Buckingway Business Park Swavesey, Cambridge CB24 4FQ, U.K.

Carbon Nanotubes (CNTs) and various types and morphologies of nanofibers (NWs) can be controllably grown. These systems are presently used for development of CNTs based transistors, interconnects, sensors, displays, thermal interfaces, electron guns, micro fluidics, microwave amplifiers, super capacitors and fuel cells.

Here, CNTs and NWs were grown by the "black magic II" by Aixtron Ltd., which enables us to use both plasma enhanced and thermal chemical vapor depositions (PECVD/thermal CVD modes) by the same system. This CVD system employs rapid heating and plasma technologies. Therefore, the proper choice of CVD modes according to desired CNT, we demonstrate a straightforward approach for both multi-walled CNTs by PECVD and Rapid-Growth of wall-number selected high density CNTs. This is good advantage for this CVD system over the other CVD systems because the PECVD and the thermal CVD are totally different processes for CNT growth. In addition, we have already manufactured the extended CVD system based on the black magic II, which enables us to grow very uniform and well reproduced CNTs on the large wafer size up to 12-inchs.

CNTs were grown by catalytic decomposition of acetylene on nickel at different substrate temperature using $Ni/SiO_2/Si$ substrate by PECVD, as shown in Fig 1. In case of Rapid-Growth CNTs by thermal CVD, as shown in Fig 2, we have investigated the effect of growth time, temperature rump rate and other parameters using $Fe/Al_2O_3/Si$. We characterized samples by Raman scattering, scanning electron microscopy (SEM), transmission electron microscope (TEM) and atomic force microscope (AFM), sequentially

In this study, we report the primary results of PECVD grown CNTs as well as Rapid-Growth CNTs by thermal CVD.

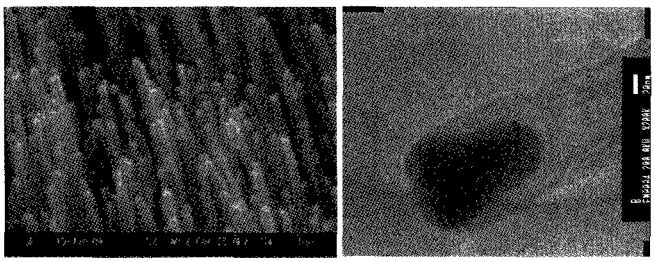

Fig1. SEM and TEM images of CNTs by PECVD.

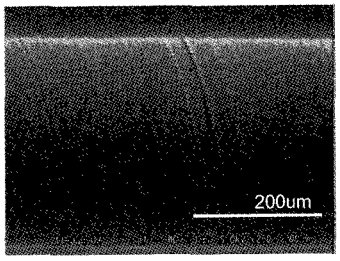

Fig2. SEM image of CNTs by Rapid- Growth.

Masato Miyake : E-mail : m.miyake@aixtron.com,
Tel&Fax : +81-3-5781-0931, +81-3-5781-0940

2P-37

Carbon Nanotubes Synthesis in Liquid Xylene by Arc Discharge Using Metal Electrodes

○Takio Kizu, Shinya Aikawa, Eiichi Nishikawa

Department of Electrical Engineering, Tokyo University of Science, 1-3 Kagurazaka, Shinjuku, Tokyo 162-8601, Japan

Carbon nanomaterials including carbon nanotubes (CNTs) are discriminating in mechanical, chemical and physical properties, so it is expected as one of promising next-generation carbon material. The method of synthesis of nanocarbon is arc discharge, laser ablation and chemical vapor deposition (CVD) method. Electrical arc discharge in water was particularly cost effective process because of without use of vacuum devices [1,2]. In almost all of the research employing an arc discharge method in liquid phase, the nanomaterials produced are composed of carbon atoms supplied from the graphite electrodes. Several groups have achieved synthesis of nanocarbon materials from liquid hydrocarbons. We have previously demonstrated producing carbon nanospheres from sucrose solution in an experiment using arc method with copper electrodes [3]. Shibata et al. added ultrasonically irradiation in this method and amorphous carbon could be synthesized from liquid benzene [4]. Also according to Okada et al.'s report [5], tube-like nanocarbons were formed from toluene by an arc discharge method between nickel electrodes.

Here we present carbon nanomaterials such as CNT could be synthesized from liquid xylene using arc discharge method with copper electrodes. This process successfully yields various nanocarbon materials having a graphite layer structure of high crystallinity.

[1] N. Sano, H. Wang, M. Chhowalla, I. Alexandrou, G. A. J. Amaratunga, Nature 414, 506 (2001).
[2] Y. L. Hsin, K. C. Hwang, F.-R. Chen, J.-J. Kai, Adv. Mater. 13, 830 (2001).
[3] S. Aikawa, T. Kizu, E. Nishikawa, T. Kioka: Chem. Lett. 36, 1426 (2007).
[4] E. Shibata, R. Sergiienko, H. Suwa, T. Nakamura, Carbon 42, 885 (2004).
[5] T. Okada, T. Kaneko, R. Hatakeyama, Thin Solid Films 515, 4562 (2007).

Corresponding Author: Eiichi Nishikawa
TEL: +81-3-3260-4271, FAX: +81-3-5213-0976, E-mail: nisikawa@ee.kagu.tus.ac.jp

2P-38

Selective dispersion of single-walled carbon nanotubes using polycarbazole derivative

○Hiroaki Ozawa[1], Natsuko Ide[1], Tsuyohiko Fujigaya[1], Suhee Song[2], Hongsuk Suh[2], and Naotoshi Nakashima[1,3]

[1]*Department of Applied Chemistry, Graduate School of Engineering, Kyushu University, Fukuoka 819-0395, Japan*
[2]*Department of Chemistrya and Chemistry Institute for Functional Materials, Pusan National University, Busan 609-735, Korea,*
[3]*JST-CREST, 5 Sanbancho, Chiyoda-ku, Tokyo 102-0075, Japan*

Selective dispersion of single-walled carbon nanotubes (SWNT) has attracted much attention due to potential applications in the fields of energy, electronics, sensing and so forth. However, the coexistence of SWNTs having many chiralities makes application difficult. Therefore, it is desirable to find ways to selectively separate semiconducting SWNTs from commercially available SWNTs. Recently, approaches to selective dispersion of SWNT were explored using polyfluorenes [1,2]. We made effort to find another type of compounds that are able to selective SWNT solubilization. Here we report the finding that polycarbazole derivatives **1** (Figure 1) carrying carbazole, thiophene, and benzothiadiazole shows an unique SWNT solubilization behavior.

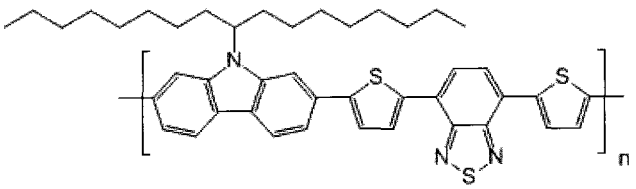

Figure 1. Chemical structure of polycarbazole derivatives **1.**

HiPco-SWNTs were added to a toluene solution of **1** and sonicated for 1h followed by centrifugation at 10000 g. As shown in Figure 2, very sharp S11 bands of the SWNTs are observed in the range of 1000-1500 nm, which resembles the spectra of the SWNTs dissolved in a PFO toluene solution. Details will be reported at the meeting.

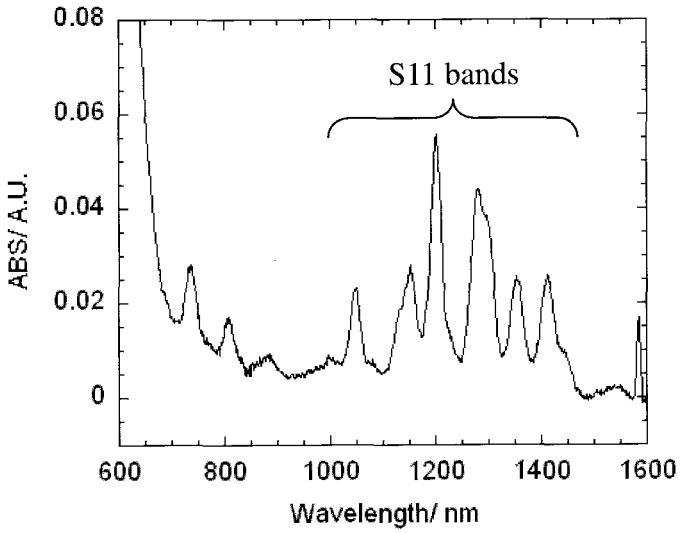

Figure 2. UV-Vis-NIR spectrum of SWNT dissolved in a **1** toluene solution.

[1] A. Nish, J. Y. Hwang, J. Doig, R. J. Nicholas, *Nature Nanotechnology* **2**, 640 (2007).
[2] F. M. Chen, B. Wang, Y. Chen, L. J. Li, *Nano Letters* **7**, 3013 (2007)

Corresponding Author: Naotoshi Nakashima
TEL/FAX: +81-92-802-2840, E-mail: nakashima-tcm@mail.cstm.kyushu-u.ac.jp

2P-39

Diameter-Dependence of Host-Guest Interaction between Single-Wall Carbon Nanotubes and Encapsulated Fullerenes Probed by Resonance Raman Spectroscopy

○Soon-Kil Joung[1], Toshiya Okazaki[1,2], Susumu Okada[3], and Sumio Iijima[1]

[1]*Nanotube Research Center, AIST, Tsukuba 305-8565, Japan*
[2]*PRESTO, JST, 4-1-8 Honcho, Kawaguchi 332-0012, Japan*
[3]*Institute of Physics, Center for Computational Science, University of Tsukuba, Tsukuba 305-8571, Japan*

In supramolecular systems, two or more molecular entities held together and are organized by means of intermolecular (noncovalent) binding interaction such as van der Waals forces, π-π stacking, hydrogen bond and so on. Based on these interactions, host molecule can recognize the guest molecule and form a supramolecular structure with useful functions. Fullerene encapsulated single-wall carbon nanotubes (SWCNTs), so-called nanopeapods (NPDs), can be regarded as one of the best model systems for investigating the host-guest interaction in aromatic supramolecules because the distance between fullerenes and SWCNTs can be varied finely and systematically in the angstrom scale. We here report the fullerene encapsulation effects on the radial breathing mode (RBM) of semiconducting and metallic SWCNTs, in which the interspacing between SWCNT and fullerene varies from 2.7 Å to 4.2 Å (corresponds to 1.25 nm to 1.55 nm in tube diameter).

Figure 1 shows the RBM frequency shifts obtained from semiconducting and metallic C_{60} NPDs as a function of tube diameter. Even though metallic SWCNTs are not luminescent, their resonance Raman signals are observable. For smaller diameter tubes (d_t < ~1.3 nm), the changes in the RBM frequencies of semiconducting SWCNTs after C_{60} insertions are shifted to higher frequencies, which is reasonably explained by the repulsive forces (from electron repulsions) between C_{60} and SWCNTs [1]. On the other hand, for larger diameter regime (d_t > ~1.3 nm), $\Delta\omega$ shows the negative values and approaches to zero again as increasing tube diameter. Interestingly, the semiconducting C_{60} NPDs are prominently downshifted up to -7 cm^{-1} around d_t ~1.4 nm due to π-π hybridization interaction between SWCNTs and C_{60} [1] while metallic C_{60} nanopeapods are only shifted downward up to -2 cm^{-1}. The difference in the intermolecular interactions between metallic and semiconducting SWCNTs may come from the difference in the Coulomb interaction with C_{60}.

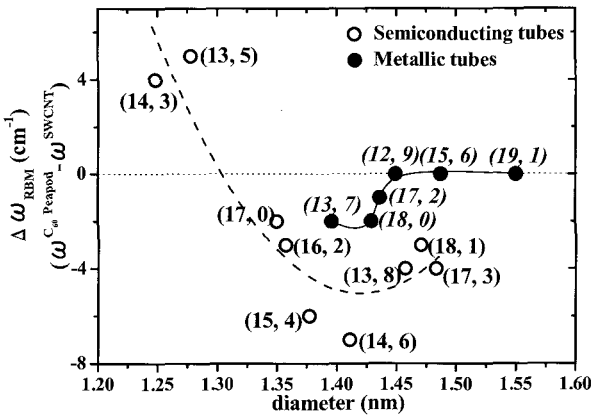

Figure 1. $\Delta\omega_{RBM}$ of semiconducting tubes (●) and metallic tubes (○) as a function of tube diameter.

[1] S.-K. Joung, T. Okazaki, N. Kishi, S. Okada, S. Bandow, S. Iijima, ***Phys. Rev. Lett.*** in press.

Corresponding Author: Toshiya Okazaki, **E-mail:** toshi.okazaki@aist.go.jp, **Tel:** 029-861-4173, **Fax:** 029-861-6241

2P-40

Room-Temperature Y-Emission from Perylene Molecules Confined in Single-Wall Carbon Nanotubes

○Masayoshi Tange[1], Toshiya Okazaki[1,2], Zheng Liu[1], Kazu Suenaga[1], and Sumio Iijima[1]

[1]*Nanotube Research Center, AIST, Tsukuba, 305-8565, Japan*
[2]*PRESTO, JST, Kawaguchi 332-0012, Japan*

Confinement of materials in individual single-wall carbon nanotubes (SWCNTs) is effective in the synthesis of functional nanocomposites. One of the materials characterized by molecular arrangement is perylene. A perylene crystal with dimeric structures (i.e., α-perylene) forms two kinds of excited dimer (excimer) states, which are attributed to the coupling between excitons and phonons. One is the E-state observed at high temperatures > 50 K. The other is the Y-state, which is observable at low temperatures, but is not observed at high temperatures because of the metastability of the state. In this study, we have investigated the optical properties of the perylene molecules (with monomeric and dimeric structures) encapsulated in SWCNTs.

Figure 1 shows fluorescence spectra in the perylene@SWCNTs and perylene monomers dispersed in D_2O with the sodium dodecylbenzene sulphonate (SDBS) surfactant. At a excitation wavelength λ_{ex} of 380 nm, the perylene@SWCNTs solution exhibits a complicated spectrum including a monomer emission due to the monomeric structure of encapsulated perylene molecules. On the other hand, at λ_{ex} = 310 nm, where the excitation energy deviates from the optical absorption band of a perylene monomer, the perylene@SWCNTs solution exhibits a fluorescence spectrum with several vibrational structures without the monomer-like emission. The spectrum at λ_{ex} = 310 nm is similar to the Y-emission rather than the broad, structureless E-emission of α-perylene. Moreover, in the shape and peak positions of the spectrum, the fluorescence from perylene@SWCNTs resembles that of the dimer perylene examined at T = 2 K by Mahrt *et al.*[1] The Y-emission-like spectrum found at a room temperature in the present work suggests that the confinement of perylene molecules in SWCNTs suppresses the influence of thermal fluctuations on the metastable Y-state.

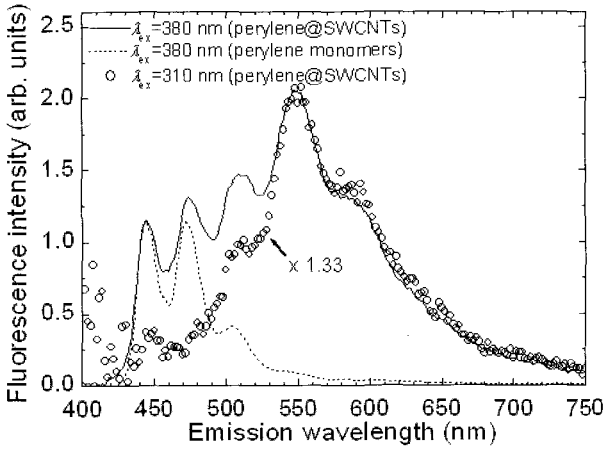

Fig. 1. Fluorescence spectra of perylene@SWCNTs and monomer perylene solutions.

[1] J. Mahrt *et al.*, J. Phys. Chem. **98** (1994) 1888.

Corresponding Author: Toshiya Okazaki
E-mail: toshi.okazaki@aist.go.jp
Tel: +81-29-861-4173
Fax: +81-29-861-6241

2P-41

Energetics and Electronic Structure of Carbon Nanotube Encapsulating Coronene Molecules

Susumu Okada

Graduate School of Pure and Applied Sciences, Center for Computational Sciences, University of Tsukuba, Tennodai, Tsukuba 305-8577, Japan
CREST, JST, 4-1-8 Honcho, Kawaguchi, Saitama 332-0012, Japan

Space inside the carbon nanotubes is applicable to contain foreign atoms and molecules resulting in one-dimensional structures which are completely different from conventional bulk structures. For instance, C_{60} and other higher fullerenes are indeed encapsulated in single-walled and double-walled carbon nanotubes in which the fullerenes form one-dimensional chains. In addition to fullerenes, metal atoms, water molecules, and organic molecules have been encapsulated into inner space of nanotubes. These hybrid structures comprising of nanotube and encapsulated species exhibit different structural and electronic properties to those obtained by the simple sum of constituents.

Here we examine the energetics and electronic structures of single-walled nanotube encapsulating coronene molecules (a polycyclic aromatic hydrocarbon: $C_{24}H_{12}$) based on the first-principle total-energy calculations in the framework of the density functional theory. Our calculations show that stacked coronene molecules are stable in carbon nanotubes with diameter of 1.35 nm or larger. In the nanotube with diameter of 1.47 nm, the encapsulation results in the largest energy gain of about 1eV. It is also found that the encapsulated coronene are slightly tilted to the tube axis. This tilting arrangement of coronene results in the substantial hybridization between the π states of nanotube and coronene, which induces the modulation of electronic structures of each constituent unit.

Corresponding Author: Susumu Okada, sokada@comas.frsc.tsukuba.ac.jp

2P-42

Ceramide-conjugated PEG: an Outstanding Dispersant for SWNHs

O Jianxun Xu,[1] Sumio Iijima,[1,2] Masako Yudasaka[2]

[1] Meijo University, 1-501 Shiogamaguchi, Tenpaku-ku, Nagoya 468-8502, Japan

[2]Nanotube Research Center, National Institute of Advanced Science and Technology (AIST), Central 5, 1-1-1 Higashi, Tsukuba, 305-8565, Japan

In this study, we compared the abilities of two types of poly(ethylene glycol) (PEG)-based materials to disperse single wall carbon nanohorns (SWNHs): they were phospholipid-conjugated PEG (DPEG) and ceramide-conjugated PEG (CPEG), as shown in Fig. 1. DPEG is a widely used dispersant for nano-carbon materials. According to our results, CPEG showed better dispersion ability than DPEG, in both water and phosphate buffer saline (PBS). The size of CPEG-wrapped SWNHs was obviously smaller than that of DPEG-wrapped SWNHs, according to our dynamic light scattering measurements and electron microscopy observations (Fig. 2). Furthermore, the dispersion of CPEG-SWNHs was very stable as concluded from the light transmittance monitoring.

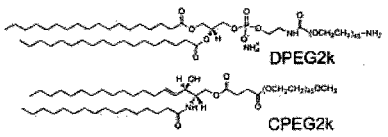

Figure 1. The structures of the PEG-based dispersants used in this work.

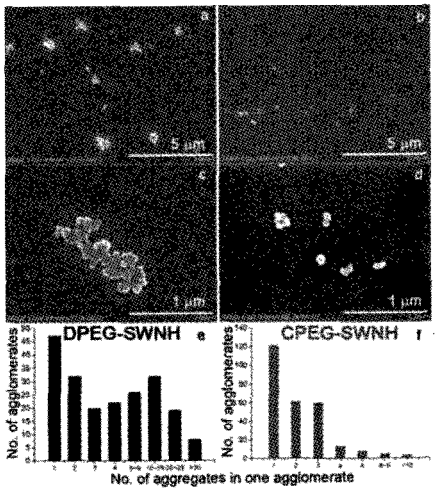

Figure 2. SEM images of (a, c) DPEG-SWNH and (b, d) CPEG-SWNH in H_2O. (e, f) The agglomeration number histograms of these two samples.

Apparently the high surface charge of CPEG-SWNHs in H_2O, as revealed by zeta potential measurements, generates strong Coulomb repulsion force between SWNH aggregates. The high stability in PBS may be ascribed to the attached PEG chains, which wrap the SWNH aggregates and extend into the aqueous environment to prevent agglomeration. We believe that the neutral structure of CPEG, compared to the charged phosphoethanolamino group of DPEG, results in its stronger interaction with the SWNHs, leading to better dispersion ability.

Contact: m-yudasaka@aist.go.jp

2P-43

Formation of honeycomb nano-pore array on graphene using by nanoporous alumina template and edge electronic structures

○J.Nakamura, J. Haruyama, T. Shimizu, S.Oikawa, S.Enomoto

School of Science and Engineerings, Material Science course, Aoyama Gakuin University, 5-10-1 Fuchinobe, Sagamihara, Kanagawa 229-8558, Japan

Abstract

Recently, graphene is attracting significant attention. A variety of interesting phenomena has been reported; *e.g.*, anomalous quantum Hall effect with half branch ($R_{xy}^{-1} = 4(N+1/2))e^2/h$) [1], its appearance at room temperature [2], residual quantum resistance [3] and Cooper-pair transport [4] at Dirac point, high electronic density of states (EDOS) at ZIG-ZAG edges [5]. Moreover, application to devices has been realized; e.g., f_t=26GHz FET [6], band-gap engineering by using graphene nano-ribbon [7] and a few layer graphenes.

In particular, research of chirality, electronic states, and spin transport at graphene edges, and also those applications is of great interest. Possibility of extremely high EDOS and polarized spin transport at ZIG-ZAG edge is highly expected. However, region of such edge states is at most a few-nm width and it is difficult to make current flow through such a small region. Thus, expansion of the edge region is indispensable.

In the present study, we fabricated honeycomb like array of nano-pores on graphene by using nano-porous alumina template (NPAT) as a mask for etching. We expect that the edges of nanopores partially have ZIG-ZAG structure and those highly dense location results in expansion of edge states. NPAT was fabricated by anodic oxidation of pure aluminum substrate (99.99%) with pore diameter of 20 ~ 80 nm. After anodization, NPAT was detached from aluminum substrate and placed on graphene sheet, which was fabricated by following Geim's method [8] on Si substrate. Then, graphene was etched using the NPAT as a mask and honeycomb nano-pore array of the NPAT was transferred to graphene. Observation of edge structure of the nano-pores and those electronic states will be reported in the poster.

References

1. Y. Zhang, Y.-W. Tan, H. L. Stormer, P. Kim, *Narture* **438**, 201 (2005)
2. K. S. Novoselov, H. L. Stormer, P. Kim, A. K. Geim et al., *Science* **315**, 1379 (2007)
3. Y.-W. Tan, H. L. Stormer, P. Kim et al., *Phys.Rev.Lett.* **99**, 246803 (2007)
4. H.B. Heersche, P. Jarillo-Herrero, et al., *Nature* **446**, 56 (2007)
5. K. Nakada, M. S. Dresselhaus et al., *Phys. Rev. B* **54**, 17954 (1996)
6. J. P. Small, D. B. Farmer, P. Avouris et al., *Nano Lett.* **9**, 422 (2009)
7. X. Jia, et al., *Science* **323**, 1701 (2009); X. Li, H. Dai et al., *Science* **319**, 1229 (2008)
8. K. S. Novoselov, A. Geim et al,. *Science* **306**, 666 (2004).

Corresponding Author: Junji Haruyama **E-mail: J-haru@ee.aoyama.ac.jp**

Tel&Fax: 042-759-6256 (Fax: 6524)

2P-44

Characterization of Graphene by Scanning Electron Microscopy

○Hidefumi Hiura[1,2], Hisao Miyazaki[2,3] and Kazuhito Tsukagoshi[2,3]

[1]*Nano Electronics Research Laboratories, NEC Corporation, Tsukuba 305-8501, Japan*
[2]*International Center for Materials Nanoarchitectonics (MANA), National Institute for Materials Science (NIMS), Tsukuba 305-0044, Japan*
[3]*CREST, Japan Science and Technology Agency, Kawaguchi, Saitama 332-0012, Japan*

Graphene has attracted broad attention since the electric field effect in graphene was first discovered [1]. Interesting phenomena of graphene in nanoelectronics has been found mostly in monolayer [1-3], bilayer [4,5], trilayer [6] and several layers graphene [7]. Therefore, it is of great importance to identify the number of graphene layers when fabricating the devices well defined with them. There are several ways to count the number of graphene layers, such as optical microscopy [8], atomic force microscopy [9] and Raman microscopy [10]. Among them, the common method is optical microscopy because it is the most reliable and undestructive. Besides the above-mentioned counting measures for graphene, scanning electron microscopy (SEM) is also used, but is only subsidiary to them because no decisive technique to characterize the number of graphene layers using SEM has been definitely established. Here we report the systematic SEM investigation of few layer graphene on a silicon substrate.

We peeled off graphene flakes mechanically from natural graphite and stuck onto a silicon substrate with a thermal SiO_2 surface. We then checked the number and location of graphene flakes using optical microscope as criteria for the following SEM investigations. Our SEM observations revealed that the contrast of graphene flakes to the SiO_2 surface changed gradually depending on the acceleration voltage of the primary electrons, V_{acc}, *e.g.*, the graphene flakes are brighter than SiO_2 when V_{acc} < ~1.5 kV, while they are darker than SiO_2 when V_{acc} > ~2.0 kV. The contrast reversal point around V_{acc} = 1.5 to 2.0 kV was independent on the thickness of SiO_2. As the number of graphene layers increases, the brightness of them always decreases in a proportionate manner, indicating SEM can be potentially used for counting the number of graphene layers. Opposite to the graphene flakes within about 10 layers, a cake of graphite exhibits no such a trend and remains darker than the SiO_2 at any acceleration voltages we used. The extraordinary contrast of SEM images in graphene is reminiscent of that in single-walled carbon nanotubes [11-13]. Based on our SEM observations, the contrast reversal of graphene can be primary explained in terms of a charging effect, whether the primary electron beam makes the SiO_2 surface positively charged at the lower voltage below 1.5 kV or negatively charged at the higher voltages over 2.0 kV.

References: [1] K. S. Novoselov *et al.*, *Science* **306**, 571 (2004). [2] K. S. Novoselov *et al.*, *Nature* **438**, 197 (2005). [3] Y. Zhang eta al., *Nature*, **438**, 201 (2005). [4] H. Miyazaki *et al.*, *to be published.* [5] Y. Zhang *et al.*, *Nature* **459**, 820 (2009). [6] M. F. Craciun *et al.*, Nature Nanotechnology **4**, 383 (2009). [7] H. Miyazaki **et al.**, *Appl. Phys. Express* **1**, 034007 (2008). [8] Z. H. Ni et al., *Nano Lett.* **7**, 2758 (2007). [9] T. W. Ebbesen & H. Hiura., *Adv. Mater.* **7(6)**, 582-586 (1995). [10] A. C. Ferrari *et al.*, *Phys. Rev. Lett.* **97** 187401 (2006). [11] Y. Homma *et al.*, *Appl. Phys. Lett.* **84**, 1750 (2004). [12] R.Y. Zhang *et al.*, *Nanotechnology*, **17**, 272 (2006). [13] Yu. A. Kasumov *et al.*, *Appl. Phys. Lett.*, **89**, 013120 (2006).

Corresponding Author: Hidefumi Hiura
TEL: +81-29-850-1116, FAX: +81-29-856-6139, E-mail: h-hiura@bq.jp.nec.com, HIURA.Hidefumi@nims.go.jp

2P-45

Fabrication of graphene nano-ribbons and observation of those structures and electrical features

○T. Shimizu, J. Haruyama, J. Nakamura, Y. Tanabe, Y. Yamakawa
School of Science and Engineerings, Material Science course, Aoyama Gakuin University, 5-10-1 Fuchinobe, Sagamihara, Kanagawa 229-8558, Japan

Abstract

Graphene is attracting considerable attention with respects both to basic physics and to application to novel nano-devices. A variety of interesting phenomena has been reported; *e.g.*, anomalous quantum Hall effect with half branch ($R_{xy}^{-1} = 4(N+1/2))e^2/h$) [1], residual quantum resistance [2] and Cooper-pair transport [3] at Dirac point, high electronic density of states (EDOS) at zigzag edges [4].

In particular, research of graphene nano-ribbon (GNR), which is one-dimensional strip line of graphene, is highly active. One reason is for band gap engineering of graphene [5], because graphene is basically semi-metal without band gap, while appearance of band gap is predicted in GNR depending on the ribbon width. The other reason is for investigation of electron-spin transport along edge states [4], because current flow along edge can govern charge flow through GNR due to its narrow width. However, formation of GNR and research of electron transport in it are still hard, because even small volume of defects and impurities tends to obstruct the current flow. Moreover, edge structure (chirality) is difficult to control.

In the present study, we fabricated GNR by the following two methods; (1) etching of graphene by lithographic method [5] and (2) longitudinal unzipping of multi-walled carbon nanotubes [6]. After fabrication of GNRs, high temperature annealing was carried out for control of edge chirality [7]. The GNRs fabricated from (1) have width of about 20 – 50 nm. Current level observed in 50 nm-width GNR is below 10^{-6} A order at room temperature, while that in 20nm-width GNR is below 10^{-8} A. As temperature decreases, current decreases and it is difficult to measure clear relationships conductance vs. temperature due to noise at current stage. After improving fabrication process, whether GNR has semiconductive behavior or single electron charging effect will be shown in the poster. The GNR fabricated by (2) exhibit no current. Optimization of process is required. Observation of edge structures will be also shown in the poster.

References

1. Y. Zhang, Y.-W. Tan, H. L. Stormer, P. Kim, *Narture* **438**, 201 (2005)
2. Y.-W. Tan, H. L. Stormer, P. Kim et al., *Phys.Rev.Lett.* **99**, 246803 (2007)
3. H.B. Heersche, P. Jarillo-Herrero et al., *Nature* **446**, 56 (2007)
4. K. Nakada, M. S. Dresselhaus et al., *Phys. Rev. B* **54**, 17954 (1996)
5. M. Y. Han, P. Kim et al., *Phys. Rev. Lett.* **98**, 206805 (2007)
6. D.V.Kosynkin, et al., *Nature* **458**, 7822 (2009)
7. X Jia, M.Dresselhaus et al., *Science* **323**, 1701 (2009)

Corresponding Author: Junji Haruyama **E-mail: J-haru@ee.aoyama.ac.jp**
Tel&Fax: 042-759-6256 (Fax: 6524)

2P-46

Promotion of Polyhedral Graphite Growth in Laser Vaporization by Adding Silicon or Boron

Hajime Chigusa, Iori Nozaki, Akira Koshio, and ○Fumio Kokai

Division of Chemistry for Materials, Graduate School of Engineering, Mie University
1577 Kurimamachiya, Tsu, Mie 514-8507, Japan

Graphitic carbon nanostructures are of great interest in fundamental research and application in various fields. We previously fabricated polyhedral graphite (PG) particles with diameters of 100–1000 nm by CO_2 laser vaporization of graphite at room temperature [1]. To form PG particles with a 90% yield, we require high-pressure (>0.8 MPa) Ar gas to confine laser-vaporized carbon species and maintain their high temperatures. Transmission electron microscopy (TEM) images of the central parts of PG particles showed closed shells (~5 nm in diameter) and concentric frameworks of graphene layers [2, 3]. The PG particles exhibited interesting behavior under high-pressure compression, probably due to a topological difference from bulk graphite [3]. However, for further investigation of other properties and applications of PG particles, such as tribology [4], development of a larger-scale production method is favorable. We report here the coexistence of a small amount of silicon or boron promotes the growth of PG particles.

Laser vaporization of graphite containing Si or B was carried out in the presence of Ar gas in the same way as reported in previous studies [1, 2]. A powder of Si or B_4C was mixed with a graphite powder and was pressed into pellets. The laser beam from a continuous wave Nd:YAG laser was focused on the pellet targets through a quartz window installed in a stainless-steel chamber filled with Ar gas at room temperature. The laser spot size and the power density on the target were adjusted to 2 mm and about 18 kW/cm^2, respectively, and the laser irradiation time was set to 2 s. Products were examined by TEM.

Using graphite containing Si or B atoms (1–5 at.%), we investigated the formation of PG particles in Ar gas (0.1 to 0.4 MPa). Figure 1 shows TEM micrographs of products obtained from pure graphite or graphite containing 1 at.% Si in 0.3-MPa Ar, which reveal the presence of single-wall carbon nanohorn particles, platelet graphite particles, and PG particles. Adding small amount (<2 at. %) of Si or B to graphite was found to enhance the formation of PG particles in Ar, even at low pressures. The reason for the enhanced formation of PG particles is unclear. However, one possibility is that a Si or B atom could bind to a carbon atom and act as a seed to enhance the formation of carbon clusters and/or nanoparticles. As a result, the presence of high-density carbon clusters and/or nanoparticles may result in an efficient PG particle formation in Ar, even at low pressures.

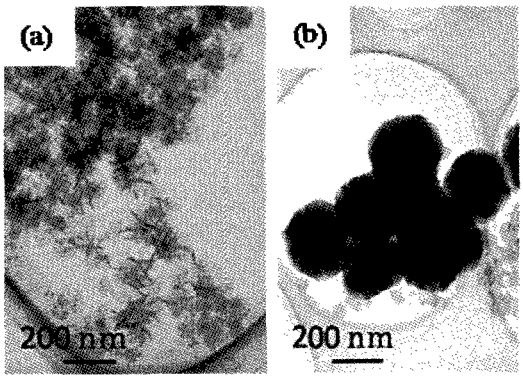

Fig. 1. TEM images of products prepared from (a) pure graphite and (b) graphite containing Si (1 at.%).

[1] F. Kokai *et al.*, Appl. Phys. A **77**, 69 (2003).
[2] F. Kokai *et al.*, Carbon **42**, 2515 (2004).
[3] A. Nakayama *et al.*, Appl. Phys. Lett. **84**, 5112 (2004).
[4] M. Ishihara *et al.*, Carbon **45**, 880 (2007).

Corresponding Author: Fumio Kokai, **E-mail:** kokai@chem.mie-u.ac.jp, **Tel:** +81-59-231-9424.

2P-47

Photo-induced formation of Polyyne-Bromine Complex in Solution

○Yasunori Kai[1], Tatsuhisa Kato[1*], Yoriko Wada[2], and Tomonari Wakabayashi[2*]

[1]*Department of Chemistry, Josai University, Sakado, 350-0295, Japan*
[2]*Department of Chemistry, Kinki University, Higashi-Osaka 577-8502, Japan*

We have reported the formation of Polyyne ($C_{10}H_2$, $C_{12}H_2$)–Iodine (I_2) complexes in solutions [1, 2]. It has been found that the allowed absorption bands of $C_{10}H_2$ or $C_{12}H_2$ diminished with increasing I_2 concentration, while the forbidden bands were enhanced. The stoichiometry of the polyyne-iodine complex was deduced with a titration analysis, and the well-defined structure of the complex was confirmed by a ^{13}C-NMR measurement. Recently we found that the formation of the complex was triggered by the irradiation of a fluorescent lamp.

In this paper we report that the similar photo-induced formation of the complex of $C_{10}H_2$ with bromine (Br_2) was observed in solution, and the system exhibited higher sensitivity to the irradiation of a fluorescent lamp than the iodine system. The difference between the formation processes of iodine and bromine is clarified.

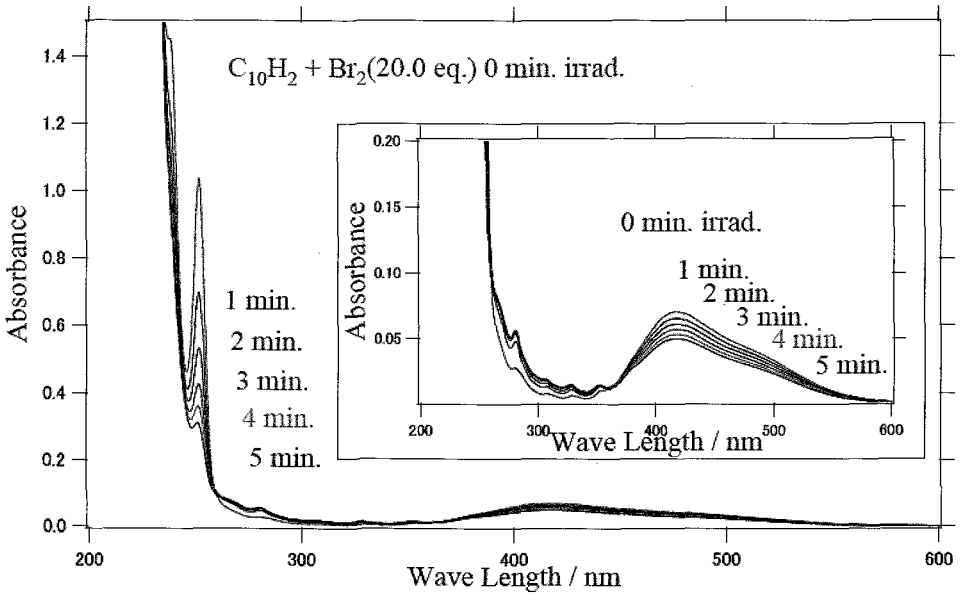

Absorption spectra of $C_{10}H_2$ + Br_2 (1:20 molar eq.) in n-hexane with 0, 1, 2, 3, 4, 5 min. irradiation of fluorescent lamp.

References:

1. Y. Wada et al., The 36th Fullerene Nanotube General Symposium Abstract 1P-31.
2. R. Osada and T. Kato, Abstract of the Oral Presentation for Thesis 2008, p.62.

Corresponding Author: Tatsuhisa Kato
E-mail: rik@josai.ac.jp
Tel. 049-271-7295&Fax 049-271-7985

2P-48

Raman and TEM Studies of Heat-Treated La Fullerene Soot

○Kazunori Yamamoto[1], Shin-ichi Shamoto[1], Takeshi Akasaka[2], Takatsugu Wakahara[3], and Kun'ichi Miyazawa[3],

[1]*Nanomaterials Research Group, Quantum Beam Science Directorate, Japan Atomic Energy Agency, Tokai-mura, Naka-gun, Ibaraki 319-1195, Japan*
[2]*Center for Tsukuba Advanced Research Alliance, University of Tsukuba, Ibaraki 305-8577, Japan*
[3]*Fullerene Engineering Group, Advanced Nano Materials Laboratory, National Institute for Materials Science, 1-1 Namiki, Tsukuba, Ibaraki, 305-0044,Japan*

Although the microstructural properties of so-called "fullerene soot" have been studied for nearly two decades, the general understanding of the structure and properties of the fullerene soot particles is still incomplete. Recently, multi-shell single-digit nanoparticles filled with La have been found in La fullerene arc soot synthesized in lower He atmosphere of 20-50 Torr [1], where most of the single-digit nano-particles contain La. Furthermore, the heat-treated "La fullerene soot" produces carbon nanocapsules. The soot was treated at high temperatures between 1000 and 2200°C in vacuum. In this study the modifications resulting from the heat treatment have been followed by Raman spectroscopy as well as transmission electron microscopy (TEM). The vibrational frequencies of raw (as-arced) and heat-treated La fullerene soot were measured using Raman spectrophotometer (JASCO, NRS-3100) equipped with a microscope. A 100× objective was used to focus the laser beam on the sample surface. TEM observation revealed that the single-digit nanoparticles have been transformed by the treatment into larger multi-shell nanocapsules filled with LaC_2 [1].

In the Raman spectrum of highly oriented pyrolitic graphite (HOPG) only one peak centered at 1580 cm^{-1} can be found (G-band). However, in fullerene soot spectra, this peak is accompanied by another band centered at about 1345 cm^{-1} (D-band). When temperature is increased, the shape of both bands changes. One of two noteworthy features of this group of spectra are the narrowing of both peaks, which is quite similar to the other carbonaceous materials such as carbon black [2]. Another noteworthy features of this group of spectra are the dramatic increase in intensity of the disordered D peak at 1345 cm^{-1} with respect to the higher frequency peak (G-band) after 1850 C^{o} treatment, which is not seen in usual carbonaceous materials. Detailed results of characterization will be presented in the presentation.

[1] K.Yamamoto, et. al., The 34th Fullerene Nanotube General Symposium Abstract 2-14.

[2] T. Gruber, et al., *Carbon*, **32**, 1377(1994).

Corresponding Author: Kazunori Yamamoto

Tel&Fax: +81-29-282-6474 & +81-29-284-3813.

E-mail: yamamoto.kazunori@jaea.go.jp

3P-1

Preparation of [60]Fullerene-Based Interlocked Compounds Using Axle Molecules Including Donor Units

○Chika Sakamoto, Naoki Muroya, Yosuke Nakamura, and Jun Nishimura

Department of Chemistry and Chemical Biology, Graduate School of Engineering, Gunma University, Kiryu, Gunma 376-8515, Japan

Recently, we have developed new synthetic strategies of neutral fullerene-based [2]catenanes and [2]rotaxanes, consisting of a fullerene derivative carrying an aromatic diimide moiety as another electron-acceptor and an electron-donating macrocycle such as a dibenzocrown ether [1]. In the presence of 1,5-dinaphtho-38-crown-10 ether at low temperatures, the *inter*molecular Bingel reactions of [60]fullerene monoadducts bearing a naphthalenetetracarboxylic diimide moiety with [60]fullerene successfully afforded novel [2]rotaxanes, while their *intra*molecular Bingel reactions gave [2]catenanes with D–A–D–A stacking structure. Herein, we have examined the synthesis of [60]fullerene-based [2]rotaxanes **1** by using [60]fullerene derivatives **2** carrying electron-donating moieties, such as 1,5-dialkoxynaphthalene, TTF, or bithiophene, and macrocycles **4**–**6** bearing electron-deficient aromatic diimide moieties (Scheme 1).

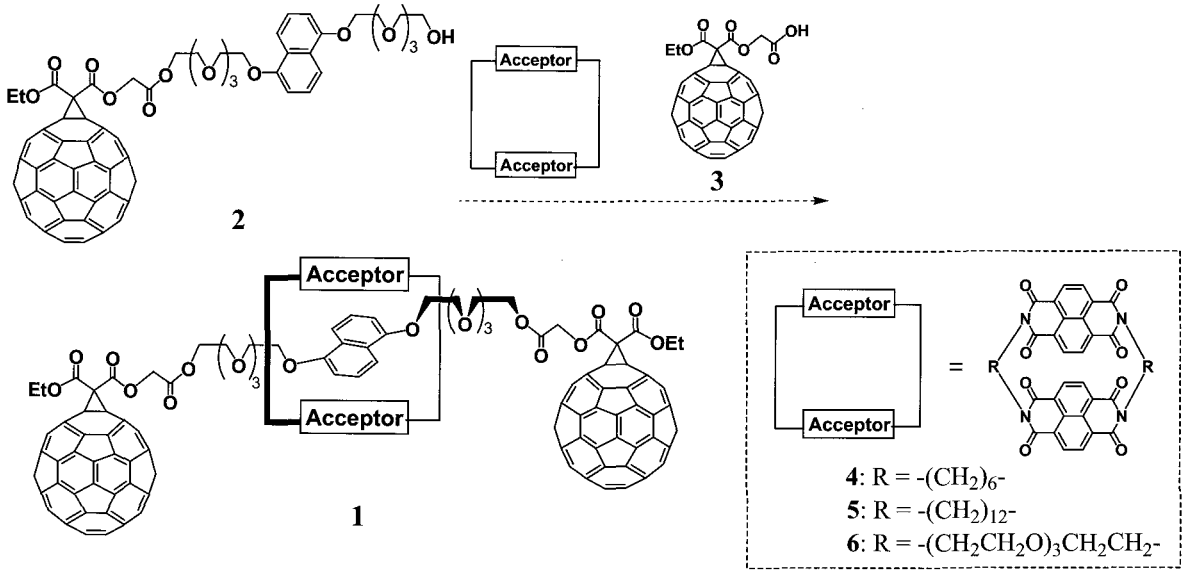

Scheme 1

Prior to the synthesis of **1**, the pseudorotaxane formation between **2** and **4**–**6** was investigated by ^{1}H NMR spectroscopy. The ^{1}H NMR spectra of a mixture of **2** and **4** in $CDCl_3$ showed remarkable broadening and peak shifts, suggesting the pseudorotaxane formation, while only negligible spectral change was observed in cases of using **5** and **6**. The reaction of **2** with **3** in the presence of **4** is now being investigated.

[1] Y. Nakamura, S. Minami, K. Iizuka, and J. Nishimura, *Angew. Chem., Int. Ed.*, **42**, 3158–3162 (2003).

Corresponding Author: Yosuke Nakamura
Tel: +81-277-30-1310, Fax: +81-277-30-1314, E-mail: nakamura@chem-bio.gunma-u.ac.jp

3P-2

Synthesis and Photophysical Properties of Oligocarbazole-[60]Fullerene Adducts Bearing Various Spacer Units

○Kounosuke Kobayashi, Keisuke Kinoshita, Yosuke Nakamura, and Jun Nishimura

Department of Chemistry and Chemical Biology, Graduate School of Engineering, Gunma University, Kiryu, Gunma 376-8515, Japan

[60]Fullerene–donor dyads linked by covalent bondings have attracted much interest from the aspects of charge-separated states arising from the intramolecular photoinduced electron transfer. Recently, we have successfully prepared [60]fullerene adduct **1** bearing two carbazole trimer residues by using Bingel reaction [1]. For **1**, charge-separation takes place via the excited singlet state of the C_{60} moiety in polar solvents and the lifetime of the radical ion-pairs (τ_{RIP}) is ca. 300 ns, as revealed by the combination of the C_{60}-fluorescence quenching and transient absorptions of the radical ion pair. Herein, in order to clarify the effects of the spacer units between the donor and C_{60} moieties on τ_{RIP} and enhance τ_{RIP}, oligocarbazole-[60]fullerene adducts **2**–**5** bearing various spacer units were prepared and their photophysical properties were investigated.

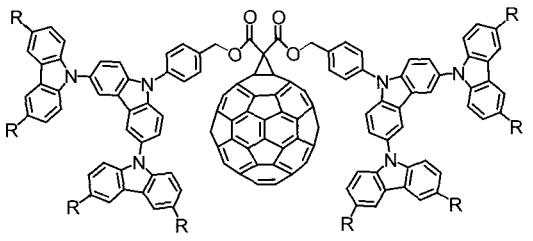

1: R = *t*-Bu

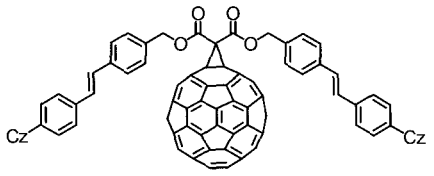

2

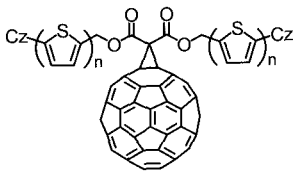

4a: n = 1
4b: n = 2

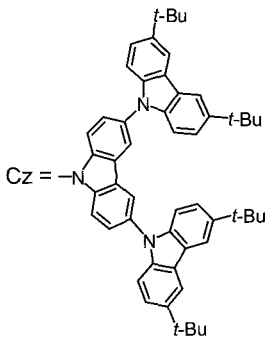

Cz = –N

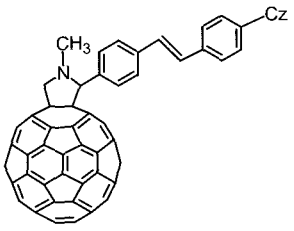

3

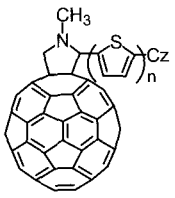

5a: n = 1
5b: n = 2

Adducts **2**, **4a**, and **4b** were prepared by Bingel reaction using the corresponding malonates, while **3**, **5a**, and **5b** by Prato reaction using the corresponding aldehydes. In all of **2**–**5**, the fluorescence of C_{60} moiety was extremely quenched in polar solvents, suggesting the intramolecular photoinduced electron transfer via the excited singlet state of the C_{60}.

[1] T. Konno, M. E. El-Khouly, Y. Nakamura, K. Kinoshita, Y. Araki, O. Ito, T. Yoshihara, S. Tobita, and J. Nishimura, *J. Phys. Chem. C*, **112**, 1244–1249 (2008).

Corresponding Author: Yosuke Nakamura
Tel: +81-277-30-1310, Fax: +81-277-30-1314, E-mail: nakamura@chem-bio.gunma-u.ac.jp

3P-3

Synthesis and Liquid Crystallinity of Fullerodendron Having Cyanobiphenyl Groups at the Terminals

○Yutaka Takaguchi, Yuuki Sako, Tomoyuki Tajima

Graduate School of Environmental Science, Okayama University, Okayama 700-8530, Japan

C_{60} derivatives showing liquid-crystallinity have attracted a lot of attention because of promising applications for electronic devices. In particular, several reports have described that dendritic substituent is effective to construct the liquid-crystalline fullerene derivatives. However, there is no report on the fullerene derivatives showing smectic B phase, of which C_{60} moieties aligned with hexagonal 2D-sheet. During our studies on self-organization of fullerodendrons,[1-3] we found that fullerodendron having cyanobiphenyl terminals self-organized to form thermotropic liquid crystal.[4] To our knowledge, this is the first example of liquid-crystalline C_{60} derivatives showing smectic B phase.

Liquid-crystalline fullerodendron (**1**) having cyanobiphenyl terminals was synthesized via Diels-Alder reaction of corresponding anthryl dendron (**2**) and C_{60}. The liquid-crystalline properties of the fullerodendron was investigated by polarized optical microscopy, differential scanning calorimetry, and X-ray diffraction. Interestingly, the fullerodendron give rise to thermotropic smectic B phase, in which the hexagonal packing arrangement of C_{60} moiety is observed (Figure 1).

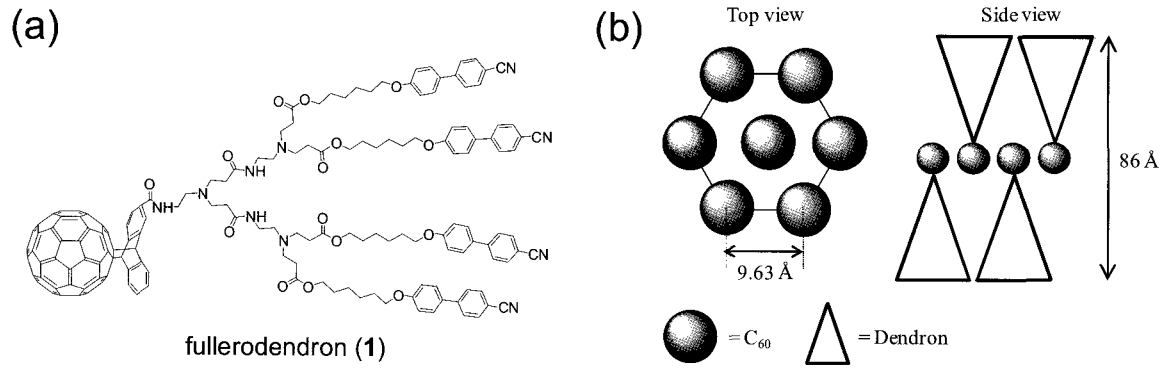

Figure 1. (a) Molecular structure of fullerodendron (**1**). (b) An assumed mesophase structure of the smectic B phase for fullerodendron (**1**).

[1] C. Hirano, T. Imae, S. Fujima, Y. Yanagimoto and Y. Takaguchi, *Langmuir*, **2005**, 21, 272.

[2] H. Kusai, T. Nagano, K. Imai, Y. Kubozono, Y. Sako, Y. Takaguchi, N. Akima, Y. Iwasa, and S. Hino, *Appl. Phys. Lett.*, **2006**, 88, 173509.

[3] N. Kawasaki, T. Nagano, Y. Kubozono, Y. Sako, Y. Morimoto, Y. Takaguchi, A. Fujiwara, C.-C. Chu, and T. Imae, *Appl. Phys. Lett.*, **2007**, 91, 243515.

[4] Y. Sako, Y. Takaguchi, M. Ichihara, K. Ohta, *Sen'i Gakkaishi*, **2008**, 64, 324.

Corresponding Author: Yutaka Takaguchi

TEL: +81-86-251-8903, FAX: +81-86-251-8903, E-mail: yutaka@cc.okayama-u.ac.jp

3P-4

The Diels-Alder Reaction of C_{60} and Dienes in Mesoporous Silica as a Reaction Medium

Satoshi Minakata ○Toshiki Nagamachi and Kazuhisa Nakayama

Department of Applied Chemistry, Graduate School of Engineering, Osaka University, Suita, Osaka 565-0871, Japan

The development of a basic and facile method for the functionalization of C_{60} remains an important challenge because of recent demands for carbon nanomaterials. A convenient chemical modification is significantly hampered by the poor solubility of C_{60} in commonly used organic solvents. As one potential strategy for overcoming this problem, a potential process was devised based on the concept of a solid solvent.

We recently reported on an efficient and convenient method for the inclusion of C_{60} in a mesoporous silica, MCM-41, by a solvophobic process [1].

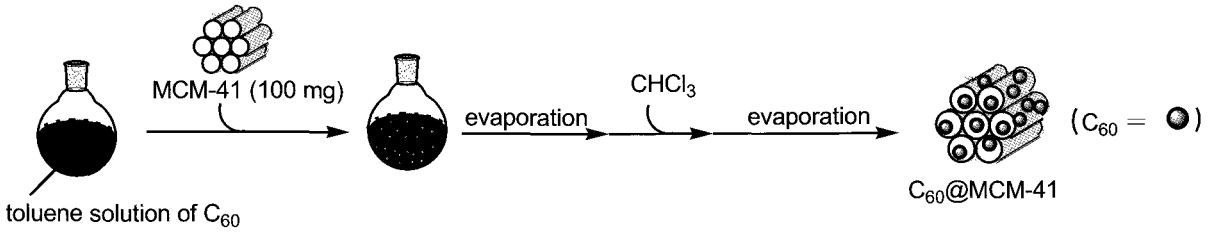

Since the inorganic porous material enables C_{60} to disperse at the molecular level, the mesoporous silica can be regarded as a potential solvent for reactions of C_{60}. We report herein on a novel and unique chemical modification of C_{60} in silica gel solvent, namely, a Diels-Alder reaction between C_{60} and a diene. The Diels-Alder reaction of C_{60} and cyclopentadiene in *n*-hexane for 6 hours at 35 °C did not proceed at all because of the insolubility of C_{60} in *n*-hexane. The same reaction in toluene, in which both C_{60} and cyclopentadiene are soluble, gave the monoadduct in 34% yield (36% selectivity).

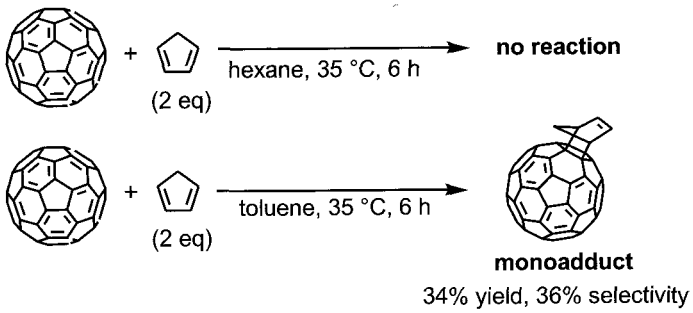

Using the strategy described here, when cyclopentadiene was added to a suspension of C_{60}@MCM-41 in *n*-hexane, the desired adduct was obtained in good yield and selectivity compared with the homogeneous reaction in toluene.

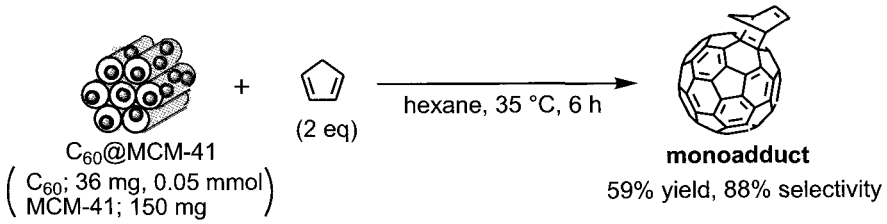

[1] Minakata, S.; Tsuruoka, R.; Komatsu, M. *J. Am. Chem. Soc.* **2008**, *130*, 1536-1537.

Corresponding Author: Satoshi Minakata
TEL: +81-6-6879-7403, FAX: +81-6-6879-7402, E-mail: minakata@chem.eng.osaka-u.ac.jp

3P-5

Synthesis and Thermally Morphological Control of 1,4-Bis(silylmethyl)[60]fullerene Derivatives

○Keiko Matsuo[1], Yutaka Matsuo[1,2], and Eiichi Nakamura[1,2]

[1]*Department of Chemistry, The University of Tokyo, Hongo, Bunkyo-ku, Tokyo 113-0033, Japan*

[2]*Nakamura Functional Carbon Cluster Project, ERATO, Japan Science and Technology Agency, Hongo, Bunkyo-ku, Tokyo 113-0033, Japan*

Rational design of functional molecules and construction of ordered structures in solid states are central issue in the researches of organic electronic devices. The 58π-electron [60]fullerene 1,2-adducts such as PCBMs ([6,6]-Phenyl C61 butyric acid methyl esters) are widely used as acceptor materials in organic photovoltaic (OPV) cells. However, fullerene derivatives that are synthesized in good yield and show higher OPV performances than PCBMs are strongly desired in this research area.

We have recently reported the efficient synthesis and design of 58π-electron 1,4-bis(silylmethyl)[60]fulleren es, SIMEFs (Figure 1a), which have allowed us to control electrochemical and thermal properties. In this work, we discuss thermal morphology change from amorphous to crystalline state (Figure 1b) of SIMEFs (Figure 1c). Honeycomb-like arrangement and columnar array of the fullerene part (Figure 1b) play a key role for high performance in OPV devices using SIMEF and donor porphyrin derivatives.

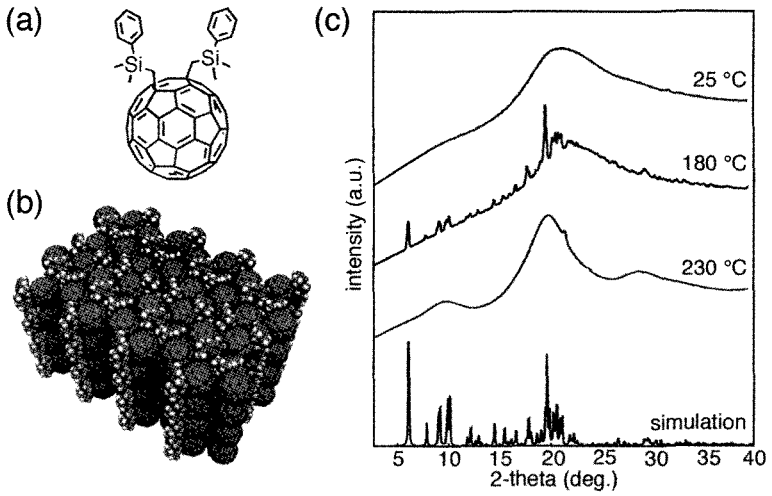

Figure 1. Structure and thermal property of SIMEF. (a) Molecular structure. (b) Crystal packing structure. (c) XRD patterns of SIMEF at different temperatures and a simulated powder XRD pattern obtained from the single crystal X-ray crystallography data of SIMEF (bottom).

Reference:

Y. Matsuo, A. Iwashita, Y. Abe, C.-Z. Li, K. Matsuo, M. Hashiguchi, E. Nakamura, *J. Am. Chem. Soc.* **130**, 15429 (2008).

Corresponding Authors: Yutaka Matsuo and Eiichi Nakamura

Tel/Fax: +81-3-5841-1476; E-mail: matsuo@chem.s.u-tokyo.ac.jp; nakamura@chem.s.u-tokyo.ac.jp

3P-6

Synthesis and Properties of Novel Open-Cage C_{60} Derivatives

○Kei Kurotobi, Michihisa Murata, Yasujiro Murata

Institute for Chemical Research, Kyoto University, Uji Kyoto 611-0011, Japan

Recently, studies on functionalization of fullerenes have attracted much attention. Especially, that of open-cage fullerene derivatives[1] by transformation of fullerene skeleton is very interesting for the synthesis of endohedral fullerenes and heterofullerenes. Herein, we report the synthesis of novel open-cage fullerene derivatives by functionalization at the rim of an orifice. Thermal reaction of C_{60} with 3,6-bis(4-octylphenyl)pyridazine gave **1**, whose orifice was enlarged to afford diketone **2**. The reaction of **2** with $P(OEt)_3$ in toluene proceeded at room temperature to give epoxide **3** as relatively unstable solid. Then, diol **4** was obtained by the reaction of **3** with AcONa/CuCl in THF at room temperature followed by hydrolysis. Transformation to new open-cage fullerene **5** which has C_s-symmetry was accomplished by oxidative ring-opening reaction of **4** with $PhI(OAc)_2/I_2$ under irradiation with visible light. UV-Vis spectrum of **5** showed maximum absorptions at 330 (sh), 400 (sh), 450 (sh) and 730 nm extended to ca. 900 nm. This is assumed to be due to expansion of the π-conjugated system of the C_{60} cage. The redox properties were investigated by cyclic voltammetry in benzonitrile. The first reduction wave was observed in much less negative potential by 0.3 V from that of C_{60}, indicating the lower-lying LUMO level. Furthermore, an irreversible oxidation wave was detected at 1.0 V, which was less positive than that of C_{60}.

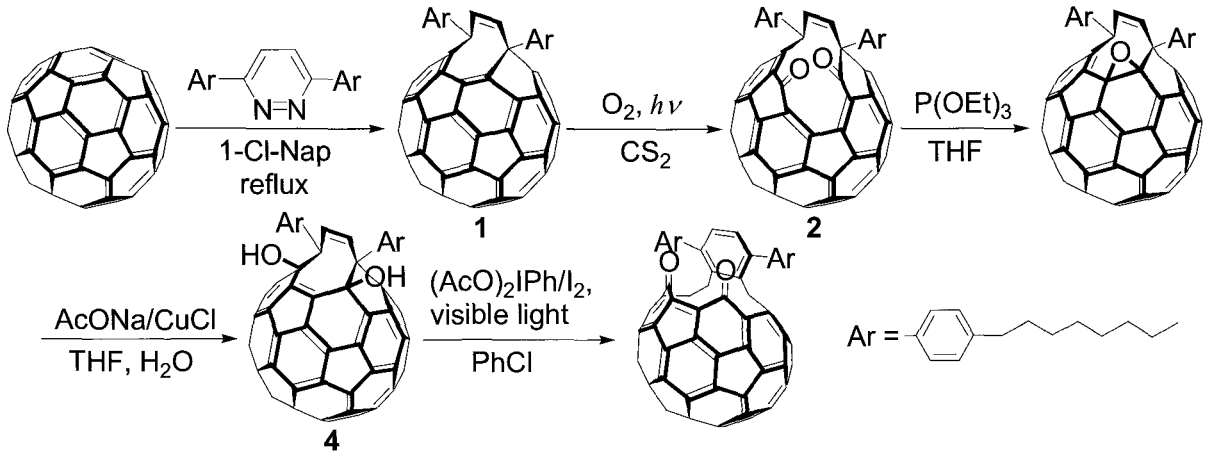

[1] For example, (a) Hummelen, J. C.; Prato, M.; Wudl, F. *J. Am. Chem. Soc.* **1995**, *117*, 7003. (b) Schick, G.; Jarrosson, T.; Rubin, Y. *Angew. Chem. Int. Ed.* **1999**, *38*, 2360. (c) Murata, Y.; Murata, M.; Komatsu, K. *Chem. Eur. J.* **2003**, *9*, 1600. (d) Iwamatsu, S.; Uozaki, T.; Kobayashi, K.; Re, S.; Nagase, S.; Murata, S. *J. Am. Chem. Soc.* **2004**, *126*, 2668. (e) Xiao, Z.; Yao, J.; Yang, D.; Wang, F.; Huang, S.; Gan, L.; Jia, Z.; Jiang, Z.; Yang, X.; Zheng, B.; Yuan, G.; Zhang, S.; Wang, Z. *J. Am. Chem. Soc.* **2007**, *129*, 16149.

Corresponding Author: Yasujiro Murata

TEL: +81-774-38-3172, FAX: +81-774-38-3178, E-mail: yasujiro@scl.kyoto-u.ac.jp

3P-7

Construction of Ordered Fullerene Arrays by Supramolecular Fullerene-Perfluorobenzene interaction

○ Chang-Zhi Li[1], Yutaka Matsuo[1,2], Eiichi Nakamura[1,2]

[1]*Nakamura Functional Carbon Cluster Project, ERATO, Japan Science and Technology Agency (JST), Hongo, Bunkyo-ku, Tokyo 113-0033, Japan*
[2]*Department of Chemistry, The University of Tokyo, Hongo, Bunkyo-ku, Tokyo 113-0033, Japan*

Generally, charge transportation in organic materials occurs via the hopping mechanism, which depends on the degree of orbital overlap between the molecules. Charges are preferentially transported along the π–π stacking direction in organic semiconductors. [1] Inspired by stable benzene (C_6H_6)/perfluorobenzene (C_6F_6) dimerization [2], we report herein the efficient construction of ordered fullerene arrays through the interaction of C_{60} and pentafulorobenzene (C_6F_5), by means of thermal-induced phase transition from glass to crystalline phase.

In solution, the aggregation of compound **1** was varied from monomers to aggregators (diameter of 190 nm) by addition of C_6F_6 or not. Accordingly, the precipitated samples were found to have a thermal-induced phase transition from glass to crystalline phase, which have been characterized by single crystal analysis, variable temperature X-ray diffraction (VT-XRD) and differential scanning calorimetry (DSC). Furthermore, through introducing third addend to C_{60} core, the LUMO level of adducts varied from −3.80 eV (**1**) to −3.70 eV (**2b**), and −3.67 eV (**2a**). Together with thermal-induced ordered morphology in solid phase and tunable energy level of adducts, studies toward organic photovoltaic (OPV) cell [3] will be conducted with the use of these samples as n-type semiconductor materials.

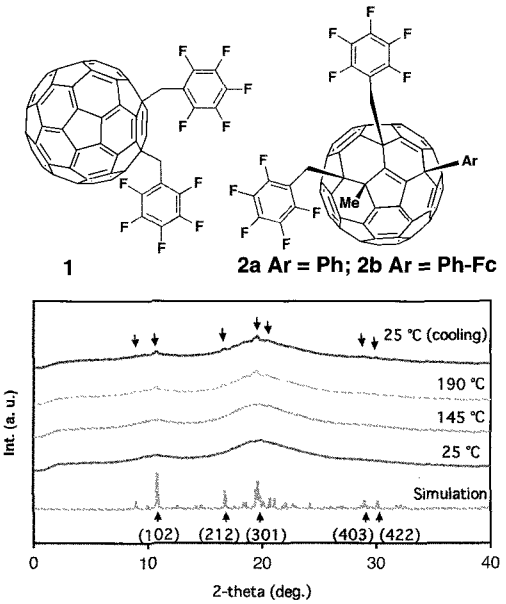

Fig. 1. Chemical structures of 1 and 2 (top). And VT-XRD studies of thermal-induced crystallization of **1** (bottom).

[1] Liu, S. H.; Wang, W. M.; Briseno, A. L.; Mannsfeld, S. C. B.; Bao, Z. N. *Adv. Mater.* **2009**, *21*, 1217.
[2] Wheeler, S. E.; Houk, K. N. *J. Am. Chem. Soc.* **2008**, *130*, 10854.
[3] Niinomi, T.; Matsuo, Y.; Sato, Y.; Nakamura, E. *J. Mater. Chem.* in press.

Corresponding Authors: Yutaka Matsuo and Eiichi Nakamura
TEL/FAX: +81-3-5841-1477 E-mail: matsuo@chem.s.u-tokyo.ac.jp; nakamura@chem.s.u-tokyo.ac.jp

3P-8

Highly Regioselective Adiridination of C_{60} with Sulfilimines

○Midori O. Ishitsuka[1], Mitsunori Okada[1], Tsukasa Nakahodo[2], Hidefumi Nikawa[1], Takahiro Tsuchiya[1], Takeshi Akasaka[1], Tetsuo Fujie[3], Toshiaki Yoshimura[3], Zdenek Slanina[1] and Shigeru Nagase[4]

[1]*Center for Tsukuba Advanced Research Alliance, University of Tsukuba, Tsukuba, Ibaraki 305-8577, Japan*
[2]*Department of Applied Chemistry, Kinki University, Higashi-Osaka, Osaka 577-8502, Japan*
[3]*Department of Applied Chemistry, Graduate School of Science and Engineering, University of Toyama, Gofuku, Toyama 930-8555, Japan*
[4]*Institute for Molecular Science, Okazaki, Aichi 444-8585, Japan*

In the course of our study on the development of synthetic methodology for the aziridination of fullerenes, we have recently reported the photochemical [2+1]cycloaddition reaction of the nitrene onto C_{60} which are generated from the sulfilimine.[1] Meanwhile, it is well known that the sulfilimines with electron-donating group on N atom undergo the Michael-type reactions, which are followed by concomitant elimination of sulfide to afford the corresponding aziridines. In these reactions, sulfilimines act as a nucleophile to the electrophilic olefins. Since C_{60} has a characteristic feature of its low LUMO level and electron-accepting property, it can be an electrophilic olefin. In this context, sulfilimines may react with C_{60} to afford the corresponding aziridinofullerenes.

We have studied the thermal reaction of S,S-diphenylsulfilimines (**1-3**) with C_{60} and succeeded in the regioselective syntheses of multi-substituted aziridinofullerenes. Among these, the structure of $C_{60}(NCH_3)_2$ was successfully determined by the single-crystal X-ray analysis.

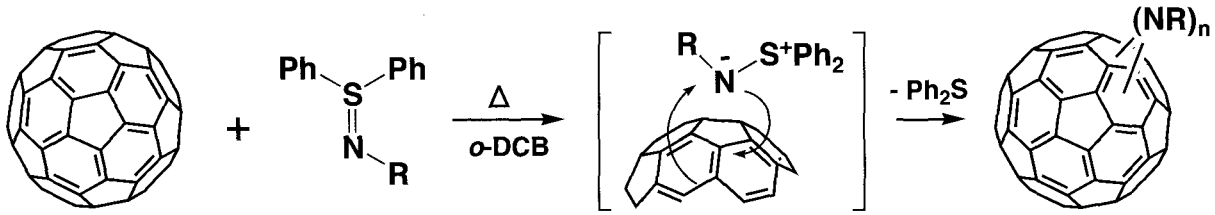

1: R = H
2: R = Me
3: R = Ph

[1] T. Nakahodo, M. Okada, H. Morita, T. Yoshimura, M. O. Ishitsuka, T. Tsuchiya, Y. Maeda, H. Fujihara, T. Akasaka, X. Gao, S. Nagase, *Angew. Chem. Int. Ed.* **47**, 1298-1300 (2008).

Corresponding Author: Midori O. Ishitsuka
TEL & FAX: +81-29-853-7289, E-mail: moinuma@tara.tsukuba.ac.jp

3P-9

Behavior of the photocurrent on Mg-doped C_{60} films

C. Morales, N. Kojima, M. Natori, S. Nishi and M. Yamaguchi

Toyota Technological Institute, 2-12-1 Hisakata Tenpaku, Nagoya 468-8511, Japan

Research on conjugated organic systems is a field that expands rapidly in chemistry, condensed matter physics, material science and device physics due to the promising opportunities for applications of these π -electron semiconductors in electronics and photonics. Due to their interdisciplinarity, this class of materials attracted the attention of a large number of researchers and originated the beginning of a revolution in "Organic Electronics". Fullerenes, such as C_{60} and C_{70}, are known to show photoconductive properties because of their unusual structure and extended π-electron system [1]. So far several papers have reported that the conductivity of C_{60} molecules can be increased by doping with different atoms. In this respect, Mg is one of the promising materials for guest metal showing semiconductor properties [2, 3].

For this work, thin-film samples were deposited on mica substrates by molecular beam epitaxy, the growth temperature was of 165°C. The resulted film composition of Mg/C_{60} was confirmed by X-ray photoelectron spectroscopy. The epitaxial growth was confirmed by XRD measurement. Photocurrent measurements were performed in vacuum to avoid the oxidation. Figure 1 is presented the photocurrent spectrum of Mg-doped C_{60} and un-doped C_{60} films where it is can observe the presence of a new peak at wavelengths of $900 < \lambda < 1200$ nm. The detailed analysis of the new peak will be discussed at the conference.

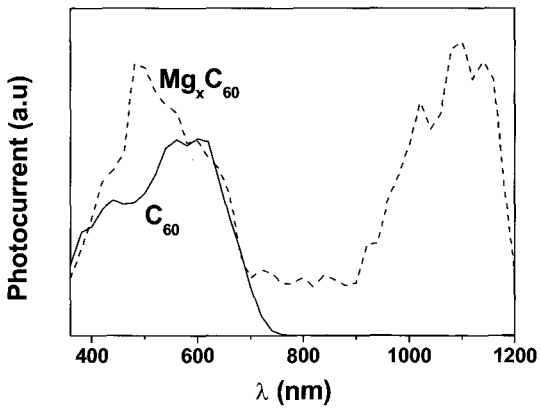

Figure 1. Photocurrent spectrum of Mg-doped C_{60} and un-doped C_{60}.

REFERENCES

[1] H.W. Kroto, J.R. Heath, S.C. O'Brien, R.F. Curl, R.E. Smalley, *Nature* 318 (1985) 162.

[2] R. P. Gupta and M. Gupta *Physica* C 219 (1994) 21.

[3] M. Chikamatsu, T. Taima, Y. Yoshida, K. Saito and K. Yase, *Appl. Phys. Lett.* 84 (2004) 127.

Corresponding Author: C. Morales

TEL: (052) 809-1877, FAX: (052) 809-1879, E-mail: crisomr@toyota-ti.ac.jp

3P-10

C_{60} Crystal Growth Directly between Electrodes from Solution

○Nobuyuki Iwata, Kohei Kurihara, Yasunari Iio, and Hiroshi Yamamoto

Department of Electronics & Computer Science, College of Science & Technology, Nihon University, 7-24-1 Narashinodai, Funabashi-shi, Chiba, 274-8501 Japan

The C_{60} crystals are promising candidate for cannel of organic field effect transistor (FET). For example, an ambipolar operation of C_{60} film is demonstrated between the gold electrodes with modified work function by self-assembled monolayer[1]. The measured mobility of C_{60} evaporated film is 1.4 $cm^2/(Vs)$ with the top-gate type fabricated in-situ[2]. However as well known, the FET performance degrades rapidly in air. Therefore it seems difficult to apply C_{60} film to FET devices. By the way, C_{60} nano-whisker (C_{60}-NW) is able to be grown by the liquid liquid interfacial precipitation (LLIP) method, and C_{60} needle is grown by simply evaporating the solvent from C_{60} solution[3-5]. Furthermore the C_{60}-NW includes solvent in its crystal, and the crystal is polymerized from the results of X-ray diffraction and Raman spectra[6]. Focusing on the application, the solution including the C_{60}-NW grown by LLIP is dropped between electrodes and then measured, which is very far from the realization of C_{60} FET devices[7]. We propose a simple C_{60}-NW growth technique directly between electrodes from solution. Such the grown crystal, which includes solvent and is polymerized, is expected to be prevented from oxidization and degradation of performance for FET until the FET structure is fabricated. The C_{60}-NW also has the advantage toward nano-scale devices.

The electrodes were deposited on the substrate of SiO_2/Si cleaned in acetone and ethanol. The electrodes deposited substrate was soaked and drawn up with speed of 1 or 100 μm/s. Electrodes deposited were Au in figure 1(a) and Cu in figure 1(b). Needle-like C_{60} crystal grew between electrodes, but the crystal did not bridge over the electrodes. The crystal was composed of C_{60} molecules, confirmed by Raman spectrum. It is expected that the crystal structure, crystallinity, shape, and growth direction *etc.* are expected to depend on solvent, dipping speed, and solution temperature, electrode's shape, difference in surface tension between solvent and the substrate surface (wettability).

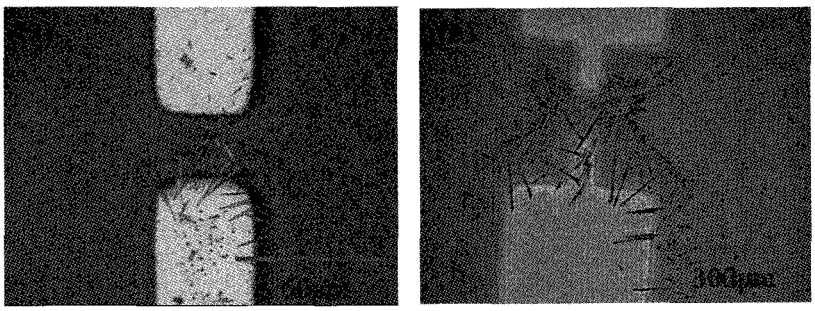

Figure 1 : (a) C_{60} needles between Au electrodes dipped with 100 μm/s. (b) C_{60} needles between Cu electrodes dipped with 1 μm/s.

[1] T. Nishikawa et al., J.Appl.Phys. 97 (2005) 104509.
[2] J. Yamaguchi et al., Jpn. J. Appl. Phys. 44 (2005) 3757.
[3] K. Miyazawa et al., J. Mater. Res. 17 (2002) 83.
[4] R. Ceolin et al., Chem. Phys. Lett. 314 (1999) 21.
[5] L. Wang et al., Adv. Mater 18 (2006) 1883.
[6] J. Minato et al., Carbon 43 (2005) 2837.
[7] K. Ogawa et al., Appl. Phys. Lett. 88 (2006) 112109.
iwata@ecs.cst.nihon-u.ac.jp

3P-11

Extraction Selectivity of Fullerenes: Dependence on Solvents

○Takashi Inoue, Rie Tao, Yuji Takimoto

Toyo Tanso Technology Center, Toyo Tanso Co., Ltd., 2181-2 Nakahime, Ohnohara-cho, Kanonji, Kagawa 769-1612 Japan

Investigation of extraction and solubility behavior of fullerenes is important for industrial separation of them. For example, metal endohedral fullerene Ce@C_{82} was effectively extracted against empty fullerenes by using a polar solvent *N*, *N*-dimethylformamide (DMF) [1]. The extraction by using DMF is generally favorable for the separation of Ce@C_{82} in comparison with non-polar solvents such a as xylene.

In this study, we have investigated the extraction selectivity of fullerenes using HPLC with a multi-wavelength detector and a Buckyprep column. Fig. 1 shows contour maps of absorption wavelength against retention time. A fullerene eluted around 25min in Fig. 1(b) exhibits a characteristic absorption at 600 nm. The fullerene was assigned to C_{80}(II) [2] which was the most ellipsoidal fullerene so far isolated (Fig. 2). C_{80}(II) was not observed in xylene extracts (Fig. 1(a)). Consequently, C_{80} (II) was selectively extracted by DMF. We will present the selective extraction of other fullerenes.

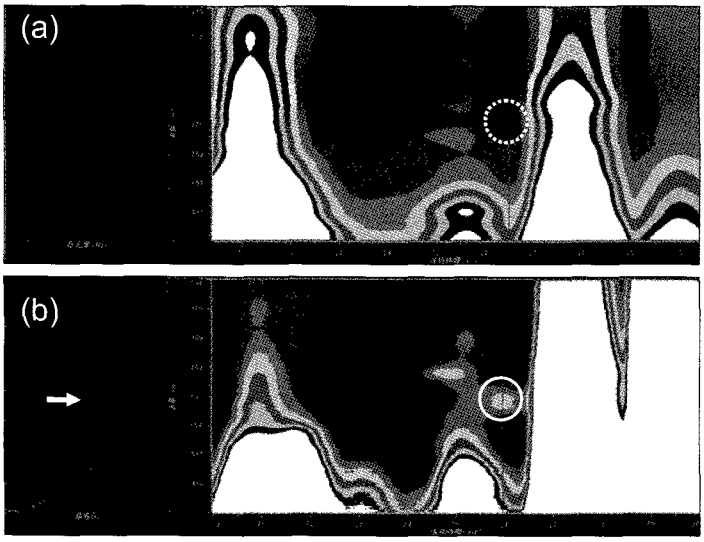

Fig. 1 Contour maps of absorption wavelength against retention time around C_{86} fraction obtained by multi-wavelength detector. (a) Xylene extracts (b) DMF extracts.

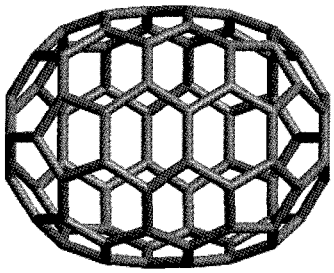

Fig. 2 Molecular structure of ellipsoidal C_{80}(II) with D_{5d} symmetry.

References: [1] J. Ding and S. Yang, *Chem. Mater.*, **1996**, *8* 2824-2827.
[2] C.-R. Wang, T. Sugai, T. Kai, T. Tomiyama and H. Shinohara, *Chem. Commun.*, **2000**, 557-558.

Corresponding Author: Takashi Inoue
E-mail: t_inoue@toyotanso.co.jp
Tel: +81-875-54-2627, **Fax:** +81-875-54-4442

3P-12

Application of Metal Endohedral Fullerenes for High Power Conversion Efficiency in Bulk-heterojunction Solar Cells

○Morihiko Saida[1], Haruna Oizumi[1], Hiroyuki Sagami[1], Yuzo Mizobuchi[1], Kenji Omote[1], Yasuhiko Kasama[1], Kuniyoshi Yokoo[1], Shoichi Ono[1], Shigehiko Yamamoto[1,2], Takayuki Kuwabara[3] and Kohshin Takahashi[3]

[1]*Ideal Star Inc., Sendai 989-3204, Japan*
[2]*National Institute of Advanced Industrial Science and Technology (AIST), Tsukuba 305-8562, Japan*
[3]*Graduate School of Natural Science and Technology, Kanazawa University, Kanazawa 920-1192, Japan*

Bulk-heterojunction (BHJ) organic solar cells based on the composite of an electron-donating conjugated polymer and an electron-accepting fullerene are focused to be developed in the potential applications as low-cost, printable and flexible electric sources. The BHJ has been expected to have higher power conversion efficiency (PCE) than that of bilayer solar cells thanks to efficient optical absorption and exciton dissociation at the donor-acceptor interface. Up to now, the BHJ solar cells with regio-regular poly(3-hexylthiophene) (P3HT) as the electron donor and [6 6]-phenyl C61-butyric acid methyl ester (PCBM) as the acceptor have achieved the PCE around 5 % [1].

We have constructed the BHJ solar cells on ITO substrates with TiOx and PEDOT:PSS as hole and electron blocking layers, respectively. This is a so-called "inverted-type solar cell" which is robust against air permeation and non-corrosive, resulting in a longer life time [2]. Figure 1 shows the *I-V* characteristics of the inverted-type solar cell under the light irradiation of metal halide lump with the power of 150 mW/cm^2. The PCE is about 3 % and is stable for over 500 hours.

One of the approaches to improve the PCE further is the application of an acceptor with a shallow LUMO energy level to enhance the open circuit voltage (Voc). We have synthesized endohedral Li-fullerene by plasma shower method [3] to apply in the BHJ solar cell as the acceptor material. It is expected that Li@C_{60} has a shallow LUMO energy level. The improvement of Voc in the BHJ solar cell has recently been reported by applying Lu_3N@C_{80}-PCBH [4].

We will present a recent progress in development of the BHJ solar cells and Li@C_{60} synthesis.

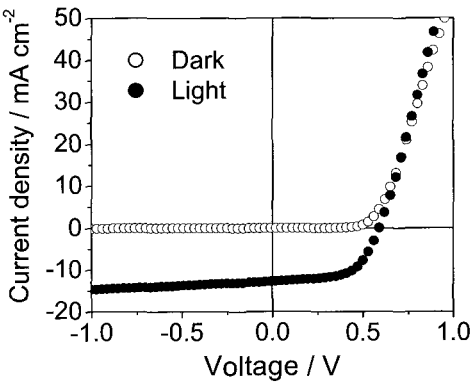

Fig. 1. *I-V* curves of inverted-type solar cell under light irradiation of metal halide lump with the power of 150 mW/cm^2 and in the dark.

[1] M. R. Reyes, K. Kim and D. L. Carroll, Appl. Phys. Lett. **87**, 083506 (2005).
[2] T. Kuwabara, T. Nakayama, K. Uozumi, T. Yamaguchi and K. Takahashi, Sol. Energy Mater. Sol. Cells **92**, 1476 (2008).
[3] Y. Kasama, K. Omote, H. Okada and K. Yokoo, *NDNC 2007 abstract book, 119* (2007).
[4] R.B.Ross, C. M. Cardona, D. M. Guldi, S. G. Sankaranarayanan, M. O. Reese, N. Kopidakis, J. Peet, B. Walker, G. C. Bazan, E. V. Keuren, B. C. Holloway and M. Drees, Nat. Mater. **8**, 208 (2009).
Corresponding Author : Morihiko Saida
TEL&FAX : +81-22-303-7336, +81-22-303-7339, E-mail : morihiko.saida@idealstar-net.com

3P-13

Rotational Sub-levels of Ortho-Hydrogen Molecule Encapsulated in Isotropic C_{60} Fullerene Cages

Katsumi Tanigaki,*[1] Yoshimitsu Kohama,*[2] Takeshi Rachi,[1] Ju Jing,[1] Zhaofei Li,[1] Jun Tang,[1] Ryotaro Kumashiro,[1] Satoru Izumisawa,[2] Hitoshi Kawaji,[2] Tooru Atake,[2] Hiroshi Sawa,[3] Yasujiro Murata,[4] and Koichi Komatsu[5]

[1]Department of Physics, Tohoku University, 6-3 Aoba Aramaki Aoba-ku, Sendai, 980-8578, Japan.,[1]Materials and Structures Laboratory, [2]Tokyo Institute of Technology, 4259 Nagatsuta-cho, Midori-ku, Yokohama, 226-8503 Japan. [3]Department of Applied Physics, Nagoya University, Furyo-cho, Chidane-ku, Nagoya, 464-8603, Japan.,[4]Institute for Chemical Research, Kyoto University, Uji, Kyoto 611-0011, Japan, [5]Fukui University of Technology, Gakuen, Fukui 910-8505, Japan.

Molecular hydrogen (H_2), the simplest system among all molecules, has been studied extensively to date, and its electronic spectra have been fundamental in establishing the fundamentals of quantum mechanics. An H_2 molecule is not expected to be completely localized at lattice sites even in the solid state at 0 K due to its large zero point motion. H_2 retains translational freedom as a translational quantum solid. The rotational motion of the H_2 molecule also persists and thus an H_2 crystal is also an orientational quantum solid. The unique free-rotor description is a result of the nuclear spin isomers denoted by para-H_2 $J = 0, 2, 4$ and ortho-H_2; $J = 1, 3, 5\ldots$, where J is the rotational quantum number. Fullerene encapsulated H_2 molecules ($H_2@C_{60}$) have been only recently macroscopically synthesized by organic reactions known as the "molecular surgery method", [1] and offer an unprecedented opportunity to studying the rotational and translational states of the H_2 molecule. In this talk, we discuss the first specific heat results of 99% pure $H_2@C_{60}$ from room temperature down to 0.085 K [2]. An anomaly observed at $T = 0.6$ K, is attributed to almost degenerate quantized rotational levels state. The observed small 0.1-0.2 meV energy splitting between states allows us to conclude that the encapsulated H_2 in the C_{60} cage can be regarded as an almost 3-D free quantum rotor.

References:

[1] K. Komatsu, M. Murata, and Y. Murata, *Science* **307**, 238 (2005)
[2] Y. Kohama, T. Rachi, J. Jing,[2] Z. Li, J. Tang,[2] R. Kumashiro, S. Izumisawa, H. Kawaji, T. Atake, H. Sawa, Y. Murata, K. Komatsu, and K. Tanigaki, submitted.

Corresponding Author: Katsumi Tanigaki
E-mail: Tanigaki@sspns.phys,tohoku.ac.jp
Tel&Fax: 022-795-6469 (TEL) 022-795-6470 (FAX)

3P-14

Structure and Relative Stabilities of $Sc_2@C_{74}$ and $La_2@C_{74}$

T. Ren, X. Zhao*, H. Zheng, J. S. Dang

Institute for Chemical Physics and Department of Chemistry, Xi'an Jiaotong University, Xi'an 710049, P. R. China

For fullerene C_{74}, there is just one cage that obeys the isolated pentagon rule (IPR), namely of D_{3h} symmetry [1]. In order to evaluate the relative stabilities of metallofullerenes $La_2@C_{74}$ and $Sc_2@C_{74}$, 476 C_{74} isomers (all species with one, two, three adjacent pentagon pairs and IPR structure) have been screened at hexa-anion state by semi-empirical MO methods. Eight stable isomers were chosen and re-optimized at B3LYP/6-31G(d) levels of theory. A non-IPR isomer (Spiral No. 13295) of C_2 symmetry with two pentagon pairs is found to be the lowest energy structure. Another non-IPR isomer 13333:C_2 is the second stable structure of C_{74}^{6-}.

Further geometry optimizations of metallofullerenes $Sc_2@C_{74}$ and $La_2@C_{74}$ systems have been carried out using B3LYP hybrid density functional method in the following basis set: 6-31G(d) for C atoms and LanL2dz for Sc and La atoms. Our results show that isomer $Sc_2@C_{74}$-13333 is the most stable structure. The second lowest energy isomer $Sc_2@C_{74}$-13295 with a rather big HOMO-LUMO gap (1.78eV) and small energy difference of 0.73kcal/mol to 13333:C_2 is more stable than the IPR isomer $Sc_2@C_{74}$-14246. In order to probe all stable conformations found are true minimal energy structures, harmonic vibrational frequencies were calculated. All vibrational frequencies are found without any imaginary frequency, whereas IPR isomer $Sc_2@C_{74}$-14246 has a quite low frequency, 28.85 cm^{-1}. The results are consistent with the finding of Liu *et al.*, who found that $Sc_2@C_{74}$-14246 could be realized as a spin triplet [2]. The spin singlet energy of IPR ($Sc_2@C_{74}$-14246) exceeds the ground state of $Sc_2@C_{74}$-13333 by 19.24kcal/mol, whereas for spin triplet of ($Sc_2@C_{74}$-14246) only 6.57 kcal/mol higher than $Sc_2@C_{74}$-13333.

In the case of $La_2@C_{74}$, the energy of the $La_2@C_{74}$-13295 conformation is 0.81kcal/mol lower than the $La_2@C_{74}$-13333 conformation.

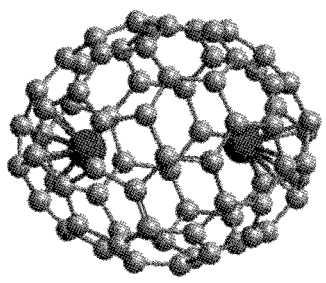

$Sc_2@C_{74}$-13295:C_2

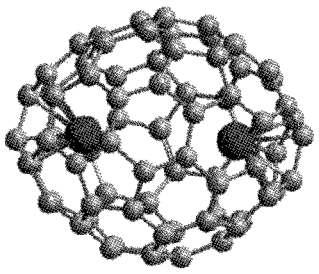

$Sc_2@C_{74}$-13333:C_2

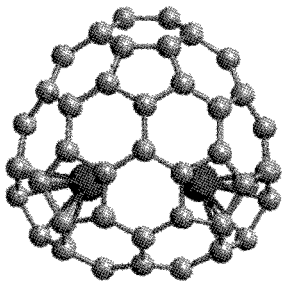

$Sc_2@C_{74}$-14246:D_{3h}

[1] Fowler, P. W.; Manolopoulos, D.E. *An Atlas of Fullerenes*; Clarendon Press: Oxford, U. K., 1995.

[2] Dan Liu, Frank Hagelberg. *Int. J. Quant. Chem.*, **2007**, *107*, 2254-2260.

Corresponding Author: X. Zhao, xzhao@mail.xjtu.edu.cn, or x86zhao@yahoo.co.jp

3P-15

Evaluation of Multi-Walled Carbon Nanotubes by Ultraviolet Raman Spectroscopy

○Hiroyuki Nii, Ken-ichi Hongyou, and Hamazo Nakagawa

UBE Scientific Analysis Laboratory, Inc., 1978-5 Kogushi, Ube, Yamaguchi 755-8633, Japan

Raman spectroscopy is an analytical technique mainly used to characterize carbon materials such as graphite, glassy carbon, and carbon nanotubes (CNTs). So-called D band and G band in Raman spectrum are mainly used to estimate the crystalline quality of carbon materials. It is, however, difficult to evaluate Multi-Walled Carbon Nanotubes (MWNTs) that contain SWNTs or DWNTs by visible Raman spectroscopy because Raman spectrum of them has limited information of specific SWNTs or DWNTs on resonance. On the other hand, it has recently been reported that ultraviolet (UV) Raman spectroscopy could be used to characterize averaged feature of SWNTs reflecting less selective resonance condition [1]. In this study, CNTs composed of SWNTs, DWNTs, and MWNTs are analyzed by Raman spectroscopy at an excitation wavelength of 325 nm, and we discuss the availability of UV Raman spectroscopy to evaluate MWNTs that contain SWNTs or DWNTs.

Figure 1 shows the Raman spectra of CNTs using two different excitation laser wavelengths: (1) 532 and (2) 325 nm. Measurements were performed at four points on the CNTs. G-band intensities were used to normalize the spectra. The Raman spectra excited by 325 nm line exhibit a higher reproducibility of the D-band intensity than those excited by 532 nm line. The low reproducibility of the D-band intensity excited by 532 nm line is attributed to the inhomogeneous distribution of SWNTs or DWNTs that satisfy the resonance condition. Table 1 shows the G/D band intensity ratios of the CNTs before and after an anneal at about 700 ℃ in reductive atmosphere. The peak intensities were determined by curve fitting of the Raman spectra excited by 325 nm line. The intensity ratios of as-received CNTs vary from 5.98 to 11.92, while those of annealed CNTs vary from 8.24 to 9.66. The data indicate that the as-received CNTs are composed of SWNTs, DWNTs, and MWNTs with various crystalline quality, and that the crystallinity of the annealed CNTs is higher than that of the as-received CNTs.

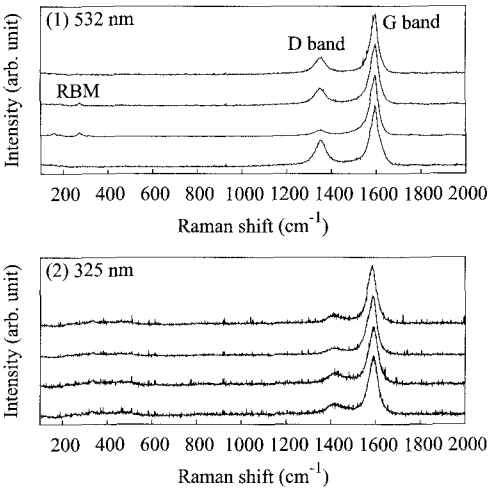

Fig. 1 Raman spectra of carbon nanotubes using two different excitation laser wavelengths: (1) 532 and (2) 325 nm.

Table 1 G/D band intensity ratios.

As received	Annealed
6.77	8.40
5.98	9.66
11.92	8.69
8.55	8.24

[1] H. Kataura, Y. Miyata, Y. Maniwa, and K. Yanagi: Abstract of the 33rd Fullerene-Nanotubes General Symposium, 2007, p. 117.

Corresponding Author: Hiroyuki Nii

TEL: 0836-31-0987, FAX: 0836-31-0956

E-mail: hiroyuki.nii@ube-ind.co.jp

3P-16

Near-infrared Absorption Properties of Single-walled Carbon Nanotubes under Ultra-high Magnetic Fields

○Hiroyuki Yokoi[1], Eiji Kojima[2], Shojiro Takeyama[2], Nobutsugu Minami[3]

[1]*Department of Materials Science and Engineering, Kumamoto University, Kumamoto 860-8555, Japan*
[2]*Institute for Solid State Physics, University of Tokyo, Kashiwa, 277-8581, Japan*
[3]*Nanotechnology Research Institute, National Institute of Advanced Industrial Science and Technology, Tsukuba 305-8565, Japan*

Optical properties of single-walled carbon nanotubes (SWNTs) are governed largely by excitonic states because the exciton exists stably even at room temperature due to the one-dimensionality of their structures. It has been predicted theoretically that the excitonic state is split into singlet and triplet states due to valley mixing and exchange at K and K' points of the Brillouin zone because the electronic states are degenerate at the points [1]. Among these excitonic states, only the symmetric combination of direct excitons at the K and K' valleys is optically active ("bright") and the others are optically inactive ("dark"). It has been one of the most important problems in the properties of SWNTs which state locates lower energetically between the singlet "bright" and "dark" excitonic states.

In order to approach this subject, we have developed a measurement system for near-infrared absorption spectra under ultra-high magnetic fields. Ultra-high magnetic fields to 107 T were generated using a single-turn coil system without destroying an optical probe and a sample at each field generation. An absorption spectrum was recorded at the top of a pulsed field by exposing an InGaAs photodiode array for 1 μs. Magnetic fields were applied to stretch-aligned SWNT(CoMoCAT)/SDBS/gelatin films in parallel to the alignment in the Voigt configuration. Incident light was also polarized in parallel to the alignment with a near-infrared polarizer.

Absorption peaks corresponding to the first sub-band excitons in (8, 4), (7, 5), and (6, 5) SWNTs were observed at 0 tesla in the energy range between 1.05 and 1.28 eV. With increasing magnetic fields, the following spectral changes were observed. The absorption peak for (8, 4) SWNT shifted toward lower energies and a new absorption peak appeared at the higher energy side above 40 T. On the other hand, the absorption peaks for the (6, 5) and (7, 5) SWNTs shifted toward higher energies and a new peak appeared at the lower energy side of each of the absorption peaks. These experimental results suggest strongly that it is the "bright" excitonic state in (8, 4) SWNT and the "dark" one in (6, 5) and (7, 5) SWNTs that situates at the lower energy side in the case of the singlet splitting of the first sub-band excitonic state. Disagreement between our results and the previous works [2-5] will be discussed in detail.

[1] T. Ando, *J. Phys. Soc. Jpn.*, **75**, 024707 (2006).
[2] I.B. Mortimer and R.J. Nicholas, *Phys. Rev. Lett.*, **98**, 027404 (2007).
[3] J. Shaver et al., *Nano Lett.*, **7**, 1851 (2007).
[4] A. Srivastava et al., *Phys. Rev. Lett.*, 101, 087402 (2008).
[5] R. Matsunaga et al., *Phys. Rev. Lett.*, 101, 147404 (2008).

Corresponding Author: Hiroyuki Yokoi
TEL.: +81-96-342-3727, FAX: +81-96-342-3710, E-mail: yokoihr@kumamoto-u.ac.jp

3P-17

Molecular Dynamics Simulation of Adsorption of Polysaccharide on Carbon Nanotubes

Hiroyuki Shinomiya, Katsumi Uchida, Koji Tsuchiya, Tadahiro Ishii, and Hirofumi Yajima*

Department of Applied Chemistry, Faculty of Science, Tokyo University of Science
12-1 Funagawara-machi, Shinjyuku-ku, Tokyo 162-0826, Japan

We have investigated about the dispersion of the single-walled carbon nanotubes (SWNTs) in water using polysaccharide such as carboxymethylcellulose (CMC), chitosan, and xylan. CMC possessed the high ability to disperse SWNTs in water. The SWNTs dispersed by CMC were treated with the density gradient ultracentrifugation, resulting in changing the metal-to-semiconducting ratio for the SWNTs in water. This finding indicates that CMC is an effective agent for chiral separation of SWNTs. In this study, to discuss about the interaction between polysaccharide and the chirality of SWNT, we have studied about the molecular dynamics (MD) simulations of polysaccharide adsorption on a single-walled carbon nanotube (SWNT) in an aqueous environment. We calculated the interaction between SWNT and polysaccharide (in this study, chitosan, xylan and CMC were used) using the condition of (6,5) (8,6) (9,6) (11,2) SWNTs as chirality, 20 units segments as the polysaccharide's chain length, and water as external environment.

The MD simulation using Xylan and (6,5) SWNT showed that Xylan chain was helically-wrapped around the SWNT (Fig.1), additionally, the SWNTs' six-membered ring atracted to Xylan's pyranoside ring through CH- π interactions. Now, we have investigated about the interaction between helical pitch of polysaccharide and chirality of SWNT by calculating the stabilization energy of the helically-wrapped polysaccharide around SWNT.

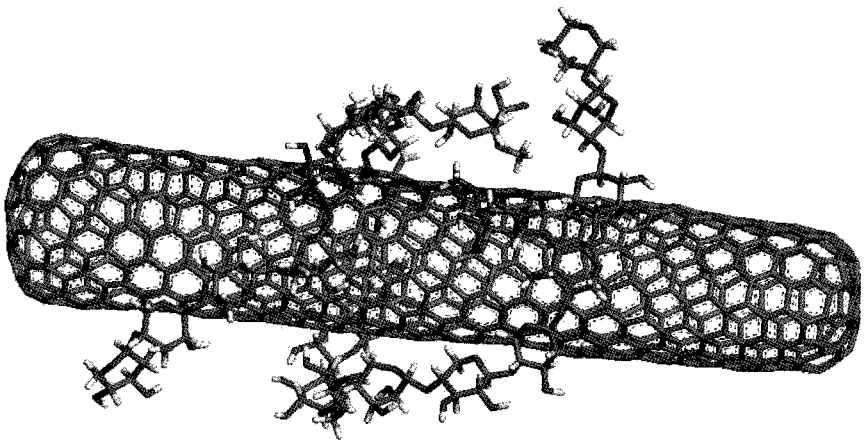

Fig.1 Structure of Xylan wrapping around (6,5) SWNT.

Corresponding Author: Hirofumi Yajima
E-mail: yajima@rs.kagu.tus.ac.jp
Tel:+81-3-3260-4272(ext.5760), FAX: +81-3-5261-4631

3P-18

Field emission study on a single Ti-coated multi-wall carbon nanotube

○Y. Yamamoto, H. Liu, K. Nomura, H. Nakahara and Y. Saito
Dept. of Quantum Eng., Nagoya University, Furo-cho, Nagoya 464-8603, JAPAN

It has been reported that aluminum coating on multi-walled carbon nanotubes (MWNTs) remarkably stabilize field emission (FE) currents [1]. We here investigated influence of thin titanium (Ti) film coating on FE characteristics of a single MWNT emitter.

A single MWNT with diameter of ~10 nm was mounted on a tungsten tip by a nano-manipulator. A Ti film with thickness from 0.2 to 7.2 nm was deposited on the MWNT, and FE characteristics were measured in situ by a field emission microscope (FEM).

Fig. 1 exhibits emission current versus applied voltage (*I-V*) characteristics for a bare emitter (Ti thickness, 0 nm) and the emitter with a Ti film of several different thicknesses. The *I-V* curve shifts remarkably to lower voltage by increasing the film thickness from 0 to 0.9 nm, however, further increase in the film thickness from 0.9 to 7.2 nm results in the curve shifts to higher voltage.

An emission area and a field enhancement factor (voltage to filed conversion factor) of an emitter can be calculated based on the Fowler-Nordheim theory. Fig. 2 shows Ti film thickness dependence of the emission area and the field enhancement factor of the emitter shown in Fig. 1. It is considered that the observed increase in emission (thickness from 0 to 0.9 nm) is caused by drastic increase in the emission area, and the emission decrease (0.9 to 7.2 nm) is caused by the decrease in the field enhancement factor.

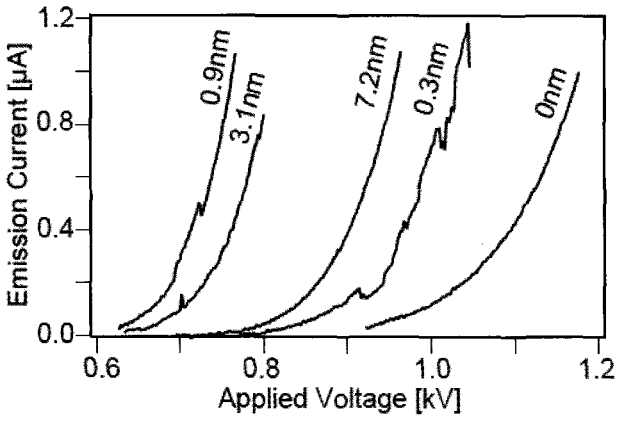

Fig. 1: *I-V* curves for different Ti thicknesses on a MWNT.

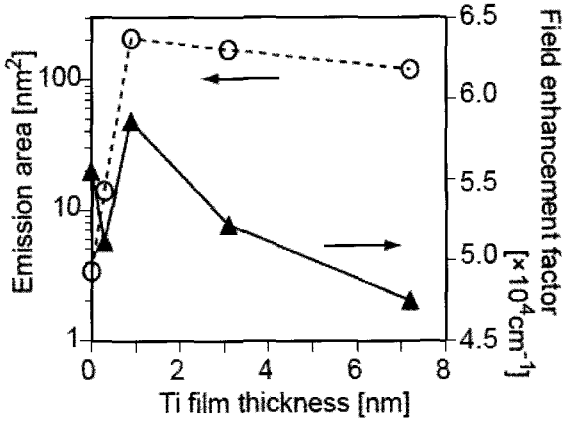

Fig. 2: Field enhancement factors and emission areas vs. Ti film thickness.

[1] Y. Saito *et al.*, 14th Int. Display Workshop, Dec. 5-7, 2007, Sapporo, Japan

Corresponding Author: Yuuta Yamamoto
E-mail: yamamoto@surf.nuqe.nagoya-u.ac.jp, Tel: +81-52-789-4659, Fax: +81-52-789-3703

3P-19

Reduction of Single-walled Carbon Nanotubes in Organic Solvent

○Yutaka Maeda,[1,2], Atsushi Tashiro[1], Tadashi Hasegawa[1], Takahiro Tsuchiya[3], Takeshi Akasaka[3], Jing Lu[4], Shigeru Nagase[4]

[1]*Department of Chemistry, Tokyo Gakugei University, Koganei 184-8501, Japan*
[2]*PRESTO, Japan Science and Technology Agency, Chiyoda, Tokyo 102-0075, Japan*
[3]*Center for Tsukuba Advanced Research Alliance, University of Tsukuba, Tsukuba, Ibaraki 305-8577, Japan*
[4]*Department of Theoretical and Computational Molecular Science, Institute for Molecular Science, Okazaki, Aichi 444-8585, Japan*

Single-walled carbon nanotubes (SWNTs) have excellent mechanical and electrical properties that have led to the proposal of many potential applications. Depending on their chirality and diameter, SWNTs can be classified into two categories: metallic and semiconducting. It has been experimentally reported that the oxidation rate depends on the electronic type and the diameter of the SWNTs, following the order: metallic SWNTs > large-diameter semiconducting SWNTs > small-diameter semiconducting SWNTs. By taking advantage of the difference in oxidation rates, separation of metallic SWNTs from semiconducting SWNTs. We investigate the chemical reduction of dispersed SWNTs using two strong donor molecules, tetrakis(dimethylamino)ethylene (TDAE) and cobaltocene (CoCp2).

The titration of SWNTs using TDAE or $CoCp_2$ was performed under argon atmosphere. The reduction of SWNTs was monitored by means of absorption spectra. When the SWNTs are reduced, the Van Hove singularity in the conduction band is filled, and thus the absorption and Raman peaks diminish. This enables the monitoring of the extent of the reduction of the SWNTs. The S11 peak of large-diameter semiconducting SWNTs decays more quickly than that of small-diameter semiconducting SWNTs. On the other hand, the decay rates of the M11 peaks of metallic SWNTs are comparable to those of the S11 peaks of large-diameter semiconducting SWNTs. The similarity between the decay rates of the M11 absorption peaks of metallic SWNTs and the S11 absorption peaks of semiconducting SWNTs does not imply a similar reduction extent. Then, the optical absorption is calculated by using the CASTEP package. The changes of the calculated optical absorption peaks of the semiconducting (10,0) and metallic (6,6) SWNTs with the electron doping concentration reveal that the S11 peak is sensitive to electron doping, and an electron-doping concentration of 0.01 e/C atom. By contrast, the M11 peak is rather insensitive to electron doping. It is nearly intact at an electron concentration of 0.07 e/C atom, and only loses 41% of its intensity even if the electron doping concentration reaches 0.1 e/C atom. The reduction rate derived from the absorption spectra decreases in the order: metallic SWNTs > large diameter semiconducting SWNTs > small diameter semiconducting SWNTs. We also monitored the SWNTs reduction by means of Raman spectra.

References: *Small,* **2009**, *5,* 244.

Corresponding Author Yutaka Maeda
E-mail ymaeda@u-gakugei.ac.jp
Tel&Fax +81-42-329-7512

3P-20

Solvent Effect On Single-walled Carbon Nanotubes in Organic Solvent

○Tomohisa Okita[1], Yutaka Maeda,[1,2], Katsuya Sode[1], Tadashi Hasegawa[1], Takahiro Tsuchiya[3], Takeshi Akasaka[3], Shigeru Nagase[4]

[1]*Department of Chemistry, Tokyo Gakugei University, Koganei 184-8501, Japan*
[2]*PRESTO, Japan Science and Technology Agency, Chiyoda, Tokyo 102-0075, Japan*
[3]*Center for Tsukuba Advanced Research Alliance, University of Tsukuba, Tsukuba, Ibaraki 305-8577, Japan*
[4]*Department of Theoretical and Computational Molecular Science, Institute for Molecular Science, Okazaki, Aichi 444-8585, Japan*

Single-walled carbon nanotubes (SWNTs) have excellent mechanical and electrical properties. Smalley and co-workers reported that *o*-dichlorobenzene (ODCB) is one of the suitable organic solvents for dispersing SWNTs. Herein, we report the reversible and non-bonding interaction between SWNTs and ODCB, which could be a possible driving force for the dispersion of SWNTs in ODCB.

SWNTs were dispersed in ODCB (SWNTs-ODCB), 1 M octylamine solution in tetrahydrofuran (SWNTs-OA, tetrahydrofuran: THF), and 1 M pyrene solution in THF (SWNTs-P). These dispersions were analyzed by means of absorption and Raman spectra.

The intensity of the absorption bands corresponding to S_{11} decreased in ODCB compared to those in SWNTs-OA and SWNTs-P. On the other hand, the S11 band of SWNTs (SWNTs-ODCB-OA), which was prepared from SWNTs-ODCB by displacement of the solvent, in THF solution containing octylamine, is clearly observed. These results suggest that the interaction between SWNTs and ODCB is reversible. These phenomena are similar to those in the acid treatment of SWNTs. It is reported that proton on SWNTs effectively oxidize the SWNTs. The interaction between SWNTs and an acid increases the solubility of SWNTs. This interaction should not involved covalent bond formation and may be important for stable and high concentrated dispersion of SWNTs in ODCB.

The intensity of large Breit-Wigner-Fano (BWF) line at the lower energy side of the G-band decreased in ODCB. In the region from 200 to 300 cm^{-1}, two radial breathing mode (RBM) peaks due to metallic SWNTs were observed in the case of SWNTs-OA. In the spectrum of SWNTs-ODCB at the same region, there was a decrease in the intensity of RBM peaks that appeared at a lower wavenumber and the peaks at higher wavenumbers shifted to even higher wavenumbers. Similar shifts were observed in case of SWNTs doped with iodine. Haddon et al reported that the intensity of the D-band increases and those of the RBM and G-band decrease with an increase of the degree of sidewall functionalization. Increase of the relative ratio of the D/G intensities was not observed in SWNTs-ODCB. This indicates strongly that the interaction of SWNTs and ODCB is non-covalent.

References: *ChemPhysChem*, **2009**, *10*, 926.

Corresponding Author Yutaka Maeda
E-mail ymaeda@u-gakugei.ac.jp
Tel&Fax +81-42-329-7512

3P-21

Mechanism of thermal boundary conductance between SWNTs and surrounding materials

○Jin Hyeok Cha, Junichiro Shiomi and Shigeo Maruyama

Department of Mechanical Engineering, The University of Tokyo
7-3-1 Hongo, Bunkyo-ku, Tokyo 113-8656, Japan

Thermal boundary conductance (TBC) between SWNTs and surrounding materials is one of the crucial characteristics for various electrical and thermal devices applications. Although there have been many reported studies that experimentally and numerically investigated the TBC for specific systems [1,2], the mechanism of the interfacial energy transfer is far from being understood.

In this study, we investigate the TBC between an SWNT and the various surrounding materials in wide density and temperature ranges (Fig. 1). Our primary aim here is to identify the general scaling law that explains the TBC for various surrounding materials. Such a general law would be of practical importance to predict and design the interfacial thermal transport and also would serve to identify its mechanism.

We employed classical molecular dynamics (MD) simulations to investigate the TBC between a 25 nm long SWNT and a surrounding Lennard-Jones (LJ) medium, as shown in Fig. 1. Using the non-stationary approach, the TBC can be obtained adopting the lumped-heat-capacity method [3]. Figure 2 shows typical density dependence of the TBC for various interfaces, where the axes are nondimensionalized based on the bulk properties of the LJ medium. Different scalings will be tested to identify the general law and to investigate the mechanism of the interfacial energy transfer. Furthermore, the analysis will be extended to examine more complicated aspects such as influence of phase change of the medium and bundling of SWNTs.

References

[1] S. T. Huxtable, et al, Nature Mater. 2, 731 (2003).

[2] M. Hu, S. Shenogin, and P. Keblinski, Appl. Phys. Lett. 90, 231905 (2007).

[3] F. Carlborg, J. Shiomi and S. Maruyama, Phys. Rev. B 78, 205406 (2008).

Corresponding Author: Shigeo Maruyama

E-mail: maruyama@photon.t.u-tokyo.ac.jp.

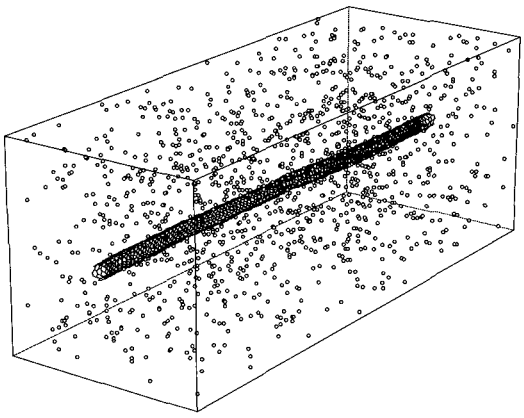

Fig. 1 Snapshot of the simulation.

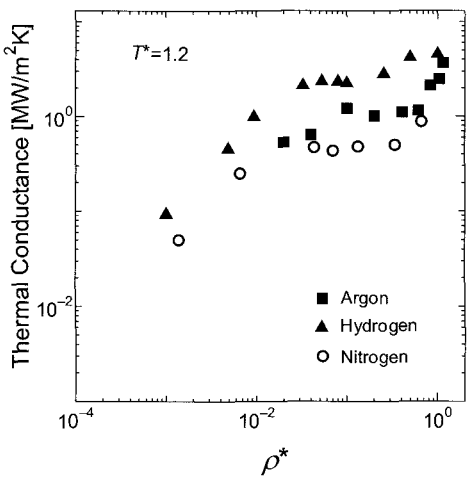

Fig. 2 Density dependence of TBC between SWNT and L-J molecules.

3P-22

The Raman scattering of chain like carbon materials observed in MWNTs and SWNTs produced by hydrogen gas arc discharge using Fe catalyst

○ Makoto Jinno and Yoshinori Ando

Department of Materials Science and Engineering, Meijo University, 1-501 Shiogamaguchi, Tenpaku, Nagoya 468-8502, Japan

Multiwall carbon nanotube (MWNT) produced by dc arc discharge using hydrogen as ambient gas, included very thin innermost diameters tube, 1nm or less. In Raman scattering spectra for H_2-arc driven MWNTs, G-band at 1582 cm^{-1} and characteristic band at 1860cm^{-1} appeared [1, 2]. The new 1860 cm^{-1} band was assigned to liner carbon chain existed inside space of MWNTs. Recently, Raman scattering for liner polyyne molecules encapsulated inside single wall carbon nanotubes (SWNTs) was reported in the region of 2000 ~ 2200cm^{-1} [3]. We report that chain like carbon materials can be synthesized from cathode deposit including MWNTs and web of SWNTs produced by hydrogen arc discharge using Fe catalyst.

H_2-arc driven MWNTs and SWNTs were prepared by DC arc discharge evaporation of carbon anode electrode containing 1 at% Fe in hydrogen pressure of 50 Torr and dc current 60 A. As shown Fig.1, for H_2-arc driven MWNTs, the Raman band appears at ≈1850 cm^{-1} with very strong intensity when the spectrum was taken by a 532 nm excitation wavelength. For H_2-arc driven SWNTs, the new Raman peaks at 2064 and 2120 cm^{-1} were observed, but the intensity of Raman band was weaker than the G-band. We considered that the materials giving the ≈2064 and ≈2120cm^{-1} Raman peaks can be formed in the confined nano-space inside SWNTs.

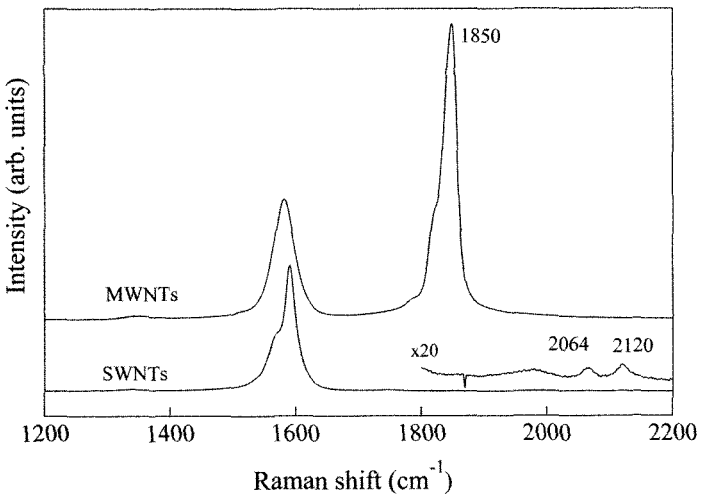

Fig.1 Raman spectra taken for MWNTs and SWNTs.

References:

[1] X. Zhao, Y. Ando, Y. Liu, M. Jinno and T. Suzuki: *Phys. Rev. Lett.* 90 (2003), 187401.

[2] M. Jinno, Y. Ando, S. Bandow, J. Fan, M. Yudasaka and S. Iijima: *Chem. Phys. Lett.* 418 (2006) 109.

[3] D. Nishide, T. Wakabayashi, T. Sugai, R. Kitaura, H. Kataura, Y. Achiba and H. Shinohara: *J. Phys. Chem.* C 111 (2007) 5178.

Corresponding Author: Makoto Jinno

E-mail: mjinno@ccmfs.meijo-u.ac.jp, Tel: +81-52-838-2409

3P-23

Fabrication of plastic lens for glasses with anti-static property using single wall carbon nanotubes.

○Hirotoshi Takahashi[1], Tsuyoshi Fukagawa[1], Takeshi Hashimoto[2]

[1]*TOKAI OPTICAL CO., LTD., R&D Department, Okazaki, Aichi 444-2192, Japan*
[2]*MEIJO NANO CARBON CO., LTD., Nagoya, Aichi 460-0002, Japan*

The plastic lens for glasses with the anti-static property was fabricated using single wall carbon nanotubes (SWNTs). Method for fabricating the plastic lens is follows: first we prepared plastic substrate and SWNTs dispersed to EtOH (concentration: 0.0128wt %). Then, SWNTs dispersed to EtOH were spin-coated onto a plastic substrate. After drying for 10min at 60℃, the organic hard coating was coated on the plastic substrate where SWNTs exists, and it cured for 1.5hr at 120℃ (a few microns thickness). As the final process, the anti-reflection (AR) coating with 5 layer configurations and hydrophobic coating were deposited on the hard coating by vacuum deposition. The index of absorption of this lens was 2.5%.

Table 1 shows the result of before and after the durability test. The anti-static property was evaluated by measuring the electrification potential after the plastic lens had been rubbed with the unwoven cloth by 20 round trips for 10sec at 1kgf. The anti-static property is maintained after various tests, and durability is very excellent. Moreover, there was not a film peeling off. We think that durability is excellent because SWNTs are bonded with the organic hard coating. Detail of the evaluations will be presented in the poster.

Table 1

durability tests	before		after					
description of tests	-		soak in artificial perspiration(1 day)		constant temperature and humidity (5days at 60℃-95%RH)		weather resistance test (120hr)	
electrification potential [kV]	convex	concave	convex	concave	convex	concave	convex	concave
	0.00	0.00	0.00	0.00	0.00	0.00	0.00	0.00
anti-static property	○	○	○	○	○	○	○	○

Corresponding Author: Hirotoshi Takahashi
E-mail: hi-takahashi@tokaiopt.co.jp
Tel: +81-564-27-3025, Fax: +81-564-27-3038

3P-24

Super-growth: Low Threshold Voltage, High Uniformity, and High Stability Field Emission from As-Grown Carbon Nanotubes

○ Hiroe Kimura[1], Don N. Futaba[1], Takeo Yamada[1], Tatsuo Toida[1], Bin Zhao[1], Hiroyuki Kurachi[2], Sashiro Uemura[2], and Kenji Hata[1]

[1]*Nanotube Research Center, National Institute of Advanced Industrial Science and Technology (AIST), Tsukuba, 305-8565, Japan.*

[2]*Noritake Company Ltd., 728-23 Tsumura-cho, Ise, Mie 516-1103, Japan.*

Carbon nanotubes (CNT) are excellent candidates for electron field emission from their intrinsic physical and electrical properties, i.e. crystallinity, electrical conductivity, and high aspect ratio. Yet, uniform and stable field emission at low voltages over large areas has been a major obstacle for carbon nanotubes, as thin diameter CNTs (required for low power operation) cannot be grown vertically in low density. As a result, the high electric field concentration from their small diameters is offset by the shielding effects from neighboring CNTs. As a result various methods have been developed involving patterning or composites to achieve low threshold voltages (voltage at the onset of emission). However, CNT-based field emission devices has failed in achieving the strict industrial benchmarks for commercial applications, such as displays, such as low threshold voltage, emission uniformity, and stable emission over long time-scales.

Here, we report low average threshold voltage (1.09 V/μm), high uniformity, and high stability emission from as-grown CNTs grown by the Super-Growth CVD method [1]. Central to this result was the uniform growth of an ultra-low density film of quasi-standing CNTs (~few/μm^2) necessary for achieving low voltage emission. Uniform growth led to high emission uniformity, and when combined with the low threshold voltage, afforded exceptional stable emission.

References:

[1] K. Hata *et al*, Science, **306**, 1241 (2004)

Corresponding Author: Don N. Futaba

TEL: (029) 861-44402, FAX: (029) 861-4851, E-mail: d-futaba@aist.go.jp

3P-25

Aligned SWNT Prepreg Sheets and Their Reinforcing Effects

○Kazufumi Kobashi, Hidekazu Nishino, Takeo Yamada, Don N. Futaba and Kenji Hata

Nanotube Research Center, National Institute of Advanced Industrial Science and Technology (AIST), 1-1-1 Higashi, Tsukuba, Ibaraki 305-8565, Japan

Carbon nanotubes (CNT) have the highest Young's modulus and strength among any known material and, combined with their one-dimensional nature, have the potential to serve as outstanding reinforcing fillers. An interlaminar reinforcement with aligned CNTs was demonstrated for carbon fiber/epoxy prepreg [1]. To fully reinforce polymer composites with CNTs, following parameters are essential, such as large aspect ratio of nanotubes, unbundling nanotubes, high loading of nanotubes, large nanotube-matrix interface area, nanotube alignment, and effective interfacial stress transfer. We reported a rational approach to fabricate single-walled carbon nanotube (SWNT)/epoxy prepreg sheets highly-loaded with long, pure aligned, and unbundled SWNTs. The facile fabrication process is comprised of roll-pressing vertically aligned SWNT forest and filling epoxy resin in the SWNT sheet.

Here we present the aligned, roll-pressed SWNT sheet with nanoporosity, which is an excellent template for epoxy filling (Figure 1). XRD patterns revealed that the alignment of nanotubes was kept after the epoxy filling. The optimization of composite fabrication process led to an increase of nanotube loading to 33 wt%, giving the higher Young's modulus, 15 GPa (5.4 times enhancement). Thicknessess of composite sheets are controllable in the range of 20-40 μm. Thinner films resulted in the higher nanotube loading and the enhanced mechanical properties.

More generally, the present approach to make aligned SWNT prepreg sheet can be extended to other thermosetting polymers like polyimides, and also be applied to design a wide range of multifunctional CNT composites with excellent electronic, mechanical, and thermal properties derived from the nanotubes.

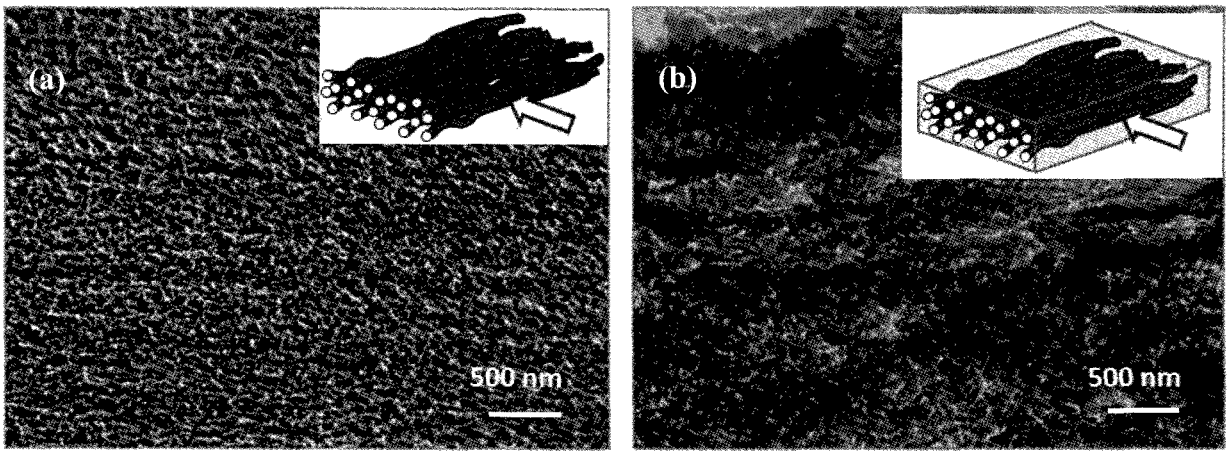

Figure 1 SEM images of cross sections (a) of SWNT roll-pressed sheet showing the nanoporosity and (b) of SWNT/epoxy prepreg sheet in which SWNTs were well impregnated.

[1] J. E. Garcia, B. L. Wardle and A. J. Hart, *Composite A*, **39**, 1065 (2008).

Corresponding Author: Kenji Hata
TEL: +81-29-861-4654, FAX: +81-29-861-4851, E-mail: kenji-hata@aist.go.jp

3P-26

Enhanced Photocurrent in a Dye-Sensitized Solar Cell Consisting of an FTO glass/SnO_2/*p*3HT Electrode by Coating with MWCNTs

○Toru Arai, Atsushi Furuta, Tatsunori Kuramoto

Department of Applied Chemistry, Kyushu Institute of Technology, Kitakyushu 804-8550, Japan

The thin film of *poly*(3-hexylthiophene)s (*p*3HT) is often used as the light-harvesting material for the dye-sensitized solar cell. Here, the *p*3HT-modified electrode was coated with MWCNTs, expecting an improved photovoltaic performance. Figure 1 depicts the modified electrode consisting of a glass electrode (F-doped SnO_2 and the nano-structured SnO_2), *p*3HT (synthesized via electro-chemical polymerization), and MWCNTs.

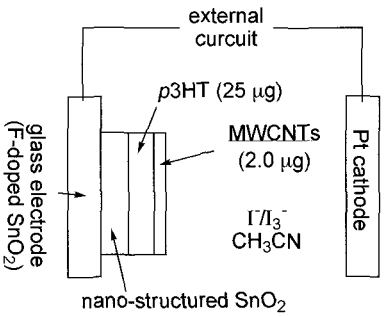

Fig. 1 Photovoltaic cell with *p*3HT-modified glass electrode coated by MWCNTs.

The *p*3HT-modified glass electrode and the counter electrode were dipped in the electrolyte solution (CH_3CN containing 50 mM I_2/0.50 M NaI). Under Xe light (>390 nm) illumination, the moderate photocurrent (J_{sc}= –0.80 mA cm^{-2}) and photovoltage (V_{oc}=0.39 V) were observed (Figure 2, curve b). The photoexcited *p*3HT* released an electron to the glass electrode.

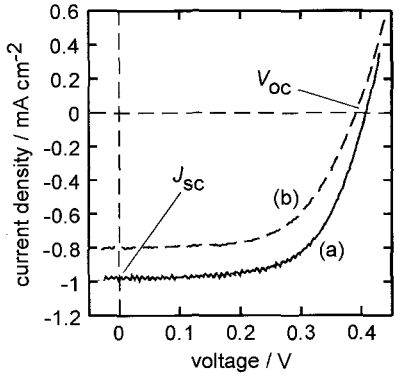

Fig. 2 Photo-voltaic properties of the solar cells with (a) glass/*p*3HT and (b) glass/*p*3HT/MWCNTs electrode under (>390 nm) illumination.

The *p*3HT-modified glass electrode was further coated with MWCNTs (THF suspension). The solar cell coated with 2.0 μg MWCNTs showed an increased photocurrent (J_{sc}= –0.97 mA cm^{-2}), essentially unchanged photovoltage (V_{oc}=0.41 V), and the 35 % increased maximum power output upon illumination (Figure 2, curve a). The photo-current represents the charge injection from the photo-excited *p*3HT* to the electrode. MWCNTs may extract a hole from the photoexcited *p*3HT* to effectively generate the charge separation state, in which the undesired charge recombination may be avoided. The electron transfers from the *p*3HT* to SnO_2, and in turn, the hole transfers from *p*3HT* to the MWCNTs, electrolyte, and to the Pt cathode.

Interestingly, the use of SWCNTs instead of MWCNTs only resulted in a slightly increased the photocurrent (–0.83 mA cm^{-2} with 1.0 μg SWCNTs). SWCNTs may accept an electron but not extract a hole like MWCNTs. The energy transfer from the photoexcited *p*3HT* to SWCNTs might occur, which resulted in the decreased photocurrent. In fact, the addition of MWCNTs decreased the fluorescence emission of *p*3HT to 48% intensity, without changing the emission wavelength. Contrary, the addition of the same amount of SWCNT decreased the emission of *p*3HT only to 85% intensity. These facts indicated that MWCNTs more efficiently quenched the excited state of *p*3HT* in THF than SWCNTs.

[1] A. Furuta, T. Kuramoto, and T. Arai, *Energy Environ. Sci., in press.*

Corresponding Author: Toru Arai
TEL: +81-93-884-3303, FAX: +81-93-884-3300, E-mail: arai@che.kyutech.ac.jp

3P-27

Solubilization of Single-walled Carbon Nanotubes by Using meso-meso Linked Porphyrin oligomer

○Takeshi Uchinoumi[1], Tsuyohiko Fujigaya[1], and Naotoshi Nakashima[1,2]

[1]*Department of Applied Chemistry, Graduate School of Engineering. Kyushu University, 744, Motooka Nishi-ku Fukuoka, Japan*
[2]*JST-CREST, 5 Sanbancho, Chiyoda-ku, Tokyo 102-0075, Japan*

Porphyrins are functional dyes with a variety of unique photophysical, electrochemical properties. We have reported porphyrin can adsorbed on the single-walled carbon nanotubes (SWNT) through π-π interaction and give stable SWNT dispersion[1)]. Here meso-meso linked porphyrin (por oligomer) was synthesized and used as a new solubilizer. Optical and electrochemical properties of meso-meso linked porphyrin/SWNT complex were investigated in targeting the novel functional materials.

Zinc(II)-5,15-bis-(3,5-di-tert-butylphenyl) porphyrin was polymerized to give oligo(Zn(II)-porphyrinylene) (por oligomer) (Fig.1) in the reaction with $AgPF_6$ in $CHCl_3$ upon heating[2)]. SWNT was added to the oligo(Zn(II)-porphyrinylene) solution dissolved in THF containing 5% trifluoroacetic acid (TFA). This solution was sonicated for 60 min to dissolve SWNT, followed by the centrifugation (4000 *g*). Fig.2 (a) shows the absorption spectra of the surpernatant solution after the centrifugation. For comparison, the same operation without Por oligomer was carried out and absorption of the solution spectra was shown in Fig.2 (b).

In the case of the solution including por oligomer (Fig.2 (a)), the characteristic spectral features due to dissolved SWNT were clearly observed in the near-IR region. On the other hand, the characteristic absorption due to SWNT was not observed in the absence of por oligomer (Fig.2 (b)). The result indicates the por oligomer act as a nice solubilizer for SWNT.

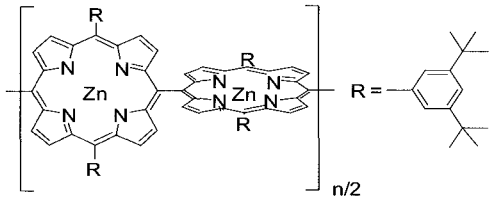

Fig.1 Chemical structure of por polymer.

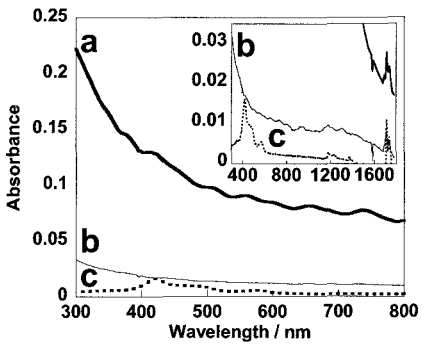

Fig.2 Absorption spectra of (a) Por oligomer/SWNT, (b) SWNT and (c) Por oligomer in THF/TFA mixture solution.

References:

1) N. Nakashima et al., *Chem. Phys. Lett.* **2003**, *378*, 481-485.

2) A. Osuka et al., *Chem. Commun.*, **2000**, 197-198.

Corresponding Author: Naotoshi Nakashima

E-mail: nakashima-tcm@mail.cstm.kyushu-u.ac.jp

Tel&Fax: +81-92-802-2840

3P-28

Preparation of Conductive Film Composed of Polyaniline Sulfonic Acid and Single-walled Carbon Nanotubes

Tomoyuki Kuriyama, Syuku Ono, Yosiya Kaminosono, Katsumi Uchida,
Koji Tsuchiya, Tadahiro Ishii, and Hirofumi Yajima

Department of Applied Chemistry, Faculty of Science, Tokyo University of Science
1-3Kagurazaka Shinjyuku-ku, Tokyo 162-0826, Japan

The formation of carbon nanotube and polymer composites has been explored for possible improvement in the electrical and mechanical properties of polymers. In particular, composite materials based on the coupling of conducting polymer and carbon nanotubes have been shown to possess properties of the individual components with a synergistic effect. Thus, we have investigated about the conductive film composed of polyaniline sulfonic acid (PAS) as conducting polymer and single-walled carbon nanotube (SWNT). In particular, we have paid attention to the effect of the dispersibility and the amount of SWNTs included the PAS film to the electronic property of the composited film. PAS is one of the more important conducting polymers because of its good electrochemical activity and chemical stability. In this study, we have discussed about the dispersion-condition of the SWNTs in water using PAS as a dispersing agent. 2.5 mg-SWNT was added in 10 ml 1 wt% PAS aqueous solution, and the mixture was ultrasonicated. The optical adsorption intensity of the mixture solution was estimated by UV-vis-NIR absorption measurement. The adsorption intensity was dependent on the treated time of ultrasonication. The adsorption intensity was increased with the treated time up to 1 hour, and then leveled off, indicating that the amount of the dispersed SWNT was dependent on the ultrasonication time. Resonance Raman scattering measurements showed no damage to PAS and SWNT by ultrasonication for 3 hours. From UV-vis-NIR absorption measurement, the adsorption intensity for the mixture of PAS and SWNT was increased in proportion to the amount of the SWNTs (up to 1 wt%) added to 1 wt% PAS solution. However, from Dynamic Light Scattering (DLS) measurements, the size of the dispersed SWNT was increased as the added amount of SWNT to the PAS solution was increased, indicating that the dispersibility of SWNT was dependent on the added amount of SWNT in the PAS solution.

Corresponding Author: Hirofumi Yajima
TEL: +81-3-3260-4272(ext.5760), FAX: +81-3-5261-4631, E-mail: yajima@rs.kagu.tus.ac.jp

3P-29

Facile Fabrication and Characterization of a Field Effect Transistor using As-grown Single-Walled Carbon Nanotubes

○Shinya Aikawa[1,2], Rong Xiang[1], Erik Einarsson[1], Junichiro Shiomi[1], Eiichi Nishikawa[2] and Shigeo Maruyama[1]

[1]*Department of Mechanical Engineering, The University of Tokyo, 7-3-1 Hongo, Bunkyo-ku, Tokyo 113-8656, Japan*
[2]*Department of Electrical Engineering, Tokyo University of Science, 1-3 Kagurazaka, Shinjuku, Tokyo 162-8601, Japan*

A single-walled carbon nanotube (SWNT) with small diameter (1-2 nm) is one of the most promising materials for application as an electron transporter, owing to its quasi one-dimensional structure. A carbon nanotube field effect transistor (CNT-FET) having an SWNT as its gate channel has been particularly investigated as a favorable nanoscale device for next-generation electronics [e.g., 1]. However, in most previous reports SWNTs were dispersed or transported during the device fabrication process, which may induce significant damage and/or doping of the SWNTs. A CNT-FET consisting of as-grown high-quality SWNTs may be obtained by depositing electrodes on as-grown SWNTs, but fabrication of fine structures (e.g., channel width < 1 μm) is still challenging.

Recently we succeeded in restricting the catalyst-coating area by patterning a self-assembled monolayer (SAM) on a Si substrate [2]. The growth location in this process can be precisely controlled down to 10 nm. This method has two primary advantages compared with conventional MEMS techniques (e.g., lift-off). Firstly, since the SAM surface is very hydrophobic it is possible to easily prepare substrates using a scalable liquid-based dip-coating method for catalyst deposition [3]. Secondly, the SAM can also be patterned with high resolution (~10 nm) using the electron beam of a scanning electron microscope (SEM), which makes the patterning process visible. A back-gate-type CNT-FET with an as-grown SWNT bridge and pre-deposited source and drain electrodes was fabricated using this method. The CNT-FET fabrication process is as follows. After SAM formation on a SiO_2/Si substrate with pre-patterned electrodes, the substrate was installed into a SEM to selectively remove the SAM using the electron beam. Catalyst was then deposited by dip-coating the substrate into a Co solution, and SWNTs were grown by ACCVD [4]. The *I-V* characteristics were measured using the Si substrate as a back-gate. Here we discuss the fabrication process and measured properties of the device.

[1] S. J. Tans et al., Nature **393**, 49 (1998).
[2] R. Xiang et al., submitted.
[3] Y. Murakami et al., Chem. Phys. Lett. **377**, 49 (2003).
[4] S. Maruyama et al., Chem. Phys. Lett. **360**, 229 (2002).

Corresponding Author: Shigeo Maruyama
TEL: +81-3-5841-6421, FAX: +81-3-5800-6983, E-mail: maruyama@photon.t.u-tokyo.ac.jp

3P-30

Improvement of carbon nanocoil yeild by using vacuum-evaporated Sn thin film

○K. Takimoto[1], M. Yokota[1], T. Kawabata[1], Y. Suda[1], S. Oke[1], H. Takikawa[1], Y. Fujimura[2], S. Itoh[2], H. Ue[3], M. Morioki[4], K.Shimizu[5]

[1] *Department of Electrical and Electronic Engineering, Toyohashi University of Technology*
[2] *Research and Development Center, Futaba Corporation.*
[3] *Fuji Research Laboratory, Tokai Carbon Co., Ltd.*
[4] *Fundamental Research Department, Toho Gas Co., Ltd.*
[5] *Development Department Shonan Plastic Mfg. Co., Ltd*

Carbon nanocoil (CNC) is a material of carbon nanofiber with helical shape. CNCs are synthesized by chemical vapor deposition on a substrate using a composite catalyst, Fe and Sn. So far, we have prepared CNC catalyst from Fe-powder-mixed Sn solution. In this study, Sn catalyst was deposited on Si substrate by vacuum evaporation so that catalyst metal could be a fine grain. Experimental apparatus used in this study is the same as that in past time [1]. Sn catalyst films of 2.5, 25, and 50 nm thicknesses were deposited on Si substrate. Solution of Fe catalyst was dropped on Sn-catalysed substrate. Fe/Sn-coated substrate was placed in the center of a quartz tube. The reaction temperature, the gas flow rates of nitrogen as a dilution gas and acetylene as a source gas, and the reaction time were 700°C, 1000 sccm, 50 sccm, and 10 min, respectively. After experiment, many CNCs were observed by field emission scanning electron microscopy (FE-SEM) as shown in Fig.1. Then as-grown CNCs were mixed in distilled water and dispersed for 1 h by an ultrasonic cleaner. The distilled solution was dropped on Si substrate and dried. After drying, CNCs were observed by FE-SEM and CNC yield was evaluated. Fig.2 shows the dependence of CNC yield on Sn film thickness. This result shows that the yield of CNC is higher than 40% for each film thickness. Particularly 50 nm Sn film obtained a high yield up to 60%.

This work has been partly supported by the Outstanding Research Project of the Research Center for Future Technology, Toyohashi University of Technology (TUT); the Research Project of the Venture Business Laboratory (TUT); Global COE Program "Frontiers of Intelligent Sensing" from the Ministry of Education, Culture, Sports, Science and Technology (MEXT); The Japan Society for the Promotion of Science (JSPS) and Core University Programs (JSPS-CAS program in the field of "Plasma and Nuclear Fusion")

Fig.1 SEM image of as-grown CNC

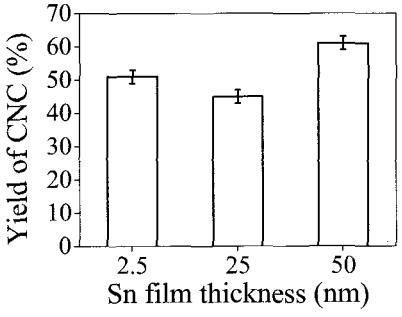

Fig.2 Yeild of CNC

[1] Guochun Xu et al, Japanese Journal of Applied Physics, Vol. 44, No. 4A, 2005, pp. 1569-1576

Corresponding Author: Yoshiyuki Suda
E-mail: suda@eee.tut.ac.jp, Tel: +81-532-44-6726

3P-31

Improvement of bulk-density of brush-like carbon nanotubes

○Gen Kubo, Takayuki Arie and Seiji Akita

[1]*Department of Physics and Electronics, Graduate School of Engineering, Osaka Prefecture University, 1-1 Gakuen-cho, Naka-ku, Sakai, Osaka 599-8531, Japan.*

Brush-like carbon nanotubes (CNTs) are expected to have wide applications due to their structural anisotropy. It is important to control the formation of the catalyst particles in order to enhance the growth of the blush-like CNTs. Recently, it has been reported that both the kind of substrates and water concentration in a reactor on the growth of CNTs are very crucial for formation of appropriate catalyst particle [1]. The bulk density is one of important parameters for practical applications of the brush-like CNTs. In this report, we investigate the effect of buffer layer and water concentration on the growth of CNTs in terms of the bulk density of the grown CNTs.

A Si_3N_4 film with a thickness of 115 nm sputtered on the SiO_2/Si substrates at room temperature was used as a buffer layer. A Fe layer with a thickness of 4 nm deposited on the buffer layer was used as the catalyst. For the reference, the Fe layer with the same thickness was deposited directly on SiO_2/Si substrates. The substrates thus prepared were heated up to 700 °C in He atmosphere. After holding the temperature at 700°C for 2 min, the C_2H_2 gas of 15 sccm mixed with He gas of 245 sccm was introduced into the reactor for 10 min for the growth of CNTs. Water vapor with a certain concentration was also introduced during both processes of the heat-up and the growth of CNTs.

Figures 1(a) and 1(b) show the water concentration dependence of the height and the bulk density of the brush-like CNTs grown on the Si_3N_4/SiO_2/Si substrate. Both the length and the density are bigger than those of the SiO_2/Si substrate at the condition of no additional water and are maximum around the water concentration of 20 ppm. In the case of SiO_2/Si substrate, the height and the bulk density of grown CNTs are maximums of 184 μm and 28 mg/cm^3 at the water concentration less than 2 ~ 3 ppm, respectively. Additional water affected the growth of CNTs and both of the height and the bulk density were reduced. Thus, the high bulk density of ~ 70 mg/cm^3 has been achieved by using the Si_3N_4 buffer layer and the water.

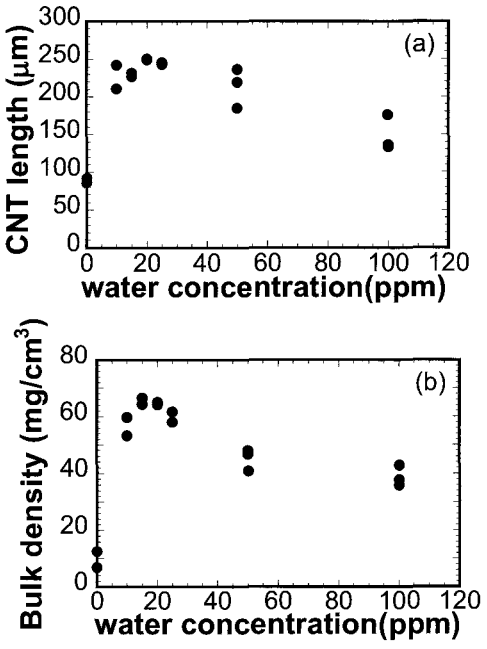

Fig.1 (a) CNT length and (b) bulk density grown on the Si_3N_4/SiO_2/Si substrate as a function of water concentration.

Acknowledgement: This work was partially supported by the Osaka Prefecture Collaboration of Regional Entities for the Advancement of Technological Excellence, JST.

[1] T. Nagasaka *et al*, Jpn. J. Appl. Phys. in press.

Corresponding Author: Seiji Akita
Tel&Fax: 072-254-9261, E-mail:akita@pe.osakafu-u.ac.jp

3P-32

Influence of Water Addition on Carbon Nanotube Growth by Alcohol Gas Source Method in High Vacuum

○Kuninori Sato, Takahiro Maruyama, Shigeya Naritsuka

Department of Materials Science and Engineering, Meijo University,
1-501 Shiogamaguchi, Tempaku, Nagoya 468-8502

Carbon nanotube (CNT) is a specific material expected to be applied to nanoscale devices. Recently, we have reported CNT growth by alcohol gas source method in an ultra-high vacuum (UHV) chamber. This growth technique enables CNT growth at 400°C [1]. However, the CNT yield was not sufficient and it is necessary to increase the yield at low temperature growth. So far, it has been reported that addition of a small amount of water enhances the yield in the CNT growth with hydrocarbon sources [2]. In this study, we investigated effect of water addition on CNT growth at low temperature by the alcohol gas source method.

SiO_2(100nm)/Si substrates were introduced into a UHV chamber and Co catalysts (~0.1 nm in thickness) were deposited on them by electron beam evaporation. Then, the substrates were heated at 400°C and ethanol gas was supplied onto the substrate surfaces through a stainless steel nozzle for the CNT growth. In this study, we carried out CNT growth at a fixed ethanol pressure of 1.0×10^{-4} Pa, while the water partial pressure was varied between 0 and 1.0×10^{-4} Pa. The ethanol pressure and water pressure were controlled by monitoring the ambient pressure of the UHV chamber and quadrupole mass spectra.

Fig.1 shows Raman spectra of CNTs grown under various amounts of the additional water. When the growth pressure (ethanol + water pressure) was 1.2×10^{-4} Pa, G band intensity reached its maximum, indicating that this is the optimum condition for CNT growth. Irrespective of the amount of water, the G/D ratio did not show distinct change. Out result showed that the water addition is effective to enhance the CNT yield in low temperature growth using alcohol gas source method. Compared with the growth using the hydrocarbon sources, the enhancement effect was much smaller. This may be due to the effect of OH group in an ethanol molecule and/or the fact that the water amount was still not optimized.

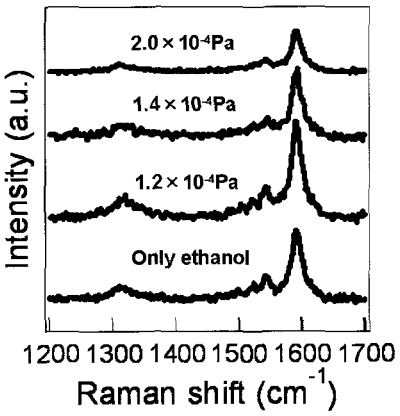

Fig.1

[1] K.Tanioku et al., *Diam. Relat. Mater. 17(2008)589.*

[2] S. Noda et al. *Jpn.J. Appl. Phys. 17 (2007) L399.*

Corresponding Author: Takahiro Maruyama

Tel: +81-52-838-2386, **Fax**: +81-52-832-1172, **E-mail**: takamaru@ccmfs.meijo-u.ac.jp

3P-33

Optical Emission Spectroscopy Study of Plasmas during the growth of Single-Walled Carbon Nanotubes with Au Catalyst

○ Z. Ghorannevis, T. Kato, T. Kaneko, and R. Hatakeyama

Department of Electronic Engineering, Tohoku University, Sendai 980-8579, Japan

We investigated the plasma diagnostic consisted of CH_4 and H_2 gas mixtures using optical emission spectroscopy (OES) during the growth of single-walled carbon nanotubes (SWNTs) [1,2] from Au catalyst [3]. H_2 flow rate has been varied to modify the chemical species in plasmas, which have an important role in the growth of SWNTs. Based on Raman scattering spectra analysis, it was found that SWNTs can be grown only when fairly low H_2 flow rate conditions with Au catalyst. OES analysis shows that the intensity of CH radical obviously decreased by increasing the hydrogen flow rate, whereas the intensity of hydrogen related radicals increased as shown in Figure 1. Interestingly, the intensity ratio of CH/H_α shows similar tendency of G-band intensity as function of H_2 flow rate, i.e. SWNTs could be grown only when high CH/H_α conditions. This should be related with the balance between supplying and etching of carbon precursors for SWNTs growth. Since Au catalyst has lower adsorption efficiency with hydro carbons compared to general magnetic catalysts such as Fe and Co, the balance effects must be much more sensitive. Our result suggests that CH/H_α intensity ratio can be useful to identify the optimum growth condition for SWNTs growth from Au catalyst.

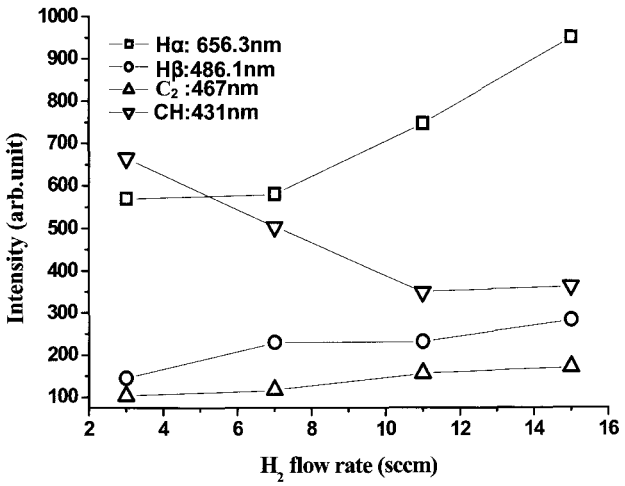

Fig. 1: The emission intensity of various radicals as a function of H_2 flow rate in plasmas.

References:

[1] T. Kato, R. Hatakeyama, and K. Tohji, Nanotechnol. **17**, 2223 (2006).

[2] T. Kato and R. Hatakeyama, Appl. Phys. Lett. **92** , 031502 (2008).

[3] D. Takagi, Y. Homma, H. Hibino, S. Suzuki, and Y. Kobayashi, Nano Lett. **6**, 2642, (2006)

Corresponding Author:

E-mail: zohreh@plasma.ecei.tohoku.ac.jp

Tel & Fax: 022-795 7046 , 022-263 9225

3P-34

Super-growth: How to Make Fast Growth Even Faster (and keep its quality)

○ Junichi Sato[1], Satoshi Yasuda[1], Don N. Futaba[1], Takeo Yamada[1], Motoo Yumura[1], and Kenji Hata[1,2]

[1]*National Institute of Advanced Industrial Science and Technology (AIST), Tsukuba, 305-8565, Japan*
[2]*Japan Science and Technology Agency (JST), Kawaguchi, 332-0012, Japan*

The development of carbon nanotube (CNT) technology (and consequently a CNT-based industry) is reliant upon the economical availability of CNTs and single-walled carbon nanotubes (SWNTs). One critical hurdle in the journey to establish a CNT industry is to use a highly efficient growth process for the synthesis of SWNTs. Previously we demonstrated the highly pure and highly efficient synthesis of SWNTs ("Super-growth" chemical vapor deposition (CVD)) [1] which simultaneously addressed problems, such as scalability, purity and cost. By the Super-growth method, SWNT growth rates as high as ~200 μm/min were possible [2]. As the levels of carbonaceous impurities increase nonlinearly with exposure to the growth ambient [3], simply extending the length of the growth process was not a viable option. Here, we address the issue of efficiency without extending the growth process by optimizing the gas heating time and carbon flux. In doing so, growth rates could be increased by up to 300% while maintaining catalyst lifetime and SWNT purity and selectivity. We believe that this maybe a key technological advancement in realizing a CNT-based industry.

References:

[1] K. Hata *et al*, Science, **306**, 1241 (2004).

[2] D.N. Futaba, K. Hata, T. Yamada, K. Mizuno, M. Yumura, S. Iijima, Phys. Rev. Lett. **95**, 50561041 (2005).

[3] S. Yasuda, T. Hiraoka, D.N. Futaba, T. Yamada, M. Yumura, K. Hata, *Nano Lett.* **9**, 769 (2009)..

Corresponding Author: Don N. Futaba

TEL: (029) 861-44402, FAX: (029) 861-4851, E-mail: d-futaba@aist.go.jp

3P-35

Effect of the support materials on catalyst chemical vapor deposition (CCVD) growth of carbon nanotubes

T. Nakayama, R. Kitaura, and, H. Shinohara,

Department of Chemistry & Institute for Advanced Research, Nagoya University, Nagoya 464-8602

Effects of support materials are one of the most important factors in heterogeneous catalytic reactions. In the case of catalyst-supported CVD (CCVD) growth of carbon nanotubes, the effects of support materials have not been well addressed even though the size of catalyst nanoparticles, kind of carbon sources and reaction condition (reaction temperature and flow rate) have been well investigated[1]. Therefore, in this study, we have performed a systematic study on the effect of support material in CCVD growth of CNTs using Al_2O_3, SiO_2, MgO, CaO and SrO; these support materials have different solid basicity.

CCVD growth of CNTs was carried out using EtOH as carbon source at 1000 K. In all reactions, a surface density of Co and Fe metal catalyst deposited on support materials was fixed to 0.31mmol/m^2 and 0.16mmol/m^2, respectively. Figure 1 shows typical TEM image of the products. As clearly shown in the figure, products strongly depend on kinds of support materials. TEM investigation of the catalyst nanoparticles size after CCVD reaction reveals that degree of aggregation of catalyst nanoparticles significantly depends also on kinds of support materials. In the case of MgO, interaction between catalyst nanoparticles and surface of MgO is strong due to strong solid basicity. Therefore, the size of catalyst nanoparticles remains small after CCVD reaction, which leads to the growth of small diameter SWCNTs. In contrast, in the case of SiO_2, interaction between catalyst nanoparticles and SiO_2 is weak leading to aggregation of catalyst nanoparticles to form large Co and Fe particles. In this case, not CNTs but graphitic carbon materials tend to grow. In the study, further experimental results including TEM and Raman spectroscopy of synthesized CNTs and significance of the effect of support materials are discussed.

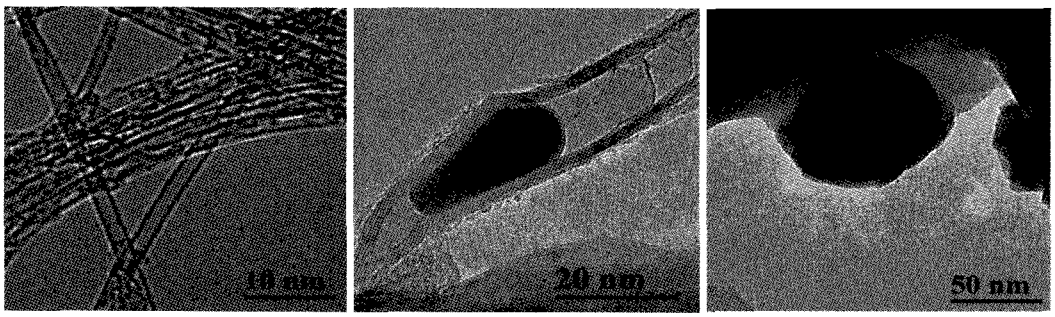

(a) (b) (c)

Figure1 TEM image of typical product using (a) MgO (b) Al_2O_3 (c) SiO_2

References: [1] Li, Q. et al., *J. Mater. Chem.* **2001**, 12, 1179

Corresponding Author: Shinohara Hisanori

Tel&Fax: +81-52-789-2482/+82-52-747-6442 **E-mail**: noris@nagoya-u.jp

3P-36

Direct Growth of Orthogonal Single-Walled Carbon Nanotube Arrays

○Tetsushi Nishi,[1] Hiroki Ago,[*,1,2,3] Carlo M. Orofeo,[1] Naoki Ishigami,[1]
Masaharu Tsuji,[1,2] Tatsuya Ikuta,[4] and Koji Takahashi[4]

[1] *Graduate School of Engineering Sciences, Kyushu University, Fukuoka 816-8580, Japan*
[2] *Institute for Materials Chemistry and Engineering, Kyushu University*
[3] *PRESTO, Japan Science and Technology Agency*
[4] *Graduate School of Engineering, Kyushu University*

Horizontally-aligned single-walled carbon nanotubes (SWNTs) grown on single crystal substrates, such as sapphire and quartz, have attracted great interest because of its importance to device applications. The aligned SWNTs are oriented along a specific crystallographic direction due to anisotropic van der Waals interaction between SWNTs and atomic surface of the crystal [1,2]. However, it is still unclear why the SWNTs are oriented along one unique direction even though there are several possible crystallographic directions with anisotropic atomic arrangement.

Here, we show a new SWNT growth direction that is orthogonal to its original growth direction. In our previous studies, SWNTs normally grow in [$1\bar{1}01$] direction on the r-plane sapphire [1]. When we used the sapphire with intentional miscut orientation, the SWNT growth direction completely changed to its orthogonal direction (Fig. 1a,b). We have confirmed that SWNTs grow in this direction regardless of the gas flow, and no remarkable steps were found in our substrate. Figure 1c,d show the corresponding surface atomic arrangements viewed from the aligned directions. We infer that a new anisotropic atomic arrangement appeared on the miscut r-plane, thus guiding the SWNT growth (Fig. 1d). Moreover, we can recover the original growth direction by thermal treatment, and orthogonal SWNT arrays are also demonstrated through surface patterning. Our new method of constructing nanotube architectures would contribute to SWNT device applications as well as further understanding of the alignment mechanism.

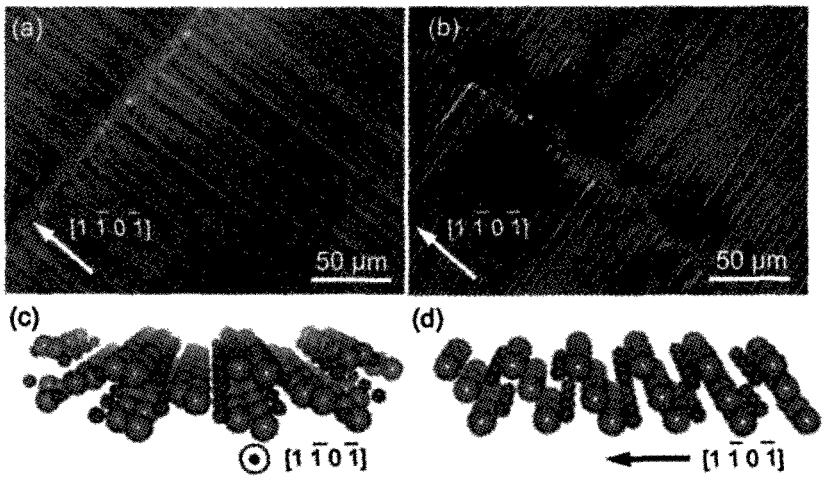

Figure 1. SEM images of the aligned SWNTs on the plain (a) and miscut (b) r-plane sapphire substrates. (c,d) Corresponding atomic arrangements of r-plane surface viewed from the aligned direction. The small and large atoms indicate Al and O, respectively.

[1] H. Ago *et al.*, *Chem. Phys. Lett.*, **408**, 433 (2005). [2] C. Kocabas *et al.*, *J. Phys. Chem. C*, **111**, 17883 (2007).

Corresponding Author: Hiroki Ago (Tel&Fax: +81-92-583-7817, E-mail: ago@cm.kyushu-u.ac.jp)

3P-37

High Precision Site-selective Growth of SWNTs and its Applications

○Rong Xiang, Shinya Aikawa, Erik Einarsson, Junichiro Shiomi, Shigeo Maruyama

Department of Mechanical Engineering, the University of Tokyo

We recently proposed a versatile wet chemistry method to localize the growth of SWNTs to desired regions via surface modification. By functionalizing the silicon surface using a classic self-assembled monolayer (SAM) and then selectively removing the SAM by ultraviolet (UV) light, the catalyst can be dip-coated onto only the hydrophilic areas of the substrate. Using the e-beam in a conventional SEM, a 50 nm SWNT pattern can be easily obtained. This technique was successful in producing both random and aligned SWNTs with various patterns.[1]

In this work, we will further discuss the mechanism of such growth selectivity. By AFM imaging of the SAM formation process, we clearly reveal the effect of wettability on the density of SWNTs grown on the surface. Meanwhile, the compatibility and scalability of this method will be presented. Large area pattern can be obtained by applying this technique into commercial e-beam lithography. Since monolayer (~2 nm high) reduces the electron scattering, the resolution is further improved. In the end, the application of current method for the easy fabrication of a field effect transistor will be demonstrated.

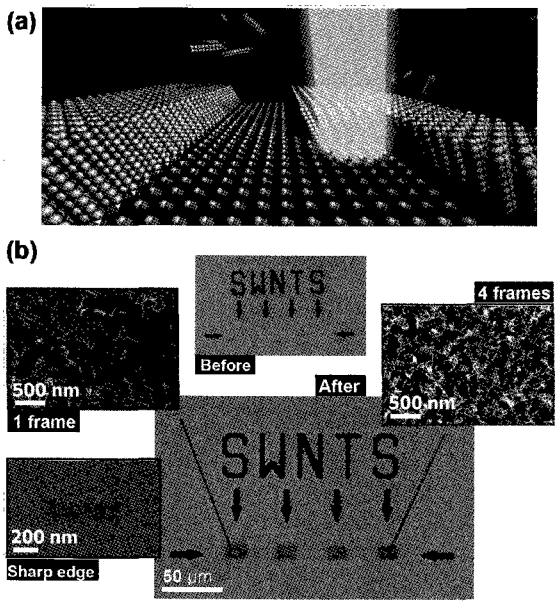

Figure 1: (a) Schematics describing the process of removing OTS by nanometer-size electron beam; (b) SEM images of SWNTs grown in the regions where OTS were selectively removed, suggesting the location and density of SWNTs can be controlled.

References:

1. R. Xiang, T. Wu, E. Einarsson, Y. Suzuki, Y. Murakami, J. Shiomi, S. Maruyama, *J. Am. Chem. Soc.*, submitted.

Corresponding Author: Shigeo Maruyama
E-mail: maruyama@photon.t.u-tokyo.ac.jp

3P-38

Observation of Photoreaction Process of Molecules within Single-Wall Carbon Nanotube by High Resolution Transmission Electron Microscopy

○Keita Kobayashi, Kazutomo Suenaga, Takeshi Saito and Sumio Iijima

Research Center for Advanced Carbon Materials, National Institute of Advanced Industrial Science and Technology (AIST), Tsukuba 305-8565, Japan

The inner space of single-wall carbon nanotubes (SWCNTs) provides an effective space for the hold of many kinds of molecules. Since the molecules in the low-dimensional nanospace, such as an inner space of SWCNT, show unique properties and behaviors that differ from bulk materials, considerable research efforts have been devoted to encapsulation of molecules within inner space of SWCNTs [1-4]. Moreover, graphene sheets are almost transparent for electron beams much like glass is transparent for visible light. Thus it is expected that the behaviors of molecules within the inner space of SWCNTs during chemical and physical reaction of them can be observation directly by using high resolution transmission electron microscope (HR-TEM), much like the observation of a reaction within a test tube [5-8]. The HR-TEM observation of the reaction process of the molecules within SWCNTs is very important for understanding the reaction mechanisms of them. In addition, since such molecules within the low-dimensional nanospaces, therefore, are expected to exhibit unusual behaviors that differ from bulk materials during reaction processes, HR-TEM observations of photoreaction of AgBr within SWNTs on the atomic scale are a subject of considerable interest.

In this study, the photo-reactive molecules, such as metal-halides and organic molecules, within SWCNTs are prepared with the aim of observing the detail of photoreaction process. The photo-reactive molecules within SWCNTs obtained were exposed by continuous-wave UV semiconductor laser light at a wavelength of 375 nm (COHERENT, CUBE 375-16C) and 406 nm (COHERENT, CUBE 406-150C) in air atmosphere or within the TEM column. The structure changes of the molecules within SWCNTs due to the UV laser light irradiation was investigated by comparing to the pristine molecules within SWCNTs by HR-TEM (JEOL, JEM-2100F/UHR) operating at 120 kV.

In the presentation, we will discuss about photoreaction process due to UV laser light irradiation based on the HR-TEM observations.

References

[1] B. W. Smith, M. Monthioux and D. E. Luzzi, *Nature*, **396**, 323 (1998)

[2] M. Monthioux, *Carbon*, **40**, 1809 (2002).

[3] R. Kitaura and H. Shinohara, *Chem. Asian J.*, **1**, 646 (2006).

[4] R. Kitaura and H. Shinohara, *Jpn. J. Appl. Phys.*, **46**, 881 (2007).

[5] J. Sloan, A. I. Kirkland, J. L. Hutchison and M. L. H. Green, *Chem. Commun.*, 1319 (2002).

[6] G. A. Britz, A. N. Khlobystov, K. Porfyrakis, A. Ardavan and G. A. D. Briggs, *Chem. Commun.*, 37 (2005)

[7] Z. Liu, K. Yanagi, K. Suenaga, H. Kataura and S. Iijima, *Nat. Nanotechnol.*, **2**, 422 (2007).

[8] K. Kobayashi, Ph. D. Thesis, Nagoya Univ. (2009).

Corresponding Author: Kazutomo Suenaga

TEL: +81-29-861-5694, FAX: +81-29-861-4806, E-mail: Suenaga-kazu@aist.go.jp

3P-39

Host-Guest Interaction between Azafullerene And Single-Wall Carbon Nanotubes in Peapod Structure

○Yoko Iizumi,[1,2] Toshiya Okazaki,[1,2,3] Zhen Liu,[2] Kazu Suenaga,[2] Takeshi Nakanishi,[2] Sumio Iijima,[2] and Nikos Tagmatarchis[4]

[1]*Department of Chemistry, University of Tsukuba, Tsukuba 305-8577, Japan*
[2]*Nanotube Research Center, AIST, Tsukuba 305-8565, Japan*
[3]*PRESTO, JST, Kawaguchi 332-0012, Japan*
[4] *Theoretical and Physical Chemistry Institute, National Hellenic Research Foundation, Athens 11635, Greece*

Control of physical properties of solids by doping molecules or atoms is the common practice in the materials science. For single-wall carbon nanotubes (SWCNTs), such doping technique is extremely important from the viewpoints of both basic science and practical applications. One of the most characteristic features of SWCNTs is to have an inner space equivalent to molecule sizes. Doping molecules to the inner space, compared with the outside, is expected to be a useful technique for realistic applications of SWCNTs in terms of increasing their stability and durability. Indeed, controlled doping states of SWCNTs have been achieved by encapsulating various fullerenes, so-called nanopeapods (NPDs), and the other organic molecules. Among these, azafullerene NPDs have recently gained attention because it has been reported that encapsulated azafullenes change the transport properties of SWCNTs from *p*-type to *n*-type in FET structure [1]. However, the azafullerene encapsulation effect on the electronic structure of SWCNTs still remains unclear.

We here report the interaction between host SWCNTs and the guest azafullerenes in detail by photoluminescence (PL) and chemical doping studies. UV–vis–NIR absorption spectra of azafullerene NPDs, C_{60} NPDs and control-SWCNTs films are depicted in Fig. 1. The similarity in shapes of these spectra suggests absence of strong interaction such as charge transfer between encapsulated fullerenes and the host tubes. In order to investigate the effects of azafullerene on SWCNTs in terms of individual chiral indices, we carried out PL excitation/emission (PLE) study on the azafullerene NPDs dissolved in micellar solution (Fig. 2). The feature of the PLE map is considerably similar to that of C_{60} NPDs and the PL peak positions are coincident with those of C_{60} NPDs within 0.01 eV [2]. These observations indicate that interaction between SWCNTs and azafullerene can be explained in terms of the repulsive and the π-π attractive forces between them which has been observed in the case of C_{60} nanopeapods [2].

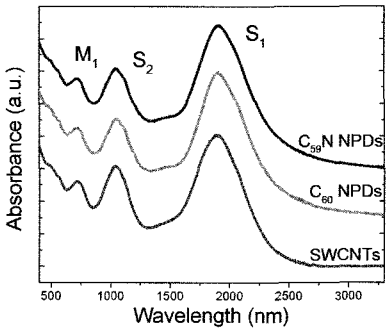

Figure 1. Optical absorption spectra of azafullerne NPDs, C_{60} NPDs and control-SWCNTs (from bottom to up).

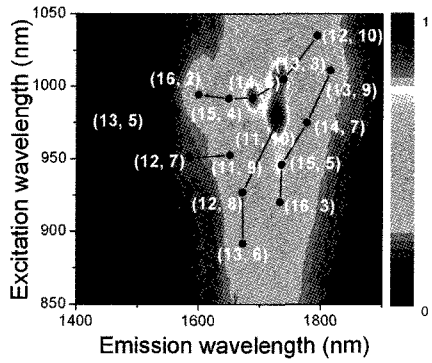

Figure 2. 2D-PL mapping of azafullerene NPDs

[1] T. Kaneko *et al.*, *J. Am. Chem. Soc.* **2008**, *130*, 2714. [2] S. Okubo *et al.*, *J. Phys. Chem. C* **2009**, *113*, 571.

Corresponding Author: Toshiya Okazaki **E-mail:** toshi.okazaki@aist.go.jp **Tel:** 029-861-4173 **Fax:** 029-861-6241

3P-40

Creation and Property Evaluation of Calcium Encapsulated Single-Walled Carbon Nanotubes

○Y. Osanai, T. Shimizu, T. Kato, W. Oohara*, and R. Hatakeyama

Department of Electronic Engineering, Tohoku University, Sendai 980-8579, Japan
** Graduate School of Science and Engineering, Yamaguchi University, Yamaguchi 755-8611, Japan*

Carbon nanotubes (CNTs) with nanometer-order diameter and millimeter-order length attract a great deal of attentions due to their novel applications such as next-generation nanoelectronic devices. Accommodation of various dopant atoms, molecules, and compounds makes it possible to modify the intrinsic electronic and optical properties of single-walled carbon nanotubes (SWNTs). According to our past research, alkali-metal- and halogen-encapsulated SWNTs are found to exhibit n-type and p-type semiconducting behaviors under the field-effect transistor (FETs) configuration [1], respectively. This indicates that alkali-metal and halogen atoms, which form singly-charged positive and negative ions, operate as an electron donor and an electron acceptor, respectively [2, 3]. If alkali-earth metal atoms which form doubly-charged positive ions are encapsulated in SWNTs, the n-type property would be expected to be enhanced. With this aim, an alkaline-earth plasma consisting of calcium (Ca) positive ions has been developed and utilized to encapsulate them in the hollow space of SWNTs. Electronic transport characterization of Ca encapsulated SWNTs (Ca@SWNTs) under the FET configuration is also precisely investigated.

Transmission electron microscopy (TEM) is used to observe the formation of Ca@SWNTs, which is realized by applying a negative bias (−100 V) to a substrate covered with dispersed SWNTs. A few chains like structure is observed in SWNTs, as shown in Fig. 1, which indicates that the formation of Ca@SWNTs can be achieved in this experimental system. Furthermore, the thin film of SWNTs with an n-type behavior is possibly made, and such film is expected to be used in various kinds of nano electronics devices.

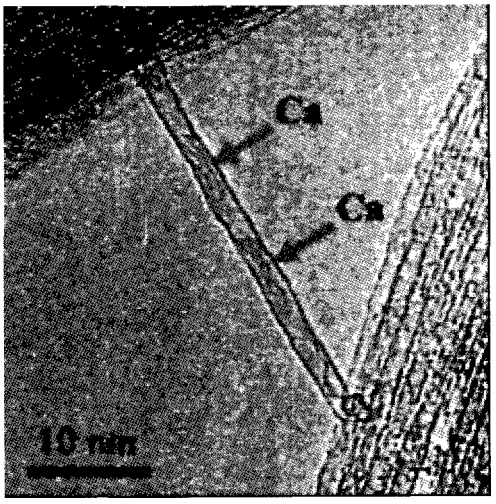

Fig. 1. TEM images of Ca@SWNTs.

Reference:
[1] V. Derycke, R. Martel, J. Appenzeller, and Ph. Avouris, Appl. Phys. Lett. **80**, 2773 (2002).
[2] T. Izumida, R. Hatakeyama, Y. Neo, H. Miura, K. Omote, and Y. Kasama, Appl. Phys. Lett. **89**, 093121 (2006).
[3] J. Shishido, T. Kato, W. Oohara, R. Hatakeyama, and K. Tohji, Jpn. J. Appl. Phys. **47**, 2044 (2008).

Corresponding Author Y. Osanai

E-mail: osanai@plasma.ecei.tohoku.ac.jp

Tel&Fax: +81-22-795-7046 / +81-22-263-9225

3P-41

Spectroscopic Characterization on the High-Yield Filling of Eu-Nanowires inside Single-Wall Carbon Nanotubes.

○R. Nakanishi[1], R. Kitaura[1], T. Yoshimoto[1], T. Saito[2,3], Y. Miyata[1] and H. Shinohara[1]

[1]*Department of Chemistry & Institute for Advanced Research, Nagoya University, Nagoya 464-8602, Japan*
[2]*Reseach Center for Advanced Carbon Materials, AIST, Tsukuba 305-8565, Japan*
[3]*PRESTO, Japan Science and Technology Agency, Kawaguchi 332-0012, Japan*

Single-wall carbon nanotubes (SWCNTs) have narrow diameters (typically 1~2 nm), which form chemically and thermally stable one-dimensional (1D) nano space. They can be used as a nano-sized reaction vessel to fabricate novel low-dimensional nanomaterials such as peapods [1], nanoclusters [2] and nanowires [3]. So far, we have developed a high yield fabrication technique of metal nanowires in 1D space of CNTs and found that the nanowires possesses low-dimensional characteristic structures that are much different from that of bulk crystals. In this study, we have focused on a large amount of synthesis of Eu-nanowires@SWCNTs and investigated their electronic structure by using absorption, photoluminescence and Raman spectroscopy.

We have synthesized Eu-nanowires@SWCNTs according to the previously reported procedures: vacuum sealing of cap-opened SWCNTs together with Eu in a Pyrex glass tube under 10^{-4} Pa followed by thermal heating at 823 K for 2 days. From high-resolution TEM (HRTEM) observations after removing Eu attached on the outer surface of SWNTs, we can estimate the filling ratio of Eu as high as ca.90 % (Fig.1). Based on Raman measurements (Fig.2), UV-Vis absorption and photoluminescence spectroscopy, a charge transfer induced electronic structure change is discussed.

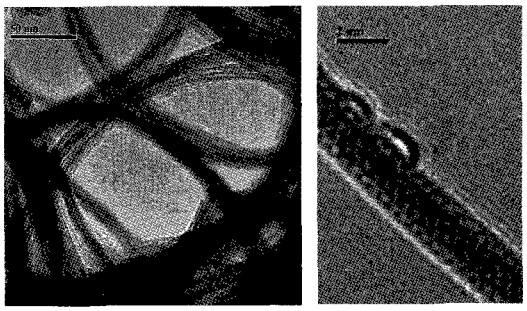

Figure. 1 HRTEM images of Eu-nanowires @SWCNTs at Low (left) and High (right) magnification.

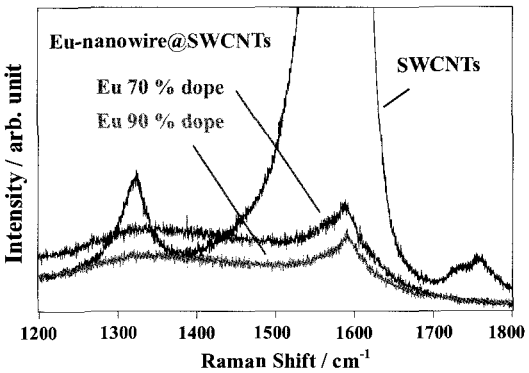

Figure. 2 Raman spectra of SWCNT and Eu-nanowires@SWCNTs at 633 nm excitation.

Reference:
[1] K. Hirahara et al., *Phys. Rev. Lett.* **85**, 5384 (2000).
[2] F. Stercel et al., *Mater. Res. Soc. Symp. Proc.* **706** Z7.8.1 (2002).
[3] R. Kitaura et al., *Nano Lett.* **8**, 693 (2008).

Corresponding Author: Shinohara Hisanori
E-mail: noris@nagoya-u.jp
Tel: (+81) 52-789-2482, **Fax:** (+81) 52-747-6442

3P-42

Evolution and Growth of Linear-Polyynes Inside Thin Double-Wall Carbon Nanotubes

○Chen Zhao, Ryo Kitaura, Hironori Hara, Stephan Irle and Hisanori Shinohara

Department of Chemistry & Institute for Advanced Research, Nagoya University, Nagoya 464-8603, Japan

One-dimensional (1D) nano-space of carbon nanotubes (CNTs) provides us an ideal nano-reaction space to fabricate novel low-dimensional nanomaterials that are difficult to synthesize in bulk reactions. In this study work, we have successfully fabricated long linear carbon chains, whose lengths correspond was estimated to those of be more than 50 atoms, in 1D space of CNTs by fusion reaction of polyyne molecules. In this reaction, ultra thin 1D nano-space of a double wall carbon nanotube (DWCNTs) plays a crucial role. Formation of long linear chains is investigated by Raman spectroscopy and a Density Functional based Tight Binding (DFTB) simulation. After encapsulation of polyyne molecules in DWCNTs, the sample was annealed at 1273 K under high vacuum for 24 hours. After the high temperature annealing, Raman bands arising from encapsulated polyyne molecules completely disappear and new Raman bands appear at 1800-1850cm^{-1}. Raman spectra of annealed empty DWCNTs, pristine and annealed $C_{10}H_2$@DWCNTs are shown in Fig. 1. This is clear evidence that fusion reaction occurs to form long linear carbon chains inside 1D space of DWCNTs. The presence of such fusion reaction of polyynes has verified by Molecular Dynamics (MD) simulation based on DFTB calculations as shown in Fig. 2.

In this presentation, we report detailed characterization of the fusion reaction inside DWCNTs with Raman spectroscopy, high-resolution transmission electron microscopy and DFTB calculations.

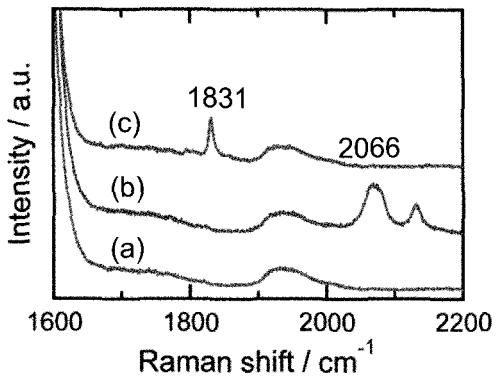

Fig. 1: Raman spectra of (a) annealed DWCNTs, (b) Pristine $C_{10}H_2$@DWCNTs and (c) annealed $C_{10}H_2$@DWCNTs (ex. @514)

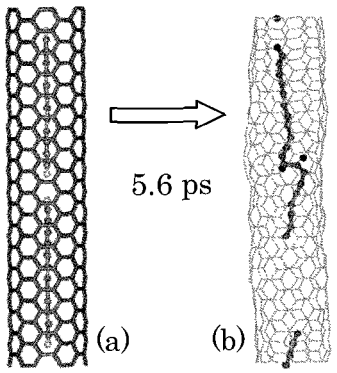

Fig.2: MD simulation of fusion reaction: (a) Initial structure model of $C_{12}H_2$@SWCNTs, (b) Structure after 5.6 ps MD simulation at 3000 K.

Corresponding Author: Hisanori Shinohara,

E-mail: noris@nagoya-u.jp, **TEL:** +81-52-789-2482, **FAX:** +81-52-747-6442

3P-43

Structure Analysis of Single-Wall Carbon Nanohorns

M. Irie[1], J. Xu[2], R. Yuge[3], S. Iijima[1,2,3], M. Yudasaka[1]

[1] *AIST, 1-1-1 Higashi, Tsukuba*
[2] *Meijo University, Tenpaku-ku, Nagoya*
[3] *NEC Corporation, Miyukigaoka, Tsukuba*

Studies on the structure of aggregate of single-wall carbon nanohorns (SWNHs) have shown that the aggregate with a diameter of about 100 nm is composed of approximately two thousands of SWNHs, and often several SWNHs aligned almost in parallel in the aggregate. The aggregate also contains few graphene sheets, called "Petal". Recent research revealed that a big population of the aggregates have caves (diameters; 10~20 nm) near their centers. We previously revealed that there were high-temperature-combustion components (~35%) in the aggregates which were assigned to the Petals and thermo-chemically metamorphosed parts of densely-packed SWNHs. We show in this report that reduction of the high-temperature-combustion parts was possible by mild oxidation.

We treated as-grown SWNHs with aqueous solution of H_2O_2, washed with pure water, and dried at 60°C in vacuum. Thermogravimetric analysis showed that the high-temperature combustion components for the obtained SWNHs decreased to 20% from the 35% for the as-grown SWNHs (Fig. 1). We consider that the mild H_2O_2 treatments made the Petals to combust preferentially. The mild H_2O_2 treatment also combusted the defects sites of SWNHs, leading to the hole opening as confirmed by the increase of m-xylene adsorption by SWNHs.

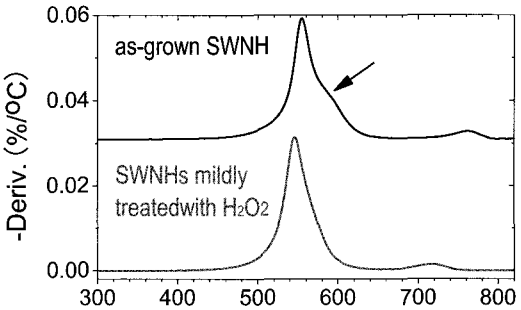

Fig. 1 Thermogravimetric analysis of as-grown SWNHs and SWNHs mildly treated with H_2O_2. The high-temperature component is indicated with an arrow.

References
[1] M. Irie, R. Yuge, S. Iijima, and M. Yudasaka, The 33rd Fulleren-Nanotube Symposium, 2009

Corresponding Author
M. Yudasaka
E-mail: m-yudasaka@aist.go.jp
Tel: 029-861-4818

3P-44

Cytotoxicity of Single-Wall Carbon Nanohorns

T. Fujinami[1], J. Xu[2], Y. Myouhara[1], S. Iijima[1,2], M. Yudasaka[1]

[1] *AIST, Higashi, Tsukuba*
[2] *Meijo University, Tenpaku, Nagoya*

Studies on potential application of single-wall carbon nanohorn (SWNH) have suggested that SWNH will be practically useful for materials storages or adsorption. For the practical uses, toxicity of SWNHs has been examined both in vitro and in vivo, and, as previously reported, no toxicity of SWNHs has been found. In this study, we have compared the cytotoxicity of as-grown SWNH (asSWNH) and hole-opened SWNHs (oxSWNHs) up to high dosages.

The asSWNHs and oxSWNHs were dispersed in PBS or culture medium using a dispersant, DSPE-PEG. The dispersion states in the physiological solutions were evaluated by the measurements of dynamic light scattering and optical absorbance change with time. In our experiments, the cell (HeLa, NIH3T3) viabilities were examined with WST-1 assay by rearranging the assay protocol for the least contact of the dyes to the nanohrns. Since the dyes easily adsorbs on the nanocarbons, the least contact of dyes with nanohorns was important to avoid the false results [1]. To confirm the WST-1 assay results and to find the differences of the interactions of cells with asSWNHs and oxSWNHs, we observed the cells with confocal microscopy.

The results indicated that asSWNHs showed no cytotoxicity up to 1 mg/mL of asSWNH in the culture medium, which agrees with the previous results [1]. On the other hands, oxSWNH showed higher toxicity. This tendency was confirmed by the confocal microscopy observation. The cell uptakes were similarly observed for both asSWNHs and oxSWNHs, however, a major difference was that the number of oxSWNHs attached to the cell surfaces was extremely larger than that of asSWNHs. The large amount of oxSWNHs covering the cells might hinder the uptake of nutrients, leading to the cell death. The abundant adhesion of oxSWNH on the cell surfaces may have the relation with the poor dispersion of oxSWNH in the medium.

References
[1] H. Isobe et al. "Preparation, Purification, Characterization, and Cytotoxicity Assessment of Water-Soluble, Transition-Metal-Free Carbon Nanotube Aggregates" *Angew. Chem. Int. Ed.* 45, 6676-6680(2006).

Corresponding Author
M. Yudasaka
E-mail: m-yudasaka@aist.go.jp
Tel: 029-861-4818

3P-45

The edge-shape dependence of Raman spectra for Graphene

○T. Mori[1], K. Takai[1], K. Sasaki[2], K. Wakabayashi[2,3], and T . Enoki[1]

[1]*Department of Chemistry, Tokyo Institute of Technology, Ookayama, Meguroku, Tokyo 152-8551, Japan*

[2]*National Institute for Materials Science, Namiki, Tsukuba 305-0044, Japan*

[3]*PRESTO, Japan Science and Technology Agency, Kawaguchi 332-0012, Japan*

The investigation of nano-sized graphene (nanographene) is one of the most important aspects among the current topics for graphene. For nanographene, the large contribution of the edge results in the edge-shape effect on the electronic structure [1, 2]. To characterize graphene related materials, Raman spectroscopy is useful in acquiring information on the structure and electronic properties. In this study, we present the results of Raman spectroscopy for graphene edge and their edge-shape dependence.

Figure 1(a) shows optical image of the exfoliated graphene with the edges crossing each other with the angle of ~30°. In many cases, graphene samples obtained by cleavage method are found with the edges having an angle of a multiple of 30° with respect to the adjacent edges. This angle can be interpreted as an evidence for the presence of the edges predominantly composed of zigzag or armchair edges. Thus, one of the edges is assigned to the zigzag direction edge in Fig.1 (b), while the other directs along the armchair. Based on the Raman 2D band, the obtained sample is characterized as the multi-layer graphene (~5 layers). The position dependence of the Raman G-band is shown in Fig. 1(b), where the laser spot diameter is about 1 μm. When the spot is positioned near the upper edge (A) or far from the edge, the G-band position is almost similar to that for bulk graphite (1582 cm^{-1}). However, a softening of G-band is clearly seen in the vicinity of the lower edge (B). The observed edge direction dependence of the G-band shift cannot be simply related to the local variation of the doping level around the edge. The present results suggest that G-band can be used for identification of the edge geometry in graphene.

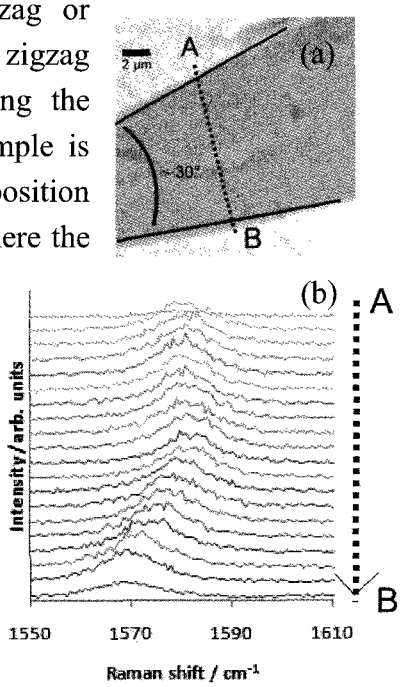

Fig.1 The optical image of graphene sample (a), and the position dependence of Raman G-band (b)

[1] M. Fujita, K. Wakabayashi *et al.*, J. Phys. Soc. Jpn. **65**, 1920 (1996).

[2] T. Enoki and K. Takai, Dalton Trans., 3773 (2008)

Corresponding Author: Kazuyuki Takai

TEL: +81-3-5734-2610, FAX: +81-3-5734-2242, e-mail: ktakai@chem.titech.ac.jp

3P-46

Nano-graphitization and mesoscopic large corrugation of amorphous carbon thin films by high temperature post-annealing

○Takuya Noguchi[1], Toshihiro Shimada[1], Takashi Chiba[2], Masao Terada[2], Tetsuya Hasegawa[1]

[1] *Department of Chemistry, The University of Tokyo, Tokyo 113-0033, Japan*
[2] *R&D Center, Sakaguchi E.H. VOC. Corporation, Tokyo 101-0021, Japan*

Graphene has attracted much attention for electronic applications because it exhibits carrier mobility much higher than those of other electronic materials used today [1]. Mass-production and direct preparation techniques of graphene on an insulating substrate, however, have not been established yet, while transfer of graphene deposited on a metal surface to an arbitrary substrate including SiO_2/Si has come to a certain degree of success [2]. We are pursuing graphene fabrication methods employing very high temperature process without transition metal catalysts [3, 4]. In this study, we report the effects of post-annealing of amorphous carbon thin films deposited by a pulsed laser deposition method. To achieve very high temperatures (1600–3000 K) without graphite contamination from the heater during annealing, we used refractory oxides (MgO, Al_2O_3 and yttria-stabilized zirconia (YSZ)) as substrates. All annealing experiments were conducted in a high vacuum chamber with the base vacuum pressure under 10^{-4} Pa.

Through post-annealing as-deposited thin films (< 100 nm thick) on oxide substrates, nano-scale graphitization (nano-graphitization) of the films was confirmed by Raman analysis of carbon G/D peaks, which is consistent with similar experiments using thicker films (> 1 μm thick) reported before [5, 6]. Besides of this microscopic structural difference, surface morphology drastically changed, which has never been reported. A protrusion on the film surface with the height of more than 1 μm was observed after annealing by both optical and atomic force microscopes (AFM) as shown in Fig. 1. These protrusions vanished after focused laser beam was irradiated (power density: ~10^5 W/cm^2, spot size: ~ 1 μm^2), indicating that these are corrugation caused by gases generated at the film/substrate interface during the annealing [7].

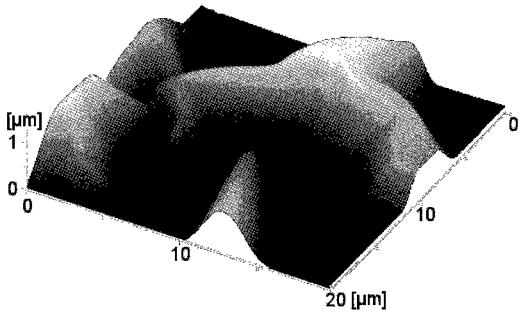

Fig. 1 A typical AFM image of the annealed film surface (20×20 μm^2).

References: [1] A. K. Geim and K.S. Novoselov, *Nature Materials* **6**, 183 (2007). [2] A. Reina, X. Jia, J. Ho, D. Nezich, H. Son, V. Bulovic, M. S. Dresselhaus and J. Kong, *Nano Letters* **9**, 30 (2009). [3] X. Li, W. Cai, J. An, S. Kim, J. Nah, D. Yang, R. Piner, A. Velamakanni, I. Jung, E. Tutuc, S. K. Banerjee, L. Colombo and R. S. Ruoff, *Science* **324**, 1312 (2009). [4] T. Noguchi, T. Shimada, A. Hanzawa and T. Hasegawa, *Thin Solid Films*, in press.; T. Noguchi et al., Abstract of The 35th Fullerene-Nanotubes General Symposium, 3P-23 (p. 153) (2009). [5] K. Takai, M. Oga, H. Sato, T. Enoki, Y. Ohki, A. Taomoto, K. Suenaga and S. Iijima, *Phys. Rev. B* **67**, 214202 (2003). [6] L. G. Cançado, K. Takai, T. Enoki, M. Endo, Y. A. Kim, H. Mizusaki, A. Jorio, L. N. Coelho, R. Magalhães-Paniago and M. A. Pimenta, *Appl. Phys. Lett.* **88**, 163106 (2006). [7] T. Noguchi, T. Shimada, T. Chiba, M. Terada and T. Hasegawa, *submitted.*

Corresponding Author: Toshihiro Shimada
E-mail: shimada@chem.s.u-tokyo.ac.jp **Tel & Fax:** +81-3-5841-9575

3P-47

Electronic Structures of Folded Graphene

Yoshiteru Takagi[1,2] and Susumu Okada[1,2]

[1]*Center for Computational Sciences and Graduate School of Pure and Applied Science, University of Tsukuba, Tsukuba 305-8577, Japan*
[2]*CREST, Japan Science and Technology Agency, 4-1-8 Honcho, Kawaguchi, Saitama 332-0012, Japan*

Recently, edge reconstruction has been observed in thermally treated graphite by means of atomically resolved high resolution transmission electron microscope [1]. Atomic structure of the edge reconstruction is now considered to be a pair of graphene sheets one of which edges are smoothly connected each other by a part of carbon nanotubes with appropriate diameter and chirality [Fig 1(a)]. The structure gives us a question that the electronic structure of the folded graphene is the same as that of the conventional graphene sheet or that of the bilayer graphene. To elucidate the issue, we performed the electronic structure calculations on the folded graphene as shown in Fig. 1(a) based on the generalized tight-binding model. Surprisingly, electronic structures of a folded graphene differ from those of graphene and bilayer graphene. π-electronic band structures for a folded graphene are asymmetric with respect to the Fermi energy, although those for graphene and graphite almost are symmetric with respect to the Fermi energy. Calculated STM image of the folded graphene reflects the asymmetry.

Fig.1 (a)

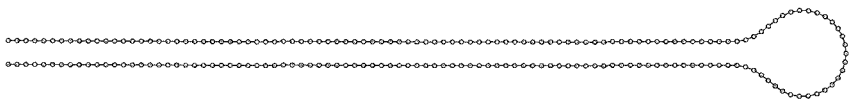

(b)

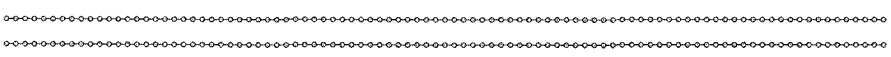

Geometric structure of (a) folded graphene and (b) bilayer graphene.

[1] Z. Liu, K. Suenaga, P.J.F. Harris, and S. Iijima: Phys. Rev. Lett. **102** (2009) 015501.

Corresponding Author: Yoshiteru Takagi
E-mail: ytakagi@comas.frsc.tsukuba.ac.jp, TEL: +81-29-853-5600(8233), FAX:+81-29-853-5924

3P-48

Combinatorial study on Fe-SnO_2 catalyst for synthesis of carbon nanocoils

○Hiroshi Fujita, Takayuki Arie, and Seiji Akita

Department of Physics and Electronics, Osaka Prefecture University, 1-1 Gakuen-cho, Naka-Ku, Sakai, Osaka 599-8531, Japan

It has been reported that multiwalled carbon-nanocoils (CNCs) can be synthesized by using thin Fe-Sn catalysts with the thickness less than 5 nm[1]. However, the detailed analysis for the structural and morphological changes of layered catalysts for growth of CNCs is still an open subject. In this report, we investigate the influences of both the thickness and the composition ratio of the Fe-SnO_2 catalyst for synthesis of CNCs by combinatorial method[2].

Two elements of Fe and SnO_2 were used as the catalysts. To perform the combinatorial study, each catalyst was deposited layer-by-layer using a sputtering method, where the thickness of each layer was gradually changed on the same substrate. Thus, the catalyst with the different composition ratio and the thickness was successfully fabricated as shown in Fig. 1. Carbon nanocoils were synthesized by the thermal chemical vapor deposition (CVD) at 700 °C using C_2H_2 as a source gas at atmospheric pressure.

Figure 1 shows a photograph of the substrate after the CVD. The CNC growth is observed at gray area surrounded by dotted line. In the region of Fe layer thicker than 4 nm, the CNC growth was observed at a thin SnO_2 layer region. This indicates that the enough iron is required to grow CNCs. The coil diameter becomes small with decreasing the total thickness of the catalyst layer in this region. Non-coil shape products such as twist-coils increases with decreasing the total thickness, even under the same composition ratio. Figures 2(a) and 2(b) show respectively scanning electron microscopy (SEM) images of the grown CNCs at (a) and (b) indicated in Fig. 1, corresponding to the different composition ratio of the catalyst. The coil diameter becomes small with decreasing the Sn ratio and non-coil shape products such as twist-coils increases with the ratio, which are similar to those in the case of thickness reduction. Thus, not only the composition ratio of Sn but also the total thickness of catalysts play a crucial role for both the formation of coiled structure and the determination of the coil-line diameter.

Acknowledgement: This work was supported by the Osaka Prefecture Collaboration of Regional Entities for the Advancement of Technological Excellence, JST.

[1] R. Kanada *et al*, Jpn. J. Appl. Phys.**47** (2008) 1949. [2] S. Noda et al, Carbon **44** (2006) 1414.

Corresponding Author: Seiji Akita, Tel&Fax: 072-254-9261, E-mail: akita@pe.osakafu-u.ac.jp

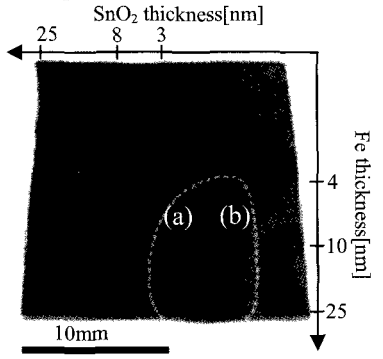

Fig. 1 Photograph of the substrate after CVD process.

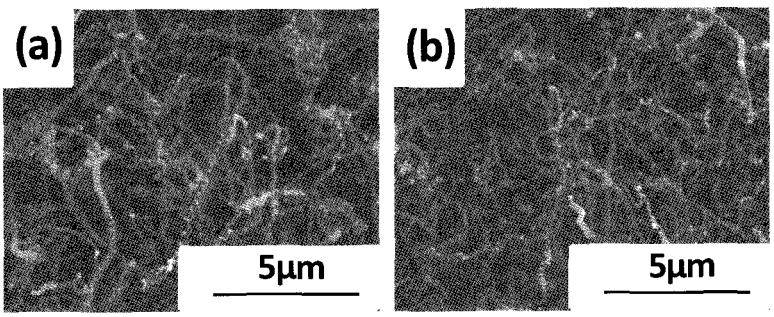

Fig. 2 SEM images of grown CNCs at (a) and (b) in Fig.1, corresponding to the different composition ratio of the catalyst.

発表索引
Author Index

Author Index

~A~

Abe, Katsuyoshi 2P-36
Achiba, Yohji 1-10, 2-16, 1P-34, 2P-31
Ago, Hiroki 1-5, 2P-34, 3P-36
Aida, Takuzo 2-3, 2-12
Aikawa, Shinya 2P-37, 3P-29, 3P-37
Akasaka, Takeshi 2-2, 2-3, 2-17, 1P-6, 1P-8, 1P-9, 1P-11, 1P-12, 2P-5, 2P-6, 2P-7, 2P-8, 2P-9, 2P-10, 2P-48, 3P-8, 3P-19, 3P-20
Akita, Seiji 1P-14, 1P-27, 3P-31, 3P-48
Ando, Tsuneya 2P-21
Ando, Yoshinori 3P-22
Aoki, Yusuke 1P-10, 2P-14
Aono, Takayuki 2P-12
Aoyagi, Shinobu 2P-12
Aoyama, Ryo 2P-9
Arai, Toru 3P-26
Araujo, Paulo T. 1P-15
Arie, Takayuki 1P-14, 1P-27, 3P-31, 3P-48
Asada, Yuki 3-11
Asai, Tomohito 1P-19
Asaka, Koji 2-1, 1P-19
Asano, Hirohito 1P-45
Asano, Takeshi 2-5
Atake, Tooru 3P-13
Awa, Shigeki 2-13
Ayala, P. 1P-20

~B~

Bandow, Shunji 1P-44, 1P-45
de Blauwe, K. 1P-20

~C~

Cha, Jin Hyeok 3P-21
Chiba, Takashi 3P-46
Chigusa, Hajime 2P-46

~D~

Dang, J. S. 3P-14
Dorn, Harry C. 2S-2
Dresselhaus, Mildred S. 3-5, 1P-15
Dressselhaus, Gene 3-5

~E~

Einarsson, Erik 1-14, 2P-33, 3P-29, 3P-37
Endo, Hiroki 1P-44, 1P-45
Endoh, Hiroyuki 1-15
Enoki, T. 3P-45
Enoki, Toshiaki 1-1
Enomot, S. 2P-43

~F~

Feng, Y. 1P-20
Follath, R. 1P-20
Fueno, Hiroyuki 1P-29
Fujie, Tetsuo 3P-8
Fujigaya, Tsuyohiko 3-4, 1P-25, 2P-38, 3P-27
Fujii, Motoo 1-6
Fujimoto, Yoshitaka 2P-23
Fujimura, Yohhei 1P-26, 2P-27, 3P-30
Fujinami, Takako 1-9, 1P-41, 3P-44
Fujino, Masahisa 3-9
Fujita, Hiroshi 3P-48
Fujita, Wataru 2-16
Fujita, Yasuhiko 2P-1
Fukagawa, Tsuyoshi 3P-23
Fukami, Shun 1P-14
Fukui, Munetoshi 2P-34
Fukumaru, Takahiro 1P-25
Fukuoka, Tomoko 1-7
Furuta, Atsushi 3P-26
Futaba, Don N. 1-11, 1P-30, 3P-24, 3P-25, 3P-34

~G~

Gao, Xingfa 1-4
Ghorannevis, Z. 3P-33
Gotou, Jundai 1-11

~H~

Hajjaj, Fatin 2-3
Hara, Hironori 3P-42
Harigaya, Kikuo 2-8
Haruyama, J. 2P-43
Haruyama, Junji 2P-45
Hasegawa, Tadashi 2-17, 1P-12, 3P-19, 3P-20

Hasegawa, Tetsuya 3P-46
Hashiguchi, Masahiko 1P-7
Hashimoto, Takeshi 3P-23
Hata, Kenji 3S-2, 1-11, 1P-30, 3P-24, 3P-25, 3P-34
Hatakeyama, R. 3P-33
Hatakeyama, Rikizo 3-10, 1P-23, 2P-29
Hatakeyama, Rikizou 3P-40
Hayamizu, Yuhei 1P-30
Hayashi, Yasuhiko 1P-24, 2P-36
Heguri, Satoshi 1P-47
Hino, Shojun 1P-10, 2P-14, 2P-15
Hirana, Yasuhiko 2-4
Hirose, Kaori Takai 1P-38
Hirotsu, Takahiro 1P-22, 2P-26
Hiura, Hidefumi 2P-44
Hizume, Yumi 2-12
Homma, Yoshikazu 2-6
Hongyou, Ken-ichi 2P-20, 3P-15
Honma, Itaru 1-2
Horikawa, Kazunori 2P-36
Hosono, Eiji 1-2
Hu, Chunping 1-19
～I～
Ichihashi, Toshinai 1-9
Ichiki, Takahiko 1P-4
Ide, Natsuko 2P-38
Ihara, Kazuki 1-15
Iijima, Hiroaki 2P-11
Iijima, S. 3P-43
Iijima, Sumio 1-7, 1-9, 1-17, 1P-41, 1P-44, 1P-45, 2P-22, 2P-39, 2P-40, 2P-42, 3P-38, 3P-39, 3P-44
Iijima, Toru 2P-36
Iio, Yasunari 2P-2, 3P-10
Iizumi, Yoko 1P-38, 3P-39
Ikeda, Ken-ichi 1-5
Ikeda, Takashi 2P-27
Ikuta, Tatsuya 1-6, 2P-34, 3P-36
Imahori, Hiroshi 3-7
Imamoto, Kenta 2P-34
Inada, Koji 2-17
Inoue, Akihito 1-10
Inoue, Akira 2P-31
Inoue, Takashi 3P-11
Inoue, Takumi 2-15
Irie, Hiroshi 1-9
Irie, M. 3P-43
Irle, Stephan 3P-42
Ishiduka, Daisuke 1P-35
Ishigami, Naoki 3P-36
Ishii, Tadahiro 1P-33, 2P-32, 3P-17, 3P-28
Ishii, Yosuke 1P-13
Ishitsuka, Midori O. 2-2, 1P-8, 2P-6, 3P-8
Ishizuki, Yoshikatsu 3-9
Ito, Masayuki 2-15
Ito, Osamu 1-19
Ito, Shigeo 3P-30
Ito, Tsuyoshi 1P-9, 2P-7
Ito, Yasuhiro 1P-10
Ito, Yohei 1-6
Itoh, Shigeo 1P-26, 2P-27
Itoh, Tamitake 2P-26
Iwai, Taisuke 3-9
Iwamatsu, Sho-ichi 2-10
Iwasa, Yoshihiro 2-5
Iwata, Atsushi 1P-13
Iwata, Iori 1P-44
Iwata, Nobuyuki 1P-35, 2P-2, 3P-10
Izumi, Noriko 2P-11, 2P-13, 2P-15
Izumisawa, Satoru 3P-13
～J～
Jimbo, Takashi 1P-24
Jinno, Makoto 3P-22
Jorio, Ado 1P-15
Joung, Soon-Kil 2P-39
Ju, Jing 3P-13
～K～
Kai, Yasunori 1-8, 2P-47
Kakeda, Daisuke 2-16
Kako, Masahiro 1P-12, 2P-6
Kaminosono, Yoshiya 1P-33

Kaminosono, Yosiya 3P-28
Kaneki, Kunihide 1P-35
Kaneko, T. 3P-33
Kaneko, Toshiro 3-10, 1P-23, 2P-29
Kanemitsu, Yoshihiko 1P-16
Kasama, Yasuhiko 3P-12
Kataura, H. 1P-20
Kataura, Hiromichi 1-7, 1-16, 2-5, 3-1, 2P-18
Kato, Koichiro 2-4, 1P-18
Kato, Ryoei 2P-3
Kato, Ryogo 1-12
Kato, Shinya 1P-24
Kato, T. 3P-33
Kato, Takaaki 1P-12
Kato, Tatsuhisa 1-8, 2-2, 2-3, 2-17, 2P-47
Kato, Tatsuya 2P-29
Kato, Toshiaki 3P-40
Kato, Yoshitaka 1P-29
Kawabata, Takahiro 2P-27, 3P-30
Kawai, Takazumi 3-2
Kawaji, Hitoshi 3P-13
Kawamoto, Akira 3-8
Kawarada, Hiroshi 1-12
Kawasaki, Shinji 1P-13
Kawase, Takeshi 2-13
Kawata, Satoshi 2P-19
Kikitsu, Tomoka 1P-32, 1P-37
Kikuchi, Koichi 2-16
Kim, Jedeok 1-2
Kimura, Hiroe 3P-24
Kinoshita, Keisuke 3P-2
Kishi, Naoki 1P-24
Kitai, Ryuhei 3-8
Kitamura, Hiroshi 1P-28
Kitaura, Ryo 3-11, 2P-12, 2P-13, 3P-35, 3P-41, 3P-42
Kizu, Takio 2P-37
Kizuka, Tokushi 2-1
Kobashi, Kazufumi 3P-25
Kobayash, Yuki 1-13
Kobayashi, Keita 3P-38
Kobayashi, Kounosuke 3P-2
Kobayashi, Minoru 3-3
Kobayashi, Mototada 1P-47
Kobayashi, Yoshihiro 2-6
Kobayshi, Yoshihiro 2P-19
Kodaka, Ryosuke 2-14
Kodama, Takeshi 1-10, 2-16
Kohama, Yoshimitsu 3P-13
Kojima, Eiji 3P-16
Kojima, Nobuaki 1-18, 3P-9
Kokai, Fumio 2P-46
Komatsu, Koichi 1P-5, 3P-13
Kondo, Daiyu 3-9
Koretsune, Takashi 2P-4
Koshio, Akira 2P-46
Kramberger, C. 1P-20
Krueger, Anke 2-7
Kubo, Gen 3P-31
Kubota, Toshihiko 3-8
Kudo, Tetsuichi 1-2
Kuga, Hidenori 1P-9
Kumashiro, Ryotaro 3P-13
Kumazawa, Akira 2P-32
Kunishige, Atsuhiro 2P-20
Kurachi, Hiroyuki 3P-24
Kuramoto, Tatsunori 3P-26
Kurihara, Hiroki 2P-5
Kurihara, Kohei 2P-2, 3P-10
Kuriyama, Tomoyuki 3P-28
Kurotobi, Kei 3P-6
Kushita, Shinya 1P-28
Kuwabara, Takayuki 3P-12
Kuwano, Jun 1P-32, 1P-37
Kyakuno, Haruka 1-7

～L～

Li, Chang-Zhi 3P-7
Li, Yongfeng 3-10, 1P-23, 2P-29
Li, Zhaofei 3P-13
Liang, Yuejiang 2-7
Liu, Dian 2-13
Liu, Huarong 3P-18

Liu, Zhen 3P-39
Liu, Zheng 2P-40
Lu, Jing 3P-19
Lu, Xing 1P-8
～M～
Maeda, Shuhei 1P-5
Maeda, Yutaka 2-2, 2-17, 1P-8, 1P-11, 1P-12, 3P-19, 3P-20
Makimoto, Natsumi 1P-30
Maniwa, Yutaka 1-7, 2P-18
Maruyama, Masashi 1P-2
Maruyama, Shigeo 1-14, 3-9, 2P-25, 2P-33, 3P-21, 3P-29, 3P-37
Maruyama, Takahiro 3P-32
Mashino, Tadahiko 2-15
Matano, Yoshihiro 3-7
Matsubara, Tohoru 2P-20
Matsuda, Kazunari 1P-16
Matsuda, Kazuyuki 1-7, 2P-18
Matsukawa, Junpei 2P-1
Matsumoto, HIbiki 1P-40
Matsumura, Sachiko 1-9
Matsunaga, Ryusuke 1P-16
Matsuo, Keiko 3P-5
Matsuo, Yutaka 1P-1, 1P-2, 1P-3, 1P-4, 3P-5, 3P-7
Mibu, Ko 1P-31
Minakata, Satoshi 3P-4
Minami, Nobutsugu 3P-16
Minowa, Mari 2P-6
Mitoma, Nobuhiko 1P-42
Miyake, Masato 2P-36
Miyako, Eijiro 1P-22, 2P-26
Miyamoto, Yoshiyuki 3-2, 1P-46
Miyata, Y. 1P-20
Miyata, Yasumitsu 1-7, 2-5, 3-1, 3-11, 2P-11, 3P-41
Miyawaki, Jin 1-9
Miyazaki, Hisao 2P-44
Miyazaki, Takafumi 1P-10, 2P-14, 2P-15
Miyazawa, Kun'ichi 1-19, 2-1, 2P-3, 2P-17, 2P-48
Mizobuchi, Yuzo 3P-12
Mizorogi, Naomi 2-2, 2-17, 1P-8, 1P-9, 2P-5, 2P-7, 2P-10
Mizukoshi, Masataka 3-9
Mizusawa, Takashi 1P-34
Mizutani, Takashi 3-11
Morales, Crisoforo 3P-9
Mori, T. 3P-45
Mori, Takanori 1-1
Morinaka, Yuta 1P-5
Morioki, Masakatsu 1P-26, 2P-27, 3P-30
Morishima, Yotaro 2-13
Moriyama, Hiroshi 3-12
Motomiya, Kenichi 2P-35
Murakami, Mutsuaki 3S-1
Murakami, Tatsuya 1-9
Murakami, Yoichi 1-14
Muraki, Susumu 1P-44
Murata, Michihisa 1P-5, 3P-6
Murata, Yasujiro 1P-5, 3P-6, 3P-13
Muroya, Naoki 3P-1
Myouhara, Yuri 3P-44
～N～
Nagamachi, Toshiki 3P-4
Nagasaki, Yukio 2-14
Nagase, Shigeru 1-4, 2-2, 2-17, 1P-8, 1P-9, 1P-12, 2P-5, 2P-7, 2P-8, 2P-10, 3P-8, 3P-19, 3P-20
Nagashima, Keisuke 1P-17
Nagashima, Yuki 2P-8
Nakagawa, Hamazo 3P-15
Nakahara, Hitoshi 1P-19, 3P-18
Nakahodo, Tsukasa 3P-8
Nakamura, Eiichi 1S-1, 1P-1, 1P-2, 1P-3, 1P-4, 3P-5, 3P-7
Nakamura, J. 2P-43
Nakamura, Jin 2P-45
Nakamura, Shigeo 2-15
Nakamura, Takayuki 1P-12

Nakamura, Yosuke	1S-2, 3P-1, 3P-2
Nakanishi, Ryo	3P-41
Nakanishi, Takeshi	2P-21, 3P-39
Nakashima, Kenichi	2-13
Nakashima, Naotoshi	2-4, 3-4, 1P-25, 2P-38, 3P-27
Nakayama, Kazuhisa	3P-4
Nakayama, Takuya	3P-35
Namura, Masaru	2P-35
Naritsuka, Shigeya	3P-32
Natori, Masato	1-18, 3P-9
Nemoto, Yoshihiro	1-19
Nihey, Fumiyuki	1-15
Nii, Hiroyuki	2P-20, 3P-15
Nikawa, Hidefumi	2-2, 2-17, 1P-6, 1P-8, 1P-9, 2P-5, 2P-7, 3P-8
Nishi, Seiji	1-18, 3P-9
Nishi, Tetsushi	2P-34, 3P-36
Nishibori, Eiji	2P-12
Nishii, Ryosuke	1P-27
Nishikawa, Eiichi	2P-37, 3P-29
Nishimura, Jun	3P-1, 3P-2
Nishino, Hidekazu	3P-25
Noguchi, Takuya	3P-46
Nomura, Koudai	3P-18
Nouchi, Ryo	1-3
Nozaki, Iori	2P-46
Nozaki, Takayuki	1P-42
Nudejima, Shin-ichi	2P-17
Nugraha, Ahmad R.T.	1P-15
Numata, Youhei	2-9
～O～	
Oda, Kota	1P-27
Ohfuchi, Mari	1P-36
Ohmori, Shigekazu	1-17, 2P-22
Ohno, Masatomi	1P-28
Ohno, Yutaka	3-11
Ohshima, Satoshi	1-7
Oikawa, S.	2P-43
Oizumi, Haruna	3P-12
Okada, Mitsunori	3P-8
Okada, Susumu	3-13, 1P-43, 2P-39, 2P-41, 3P-47
Okamoto, Hiroshi	3-1
Okazaki, Toshiya	1-10, 1P-34, 1P-38, 2P-11, 2P-31, 2P-39, 2P-40, 3P-39
Oke, Shinichiro	1P-26, 2P-27, 3P-30
Okimoto, Haruya	2-5, 1P-10
Okita, Tomohisa	3P-20
Okuda-Shimazaki, Junko	2P-17
Omote, Kenji	3P-12
Ono, Shoichi	3P-12
Ono, Syuku	3P-28
Onuma, Kenjirou	2P-36
Oohara, Wataru	3P-40
Orofeo, Carlo M.	3P-36
Osada, Ryoichi	1-8
Osanai, Yosuke	3P-40
Oshima, Hisayoshi	1P-31
Oshima, Yugo	2P-18
Ota, Taisuke	3-3
Oyama, Hiromi	1P-3
Ozawa, Hiroaki	2P-38
Ozawa, Masaki	2-7
～P～	
Park, Jin Sung	3-5
Pichler, T.	1P-20
～Q～	
Qiu, Hanxun	1P-11
～R～	
Rachi, Takeshi	3P-13
Ren, T.	3P-14
Richard, Charvet	2-12
Rupesinghe, Nalin	2P-36
～S～	
Sagami, Hiroyuki	3P-12
Sagitani, Satoshi	2P-18
Saida, Morihiko	3P-12
Saikawa, Mao	2P-16
Saito, Riichiro	3-5, 1P-15, 2P-25

Saito, Susumu 2-4, 1P-18, 2P-4, 2P-23
Saito, Takeshi 1-7, 1-17, 1P-24, 1P-38, 2P-22, 3P-38, 3P-41
Saito, Tatsuya 1-3
Saito, Yahachi 2-1, 1P-19, 3P-18
Sakai, Keijiro 1P-35
Sakamoto, Chika 3P-1
Sakamoto, Shingo 1P-17, 2P-28
Sakata, Makoto 2P-12
Sakata, Wakako 3-6
Sako, Yuuki 3P-3
Sano, Masahito 1-13, 1P-40
Sasaki, K. 3P-45
Sasaki, Kenich 1-1, 3-5
Sasaki, Toshio 1-19
Sathish, Marappan 1-19
Sato, Junichi 3P-34
Sato, Kentaro 1P-15, 2P-25
Sato, Kuninori 3P-32
Sato, Satoru 2-17
Sato, Shigeo 1-9
Sato, Yoshinori 2P-35
Satoh, Masayuki 2P-36
Sawa, Hiroshi 2S-1, 2P-12, 3P-13
Seki, Shu 2-12
Sekido, Masaru 1P-28
Shamoto, Shin-ichi 2P-48
Shiba, Kiyotaka 1-9
Shimada, Toshihiro 3P-46
Shimazu, Tomohiro 1P-31
Shimizu, Kazuki 1P-26, 2P-27
Shimizu, T. 2P-43
Shimizu, Taisei 2P-45
Shimizu, Tetsuhiro 3P-40
Shinjo, Teruya 1P-42
Shinohara, H. 1P-20
Shinohara, Hisanori 3-11, 1P-10, 2P-11, 2P-12, 2P-13, 2P-15, 3P-35, 3P-41, 3P-42
Shinohara, Yuichiro 3P-30
Shinomiya, Hiroyuki 3P-17
Shiomi, Junichiro 1-14, 3-9, 2P-33, 3P-21, 3P-29, 3P-37
Shiozawa, H. 1P-20
Shiozawa, Kazunari 2P-13
Shiraishi, Masashi 1P-42
Shoji, Satoru 2P-19
Shukla, Bikau 1-17, 2P-22
Silva, R. 1P-20
Siry, Milan 1P-31
Slanina, Zdenek 2-2, 2-17, 1P-8, 2P-7, 2P-8, 3P-8
Sode, Katsuya 3P-20
Soga, Ikuo 3-9
Soga, Tetsuo 1P-24
Song, Suhee 2P-38
Sonomura, Takuya 1P-35
Suda, Yoshiyuki 1P-26, 2P-27, 3P-30
Suenaga, Kazu 1P-38, 2P-40, 3P-39
Suenaga, Kazutomo 3P-38
Suga, Tadatomo 3-9
Sugai, Toshiki 3-11
Suh, Hongsuk 2P-38
Sumii, Ryohei 1P-10
Suzuki, Shinzo 2-16, 1P-34
Suzuki, Yoshishige 1P-42
—T—
Tagmatarchis, Nikos 3P-39
Tajima, Isamu 2P-32
Tajima, Tomoyuki 3-6, 2P-1, 3P-3
Tajima, Yusuke 2-9
Takada, Tadao 2-13
Takagi, Daisuke 2-6, 2P-19
Takagi, Yoshiteru 3-13, 3P-47
Takaguchi, Yutaka 3-6, 2P-1, 3P-3
Takahashi, Hirotoshi 3P-23
Takahashi, Katsumune 2P-30
Takahashi, Kohshin 3P-12
Takahashi, Koji 1-6, 2P-34, 3P-36
Takahashi, Kyoko 2-15
Takahashi, Tsukasa 1P-9

Takai, K. 3P-45
Takai, Kazuyuki 1-1
Takamizu, Naoko 1-10
Takano, Takumi 1P-42
Takano, Yoshihiko 2P-24
Takano, Yuta 2-2, 2P-8
Takata, Masaki 2P-12
Takenobu, Daishi 2P-18
Takenobu, Taishi 2-5
Takeshita, Hiroaki 1P-35
Takeuchi, Hisato 1P-28
Takeuchi, Masayuki 2-11
Takeyama, Shojiro 3P-16
Takikawa, Hirofumi 1P-26, 2P-27, 3P-30
Takimoto, Kotaro 2P-27, 3P-30
Takimoto, Yuji 3P-11
Tanabe, Yuki 2P-45
Tanaka, Izumi 1-5
Tanaka, Kazuyoshi 1P-29
Tanaka, Takeshi 1-16
Tanaka, Tatsuya 2P-10
Tanaka, Yasuhiko 2-4
Tang, Jun 3P-13
Tange, Masayoshi 2P-11, 2P-40
Tanigaki, Katsumi 1-3, 3P-13
Taniguchi, Akiyoshi 2P-17
Tao, Rie 3P-11
Tao, Shoichi 3-1
Tashiro, Atsushi 3P-19
Tashiro, Kentaro 2-3, 2-12
Tateyama, Yoshitaka 1-19
Teduka, Noriyasu 3-7
Teo, Kenneth 2P-36
Terada, Masao 3P-46
Teshiba, Masashi 2P-16
Thurakitseree, Theerapol 2P-33
Tohji, Kazuyuki 2P-35
Toida, Tatsuo 3P-24
Tokumoto, Youji 1P-10, 2P-15
Tomida, Akihiro 1-9
Tominaga, Masato 1P-17, 2P-28
Toyama, Kiyohiko 1-15
Tsuboi, Toshiyuki 1P-21
Tsuchida, Kunihiro 1-9
Tsuchiya, Koji 1P-33, 2P-32, 3P-17, 3P-28
Tsuchiya, Takahiro 2-2, 2-17, 1P-6, 1P-81P-9, 2P-5, 2P-6, 2P-8, 2P-9, 2P-10, 3P-8, 3P-19, 3P-20
Tsuda, Shunsuke 2P-24
Tsuji, Masaharu 1-5, 2P-34, 3P-36
Tsukagoshi, Kazuhito 2P-44
Tsuruo, Takashi 1-9
Tsuruoka, Yasuhiro 2P-31
Tsutiya, Takahiro 2P-7

~U~

Uchida, Katsumi 1P-33, 2P-32, 3P-17, 3P-28
Uchinoumi, Takeshi 3P-27
Uchiyama, Tomoya 3-3
Udoguchi, Hiroki 2P-18
Ue, Hitoshi 1P-26, 2P-27, 3P-30
Ueda, Nobuaki 1P-6
Uemura, Sashiro 3P-24
Umemoto, Hisashi 1P-10, 2P-13
Umeyama, Tomokazu 3-7
Urabe, Yasuko 1-16

~W~

Wada, Yoriko 1-8, 2P-16, 2P-47
Wakabayashi, K. 3P-45
Wakabayashi, Katsunori 1-1
Wakabayashi, Tomonari 1-8, 2P-16, 2P-47
Wakahara, Takatsugu 1-19, 2P-48
Wang, Qiguan 3-12
Wang, Zheng-Ming 2P-3
Watanabe, Hikaru 2P-35
Watanabe, Kazuhiro 1P-7
Watanabe, Tohru 2P-24

~X~

Xiang, Rong 1-14, 2P-33, 3P-29, 3P-37
Xiao, Zuo 1P-1
Xu, J. 3P-43
Xu, Jianxun 1P-41, 2P-42, 3P-44

~Y~

Yagi, Hajime 2P-15

Yahiro, Hitomi 1-7
Yajima, Hirofumi 1P-33, 1P-35, 2P-30, 2P-32, 3P-17, 3P-28
Yamada, Michio 2-2, 2-17, 2P-6
Yamada, Sachiko 1P-30
Yamada, Takeo 1-11, 1P-30, 3P-24, 3P-25, 3P-34
Yamagiwa, Kiyofumi 1P-32, 1P-37
Yamago, Shigeru 2-13
Yamaguchi, Masafumi 1-18, 3P-9
Yamaguchi, Takahide 2P-24
Yamaguchi, Takashi 1P-41
Yamaguchi, Yoshihiro 1P-32, 1P-37
Yamakawa, Yusuke 2P-45
Yamamoto, Hiroshi 1P-35, 2P-2, 3P-10
Yamamoto, Kazunori 2P-48
Yamamoto, Shigehiko 3P-12
Yamamoto, Yohei 2-12
Yamamoto, Yuki 3-4, 1P-30
Yamamoto, Yuuta 3P-18
Yamana, Shuichi 2-15
Yamashita, Shunsuke 1P-32, 1P-37
Yamaura, Tatsuo 3P-30
Yamazaki, Yuko 2P-5
Yanagi, K. 1P-20
Yanagi, Kazuhiro 1-7, 2-5, 3-1, 2P-18
Yasuda, Satoshi 1-11, 3P-34
Yasukawa, Koichi 2P-28
Yasumitsu, Miyata 3P-41
Yokoi, Hiroyuki 3P-16
Yokoo, Kuniyoshi 3P-12
Yokosawa, Yuya 2P-9
Yokota, Masasgi 1P-26
Yokota, Masashi 2P-27, 3P-30
Yoo, EunJoo 1-2
Yoshikawa, Airi 2P-16
Yoshimoto, Takahisa 3P-41
Yoshimura, Masamichi 3-3
Yoshimura, Toshiaki 3P-8
Yudasaka, M. 3P-43
Yudasaka, Masako 1-9, 1P-41, 2P-42, 3P-44
Yuge, R. 3P-43
Yuge, Ryota 1-9
Yumura, Motoo 1-7, 1-11, 1-17, 2P-22, 3P-34
Yumura, Takashi 1P-39
Yusa, Shin-ichi 2-13

〜Z〜

Zhang, Hong 1P-46
Zhang, Minfang 1P-41
Zhang, Xiaoyong 1P-4
Zhang, Xing 1-6
Zhang, Xuan 2-11
Zhao, Bin 3P-24
Zhao, Chen 3P-42
Zhao, Pei 1-14, 2P-33
Zhao, X. 3P-14
Zheng, H. 3P-14
Zhou, H.S. 1-2

複写される方へ

フラーレン・ナノチューブ学会は、有限責任中間法人　学術著作権協会（学著協）に複写に関する権利委託をしていますので、本誌に掲載された著作物を複写したい方は、学著協より許諾を受けて複写して下さい。

但し、社団法人日本複写権センター（学著協より複写に関する権利を再委託）と包括複写許諾契約を締結されている企業の社員による社内利用目的の複写はその必要はありません。（※社外頒布用の複写は許諾が必要です。）

権利委託先：有限会社中間法人　学術著作権協会
〒107-0052　東京都港区赤坂 9-6-41　乃木坂ビル 3 階
電話：03-3475-5618　　FAX：03-3475-5619　　E-Mail：info@jaacc.jp

注意：複写以外の許諾（著作物転載・翻訳等）は、学著会では扱っていませんので、直接、フラーレン・ナノチューブ学会へご連絡下さい。

Notice for Photocopying

If you wish to photocopy any work of this publication, you have to get permission from the following organization to which licensing of copyright clearance is delegated by the copyright owner.

＜All users except those in USA＞
Japan Academic Association for Copyright Clearance, Inc. (JAACC)
6-41 Akasaka 9-chome, Minato-ku, Tokyo 107-0052 Japan
TEL：81-3-3475-5618
FAX：81-3-3475-5619　　E-Mail：info@jaacc.jp

＜Users e in USA＞
Copyright Clearance Center, Inc.
222 Rosewood Drive, Danvers, MA 01923 USA
Phone：1-978-750-8400　　FAX：1-978-646-8600

2009 年 9 月 1 日発行

第３７回フラーレン・ナノチューブ総合シンポジウム
講演要旨集

＜フラーレン・ナノチューブ学会＞
〒464-8602　愛知県名古屋市千種区不老町
名古屋大学大学院理学研究科　物質理学専攻
篠原研究室内
Tel：052-789-5948
Fax：052-747-6442
E-mail：fullerene@nano.chem.nagoya-u.ac.jp
URL：http://fullerene-jp.org
印刷　/　製本　株式会社イセブ

kleindiek
nanotechnik

for Electron microscope

マイクロマニピュレータ
サブステージ

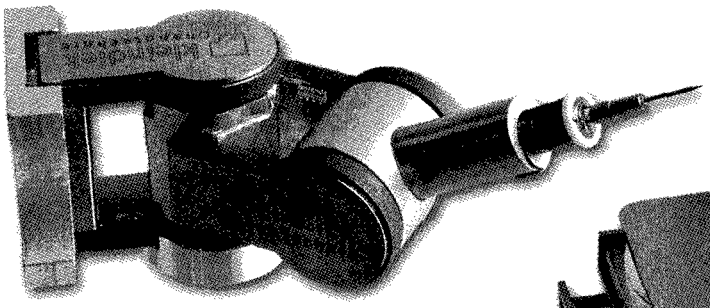

MM3A-EM

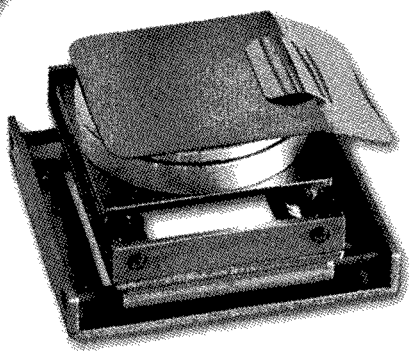

LT3310XYR

Semiconductor/R&D/Material Science

■電気特性評価
- ナノプロービング(I-V測定,Vias印加)
- EBIC(ElectronBeamInducedCurrent)
- RCI(ResistiveContrastImage)

■マニピュレーション

■TEM試料リフトアウト

■応力・引っ張り測定

■マイクロインジェクション

■Cellカウンティング

■CAD Navigation

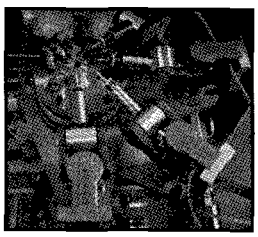

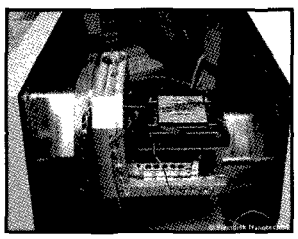

ADS 株式会社アド・サイエンス

〒273-0005 千葉県船橋市本町2-2-7サンテックビル TEL:047-434-2090 FAX:047-434-2097 http:// www.ads-img.co.jp

Quantum Wise

密度汎関数理論と非平衡グリーン関数による電子輸送計算プログラム

Atomistix ToolKit & Virtual NanoLab

Atomistix ToolKit

Atomistix ToolKit(ATK)は、2つの半無限の電極に挟まれたナノスケール構造体(2プローブ系)の電気伝導特性を解析するためのソフトウェアです。密度汎関数理論(DFT)と非平衡グリーン関数(NEGF)の手法に基づき、バイアス電圧が印加された2プローブ系の非平衡電子状態の第一原理計算が実現されます。

Virtual NanoLab

Virtual NanoLabは、Atomistix ToolKitのためのユーザーフレンドリーな操作環境を提供します。モデルのセットアップからAtomistix ToolKitを用いた計算の実行、結果の表示までGUIを使って簡便に行うことができます。

計算理論

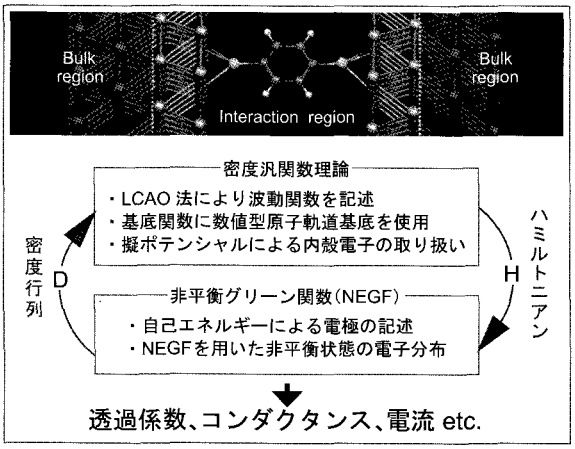

Atomistix ToolKitの計算理論概念図

適用分野

Atomistix ToolKitは、分子デバイス、ナノチューブ/フラーレン、Si/SiO_2絶縁膜などの多様なデバイス構造の電気伝導特性をシミュレーションできます。

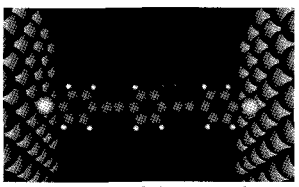

金電極に架橋された分子素子

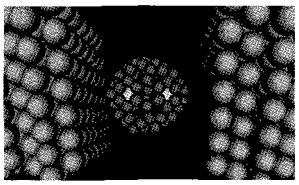

金属内包フラーレン

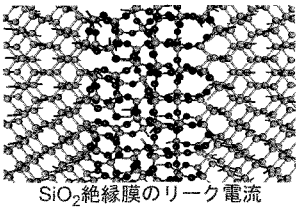

SiO_2絶縁膜のリーク電流

カーボンナノチューブ

Atomistix ToolKitによるカーボン材料のデバイスシミュレーション

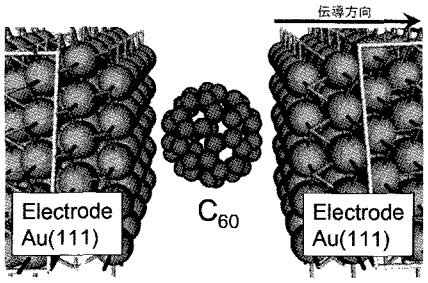

サイバネットシステムでは Au 電極に挟まれた C_{60} の単分子デバイス特性を解析を Atomistix ToolKit を用いて実施し、"Atomistix ToolKit によるナノデバイスシミュレーション" と題して 日本化学会情報化学部会誌，Vol. 26, 118 (2008) に発表しました。

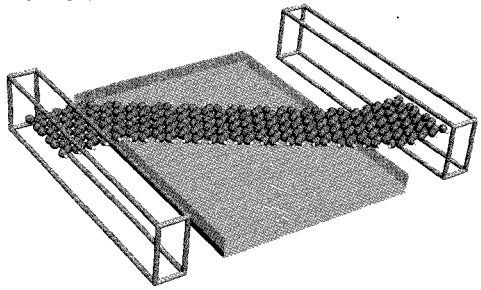

Z 形状グラフェンナノリボン 2 プローブ構造。グラフェンナノリボン下部のグレーの領域は連続体近似で記述されたゲート電極・絶縁膜を表しています。2009 年リリース予定の新バージョンの Atomistix ToolKit ではゲート電極による電圧印加を顕に考慮したデバイスシミュレーションが可能となる予定です。

Atomistix ToolKit & Virtual NanoLab には1ヶ月無料ですべての機能をお試しいただける評価版がございます。お申し込みは下記まで。

http://www.cybernet.co.jp/quantumwise/index.html

サイバネットシステム株式会社
本　社　〒101-0022 東京都千代田区神田練塀町3 富士ソフトビル
Tel:03-5297-3247 Fax:03-5297-3637
http://www.cybernet.co.jp/quantumwise/index.html
e-mail: atomistix-info@cybernet.co.jp

nacalai tesque
The quality for certainty.

可溶化カーボンナノチューブ分離用カラム

COSMOSIL® CNT

- 可溶化カーボンナノチューブをサイズで分離！
- 親水性基(中性)コーティングタイプ！
- 3種類の細孔径(300 Å,1000 Å,2000 Å)！
- 高い耐久性！

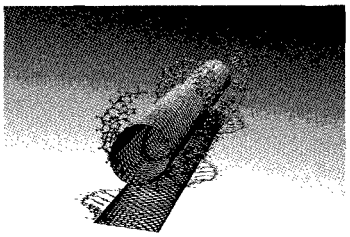

Image courtesy of Dr. Y. Ito, Univ. of Oxford

■分離例

カーボンナノチューブのサイズ分離

細孔径の異なる3種類のカラムを連結し、DNAでラッピングされたカーボンナノチューブを分離しました。

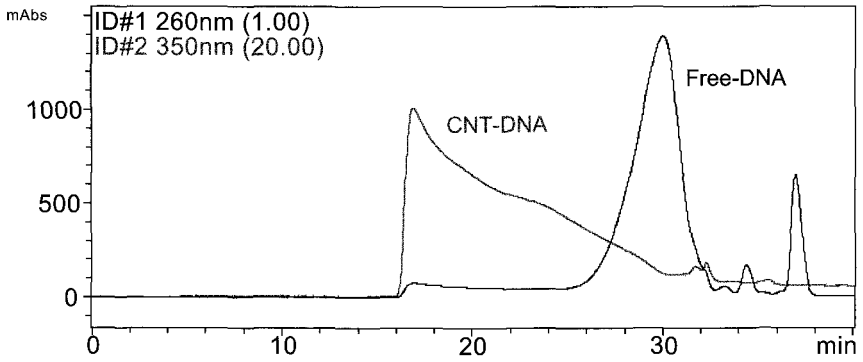

分析条件

カラム	COSMOSIL CNT-300 7.5mmI.D.×300mm	温　度	40 ℃
	COSMOSIL CNT-1000 7.5mmI.D.×300mm	検　出	UV260nm(×1), 350nm(×20)
	COSMOSIL CNT-2000 7.5mmI.D.×300mm	サンプル	DNA-wrapped CNT(CNT-DNA)
移動相	0.5mmol/l EDTA, 200mmol/l NaCl, 40mmol/l Tris-Tris HCl(pH7.0)	注入量	500μl
流　速	1.0ml/min	圧　力	8.1MPa

【サンプルのご提供 ： 名古屋大学大学院理学研究科物質理学専攻 篠原研究室】

AFM(原子間力顕微鏡)によるサイズ観察

上記分離時に分取した各フラクションをAFMにて観測し、CNTの長さを測定しました。

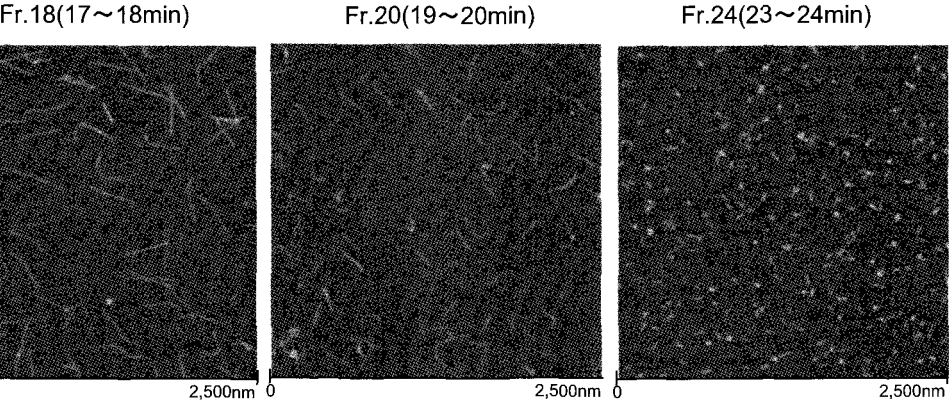

【撮影・データのご提供 ： 名古屋大学大学院理学研究科物質理学専攻 篠原 久典教授・浅田 有紀様】

詳しい情報はWeb siteをご覧ください。

ナカライテスク株式会社

〒604-0855 京都市中京区二条通烏丸西入東玉屋町498

価格・納期のご照会 フリーダイヤル 0120-489-552
製品に関するご照会 TEL : 075-211-2746 FAX : 075-211-2710
Web site :http://www.nacalai.co.jp

Access to your success

SHIMADZU

Best for Our Customers

～すべてはお客様のために～ を合言葉にナノテク新材料における最高のソリューションを提供します。

(1 微量測定) (2 純　度) (3 直　径) (4 観　察) (5 カイラリティ) (6 凝集分散)

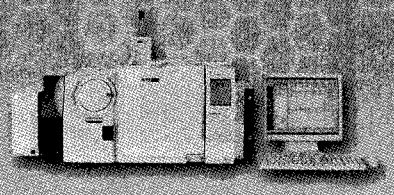

① 熱分解生成物・発生ガスの分析
ガスクロマトグラフ質量分析計
GCMS-QP2010 Plus

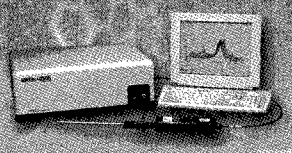

②③直径測定
②④結晶性と耐熱性の評価
ラマン分光光度計
Holo-Probe モニタリングシステム

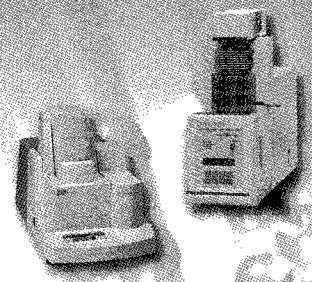

① 微量CNTの純度・熱特性評価
① CNTの結晶性と耐熱性の評価
ミクロ熱重量測定装置
TGA-50
TG/DTA同時測定装置
DTG-60/60H

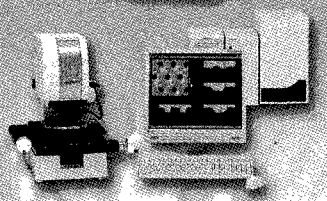

③④あらゆるナノテク材料を観察・測定
ナノサーチ顕微鏡
SFT-3500

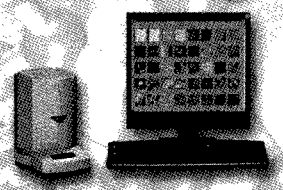

③④直径測定
③④精製前後の観察
③④CNTとポリマーコンポジット試料の観察
走査型プローブ顕微鏡
SPM-9600

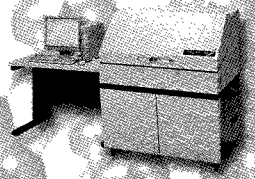

①②CNTの紫外可視近赤外吸収スペクトル測定
紫外可視近赤外分光光度計
SolidSpec-3700
紫外可視近赤外分光光度計
UV-3600

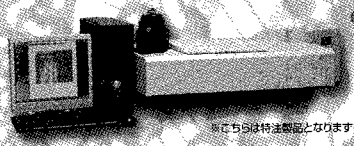

⑤SWNTの近赤外PL 3次元分布測定
近赤外フォトルミネッセンス測定システム
NIR-PL System
※こちらは特注製品となります

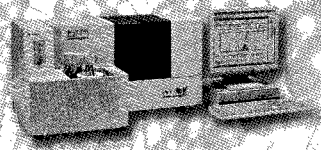

⑥分散・凝集過程評価
ナノ粒子径分布測定装置
SALD-7100

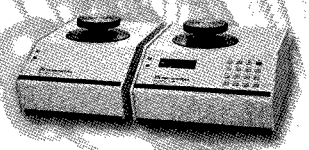

② CNTの密度測定
乾式自動密度計
アキュピックII 1340シリーズ

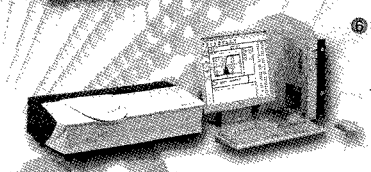

⑥独自のIG法による シングルナノ領域の粒子径評価
シングルナノ粒子径測定装置
IG-1000

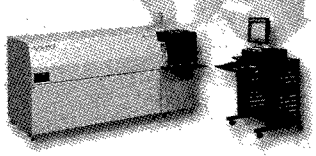

② 触媒元素の測定
ツインシーケンシャル形ICP発光分析装置
ICPS-8100

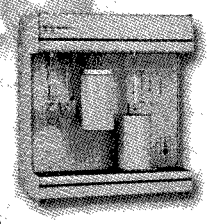

⑥比表面積と吸着特性
マイクロメリティックス
高速比表面積/細孔分布測定装置
アサップ2020シリーズ

nanotech
SHIMADZU

Total solutions for the future of nanotechnology

株式会社島津製作所
分析計測事業部　マーケティング部　プロモーションG
〒604-8511 京都市中京区西ノ京桑原町1
TEL075-823-1468 FAX075-823-1380 http://www.an.shimadzu.co.jp

波長可変チタンサファイアレーザー

3900S

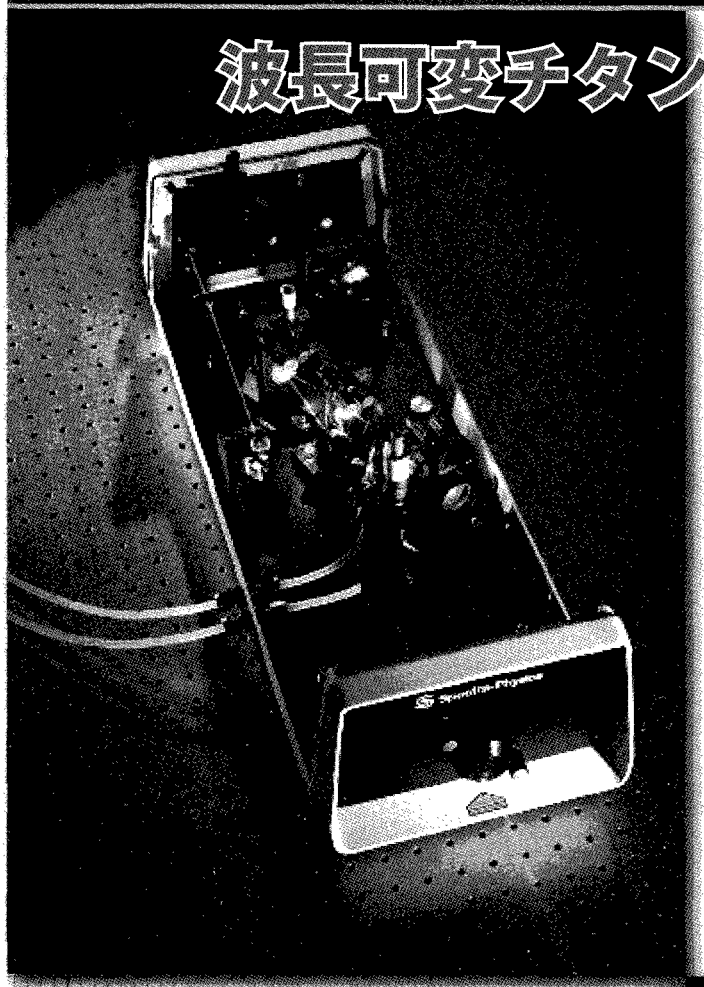

- 優れた操作性、メンテナンス性と高い変換効率
- 高い安定性を実現し、675～1100nmの超広帯域発振が可能
- フラーレン・ナノチューブの分光用およびフォトルミネッセンス光源として最適

【主な仕様】

平 均 入 力 ： 5Wおよび10W
発振波長域 ： 700-1000nm (5W励起)
発振波長域 ： 675-1100nm (10W励起)
線　　幅 ： 40GHz以下 (1GHz以下のオプション有り)
ノ　イ　ズ ： 1%以下
安　定　性 ： 3%以下
空間モード ： TEM_{00}

コンパクトCW固体レーザー

Excelsior®

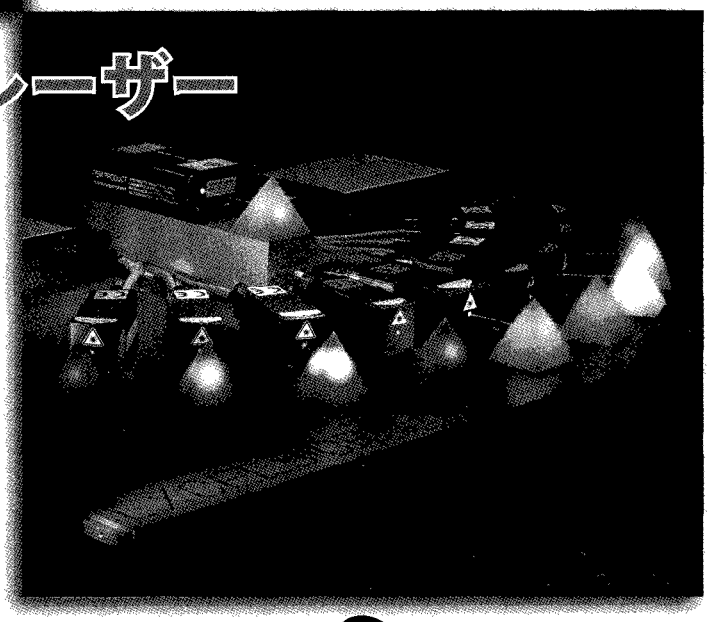

- 375, 405, 440, 473, 488, 505, 515, 532, 561, 594, 635, 785,1064nm をラインナップし、市場での要求波長すべてを網羅
- コンパクト設計、統一された共通筐体寸法で装置組込みに最適
- アクティブパワーループによる卓越した出力安定性
- 優れたビーム品質
- 高信頼性、長寿命、低RMSノイズ、低消費電力(30W以下)
- CDRHモデル、ファイバー付モデルにも対応

Spectra-Physics
A Division of Newport Corporation

スペクトラ・フィジックス株式会社
本　　社 〒153-0061 東京都目黒区中目黒4-6-1 大和中目黒ビル　TEL(03)3794-5511 FAX(03)3794-5510
大阪支社 〒550-0005 大阪府大阪市西区西本町3-1-43 西本町ソーラービル　TEL(06)4390-6770 FAX(06)4390-2760

MAKE LIGHT | MANAGE LIGHT | MEASURE LIGHT

製品情報・お問い合わせは　http://www.spectra-physics.jp

取扱いナノテク材料一覧

フラーレン材料

【60】PCBMフラーレン　純度99% 99.5% 99.9%
【70】PCBMフラーレン　純度99%
【84】PCBMフラーレン　純度99%
bis【60】PCBMフラーレン 純度99.5%
d5-60PCBMフラーレン　純度99.5%
Gd@C82金属内包フラーレン
La@C82金属内包フラーレン
Ce@C82金属内包フラーレン
Sc3N@C80内包フラーレン
C60F36,C60F48,C60Br24フラーレン
高次フラーレン[C76,C78,C84]
C13安定同位体置換フラーレン 純度98% 99%
Anti-HIVフラーレン
水溶性フラーレン
C60(OH)6, C60(OH)22-26, C60(OH)24
C60(OH)18-22(O^-K^+)4フラーノール
アミノ酪酸フラーレン誘導体
アミノカプロン酸フラーレン
ビスマロン酸エチルフラーレン
ビスマロン酸ジエチルフラーレン

カーボンナノチューブ

単層カーボンナノチューブ
純度50% 径1.1nm 長さ5-15μm
純度60% 径1.1nm 長さ0.5-2μm
純度60% 径1-2nm 長さ5-30μm
純度90% 径1-2nm 長さ5-30μm
SWNT-COOH, SWNT-NH2, SWNT-PEG
SWNT-SHSWNTs-OH 純度90%
SWNTs-COOH　純度90%

多層カーボンナノチューブ
純度95+% 外径8nm　内径2-5nm　長さ10-30μm
純度95+% 外径8nm　内径2-5nm　長さ0.5-2μm
純度95+% 外径10nm　内径2-7nm　長さ5-15μm
純度95+% 外径3-20nm　内径1-3nm　長さ0.1-10μm
純度95+% 外径8-15nm　内径3-5nm　長さ10-50μm
純度95+% 外径8-15nm　内径3-5nm　長さ0.5-2μm
純度95+% 外径10-20nm 内径5-10nm 長さ10-30μm
純度95+% 外径10-20nm 内径5-10nm 長さ0.5-2μm
純度90+% 外径10-30nm 内径3-10nm 長さ1-10μm
純度95+% 外径10-30nm 内径5-10nm 長さ5-15μm
純度95+% 外径10-30nm 内径5-10nm 長さ1-2μm
純度95+% 外径20-30nm 内径5-10nm 長さ10-30μm
純度95+% 外径20-30nm 内径5-10nm 長さ0.5-2μm
純度95+% 外径20-40nm 内径5-10nm 長さ5-15μm
純度95+% 外径20-40nm 内径5-10nm 長さ1-2μm
純度85%　外径20-40nm 長さ0.5-5nm 壁厚5-15nm
純度95%　外径20-40nm　長さ0.5-5nm　壁厚5-15nm
純度99%　外径20-40nm　長さ0.5-5nm　壁厚5-15nm
純度94+% 外径20-50nm　壁厚1-2nm　長さ0.5-2μm
純度95+% 外径30-50nm　内径5-15nm　長さ10-20μm
純度95+% 外径30-50nm　内径5-15nm　長さ0.5-2μm
純度95+% 外径40-60nm　内径5-10nm　長さ5-15μm
純度85%　外径40-70nm　長さ0.5-5μm 壁厚5-30nm
純度90%　外径40-70nm　長さ0.5-5μm 壁厚5-30nm
純度95%　外径40-70nm　長さ0.5-5μm 壁厚5-30nm
純度95%　外径40-60nm　長さ1-2μm
純度99%　外径40-70nm　長さ0.5-5μm 壁厚5-30nm
純度99%　外径40-60nm　長さ1-2μm
純度95+% 外径50-80nm　内径5-15nm　長さ10-20μm
純度95+% 外径50-80nm　内径5-15nm　長さ0.5-2μm
純度95+% 外径60-100nm 内径5-10nm　長さ5-15μm
MWNT-COOH, MWNT-NH2, MWNT-PEG, MWNT-SH

2層カーボンナノチューブ
径1.3-5nm 長さ5-15nm 純度50%
径1.3-5nm 長さ5-15nm 純度20%

その他カーボンナノチューブ
カーボンナノチューブ・フィルム【Cu,Si,Ni,Graphite】
カーボンナノチューブ・カソード【Cu,Si】
カーボンナノファイバー

金ナノ微粒子

金ナノ微粒子　0.01%金　2～50nm
Dextranコート 0.01%金 10～50nm
PEGコート　0.01%金　0～50nm
Biotinラベル　0.01%金 5～50nm
Streptavidinラベル 0.01%金 5～50nm
その他銀ナノ微粒子

電気鋳造精密メッシュ

金,銅,ニッケル　透過率(36～98%) 標準サイズ279×279mm

詳しいお問合せはこちら **http://atr-atr.co.jp**

株式会社ATR
Advanced Technology Research
〒270-0021 千葉県松戸市小金原 7-10-25
TEL：047-394-2112　FAX：047-394-2100
Mail：sales@atr-atr.co.jp

日本初上陸！

デジタル顕微鏡

10万円以下の低価格･高性能･高品質

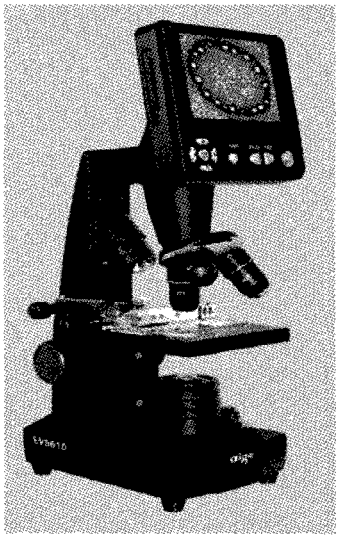

中 国 製
EV5610 型

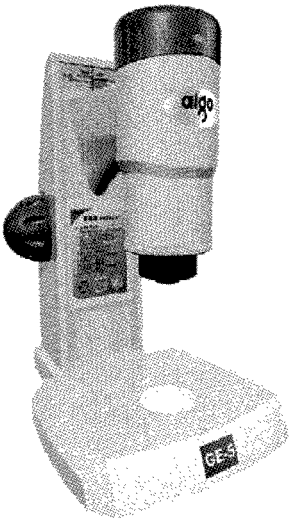

ＧＥ－５型
中 国 製

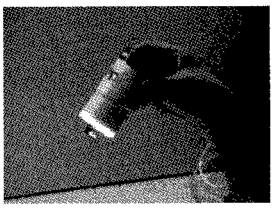

サンプル試料を大きく拡大して見れます。
88 ミリ カラー液晶画面を見るだけ
（覗きこむことはなくなりました）

対物レンズ	：	4倍、10倍、40倍が標準で装着
デジタル倍率	：	40倍から400倍まで
ﾃﾞｼﾞﾀﾙｽﾞｰﾑ	：	～1600倍まで
SDカード	：	データは簡単に保存
USBケーブル	：	パソコンに簡単にデータ転送
ﾃﾞｼﾞﾀﾙｶﾒﾗ	：	2ﾒｶﾞﾋﾟｸｾﾙ、CMOS、512MB内部ﾒﾓﾘ 192万画素、最大解像度1600×1200
XYｽﾃｰｼﾞ	：	手動で X軸 Y軸 に微調整 可
オプション	：	加熱･冷却機構

顕微鏡ヘッド部がはずれ任意な箇所に取り付け可能
このヘッド部のみも供給可能（ご相談ください）

標準倍率	：	60倍と180倍　ｵﾌﾟｼｮﾝで540倍
標準素子	：	1.3ﾒｶﾞﾋﾟｸｾﾙ、ｶﾗｰCMOS
ﾋﾟｸｾﾙｻｲｽﾞ	：	5.2×5.2 ﾐｸﾛﾝ
分解能	：	1280×1024 ﾋﾟｸｾﾙ
波長範囲	：	400～1000ﾅﾉﾒｰﾀ
ﾀﾞｲﾅﾐｯｸﾚﾝｼﾞ	：	62 dB
ﾃﾞｰﾀ出力	：	USB 2.0 でﾊﾟｿｺﾝに接続
対応OS	：	WinXP、Vista
フレームレート	：	10f/s　1280×1024
使用箇所	：	生産工場向き、工程作業、 品質管理、部品の詳細ﾓﾆﾀｰ

詳細については下記までお問い合わせ下さい

和貴ビジネスグループ
〒270-0021　千葉県松戸市小金原7丁目10番地25
TEL/FAX:047-309-8312
k.maeda@sea.plala.or.jp
http://www15.plala.or.jp/WBG/

BELSORP-miniII
自動比表面積／細孔分布測定装置

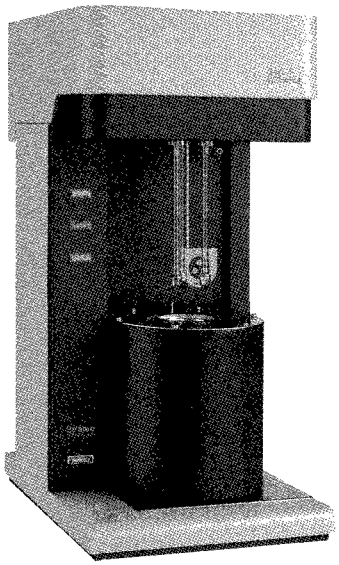

定容量法により吸脱着等温線を自動測定し、BET多点法による比表面積及び細孔分布を求める装置です。独自の死容積測定法により液体窒素の液面コントロールが不要となり、低価格・コンパクトな専用装置を開発致しました。

- ●全自動吸脱着等温線測定
- ●3検体同時測定
- ●JIS Z 8830対応品
- ●比表面積:0.01m^2/g以上
- ●細孔分布:直径0.7～400nm
- ●吸着ガス:N_2,その他非腐食性ガス（オプション）
- ●価格:¥4,720,000～（税別）

低価格 高性能

※別途パソコンが付属します。

NEW 高精度ガス/蒸気吸着量測定装置

ー高精度なマイクロ孔解析（超低相対圧$P/P_0=10^{-9}$から測定可能）ー

BELSORP-max

特 徴

- ●業界初のフルスケール0.013KPa圧力計を搭載しており、$P/P_0=10^{-9}$ の超低相対圧から再現性良く吸着等温線を測定し、高精度なマクロ孔解析が可能です。
- ●各測定ポートに圧力センサーが取り付けられており最大3検体同時測定可能
- ●弊社が開発したAFSM^{TM}法により定容量法測定が次世代へと進化しました。試料管の死容積変化を連続測定する事により高精度で再現性の良いデータが得られます。(Patent #3756919)
- ●データ解析ソフトBELMaster^{TM} にさらに進化したNLDFT/GCMC細孔分布シュミレーションソフトウエアー（BELSim^{TM}）が付属

基本仕様

- ●測定内容　：比表面積、細孔分布、蒸気吸着等温線
- ●測定試料数　：超低圧モード 2検体、標準モード 3検体同時測定
- ●最少比表面積: 0.0005m^2/g以上(Kr)
- ●細孔分布範囲: 0.35～500nm（直径）
- ●吸着ガス　：N_2,Ar,Kr,CO_2,H_2,O_2, NH_3,H_2Oその他有機蒸気

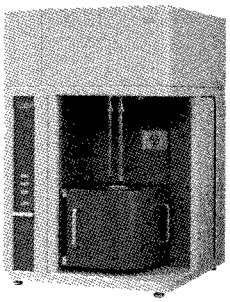

触媒分析装置

BEL-CAT

ダイナミック法（流通法）により各種触媒表面特性を低コストで、しかも自動分析する事ができます。

主な機能

- ●アンモニアTPD
- ●昇温還元/酸化（TPReduction, TPO）
- ●金属分散度測定/化学吸着量測定（パルス法）
- ●比表面積測定（BET1点法）

基本仕様

- ●測 定 法 ：ダイナミック法（流通法）
- ●検 出 器 ：熱伝導度検出器
- ●昇温範囲 ：1100℃
- ●使用ガス ：H_2, O_2, N_2, NO, NH_3等
- ●そ の 他 ：Q-mass（オプション）を使用し、TPReactionなどの生成ガスの同時分析が可能です。

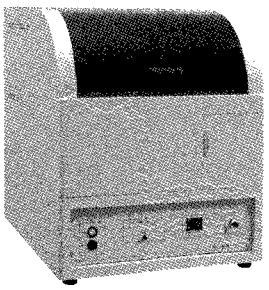

BEL JAPAN, INC.
吸着現象を考える
日本ベル株式会社

大 阪 本 社　〒561-0807 大阪府豊中市原田中1丁目9番1号
西日本営業所　TEL 06-6841-2161　FAX 06-6841-2767
東 京 支 店　〒130-0021 東京都墨田区緑2丁目7番3号 ダイコービル4F
TEL 03-5638-4271　FAX 03-5638-4277
E-mail: sales@nippon-bel.co.jp　URL: http//www.nippon-bel.co.jp

シミュレーションを高速化

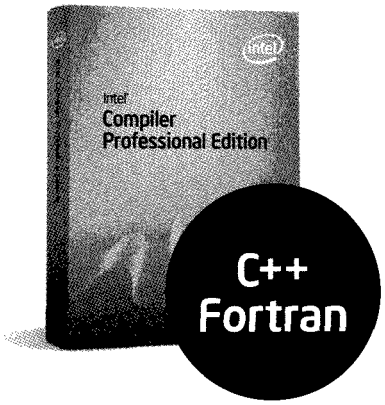

アプリケーションを高速化するコンパイラーです。

コンパイラーの最適化機能により、プロセッサーの機能を最大限に生かし、

高速に演算を行うことができます。

- ☑ **自動最適化 / 並列化により演算速度を向上**
- ☑ **ISO 標準の Fortran 77/90/95 とより多くの Fortran 2003 規格に対応**
- ☑ **C++ 非同期ファイルストリームを提供**
- ☑ **BLAS/LAPACK を並列化し、より高速になったインテル® MKL 最新版をバンドル**

Windows*/Linux*/Mac OS*

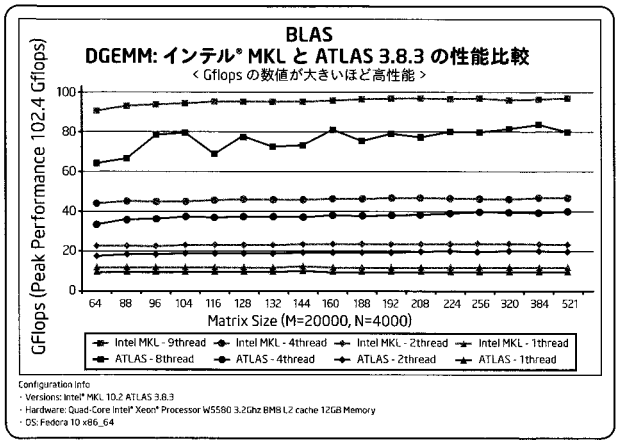

他にも以下の性能向上が確認されています。

- インテル® Core™ i7 プロセッサーにて DGEMM が最大 50% 向上
- インテル® Xeon® 7460 番台プロセッサーにて DGETRF が 25% 向上

サイエンス・テクノロジー分野の研究、開発に最適！

高速化で研究コストを削減！

Voice お客様の声

「インテル® Fortran コンパイラーにより、アプリケーションが 24.5% から 31.5% ほど高速化されました。このパフォーマンスの改善は、劇的な変化をもたらしました。」

某大学天体物理学博士 殿

「非線形構造解析プログラムで計算時間の多くを占める行列の求解において、インテル® コンパイラーに含まれるインテル® MKL を用いることにより非常に高速化できました。今まで一昼夜かけて計算していたものが半日で行えることになり、非常に有効です。」

株式会社 計算力学研究センター 殿

インテル® コンパイラー 11.1 好評発売中

ご購入に関するお問い合わせ先：

HPC システムズ株式会社
www.hpc.co.jp
TEL：03-3599-3652

住商情報システム株式会社
www.clubscs.com
TEL：03-5859-3011

HPC テクノロジーズ株式会社
www.hpc-technologies.co.jp
TEL：03-6410-6070

株式会社 HPC ソリューションズ
www.hpc-sol.co.jp
TEL：03-5640-7858

製品の詳細に関するお問い合わせ先：XLSOFT エクセルソフト株式会社 Tel: 03-5440-7875 www.xlsoft.com/intel

Intel、インテル、Intel ロゴ、Intel Core、Xeon は、アメリカ合衆国およびその他の国における Intel Corporation の商標です。* その他の社名、製品名などは、一般に各社の表示、商標または登録商標です。 ©2009 Intel Corporation. 無断での引用、転載を禁じます。

BIOCOMP

密度勾配遠心用装置

グラジェント・マスター 107-201M

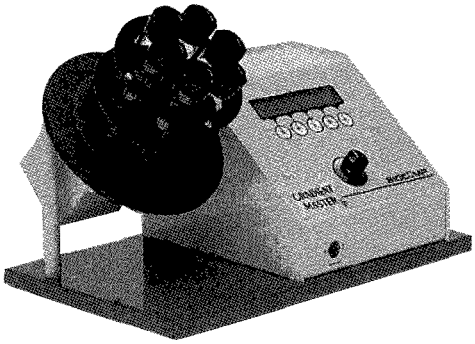

パテントである「Tilted tube rotation」の技法を使用して、短時間に、一度に6本の遠心チューブ内に、希望するグラジェントが作成できます。付属のマーカーブロックを用いて、チューブの下半分に希望するSolutionのBottom%溶液を入れ、上半分にTop%溶液を入れ、あとはDisplayに従って、2～3回ボタンを押すだけ! 誰にでも容易に再現性の良いリニアグラジェントが作成できます。

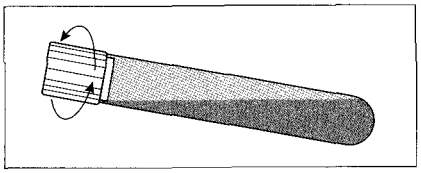

Tilted tube rotation

■価格 ¥710,000(本体のみ)～

ピストン・グラジェント・フラクショネーター 152-001

パテントである「Trumpet Tip」を用い、チューブ内に形成されたバンド(目に見えても、見えなくても)を上から順番に、水平に、上下のグラジェントとコンタミ無く、分離回収することができます。またair、rinse機構により、非常に狭い巾のバンド(通常は0.3mm巾以上)も回収可能です。カーボンナノチューブの分離、精製には最適です。(Arnold et al, 2006, Nature Nanotechnology. 1 : 60)

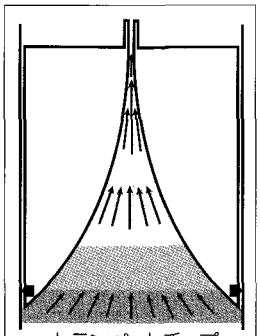

トランペットチップ

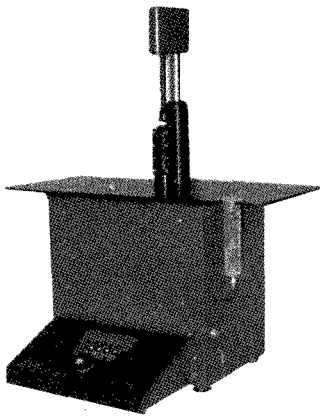

■価格 ¥1,960,000(本体のみ)～

グラジェント・ステーション 153-001

グラジェント・マスターとピストン・グラジェント・フラクショネーターを一体化した省スペースタイプです。

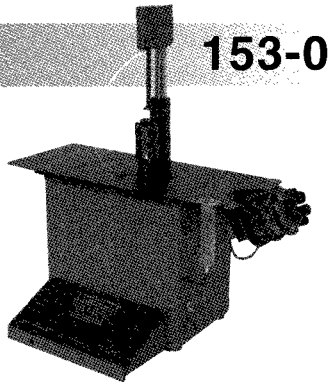

■価格 ¥2,600,000(本体のみ)～

●詳細については下記にお問合せ下さい。

日本総代理店
エスケーバイオ・インターナショナル株式会社
〒113-0033 東京都文京区本郷3-41-9
TEL 03-5689-9888 FAX 03-5689-9890
E-mail : info@skbio.co.jp
URL: http://www.skbio.co.jp

真空・酸素雰囲気中のクリーン加熱

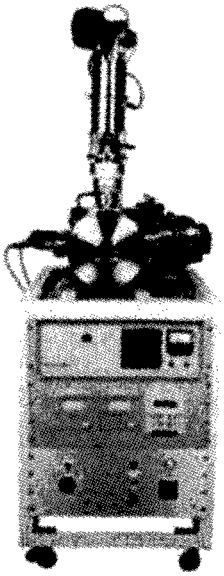

超高速昇温型を取付けた赤外線導入加熱システム

赤外線導入加熱装置
（GVL298・GVH298）

新しい赤外線加熱方式を採用し、真空中や狭い空間に赤外線を導入、試料に照射・昇温ができる

＜特長＞
- ●周りを加熱せずに試料のみクリーン加熱
- ●ノイズや電気誘導が発生しない
- ●少ない電力で高温まで加熱
- ●高真空、超高真空中、O_2、Ar中の試料加熱

＜仕様＞

	超高速昇温型（GVL298）	超高真空型（GVH298）
最高到達温度	1500℃	1400℃
対応真空度	5×10^{-7}Pa	5×10^{-9}Pa

＜用途＞
- ●シリコン、炭化珪素等の超高速昇温
- ●昇温脱離分析、酸素雰囲気中加熱
- ●X線光電子分光装置内試料の加熱

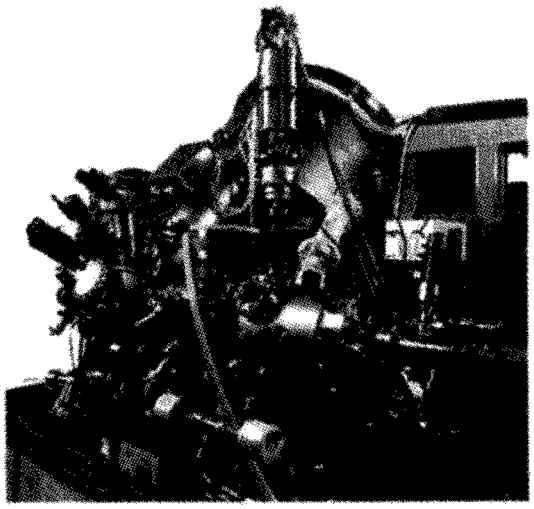

超高真空型のX線光電子分光装置取付例

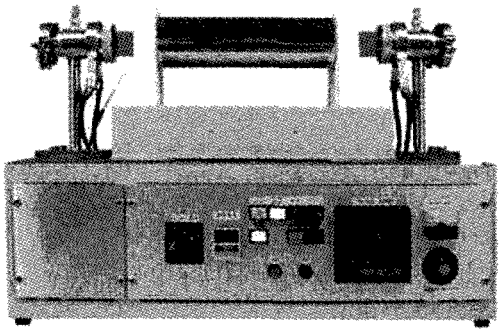

均温熱処理装置（GFA430VN）

均一な温度分布で、試験試料の熱処理！

＜特長・仕様＞
- ● 温度分布　：　1000℃ ±5℃
- ● 均温容積　：　φ36×200mm
- ● 透明電気炉　：　昇温中試料が見える
- ● 雰囲気　：　真空、ガスフロー中

＜用途＞
フラーレン・ナノチューブの生成、新素材の熱処理

貴社試料による依頼試験も受付けております。詳細は下記にお問い合わせ下さい

熱と共に歩む
株式会社サーモ理工

〒181-0013
東京都三鷹市下連雀8-7-3三鷹ハイテクセンター
TEL 0422-76-2511　FAX 0422-76-2514

★詳しくはWEBで　サーモ理工　検索

okamura

研究者の創造性を刺激し、あらゆる実験・研究にフレキシブルに対応。
いま、研究施設に求められるもの —— オカムラからの答えです。

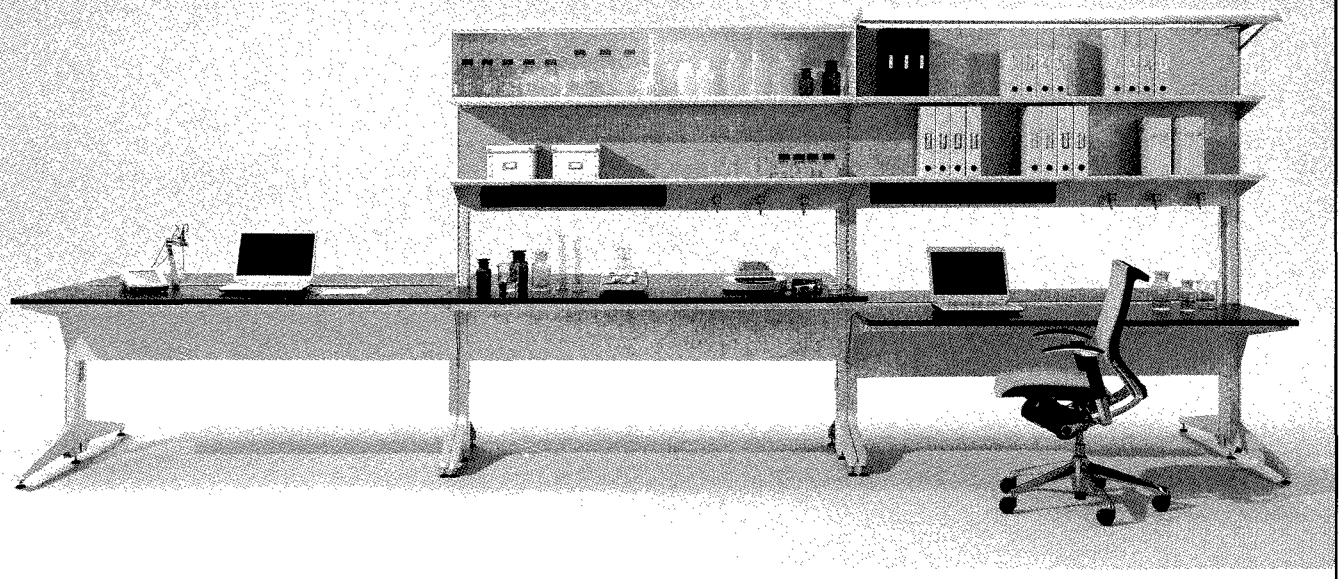

RIFORMA

ラボ・システム[リフォルマ]

豊富なオプションパーツにより、用途や使用する機器に合わせて自由自在に組合せ・組替えができる実験台です。機能性と同時にスマートなデザインを追求、研究施設にこれまでにない洗練された雰囲気をつくります。

DESIGN
研究者が快適に実験・研究に集中できるシンプルでスマートなデザイン。

FUNCTION
高さ調整可能な天板、支柱を用いた配線機能など、隅々にまで使いやすさを追求。

ABILITY
安全性や耐久性に加えて、点検もスムーズに行える高いメンテナンス性を確保。

FLEXIBILITY
オプションを用いて自由自在にカスタマイズ可能。拡張性に優れ、組替えも簡単に行えます。

試薬ボックス・スタイル
薬品や備品の
一時保管に最適

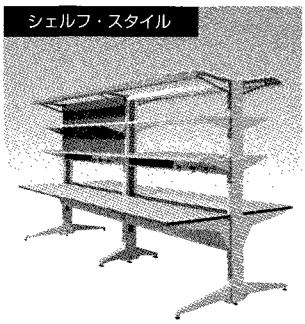
シェルフ・スタイル
天板を広く使いながら
十分な収容スペースを確保

フラット・スタイル
天板だけを広く
シンプルに活用

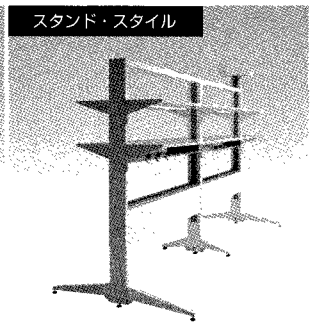
スタンド・スタイル
大型機器を配置するなど
天板を使わないスタイル

ホームページアドレス **http://www.okamura.co.jp/**

お問い合わせ・ご相談は お客様サービスセンターへ フリーダイヤル **0120-81-9060** 月曜～金曜(祝日を除く) 9:00～18:00

よい品は結局おトクです
オカムラ
株式会社 岡村製作所

Rigaku

VariMax Mo for Small Molecule

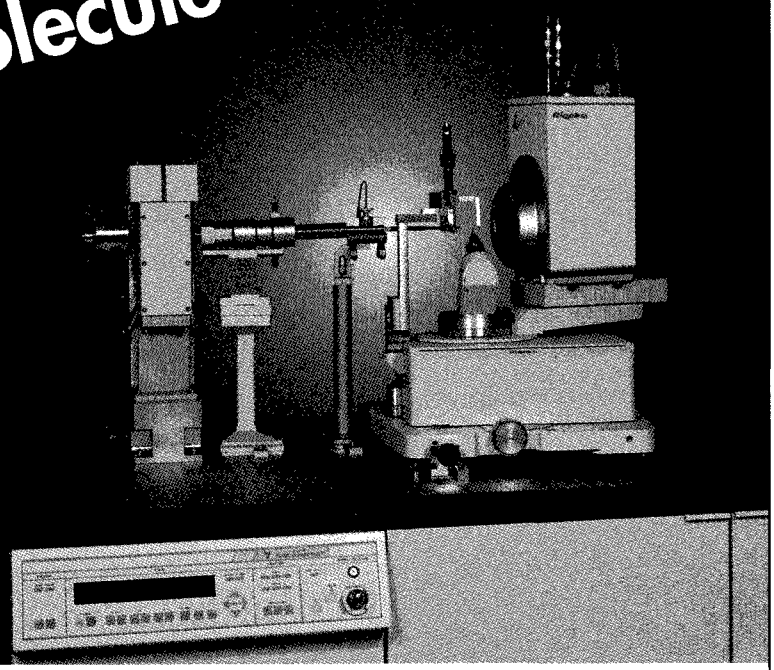

極微小結晶用単結晶構造解析装置

微小焦点X線発生装置RA-Micro7と新開発Moターゲット用 Confocal Mirror "VariMax Mo" を組み合わせたX線源は、従来比*約10倍のX線強度アップを実現しました。"VariMax Mo"は、測定目的に応じてビーム集光角を可変できるため、強度優先／分解能優先（格子定数の大きい結晶に有効）の選択が可能です。

＊X線発生装置 ultraX 18＋Graphite monochromatorとの比較

測定例

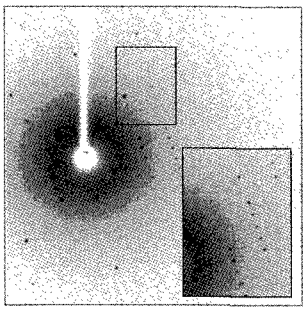

RA-Micro7+VariMax 50kV,16mA
微小試料からの弱い回折線も明瞭に捉えています。

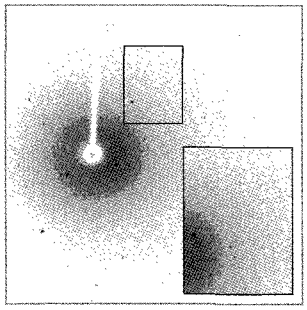

ultraX18+Graphite monocromator
60kV, 90mA
弱い回折線を捉えることが困難です。

【測定条件】
試　　料：Cytidine
結　　晶：0.02×0.02×0.02mm
カメラ長：45mm
検 出 器：Saturn70 CCD
波　　長：MoKα

従来比10倍の輝度

RA-Micro7とVariMaxの組み合わせによる相対強度比は、Graphite monochromatorを使用した光学系に比べ、約10倍（φ0.1mmのピンホールにて測定）を実現しました。

X線発生装置	光学系	相対強度比	
		φ0.3mmピンホール	φ0.1mmピンホール
RA-Micro7	VariMax	3.2	9.5
ultraX18	Graphite monochromator	1	
Sealed tube		0.25	

＊ピンホールはサンプル位置に設置し、強度を観測しました。

理想に近い円形ビーム

Osmic社により開発されたMoKα用のVariMaxは、高い技術力により、焦点位置で理想的な円形状ビームを作り出します。この高輝度のX線ビームは、約φ0.3mm程度の結晶から微小結晶に至る測定に対して、Graphitemonochromatorの光学系より効果を発揮します。

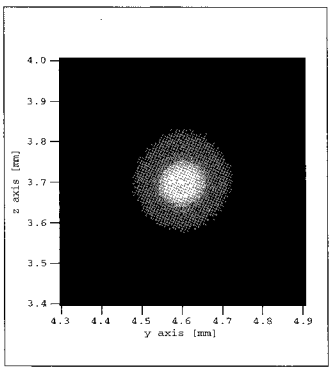

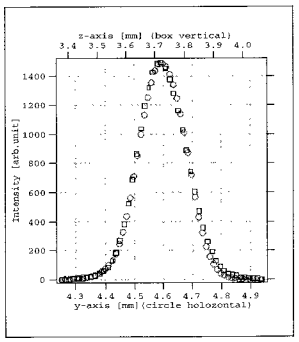

Horizontal：FWHM =0.193 mm
FW10M=0.334 mm
Vertical：FWHM =0.194 mm
FW10M=0.346 mm

微小結晶に対して威力を発揮

0.02mmのシチジン結晶により比較

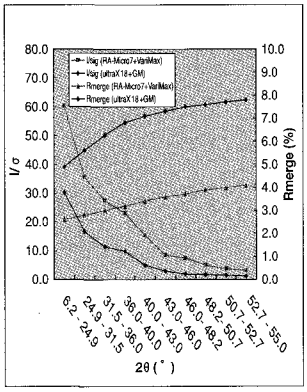

RA-Micro7 + VariMax Moは、現在ご利用いただいておりますMERCURY CCDシステムおよびSaturn CCDシステムと組み合わせが可能です。
詳しくはお問い合わせください。

株式会社リガク
〒196-8666 東京都昭島市松原町3-9-12 電話(042)545-8111<代表電話案内> FAX.(042)544-9795
●東京(03)3479-6011 ●東北(022)264-0446 ●大阪(072)696-3387 ●名古屋(052)931-8441 ●九州(093)541-5111
●URL http://www.rigaku.co.jp/

超小型最先端デジタルNMR 装置

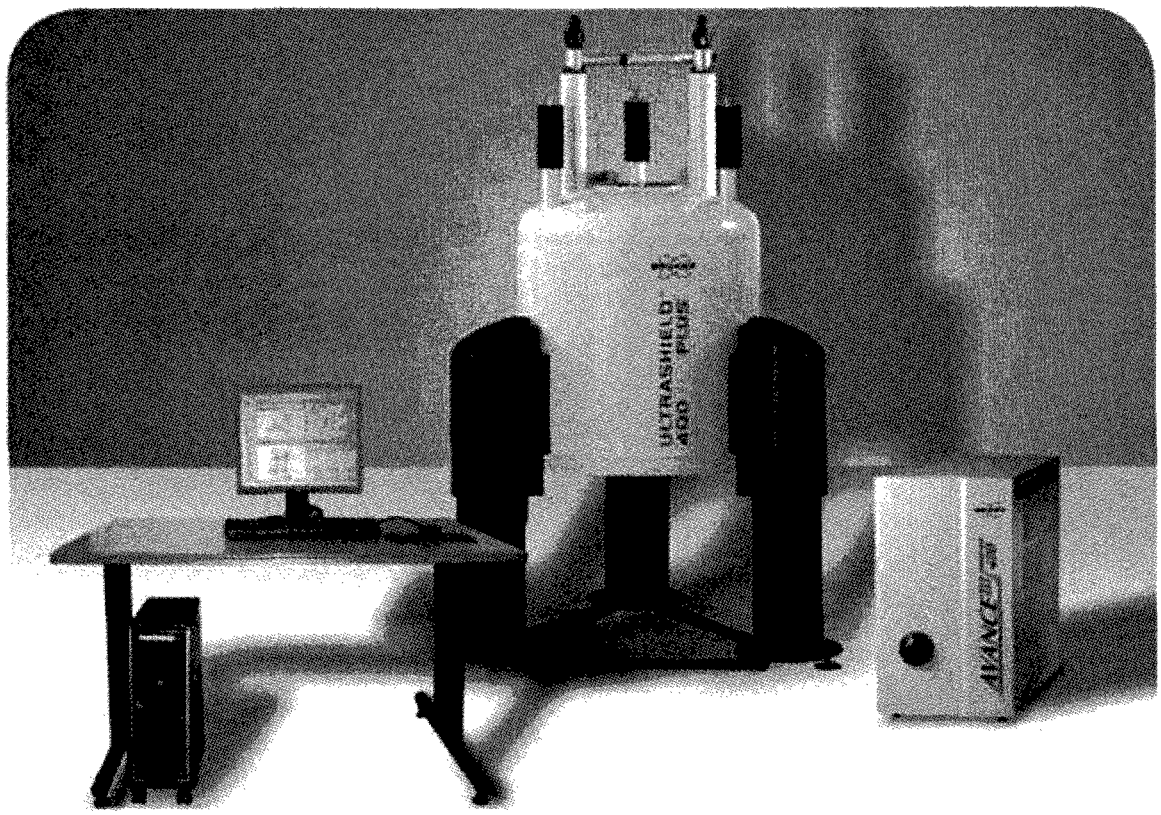

Avance™ III NanoBay

最新型Avance™III NanoBayは集積度が最高レベルの最先端デジタルNMR装置です。ブルカー・バイオスピンの高性能Avance™ III NMR分光計技術が超小型の筐体に大胆に収納されているところにNanoBayの革新的デザインを見ることができます。NanoBayは医薬品や工業化学、大学での基礎研究、学生実験、食品分析、病気の診断、その他低分子研究用途など幅広い分野の方々に高い生産性と最高品質のNMR情報を提供いたします。

- 超小型、革新的デザインの高性能NMR分光計
- 拡張性の高いAvance™III MicroBayも選択可能
- 適応機種は300、400MHz
- 超伝導磁石はUltraShield™ Plusも選択可能
- 小スペースにも容易に設置可能
- 分かりやすいTopSpin®ユーザーインターフェース
- 日本語で画面表示可能
- 実績あるAvance™ III技術を搭載
- 広範囲の研究分野に信頼性の高いNMR情報を提供

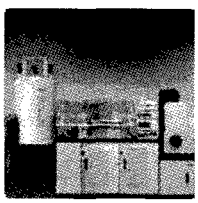
Metabolic Profiler

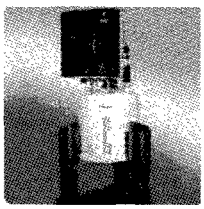
SampleJet

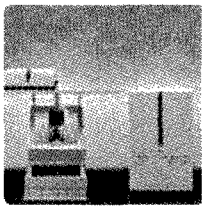
EMXplus

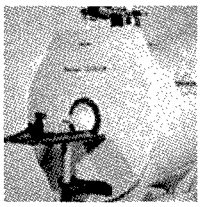
BioSpec MRI

ブルカー・バイオスピン株式会社

Bruker BioSpin

本社　〒221-0022　神奈川県横浜市神奈川区守屋町3-9　Tel.045-444-1390(代)　Fax.045-453-2457
大阪　〒532-0004　大阪府大阪市淀川区西宮原1-8-29 テラサキ第2ビル2階 Tel.06-6394-8989(代)　Fax.06-6394-9559
ホームページアドレス：http://www.bruker-biospin.com　メールアドレス：info@bruker-biospin.jp

BRUKER

Bruker AXS

SMART APEX II ULTRA

高輝度X線源搭載CCD単結晶X線構造解析装置

- 高輝度微小焦点X線源と集光型多層膜ミラーにより、100μm以下の微小結晶が測定可能
- Mo線源、Cu線源のどちらかを選択可能
- 今まで放射光施設を必要としたサンプルが、実験室で測定・解析可能

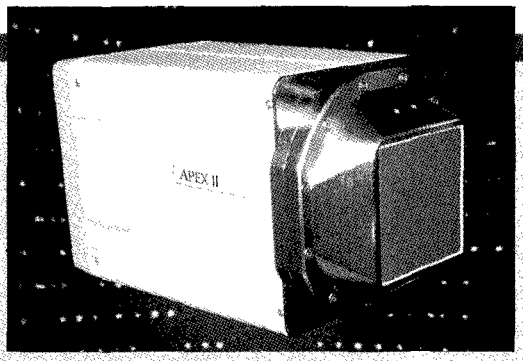

60×60mm 4KCCD搭載 APEXII 検出器

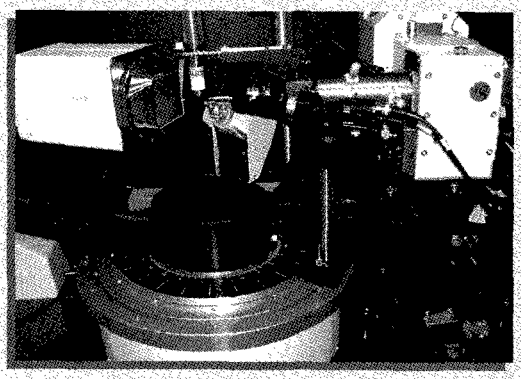

高輝度微小焦点＋集光ミラー光学系

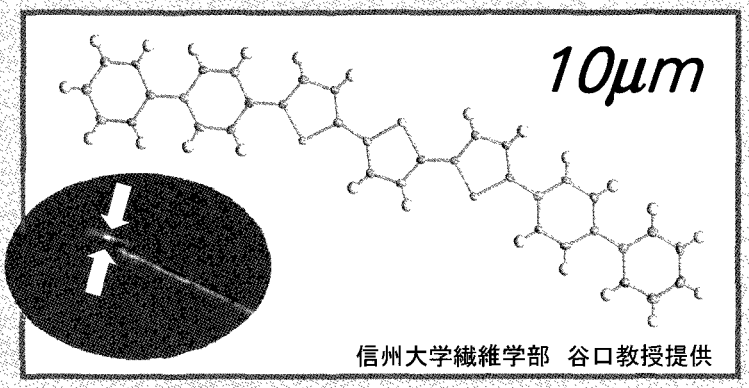

信州大学繊維学部 谷口教授提供

SMART APEX II DUO

2波長X線源搭載CCD単結晶X線構造解析装置

- 封入管球式のMo線源とCu線源の2つを1つの回折計に搭載、各線源による測定が自動的に続けて実行可能
- CCD検出器の感度はMo線源とCu線源の両方に対応
- スタンダードなMo線源による錯体・天然物などの低分子化合物の構造解析から電子密度解析、Cu線源を利用した絶対構造決定まで幅広いアプリケーションに1台で対応

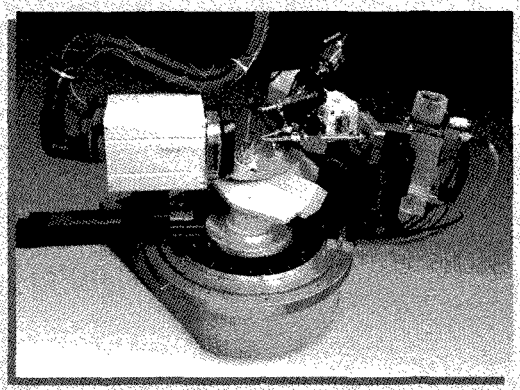

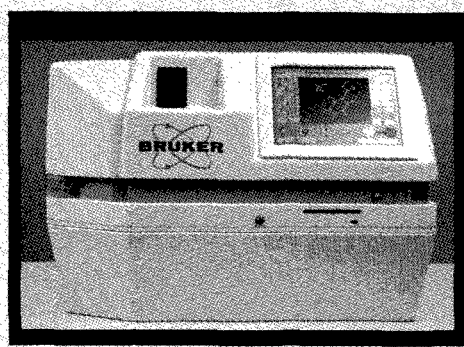

SMART X2S

卓上型CCD単結晶X線構造解析装置

- 卓上型のX線構造解析システム
- サンプルセッティング、アライメント、測定、解析まで全自動化
- タッチパネル式で操作も簡単
- 冷却水の不要な空冷タイプ

ブルカー・エイエックスエス株式会社

横　浜 〒221-0022 神奈川県横浜市神奈川区守屋町3-9
Tel.045-453-1960（代） Fax.045-453-1825

大　阪 〒532-0004 大阪府大阪市淀川区西宮原1-8-29テラサキ第2ビル2F
Tel.06-6393-7822（代） Fax.06-6393-7824

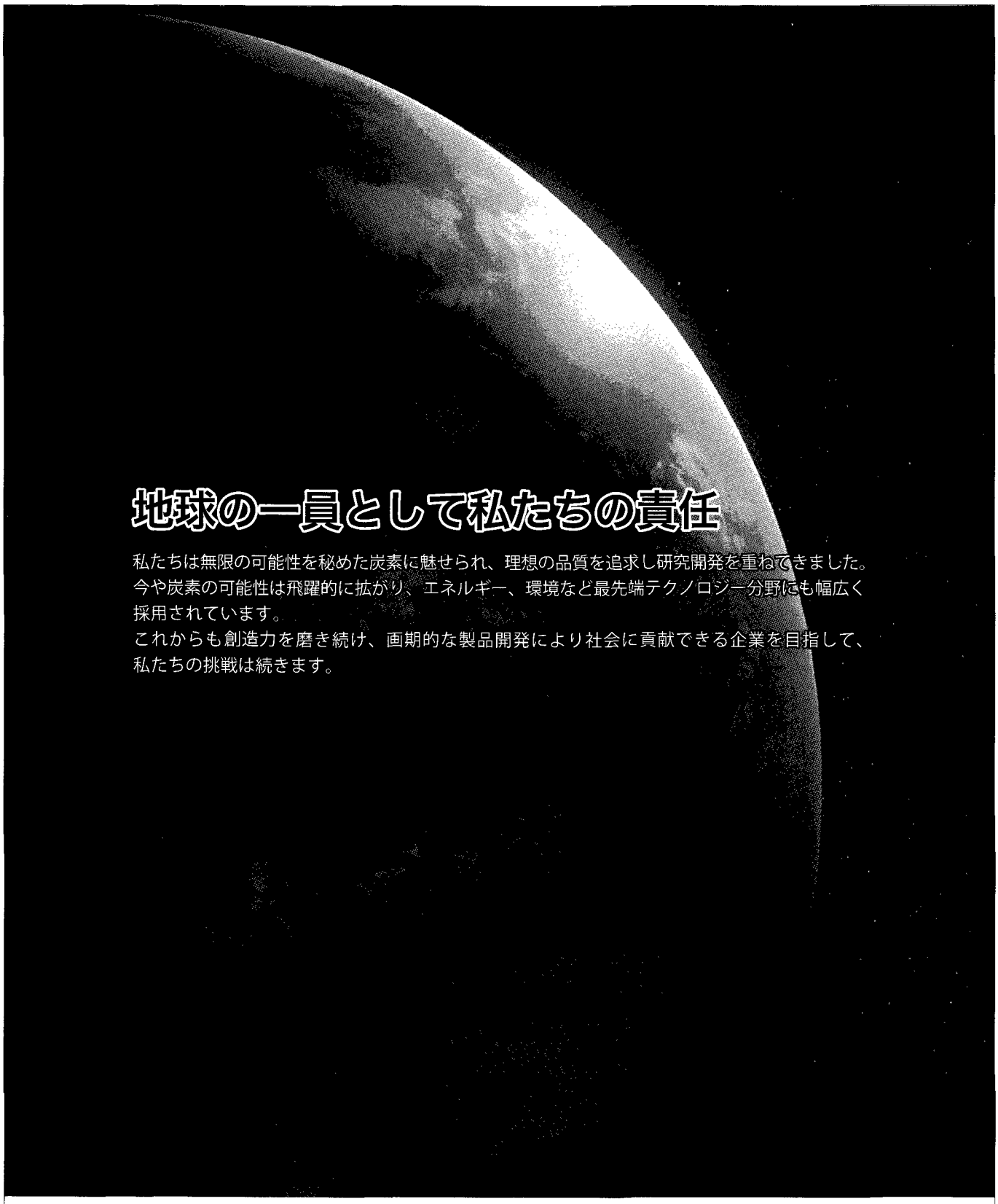

地球の一員として私たちの責任

私たちは無限の可能性を秘めた炭素に魅せられ、理想の品質を追求し研究開発を重ねてきました。
今や炭素の可能性は飛躍的に拡がり、エネルギー、環境など最先端テクノロジー分野にも幅広く採用されています。
これからも創造力を磨き続け、画期的な製品開発により社会に貢献できる企業を目指して、私たちの挑戦は続きます。

TOYO TANSO
Inspiration for Innovation

東洋炭素株式会社
本社　〒530-0001 大阪市北区梅田3-3-10 梅田ダイビル10F　Tel 06-6451-2114　Fax 06-6451-2186　www.toyotanso.co.jp

究極のナノ分散評価技術「複合化燃焼法」をご紹介します。

この技術は、私が2005年ごろに、当時勤務しておりました某企業内に於きまして、独力で、セレンディピティ的に開発した技術です。

しかし、都合により、その企業に在籍している間には、この技術を世に出すことはできませんでした。

昨年末、私は転身支援制度（早期退職者優遇制度）を利用して退職し、私費を投じて、この技術を世に出すことにしました。

発明した技術、およびその発明の過程は、学術的、教育的には、極めて興味深く、意義深い内容であると自負しており、これを世に出すことに人生をかけて取り組んでおります。

すなわち、

「リストラドクターがナノテクの歴史を変える！」

―自称:ナノテク界のブラックジャックの挑戦― を実行しているところなのです。

（注）ナノテク界のブラックジャック ≒ 企業人として13年間ナノカーボン界で活躍したが、現在は無職の天才科学者

今回の発表の見どころは　、

・カーボンナノチューブの超音波分散状態を瞬間的に封じ込める魔法（「魔法の立体網効果」の発見）。

・「魔法の立体網」で捕まえたカーボンナノチューブの料理方法（複合化燃焼法の開発）。

・開発過程で発掘したナノカーボン界のスーパースター（BP2000：CABOT）　です。

なお、退職時にデータ、資料等の持ち出し禁止、守秘義務等の誓約があります。

さらに、（失業中ですので）再現実験を行うことができない状況にあります。

したがって、当時の記憶を頼りに発表用資料を作成している状況にあることをご理解いただきたく存じます。

公的目標：「複合化燃焼法」が世界中の高校の化学の教科書に掲載されること。

私的目標：この活動により、人並み以上の収益が得られること。

皆様のご理解とご協力をお願いします。

無所属　工学博士　坪井利行

携帯電話　090-8439-7432　　e-mail:　marobonta@yahoo.co.jp

調べる作業をお手伝い！
試薬・消耗品の総合カタログサイト

登録料・利用料 無料！

LabIT Chemistry for Life Science for Future www.labit.jp （ラビット）

研究室に必要な、試薬・消耗品などをインターネットで簡単検索。
面倒だった「ものを探す」作業をお手伝いします。

http://www.labit.jp

◆ メーカー各社より提供を受けた豊富なカタログデータをご用意
◆ WEBカタログで調べた商品をそのまま見積依頼・注文することができます
◆「お気に入り」や「購買履歴」から注文でき、繰り返し注文が簡単
◆ カタログ掲載品以外の商品もフリーハンドで注文可能
◆ 検索、申請、承認、発注、伝票管理に至るまで、一貫して行えます
◆ 申請・承認機能により、申請の為の書類づくりが不要です
◆ 注文・購入実績データをダウンロード(CSV)することができます
◆ パソコンとインターネットの環境だけ、登録料・利用料は一切かかりません

中山商事では、WEBカタログ購買ツール「LabIT(ラビット)」を推奨・提案しています。
ご利用に関するお問い合わせは、弊社営業所もしくはラビットカスタマーセンター(TEL 029-847-9475)までご連絡下さい。詳しくはこちら(http://www.nakayama-co.jp/labit/)をご参照下さい。

Nakayama

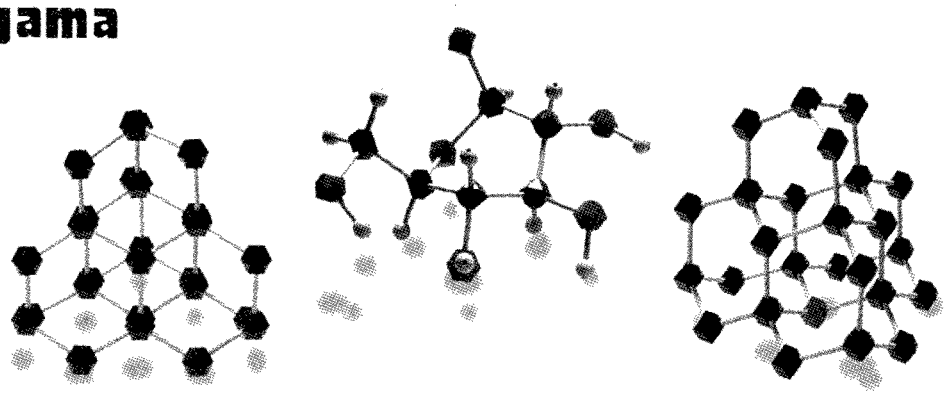

中山商事株式会社

http://www.nakayama-co.jp

〒317-0075 茨城県日立市相賀町17-9
TEL 0294-22-5291 FAX 0294-25-1077 info@nakayama-co.jp
茨城県：日立営業所・水戸営業所・筑波営業所・鹿島営業所・下館営業所・配送センター
栃木県：栃木営業所
福島県：いわき営業所・郡山営業所・原町営業所・白河営業所
宮城県：仙台営業所

実験研究用試薬・化学工業薬品・臨床試薬・水処理薬品・防災設備・理化学機器・研究試作装置・実験室設備
環境分析装置・産業廃棄物収集運搬・機械器具設置工事・環境エンジニアリング・各種オーダーメイド機器製作

溶液中の粒子のナノレベル微細化・分散に

BRANSON 超音波ホモジナイザー

ホーン先端部の振幅の安定性を、より高めた Advance タイプ になりました。

近年のナノテクノロジーの発展及び粉体関連技術の向上により、より微細な粒子に対する乳化分散処理の要望が増えてまいりました。
超音波ホモジナイザーを使用し、均質な乳化分散処理を行い、安定させることにより製品の機能は向上します。
ブランソン社では 20kHz 機と、40kHz 機の 2 タイプを用意しております。
1 次粒子の凝集力にも拠りますが、20kHz 機では 100nm 程度までの分散力があります。40kHz 機は、さらに細かいレベルで分散ができる可能性があります。

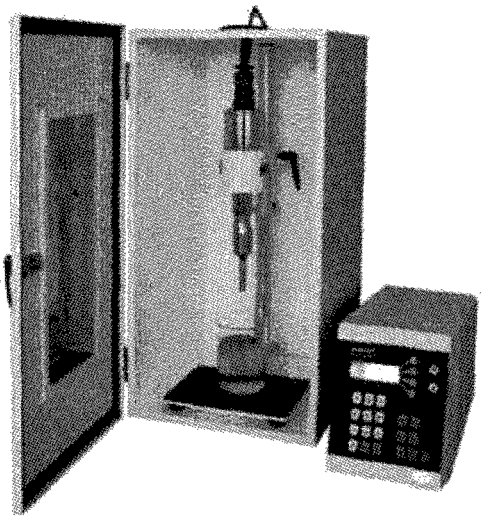

20KHz 超音波ホモジナイザー
BRANSON　SONIFIER シリーズ

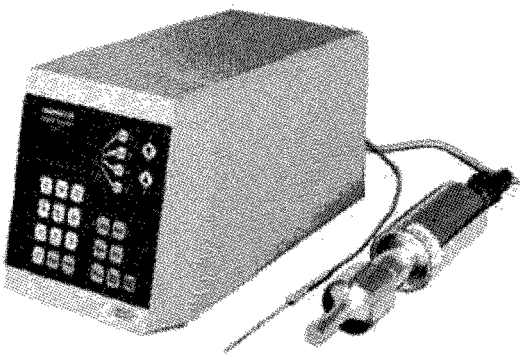

高周波 40KHz 超音波ホモジナイザー
BRANSON SLPe シリーズ

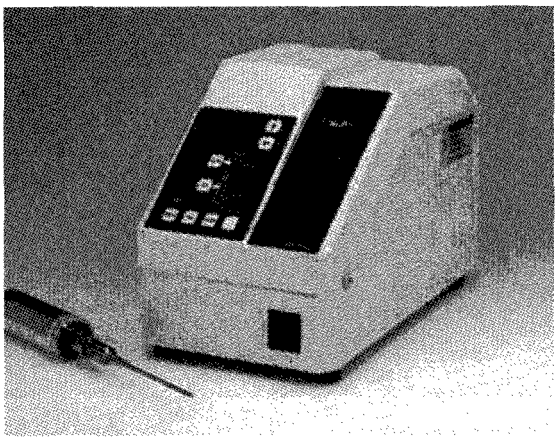

ブランソン社の製品は、ホーン先端部の振幅の安定性が高く、強力なキャビテーションが得られ、効率良く、再現性の高い分散処理が行えます。

主なアプリケーション

分散

カーボンナノチューブ　有機顔料　無機顔料　セラミック　セメント　感光体　記録材料
磁性粉　粉末冶金　酸化鉄　金属酸化物　シリカ　アルミナ　カーボンブラック
ポリマー　ラテックス　製紙　ファンデーション
研磨剤　電池　フィラー　光触媒　触媒　ワクチン　体外診断薬　歯磨き粉　シャンプー
半導体　電子基盤　液晶　貴金属　金属　宝石　タイヤ　発酵菌類　その他

乳化

エマルジョン製剤　農薬　トナー　ラテックス　界面活性剤　クリーム　乳液　クリーム　等

株式会社セントラル科学貿易
本社：111-0052 東京都台東区柳橋 1-8-1
Tel 03-5820-1500 Fax 03-5820-1515
URL http://www.cscjp.co.jp/

大阪支店：　Tel 06-6325-3171 Fax 06-6325-5180
福岡営業所：Tel 092-482-4000 Fax 092-482-3797
札幌出張所：Tel 011-764-3611 Fax 011-764-3612

新登場

逆相クロマトグラフィー用カラム

TSKgel ODS-100V 3μm / 5μm

親水性物質に対して保持が強く、また、塩基性物質・酸性物質のピーク形状が共に優れた、ODS-100Vのラインナップが強化されました。従来の5μmとハイスループット分析用3μmの驚きのピーク形状を体験してください。

特長

- 細孔径100Å、比表面積450 m²/g(当社従来カラムの1.5 倍)、炭素導入量15 %、モノレイヤー
- 水100 % 移動相でも使用可能
- グラジエントによる親水性物質から疎水性物質までの一斉分析が可能
- 新技術エンドキャッピングでシラノールの影響を低減
- 3μmシリーズはハイスループット分析が可能
- 常に3ロットのカラムを用意
- USP L1カテゴリー

LC/MS分析に、ファーストチョイス

サルファ剤の一斉分析

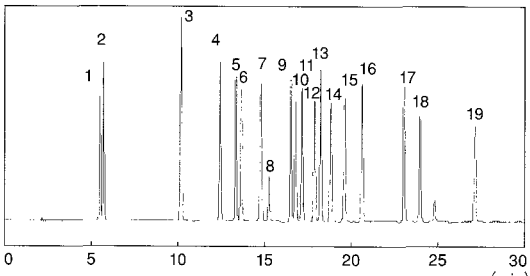

サンプル
1：sulfaguanidine
2：sulfanilamide
3：sulfacetamide
4：sulfadiazine
5：sulfathiazole
6：sulfapyridine
7：sulfamerazine
8：trimethoprim
9：sulfamethizole
10：sulfadimidin
11：sulfamethoxypyridazine
12：sulfachloropyridazine
13：sulfamethoxazole
14：sulfamonomethoxine
15：sulfadoxine
16：sulfabenzamide
17：sulfadimethoxine
18：sulfaquinoxaline
19：sulfanitran

カラム：TSKgel ODS-100V 3μm(4.6mmI.D.×15cm)
溶離液：A；0.1% formic acid in water
B；0.1% formic acid in methanol
ｸﾞﾗｼﾞｴﾝﾄ：0min(B；0%)→30min(B；70%)→32min(B；70%)
流　速：1.0mL/min
検　出：UV 270nm
温　度：40 ℃
注入量：10μL

塩基性物質のピーク形状

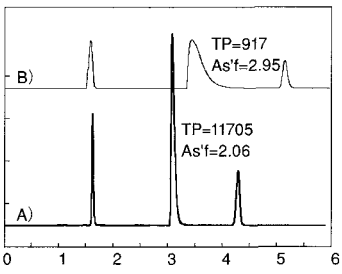

カラム：A)TSKgel ODS-100V 3μm(4.6mmI.D.×15cm)
B)他社ODS 3μm(4.6mmI.D.×15cm)
溶離液：5mmol/L $HCOONH_4$/MeOH (20/80)
流　速：1.0mL/min　　検　出：UV 254nm
温　度：40 ℃　　注入量：10μL
サンプル：1. Uracil 2. Desipramine (26mg/L)
3. Benzene

分析カラム

品　名	品　番	カラムサイズ	価　格
TSKgel ODS-100V 3μm	0021838	1.0mmI.D. × 3.5cm	28,000円
	0021839	1.0mmI.D. × 5.0cm	28,000円
	0021814	2.0mmI.D. × 1.0cm	30,000円
	0021813	2.0mmI.D. × 3.5cm	38,000円
	0021812	2.0mmI.D. × 5.0cm	40,000円
	0021811	2.0mmI.D. × 7.5cm	45,000円
	0021810	2.0mmI.D. ×15.0cm	55,000円
	0021482	3.0mmI.D. × 5.0cm	40,000円
	0021483	3.0mmI.D. × 7.5cm	45,000円
	0021484	3.0mmI.D. ×15.0cm	55,000円
	0021831	4.6mmI.D. × 5.0cm	40,000円
	0021830	4.6mmI.D. × 7.5cm	45,000円
	0021829	4.6mmI.D. ×15.0cm	55,000円

品　名	品　番	カラムサイズ	価　格
TSKgel ODS-100V 5μm	0021457	2.0mmI.D. × 5.0cm	35,000円
	0021458	2.0mmI.D. ×15.0cm	42,000円
	0021455	4.6mmI.D. ×15.0cm	42,000円
	0021456	4.6mmI.D. ×25.0cm	55,000円

ガードカラム（ガードカートリッジ）

品　名	品　番	カラムサイズ	価　格
TSKguardgel ODS-100V 5μm	0021841	2.0mmI.D. ×1.0cm*1	30,000円
	0021453	3.2mmI.D. ×1.5cm*2	35,000円

注意）カートリッジホルダは、下記が必要になります。
*1）2 mmI.D.（品番 0019308 ／45,000 円）
*2）3.2 mmI.D.（品番 0019018 ／45,000 円）

TOSOH 東ソー株式会社 バイオサイエンス事業部

東京本社営業部　☎(03)5427-5181　〒105-8623　東京都港区芝3-8-2
大阪支店バイオサイエンスG　☎(06)6209-1948　〒541-0043　大阪市中央区高麗橋4-4-9
名古屋支店バイオサイエンスG　☎(052)211-5730　〒460-0003　名古屋市中区錦1-17-13
福岡支店　☎(092)781-0481　〒810-0001　福岡市中央区天神1-13-2
仙台支店　☎(022)266-2341　〒980-0014　仙台市青葉区本町1-11-1
山口営業所　☎(0834)63-9888　〒746-8501　山口県周南市開成町4560
カスタマーサポートセンター　☎(0467)76-5384　〒252-1123　神奈川県綾瀬市早川2743-1
バイオサイエンス事業部ホームページ http://www.tosoh.co.jp/science/

M0905GX.C

Nano & Bio

――フロンティア出版のナノテクノロジー・ナノマテリアルシリーズ――

自己組織化ナノマテリアル
ーフロントランナー85人が語るナノテクノロジーの新潮流ー
企　画：理化学研究所　フロンティア研究システム
　　時空間機能材料研究グループ
監　修：国武豊喜（北九州市立大学／理化学研究所）
編集幹事：下村政嗣（北海道大学／理化学研究所）
　　山口智彦（産業技術総合研究所）
■体裁／B5判・392頁　■価格／57,750円（税込）

有機・無機・金属ナノチューブ
ー非カーボンナノチューブ系の最新技術と応用展開ー
編　集：清水敏美（産業技術総合研究所）
　　木島　剛（宮崎大学）
■体裁／B5判・330頁　■価格／57,750円（税込）

ナノ粒子の創製と応用展開
編　集：米澤　徹（東京大学）
■体裁／B5判・322頁　■価格／57,750円（税込）

ナノコンポジットマテリアル
ー金属・セラミック・ポリマー3大物質のナノコンポジットー
編　集：井上明久（東北大学）
■体裁／B5判・363頁　■価格／52,500円（税込）

ナノオプティクス・ナノフォトニクスのすべて
ーナノ光技術の基礎から実用までー
監　修：河田　聡（大阪大学／理化学研究所）
編　集：梅田倫弘（東京農工大学）
　　川田善正（静岡大学）
　　羽根一博（東北大学）
■体裁／B5判・352頁　■価格／57,750円（税込）

MEMS/NEMSの最先端技術と応用展開
編　集：前田龍太郎（産業技術総合研究所）
　　澤田廉士（九州大学）
　　青柳桂一（マイクロマシンセンター）
■体裁／B5判・285頁　■価格／52,500円（税込）

ナノインプリントの最新技術と装置・材料・応用
ーナノインプリント技術の最先端と拡がる用途ー
編　集：平井義彦（大阪府立大学）
■体裁／B5判・330頁　■価格／57,750円（税込）

ナノバイオエンジニアリングマテリアル
ーバイオインターフェイス・ナノバイオプロセッシング
　・バイオコンジュゲーション・バイオマトリックスー
監　修：石原一彦（東京大学）
■体裁／B5判・350頁　■価格／52,500円（税込）

フロンティア出版
〒110-0012 東京都台東区竜泉1-21-18　TEL:03-6802-1640　FAX:03-6802-1641　E-mail:info@frontier-books.com
http://www.frontier-books.com

株式会社　マシナックス

代表取締役　佐野隆治

〒454-0856　名古屋市中川区小碓通 2-6

ＴＥＬ　052-654-5021(代)　　ＦＡＸ 052-654-5125

HP　　http://www.mashinax.jp/

メール　mashinax@sf.starcat.ne.jp

販売
人と科学のステキな未来へ
コスモ・バイオ株式会社

製造
東湘電機株式会社

NANORUPTOR® ～サンプル密閉式超音波分散装置～

―――― バイオの技術をナノテクへ ――――

本装置はカーボンナノチューブや燃料電池用触媒を始めとする
各種ナノ粒子を溶媒に分散させる用途に最適化されています。

実施例：燃料電池用触媒評価、カーボンナノチューブの分散
納入実績：各大学、自動車メーカー、光学機器メーカー、電子部品メーカー

特　長

● **分散に最適**
各種ナノ粒子（カーボンナノチューブ、フラーレン等）
の分散処理に最適。

● **密閉処理**
溶媒の蒸発・揮散やコンタミがありません。

● **多検体同時処理**
最大 24 試料を同時に処理できます。

● **再現性良好**
回転機構の採用により均一な超音波照射が可能です。

● **低騒音**
高性能消音箱により超音波の騒音が低く抑えられます。

NR-350仕様表

品番	NR-350
品名	密閉式超音波分散装置　Nanoruptor
超音波周波数	20 kHZ
超音波出力	～350 W 可変
電源	100 V、50/60 Hz、5.5 A
最低設置スペース概寸	400 (W) × 300 (D) × 680 (H) mm
発振ユニット概寸	400 (W) × 260 (D) × 160 (H) mm
処理ユニット概寸	170 (W) × 160 (D) × 270 (H) mm
消音箱概寸	400 (W) × 300 (D) × 520 (H) mm
NR-350 全体重量	36 Kg
ランタイマー	0～99 分 59 秒、デジタル
インターバルタイマー (ON)	0～99.99 秒、デジタル
インターバルタイマー (OFF)	0～99.99 秒、デジタル
処理本数	1 本 (50 mL)
付属品	消音箱、電源ケーブル、接続ケーブル、排水ポンプ、取り扱い説明書、ユーザー登録カード
備考	NR-350 は機器のみです。別途処理量に応じたアクセサリー（ギヤ・板＋チップ）をお買い求め下さい。

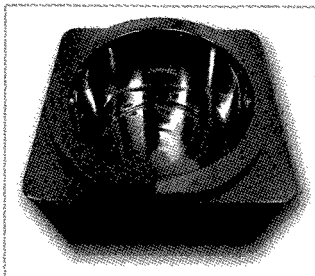

丸形超音波処理槽

丸形超音波処理槽の採用により分散の高効率化を実現。

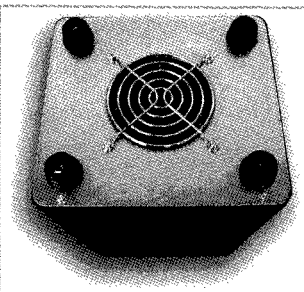

冷却ファン

冷却ファン及び専用回路の採用により長時間運転が可能。

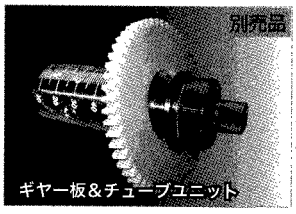

・ギヤー板（品番：NG-350-50）
・50 mL 専用共振棒 1 本入りセット（品番：MM-50WS）

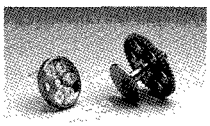
1.5mL チップ ユニット

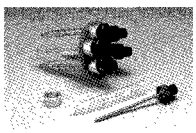
15mL チップ ユニット

メーカー略号：TOS

品名	品番	包装	希望販売価格
超音波密閉式分散装置 Nanoruptor®	NR-350	1 UNIT	¥1,950,000

*アクセサリユニットは含みません

別売品　使用可能チューブ：マルエム社製 50 mL ねじ口試験管　メーカー略号：TOS

品名	品番	包装	希望販売価格
50 mL チューブ用チップ	MM-50WS	1 SET*	¥54,000
ギヤー板	NG350-50	1 PC	¥9,000

*50 mL 専用共振棒 1 本入りセット。ギヤー板は別売品。

コンパクト&スマートな時代へ《nEXTシリーズ》

新発売!!

JAIのリサイクル分取HPLCは発売以来37年。
おかげさまで2,500台を超える装置が国内外で活躍しています。

2009年、装いを新たにnEXTシリーズを発売いたします。

"高性能"・"使いやすさ"・"メンテナンス性能"を追求した究極の装置。
1/3ボディーサイズ(従来機比較)。nEXTを皆様のラボで是非ご採用ください。

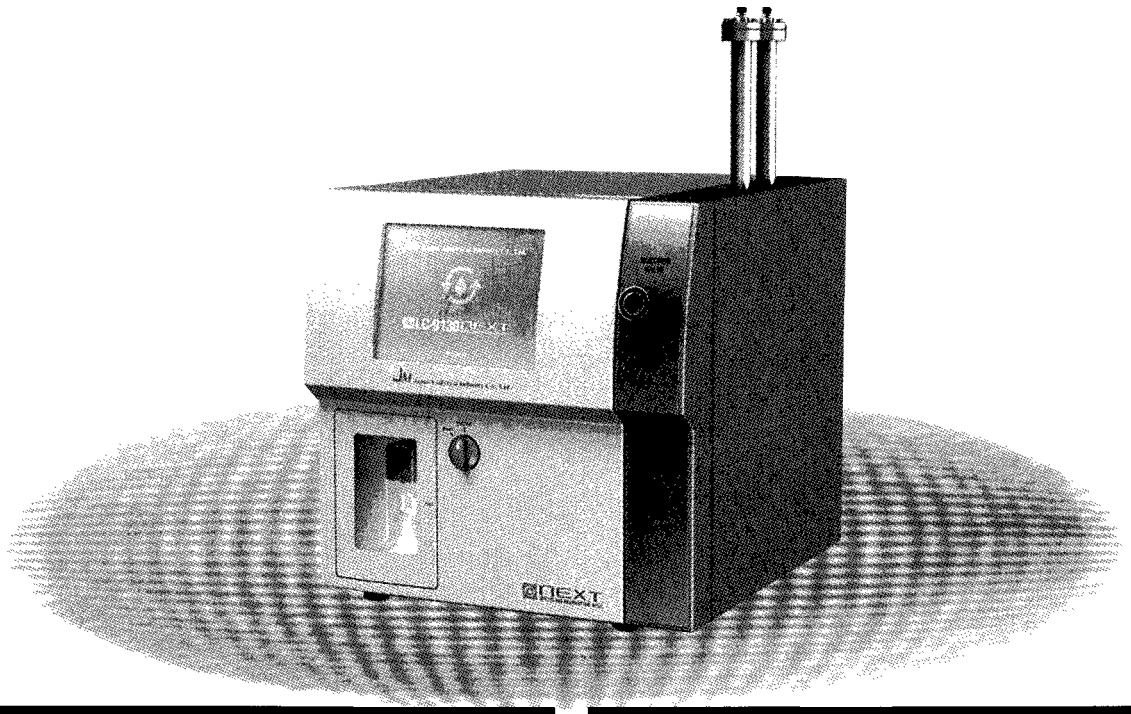

GPCリサイクルによる Macrocyclic Oligothiophenesの分離

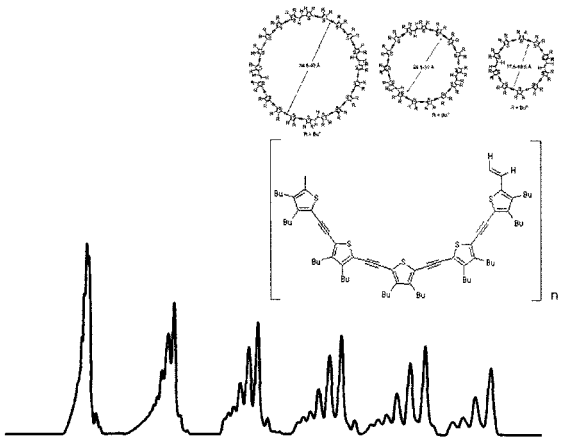

Column: JAIGEL-2.5H+JAIGEL-3H
Eluent: Chloroform
Detector: UV-310B @ 254 nm

GPCリサイクルによる位置異性体の分離

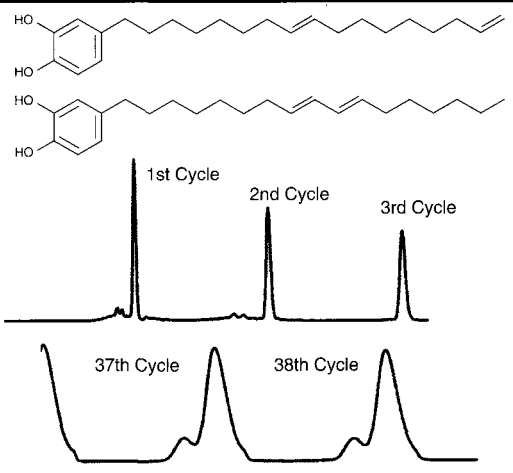

Column: JAIGEL-2H+JAIGEL-2.5H
Eluent: Chloroform
Detector: UV-310B @ 254 nm

JAI 日本分析工業株式会社

■本社・工場　〒190-1213　東京都西多摩郡瑞穂町武蔵208　TEL：042-557-2331　FAX：042-557-1892
■大阪営業所　〒532-0002　大阪府大阪市淀川区東三国5-13-8-303　TEL：06-6393-8511　FAX：06-6393-8525
■名古屋営業所　〒465-0025　愛知県名古屋市名東区上社3-609-3D　TEL：052-709-5400　FAX：052-709-5403

URL：http//www.jai.co.jp/　E-mail：sales@jai.co.jp

フロンティアカーボン(株)の フラーレンおよびフラーレン誘導体 サンプル一覧

銘柄		分子構造	純度(HPLC面積%、代表値)	取扱数量
nanom purple フラーレンC60	**ST**	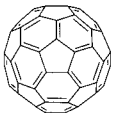	99	10g以上
	TL		99.5	5g以上
	SU		99.5/昇華精製品	2g以上
	SUH		99.9/昇華精製品	1g以上
nanom orange フラーレンC70	**ST**		97	1g以上
	SU		98/昇華精製品	0.5g以上
nanom mix 混合フラーレン	**ST**	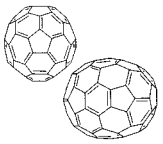	C60、C70、その他高次フラーレンの混合物 ST-FはSTの微粒化品	50g以上

銘柄	分子構造	純度(HPLC面積%、代表値)	取扱数量
nanom spectra E100 **PCBM** (phenyl C61-butyric acid methyl ester)	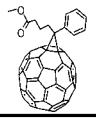	99	1g以上
nanom spectra E200 **PCBNB** (phenyl C61-butyric acid n-butyl ester)	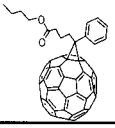	99	1g以上
nanom spectra E210 **PCBIB** (phenyl C61-butyric acid i-butyl ester)	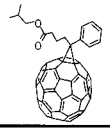	99	1g以上
nanom spectra E110 **C70PCBM** (phenyl C71-butyric acid methyl ester)	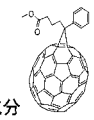 主成分	99（異性体トータル） 位置異性体の混合物	0.5g以上

銘柄	分子構造	内容	取扱数量
nanom spectra D100 水酸化フラーレン	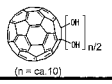	$C_{60}OH_n$ n=10を主成分とする混合物	2g以上
nanom spectra A100 水素化フラーレン	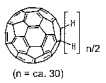	$C60H_n$ n=30を主成分とする混合物	2g以上
nanom spectra G100	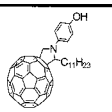	純度(HPLC面積%, 代表値) 99	1g以上

2009年2月1日現在

銘柄、取扱数量等は予告無く変更する場合がございます。予めご了承下さい。

当社製品は、下記2社から購入いただけます。詳細は直接お問い合わせください。

・関東化学株式会社 試薬事業本部
〒103-0023 東京都中央区日本橋本町3-11-5 TEL:03-3663-7631 FAX:03-3667-8277
http://www.kanto.co.jp E-mail:reag-info@gms.kanto.co.jp
・第一実業株式会社 新事業推進室 【担当:鎰広(カギヒロ)】
〒102-0084 東京都千代田区二番町11-19 TEL:03-5214-8579 FAX:03-5214-8501

＜本資料に関するお問い合わせ先＞
フロンティアカーボン株式会社 営業販売センター【担当:梶原】
〒806-0004 福岡県北九州市八幡西区黒崎城石1-1 （移転いたしました）
TEL:093-643-4400 FAX:093-643-4401 http://www.f-carbon.com
※弊社へのお問い合わせはHPよりお願いいたします。

Frontier Carbon Corporation